1-1-2015

# The Role of Intra-Articular Nerve Growth Factor in Facet-Mediated Pain: Relationships to Spinal BDNF and Neuronal Hyperexcitability

Jeffrey Kras
*University of Pennsylvania*, jkras@seas.upenn.edu

# The Role of Intra-Articular Nerve Growth Factor in Facet-Mediated Pain: Relationships to Spinal BDNF and Neuronal Hyperexcitability

**Abstract**
Traumatic neck injuries commonly result from rear-end motor vehicle collisions and are associated with a high incidence of neck pain and considerable annual costs. The facet joint is the most common source of neck pain. That joint is innervated by nociceptors that are activated by tensile stretching of the joint's capsular ligament. Although activation of those joint afferents and joint inflammation contribute to facet-mediated pain, the cellular response(s) within the joint that initiate pain via the joint afferents are unknown. Similarly, the mechanisms that induce central sensitization and maintain facet pain are not fully defined. Nerve growth factor (NGF) is a potent mediator of inflammatory cascades and is hypothesized to contribute to joint pain. Further, NGF regulates brain-derived neurotrophic factor (BDNF), which, when released in the spinal cord, sensitizes spinal neurons. Despite their roles in inflammatory pain, no studies have identified whether the neurotrophins NGF and/or BDNF contribute to facet joint-mediated pain. These studies utilize a rat model of mechanical facet joint injury to investigate the roles of NGF and BDNF in facet pain. Because joint afferents are crucial for the initiation and maintenance of facet pain, the innervation pattern of the C6/C7 facet joint in the rat is quantitatively defined. NGF expression is measured in the facet joint and the dorsal root ganglion (DRG) following a painful facet joint distraction. Further, the role of intra-articular NGF in the initiation and maintenance of facet-mediated pain and spinal neuronal hyperexcitability is evaluated by selectively blocking intra-articular NGF signaling. BDNF expression is quantified in the DRG and spinal cord after joint injury. Selective inhibition of spinal BDNF is utilized to determine its contribution to facet-mediated pain. This thesis demonstrates that throughout the peripheral and central nervous systems neurotrophins are key mediators of behavioral hypersensitivity and contribute to the hyperexcitability of spinal neurons after a painful facet joint injury. This work further establishes the need for future studies to integrate investigations throughout all aspects of the pain pathway to fully understand the mechanisms underlying facet-mediated pain.

**Degree Type**
Dissertation

**Degree Name**
Doctor of Philosophy (PhD)

**Graduate Group**
Bioengineering

**First Advisor**
Beth A. Winkelstein

**Keywords**
Brain-Derived Neurotrophic Factor, Facet Joint, Injury, Nerve Growth Factor, Neuronal Hyperexcitability, Pain

# THE ROLE OF INTRA-ARTICULAR NERVE GROWTH FACTOR IN FACET-MEDIATED PAIN: RELATIONSHIPS TO SPINAL BDNF AND NEURONAL HYPEREXCITABILITY

Jeffrey V. Kras

A DISSERTATION

in

Bioengineering

Presented to the Faculties of the University of Pennsylvania in

Partial Fulfillment of the Requirements for the

Degree of Doctor of Philosophy

2015

Supervisor of Dissertation

_____

Beth A. Winkelstein, Professor of Bioengineering

Graduate Group Chairperson

_____

Jason A. Burdick, Professor of Bioengineering

Dissertation Committee

Douglas H. Smith, Robert A. Groff Professor of Teaching and Research in Neurosurgery
Gordon A. Barr, Associate Professor of Psychology in Anesthesiology and Critical Care
Francis J. Golder, Head of Discovery Biology at Galleon Pharmaceuticals, Inc.
Arjun Raj, Assistant Professor of Bioengineering

ACKNOWLEDGMENTS

I am greatly in debt to my advisor and mentor, Dr. Beth Winkelstein, for the time, energy, and commitment she has devoted to my training and development as a professional. I hope to continue to learn from her in the years to come. I would like to thank the members of my thesis committee, Dr. Douglas H. Smith, Dr. Gordon A. Barr, Dr. Francis J. Golder, and Dr. Arjun Raj for their support and guidance on my thesis work.

I am grateful to all of the current and former members of the Spine Pain Research Lab for their invaluable support and friendship. I would like to specifically acknowledge the members who assisted with the development and completion of the research presented in this thesis, including Ben Bulka, Nate Crosby, Ben Guarino, Taylor Gilliland, Parul Pall, Julia Quindlen, Kosuke Tanaka, Christine Weisshaar, and Angel Xiao. I would also like to thank the rest of the SPRL members who all supported me throughout this process.

I would like to thank my family for their unconditional love and support over the years. Finally, I would like to thank my wife, Lauren Brooks, for her love, patience, and support that enabled me to accomplish this goal.

ABSTRACT

THE ROLE OF INTRA-ARTICULAR NERVE GROWTH FACTOR IN FACET-MEDIATED PAIN: RELATIONSHIPS TO SPINAL BDNF AND NEURONAL HYPEREXCITABILITY

Jeffrey V. Kras

Beth A. Winkelstein

Traumatic neck injuries commonly result from rear-end motor vehicle collisions and are associated with a high incidence of neck pain and considerable annual costs. The facet joint is the most common source of neck pain. That joint is innervated by nociceptors that are activated by tensile stretching of the joint's capsular ligament. Although activation of those joint afferents and joint inflammation contribute to facet-mediated pain, the cellular response(s) within the joint that initiate pain via the joint afferents are unknown. Similarly, the mechanisms that induce central sensitization and maintain facet pain are not fully defined. Nerve growth factor (NGF) is a potent mediator of inflammatory cascades and is hypothesized to contribute to joint pain. Further, NGF regulates brain-derived neurotrophic factor (BDNF), which, when released in the spinal cord, sensitizes spinal neurons. Despite their roles in inflammatory pain, no studies have identified whether the neurotrophins NGF and/or BDNF contribute to facet joint-mediated pain. These studies utilize a rat model of mechanical facet joint injury to investigate the roles of NGF and BDNF in facet pain. Because joint afferents are crucial

for the initiation and maintenance of facet pain, the innervation pattern of the C6/C7 facet joint in the rat is quantitatively defined. NGF expression is measured in the facet joint and the dorsal root ganglion (DRG) following a painful facet joint distraction. Further, the role of intra-articular NGF in the initiation and maintenance of facet-mediated pain and spinal neuronal hyperexcitability is evaluated by selectively blocking intra-articular NGF signaling. BDNF expression is quantified in the DRG and spinal cord after joint injury. Selective inhibition of spinal BDNF is utilized to determine its contribution to facet-mediated pain. This thesis demonstrates that throughout the peripheral and central nervous systems neurotrophins are key mediators of behavioral hypersensitivity and contribute to the hyperexcitability of spinal neurons after a painful facet joint injury. This work further establishes the need for future studies to integrate investigations throughout all aspects of the pain pathway to fully understand the mechanisms underlying facet-mediated pain.

TABLE OF CONTENTS

Page

LIST OF TABLES

Page

LIST OF FIGURES

Page

# Chapter 1

# Introduction and Background

## 1.1. Overview

In the United States, neck and back syndromes are the most common cause of job-related disability, with costs exceeding $50 billion each year (Strine and Hootman, 2007). The annual incidence of neck pain is estimated to be as high as 50% within the general population (Hogg-Johnson et al., 2008; van Eerd et al., 2010). Rear end motor vehicle collisions are a major cause of neck pain, with as many as one in three people involved reporting a minor neck injury (Quinlan et al., 2004; Zuby and Lund, 2010). Such motor vehicle collisions cause whiplash injuries, the most frequent symptom of which is neck pain (Berglund et al., 2000; Eck et al., 2001). Whiplash injuries incur annual costs of nearly $4 billion, including medical care, disability, and lost productivity (Eck et al., 2001; Freeman et al., 1999). As many as 50% of whiplash patients experience chronic pain (Carroll et al., 2009; Pedler et al., 2013). Yet, despite these high instances and staggering socioeconomic costs, the physiological mechanisms that lead to persistent pain from mechanical injury to the neck are still poorly understood (Chen et al., 2006; Dong and Winkelstein, 2010; Panjabi et al., 1998; Winkelstein et al., 2000). This lack of clear mechanistic understanding of the cellular signals that sensitize sensory neurons and lead to pathological pain after injury makes it challenging to develop and implement effective strategies to prevent the transition to chronic pain (Elliott et al., 2009).

Exposure to non-physiological spinal motions, particularly those associated with dynamic neck loading scenarios, has the potential to injure many innervated structures in the neck, including the vertebrae, intervertebral discs, facet joints, muscles, and ligaments, among others. Anesthetic nerve blocks have identified the cervical facet joints as the source of pain in up to 65% of neck pain patients (Barnsley et al., 1995; Lord et al., 1996; Manchikanti et al., 2002; van Eerd et al., 2010). Further, the cervical facet joints in the *lower* cervical spine are those most commonly symptomatic after neck injury (Bogduk, 2011; Bogduk and Aprill, 1993). In particular, biomechanical studies simulating whiplash identify the C6/C7 facet joint capsule as undergoing the greatest ligament strains among all of the cervical facet joints (Panjabi et al., 1998; Pearson et al., 2004). Further, those capsular ligament strains resulting from whiplash simulations are significantly larger than the corresponding strains reported for physiological neck motions (Bogduk and Aprill, 1993; Panjabi et al., 1998; Pearson et al., 2004). Together, such studies support the C6/C7 joint as being one of the most relevant to injury-induced neck pain. Although the facet joint undergoes a combination of compression, shear, and tensile loading during dynamic neck loading, tensile stretch of the capsular ligament that encloses the facet joint is, by itself, capable of activating nociceptors innervating the joint (Chen et al., 2006; Lu et al., 2005), which suggests that joint loading may be sufficient to induce pain. Moreover, tensile stretch of the facet capsular ligament induces pain in association with spinal neuronal hyperexcitability and a host of other cellular responses in both the peripheral and central nervous systems in the rat (Crosby et al., 2013; Dong and Winkelstein, 2010; Kras et al., 2014a; Lee and Winkelstein, 2009; Quinn et al., 2010). Spinal neuronal hyperexcitability is one component of central sensitization, which is a

state of increased neuronal excitability and synaptic efficacy that contributes to widespread and persistent pain (Latremoliere and Woolf, 2009). However, there is little data defining the relationship between local responses in the joint to the nociceptive, biochemical, and cellular responses of the primary sensory neurons and neurons in the central nervous system (CNS) in facet-mediated pain.

Clinically, facet joint interventions, such as anesthetic nerve blocks and radiofrequency neurotomy, are one of the largest contributors to the growth in expenditures among chronic pain patients (Manchikanti et al., 2013). The use of those treatments increased more than 300% between 2000 and 2011 (Manchikanti et al., 2013). The growing utilization of treatments targeting the nerve supply to painful facet joints supports a role for facet joints and the neurons that innervate them in chronic pain. The facet joint and its capsular ligament are densely innervated, receiving afferents from both the spinal level above and below the joint in humans (Barnsley and Bogduk, 1993; van Eerd et al., 2010). Because studies identify innervation of some facet joints as more complex in the rat, with several spinal levels contributing fibers to the joint (Ohtori et al., 2002; Ohtori et al., 2003), characterization of the specific joint innervation patterns is necessary in order to define those relevant mechanisms contributing to joint pain. Further, afferent fibers may be classified as peptidergic (those neurons expressing neuropeptides) or non-peptidergic (those neurons binding isolectin B4) (Merighi et al., 2008), and each type of neuron responds to different environmental signals and initiates different cellular responses that contribute to pain (Joseph and Levine, 2010; Merighi et al., 2008; Seybold, 2009). Peptidergic fibers have been identified in the facet joint capsules of both humans

(Kallakuri et al., 2004) and rats (Ohtori et al., 2003), yet it remains to be seen if this or other classes of neurons have an important role in facet joint pain.

Many pro-inflammatory cascades that are associated with pain, such as increased levels of cytokines and prostaglandins, are initiated in joint inflammation and arthritis (Kidd et al., 1996; Longo et al., 2013; Schaible and Grubb, 1993; Woolf et al., 1997). Inflammation in the facet joint is sufficient to induce pain (Tachihara et al., 2007), and local treatment with an anti-inflammatory drug alleviates loading-induced facet joint pain (Dong et al., 2011). Both of these studies support a role for inflammation in the evolution of pain after a mechanical facet joint injury. Although tensile loading of the facet joint differentially increases mRNA levels of cytokines in the DRG and upregulates prostaglandin and cytokine expression in the spinal cord (Kras et al., 2014a; Lee et al., 2008), it is unclear how localized inflammation in the facet joint leads to neuronal hyperexcitability in the CNS and behavioral hypersensitivity. Within inflamed tissue, increased levels of the neurotrophin nerve growth factor (NGF) sensitize neurons and increase sensitivity to mechanical, as well as thermal, stimuli (Amaya et al., 2004; McMahon, 1996; Merighi et al., 2004; Pezet and McMahon, 2006). In fact, NGF and its receptor have been identified within the synovial fluid of arthritic joints and in the adjacent synovial tissue (Barthel et al., 2009; Kidd et al., 1996; Raychaudhuri et al., 2011), as well as in degenerative facet joints (Surace et al., 2009). Although those findings suggest that intra-articular NGF and its downstream signaling cascades may contribute to facet pain after mechanical injury, such a role for NGF in joint pain remains undefined.

In addition to mechanical sensitivity, inflammation is commonly associated with an increased sensitivity to thermal stimuli (Amaya et al., 2004; Woolf et al., 1997). Moreover, pain patients suffering from whiplash report increased sensitivity to *both* heat and cold stimuli (Chien et al., 2009; Smith et al., 2014), phenomena that are alleviated by ablating the neurons innervating the facet joints in the neck (Smith et al., 2014), which suggests that facet joint injury may induce thermal sensitivity in addition to mechanical sensitivity. Studies in the rat demonstrate that painful inflammatory joint conditions such as arthritis reduce the latency to withdrawal from heat stimuli (Luo et al., 2014); yet, it is unknown if tensile loading of the facet joint is sufficient to induce thermal sensitivity in addition to the well-documented mechanical sensitivity.

Painful facet joint loading damages the primary afferent axons that innervate the joint capsule (Kallakuri et al., 2008) and also induces immediate and sustained neuronal hyperexcitability in the spinal cord (Crosby et al., 2013; Quinn et al., 2010). Of note, the neural circuits that relay painful stimuli to the central nervous system extend beyond the spinal cord. Nociceptive sensory stimuli received in the spinal cord are transmitted to higher centers in the central nervous system via the spinothalamic tract (Merighi et al., 2008), and the thalamus is believed to be the key relay for supraspinal processing and transmission of nociceptive stimuli (Slack et al., 2005). Some of the neurons projecting to the thalamus are sensitive to the neurotrophin brain-derived neurotrophic factor (BDNF), a central pain mediator whose expression is regulated by NGF (Merighi et al., 2008; Slack et al., 2005). Some neurons within the thalamus are activated by joint stimulation (Schaible et al., 2009); moreover, thalamic neurons with joint input become hyperexcitable when the innervated joint is inflamed, in association with pain (Gautron

and Guilbaud, 1982). Despite the known role of inflammation in painful mechanical facet joint injury and the sensitization of spinal neurons to mechanical stimuli, it is unknown if higher order neurons are also sensitized by painful facet joint loading.

Studies in this thesis aim to identify a mechanism through which local joint responses following tensile loading of the facet joint induce neuronal hyperexcitability in the CNS and persistent pain by specifically defining roles for the neurotrophins NGF and BDNF in the initiation and maintenance of joint pain in a rat model. Behavioral sensitivity to both mechanical and thermal stimuli is evaluated to define the pain modalities associated with mechanical facet joint injury. The innervation of the C6/C7 facet joint is determined using retrograde neuronal tracing in order to identify the distribution pattern and subtypes of neurons innervating the joint in the rat. The temporal and spatial neurotrophin responses in the DRG and spinal cord also are quantified after joint loading in order to determine if this class of proteins contributes to persistent joint pain. Complementary studies using anti-NGF antibodies and purified NGF evaluate the specific contribution of intra-articular NGF to the initiation and maintenance of facet pain and spinal neuronal plasticity. The role of spinal BDNF in the maintenance of facet-mediated pain is also determined by spinal administration of a BDNF sequestering protein after joint injury-induced pain is established. In addition, since the thalamus is a major relay center for nociceptive information (Merighi et al., 2008; Millan, 1999) and may be sensitive to spinal BDNF signaling (Slack et al., 2005), neuronal excitability is quantified in the thalamus at day seven after injury since that time point coincides with pain maintenance in this model.

## 1.2. Background

### 1.2.1. Cervical Spine & Facet Joint Anatomy

The cervical spine consists of seven bony vertebrae (C1-C7) separated by intervertebral discs between each pair of vertebrae and is stabilized by a network of soft tissues including ligaments and muscles (Figure 1.1A) (Jansen et al., 2008). On the lateral sides of each spinal motion segment, which itself consists of two adjacent vertebrae and the associated intervertebral disc, a pair of facet joints is formed at the junction of the inferior and superior facets (Figure 1.1). The facet joints are the only diarthrotic joints in the spine, and they permit articulation between the vertebrae while also providing support and absorbing loading along the axial spine (Kirpalani et al., 2008; Li et al., 2011). The facet joint space is enclosed by a capsular ligament that is innervated by primary afferent neurons that carry sensory information from the joint to the spinal cord where it is processed and further relayed to the brain.

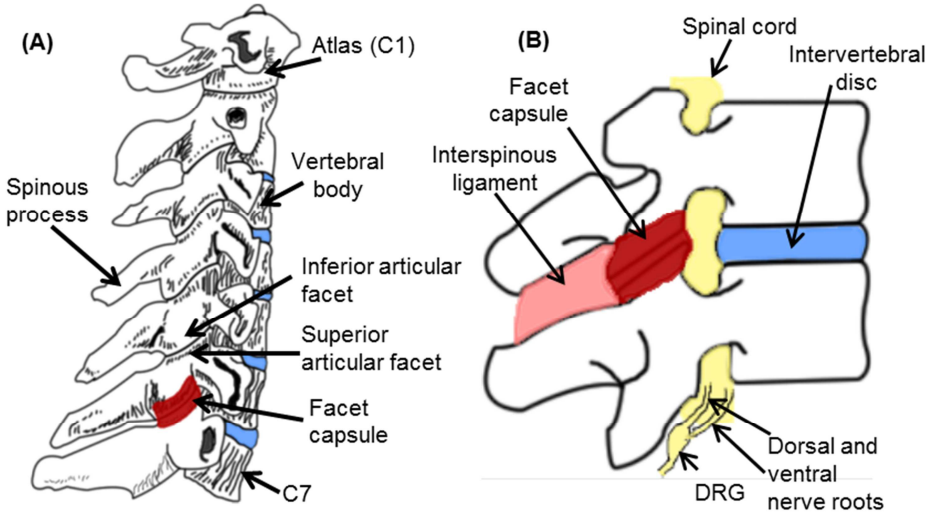


**Figure 1.1.** Right lateral view of a human cervical spinal column and generic motion segment. **(A)** The capsular ligament encloses the joint space between the inferior and superior articular facets at each cervical level. **(B)** A magnified view of a spinal motion segment shows the facet joint capsular ligament in red.

### 1.2.2. Neural Anatomy

The cervical facet joints from C3-C7 are innervated by the medial branches of the dorsal rami of the spinal nerves at the levels immediately superior and inferior to each joint (van Eerd et al., 2010). The cell bodies of those sensory neurons that innervate the joint reside in the dorsal root ganglion (DRG) proximal to the transverse foramen (Figures 1.1B & 1.2) (Kallakuri et al., 2004; van Eerd et al., 2010). Although there are only seven cervical vertebrae, there are eight DRGs in the cervical space, with C8 located caudal to the C7 vertebra. In addition to innervating the facet joints, the cervical spinal nerves also innervate the neck, shoulders, and upper limbs (Lee et al., 2008). Specifically, the sensory neurons of the C6-C8 spinal nerves have receptive fields that extend into the hands (Lee et al., 2008). In the rat, the C6-C8 dermatomes are similar to those in the human and innervate the neck, shoulders, and forepaws (Takahashi and Nakajima, 1996).

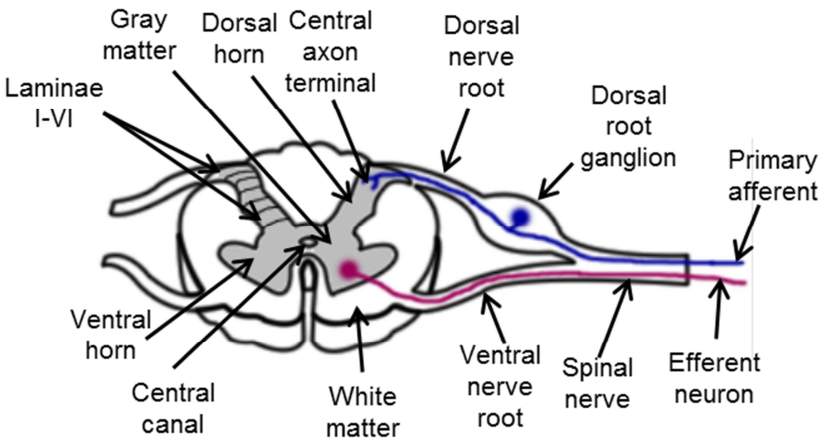


**Figure 1.2.** Anatomy of the dorsal root ganglion (DRG) and spinal cord. Sensory information is transmitted from the periphery to the spinal cord via primary afferent neurons with their cell bodies in the DRG. The afferents synapse in specific laminae in the dorsal horn (laminae I-VI), in accordance with the afferent phenotype.

Sensory neurons can be classified into several categories based on the diameter of the cell body and the thickness of the myelin sheath surrounding the axons. Aβ-fibers are large diameter myelinated neurons that typically respond to light touch or are involved in proprioception; under normal circumstances, these neurons do not transmit pain signals (Basbaum et al., 2009; Merighi et al., 2008). Both the medium diameter thinly myelinated Aδ-fibers and the small diameter unmyelinated C-fibers can function as nociceptors and transmit sensory information related to pain (Basbaum et al., 2009; Merighi et al., 2008). Among mechanoreceptive nerve fibers innervating the facet joint capsule, both proprioceptors and nociceptors that are responsive to capsular ligament stretch have been identified (Cavanaugh et al., 1989; Cavanaugh et al., 1996; Chen et al., 2006; Lu et al., 2005), suggesting that joint loading alone may be sufficient to induce pain.

Primary afferents also can be classified as either peptidergic (those neurons expressing the neuropeptides substance P (SP) and/or calcitonin gene-related peptide (CGRP)) or non-peptidergic (those neurons that bind isolectin B4) (Merighi et al., 2008). Although nociceptors include both populations of afferents, peptidergic and non-peptidergic afferents can be functionally distinct. Peptidergic afferents are sensitive to the neurotrophin nerve growth factor (NGF), whereas non-peptidergic neurons express receptors for glial cell line-derived neurotrophic factor (GDNF) (Stucky and Lewin, 1999). Moreover, the two populations exhibit distinct electrophysiological properties and sensitivities to heat stimuli (Fang et al., 2006; Stucky and Lewin, 1999). The IB4-negative neurons fire shorter duration action potentials and, when activated by noxious heat, exhibit larger inward currents than do the IB4-binding afferents (Fang et al., 2006; Stucky and Lewin, 1999). Such differences suggest that the two populations of afferents

might transmit distinct types of nociceptive information, especially given their divergent central projections (Basbaum et al., 2009; Merighi et al., 2008). Up to 11% of neurons innervating facet joints are IB4-positive (Ishikawa et al., 2005); therefore, activation of this population of afferents may contribute to facet-mediated pain. Based on expression of the neuropeptides substance P and CGRP in the facet joint (Kallakuri et al., 2004; Ohtori et al., 2003), peptidergic neurons have been reported to innervate that joint. Since both substance P and CGRP can act as neurotransmitters and are capable of sensitizing nociceptive circuits (Seybold et al., 2009), neurons expressing these peptides in the joint capsule further support the facet joint as a source of injury-induced pain.

Peripheral stimuli activate primary sensory neurons, whose cell bodies are located in the DRG, that relay the signal to the spinal cord via the dorsal nerve roots where they synapse with second order neurons in the dorsal horn (Figure 1.2). The dorsal horn, where most primary afferent neurons synapse, is arranged into laminae with distinct anatomical and electrophysiological characteristics (Basbaum et al., 2009; Merighi et al., 2008). Most large diameter sensory neurons that transmit non-noxious stimuli project to the deep laminae (III-VI) (Merighi et al., 2008), whereas small diameter peptidergic and non-peptidergic afferents primarily synapse in distinct layers of the superficial laminae (I-II), although some thinly myelinated nociceptors also reach deeper laminae (Figure 1.2) (Basbaum et al., 2009; Merighi et al., 2008). Specifically, the peptidergic afferents synapse in lamina I and the outer portion of lamina II, whereas the non-peptidergic neurons synapse in the inner portion of lamina II (Stucky and Lewin, 1999). Further, unmyelinated afferents with input from joints project to both lamina I and laminae V-VI (Millan, 1999). Second order neurons in the dorsal horn can be classified as low threshold

mechanoreceptive (LTM), nociceptive specific (NS), or wide dynamic range (WDR) based on their responses to cutaneous stimulation (Dostrovsky and Craig, 2013). LTM neurons respond to non-noxious mechanical stimuli, as opposed to NS neurons that are unresponsive to gentle cutaneous stimuli but are are activated by high threshold stimuli sufficient to induce pain. WDR neurons exhibit a graded response to innocuous and noxious stimuli (Coghill et al., 1993; Dostrovsky and Craig, 2013; Millan, 1999). NS neurons are most commonly located in the superficial laminae (I-II) of the dorsal horn, but in the deeper laminae (IV-VI), WDR neurons predominate (Coghill et al., 1993; Dostrovsky and Craig, 2013).

From the spinal cord, nociceptive information is transmitted to many higher order structures in the brain such as the brainstem, periaqueductal gray matter, amygdala, thalamus and cortex (Figure 1.3) (Basbaum et al., 2009; Merighi et al., 2008; Steeds, 2009). Neurons in laminae I and IV-VI of the dorsal horn that directly project to the thalamus constitute the spinothalamic tract (STT), which has traditionally been thought of as the main nociceptive pathway to the brain (Basbaum et al., 2009; Merighi et al., 2008; Steeds, 2009). The thalamus encodes sensory signals relating to the type, intensity, and topographical location of pain and relays nociceptive information to the somatosensory cortex (Basbaum et al., 2009; Millan, 1999; Steeds, 2009). Of the multiple distinct regions of the thalamus in which the STT terminates, the ventral posterolateral (VPL) nucleus provides intense input to the somatosensory cortex and has a role in the sensory-discriminative aspect of pain (Millan et al., 1999).

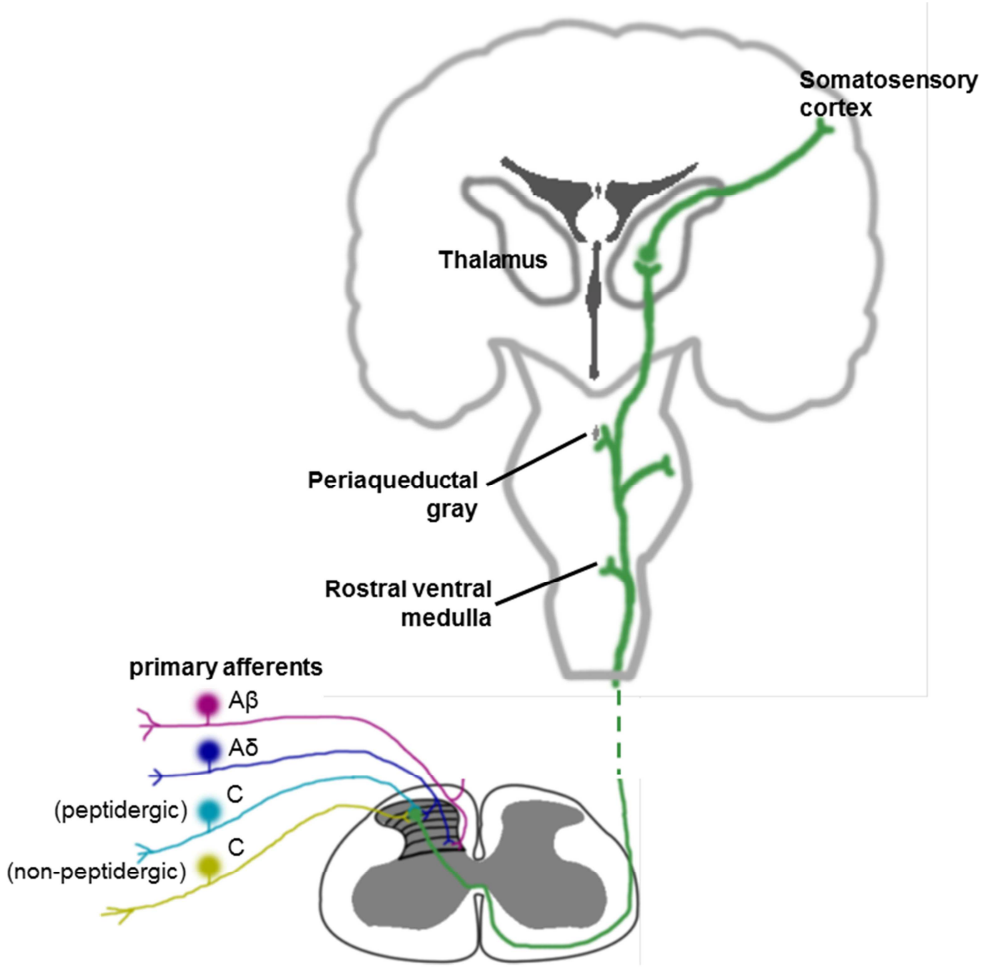


**Figure 1.3.** Schematic of the brain regions involved in nociception. A spinothalamic tract neuron (green) receives input from nociceptors in the dorsal horn and ascends to the thalamus where it synapses with thalamic neurons that project to the cortex.

### 1.2.3. Central Sensitization

In many chronic pain conditions, hyperexcitability of neurons in the CNS can lead to normally non-noxious stimuli being perceived as painful (Latremoliere and Woolf, 2009). This hyperexcitable state can persist even in the absence of ongoing tissue injury or inflammation and is thought to maintain chronic pain (Latremoliere and Woolf, 2009). In the spinal cord, enlarged receptive fields, increased neuronal responses to suprathreshold stimuli, and the conversion of neurons to the WDR phenotype all

contribute to the enhanced excitability characteristic of central sensitization (Latremoliere and Woolf, 2009; Millan, 1999). Indeed, injury to the facet joint induces hyperexcitability in spinal neurons and increases the proportion of WDRs in the spinal dorsal horn in association with pain (Crosby et al., 2013; Dong et al., 2013b, Quinn et al., 2010), supporting that central sensitization likely has a role in persistent facet-mediated pain.

During inflammation or after a peripheral nerve injury associated with pain, activation of primary afferents leads to upregulation and release of a number of molecules that sensitize spinal neurons. The molecular mediators of hyperexcitability in the spinal cord are varied, including prostaglandins, neurotrophins such as BDNF, excitatory amino acids, and neuropeptides (Latremoliere and Woolf, 2009; Merighi et al., 2008; Millan, 1999). Release of these transmitters upon stimulation of the primary afferents potentiates glutamate receptor signaling and alters sodium, potassium, and calcium currents in neurons, leading to an increase in membrane excitability (Latremoliere and Woolf, 2009; Millan, 1999). Many of the pain mediators, including substance P, prostaglandin $E_2$ ($PGE_2$), and the glutamate receptor mGluR5, that contribute to spinal neuronal sensitization are upregulated in the DRG or spinal cord after a painful facet joint injury (Crosby et al., 2014; Dong and Winkelstein, 2010; Kras et al., 2014a; Lee and Winkelstein, 2009). Such increases occur at times when spinal neurons are hyperexcitable after facet injury, supporting their contribution to central sensitization in facet-mediated pain.

Central sensitization cannot be explained simply as an increased expression and/or release of pro-nociceptive mediators in the spinal cord. Rather, structural reorganization can occur in the spinal cord in response to injury, with the Aβ-fibers that

normally transmit innocuous mechanical sensation sprouting into the superficial dorsal horn (Latremoliere and Woolf, 2009; Millan, 2002). Typically, only nociceptors synapse in the superficial dorsal horn, and sprouting of Aβ-fibers into that region can cause those fibers to activate nociceptive second order neurons (Millan, 2002). Such Aβ-fiber sprouting is one mechanism thought to underlie the perception of innocuous stimuli as painful in the sensitized nervous system. Additionally, peripheral inflammation can induce Aβ-fibers to begin expressing neuropeptides and neurotrophins that are normally expressed by smaller diameter nociceptors (Latremoliere and Woolf, 2009; Millan, 2002). Activation of those Aβ-fibers then induces release of the pro-nociceptive neuropeptides, leading to further sensitization at the level of the spinal cord in association with pain (Millan, 2002). Although direct evidence of Aβ-fiber sprouting has not been demonstrated after facet joint injury, excitatory synapses are more abundant after painful facet loading (Crosby et al., 2015). Such an increase in excitatory synapses suggests that other forms of neuronal plasticity may also contribute to spinal neuronal hyperexcitability that is associated with facet pain.

In addition to neuronal mechanisms of central sensitization, glial cells can also increase neuronal excitability (Latremoliere and Woolf, 2009). Normally, glial cells such as astrocytes and microglia function to maintain homeostasis in the CNS (Bradesi, 2010). Yet, under inflammatory conditions or after neural tissue injury, both microglia and astrocytes become activated and release pro-inflammatory cytokines, such as IL-1β and TNFα, that can enhance neuronal excitability (Bradesi, 2010; Latremoliere and Woolf, 2009). Painful facet joint injury consistently activates astrocytes in the spinal cord by day seven after injury, but microglial activation varies with age (Crosby et al., 2014; Dong et

al., 2013a; Weisshaar et al., 2010; Winkelstein and Santos, 2008). Adolescent rats exhibit increased microglial activation seven days after injury, but microglia are not activated at that time in association with facet pain in adult rats (Weisshaar et al., 2010; Winkelstein and Santos, 2008). Further, astrocytes have a significant role in the clearance of glutamate from the synaptic cleft, but facet joint injury downregulates astrocytic glutamate transporters while upregulating glutamate receptor expression and activation (Crosby et al., 2014; Dong and Winkelstein, 2010). This combination of diminished glutamate clearance together with increased glutamate receptor expression could directly increase the excitability of spinal neurons and contribute to the behavioral sensitivity that develops and persists after a joint injury. As such, the glial response to facet joint injury, in particular the activation of spinal astrocytes, has important implications for the maintenance of central sensitization in facet pain through the regulation of extracellular glutamate and the potential release of inflammatory mediators that collectively increase the excitability of neurons in the CNS.

Such adaptive responses of resident cells in the CNS are not restricted to the spinal cord but can also occur in supraspinal centers such as the thalamus (Iwata et al., 2011; Merighi et al., 2008; Millan, 1999; Slack et al., 2005). In fact, neuronal firing patterns are altered in the thalamus in neuropathic and inflammatory pain (Huh et al., 2012; Iwata et al., 2011; Millan, 1999; Syré et al., 2014). As a result, efforts to treat chronic pain may benefit from targeting supraspinal sites in order to achieve pain relief. Further, descending pathways also alternately contribute to the inhibition or facilitation of spinal neuronal hyperexcitability (Millan, 1999; Millan, 2002). Inflammatory joint pain is maintained in part due to descending facilitation via the rostroventral medulla (Carr et al.,

2014). Yet, it is not known if supraspinal mechanisms contribute to facet joint-mediated pain. Although increased excitability of neurons in the CNS is a major component of persistent pain, there is no single mechanism that produces neuronal hyperexcitability (Latremoliere and Woolf, 2009). However, the neurotrophins are one family of molecules that is expressed throughout the nervous system, and they are able to sensitize both primary afferents and neurons in the CNS (Pezet and McMahon, 2006). Consequently, increased neurotrophin expression and signaling may initiate and/or sustain facet joint injury-induced neuronal hyperexcitability and the associated pain.

### 1.2.4. Neurotrophins & Pain

In general, inflammation is a common local response in injured tissues that helps initiate tissue repair (Watkins et al., 1995). However, inflammatory cascades also have the potential to contribute to persistent pain via the release of various chemicals, among which nerve growth factor (NGF) has a major role (Kras et al., 2014a; McMahon, 1996; Woolf et al., 1997). NGF released during inflammation sensitizes nociceptors and increases the excitability of sensory neurons (Dawes et al., 2013; Woolf et al., 1997). NGF is a member of the neurotrophin family of growth factors that has a major role in the growth, development, and survival of sensory neurons through activation of its high affinity receptor, tyrosine receptor kinase A (trkA) (Pezet and McMahon, 2006). In adulthood, NGF is also capable of sensitizing sensory neurons and contributing to pain through post-translational regulation of ion channels as well as increased expression of many pain-associated genes, such as substance P, CGRP, and BDNF (Dawes et al., 2013; Pezet and McMahon, 2006). NGF levels are increased in injured and inflamed tissues

through release from a number of different types of immune cells, such as macrophages (McMahon, 1996). Increased levels of NGF have profound effects on responses to thermal stimuli, via increased expression and phosphorylation of the heat sensitive transient receptor potential vanilloid 1 (TRPV1), and mechanical sensitivity (Figure 1.4) (Amaya et al., 2004; Dawes et al., 2013; Longo et al., 2013; Sah et al., 2003; Woolf, 1996). Both intradermal and intramuscular injections of NGF in human volunteers elicit decreases in the heat pain threshold as well as increased sensitivity to mechanical stimuli (Dyck et al., 1997; Gerber et al., 2011; Rukwied et al., 2010). Similarly, NGF injection induces both thermal and mechanical pain in the rat (Amann et al., 1995; Malik-Hall et al., 2005; Woolf, 1996). Since NGF levels are increased in inflamed tissue, NGF is considered to be a major contributor to inflammatory pain (Amaya et al., 2004; Ma and Woolf, 1997; McMahon, 1996). Recent studies identify upregulation of inflammatory cytokines and prostaglandin $E_2$ in association with loading-induced facet pain in the rat (Kras et al., 2014a; Lee et al., 2008). Moreover, intra-articular injection of the non-steroidal anti-inflammatory drug ketorolac one day after a painful facet joint injury alleviates behavioral hypersensitivity (Dong et al., 2013a). Those findings support a role for joint inflammation in facet-mediated pain. Because inflammation is necessary for persistent pain following facet joint injury, it is likely that NGF contributes to the development of facet pain.

NGF and its receptor have been identified in arthritic joints and degenerative facet joints (Barthel et al., 2009; Surace et al., 2009). Further, systemic anti-NGF therapy has shown success in alleviating osteoarthritis pain in clinical trials (Brown et al., 2012; Lane et al., 2010), demonstrating a role for NGF in that form of joint pain. Although animal

studies implicate NGF as contributing to arthritis pain (Longo et al., 2013; McNamee et al., 2010; Orita et al., 2011), very little is known about the potential relationship between NGF and loading-induced facet joint pain; in addition, the mechanism(s) through which NGF contributes to joint pain is poorly understood.

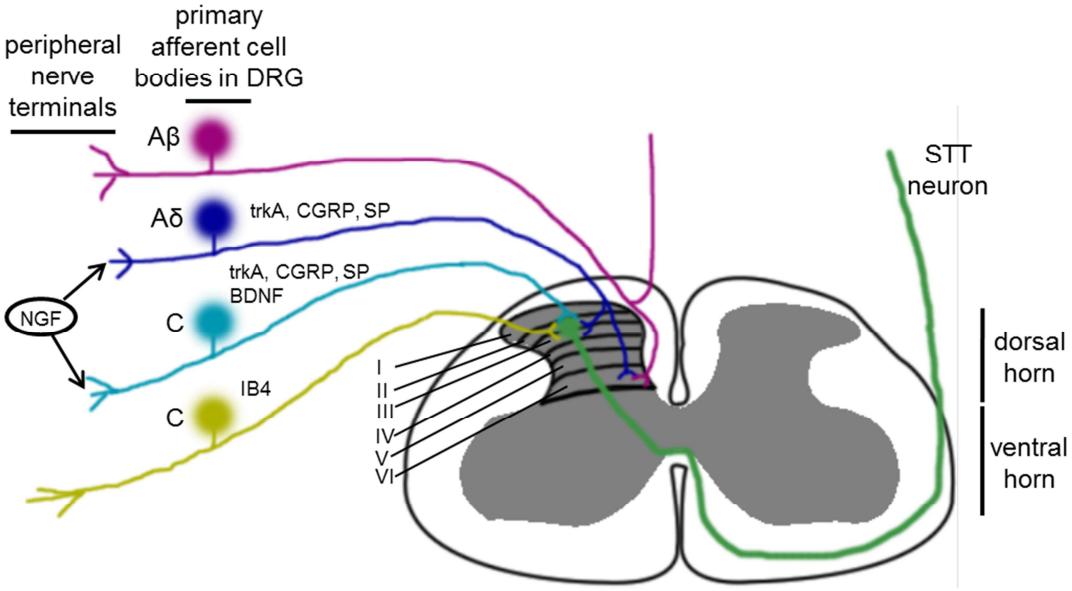


**Figure 1.4.** NGF activation of primary afferent neurons innervating peripheral targets. NGF binds to trkA receptors expressed on the peripheral terminals of peptidergic Aδ- and C-fiber sensory neurons resulting in increased expression of CGRP, substance P (SP) and BDNF. The C-fibers enter the spinal cord and synapse in the superficial dorsal horn; the Aδ-fibers synapse in both the superficial laminae and deeper laminae.

In parallel with the overall behavioral effects that are induced by NGF exposure, NGF acts on peptidergic afferents to increase expression of the neuropeptides CGRP and substance P, as well as the neurotrophin BDNF, in the rat (Figure 1.4) (McMahon, 1996; Pezet and McMahon, 2006; Woolf, 1996). Because these proteins are transported to, and released in, the spinal cord where they contribute to the activation and sensitization of second order sensory neurons, NGF has a role in central sensitization despite its not reaching the spinal cord itself (Dawes et al., 2013; McMahon, 1996). In fact, peripheral

injection of NGF is associated with increased excitability of spinal neurons (Hoheisel et al., 2007). Despite increased expression of neuropeptides and hyperexcitability of spinal neurons after painful facet joint injury (Crosby et al., 2013; Lee and Winkelstein, 2009; Quinn et al., 2010), no study has determined if NGF contributes to that spinal hyperexcitability or altered protein expression in association with facet-mediated pain.

BDNF expression is regulated by NGF and is a central mediator of pain in nerve injury and inflammation induced chronic pain (Li et al., 2006; Mannion et al., 1999; Merighi et al., 2008; Pezet and McMahon, 2006). Peptidergic neurons produce BDNF and transport it to the superficial dorsal horn in the spinal cord where its release activates tyrosine receptor kinase B (trkB) receptors (Merighi et al., 2008; Pezet and McMahon, 2006). BDNF-trkB signaling contributes to central sensitization by facilitating spinal neurotransmission through a combination of increased neuropeptide release and potentiation of ion channels such as glutamate receptors (Merighi et al., 2008; Pezet and McMahon, 2006). BDNF released in the dorsal horn activates pre-synaptic trkB receptors and induces the release of substance P and CGRP into the synaptic cleft (Merighi et al., 2008). Those neuropeptides, in turn, facilitate neurotransmission via their downstream effects on glutamate receptor activation (Seybold, 2009). Increased spinal BDNF expression and release also activates glutamate receptors in association with pain in both neuropathic and inflammatory injury models (Geng et al., 2010; Matayoshi et al., 2005; Slack et al., 2004). Moreover, the increased expression of the glutamate receptor mGluR5, as well as phosphorylation of the NR1 subunit of NMDA glutamate receptors, in the spinal cord that is induced by painful joint injury demonstrates altered glutamate signaling in facet-mediated pain (Crosby et al., 2014; Dong and Winkelstein, 2010).

Because spinal BDNF induces phosphorylation of NR1 (Slack et al., 2004), BDNF might affect spinal glutamate signaling associated with facet-mediated pain. Pharmacological inhibition of BDNF-trkB signaling alleviates behavioral sensitivity in many experimental neural tissue injury models (Coull et al., 2005; Matayoshi et al., 2005; Zhang et al., 2011), further demonstrating a role for spinal BDNF in persistent pain. Although increased BDNF expression has been identified in the synovial tissue of arthritic joints (Grimsholm et al., 2008), the contribution of BDNF to joint pain, particularly from mechanical injury, has not been investigated.

In addition to sensitizing spinal neurons in association with persistent pain, BDNF can also activate supraspinal targets, including those in the thalamus (Merighi et al., 2008; Millan, 1999). A majority of the STT neurons projecting from the superficial and deep laminae of the dorsal horn are sensitive to BDNF, and increased activity of thalamic neurons is associated with elevated thalamic BDNF expression (Millan, 1999; Slack et al., 2005), which supports the potential for thalamic plasticity in painful conditions via BDNF signaling. Moreover, joint inflammation is associated with thalamic plasticity; arthritic rats exhibit altered gene expression in the thalamus as well as increased excitability of thalamic neurons with joint input (Gautron and Guilbaud, 1982; Millan, 1999; Neto et al., 2008). Despite evidence of joint inflammation and increased excitability of neurons in the dorsal horn in response to painful facet joint injury (Crosby et al., 2013; Dong et al., 2013a; Quinn et al., 2010), thalamic plasticity has not been investigated in facet-mediated pain.

### 1.2.5. General Neck Injury Kinematics & Symptoms

The kinematics of the cervical spine during rear-end motor vehicle impacts have been extensively studied using both cadaveric simulations and studies of human volunteers (Berglund et al., 2000; Bogduk and Yoganandan, 2001; Cusick et al., 2001; Panjabi et al., 1998; Pearson et al., 2004; Yoganandan et al., 2002). Beginning approximately 50ms after the rear-end impact of the car, the cervical spine takes on an S-shaped curvature as the lower cervical spine extends while the upper segments flex (Bogduk and Yoganandan, 2001; Pearson et al., 2004). By 120ms after the impact, the full cervical spine extends to form a C-shape (Bogduk and Yoganandan, 2001). During these spinal motions, the lower cervical facet joints undergo compressive, shear, and tensile motions, which can stretch the capsular ligament surrounding the joint space (Cusick et al., 2001; Panjabi et al., 1998; Pearson et al., 2004). Between 50 and 150ms after the impact, the capsular ligaments of the lower cervical joints sustain the peak ligament strain, with the greatest strains being reported in the C6/C7 facet joints (Panjabi et al., 1998; Pearson et al., 2004). This excessive ligament stretch, which is beyond the physiologic range, has been proposed as an injury mechanism underlying neck pain (Pearson et al., 2004; Siegmund et al., 2001; Yoganandan et al., 2002). Furthermore, the peak capsular ligament strains recorded during human cadaveric whiplash simulations reach 39.9±26.3% in the C6/C7 facet joint (Pearson et al., 2004) and are greater than the average capsule strain reported to be sufficient to induce persistent pain symptoms in rat models of both quasistatic (27.7±11.9% strain) and dynamic (24.0±10.0% strain) facet capsular ligament stretch (Dong et al., 2008; Dong and Winkelstein, 2010; Lee et al., 2004). As such, the nearly 40% capsular ligament strain that is induced during whiplash

simulations supports the facet joint as being susceptible to painful loading during rear-end motor vehicle impacts and the facet capsule as being a potential source of chronic pain when ligament strains exceed physiological limits.

Loading-induced neck injuries are associated with hypersensitivity extending beyond the region of the neck. In addition to the neck, many whiplash patients report pain extending into the shoulders and arms (Chien et al., 2009; Ferrari et al., 2005; Moog et al., 2002). Further, whiplash is associated with an increased sensitivity to heat in the neck, shoulder, and arm; pressure pain thresholds are decreased in these same regions as well as in the hand (Fernandez-Perez et al., 2012; Scott et al., 2005; Sterling et al., 2003). This widespread sensitivity in regions outside the primary site of injury supports central sensitization as being established in whiplash patients. For many patients, this increased sensitivity only persists for an acute (less than six months) time period before resolving (Borchgrevink et al., 1998; Sterling et al., 2003). However, in 14-42% of the patients, hypersensitivity can become chronic, persisting for longer than six months (Barnsley et al., 1994; Carroll et al, 2009; Sterling et al., 2003). Although clinical studies of whiplash patients document symptoms of neck injury, such studies do not relate those pain symptoms with the cellular responses to loading-induced joint injury, necessitating the use of animal models to better understand the mechanisms underlying chronic neck pain.

Since the neurons that innervate the neck at the lower cervical levels are located in the same dermatomes (C6-C8) that innervate the shoulders, arms, and hands (Lee et al., 2008), it is not surprising that injury to the neck may result in pain in those remote sites. In the rat, the C6-C8 dermatomes similarly innervate the shoulder, forelimb, and forepaw, suggesting neck injury in the rat may also induce pain extending into the upper

extremities. A facet joint injury model that applies tensile loading to the C6/C7 facet joint in the rat induces hypersensitivity to mechanical stimulation in *both* the shoulders and the forepaws (Dong and Winkelstein, 2010; Lee et al., 2008; Lee and Winkelstein, 2009). This facet injury-induced sensitization of tissues is similar to that reported in humans (Fernandez-Perez et al., 2012; Scott et al., 2005); yet, it is unknown if that rat model also induces an immediate development and persistence of thermal sensitivity. Recent studies in which the non-steroidal anti-inflammatory drug (NSAID) ketorolac was injected into the facet joint after its injury demonstrate that joint inflammation may be necessary for the maintenance, but not initiation, of loading-induced facet pain (Dong et al., 2011; Dong et al., 2013a). In those studies, the intra-articular anti-inflammatory treatment alleviates facet-mediated mechanical hypersensitivity when given one day after joint injury but is ineffective when given at the time of injury (Dong et al., 2011; Dong et al., 2013a). Joint inflammation and arthritis in animal models are associated with both mechanical *and* thermal hypersensitivity (Longo et al., 2013; Luo et al., 2014; Tachihara et al., 2007), suggesting that the joint inflammation associated with painful facet joint loading may also induce thermal sensitivity in addition to mechanical hyperalgesia. Yet, no study has investigated if facet joint injury is sufficient to induce thermal sensitivity.

### 1.2.6. Clinical Treatment of Joint Pain in the Spine

Clinically, several treatments are used currently to relieve facet joint-mediated pain. As described in Section 1.2.2, the medial branches of the dorsal rami innervate the cervical facet joints. Anesthetic blocks of those nerve branches using the sodium channel blocker bupivacaine alleviate facet-mediated pain and have been used to identify the facet

joint as the source of neck pain (Lord et al., 1996; van Eerd et al., 2010). However, such nerve blocks have also been utilized to treat facet pain, with one study reporting pain relief lasting fourteen to sixteen weeks in some patients suffering from chronic (greater than six months) facet-mediated neck pain (Manchikanti et al., 2008). Yet, anesthetic nerve blocks do not always provide such prolonged pain relief; a similar study with bupivacaine-induced medial branch nerve blocks reports pain relief lasting on the order of several hours in most patients, with only a small group experiencing sustained relief for several days (Barnsley et al., 1993). Of note, those two studies use different patient populations. All patients in the study by Barnsley exhibited facet-mediated pain after a motor vehicle collision (Barnsley et al., 1993); however, only 32% of the neck pain patients in the study by Manchikanti had experienced a motor vehicle impact prior to the initiation of pain (Manchikanti et al., 2008). The difference in the patient populations between those two studies might contribute to the differing effectiveness of anesthetic nerve blocks in alleviating facet pain, despite the use of similar injection techniques and anesthetic doses. Moreover, injection of bupivacaine into the intra-articular space of symptomatic facet joints, as opposed to blocking the nerves innervating those joints, also provides only temporary pain relief; fewer than 50% of patients report pain relief beyond one week (Barnsley et al., 1994). Ablation of the nerves innervating the painful facet joint via radiofrequency neurotomy is effective in alleviating facet pain in approximately 60% of patients, with pain relief lasting at least three months (Lord et al., 1996; Smith et al., 2014). In fact, Lord reports average pain relief lasting 263 days using that technique (Lord et al., 1996); yet, when the pain returns, a second radiofrequency neurotomy is not always effective (Lord et al., 1996). Although the effectiveness of anesthetic nerve blocks

and radiofrequency neurotomy in facet joint pain relief identifies the facet joint as the source of pain and supports ongoing input from the joint as driving persistent pain, such techniques only provide temporary pain relief of variable duration.

Anti-NGF is a targeted treatment for joint pain that is currently undergoing clinical trials. Indeed, a single dose of intravenous anti-NGF alleviates hip and knee joint pain in osteoarthritis as well as non-radicular low back pain for at least eight weeks (Katz et al., 2011; Lane et al., 2010; Schnitzer et al., 2014). The anti-NGF therapy is only applied every eight weeks; yet, it alleviates joint pain to a greater extent than does daily oral NSAID treatment (Schnitzer et al., 2014). Although current systemic anti-NGF therapies show promise in alleviating joint pain from osteoarthritis and chronic low back pain, those treatments are associated with several adverse events, including headache, hyperesthesia, paresthesia, and even joint degeneration (Brown et al., 2012; Katz et al., 2011; Lane et al., 2010). The occurrence of rapidly progressing osteoarthritis is more frequent with systemic anti-NGF therapy than it is with NSAID treatment (Schnitzer et al., 2014), and accelerated osteoarthritis progression exhibits a trend of increased prevalence with higher doses of anti-NGF (Schnitzer et al., 2014). As such, continued efforts are underway to identify safe and effective doses for anti-NGF-mediated pain relief. In addition, although anti-NGF therapy provides pain relief for clinical osteoarthritis patients for at least sixteen weeks when doses are applied every eight weeks (Lane et al., 2010; Schnitzer et al., 2014), the long-term consequences of continued anti-NGF treatment beyond sixteen weeks are not known.

Because systemic anti-NGF alleviates low back pain, and the facet joint is the source of pain in 45% of patients with low back pain (Manchikanti et al., 1999), anti-

NGF therapy may also alleviate facet-mediated pain. Further, a possible role for intra-articular NGF in joint pain is suggested by the elevated levels of NGF that are identified in painful joints, both clinically and in pain models of inflamed or arthritic joints (Barthel et al., 2009; Orita et al., 2011; Saito et al., 2000; Surace et al., 2009). Yet, it is currently unknown if NGF contributes to facet joint pain. Because current treatments for facet-mediated pain have proven to be only transiently effective (Barnsley, 2005; Manchikanti et al., 2008; van Eerd et al., 2014), defining the role of intra-articular NGF in the development and maintenance of facet joint pain is necessary to identify if anti-NGF is an effective alternative intervention. Moreover, understanding the mechanism through which NGF contributes to joint pain will also determine whether ongoing responses within the joint maintain pain or if there is a transition to central pain maintenance, which dictates whether localized joint treatment or systemic intervention is needed.

Despite biomechanical and clinical evidence that the cervical facet joint is a common source of neck pain, the molecular mechanisms involved in the initiation and maintenance of facet joint-mediate pain are incompletely defined. Evidence suggests that the neurotrophins NGF and BDNF likely contribute to injury-induced facet pain, yet no studies have identified their contributions, if any, to behavioral hypersensitivity and central sensitization that develops after non-physiological facet joint loading (Crosby et al., 2013; Dong et al., 2013b; Quinn et al., 2010). The overall hypothesis and aims of this thesis will address many of these unknown aspects of facet pain as detailed in Chapter 2.

# Chapter 2

# Rationale, Context, and Hypotheses

## 2.1. Rationale & Context

Annually, neck pain affects nearly half of the adult population in the United States (Hogg-Johnson et al., 2008; van Eerd et al., 2010). Whiplash injuries are a frequent cause of persistent neck pain (Zuby and Lund, 2010). As a result of its rich sensory fiber innervation and susceptibility to non-physiological mechanical loading, the cervical facet joint is the most common source of pain in the neck (Barnsley et al., 1995; Bogduk and Aprill, 1993; Manchikanti et al., 2002; Panjabi et al., 1998; Pearson et al., 2004; van Eerd et al., 2010). Although cadaveric simulations and clinical studies, as well as more recent studies utilizing animal models, support the facet joints in the lower cervical spine as a source of pain (Bogduk and Aprill, 1993; Dong et al., 2010; Lee et al., 2004; Manchikanti et al., 2002; Panjabi et al., 1998; Pearson et al., 2004), the cellular mechanisms by which persistent pain is produced from facet injury are still not well-defined. Previous work in our laboratory has demonstrated that tensile loading of the facet joint capsule, as occurs during traumatic neck injury, is associated with immediate and persistent mechanical hypersensitivity (Crosby et al., 2013; Dong et al., 2013a, Kras et al., 2013c). In addition to behavioral hypersensitivity, facet joint injury also induces local inflammation in the joint, altered gene expression in the primary afferents whose dermatomes include the neck, shoulder, and upper extremity, and plasticity in spinal neurons (Crosby et al., 2013;

Dong et al., 2008; Dong et al., 2013a; Kras et al., 2013a; Kras et al., 2014a; Lee and Winkelstein, 2009; Quinn et al., 2010). However, despite the behavioral hypersensitivity and neuronal sensitization that are induced by facet joint injury, the role of neurotrophins, which are key mediators of neuronal excitability and persistent pain (Pezet and McMahon, 2006), in the development and maintenance of injury-induced facet pain is still undefined. Yet, neurotrophins are upregulated and released at the peripheral sites of tissue injury or inflammation as well as in the central nervous system (CNS) (McMahon, 1996; Merighi et al., 2008; Pezet and McMahon, 2006). Because neurotrophin signaling in peripheral tissues and the CNS is associated with pain after injury or inflammation (Pezet and McMahon, 2006), neurotrophins may be molecular mediators through which local responses in the facet joint after its injury induce central sensitization and persistent pain. Therefore, the overall aim of this thesis is to define the peripheral and central contributions of two neurotrophins, nerve growth factor (NGF) and brain-derived neurotrophic factor (BDNF), to facet loading-induced pain.

Although the afferents innervating the facet joint are believed to be crucial to the maintenance of facet-mediated neck pain clinically (Barnsley et al., 1994; Bodguk, 2011; Rambaransingh et al., 2010), the phenotypes of the afferents innervating the C6/C7 facet joint and those sensory neurons that are activated during painful facet joint loading and may initiate pain are not fully defined. A study of the C5/C6 facet joint in the rat identified that although C5/C6 joint afferents originate from the DRGs at the C3-T3 spinal levels, the C5 level contains at least twice as many joint afferents as any of the other levels (Ohtori et al., 2002). Defining the innervation pattern of the C6/C7 facet joint will similarly identify the spinal level(s) supplying the most afferents to that joint and, as

such, are the most likely to exhibit cellular modifications after its injury. In addition, identifying the joint afferents as either peptidergic or non-peptidergic will help identify potential signaling pathways that contribute to joint-mediated pain since those populations of afferents respond to distinct signals and initiate different cellular responses from one another (Joseph and Levine, 2010; Merighi et al., 2008; Seybold, 2009). Accordingly, in Aim 1, the innervation pattern of the C6/C7 facet joint was defined to determine which spinal levels contain afferents innervating that joint in the rat (Aim 1a). Further, peptidergic neurons are typically sensitive to NGF signaling and also synthesize BDNF (Pezet and McMahon, 2006). If that class of neurons does indeed innervate the facet joint, the role for neurotrophins in facet-mediated pain would be further supported. As such, the relative abundance of peptidergic afferents with projections to the C6/C7 joint was also defined (Aim 1c). NGF and BDNF levels were quantified in the dorsal root ganglion (DRG) (Aim 1b) to determine the extent to which those neurotrophins are modulated by painful facet joint distraction. Collectively, those studies identify the spinal levels most relevant to facet joint injury and establish modifications in neurotrophin signaling as associated with facet joint loading-induced pain.

Inflammation is associated with increases in many pain mediators like NGF (McMahon, 1996; Watkins et al., 1995; Woolf et al., 1997), and NGF contributes to arthritic joint pain (Brown et al., 2012; Lane et al., 2010; Longo et al., 2013; McNamee et al., 2010; Orita et al., 2011). Yet, it is not known if intra-articular NGF has a role in mechanical injury-induced joint pain. Given that painful facet joint injury is associated with local inflammation in the joint and spinal cord (Dong et al., 2013a; Kras et al., 2014a; Lee et al., 2008), studies in this thesis specifically investigate if intra-articular

NGF is sufficient to induce facet-mediated pain (Aim 2a) and also identify signaling in the different neuronal populations (peptidergic, non-peptidergic) involved in initiating behavioral sensitivity in NGF-induced pain (Aim 2b). Further, the role of intra-articular NGF in the initiation of loading-induced facet pain and subsequent spinal plasticity is determined by blocking NGF signaling in the joint using an anti-NGF antibody given intra-articularly (Aim 2c). Although NGF itself is not transported to the spinal cord (Dawes et al., 2013), it does regulate expression of the neurotrophin BDNF, which *is* transported to, and released in, the dorsal horn and has a role in the sensitization of sensory circuits (Dawes et al., 2013; McMahon, 1996; Merighi et al., 2008; Pezet and McMahon, 2006). As such, spinal BDNF mRNA and protein are quantified after painful facet joint injury at early (day one) and late (day seven) time points (Aim 3a), and the cellular sources of spinal BDNF are identified via double immunolabeling (Aim 3b). The functional role of spinal BDNF in facet-mediated pain is determined by sequestering spinal BDNF to disrupt its binding to the trkB receptor after injury-induced pain is established (Aim 3c).

## 2.2. Overall Hypothesis & Specific Aims

The goal of this thesis is to identify a cellular mechanism local to the facet joint that underlies injury-induced facet pain by defining the roles of the neurotrophins NGF and BDNF in the initiation and maintenance of facet-mediated pain after a mechanical joint injury. The **central hypothesis** of this work is that NGF acting on the primary afferent neurons that innervate the facet joint is a key initiator of facet joint-mediated pain, inducing upregulation of neurotrophins in peripheral nociceptors and increasing

spinal BDNF and neuronal excitability. Further, interruption of NGF signaling in the joint immediately after injury prevents the increase in spinal neuronal excitability while also preventing pain. This thesis defines the role of intra-articular NGF in the induction and maintenance of facet joint-mediated pain, as well as identifies the contribution of BDNF signaling in the peripheral and central nervous systems to the maintenance of pain after mechanical facet joint injury through three aims.

**Hypothesis 1.** Multiple cervical spinal levels supply sensory nerve fibers to the C6/C7 facet joint, some of which are peptidergic, and painful facet joint loading shifts the phenotype of peptidergic joint afferents from primarily small diameter neurons to larger diameter neurons. Further, mechanical joint injury increases the levels of the neurotrophins nerve growth factor (NGF) and brain-derived neurotrophic factor (BDNF) in the primary afferents having cell bodies in the dorsal root ganglion (DRG).

**Aim 1.** Characterize the innervation pattern of the C6/C7 facet joint following painful whiplash-like tensile loading of the C6/C7 facet capsular ligament in the rat. Define the neurotrophin response to joint injury by quantifying the levels of NGF and BDNF in the DRG at an early (day one) and a later (day seven) time point after joint injury.

**Aim 1a.** Identify the number and distribution of afferents innervating the facet using fluorescent retrograde tracing administered in the joint in separate groups of rats undergoing either a painful facet joint distraction or a sham procedure.

**Aim 1b.** Determine which neurotrophins undergo altered expression in the dorsal root ganglion after painful facet joint injury by quantifying mRNA and protein of NGF and BDNF.

**Aim 1c.** Define the phenotypes of the neurons that innervate the C6/C7 facet joint identified in **Aim 1a**, using immunohistochemical analysis of CGRP.

**Hypothesis 2.** Intra-articular NGF is sufficient to induce facet joint-mediated behavioral hypersensitivity and spinal neuronal hyperexcitability via activation of peptidergic, but not non-peptidergic, joint afferents. Further, intra-articular NGF contributes to the initiation of loading-induced facet pain and the subsequent hyperexcitability of spinal neurons. Immunologic blockade of intra-articular NGF prevents the development of facet-mediated pain and neuronal hyperexcitability.

**Aim 2.** Identify the role of intra-articular NGF in facet joint-mediated pain.

**Aim 2a.** Apply intra-articular NGF in naïve uninjured rats to define its effect on behavioral hypersensitivity (mechanical hyperalgesia), spinal neuronal hyperexcitability, and the expression of NGF and BDNF in the DRG at day one and day seven after NGF application.

**Aim 2b.** Inject intra-articular substance P-saporin, IB4-saporin, or blank-conjugated (control) saporin into the C6/C7 facet joints of uninjured rats to ablate peptidergic (substance P) or non-peptidergic (IB4) joint afferents, in separate groups. Two weeks after saporin injection, apply intra-articular NGF to define

which subpopulation of afferents is necessary for NGF-induced mechanical and thermal hyperalgesia and spinal neuronal hyperexcitability.

**Aim 2c.** Immediately after a painful facet joint injury, block NGF signaling in the facet joint by intra-articular application of an anti-NGF antibody to define the effect of blocking intra-articular NGF on behavioral hypersensitivity and spinal neuronal excitability at days one and seven. In separate rats, inject intra-articular anti-NGF one day after a facet joint injury to determine if intra-articular NGF is involved in maintaining injury-induced facet pain and spinal neuronal hyperexcitability that is typically observed at day seven.

**Hypothesis 3.** Painful facet joint distraction induces an upregulation of brain-derived neurotrophic factor (BDNF) in neurons in the spinal cord that contributes to the maintenance, but not the initiation, of loading-induced facet pain.

**Aim 3.** Define the role of spinal BDNF in facet joint injury in association with facet-mediated pain.

**Aim 3a.** Measure spinal BDNF levels after a painful C6/C7 facet joint injury by quantifying protein expression using immunohistochemical labeling and mRNA levels using RT-PCR at an early (day one) and a later (day seven) time point.

**Aim 3b.** Identify the cellular sources of spinal BDNF in facet-mediated pain using double immunofluorescent labeling to detect BDNF and cellular markers of spinal microglia, astrocytes, and neurons at days one and seven after injury.

**Aim 3c.** Inhibit spinal BDNF to define its temporal contribution to joint-mediated pain by applying a BDNF sequestering molecule (trkB-Fc) in the intrathecal space via lumbar puncture five days after a painful facet joint injury, and assess forepaw mechanical hyperalgesia and activation of extracellular signal-regulated kinase (ERK), a cellular marker associated with BDNF-trkB signaling, in the spinal cord using Western blot.

Although not explicitly included in any of the specific aims characterizing the roles of neurotrophins in facet-mediated pain, additional studies are included in this thesis that expand the understanding of several responses of this joint pain model. Behavioral paradigms quantifying mechanical and thermal hyperalgesia associated with facet joint injury were implemented. In addition, studies of injury-induced central sensitization quantify evoked firing in the thalamus in order to identify modifications to neuronal excitability after painful facet injury that may contribute to chronic pain. NGF-induced pain is associated with *both* mechanical and thermal hyperlagesia in rats (Hoheisel et al., 2007; Lewin et al., 1994; McMahon, 1996) and in humans (Dyck et al., 1997). Accordingly, Aim 2b quantifies behavioral responses to both mechanical and thermal stimulus modalities after intra-articular NGF injection in the facet joint. Clinically, mechanical facet joint injury is also associated with both mechanical and thermal hyperalgesia (Scott et al., 2005; Smith et al., 2014; Sterling et al., 2003; Sterling and Kenardy, 2008); yet, despite a hypothesized role for NGF in facet-mediated pain, it is unknown if our rat model of facet joint injury sufficient to induce mechanical hyperalgesia also induces thermal hyperalgesia. As such, studies in Chapter 3 expand our

behavioral testing paradigms after facet joint injury in the rat to quantify *both* mechanical and thermal hyperalgesia in order to further characterize the full array of clinically-relevant symptoms.

Although the specific aims of this thesis investigate the neurotrophin responses to facet injury in the facet joint and its primary afferents at the injured spinal level, as well as in the spinal cord, supraspinal centers such as the thalamus also contribute to chronic pain (Merighi et al., 2008; Millan, 1999). Because activation of some higher order structures, such as the thalamus, are associated with joint pain and because BDNF is capable of activating thalamic neurons (Gautron and Guilbaud, 1982; Neto et al., 2008; Slack et al., 2005), neuronal sensitization in the thalamus is also investigated in preliminary work included in Chapter 7 of this thesis in order to establish whether or not supraspinal centers are also modified by painful facet injury.

In addition to Chapters 3 and 7 described above, this thesis is organized into chapters arranged by relevant studies that summarize experiments addressing the major aims and associated hypotheses as presented in this chapter. The chapters are presented with studies investigating the molecular and neuronal responses to facet joint injury progressing anatomically from the peripheral tissues to the central nervous system. Detailed background information is provided at the beginning of each chapter as appropriate. Studies in Chapter 4 characterize the distribution pattern of neurons innervating the C6/C7 facet joint (Aim 1a) and identify the phenotypes of those joint afferents (Aim 1c). In Chapter 5, the role of intra-articular NGF in the initiation and maintenance of facet-mediated pain and spinal neuronal hyperexcitability is defined (Aims 2a and 2c), and the subpopulations of neurons necessary for NGF-induced

mechanical and thermal hyperalgesia are assessed using selective neurotoxins (saporin conjugates) (Aim 2b). Studies related to Aims 1b, 3a, and 3b are presented in Chapter 6, which characterizes the expression of BDNF following painful facet joint loading and establishes a role for spinal BDNF in the maintenance of facet pain. Finally, in Chapter 8, the overall collection of studies is integrated into the broader context of mechanisms of joint pain, specifically facet-mediated pain, and a discussion of the limitations of this work is presented, as well as directions for future studies.

# Chapter 3

# Mechanical and Thermal Sensitivity in the Rat are Mediated by Facet Capsular Ligament Loading

## 3.1. Overview

Chronic neck pain is a frequent consequence of injury to the cervical spine (Berglund et al., 2000; Eck et al., 2001; Freeman et al., 1999), with the facet joints being identified as the most frequent source of neck pain following whiplash, in particular (Lord et al., 1996). Indeed, there is biomechanical evidence suggesting that tensile loading across the facet joint capsular ligament, as occurs during whiplash-like loading of the neck, may be sufficient to induce pain (Barnsley et al., 1995; Bogduk and Aprill, 1993; Chen et al., 2006; Lu et al., 2005; Panjabi et al., 1998; Pearson et al., 2004; Sundararajan et al., 2004). Whiplash is associated with hypersensitivity to a variety of sensory modalities, such as pressure, vibration, heat, and cold stimuli (Elliott et al., 2009; Scott et al., 2005; Sterling and Kenardy, 2008). In addition, hypersensitivity is also reported in body regions that are remote from the neck, including the shoulder, arm, and leg (Chien et al., 2009; Curatolo et al., 2001; Fernandez-Perez et al., 2012; Greening et al., 2005; Sterling and Kenardy, 2008; Sterling et al., 2002); these symptoms have been reported to differentiate whiplash-associated pain from other types of neck pain (Scott et al., 2005). In order to better define the mechanisms that contribute to whiplash-like facet loading-induced pain, animal models that accurately reflect the symptoms of whiplash

patients are needed. Our lab has previously developed a model of loading-induced facet joint injury in the rat and characterized sensitivity to mechanical stimulation, as well as functional deficits after injury using that model (Dong and Winkelstein, 2010; Dunk et al., 2011; Kras et al., 2013a; Lee et al., 2004). Despite the prevalence of thermal hypersensitivity reported for whiplash pain patients (Scott et al., 2005; Smith et al., 2014; Sterling et al., 2003; Sterling and Kenardy, 2008), the *thermal responses* following mechanical facet joint injury remain undefined.

The studies presented in this chapter summarize the behavioral responses to mechanical and thermal stimuli following dynamic mechanical loading-induced facet joint injury known to produce mechanical sensitivity. Specifically, this work tests the hypothesis that non-physiologic whiplash-like tensile loading of the cervical facet joint induces both mechanical *and* thermal sensitivity in the rat. As such, a previously validated model of painful facet joint loading was used, and the withdrawal threshold to mechanical stimulation and latency for withdrawal from a thermal stimulus are quantified after a facet joint distraction of sufficient magnitude to induce persistent sensitivity (Crosby et al., 2013; Dong and Winkelstein, 2010; Kras et al., 2013a). To provide biomechanical context, the severity of loading applied to the facet joint capsular ligament is quantified using distraction and strain metrics to ensure injury consistency and to enable comparisons with previously reported findings from this model. Although studies included in this chapter do not match directly to any specific sub-aim of this thesis, the injury model and associated behavioral assessment techniques presented in this chapter are utilized in subsequent chapters to study the cellular responses to facet joint injury in the context of behavioral sensitivity.

## 3.2. Relevant Background

Several modalities of pain are observed in whiplash patients, including sensitivity to mechanical and thermal stimuli among others (Fernandez-Perez et al., 2012; Scott et al., 2005; Sterling et al., 2003; Sterling and Kenardy, 2008). Although spontaneous pain is the most commonly reported symptom in chronic pain patients and is frequently reported after neck trauma (Hagström et al., 1996; Mogil et al., 2010), metrics for quantifying this type of pain in animal models, such as food intake, grooming, and paw guarding, have proven unreliable in their specificity due to inherent susceptibility to confounding factors unrelated to pain (Mogil and Crager, 2004; Mogil et al., 2010). Evoked pain measures, such as allodynia and hyperalgesia, provide a repeatable method to quantify sensitivity, both clinically and in pre-clinical animal models (Boivie, 2003; Chaplan et al., 1994; Gregory et al., 2013; Lee and Winkelstein, 2009; Mogil and Crager, 2004; Sterling and Kenardy, 2008). Allodynia is the perception of pain in response to a non-noxious stimulus, whereas hyperalgesia is an increased response to a noxious stimulus and includes all states of heightened pain sensitivity (Loeser and Treede, 2008; Ringkamp et al., 2013). One of the characteristics of hyperalgesia is a decreased pain threshold (Ringkamp et al., 2013). In fact, decreased thresholds to thermal and mechanical stimuli are evident in whiplash pain patients in the neck, as well as in remote locations like the shoulder, arm, and hand (Fernandez-Perez et al., 2012; Herren-Gerber et al., 2004; Scott et al., 2005; Sterling et al., 2003; Sterling et al., 2008). Evoked response thresholds to mechanical and thermal stimuli can be measured in both humans and animals (Chaplan et al., 1994; Hargreaves et al., 1988; Scott et al., 2005). Because whiplash patients with pain frequently exhibit hyperalgesia for both stimulus modalities,

quantification of those evoked responses in animal models of whiplash-like neck injury collectively offers a suitable measure of pain in those animal models that mimic the human condition.

Painful mechanical and thermal stimuli can activate both unmyelinated C-fibers and thinly myelinated Aδ-fibers (Ringkamp et al., 2013; Yeomans et al., 1996; Ziegler et al., 1999). Aβ-, Aδ-, and C-fibers all innervate articular joints, including the facet joint (Cavanaugh et al., 1996; Lu et al., 2005; Schaible and Grubb, 1993). With the exception of the cartilage, free nerve endings extend into all of the structures within joints, including the capsular ligament (Cavanaugh et al., 1996; Schaible and Grubb, 1993; Schaible et al., 2009), supporting the potential for injury to the joint tissues to induce pain. As reviewed more extensively in Section 1.2.2 of Chapter 1, non-physiologic loading of the facet capsular ligament is a potential mechanism thought to contribute to facet-mediated pain (Pearson et al., 2004; Siegmund et al., 2001; Yoganandan et al., 2002). In a goat model of loading-induced facet joint injury, both Aδ- and C-fibers innervating the cervical facet joint capsular ligament are activated by tensile stretch of that ligament (Chen et al., 2006; Lu et al., 2005). Since both Aδ- and C-fibers are able to detect thermal and mechanical stimuli, loading-induced activation of capsule afferents may contribute to the hypersensitivity to heat and mechanical stimulation that is observed in patients after neck trauma (Fernandez-Perez et al., 2012; Herren-Gerber et al., 2004; Scott et al., 2005; Sterling et al., 2008). In our rat model of facet joint loading that simulates a traumatic neck injury and induces non-physiological distraction of the C6/C7 facet joints, facet capsular ligament strains of 24.0±10.0% are sufficient to induce immediate and sustained mechanical hypersensitivity in the shoulders as well as the

forepaws (Dong and Winkelstein, 2010; Kras et al., 2014a; Lee et al., 2004; Lee et al., 2008). Despite the fact that thermal hypersensitivity is also evident in whiplash patients (Scott et al., 2005; Sterling and Kenardy, 2008) and sensory fibers in the joint capsule that may be capable of transducing thermal stimuli are activated (Chen et al., 2006; Lu et al., 2005; Ringkamp et al., 2013; Yeomans et al., 1996), it is not known if facet joint injury induces an immediate development and persistence of thermal sensitivity.

Standardized methods for quantifying withdrawal responses to mechanical and thermal stimulation of many body regions in the rat, including the head, shoulders, and paws, have been developed and validated (Chaplan et al., 1994; Hargreaves et al., 1988; Ivanusic et al., 2011; Lee et al., 2008). Mechanical sensitivity can be evaluated by measuring the withdrawal response threshold to stimulation using a calibrated series of von Frey filaments to apply localized pressure to the target anatomic region (Berge et al., 2013; Chaplan et al., 1994; Decosterd and Woolf, 2000; Hubbard and Winkelstein, 2005; Le Bars et al, 2001; Lee et al., 2008). Because hyperalgesia is a frequent characteristic of pain in humans (Chaplan et al., 1994), decreases in the withdrawal threshold provide a quantitative measure of that sensitivity in animal models designed to mimic human pain states (Le Bars et al., 2001). Variations of the up-down method originally described by Chaplan have been widely utilized to detect differences in withdrawal thresholds in response to nerve injury, peripheral inflammation, and joint inflammation and arthritis (Chaplan et al., 1994; Coull et al, 2005; Decosterd and Woolf, 2000; Gong et al., 2011; Hubbard and Winkelstein, 2005; Longo et al., 2013; Mannion et al., 1999; Matayoshi et al., 2005). In one variation, an ascending series of von Frey filaments is applied to the forepaw, and a filament that elicits a paw withdrawal is recorded as the withdrawal

threshold if the next higher filament in the series also elicits a positive response (Dong et al., 2011; Kras et al., 2013b; Lee et al., 2008; Lee and Winkelstein, 2009). That modified method has been used to quantify differences in withdrawal threshold in the shoulder and the forepaw between injured and control rats throughout the post-injury time period in a model of facet joint loading-induced pain (Dong et al., 2011; Kras et al., 2013b; Lee et al., 2008; Lee and Winkelstein, 2009). Thermal hyperalgesia can be measured by recording the length of time that a rat is able to tolerate a focused heat stimulus applied to the paw before withdrawing it (Hargreaves et al., 1988). A radiant heat source is applied to the paw and synchronized with a timer that stops automatically when the paw is withdrawn from the testing surface (Hargreaves et al., 1988; Nicholson et al., 2014). This method of evaluating withdrawal latency as a measure of sensitivity has been used to detect temporal changes in thermal sensitivity following a nerve root injury or inflammation-induced arthritis, as well as to quantify the effectiveness of treatments in the alleviation of inflammatory pain (Amaya et al., 2004; Fischer et al., 2013; Longo et al., 2013; Nicholson et al., 2014; Okun et al., 2011). Because facet joint injury is associated with joint inflammation (Dong et al., 2013a), measurement of thermal hyperalgesia has utility for fully characterizing the pain response after facet injury.

Studies presented in this chapter test the hypothesis that facet joint distraction of a magnitude sufficient to produce persistent mechanical hypersensitivity in the forepaws also induces thermal hyperalgesia in the forepaws. Joint capsule distraction and ligament strains are quantified during a controlled distraction of the bilateral C6/C7 facet joints using previously validated methods (Dong et al., 2008; Dong and Winkelstein, 2010; Kras et al., 2014a) as measures of the severity of the applied joint loading. Although the

initial development of this injury model applied quasistatic joint loading, studies presented in this chapter apply a dynamic joint distraction to load the joint at a rate (500%/s) comparable to the range reported for whiplash-like injuries (150-1000%/s) (Dong et al., 2008). Forepaw withdrawal thresholds to mechanical stimulation, as well as thermal withdrawal latencies, are measured for up to seven days following joint distraction. Although studies presented here include only a small number of animals in each group, the findings define the behavioral responses for the joint loading conditions that will be used in subsequent chapters and are included to provide a basis for behavioral studies with larger group sizes in those later chapters that also define the cellular responses to facet joint injury in the context of pain.

## 3.3. Methods

### 3.3.1. Surgical Procedures & Quantification of Joint Mechanics

Male Holtzman rats (Harlan Sprague-Dawley, Indianapolis, IN) (396±21g) were housed under USDA- and AAALAC-compliant conditions with free access to food and water. All experimental procedures were approved by the University of Pennsylvania IACUC and carried out under the guidelines of the Committee for Research and Ethical Issues of the IASP (Zimmermann, 1983).

All surgical procedures were performed under inhalation isoflurane anesthesia (4% induction; 2.5% maintenance). The hair on the back of the neck was shaved, and the exposed skin was scrubbed and sterilized with betadyne. Under a surgical microscope (Carl Zeiss Inc.; Thornwood, NY), a midline incision was made along the back of the neck, and the paraspinal musculature was separated from the C4-T2 spinous processes.

The laminae and bilateral facet joints were then cleared of inserting muscles from C5-T1. The supraspinous ligament, ligamentum flavum, and interspinous ligament were resected at each level from C5-T1 in order to enable attachment of the rat to the loading device. The C6 and C7 laminae were attached to a customized loading device via microforceps (Figure 3.1), and the C6 vertebra was distracted rostrally by a stepper motor (TM-400, 20µm resolution; Danaher Precision Systems; Boxborough, MA) at 200,000 steps/sec or 15mm/s while the C7 vertebra was held fixed (n=9 rats) (Dong et al., 2008; Dong et al., 2013a; Kras et al., 2013c).

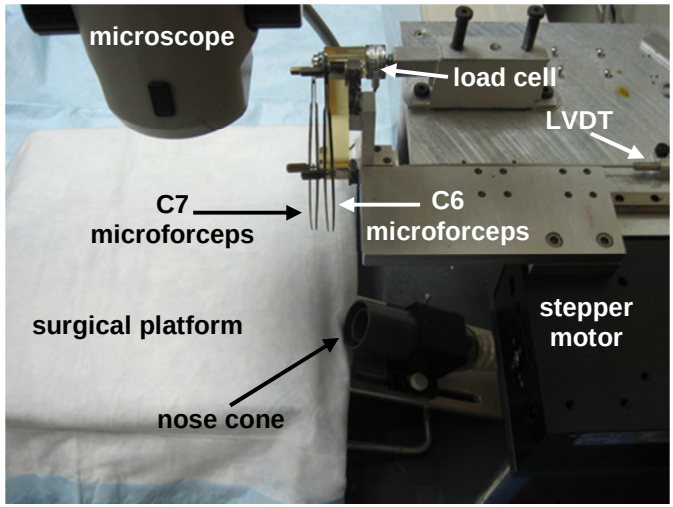


**Figure 3.1.** Customized facet joint loading device. The nose cone is used for anesthesia delivery. A surgical microscope equipped with a high speed camera mounted above the device acquires image data throughout the applied distraction. The microforceps coupled to the C6 vertebra are displaced using the stepper motor automated by a MATLAB program, and the LVDT records the displacement of the C6 forceps. The microforceps coupled to the C7 vertebra remain stationary while the attached load cell continuously records the force across the C6/C7 joint.

A linear variable differential transducer (LVDT) (S-DVRT-24; Microstrain Inc.; Williston, VT; 24mm stroke; 5.7µm resolution) coupled to the C6 microforceps continuously monitored the displacement of the forceps, while a load cell (WMC-5;

Interface Inc.; Scottsdale, AZ) attached to the C7 forceps monitored the force applied across the joint during the distraction (Figure 3.1). In order to measure the vertebral distraction, polystyrene microspheres (Spherotech Inc.; Libertyville, IL) were placed on the C6 and C7 laminae, and a grid of microspheres was placed on the joint capsular ligament in order to quantify the capsular ligament distraction and strain (Figure 3.2). A high speed camera (Phantom v5.1; Vision Research Inc.; Wayne, NJ) mounted to the surgical scope recorded the joint distraction and tracked the corresponding motion of the microspheres at a rate of 500 frames/sec. Additional rats underwent an identical sham procedure that included device attachment but no distraction applied to the facet joint (n=4). Following surgical procedures, all wounds were closed using polyester suture and surgical staples, and the incision site was cleaned with betadyne. Rats were allowed to recover in room air.

Images of the laminae and right facet joint immediately prior to initiation of distraction and at the peak of joint distraction (Figure 3.2) were digitized using ImageJ software (National Institutes of Health; Bethesda, MD) in order to calculate the vertebral and joint deformations. The capsular ligament strains were calculated using LS-DYNA software (Livermore Software Technology Corp.; Livermore, CA) according to previously established methods for study of this joint in vivo (Dong et al., 2008; Dong and Winkelstein, 2010; Kras et al., 2013a). The input file for LS-DYNA was generated using a Matlab code that is provided in Appendix A. Both the maximum principal strain and the maximum tensile strain oriented along the rostrocaudal direction were quantified for each rat to assess the severity of joint loading and to ensure consistency with previous

studies using this injury model (Dong et al., 2008; Dong and Winkelstein, 2010; Lee et al., 2008).

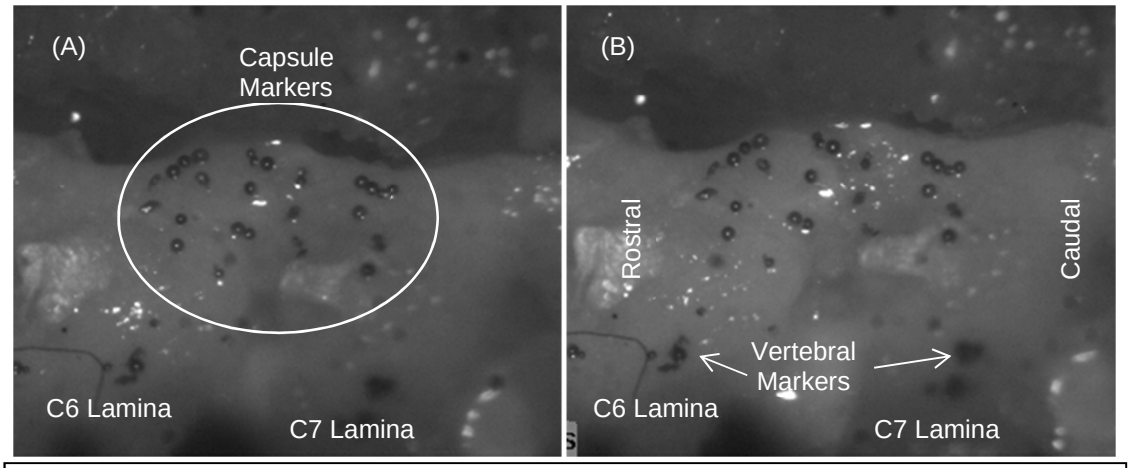


**Figure 3.2.** Representative images showing the exposed facet joint capsule prior to injury **(A)** and at the peak of distraction **(B)**. The C6 and C7 laminae are labeled with vertebral markers (arrows in **B**), and the grid of markers placed over the capsular ligament is circled in **A**. Vertebral distraction is calculated as the change in the vector length between the C6 and C7 vertebral markers before and after distraction. Capsule distraction and ligament strains are calculated from the grid of markers on the capsule.

### 3.3.2. Assessment of Mechanical Withdrawal Threshold

After the surgical procedures, mechanical sensitivity was quantified by measuring the withdrawal threshold to mechanical stimulation in each forepaw. Sensitivity was measured on day one (n=9 distraction; n=4 sham) and in a subset of those rats additionally on days three, five, and seven (n=6 distraction; n=2 sham). On each testing day, rats were placed individually into elevated cages with a wire mesh floor and allowed to acclimate to the testing environment for at least 15 minutes. Rats underwent three rounds of testing on each day with each round separated by at least ten minutes. During each testing round, a series of calibrated von Frey filaments (1.4g-26g) (Stoelting; Wood Dale, IL) was applied to the plantar surface of each forepaw in ascending order to determine the threshold filament that would elicit a response. A positive response is

defined as a rapid withdrawal of the paw following stimulation that may or may not be accompanied by vigorous shaking or licking of the paw (Chaplan et al., 1994; Crosby et al., 2013; Kras et al., 2013a; Lee et al., 2008). Each filament was applied for five consecutive stimulations at a frequency of approximately one stimulation per second. The filament strength eliciting a response was recorded as the withdrawal threshold if the next consecutive filament also elicited a positive response. If no filament elicited a response, then a threshold of 26g, corresponding to the highest magnitude filament, was recorded. For each testing round, a withdrawal threshold was determined for each paw separately, and thresholds were averaged over the three rounds and between the right and left paws in order to obtain a single withdrawal threshold for each rat on each testing day. Withdrawal thresholds were also quantified for three days prior to any surgical procedure in order to establish baseline sensitivity responses for each rat. Mechanical withdrawal thresholds were compared using a repeated-measures two-way ANOVA with Tukey's Honestly Significant Difference (HSD) test with group (distraction, sham) and testing day as factors.

### 3.3.3. Assessment of Thermal Withdrawal Latency

Thermal hyperalgesia was evaluated following mechanical behavioral assessment on day one for all rats and again on day seven for those rats that were followed to the later time point. Rats were placed in wire mesh cages on top of a glass surface and allowed to acclimate to the testing environment for 30 minutes (Figure 3.3). The glass surface was maintained at 30°C in order to reduce the effects of differences in initial skin

temperature on withdrawal latencies (Berge, 2013; Dirig et al., 1997; Nicholson et al., 2014).

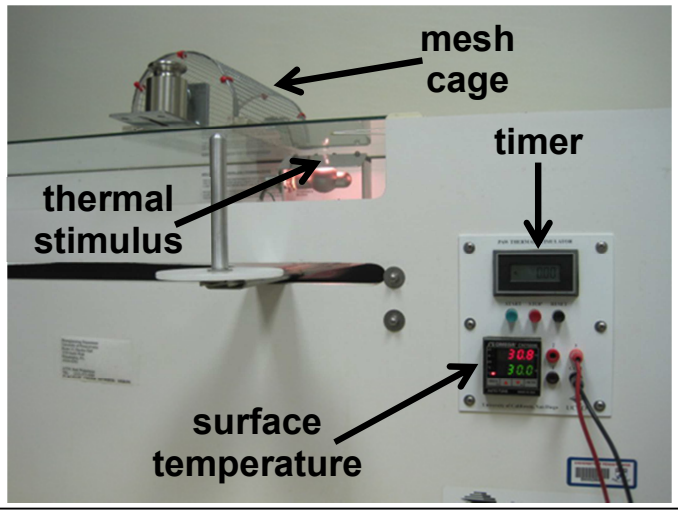


**Figure 3.3.** Device for measuring thermal sensitivity in the paws of the rat. The glass surface is warmed to 30°C, and the rat is placed in the wire mesh cage on the surface. The thermal stimulus is positioned underneath the forepaw, and the timer records the time from initiation of heating to the time when the rat withdraws the paw.

A commercially available device (UC San Diego; San Diego, CA) was used to focus a radiant heat source (projection bulb) onto the plantar surface of each forepaw (Figure 3.3) using previously validated methods to quantify the latency to paw withdrawal (Dirig et al., 1997; Hargreaves et al., 1988; Nicholson et al., 2014). An angled mirror attached to the stimulator enables accurate positioning of the heat source under the plantar surface of the forepaw. A timer synchronized to the thermal stimulus measures the latency time between the initial application of the heat source and when the paw is withdrawn (i.e. the withdrawal latency). On each testing day, the withdrawal latency was measured three to five times for each forepaw, with a ten minute rest between each measurement. Paw withdrawals associated with normal ambulation of the rat were not considered. The average withdrawal latency for each rat was calculated by averaging

results from the right and left forepaws across all testing rounds for each day. Withdrawal latencies for each rat were quantified for three days prior to any surgical procedure in order to establish baseline responses for comparison. Differences in withdrawal latency between groups were determined using a two-way repeated measures ANOVA with Tukey's HSD test with group (distraction, sham) and time point (day zero, day one, day seven) as factors. Separate paired t-tests compared differences in withdrawal latency at each time point to baseline for the distraction and sham groups.

## 3.4. Results

No adverse effects were observed following surgery, with rats displaying normal grooming behavior, mobility, and consistent weight gain. Analysis of the videos recorded during the injury, as well as visual inspection of the bilateral C6/C7 joints at the termination of each study, confirm that the joint capsules remained intact for all rats in the distraction and sham groups. The digitization error in the methods used to calculate capsule distraction and strain was only 1.5±0.8%. The joint loading device applied a consistent distraction for all rats in the distraction group, with an average displacement of the C6 microforceps of 2.50±0.02mm, corresponding to an average vertebral distraction of 0.50±0.19mm and a capsular distraction of 0.28±0.12mm (Table 3.1). The applied distraction rate was 13.58±0.66mm/sec, corresponding to an applied strain rate of 452±22% across the joint (Table 3.1). Distraction of the joint capsule produced capsular ligament strains oriented primarily in the rostrocaudal direction (Figure 3.4). Maximum principal strain in the capsule averaged 22.18±13.57%, and maximum strain in the rostrocaudal direction was 14.34±11.68% (Figure 3.4; Table 3.1). At the time of peak

joint distraction, the joint supported an average tensile load of 2.24±0.90N (Table 3.1). In addition, the individual force-displacement loading curves, capsule strain fields, and maximum vertebral and capsule distractions for each rat included in this study are detailed in Appendix B.

**Table 3.1.** Summary of maximum mechanical data for the distraction group.

| Rat | Displacement of C6 forceps (mm) | Vertebral distraction (mm) | Capsule distraction (mm) | Distraction rate (mm/s) | Maximum principal strain (%) | Rostrocaudal strain (%) | Tensile force (N) |
|---|---|---|---|---|---|---|---|
| **413** | 2.47 | 0.44 | 0.19 | 13.27 | 15.03 | 5.41 | 2.93 |
| **415** | 2.50 | 0.36 | 0.25 | 13.17 | 17.92 | 17.81 | 3.17 |
| **417** | 2.50 | 0.59 | 0.32 | 13.89 | 21.40 | 19.28 | 3.58 |
| **418** | 2.50 | 0.96 | 0.59 | 13.00 | 54.59 | 40.97 | 2.89 |
| **A** | 2.50 | 0.45 | 0.27 | 12.38 | 17.67 | 8.93 | 1.26 |
| **B** | 2.53 | 0.45 | 0.17 | 14.38 | 30.84 | 8.68 | 1.45 |
| **I** | 2.48 | 0.34 | 0.26 | 13.93 | 7.91 | 2.14 | 1.84 |
| **D** | 2.51 | 0.55 | 0.25 | 13.92 | 18.41 | 18.00 | 1.19 |
| **E** | 2.54 | 0.35 | 0.23 | 14.27 | 15.84 | 7.87 | 1.87 |
| **avg (SD)** | 2.50 (0.02) | 0.50 (0.19) | 0.28 (0.12) | 13.58 (0.66) | 22.18 (13.57) | 14.34 (11.68) | 2.24 (0.90) |

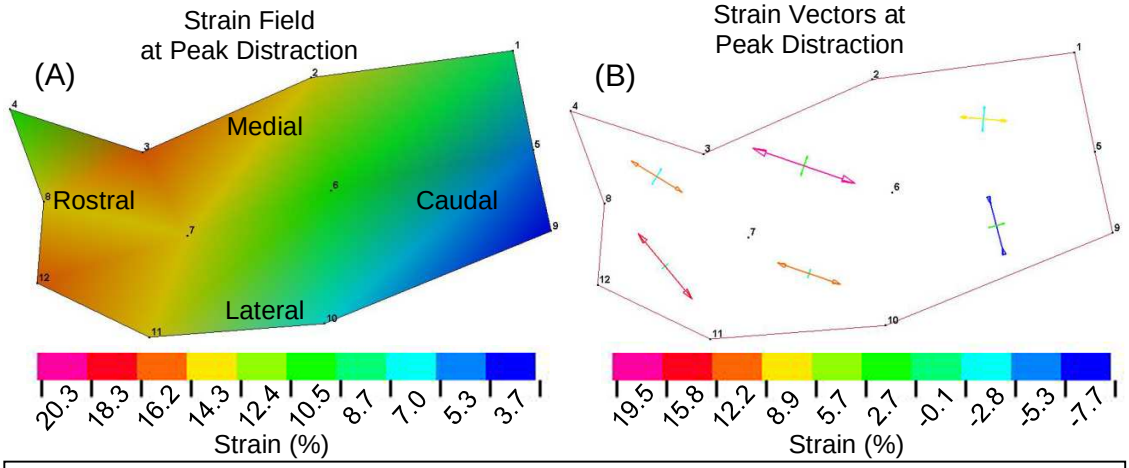


**Figure 3.4.** **(A)** Representative maximum principal strain field on the capsular ligament at its peak joint distraction. The strain field image was generated using LS-DYNA software and digitized images of the joint capsule markers just prior to joint distraction and at peak distraction. **(B)** Corresponding strain vector field of maximum principal strain at peak joint distraction. The maximum principal strain mainly occurs in the rostrocaudal direction.

Distraction of the C6/C7 facet joint induces an immediate reduction in the forepaw withdrawal threshold to mechanical stimulation by day one compared to baseline responses ($p<0.001$) (Figure 3.5). The withdrawal threshold remains significantly lower than baseline at all time points through day seven after joint distraction ($p<0.001$) (Figure 3.5). Moreover, the withdrawal threshold at day one is significantly lower after distraction than after a sham procedure ($p<0.035$); yet, statistical significance is not achieved at any other time point for comparisons between distraction and sham with these small group sizes (Figure 3.5). No change from baseline is detected in the sham group at any post-surgical time point (Figure 3.5). Detailed mechanical withdrawal threshold data for each rat in this study are included in Appendix C.

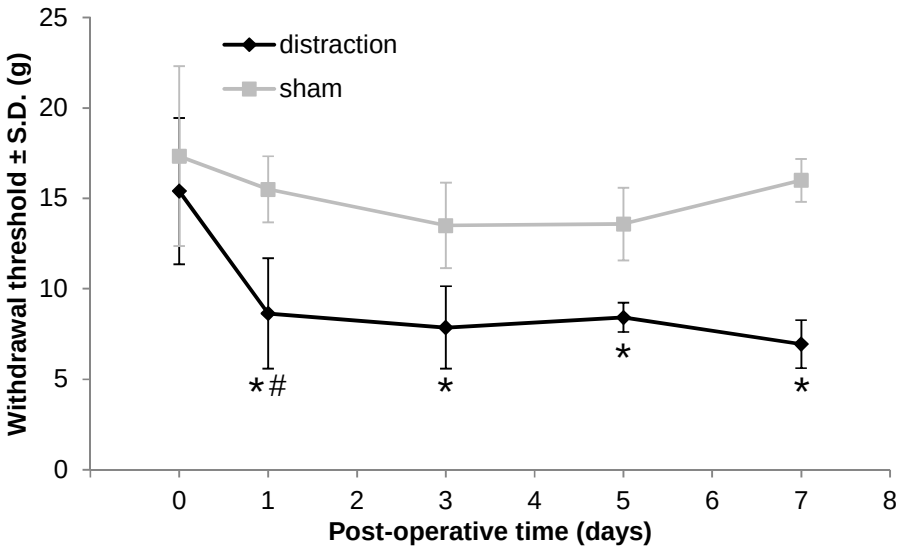


**Figure 3.5.** Mechanical sensitivity in the forepaw as measured by the withdrawal threshold in response to von Frey filament stimulation. Withdrawal threshold significantly decreases (*$p<0.001$) after joint distraction compared to baseline on all post-operative days as well as compared to sham (#$p<0.035$) at day one.

Similar to the decrease in the mechanical withdrawal threshold that is observed, joint distraction significantly reduces the withdrawal latency to thermal stimulation at day

one ($p<0.029$) compared to baseline (Figure 3.6). There is a trend towards a further decrease in latency at day seven but with no significant differences from baseline ($p<0.061$) at day seven (Figure 3.6). Withdrawal latencies in the sham group do not change significantly from baseline at either time point (Figure 3.6). No differences are detected between the distraction and sham groups at any time point. The withdrawal latency measured for each rat in this study is tabulated in Appendix C.

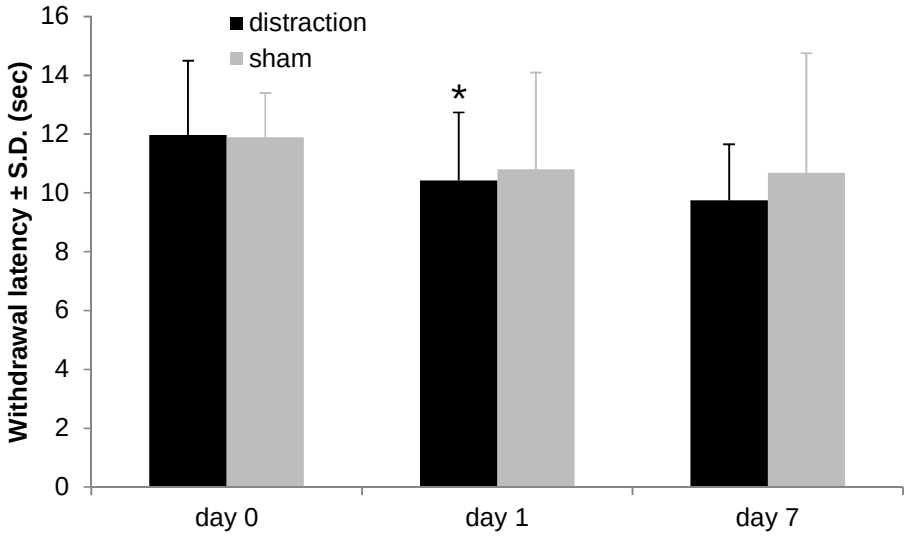


**Figure 3.6.** Thermal hyperalgesia in the forepaw as measured by the withdrawal latency to thermal stimulation. Withdrawal latency significantly decreases (*$p<0.029$) after joint distraction compared to baseline on post-operative day one and trends to significance ($p<0.061$) at day seven.

## 3.5. Discussion

The results of the studies in this chapter demonstrate that a mechanical facet joint injury sufficient to induce mechanical hypersensitivity in the rat also increases sensitivity to thermal stimuli. The 2.50±0.02mm displacement recorded by the LVDT, with a variability of only 0.8%, supports that the loading device reliably produces a consistent distraction across the rat's C6/C7 facet joint. Further, digitization errors associated with

the method of image analysis and capsule distraction and strain calculation are small (1.5±0.8%) and so are unlikely to substantially affect the distractions and strains. The metrics that quantify the mechanics of the joint distraction, including the vertebral distraction (0.50±0.19mm), tensile force across the joint (2.24±0.90N), and maximum principal strain in the capsule (22.18±13.57%) (Table 3.1), all agree closely with previous studies characterizing the mechanics of this type of injury: with (0.47-0.75mm) vertebral distractions, (3.00-4.04N) tensile forces, and (21.5-31.2%) maximum principal strains (Dong et al., 2008; Dong and Winkelstein, 2010; Dong, 2011; Dong et al., 2011; Dong et al., 2013a). This consistency in the joint loading mechanics across multiple studies further demonstrates that the dynamic mechanical joint injury used here is highly reproducible.

The injury applied to the C6/C7 facet joint in the current study closely simulates the tensile joint loading that occurs in a traumatic neck injury such as whiplash. The maximum principal strain of 22.18±13.57% is within the range of capsular ligament strains (8.7-39.9%) reported for the C6/C7 facet joint in whiplash simulations using cadavers (Panjabi et al., 1998; Pearson et al., 2004), which supports the current in vivo model as a reasonable model for further study of the behavioral and cellular effects of whiplash-like loading. In a goat model of facet joint injury, the majority of Aδ- and C-fibers innervating the capsular ligament are activated by strains of 10.7±3.3% and 10.0±4.6%, respectively (Lu et al., 2005). Since sensory fibers of these types transmit nociceptive stimuli to the spinal cord, their activation under joint loading that produces capsular ligament strains of 22.18±13.57% suggests that similar loading-induced

activation of capsule afferents in the rat may contribute to the behavioral sensitivity that is observed in the current study (Figures 3.5 & 3.6).

The significant reduction in mechanical withdrawal threshold from baseline at all time points after injury (Figure 3.5) is consistent with previous work using this injury model (Dong and Winkelstein, 2010; Lee and Winkelstein, 2009) and supports the use of this model to study both the immediate (day one) and the longer term (day seven) cellular mechanisms by which joint loading contributes to facet joint-mediated pain. Mechanical hypersensitivity is also evident when compared to sham at day one but only exhibits trends toward significance at other time points after injury (Figure 3.5). Changes in threshold after day one are not significant despite a continued decrease in the withdrawal threshold in the distraction group at the later time points. Studies using this same injury model report a significant reduction in the withdrawal threshold immediately after injury that remains significantly lower than control groups for at least seven days (Dong et al., 2011; Kras et al., 2013b); however, those studies used group sizes of at least four rats each. In the studies for this chapter, the small size of the sham group (n=2 rats) at all time points after day one likely precludes detecting any significant differences between groups because of the low power of the comparisons. Indeed, power analysis indicates that a group size of at least four is necessary to detect differences between injury and sham, a finding corroborated by the significant difference detected at day one between distraction (n=9) and sham (n=4) as well as by the studies in the later chapters (Chapters 4, 5, & 6). Because decreased threshold for withdrawal to mechanical stimulation seven days after injury has been well-documented by previous studies using this same injury model (Dong

and Winkelstein, 2010; Lee and Winkelstein, 2009), additional sham animals were not added to the current study.

Significant thermal hyperalgesia developed by day one after injury (Figure 3.6), but no significant changes in thermal sensitivity were observed in shams at either time point (Figure 3.6). Although the withdrawal latency decreases from baseline in the sham group at day one, this difference was not significant and is likely due to the response of a single animal in the sham group. Of the four rats tested at day one (see Table C.2 in Appendix C), one animal (Rat G) exhibited a decrease in withdrawal latency of 44% of its baseline, while none of the other three rats exhibited a decrease of more than 5%. These individual data suggest that the overall trend toward decreased withdrawal latency in the sham group at that day may be biased by the response of that outlier. Although additional studies are needed to fully define the thermal response to the sham procedure, such studies are not included in this thesis. However, studies identifying the contribution of intra-articular nerve growth factor and the subpopulations of joint afferents involved in the initiation of facet-mediated thermal hyperalgesia are included in Chapter 5.

Despite reports that some whiplash patients experience increased sensitivity to thermal stimuli (Scott et al., 2005; Smith et al., 2014), thermal sensitization is not a universal consequence of whiplash (Chien et al., 2008; Chien et al., 2009; Curatolo et al., 2001). Chien reports that sensitivity to heat stimuli in the hands of whiplash patients is unchanged compared to controls (Chien et al., 2009), supporting the current finding of no change in sensitivity to heat stimuli in the forepaw of injured rats compared to sham. However, data presented here (Figure 3.6) represent thermal responses measured only in the forepaw. Whiplash patients report increased sensitivity in multiple regions, including

the neck, shoulder, arm, and even the leg (Scott et al., 2005; Smith et al., 2014; Sterling et al., 2003), suggesting that sensitivity may develop in other locations not evaluated in the current study. After a neck injury, the most common body regions that patients report as painful are the posterior neck and shoulders (Hincapié et al., 2010), suggesting those regions may be more relevant to injury-induced hypersensitivity in the rat than the forepaw. In fact, mechanical sensitivity is increased in the shoulder of rats after a painful facet joint distraction (Lee and Winkelstein, 2009), supporting its potential for pain after joint injury. Additional studies characterizing thermal sensitivity with more rats and in additional relevant anatomical regions are necessary to fully define the thermal response to whiplash-like facet joint injury.

## 3.6. Conclusions & Integration

The studies in this chapter demonstrate that distraction of the C6/C7 facet joint is a highly reproducible biomechanical injury model of whiplash-like joint loading that mediates the development of both mechanical *and* thermal sensitivity (Figures 3.5 & 3.6). Because a major focus of this thesis is to define mechanism(s) through which local intra-articular responses to joint injury contribute to the development of pain, and because loading-induced mechanical and thermal sensitivity are evident at day one (Figures 3.5 & 3.6), additional experiments to increase the group sizes to determine if thermal sensitivity is maintained after injury were not carried out. Throughout the remainder of this thesis, at least four rats are included in each experimental group to ensure that statistical comparisons have enough power to detect differences between groups. Based on the finding of thermal hyperalgesia at day one after injury, thermal withdrawal latencies are

quantified at day one after intra-articular injections to determine the role of NGF in facet-mediated pain (Chapter 5).

The loading-induced strains in the joint capsule (Table 3.1) have similar magnitudes to strains that induce firing of joint capsule afferents (Chen et al., 2006; Lu et al., 2005), which suggests that loading-induced excitation of afferents innervating the facet joint may contribute to behavioral hypersensitivity after injury. The cellular mechanisms by which mechanical joint injury can induce pain remain unknown. In order to begin to define the role of the facet joint and its local responses to injury that underlie loading-induced facet pain, Chapter 4 uses neuronal tracing techniques in combination with the painful injury conditions defined in this chapter to characterize the innervation of the facet joint and the effects of painful joint loading on the afferents innervating the joint. Studies in Chapter 5 further utilize the loading condition defined in this chapter to define one mechanism through which local intra-articular responses in the joint immediately following injury contribute to the development of loading-induced facet pain.

# CHAPTER 4

# Characterization of the C6/C7 Facet Joint Afferents After Painful Joint Loading in the Rat

*Parts of this chapter are adapted from:*

Kras JV, Tanaka K, Gilliland TM, Winkelstein BA (2013). An Anatomical and Immunohistochemical Characterization of Afferents Innervating the C6-C7 Facet Joint After Painful Joint Loading in the Rat. *Spine*, 38(6): E325-E331.

## 4.1. Overview

In Chapter 3, non-physiologic loading of the facet joint was shown to induce mechanical and thermal hypersensitivity in the rat (Figures 3.5 & 3.6). In order to begin to define the molecular responses underlying loading-induced joint pain, the neuronal innervation patterns of the facet joint must be characterized. Several studies in both humans and rats have demonstrated that cervical facet joints are innervated by primary afferent neurons that originate from multiple spinal levels (Barnsley and Bogduk, 1993; Ohtori et al., 2003). Further, tensile loading of the cervical facet joint has been shown to activate the nociceptors that innervate that joint (Chen et al, 2006; Lu et al., 2005). Despite that collection of works, the distribution of primary afferents that innervate many of the cervical facet joints, and C6/C7 in particular, is unknown in the rat. Primary afferents can be classified as either peptidergic or non-peptidergic (See Chapter 1 for a more extensive review) (Merighi et al., 2008). Peptidergic afferents upregulate expression of both substance P and calcitonin gene-related peptide (CGRP) in response to

inflammation and nerve injury (Seybold, 2009; Weissner et al., 2006), and CGRP signaling has been associated with arthritis-induced spinal neuronal hyperexcitability (Bird et al., 2006). Although increased neuropeptide expression and spinal hyperexcitability both have been associated with painful facet joint distraction (Crosby et al., 2013; Lee and Winkelstein, 2009; Quinn et al., 2010), the expression of neuropeptides in afferents innervating the C6/C7 facet joint, normally or after its painful injury, has not been characterized. Studies presented in this chapter characterize the segmental innervation pattern of the C6/C7 facet joint in the rat (Aim 1a) and test the hypothesis that painful facet joint injury upregulates neuropeptide expression in those joint afferents in the dorsal root ganglion (DRG) in association with behavioral hypersensitivity. Accordingly, CGRP expression also was quantified in the DRG in those neurons innervating the C6/C7 facet joint (Aim 1c) after a painful joint distraction. Additional studies quantifying neurotrophin expression in neurons in the DRG (Aim 1b) are included as part of a later chapter (Chapter 6).

## 4.2. Relevant Background

Neck injuries are reported in up to one-in-three rear-end motor vehicle collisions (Zuby and Lund, 2011), and the cervical facet joint has been identified as the source of pain in as many as 67% of neck pain patients (Bogduk, 2011). Anesthetic nerve blocks and radiofrequency neurotomy of the branches of the nerves innervating the facet joint provide pain relief (Barnsley et al., 1994; Bodguk, 2011; Rambaransingh et al., 2010), further demonstrating facet joint innervation to have a direct relationship to pain. Mechanical facet joint injury is sufficient to activate nociceptors in the joint (Chen et al.,

2006; Lu et al., 2005) and to induce persistent pain (Dong et al., 2008; Lee et al., 2004; Quinn et al., 2010) in animal models. The C5/C6 facet joint in the rat is multi-segmentally innervated, and the expression pattern of neuropeptides is altered in the joint afferents after transection of the capsular ligament (Ohtori et al., 2003). Although the afferents innervating the cervical facet joint are suggested to be crucial to the maintenance of joint-mediated neck pain, the pattern of neurons innervating the C6/C7 facet joint is not known; it is also not known how injury to this joint affects its innervation and/or how the molecular responses of the joint afferents may contribute to pain.

Many pain mediators are upregulated in the DRG in response to joint inflammation and injury (Dong et al., 2008; Dong et al., 2011; Lee et al., 2008; Ohtori et al., 2002; Tachihara et al., 2007). Specifically, the neuropeptide CGRP, which is normally produced in 40% of the primary afferents (Lee et al., 1985), has been implicated as a contributor to joint pain and neuronal excitability (Iwakura et al., 2010; Ohtori et al., 2003; Orita et al., 2011; Staton et al., 2007; Sun et al., 2004). Moreover, CGRP is commonly used to identify peptidergic neurons due to its high expression in that subpopulation (Ferrari et al., 2010; Ohtori et al., 2003; Stucky and Lewin, 1999). Recent evidence suggests that some forms of pain can be mediated by specific subpopulations of primary sensory neurons (Ferrari et al., 2010; Hucho et al., 2005) or by a change in the phenotype of peptidergic afferents (Michael et al., 1999; Ohtori et al., 2002; Ohtori et al., 2003; Zhou et al., 1999). Despite the association of peptidergic afferents and CGRP expression with joint pain, no study has investigated the relationship between CGRP expression in facet joint afferents and painful mechanical facet injury.

Distraction of the C6/C7 facet joint, as may occur during whiplash and other neck injuries, induces persistent pain, upregulates the neuropeptide substance P in the DRG and induces neuronal hyperexcitability in spinal neurons at day 7 in the rat (Dong et al., 2008; Lee et al., 2004; Quinn et al., 2010; Dong and Winkelstein, 2010; Lee and Winkelstein, 2009). Specifically, painful joint distraction upregulates substance P in the C7 DRG at day 7 after injury (Lee and Winkelstein, 2009), which suggests that the peptidergic afferents at this spinal level have a particularly important role in joint-mediated pain. Although peptidergic fibers are identified in the human facet joint capsule (Kallakuri et al., 2004; Kallakuri et al., 2012), no study has defined the effect of a biomechanical, and clinically-relevant, painful C6/C7 facet injury on neuropeptide expression in joint afferents. The goal of this study was to identify the distribution of afferents that project to the C6/C7 facet joint after a painful joint distraction using neuronal tracing methods (Ohtori et al., 2003; Sameda et al., 2001). Because of the suspected contribution of peptidergic afferents at the C7 level to injury-induced pain, the frequency of peptidergic neurons identified in that group of joint afferents was also investigated as compared to all other neurons in the DRGs at the C7 level.

## 4.3. Methods

### 4.3.1. Surgical Procedures & Behavioral Assessment

Male Holtzman rats (Harlan Sprague-Dawley, Indianapolis, IN) (414±26g) were housed under USDA- and AAALAC-compliant conditions with a 12-12 hour light-dark cycle and free access to food and water. Experimental procedures were approved by the

IACUC and carried out under the guidelines of the Committee for Research and Ethical Issues of the International Association for the Study of Pain (Zimmermann, 1983).

All surgical procedures were performed under inhalation isoflurane anesthesia (4% induction, 2.5% maintenance). All rats received a bilateral intra-articular C6/C7 facet joint injection of 20µg of the retrograde neuronal tracing molecule cholera toxin subunit B (CTb) conjugated to the fluorescent dye Alexa Fluor 488 (Life Technologies; Carlsbad, CA) and dissolved in sterile phosphate buffered saline (PBS). The C6/C7 facet joints and their capsules were exposed according to the procedures described in Section 3.3.1 of Chapter 3 (Kras et al., 2013a; Kras et al., 2014a). A 10µL syringe (Hamilton Company; Reno, NV) with a 33-gauge beveled needle was advanced into the facet joint, and 5µL of the CTb solution was slowly injected. Following injection, the exposure was closed in layers using 3-0 polyester suture and surgical staples.

Three days after the CTb injection, a subset of rats underwent either a painful cervical facet joint distraction injury (n=4) or sham procedure (n=5), as described in Section 3.3.1 of Chapter 3 (Dong et al., 2008; Dong et al., 2011; Kras et al., 2013a). Under inhalation anesthesia, the surgical staples and suture were removed, and the C6 and C7 laminae were rigidly attached to a customized loading device via microforceps. For the painful distraction group, the bilateral C6/C7 facet joints were distracted by displacing the C6 vertebra rostrally while holding the C7 vertebra fixed (Crosby et al., 2013; Dong et al., 2011; Kras et al., 2014a). A camera mounted to a surgical dissecting scope tracked markers on the C6 and C7 laminae during injury in order to quantify the distraction. An additional group of rats underwent sham surgical procedures with device attachment but no applied joint distraction. Following surgery, the incision was closed

and rats were recovered. The remaining group of rats (normal, n=4) received no surgical procedures after the initial CTb injection.

Bilateral forepaw mechanical hyperalgesia was evaluated in those rats undergoing the painful joint injury or sham control procedure using methods identical to those described in Chapter 3 (Section 3.3.2) (Lee and Winkelstein, 2009; Quinn et al., 2010; Weisshaar et al., 2010). Baseline measurements were recorded for 2 days after the CTb injection. Hyperalgesia was measured on days 1, 3, 5 and 7 after the injury or sham procedure. A given filament was recorded as the response threshold if the next higher filament also induced a positive response. Because the applied joint distraction is a bilateral injury, response thresholds were averaged between the right and left forepaws for each rat. At each time point, response thresholds were compared between groups and to the respective baseline values using a two-way repeated measures ANOVA with Tukey's HSD test, with time and group as the factors.

### 4.3.2. DRG Harvest & CGRP Immunohistochemistry

On day 7 after the injury or sham procedures, rats were given an overdose of sodium pentobarbital (65mg/kg) and perfused transcardially with 300mL of PBS and 250mL of 4% paraformaldehyde in PBS (pH7.4). The DRGs on the right side were harvested and post-fixed in the same fixative solution for 2.5 hours at 4ºC. DRGs were then transferred to 30% sucrose for five days at 4ºC before being embedded in Tissue-Tek® OCT Compound (Sakura Finetek; Torrance, CA). Each DRG was axially sectioned at a 14µm thickness through its entire length, and sections were thaw-mounted onto slides. All sections were washed and blocked with normal donkey serum

(Chemicon; Temecula, CA) for two hours before incubation with a polyclonal rabbit anti-CGRP antibody (1:5000; T-4032; Peninsula Laboratories; San Carlos, CA) overnight at 4ºC. The following day, sections were washed and incubated with a Cy3-conjugated donkey-anti-rabbit secondary antibody (1:500; Jackson ImmunoResearch; West Grove, PA) for two hours at room temperature and cover-slipped using Fluoro-Gel anti-fade medium (EMS; Hatfield, PA).

A fluorescent microscope equipped with a digital camera (Olympus; Center Valley, PA) was used to image each DRG section that contained at least one neuron positively labeled with CTb. The total number of neurons that were positive for CTb was counted for each DRG; care was taken to avoid double-counting neurons that appeared in multiple consecutive sections. The total number of CTb-positive neurons was summed for each group at each DRG level. Also, for those CTb-positive neurons, both the cross-sectional area and the intensity of CGRP labeling were quantified using ImageJ software (National Institutes of Health; Bethesda, MD). Each neuron was identified as being either CGRP-positive or CGRP-negative based on its intensity of CGRP labeling. The number of CTb-positive neurons also positively labeled for CGRP was counted at each level for each rat; the total number of those double-labeled neurons at each level was computed for each group. The average percentage of all CTb-positive neurons that were also positive for CGRP also was determined for each group in each DRG. Also, the average cross-sectional area of CTb-positive neurons expressing CGRP was determined. The number of CTb-positive neurons at each level was compared using a two-way ANOVA with Tukey's HSD test, with group and level as the factors. A two-way ANOVA with Tukey's HSD test (with group and level as factors) compared the average

cross-sectional area of neurons positive for both CGRP and CTb; a separate two-way ANOVA with Tukey's HSD test compared the ratio of CTb-positive neurons that were CGRP-positive to the total number of CTb-positive neurons. All statistical analyses were performed using JMP 8 (SAS Institute; Cary, NC) software.

To assess the frequency of peptidergic neurons among joint afferents compared to all neurons in the DRG at the C7 level, three sections were chosen from C7 at random from each rat by an evaluator who was blinded to the rat identifications and tissue samples. The cross-sectional area and CGRP labeling intensity of all neurons were quantified. All neurons in the C7 DRG were classified as either CGRP-positive or CGRP-negative. Both the ratio of CGRP-positive neurons to all neurons in each section and the average cross-sectional area of all CGRP-positive neurons in each section were determined. Separate comparisons of the ratio and the average cross-sectional area of CGRP-positive neurons were made between two populations of neurons in the C7 DRG: (1) joint afferents (those identified as CTb-positive neurons) and (2) all other neurons. Comparisons were tested using a two-way ANOVA with Tukey's HSD and group (distraction, sham, normal) and neuron population (CTb-positive neurons, all other neurons) as factors.

## 4.4. Results

### 4.4.1. Behavioral Response Following Injury

All rats undergoing a facet joint injury received the same magnitude of distraction, and no macroscopic injuries to the facet joint capsular ligament were observed during any of the applied distractions. The average applied distraction was

0.47±0.05mm. A summary of the vertebral distractions for each rat included in this study can be found in Appendix B.

There were no differences in the baseline withdrawal threshold between the distraction and sham groups. Behavioral sensitivity was induced in all rats undergoing a joint distraction (Figure 4.1). The withdrawal threshold was significantly reduced ($p \leq 0.001$) from baseline responses in the distraction group at all time points after injury, but sham procedures did not change responses from baseline at any time point (Figure 4.1). The withdrawal threshold was significantly reduced ($p \leq 0.0002$) after distraction compared to sham at all time points (Figure 4.1). The detailed mechanical withdrawal threshold data for all individual rats are summarized in Appendix C.

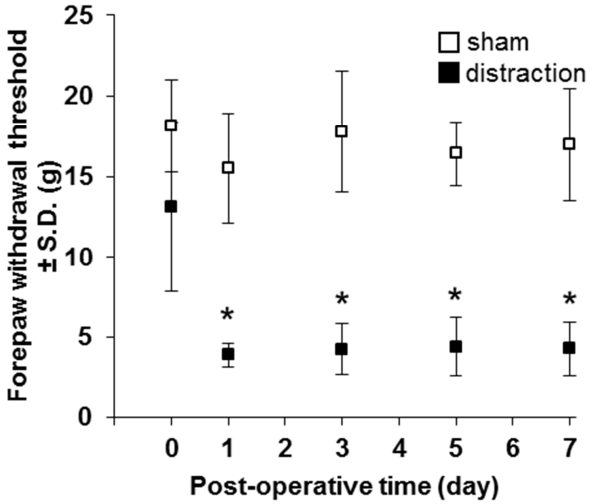


**Figure 4.1.** Mechanical hyperalgesia in the forepaw as measured by the average±S.D. withdrawal threshold (g) elicited by von Frey filament stimulation. Forepaw hyperalgesia is induced after facet joint injury compared to baseline ($p \leq 0.001$) on all days, but sham responses are unchanged from baseline. The withdrawal threshold in the distraction group is significantly reduced (*$p \leq 0.0002$) compared to sham at each post-operative time point.

### 4.4.2. CGRP Expression in Joint Afferents After Injury

Neurons positive for CTb labeling were detected in all of the DRG levels that were assayed (Figures 4.2 & 4.3, Table 4.1). Significantly more ($p \leq 0.0001$) CTb-positive neurons were identified in the C7 DRG than any other DRG (Table 4.1). The C8 DRG contained significantly more ($p \leq 0.0202$) CTb-positive neurons than either of the C6 or C5 DRGs. Although the C6 DRG contained more CTb-positive neurons than the C5 DRG (Table 4.1), that difference was not significant. Although these trends were observed within each of the distraction, sham, and normal groups, statistical significance was only achieved when considering all groups together. A summary of the CTb-positive neuron counts for each rat at each spinal level is included in Appendix H.

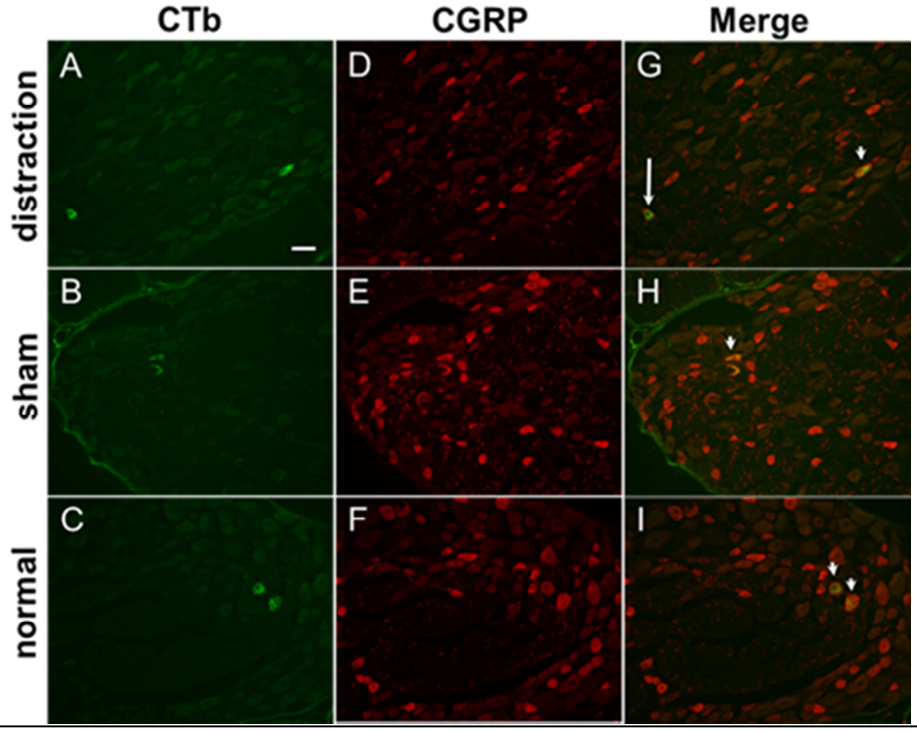


**Figure 4.2.** CTb and CGRP labeled neurons in the C7 DRG from the distraction **(A,D,G)**, sham **(B,E,H)**, and normal **(C,F,I)** groups. **(A-C)** CTb-labeled neurons are detected in all groups. **(D-F)** CGRP-labeling identifies peptidergic neurons. CTb co-localized with neurons that both express CGRP (arrowheads) and that do not express CGRP (arrow) **(G-I)**. Scale bar in **(A)** is 50µm and applies to all panels.

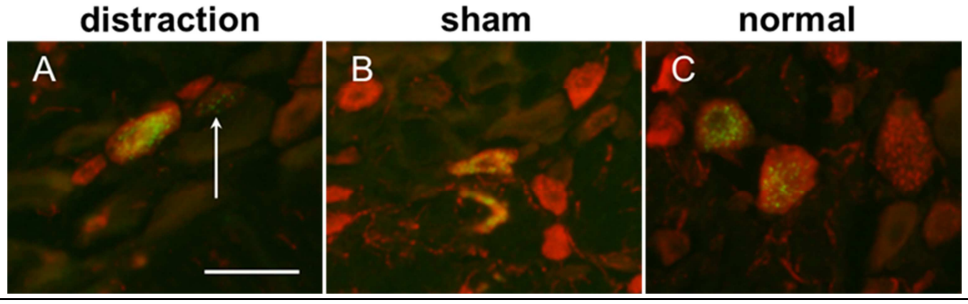


**Figure 4.3.** Magnified view of merged CTb (green) and CGRP (red) labeled neurons from the C7 DRG from distraction, sham, and normal rats showing punctate fluorescence of CTb within the cell body. In panel **(A)**, the arrow indicates a CTb-labeled neuron that is not positive for CGRP labeling. Scale bar in **(A)** is 50µm.

**Table 4.1.** Ratio and average percentages of CGRP-positive neurons that are also CTb-positive compared to the number of CTb-positive neurons.

| | **Ratio of peptidergic CTb-positive neurons*** | | | | |
|---|---|---|---|---|---|
| | **C5** | **C6** | **C7** | **C8** | **total** |
| **distraction (n=4 rats)** | 2/3 | 6/11 | 35/64 | 19/31 | 62/109 |
| **sham (n=5 rats)** | 1/4 | 16/21 | 38/61 | 30/41 | 85/127 |
| **normal (n=4 rats)** | 2/6 | 15/27 | 37/83 | 33/45 | 87/161 |
| **total (n=13 rats)** | 5/13 | 37/59 | 110/208 | 82/117 | 234/397 |
| | **Average % of peptidergic CTb-positive neurons*** | | | | |
| | **C5** | **C6** | **C7** | **C8** | **total** |
| **distraction (n=4 rats)** | 66.7±57.7 % | 45.0±33.2% | 56.2±18.4% | 61.1±13.0% | 56.4±9.4% |
| **sham (n=5 rats)** | 25.0±35.4 % | 78.4±25.5% | 59.8±14.7% | 69.4±43.3% | 66.9±18.3% |
| **normal (n=4 rats)** | 41.7±52.0 % | 47.8±32.6% | 45.9±12.6% | 75.1±19.8% | 53.1±13.7% |
| **total (n=13 rats)** | 46.9±47.1 % | 57.1±31.9% | 54.4±15.3%‡ | 68.6±28.3% | 59.4±14.8% |

***Note:** The denominator is the total number of CTb-positive neurons from all rats in each group for each DRG level; the numerator is the corresponding total number of neurons from all rats in each group that are positive for both CTb and CGRP. The percent values represent the average percent of CTb-positive neurons that are also CGRP-positive for each group and DRG level.

‡ p=0.0084 compared to the percentage of all neurons that are CGRP-positive at C7.

Further, there were no differences in the number of CTb-positive neurons between groups at any of the cervical levels evaluated (Table 4.1). There were no significant differences detected in the ratio of CTb-positive neurons that were positive for CGRP to the total number of CTb-positive neurons between any groups at any level (Table 4.1). Similarly, there were no differences in the average cross-sectional area of the neurons positive for both CTb and CGRP between any groups at any level (Table 4.2).

**Table 4.2.** Average cross-sectional area of neurons positive for both CTb and CGRP.

| | **Cross-Sectional Area ($\mu m^2$ ± S.D.)** | | | |
|---|---|---|---|---|
| | **C5** | **C6** | **C7** | **C8** |
| **distraction** | 660±353 | 840±264 | 757±142 | 825±71 |
| **sham** | 741‡ | 732±220 | 688±173 | 802±189 |
| **normal** | 599±206 | 864±139 | 738±79 | 754±134 |
| **total** | 652±212 | 804±200 | 724±133* | 794±130 |

‡ Only one neuron found.
*p=0.0005 compared to all CGRP-positive neurons in the C7 DRG.

### 4.4.3. CGRP Expression in Joint Afferents Compared to All Other Afferents

In the C7 DRG, 41.5±5.4% of all of the neurons were CGRP-positive. However, 54.4±15.3% of CTb-positive neurons at that level expressed CGRP (Table 4.1), and this difference in the ratios of CGRP-positive neurons between these two populations of neurons was significant (p=0.0084). This trend was also observed in each of the groups but was not significant for any of the groups. Interestingly, the average cross-sectional area of neurons positive for both CTb and CGRP at the C7 level ($724\pm133 \mu m^2$) was significantly smaller (p=0.0005) than the average area of all the CGRP-positive neurons in the C7 DRG ($892\pm116 \mu m^2$) (Table 4.2). Although this relationship was consistent for all of the experimental groups, the differences within each group were not significant.

Data summarizing the ratio of CGRP-positive neurons among all afferents as well as specifically among joint afferents are included in Appendix H.

## 4.5. Discussion

These data characterize a multi-segmental innervation of the C6/C7 facet joint in the rat and demonstrate that the joint innervation is unchanged at day 7 after painful mechanical joint loading (Tables 4.1 & 4.2). The applied distraction of 0.47±0.05mm in the current study is in close agreement with a previously identified distraction magnitude (0.49±0.09mm) that was found to be sufficient to induce sustained behavioral sensitivity, while a lower magnitude of distraction (0.19±0.03mm) does not induce even transient mechanical sensitivity (Dong et al., 2011). In that context, it is not likely that the joint distractions used in this study (~ 0.5mm) are induced by the normal head movements in the rat, though the physiological range of C6/C7 facet joint distraction during normal movement has not been defined explicitly. Of the spinal levels analyzed, the greatest number of neurons with projections to the C6/C7 joint had cell bodies in the C7 DRG, followed by the C8, C6, and C5 DRGs (Table 4.1). This trend in the segmental joint innervation is maintained despite an injury-induced increase in sensitivity to mechanical stimulation of the forepaw (Figure 4.1; Table 4.1). Although painful injury does not alter the percentage of joint afferents expressing CGRP in the C7 DRG, greater than one-half of the joint afferents are peptidergic (Table 4.1), but only slightly more than 40% of all neurons in the C7 DRG are peptidergic. Further, the average cell body is smaller for the peptidergic joint afferents (724±133$\mu m^2$) than for all of the peptidergic neurons (892±116$\mu m^2$) in the C7 DRG (Table 4.2). Although a previous study defined the C5/C6

facet innervation with or without a complete disruption of its capsule (Ohtori et al., 2003), that study did not quantify pain. This study is the first to characterize the innervation of the C6/C7 facet joint in the context of injury-induced pain, and by doing so suggests that future studies to identify the cellular responses to painful injury to this joint should be directed at assessments of the C7 spinal level.

The distribution pattern of neurons innervating the C6/C7 facet joint identified here is consistent with studies characterizing innervation of other cervical facet joints in that joint afferents originate from multiple spinal levels with one level (C7 in this case) having a dominant number of neurons (Ohtori et al., 2001; Ohtori et al., 2003). Indeed, multi-segmental innervation of facet joints is also evident in humans in which the lower cervical facets receive fibers from the medial branches of the dorsal rami above and below the joint (Barnsley and Bogduk, 1993). The finding that the most C6/C7 joint afferents originate in the C7 and C8 DRGs (Table 4.1) supports the observation of forepaw hypersensitivity (Figure 4.1) since the C7 and C8 dermatomes in the rat extend from the neck to the forepaw (Takahashi and Nakajima, 1996). Further, neurons innervating lumbar facet joints have been identified with dichotomizing axons projecting to peripheral targets (Sameda et al., 2001; Umimura et al., 2012), suggesting that some neurons innervating the C6/C7 facet joint may also possess dichotomizing axons extending into the forelimb and contributing to referred pain. Studies using multiple retrograde tracers are necessary to determine the incidence of dichotomizing axons projecting to the C6/C7 facet joint and forepaw. Nevertheless, these data indicate that the C7 spinal level is likely a major contributor to C6/C7 facet joint-mediated pain.

Both the ratio of CGRP-positive joint afferents and their phenotype are unchanged by injury (Figure 4.2; Tables 4.1 & 4.2). This finding is surprising since several studies have identified a shift in the phenotypic expression of pain-associated proteins like CGRP and brain-derived neurotrophic factor towards larger-diameter afferents in response to facet inflammation or traumatic injury (Ohtori et al., 2002; Ohtori et al., 2003). Despite the lack of change in the phenotype of joint afferents, injury-induced behavioral sensitivity may still result from afferent sensitization. Joint inflammation sensitizes afferents innervating the inflamed joint such that the threshold to activation is decreased and normally innocuous stimuli can be perceived as painful (Guilbaud et al., 1985; Schaible and Grubb, 1993; Schaible et al., 2009). Moreover, neuropeptides such as CGRP contribute to joint inflammation-induced pain and spinal neuronal sensitization (Schaible et al., 2009), demonstrating a role for neuropeptides in inflammatory joint pain. While it is unlikely that the discs and other spinal ligaments contribute to pain in this model, previous work with this same injury model demonstrated that intra-articular injection of an NSAID abolishes facet joint injury-induced pain (Dong et al., 2011). Joint inflammation is associated with hyperexcitability of the afferents innervating the joint and pain (Guilbaud et al., 1985; Tachihara et al., 2007), and inflammation contributes to facet joint loading-induced pain (Dong et al., 2011). Combining those observations with the findings of the current study that greater than 50% of joint afferents express CGRP supports a contribution of joint afferents to pain after facet joint distraction. Yet, the subpopulations of joint afferents contributing to injury-induced pain still remain unknown. CGRP- and substance P-containing fibers have been identified in human cervical facet capsular ligaments (Kallakuri et al., 2004;

Kallakuri et al., 2012), supporting the assertion that peptidergic afferents likely mediate pain in this joint. In the C7 DRG in the rat, CGRP-positive neurons account for a greater percentage of neurons innervating the C6/C7 joint than they do among all neurons in the C7 DRG (Table 4.1). Taken together, these data indicate that peptidergic joint afferents may make a greater contribution to facet joint pain than other neuronal subpopulations. Studies specifically investigating the roles of these and other populations of joint afferents in joint injury would determine their relative contributions to facet-mediated pain, helping to identify specific mechanisms contributing to joint pain as potential targets for its treatment.

Although these data provide insight into the innervation of the C6/C7 facet joint in the rat from C5 to C8, additional spinal levels also may contain joint afferents. In fact, Ohtori found that the C5/C6 facet joint in the rat contains fibers originating in the DRGs from C3-T3, although the vast majority originates in the cervical DRGs (Ohtori et al., 2003). Nevertheless, the C6/C7 facet joint is likely innervated by additional neurons with cell bodies in the upper thoracic DRGs. Only the right DRGs were analyzed in this study, despite the application of a bilateral joint distraction; there is not expected to be differences based on sides since this injury is symmetric (Lee et al., 2004). Of note, CTb may not label all joint afferents because not all sensory neurons express the ganglioside GM1, to which CTb binds. Since the majority of sensory neurons (85% of small, 45% of medium, and 60% of large diameter neurons) do express GM1 (Gong et al., 2002), the joint afferent count data (Table 4.1) likely represent the majority of neurons innervating the C6/C7 facet joint. However, it is possible that some neurons, especially among the larger myelinated neurons, may not be labeled by CTb because GM1 is not universally

expressed. The use of additional and distinct retrograde neuronal tracing agents would provide a more robust characterization of the full extent of the facet joint's innervation. However, because nociceptors have primarily small or medium diameter cell bodies (Merighi et al., 2008) and GM1 is expressed on 85% and 45% of these afferents, respectively (Gong et al., 2002), the majority of the nociceptive afferents are likely captured using the current technique. Further, although no visible leakage of the CTb solution from the facet joint was observed immediately after injection, a small amount may have leaked from the joint into the surrounding soft tissues. Nonetheless, any such leakage likely had only a minimal impact on the neuronal counts since the number of labeled neurons innervating the facet joint in our study is consistent with those reported in a study without joint injury in which cyanoacrylate was applied as a joint sealant (Ohtori et al., 2003).

This study identified no differences in the ratio or cross-sectional area of CGRP-positive joint afferents after injury; however, other peptides such as substance P may be differentially upregulated in these neurons. Previous work using this model identified increased substance P and the prostaglandin E2 receptor, EP2, in the DRG after painful joint injury (Lee and Winkelstein, 2009; Kras et al., 2013a), supporting that additional targets may be upregulated by afferents after injury. The lack of change in the ratio and cross-sectional area of CGRP-positive joint afferents observed in this study after injury (Tables 4.1 & 4.2) may be due to the small sample sizes. Indeed, a previous study by Ohtori required nearly twice as many rats in each group to identify changes in the ratio and size of joint afferents expressing CGRP after a joint capsule transection compared to controls (Ohtori et al., 2003). Additional studies including larger group sizes are

necessary to verify our pilot studies finding that the ratio and cross-sectional area of the peptidergic joint afferents are unchanged by painful facet joint distraction. Despite these known injury-induced changes in the DRG, the specific roles of joint afferents in the generation and maintenance of facet-mediated pain are unknown.

## 4.6. Conclusions & Integration

By characterizing the segmental innervation of the C6/C7 facet joint and identifying a greater prevalence of neuropeptide expression among joint afferents compared to all other neurons in the DRG, this study has identified the C7 spinal level as most likely contributing to facet joint pain and provides direction for future studies investigating the cellular mechanisms underlying joint injury-induced pain. Because this study identified that more C6/C7 facet joint afferents originate from the C7 spinal level than any other level, studies in later chapters investigate cellular responses to injury at that level. In addition to CGRP and/or substance P, peptidergic afferents express the trkA receptor and are thus responsive to nerve growth factor (NGF) in the innervated tissue (Merighi et al., 2004; Pezet and McMahon, 2006). The abundance of peptidergic fibers innervating the C6/C7 facet joint (Figure 4.2; Table 4.1) suggests that the peptidergic afferents, and consequently NGF signaling, may make an important contribution to the development of joint pain. In fact, elevated levels of NGF are a common component of tissue inflammation (Amaya et al., 2004; Ma and Woolf, 1997; McMahon, 1996; Merighi et al., 2004), and Dong has recently shown joint inflammation is necessary for the maintenance of loading-induced facet joint pain (Dong et al., 2011), further supporting a potential role for NGF in facet pain.

Exposure to NGF has wide-ranging effects including: upregulation and increased release of neuropeptides and brain-derived neurotrophic factor (BDNF) (Merighi et al., 2004; Pezet and McMahon, 2006), hyperexcitability of spinal neurons (Hoheisel et al., 2007), and both mechanical and thermal behavioral sensitivity (Amaya et al., 2004; Malik-Hall et al., 2005). Nearly all of the aforementioned effects of NGF exposure have been documented in the rat following painful facet joint distraction (Dong et al., 2010; Kras et al., 2013c; Lee and Winkelstein, 2009; Quinn et al., 2010), including both mechanical (Figure 4.1) and thermal hypersensitivity (Figure 3.6). The previous findings of behavioral hypersensitivity in association with joint inflammation (Dong et al., 2013a) and spinal neuronal hyperexcitability (Crosby et al., 2013; Quinn et al., 2010) strongly implicate NGF as a key contributor to facet-mediated pain. In fact, elevated levels of NGF have been reported in painful arthritic joints in humans (Aloe et al., 1992; Barthel et al., 2009; Raychaudhuri et al., 2011; Saito et al., 2000), and recent studies found that intravenous anti-NGF treatment alleviates pain from osteoarthritis and low back pain (Brown et al., 2012; Katz et al., 2011; Lane et al., 2010), suggesting NGF has a role in joint pain. Therefore, in order to begin to define the mechanisms by which initial joint injury leads to persistent pain, studies in Chapter 5 will identify the role of intra-articular NGF in facet joint loading-induced pain, as well as the role of the peptidergic and non-peptidergic afferents in mediating the onset of mechanical and thermal hyperalgesia due to NGF injection in the facet. Further, increased expression of BDNF in primary afferents and second order sensory neurons occurs downstream of NGF signaling (Merighi et al., 2004; Pezet and McMahon, 2006). Because BDNF has been linked to inflammatory and neuropathic pain as well as hyperexcitability of spinal neurons (Grimsholm et al., 2008;

Lu et al., 2009; Mannion et al., 1999; Ohtori et al., 2002), Chapter 6 will characterize the expression of BDNF after painful facet joint injury and define its role in the maintenance of facet-mediated pain.

# CHAPTER 5

# Development of Injury-Induced Facet Joint Pain and Central Sensitization: Contributions of Intra-Articular Nerve Growth Factor

*Parts of this chapter are adapted from:*

Kras JV, Kartha S, Winkelstein BA (2014). Intra-Articular Nerve Growth Factor Regulates Development, But Not Maintenance, of Injury-Induced Facet Joint Pain & Spinal Neuronal Hypersensitivity. *Osteoarthritis and Cartilage*, in revision.

## 5.1. Overview

Studies in Chapters 3 and 4 demonstrate facet joint distraction as inducing both mechanical and thermal hyperalgesia (Figures 3.5 & 3.6) and identify greater than 50% of facet joint afferents as peptidergic (Table 4.1). Despite evidence from those animal studies (Chapters 3 & 4), and from clinical studies (Lord et al., 1996; Manchikanti et al., 2002; van Eerd et al., 2010) that identifies the facet joint as a source of pain after mechanical neck injury, the local initiators of pain in the C6/C7 facet joint after its injury remain poorly defined. Inflammatory cascades, such as prostaglandin $E_2$ ($PGE_2$) signaling, are evident in the joint and spinal cord following painful facet joint injury at the time when the corresponding spinal neurons at the level of the injured joint are also hyperexcitable (Crosby et al., 2013, Dong et al., 2013a, Kras et al., 2014a). Nerve growth factor (NGF) is increased in inflamed tissues and is sufficient to induce both mechanical and thermal hypersensitivity and spinal neuronal hyperexcitability (Hoheisel et al., 2007;

Lewin et al., 1994; McMahon, 1996). During development, most small diameter primary afferent neurons require NGF for survival (Merighi et al., 2008; Pezet and McMahon, 2006); however, mainly peptidergic afferents that are capable of transmitting nociceptive information continue to express the NGF receptor, trkA, and remain sensitive to NGF in the adult (Merighi et al., 2004). Because a high proportion of joint afferents are peptidergic (Table 4.1; Kras et al., 2013b), NGF may induce joint pain by sensitizing the facet joint afferents. Animal models of pain resulting from inflammation demonstrate increased NGF as contributing to the development and maintenance of pain (Amaya et al., 2004; Woolf et al., 1994). Both clinically and in pain models of inflamed or arthritic joints, elevated levels of NGF are identified in the painful joint, suggesting a possible role for intra-articular NGF in joint pain (Barthel et al., 2009; Orita et al., 2011; Surace et al., 2009). Although increases in NGF are associated with inflammation and inflammatory responses contribute to facet joint loading-induced pain (Dong et al., 2013a; Kras et al., 2014a; McMahon, 1996; Woolf et al., 1994), it is not known if intra-articular NGF induces and/or maintains pain. NGF is a target for ongoing development of clinical treatments in several other musculoskeletal pain modalities, such as low back and knee pain (Brown et al., 2012; Katz et al., 2011). As such, defining whether or not NGF has a similar role in injury-induced facet pain will help identify if NGF signaling is a common mechanism across a range of musculoskeletal pain modalities. In addition, similarities in the mechanisms of arthritis- and injury-induced joint pain could indicate that mechanical joint injury initiates a degenerative process similar to osteoarthritis. A role for NGF in facet pain would support expanding current anti-NGF pain therapies being developed to include facet-mediated pain and local anti-NGF delivery in the joint as a new treatment.

Studies presented in this chapter summarize experiments under Aim 2, and test the hypothesis that NGF increases in the facet joint after a painful joint distraction and is both necessary and sufficient for the initiation of both behavioral and spinal neuronal hypersensitivity after injury. As such, NGF expression is quantified within the facet joint as well as in the dorsal root ganglion (DRG) to determine if joint injury modulates local NGF levels. Further, behavioral responses are evaluated after intra-articular application of NGF (Aim 2a) to assess whether or not intra-articular NGF is sufficient to induce pain. In addition to behavioral outcomes, neuronal excitability is quantified in the spinal cord after application of NGF to the facet joint to determine if intra-articular NGF is sufficient to induce central sensitization, which is a state of increased neuronal excitability and synaptic efficacy that contributes to chronic pain (Latremoliere and Woolf, 2009). Based on those findings, targeted ablation of joint afferents involved in either peptidergic or non-peptidergic signaling is performed in separate groups of rats prior to NGF application to identify those neurons that contribute to NGF-mediated joint pain (Aim 2b). The role of intra-articular NGF in the development of facet joint distraction-induced pain and spinal hyperexcitability is evaluated using an anti-NGF antibody to locally block NGF signaling in the joint (Aim 2c). Additional studies in Aim 2c also apply the anti-NGF antibody to the facet joint after the initiation of loading-induced pain to determine if intra-articular NGF also maintains pain after joint injury.

## 5.2. Relevant Background

Musculoskeletal pain, especially joint and neck/back pain, is the most common type of chronic pain (Johannes et al., 2010; Pizzo et al., 2011). Among the fibers that

innervate articular joints, the Aδ- and C-fibers exhibit increased mechanosensitivity during joint inflammation and can be activated by normal joint motions (Guilbaud et al., 1985; Schaible et al., 2009). Joint inflammation has been shown to sensitize neurons in the spinal cord and to expand receptive fields to include adjacent non-inflamed tissues in rat models (Martindale et al., 2007; Schaible et al., 2009; Woolf and Wall, 1986), supporting a role for central sensitization in joint pain.

The facet joint is the most common source of pain in chronic neck pain patients (Manchikanti et al., 2002). Non-physiological loading of the facet joint activates nociceptors in its capsule (Lu et al., 2005) and induces hyperexcitability of spinal neurons and pain (Crosby et al., 2013; Dong et al., 2013b; Lee et al., 2008; Quinn et al., 2010). Moreover, intra-articular non-steroidal anti-inflammatory drug treatment alleviates pain after mechanical facet injury (Dong et al., 2013a), suggesting inflammatory contributions to loading-induced facet pain. Because arthritis-induced joint pain and injury-induced facet joint pain exhibit similar inflammatory and neuronal responses (Boettger et al., 2008; Dong et al., 2013a; Martindale et al., 2007; Quinn et al., 2010), common mechanisms may contribute to both types of joint pain. Yet, the local molecular mechanisms that lead to the onset of facet pain are not defined.

Nerve growth factor sensitizes adult sensory neurons, and is increased in inflamed tissues (McMahon, 1996). Injection of NGF into peripheral tissues in animals (Lewin et al., 1994) and humans (Dyck et al., 1997) induces mechanical and thermal sensitivity. Treatment with anti-NGF antibodies alleviates pain from inflammation and injury in rat models (Wild et al., 2007; Woolf et al., 1994), and systemic anti-NGF reduces osteoarthritic joint pain (Brown et al., 2012), further supporting a role for NGF in joint

pain. NGF and its high-affinity receptor, trkA, have been identified in arthritic joints (Barthel et al., 2009) and degenerative facets (Surace et al., 2009). Although these studies suggest that intra-articular NGF may contribute to degenerative joint pain, its contribution, if any, to *injury*-induced facet pain is unknown.

Studies tested the hypothesis that intra-articular NGF contributes to the development of spinal neuronal hyperexcitability and behavioral hypersensitivity after facet joint injury using a validated rat model (Crosby et al., 2013). After painful injury, NGF expression was evaluated in the facet joint and in the DRG because NGF is transported to the cell bodies of mainly peptidergic primary afferents (Pezet and McMahon, 2006). Based on those findings, intra-articular NGF was administered to determine if it induces pain and spinal hyperexcitability. Targeted ablation of peptidergic or non-peptidergic joint afferents prior to intra-articular NGF application was utilized to identify which population of afferents regulates NGF-induced joint pain. An anti-NGF antibody was injected into the intra-articular space after an otherwise painful facet joint injury to determine if intra-articular NGF contributes to initiation of injury-induced spinal hyperexcitability and facet pain. In addition, the same anti-NGF antibody was injected into the joint one day after a painful facet joint injury, when behavioral hypersensitivity is evident, in order to assess whether or not joint pain is *maintained* by intra-articular NGF.

## 5.3. Methods

### 5.3.1. Facet Joint Distraction & Mechanical Behavioral Assessment

Male Holtzman rats (Harlan Sprague-Dawley, Indianapolis, IN) weighing 392±31g were housed under USDA- and AAALAC-compliant conditions with free

access to food and water. All experimental procedures were approved by the University of Pennsylvania IACUC and carried out under the guidelines of the Committee for Research and Ethical Issues of the IASP (Zimmermann, 1983). Three complementary studies were performed to: (1) first characterize NGF expression after painful facet joint injury, (2) identify whether or not intra-articular NGF is sufficient to induce pain and spinal neuronal hyperexcitability, and (3) define the contribution of intra-articular NGF to injury-induced facet pain and central sensitization.

All surgical procedures were performed under inhalation isoflurane anesthesia (4% induction; 2.5% maintenance). A detailed procedure for the painful facet joint distraction (FJD) in the rat has been reported previously (Dong et al., 2008; Kras et al., 2014a). Briefly, an incision was made along the midline of the back of the neck, and the C5-T1 laminae and facet joints were exposed and cleared of inserting muscles. The interspinous ligaments from C5-T1 were resected, and a loading device attached to the C6 and C7 laminae via microforceps applied a distraction across the bilateral C6/C7 facet joints by displacing the C6 vertebra rostrally and holding C7 fixed. The displacements of markers attached to the C6 and C7 laminae were recorded during the joint distraction by a camera mounted to the surgical dissecting scope and used to quantify the applied joint loading, as described previously (Kras et al., 2013a). The magnitude of distraction was compared between all groups of rats using an ANOVA with post hoc Tukey's HSD test. Rats (n=8) were followed for one day after distraction injury. Sham procedures including device attachment with no applied joint distraction were performed in an additional group of rats followed for one day (n=8). Wounds were closed with polyester suture and surgical staples, and rats were recovered in room air.

Forepaw mechanical withdrawal thresholds were quantified for all rats using customary methods (Dong et al., 2011; Kras et al., 2013b). Rats were individually placed in elevated cages with wire mesh floors and allowed to acclimate to the testing environment for 15 minutes. An ascending series of von Frey filaments (Stoelting; Wood Dale, IL) was applied to each forepaw, and the lower of two consecutive filaments that elicit a positive response, defined as emphatic lifting of the forepaw, was taken as the threshold for the paw being tested. Thresholds were determined for each forepaw in three testing rounds separated by at least ten minutes, and the bilateral responses were averaged to obtain the withdrawal threshold for each rat. Thresholds were quantified for three days prior to any surgical procedure to establish baseline responses as well as post-operatively until the time of tissue harvest or electrophysiological experiments. Withdrawal thresholds were compared between groups using a two-way repeated measures ANOVA with group and time as factors and a post hoc Tukey's HSD test. All statistical analyses were performed using JMP Pro v10.0.2 (SAS Institute Inc.; Cary, NC).

### 5.3.2. Facet Joint Processing & NGF Assessments

NGF expression was assessed in the facet joints of a subset of rats at day one (FJD n=3; sham n=3) using immunohistochemistry (IHC). Following behavioral assessment on day one after distraction or sham procedures, rats were given an overdose of sodium pentobarbital (65mg/kg) and transcardially perfused with phosphate buffered saline (PBS). Spinal columns from C4-T2 were harvested en bloc and post-fixed in 4% paraformaldehyde in PBS for three days. Columns were transferred to 30% sucrose in PBS for seven days and decalcified in 10% Ethylenediaminetetraacetic Acid (EDTA) in

PBS for three weeks, changing EDTA every three to four days. The C6/C7 spinal motion segment was isolated and embedded in Tissue-Tek OCT Compound (Sakura Finetek; Torrance, CA). The bilateral facet joints were sectioned (16µm) in the frontal plane, thaw-mounted onto slides, and labeled for NGF using previously published methods (Kartha et al., 2014). Endogenous peroxidase activity was quenched with 0.3% hydrogen peroxide in 0.01M PBS. Sections were incubated in DeCal Antigen Retrieval (BioGenex; Fremont, CA) solution for 30 minutes. Slides were washed, blocked with normal horse serum (Vector Laboratories; Burlingame, CA), and incubated in rabbit anti-NGF (1:250; Santa Cruz Biotechnology) primary antibody overnight at 4°C. The next day, sections were incubated with a biotinylated horse anti-rabbit secondary antibody (1:1000; Vector Laboratories) for 30 minutes and developed with 3,3-diaminobenzidine (Vector Laboratories). Sections were imaged on an Olympus BX51 microscope (Olympus; Center Valley, PA).

NGF expression was also quantified in the soft tissues of the facet joint, including the capsular ligament and synovium, from a separate group of rats at day one (FJD n=5; sham n=5) using Western blot. Following behavioral assessment on day one, rats were transcardially perfused with PBS as described above. Capsular ligament and synovial tissue was harvested from the bilateral C6/C7 facet joints, immediately frozen on dry ice, and stored at -80°C until further use. Protein was extracted from the tissue using the RIPA Lysis Buffer System (Santa Cruz Biotechnology; Santa Cruz, CA) according to the manufacturer's instructions. Proteins were prepared, separated, and transferred to an Immobilon-FL transfer membrane (Millipore; Billerica, MA) as described previously (Kras et al., 2013c). Membranes were blocked for one hour with 5% nonfat dry milk in

0.1% Tween-20 Tris-buffered saline (TBS) and incubated overnight at 4°C with a rabbit anti-NGF (1:200; Santa Cruz Biotechnology) antibody. On the following day, membranes were washed three times with 0.1% Tween-20 TBS and incubated for two hours at room temperature with a goat anti-rabbit IRDye 800CW (1:15,000; LI-COR; Lincoln, NE) secondary antibody. Membranes were imaged using the Odyssey Infrared Imaging System (LI-COR), then stripped and re-probed for β-tubulin using mouse anti-β-tubulin (1:2000; Covance; Princeton, NJ) primary and goat anti-mouse IRDye 680LT (1:15,000 with 0.02% SDS; LI-COR) secondary antibodies. Quantitative analysis of NGF and β-tubulin was performed using Image Studio Lite version 3.1 software (LI-COR). NGF expression was normalized to β-tubulin as the loading control for each sample, and NGF expression after FJD is presented relative to expression in the sham group. NGF expression in the FJD and sham groups was compared by a t-test.

### 5.3.3. Saporin Joint Injection

Because peptidergic neurons are activated by NGF, those fibers are hypothesized to have an important role in facet mediated pain. In order to identify the contribution of peptidergic signaling in joint afferents to the development of facet joint injury-induced pain, neurons expressing the NK1 receptor were ablated using a targeted substance P conjugate of the neurotoxin saporin, [$Sar^{9}$,$Met(O_2)^{11}$]-substance P-saporin (SSP-Sap) (Advanced Targeting Systems; San Diego, CA). Non-targeted saporin (Blank-Sap) served as a control (Advanced Targeting Systems). Because saporin is known to induce cell death within fourteen days (Weisshaar et al., 2014; Wiley et al., 2007), saporin was administered fourteen days prior to any joint procedures using established methods for

intra-articular injection (Dong et al., 2013a; Kras et al., 2013b). Briefly, the bilateral C6/C7 facet joints were exposed as described above. A 33-gauge beveled needle attached to a 10µL syringe (Hamilton Company; Reno, NV) was advanced into the facet joint, and 100ng of SSP-Sap in 5µL of PBS was slowly injected into the bilateral facet joints (SSP-Sap n=11). This dose of SSP-Sap was selected from the literature as sufficient to ablate spinal neurons expressing the substance P receptor when injected intrathecally (Weisshaar et al., 2014; Wiley et al., 2007). To serve as controls, 100ng of Blank-Sap was injected into the bilateral facet joints of separate rats (Blank-Sap+FJD n=7). Following joint injections, wounds were closed using polyester suture and surgical staples, and rats recovered in room air.

Fourteen days after joint injections under inhalation isoflurane anesthesia, the surgical staples and suture were removed, and rats underwent either a facet joint distraction (SSP-Sap+FJD n=7; Blank-Sap+FJD n=7) or sham (SSP-Sap+sham n=4) procedure as described above. Wounds were closed again, and rats recovered in room air. Forepaw mechanical withdrawal thresholds were determined for each rat at baseline (day 0) as well as on days one, three, five, and seven following facet joint distraction or sham procedures. Behavioral responses were compared using a two-way repeated measures ANOVA with post hoc Tukey's HSD test.

### 5.3.4. DRG Processing & NGF Immunohistochemistry

Following behavioral testing on day seven, rats were given an overdose of sodium pentobarbital and transcardially perfused with PBS followed by 4% paraformaldehyde in PBS. The bilateral C7 DRGs were harvested and post-fixed overnight in the same fixative

used for perfusion. DRGs were transferred to 30% sucrose for six days before they were embedded in OCT (Sakura Finetek; Torrance, CA). Serial axial sections (14µm) of the DRGs were thaw-mounted onto slides and incubated in DeCal Antigen Retrieval (BioGenex; Fremont, CA) solution for two hours. Slides were washed, blocked with normal goat serum, and incubated overnight with rabbit-anti-NGF antibody (1:100; Santa Cruz Biotechnology) at 4°C. The next day, sections were incubated in an Alexa488 conjugated goat-anti-rabbit secondary antibody (Life Technologies; Grand Island, NY) for two hours at room temperature, washed, and coverslipped. Sections of DRGs from naïve normal rats as well as sections with no primary antibody incubation were included as controls. Four sections from each rat were imaged on an Olympus BX51 microscope (Olympus; Center Valley, PA), and NGF labeling was quantified in each section by automated densitometry to detect the number of pixels above a detection threshold determined using the normal tissue sections (Kras et al., 2013c; Weisshaar et al., 2010). NGF expression was compared between groups using an ANOVA with a Bonferroni test.

### 5.3.5. Intra-Articular NGF Injection

In order to identify if intra-articular NGF is sufficient to induce behavioral sensitivity, rats received 3µg of rat β-NGF (R&D Systems; Minneapolis, MN) in 5µL of sterile PBS injected into the intra-articular space of the bilateral C6/C7 facet joints using the same procedure described above (NGF n=6). This dose was selected based on published reports of pain following intradermal or endoneurial injections of NGF (Amann et al., 1995; Malik-Hall et al., 2005; Obata et al., 2004). Additional rats underwent control joint injections of 5µL of sterile PBS (vehicle n=3). Mechanical

withdrawal thresholds were measured in the forepaws of all rats that underwent NGF or vehicle joint injections prior to injection to establish baseline responses, as well as at days one, three, five, and seven after injection to establish the time course of the behavioral response to the joint injections. Differences in withdrawal threshold were compared between the NGF and vehicle groups using a two-way repeated measures ANOVA with group and time as factors. Based on those behavioral time course studies of NGF or vehicle injection, additional groups of rats received the same bilateral intra-articular C6/C7 facet joint injections of either NGF (n=7) or vehicle (n=6). Rats were assessed for forepaw mechanical sensitivity at baseline and at one day post-injection and prepared for spinal electrophysiological recordings immediately following behavior testing on day one after injections.

### 5.3.6. Spinal Electrophysiological Recordings

Rats were prepared for spinal electrophysiological recordings (NGF n=7; vehicle n=6) after behavior testing on day one (Crosby et al., 2013). Rats were anesthetized with sodium pentobarbital (45mg/kg, i.p.), the mid-cervical trachea was exposed, cannulated, and ventilated (CWE Inc.; Ardmore, PA), and the rat was mounted onto a stereotaxic frame (Figure 5.1). The C6-C8 spinal cord was exposed via a bilateral laminectomy and removal of the overlying dura and bathed in 37°C mineral oil. Core temperature was maintained at 35-37°C using a feedback controlled heating plate with a rectal probe (Physitemp Instruments Inc.; Clifton, NJ). A thoracotomy was performed to minimize respiration-induced motion of the spinal cord during recordings. Anesthesia was

maintained throughout all procedures with supplementary doses of sodium pentobarbital (5-10mg/kg, i.p.) as needed.

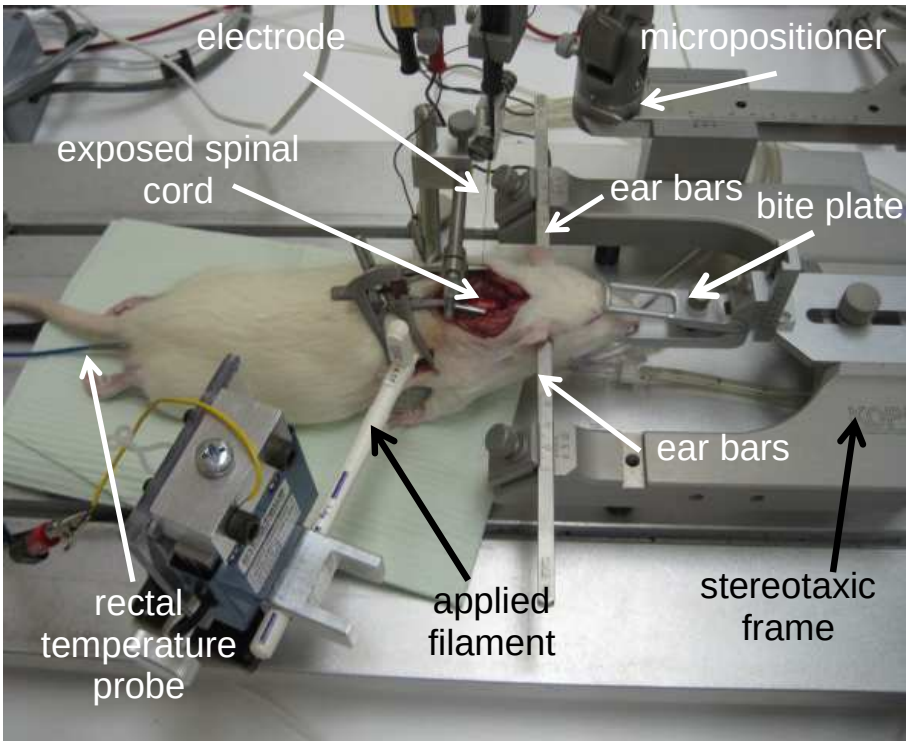


**Figure 5.1.** For electrophysiological recordings, the spinal cord was exposed from the C6-C8 levels. A tracheotomy enabled mechanical ventilation during the experiment. The rat was loaded onto a stereotaxic frame via ear bars and a bite plate. A clamp attached to the T2 spinous process held the spinal column such that the spinal cord was parallel to the ground. An electrode was lowered into the dorsal horn of the spinal cord via a micropositioner, and the stimulus train was applied to the right forepaw. Each von Frey filament was coupled to a load cell in order to synchronize stimulus application with the extracellular voltage recording.

Extracellular potentials were recorded in the C6-C7 spinal cord using tungsten electrodes lowered into the deep laminae (III-VI) of the spinal cord dorsal horn with a micropositioner. The deep laminae were selected because they include mainly wide dynamic range neurons that contribute to central sensitization (Coghill et al., 1993; Crosby et al., 2013; Dostrovsky and Craig, 2013; Quinn et al., 2010). The signal was amplified with a gain of 1,000, filtered with a passband between 300 and 3,000Hz, and

sampled at 25kHz (Dong et al., 2013b). Sensory neurons with input from the forepaw were identified by applying a light brush to the plantar surface of the forepaw using a cotton swab. A stimulus train, consisting of light brush (applied for 10 seconds), a series of non-noxious and noxious von Frey filaments (1.4g, 4g, 10g, 26g) that span the range used during mechanical withdrawal threshold testing (each applied for five stimulations of one second followed by one second of recovery), and a noxious pinch (applied for 10 seconds), was applied to the paw (Figure 5.2). Stimulus trains were applied at 30 second intervals, and the evoked spikes were recorded.

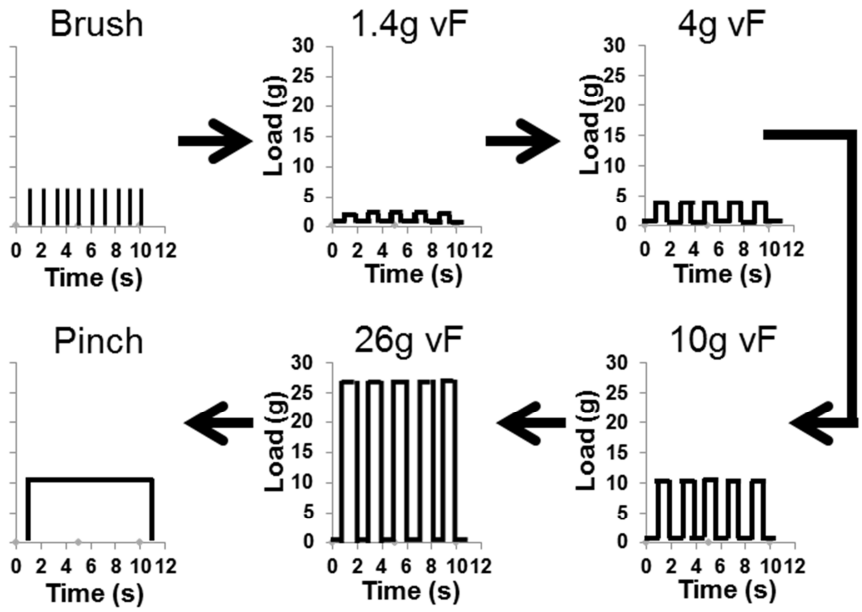


**Figure 5.2.** In the order of application, the stimulus train consisted of a light brush, followed by stimulation with the 1.4g, 4g, 10g, and 26g von Frey (vF) filaments in order of increasing strength, and a pinch applied via a 60g microvascular clip. The brush was applied ten times with a one second interval between applications. Each von Frey filament was applied for one second followed by a one second rest period for a total of five stimulations per filament. After stimulation with the 26g von Frey filament, the pinch was applied for ten seconds.

Recordings during the stimulus train were spike-sorted using Spike2 (CED; Cambridge, UK) in order to analyze individual neurons. Evoked spikes were summed

over the continuous 10-second stimulus period for both the brush and pinch stimuli. Evoked spikes during the clip stimulus were used to classify neurons as either a low threshold mechanoreceptor (LTM) or a wide dynamic range (WDR) neuron (Quinn et al., 2010). The number of spikes evoked from the initial application of a von Frey filament until one second after the $5^{th}$ application of the filament were summed for each neuron. Baseline firing was quantified by counting the number of evoked spikes one second prior to the initial application of each filament. Baseline spikes were subtracted from the total spike count for each filament. The total number of evoked spikes for each stimulus was compared between groups using a two-way nested ANOVA with group and stimulus as factors and neurons nested within rats and rats nested within group, with post hoc Tukey's HSD test. Differences in the ratio of WDR neurons were compared between groups using Pearson's chi-square test.

### 5.3.7. Saporin & NGF Injections

Additional groups of rats received intra-articular injections of the neurotoxin, saporin, separately targeted to neurons involved in peptidergic or non-peptidergic signaling in order to establish the roles of these signaling pathways in NGF-mediated joint pain. Separate groups of rats received bilateral intra-articular injections of SSP-Sap (n=28) or Blank-Sap (n=20) as described above. Fourteen days after SSP-Sap or Blank-Sap injections, rats were given an intra-articular injection of 3µg of NGF (SSP-Sap+NGF n=16; Blank-Sap+NGF n=12) or sterile PBS (SSP-Sap+veh n=12; Blank-Sap+veh n=8) as described above. Additional separate groups of rats received bilateral intra-articular injections of 5µg of saporin conjugated to isolectin B4 (IB4-Sap n=18) in 5µL of PBS to

ablate the non-peptidergic neurons. The dose of IB4-Sap was selected from a previously published report as sufficient to ablate non-peptidergic afferents (Tarpley et al., 2004). Separate rats received control injections of 5µg of unconjugated saporin (Saporin n=8) in 5µL of PBS. Fourteen days after IB4-Sap or Saporin injections, rats were given an intra-articular injection of 3µg of NGF (IB4-Sap+NGF n=12; Saporin+NGF n=8) or sterile PBS (IB4-Sap+veh n=6). In order to minimize the number of rats used, a Saporin+veh group was not included in this study since that inactive control saporin was not expected to be different from the unconjugated control group Blank-Sap+veh. Forepaw mechanical withdrawal thresholds were quantified at baseline and day one after NGF or vehicle injection for all rats and compared as described above.

### 5.3.8. Thermal Behavioral Assessment & Spinal Electrophysiological Recordings

Because NGF sensitizes neurons to both mechanical and thermal stimuli, rats were evaluated for thermal sensitivity after targeted neuronal ablation and NGF or vehicle administration (SSP-Sap+NGF n=8; SSP-Sap+veh n=8; Blank-Sap+NGF n=4; Blank-Sap+veh n=4; IB4-Sap+NGF n=8; IB4-Sap+veh n=6; Saporin+NGF n=5). Thermal hyperalgesia was evaluated in the forepaw following mechanical behavioral assessment for three days prior to NGF or vehicle joint injections and on day one using customary methods that also were detailed earlier in Chapter 3 (Nicholson et al., 2014). Rats were placed in wire mesh cages on top of a glass surface that was maintained at 30°C and were allowed to acclimate to the testing environment for 30 minutes. A commercially available device (UC San Diego; San Diego, CA) was used to focus a radiant heat stimulus onto the plantar surface of each forepaw. A timer synchronized to

the thermal stimulus measured the withdrawal latency as the time between the initial application of the heat source and when the paw was withdrawn. Paw withdrawals associated with normal ambulation of the rat were not considered. On each testing day, the withdrawal latency was measured three times for each forepaw, with a ten minute rest period between each measurement. The withdrawal latency for each rat for each day was calculated by averaging the latency from the right and left forepaws across all testing rounds. Differences in withdrawal latency between groups were tested using a two-way repeated measures ANOVA with Tukey's HSD test with group and time point as factors.

Spinal neuronal excitability was quantified in a subset of rats following behavioral testing on day one after targeted neuronal ablation and NGF or vehicle administration (SSP-Sap+NGF n=4; SSP-Sap+veh n=4; IB4-Sap+NGF n=5; IB4-Sap+veh n=4). Groups of rats received bilateral intra-articular injections of the SSP-Sap or IB4-Sap conjugates as described in Section 5.3.7. Fourteen days after the SSP-Sap or IB4-Sap injections, rats were given an intra-articular injection of 3µg of NGF or sterile PBS as described above in Section 5.3.7. In order to minimize the number of animals used and because excitability data from the NGF and vehicle groups without any saporin injections were already acquired, spinal neuronal excitability was not quantified in the non-targeted saporin groups (Blank-Sap+NGF; Blank-Sap+veh; Saporin+NGF). Following behavioral testing on day one after NGF or PBS joint injections, rats were prepared for electrophysiological recordings in the spinal cord (detailed in Section 5.3.6). Differences in neuronal excitability and the ratio of WDR neurons were compared between groups using a two-way nested ANOVA and Pearson's chi-square test, respectively, as described above in Section 5.3.6.

### 5.3.9. Facet Joint Distraction & Intra-Articular Anti-NGF Injection

In order to determine if intra-articular NGF contributes to the *development* of injury-induced joint pain, additional groups of rats underwent FJD or sham procedures as described in the first study (see Section 5.3.1 for details). Immediately following those surgical procedures and prior to wound closure, rats received bilateral intra-articular injections of either a rabbit polyclonal anti-NGF antibody or a control rabbit IgG (Millipore; Billerica, MA) in the C6/C7 facet joints, using the injection methods detailed above in Section 5.3.3. Rats undergoing joint distraction received a bilateral 10µg intra-articular injection of either a rabbit polyclonal anti-NGF antibody (FJD+anti-NGF) or a non-specific control rabbit IgG (FJD+veh) in 5µL of PBS, a dose previously used in rat models of inflammatory and neuropathic pain (Amaya et al., 2004; Obata et al., 2003). Subsets of rats undergoing sham procedures also received bilateral intra-articular injections of the anti-NGF antibody (sham+anti-NGF) or control IgG (sham+veh). Following injection, wounds were closed, and the rats were followed for either one day (FJD+veh n=5; FJD+anti-NGF n=5; sham+veh n=5) or seven days (FJD+veh n=5; FJD+anti-NGF n=6; sham+veh n=5; sham+anti-NGF n=5). Forepaw mechanical withdrawal thresholds were measured in all rats to determine baseline responses as well as post-surgically on day one or on days one, three, five, and seven, according to their designated endpoint in the study. After behavioral testing on the designated day, rats were prepared for spinal electrophysiological recordings as described in Section 5.3.6. Differences in withdrawal thresholds were compared using a two-way repeated measures ANOVA with post hoc Tukey's HSD test. Differences in neuronal excitability were compared between groups using a two-way nested ANOVA with group and stimulus as

factors and neurons nested within rats and rats nested within group, with post hoc Tukey's HSD test. Differences in the ratio of WDR neurons were compared between groups using Pearson's chi-square test.

In order to determine if intra-articular NGF also contributes to the *maintenance* of injury-induced joint pain, an additional group of rats underwent FJD procedures as described above except that no intra-articular injections were applied immediately after joint distraction. Wounds were closed with polyester suture and surgical staples, and rats were recovered in room air. Following behavioral testing on day one, rats were anesthetized with inhalation isoflurane anesthesia (4% induction; 2.5% maintenance), the surgical staples and suture were removed, and the bilateral C6/C7 facet joints were re-exposed. Those rats received a bilateral 10µg intra-articular injection of the rabbit polyclonal anti-NGF antibody (FJD+anti-NGFD1 n=8) in 5µL of PBS, and wounds were closed as described above. Forepaw mechanical withdrawal thresholds were measured at baseline as well as post-distraction on days one, three, five, and seven, at which time rats were prepared for spinal electrophysiological recordings as described above. Differences in withdrawal thresholds and neuronal excitability were compared between groups (FJD+anti-NGF, FJD+veh, FJD+anti-NGFD1) as described in the earlier methods.

## 5.4. Results

### 5.4.1. Facet Joint Distraction & Applied Joint Injury Magnitudes

All rats undergoing FJD in these studies underwent the same magnitude of joint injury. The average vertebral distraction applied to the rats that were followed for one day for either assessment of capsular ligament NGF expression or to identify the role of

intra-articular NGF in the initiation of joint pain was 0.71±0.18mm. That vertebral distraction was not different from the distraction applied to those rats (0.70±0.27mm) that were followed for seven days in order to measure NGF expression in the DRG or determine the contribution of intra-articular NGF to joint pain. There were no significant differences in the applied distraction between any of the subgroups of joint-injured rats used in the studies characterizing NGF expression after injury or administering intra-articular anti-NGF after the joint injury. As such, any outcomes from the different studies using the distraction groups can be taken as the same, with no variability due to the injury itself. The maximum vertebral and capsule distractions, as well as the associated maximum capsular ligament strains, for each rat in this study are detailed in Appendix B.

### 5.4.2. Injury-Induced Expression of NGF in the Facet Joint & DRG

Rats undergoing FJD exhibit significantly lower mechanical withdrawal thresholds on day one after facet joint distraction than their corresponding baseline responses ($p<0.001$) and also compared to the sham group at day one ($p<0.001$) (Figure 5.3A). Yet, the thresholds in the sham group are unchanged from baseline (Figure 5.3A; see Appendix C for the detailed forepaw mechanical withdrawal data for each rat included in this study. NGF labeling is evident in the C6/C7 facet joint on day one after its distraction and more dense than in the sham group at that time point (Figures 5.3B & 5.3C). Quantification of NGF expression in the bilateral C6/C7 facet capsular ligaments and synovial tissues by Western blot identifies significantly greater levels of NGF after FJD compared to sham ($p=0.031$) (Figures 5.3D & 5.3E). The quantification of NGF

expression by Western blot is summarized in Appendix F. These results demonstrate an elevation in intra-articular NGF in association with painful facet joint injury.

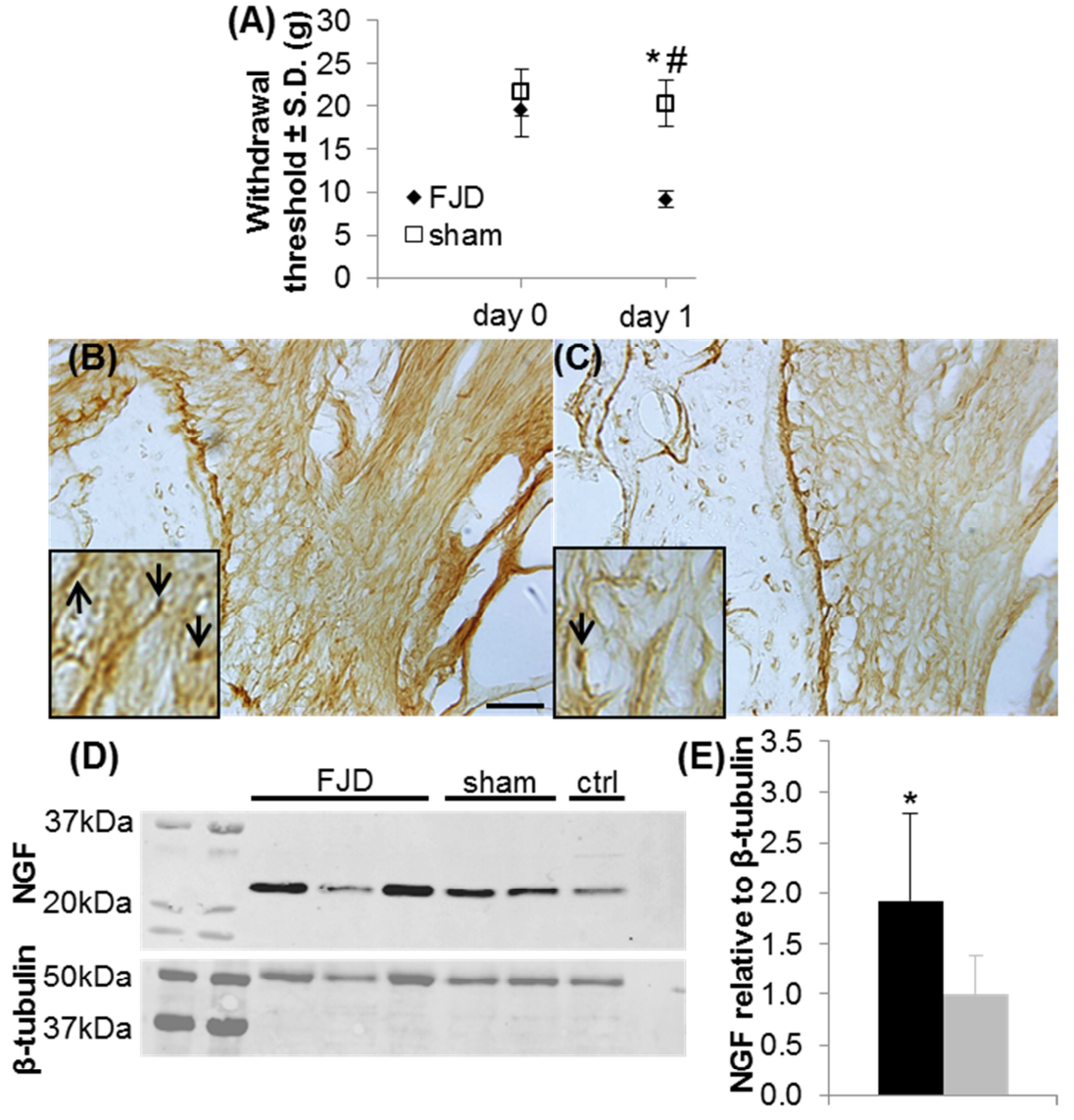


**Figure 5.3. (A)** Facet joint distraction (FJD) reduces the forepaw withdrawal threshold to mechanical stimulation at day one compared to baseline (#p<0.001) and to a sham procedure (*p<0.001). Immunolabeling for NGF is increased in the soft tissues surrounding the joint (arrows) at day one after FJD **(B)** compared to sham **(C)**. **(D)** Western blots showing NGF and β-tubulin expression in the capsular ligament and synovium. **(E)** FJD increases NGF in the capsular ligament and synovium (*p=0.031) over levels in sham at day one. Scale bar in **(B)** is 50µm and applies to **(B)** and **(C)**. The amplified inset boxes in **(B)** and **(C)** are 50µm wide.

Because NGF activates peptidergic neurons, we also evaluated if peptidergic afferents in the facet joint contribute to the development of loading-induced pain using targeted ablation of the afferents involved in peptidergic signaling. Intra-articular injection of the inactive Blank-Sap before a typically painful facet joint distraction does not alter the development of injury-induced mechanical sensitivity; the withdrawal threshold significantly decreases by day one relative to baseline and remains significantly below baseline at all post-injury points in that group ($p<0.001$) (Figure 5.4A). However, intra-articular injection of SSP-Sap to ablate neurons involved in peptidergic signaling before a distraction prevents the development of injury-induced mechanical hypersensitivity (Figure 5.4A). The withdrawal threshold of the SSP-Sap+FJD group is unchanged from baseline after distraction, a response that is also exhibited by the SSP-Sap+sham group (Figure 5.4A). Moreover, the withdrawal threshold for Blank-Sap+FJD is significantly lower than for SSP-Sap+FJD ($p<0.001$) or SSP-Sap+sham ($p<0.001$) at all post-injury days (Figure 5.4A). The individual mechanical withdrawal thresholds for each rat are summarized in Appendix C.

Immunolabeling of the C7 DRG in these groups at day seven indicates that many neurons express NGF in the C7 DRG after a FJD with no ablation of afferents (Figure 5.4B) but relatively few such NGF-labeled neurons are evident in either of the groups with the SSP-Sap injection (Figures 5.4C & 5.4D). Quantification of NGF expression with automated densitometry reveals a significant elevation of NGF expression in Blank-Sap+FJD over levels in both the SSP-Sap+FJD ($p<0.001$) and SSP-Sap+sham ($p<0.001$) groups (Figure 5.4E). A summary of the quantitative densitometry for NGF expression in the DRG for individual rats is included in Appendix E.

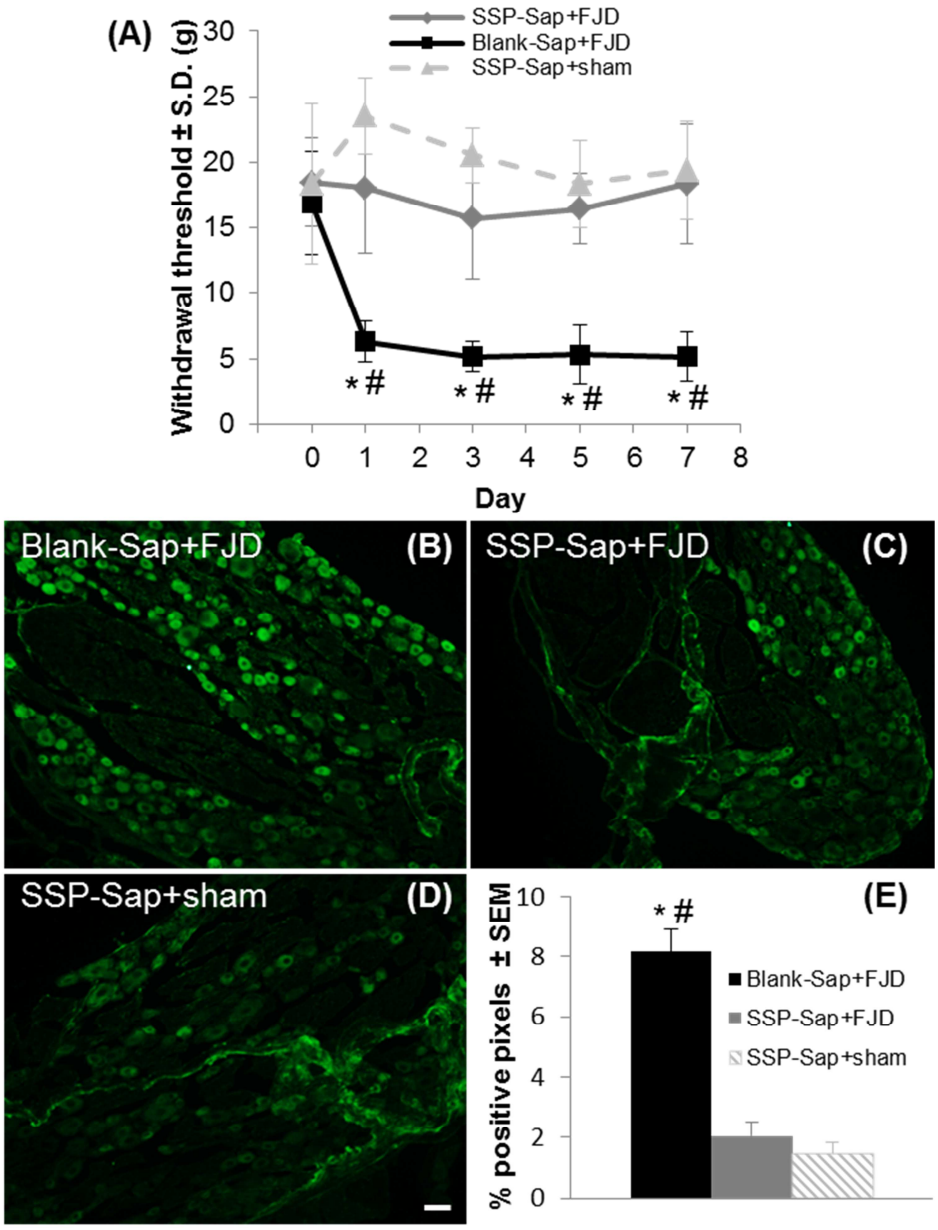


**Figure 5.4. (A)** The forepaw withdrawal threshold to von Frey filament stimulation is significantly reduced by day one and remains reduced through day seven ($p<0.001$) after intra-articular injection of Blank-Sap into the facet prior to FJD (Blank-Sap+FJD). Withdrawal thresholds for Blank-Sap+FJD are significantly lower than those for either SSP-Sap+FJD (*$p<0.001$) or SSP-Sap+sham (#$p<0.001$) at all post-surgical time points, neither of which is changed from baseline. NGF is increased at day seven in the DRG after Blank-Sap+FJD **(B)** compared to SSP-Sap+FJD **(C)** and SSP-Sap+sham **(D)**. Quantification by automated densitometry indicates these differences are significant (*$p<0.001$ vs. SSP-Sap+FJD; #$p<0.001$ vs. SSP-Sap+sham) **(E)**. Scale bar in **(D)** is 50µm and applies to all panels.

### 5.4.3. Intra-Articular NGF-Induced Pain & Neuronal Hyperexcitability

Because NGF is upregulated in the joint early after injury and along the time course of pain onset and maintenance (Figures 5.3, 5.4A, & 5.4E), we next determined if intra-articular NGF administered alone is sufficient to induce behavioral sensitivity. The withdrawal threshold at day one after intra-articular NGF injection is significantly decreased ($p<0.010$) but returns to, and remains at, baseline for all assessment times after day one (Figure 5.5A). Joint injection of vehicle does not alter the withdrawal threshold (Figure 5.5A). Because an NGF-induced reduction in withdrawal threshold is only evident on day one after injection (Figure 5.5A), additional rats were given intra-articular NGF or vehicle injections and followed for only one day to determine if intra-articular NGF also increases excitability in spinal neurons. The additional NGF injected rats used for electrophysiological assessment exhibited the same behavioral outcomes (Figures 5.5A & 5.5B), with a significant reduction in withdrawal threshold at day one compared to baseline ($p<0.001$) and to the vehicle group at day one ($p<0.001$) (Figure 5.5B). There was no change in the withdrawal threshold for the vehicle injection group (Figure 5.5B).

A total of 91 mechanosensitive spinal neurons with input from the forepaw were recorded at an average depth of 681±22μm in those rats. Representative traces during stimulation with each of the four von Frey filaments illustrate increased evoked firing in the NGF group compared to the vehicle group (Figure 5.5C). Quantification of the evoked spikes across rats and neurons demonstrates a trend towards increased firing at each von Frey filament strength in the NGF group that is significantly elevated over vehicle responses for the noxious 26g filament ($p<0.040$) (Figure 5.5D). In addition, significantly more neurons were classified as wide dynamic range (WDR) on day one

after NGF injection (93.2%) than after vehicle injection (74.5%) (p=0.016) (Figure 5.5E). Mechanical withdrawal thresholds and the spinal neuronal firing data for each rat are summarized in Appendix C and Appendix G, respectively.

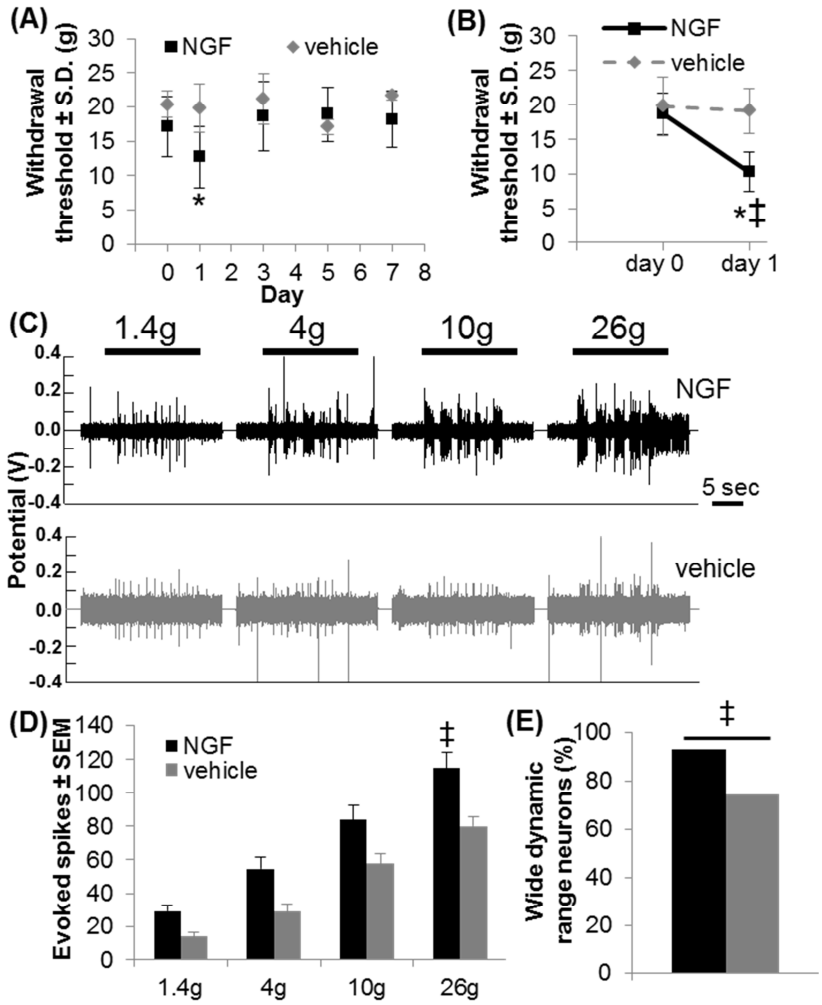


**Figure 5.5. (A)** Intra-articular application of NGF, but not the vehicle, significantly reduces the withdrawal threshold from baseline at day one (*p<0.010), but it returns to baseline by day three. **(B)** In additional rats followed for one day, intra-articular NGF reduces the withdrawal threshold at day one relative to baseline (*p<0.001) and to vehicle controls at day one (‡p<0.001). **(C)** Representative extracellular recordings in the spinal cord at day one demonstrate increased evoked neuronal firing in rats in the NGF group compared to the vehicle group. **(D)** The number of evoked spikes is significantly increased (‡p<0.040) for the noxious 26g filament after NGF injection over vehicle injection. **(E)** The number of wide dynamic range (WDR) neurons increases in the NGF group compared to the vehicle group (‡p=0.016).

Although ablating neurons in the facet joint that are involved in peptidergic signaling by administering SSP-Sap prevents the development of NGF-induced facet pain at day one, giving Blank-Sap does not alter the development of NGF-mediated pain (Figures 5.6A & 5.6B). Mechanical withdrawal thresholds for Blank-Sap+NGF are significantly reduced at day one from baseline ($p<0.001$), whereas no other groups exhibited a change from baseline (Figure 5.6A). Further, the withdrawal threshold for Blank-Sap+NGF is significantly lower at day one than any of the other groups (SSP-Sap+NGF ($p<0.001$), SSP-Sap+veh ($p<0.001$), Blank-Sap+veh ($p<0.001$)), none of which are different from each other (Figure 5.6A). When the vehicle is administered before NGF (Blank-Sap+NGF) the thermal withdrawal latency at day one is also reduced from the baseline latency ($p<0.009$) (Figure 5.6B). Similar to the mechanical response, ablation of neurons involved in peptidergic signaling prevents the development of NGF-induced thermal sensitivity (Figure 5.6B). When peptidergic signaling is intact (Blank-Sap+NGF), NGF reduces the withdrawal latency compared to both SSP-Sap+NGF ($p<0.022$) and SSP-Sap+veh ($p<0.011$). Moreover, the withdrawal latency trends towards a decrease in Blank-Sap+NGF compared to Blank-Sap+veh, but this difference does not reach significance ($p=0.098$) (Figure 5.6B). Although mechanosensitive spinal neurons with input from the forepaw were identified in both groups receiving the ablation (SSP-Sap+NGF and SSP-Sap+veh; 63 neurons; average depth of 678±21µm) (Figure 5.6C), no differences in the number of evoked spikes elicited by von Frey stimulation (Figure 5.6D) nor the proportion of WDR neurons (Figure 5.6E) were detected between groups, indicating that central sensitization driving facet injury-induced pain is driven by peptidergic input from the joint. Detailed mechanical withdrawal thresholds and thermal

withdrawal latencies for each rat are included in Appendix C; the individual spinal neuronal firing data for each rat is summarized in Appendix G.

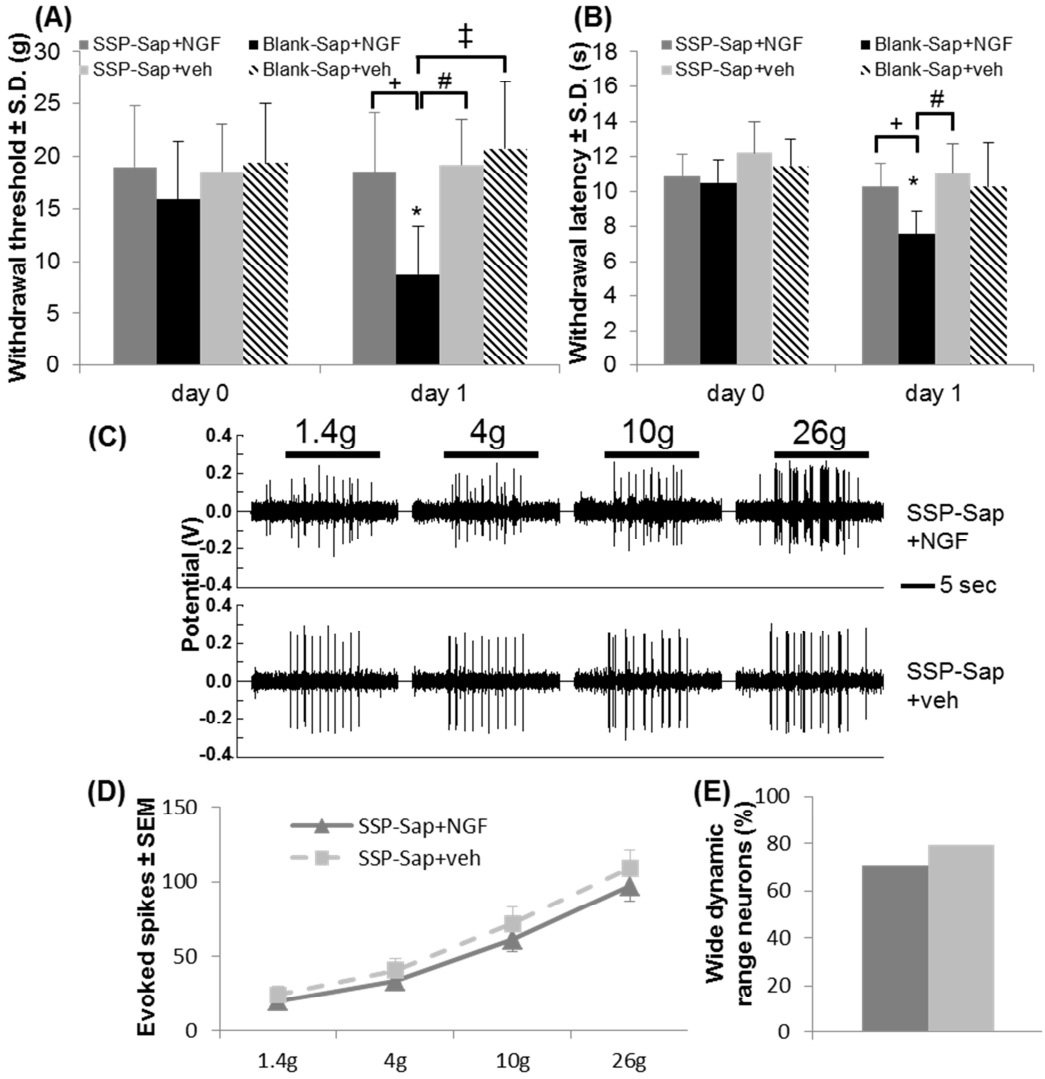


**Figure 5.6. (A)** Mechanical withdrawal threshold is reduced from baseline when intra-articular Blank-Sap, but not SSP-Sap, is given prior to NGF (Blank-Sap+NGF) (*$p<0.001$). The withdrawal threshold at day one for Blank-Sap+NGF is reduced compared to all other groups (+#‡$p<0.001$). **(B)** The thermal withdrawal latency is reduced at day one compared to baseline for Blank-Sap+NGF (*$p<0.009$) but not for any other group. Blank-Sap+NGF has a shorter withdrawal latency than either SSP-Sap+NGF (+$p<0.022$) or SSP-Sap+veh (#$p<0.011$). **(C)** Extracellular recordings in the spinal cord show similar firing between the SSP-Sap+NGF and SSP-Sap+veh groups. There is no difference in total evoked spikes for any filament **(D)** nor in the proportion of WDR neurons **(E)** between the SSP-Sap+NGF and SSP-Sap+veh groups.

In contrast to ablating the peptidergic signaling (Figure 5.6A), eliminating the non-peptidergic joint afferents does not affect the intra-articular NGF-induced sensitivity to mechanical stimuli (Figure 5.7A). In fact, mechanical withdrawal thresholds for both IB4-Sap+NGF and Saporin+NGF are reduced at day one from their respective baseline responses ($p<0.001$) and are not different from each other (Figure 5.7A). However, IB4-Sap+veh shows no change in mechanical sensitivity, and IB4-Sap+NGF and Sap+NGF both exhibit significantly lower withdrawal thresholds at day one than does IB4-Sap+veh at that time ($p<0.008$) (Figure 5.7A). Both IB4-Sap+NGF ($p<0.012$) and Saporin+NGF ($p<0.006$) exhibit shorter thermal withdrawal latencies at one day after NGF injection than at baseline; yet, the control group, IB4-Sap+veh, is unchanged from baseline (Figure 5.7B). No differences are detected between any groups at day one, despite IB4-Sap+NGF and Saporin+NGF trending lower than IB4-Sap+veh (Figure 5.7B). Mechanical and thermal hyperalgesia data for each rat in this study are summarized in Appendix C.

Representative traces of extracellular voltage spikes in neurons in the spinal cord evoked by each of the von Frey filaments demonstrate increased firing in the IB4-Sap+NGF group relative to the IB4-Sap+veh group (78 total neurons; average depth 731±20µm) (Figure 5.7C). Stimulation by the 26g von Frey filament evokes significantly more spikes in the IB4-Sap+NGF group compared to the IB4-Sap+veh group ($p<0.029$) (Figure 5.7D), but the number of WDR neurons is not different between groups (Figure 5.7E). Spinal neuronal firing data for each rat in this study is included in Appendix G.

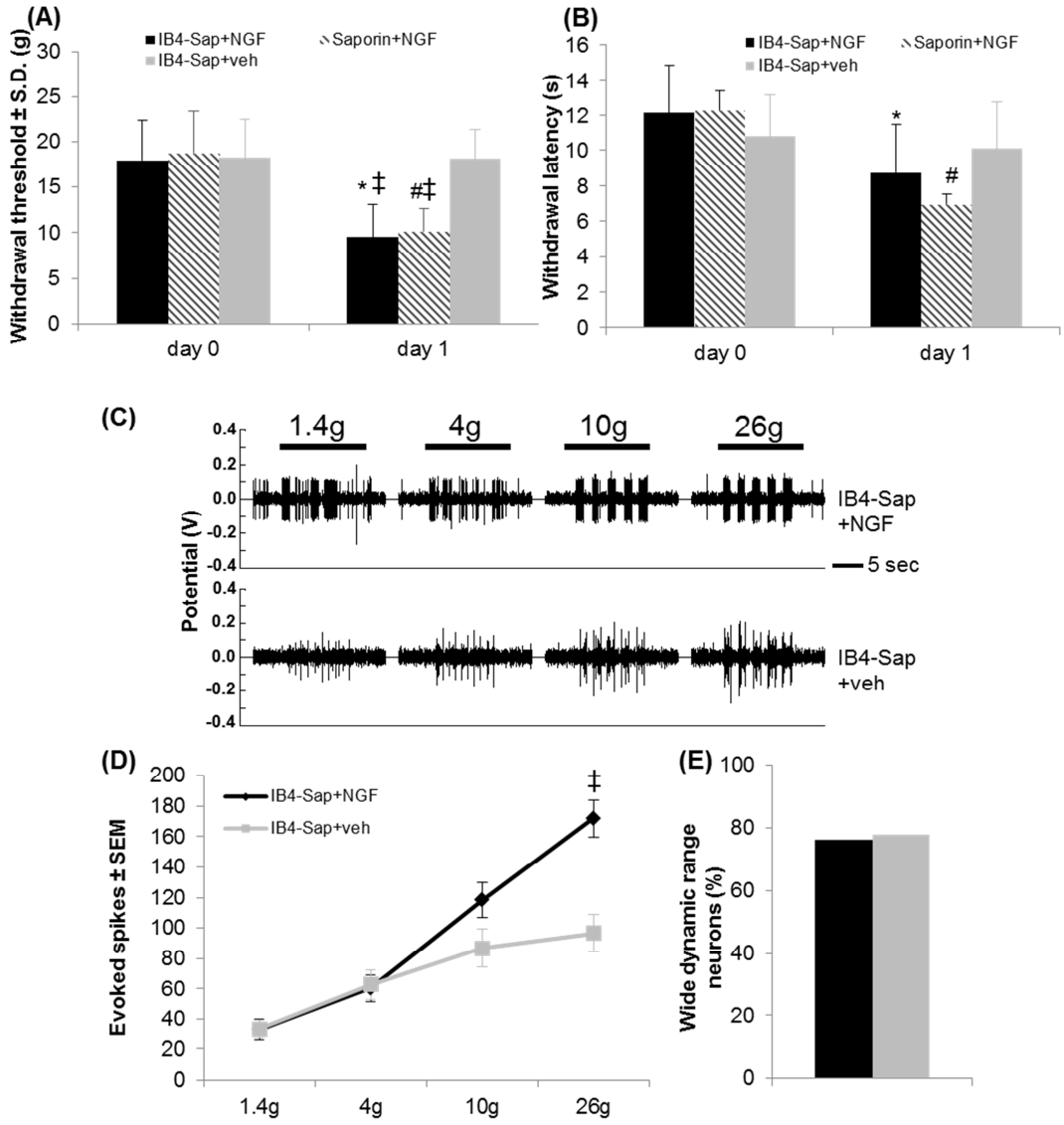


**Figure 5.7. (A)** Intra-articular NGF significantly reduces the mechanical withdrawal threshold at day one compared to baseline in rats given IB4-Sap (*p<0.001) or the unconjugated control Saporin (#p<0.001), but no change is evident in the IB4-Sap+veh control group. In addition, both IB4-Sap+NGF and Saporin+NGF exhibit significantly lower thresholds than the IB4-Sap+veh control group at day one (‡p<0.008). **(B)** Thermal withdrawal latency is reduced for both IB4-Sap+NGF (*p<0.012) and Saporin+NGF (#p<0.006) compared to baseline, but neither is different from IB4-Sap+veh at day one. Representative extracellular recordings in the spinal cord **(C)** demonstrate the increased firing that is evoked by von Frey filament stimulation for IB4-Sap+NGF compared to IB4-Sap+veh and that is significant for the 26g filament (‡<0.029) **(D)**. However, the ratio of wide dynamic range neurons is not different between groups **(E)**.

### 5.4.4. Blocking Intra-Articular NGF in Injury-Induced Facet Pain

After establishing that intra-articular NGF is sufficient to induce facet-mediated pain, we identified if intra-articular NGF contributes to the development of sustained behavioral sensitivity and spinal hyperexcitability induced by facet joint injury. By day one after facet joint distraction with a bilateral intra-articular injection of vehicle IgG (FJD+veh), the same reduction in the mechanical withdrawal threshold as is observed by injury alone (Figure 5.3) is evident, which is maintained through day seven ($p<0.001$) (Figure 5.8A). The withdrawal thresholds were unchanged from baseline after either of the sham procedures (sham+veh or sham+anti-NGF) at any time point (Figure 5.8A). However, intra-articular anti-NGF (FJD+anti-NGF) inhibits the development of mechanical sensitivity after joint injury, preventing any change in withdrawal threshold from baseline responses at any post-injury time point (Figure 5.8A). Anti-NGF treatment maintains mechanical withdrawal thresholds at a magnitude comparable to sham+veh and sham+anti-NGF (Figure 5.8A) and at a level that is significantly elevated over FJD+anti-NGF ($p<0.015$) responses (Figure 5.8A). Detailed mechanical withdrawal thresholds for each rat in this study are presented in Appendix C.

Recordings were made from 186 spinal neurons (average depth 620±13µm) at day seven after injury. Stimulation of the forepaw with either the 10g or 26g von Frey filaments evokes significantly more spikes for the FJD+veh group than for any other group (FJD+anti-NGF $p<0.001$; sham+veh $p<0.012$; sham+anti-NGF $p<0.001$) (Figure 5.8B). No differences are detected between any other groups for any of the von Frey filaments. Noxious pinch of the forepaw elicits a similar response, with more evoked spikes in the FJD+veh group than any of the other three groups ($p<0.001$) (Figure 5.8C);

no differences in evoked spikes are detected between any groups for light brushing of the paw (Figure 5.8C). Individual spinal neuronal spike counts for each rat in this study are included in Appendix G. There is a significant effect of injury group on the proportion of WDR neurons recorded in the spinal cord ($p<0.005$), with FJD+veh exhibiting the highest frequency of WDR neurons (Figure 5.8D).

The behavioral and electrophysiological studies performed at day one after injury in these same groups (Figure 5.9) mimic the results observed at day seven. The forepaw withdrawal threshold is significantly reduced in the FJD+veh group compared to the FJD+anti-NGF ($p<0.001$) and sham+veh ($p<0.001$) groups, which themselves are not different from each other, at day one (Figure 5.9A); Appendix C provides a detailed list of the withdrawal thresholds for each rat in this study. Electrophysiological recordings were made from 107 spinal neurons (average depth 729±19μm) at day one after injury or sham procedures. Similar to the findings at day seven (Figure 5.8B), stimulation of the forepaw with the 26g von Frey filament evokes significantly more spikes for the FJD+veh group at day one than for either of the other two groups (FJD+anti-NGF $p<0.006$; sham+veh $p<0.001$) (Figure 5.9B) at that time point. Although there is a trend toward an increase in the number of spikes evoked by stimulation with the 10g filament in the FJD+veh group compared to the other groups, this difference is only significant for comparison with the sham+veh group ($p<0.007$).

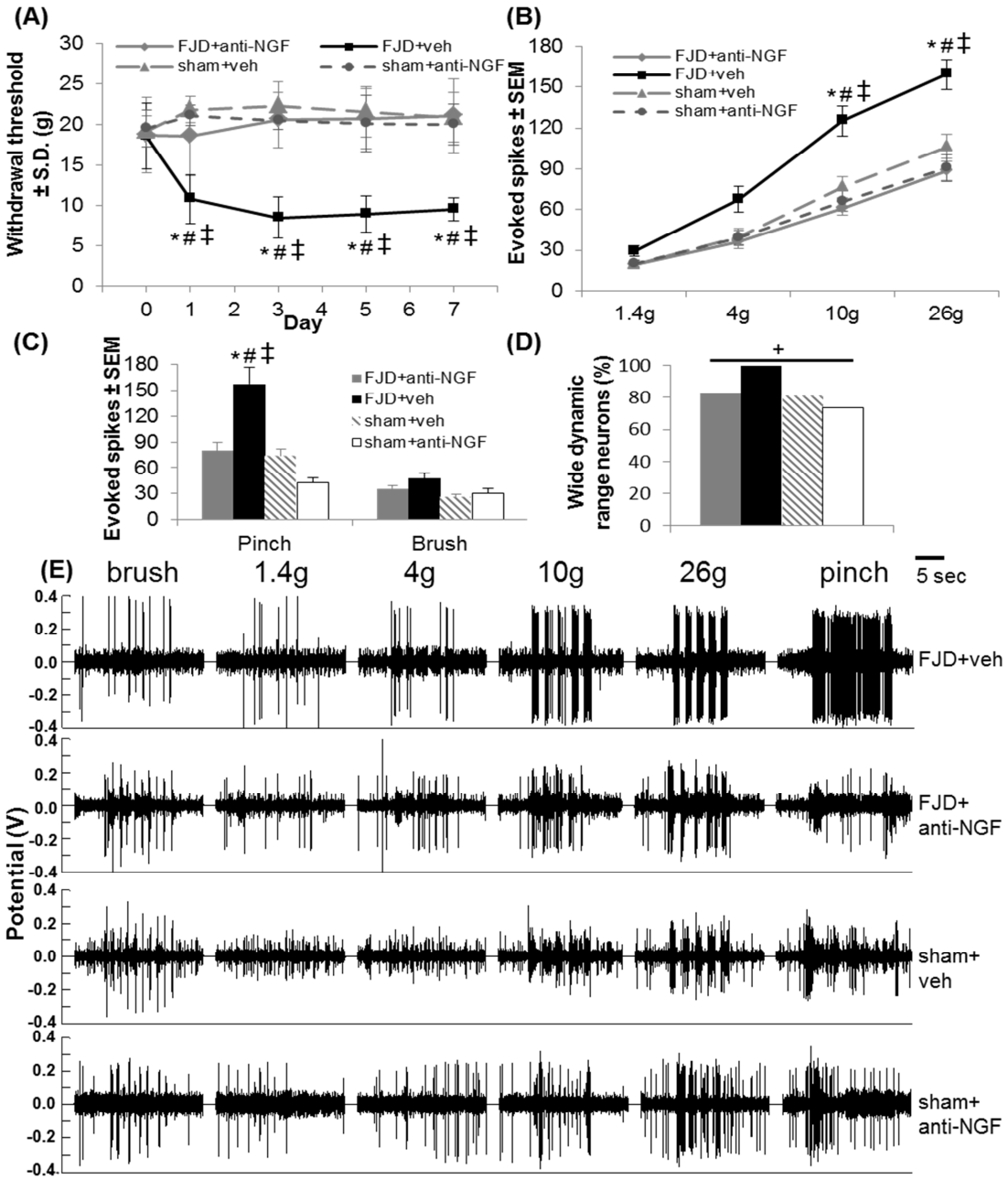


**Figure 5.8. (A)** The withdrawal threshold is reduced from baseline at all time points for FJD+veh ($p<0.001$). The withdrawal threshold is reduced for FJD+veh compared to FJD+anti-NGF (*$p<0.015$), sham+veh (#$p<0.001$), and sham+anti-NGF (‡$p<0.001$) at all post-injury days. **(B)** At day seven, the number of evoked spikes is increased in the FJD+veh group compared to all other groups (*#‡$p<0.012$) for the 10g and 26g filaments. **(C)** Pinch evokes more spikes for FJD+veh compared to all other groups (*#‡$p<0.001$). **(D)** There is an effect of group on the proportion of WDR neurons (+$p<0.005$), with FJD+veh having the largest number. **(E)** Representative recordings illustrate increased spikes in the FJD+veh group compared to the other groups.

Noxious pinch of the forepaw evokes more spikes in the FJD+veh group compared to sham+veh ($p<0.005$), but the difference between FJD+veh and FJD+anti-NGF is not significant at day one (Figure 5.9C). No differences are detected between sham+veh and FJD+anti-NGF for any of the von Frey filaments or either the brush or pinch stimuli. Mirroring the results at day seven, there is a significant effect of injury group on the proportion of WDR neurons recorded in the spinal cord ($p<0.042$), with FJD+veh exhibiting the highest frequency of WDR neurons (Figure 5.9D). Individual spinal neuronal spike counts at day one for each rat in this study are included in Appendix G. Together, these behavioral and electrophysiological findings early after injury (Figure 5.9), as well as at a later time point (day seven) after injury (Figure 5.8), support a role for intra-articular NGF in the development of persistent pain and spinal hyperexcitability after facet joint injury.

In contrast to the lack of change in mechanical withdrawal threshold after immediate anti-NGF treatment (FJD+anti-NGF), intra-articular anti-NGF injections given one day after FJD (FJD+anti-NGFD1) do *not* abolish injury-induced reductions in the withdrawal threshold (Figure 5.10A). On day one after joint distraction, the withdrawal threshold significantly decreases for the FJD+anti-NGFD1 group compared to baseline ($p<0.001$) and is not different from FJD+veh but is significantly lower than FJD+anti-NGF ($p<0.012$) at that time (Figure 5.10A). Intra-articular injection of the anti-NGF antibody after behavior testing on day one does not increase the withdrawal threshold. On the contrary, the withdrawal threshold for FJD+anti-NGFD1 remains significantly lower than baseline ($p<0.028$) as well as FJD+anti-NGF ($p<0.043$) at all post-surgical time points and is not different from FJD+veh on any day (Figure 5.10A).

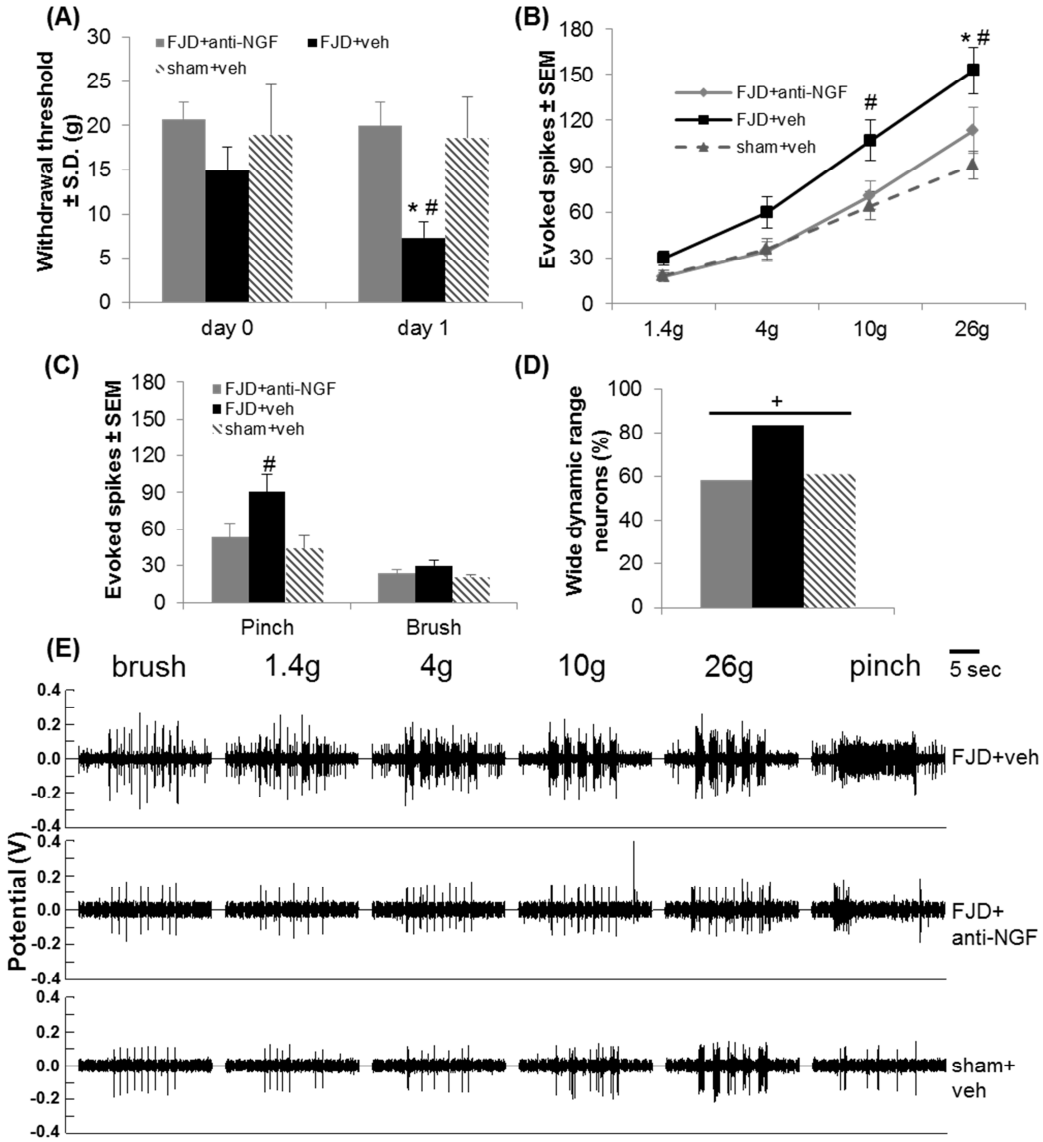


**Figure 5.9. (A)** The forepaw withdrawal threshold is reduced from baseline at day one for FJD+veh ($p<0.001$); yet, there is no change from baseline for sham+veh or FJD+anti-NGF at day one. The withdrawal threshold is reduced for FJD+veh compared to FJD+anti-NGF (*$p<0.001$) and sham+veh (#$p<0.001$) at day one. **(B)** The number of spikes evoked by von Frey filament stimulation is increased in the FJD+veh group over the FJD+anti-NGF (*$p<0.006$) and sham+veh (#$p<0.001$) groups for the 26g filament and is also increased over sham+veh (#$p<0.007$) for the 10g filament at day one. **(C)** Pinch evokes more spikes for FJD+veh compared to sham+veh (#$p<0.005$). **(D)** There is a significant effect of group on the proportion of WDR neurons (+$p<0.042$), with FJD+veh having the largest number. **(E)** Representative recordings illustrate increased spikes evoked by stimulation of the forepaw in the FJD+veh group compared to the other groups.

Quantification of evoked spikes from 61 spinal neurons (average depth 724±25µm) at day seven after FJD+anti-NGFD1 identifies significantly more firing evoked by the 26g filament compared to FJD+anti-NGF ($p<0.022$) but not with the pinch (Figures 5.10B & 5.10C). Spikes evoked by the noxious 26g von Frey filament are not different between the FJD+anti-NGFD1 and FJD+veh groups (Figures 5.10B & 5.10C). In the context of the behavioral findings (Figure 5.10A), these electrophysiological data suggest that intra-articular NGF is not a contributor to the maintenance of injury-induced facet pain or the associated spinal neuronal hyperexcitability. Detailed mechanical withdrawal thresholds for each rat included in this study are summarized in Appendix C; individual spinal neuronal firing data for each rat are included in Appendix G.

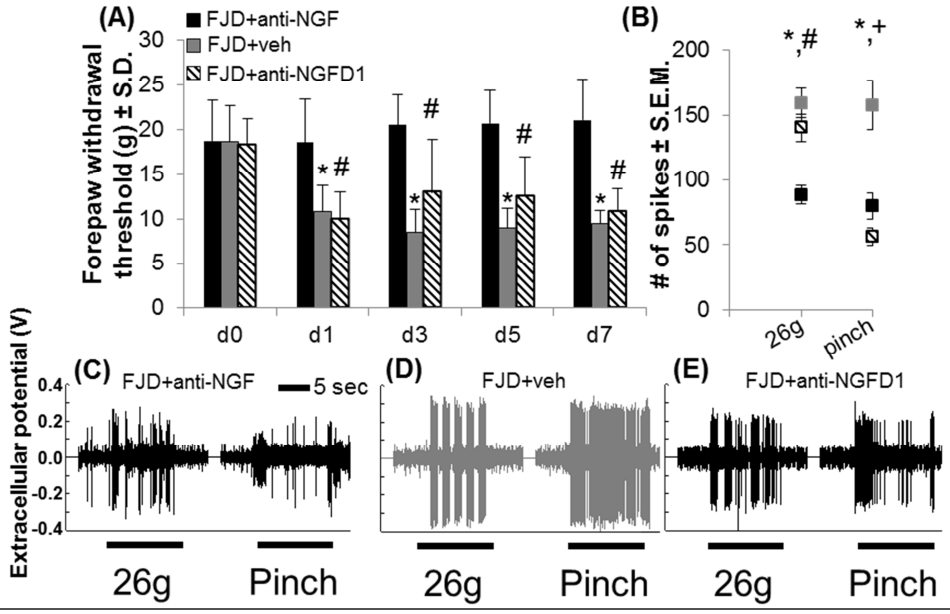


**Figure 5.10. (A)** Withdrawal threshold decreases at all days (d) after FJD+veh compared to FJD+anti-NGF (*). FJD+anti-NGFD1 also exhibits decreases in threshold at all days compared to FJD+anti-NGF (#). **(B)** At day seven, the number of spikes evoked by noxious von Frey stimulation (26g) decreases for FJD+anti-NGF relative to FJD+veh (*) and FJD+anti-NGFD1 (#), but both FJD+anti-NGF (*) and FJD+anti-NGFD1 (+) exhibit fewer evoked spikes than FJD+veh for noxious pinch. **(C)** Representative spikes are shown for the 26g and pinch stimuli for each group.

## 5.5. Discussion

This study defines a role for intra-articular NGF in the development of facet joint-mediated pain. NGF expression increases in the injured joint as early as one day after painful injury and within the DRG at day seven (Figures 5.3 & 5.4). Exogenous intra-articular NGF induces transient mechanical and thermal behavioral sensitivity lasting one day, implicating intra-articular NGF in pain initiation (Figures 5.5, 5.6, & 5.7). Intra-articular NGF induces behavioral sensitivity that is associated with spinal neuronal hyperexcitability (Figure 5.5). Pharmacologic ablation of neurons involved in peptidergic, but not non-peptidergic, signaling from the joint prevents the development of both of these NGF-induced responses, strongly supporting peptidergic signaling in NGF-mediated joint pain (Figures 5.6 & 5.7). Interruption of peptidergic signaling in the joint prevents the increases in NGF expression in the DRG that are evident with injury-induced pain (Figure 5.4). Local administration of anti-NGF in the joint immediately after its injury also prevents the development of both behavioral and spinal neuronal hypersensitivity (Figure 5.8). Yet, delayed administration of intra-articular anti-NGF one day after joint injury does not abolish behavioral sensitivity or the associated spinal neuronal hyperexcitability (Figure 5.10). Taken together, these data identify NGF as the intra-articular *initiator* of joint injury-induced pain and support early localized treatment targeting NGF as a potential effective therapy.

NGF has been shown to contribute to arthritis-related joint pain. NGF is upregulated in inflamed tissues (McMahon, 1996) and increases in the soft tissues of experimental knee arthritis in the rat (Orita et al., 2011). Increased NGF also has been reported in the synovial fluid of painful inflamed and arthritic joints in humans (Barthel

et al., 2009; Raychaudhuri et al., 2011; Saito et al., 2000). Because intra-articular NGF induces pain, albeit only transiently, in our study, elevated intra-articular NGF is a likely source of clinical joint pain, especially since NGF induces pain in humans when applied to skin or muscle tissue (Dyck et al., 1997; Svensson et al., 2003). The elevated intra-articular NGF across several types of painful conditions, including our model of painful joint trauma, together with the fact that local anti-NGF prevents pain development, suggests that regardless of the etiology, NGF likely has a role in a broad range of painful joint conditions, including other traumatic joint injuries or arthritis.

The prevention of injury-induced pain by immediate, but not delayed (day one), intra-articular anti-NGF supports traumatic joint pain being mediated by early NGF signaling cascades (Figures 5.8, 5.9 & 5.10). Yet, NGF-induced joint pain is transient and only evident for one day (Figure 5.5). As such, several mechanisms may induce persistent joint pain, with NGF as the initiator. Painful facet joint distraction is associated with increased expression of prostaglandin $E_2$ ($PGE_2$), a known regulator of inflammation and pain (Lin et al., 2006), by day one after injury (Kras et al., 2014a); NGF facilitates inflammatory hyperalgesia by inducing a switch to a PKCε-dependent mechanism for $PGE_2$ signaling (Joseph and Levine, 2010; Parada et al., 2005). Such a priming mechanism may explain why intra-articular NGF induces only short-lasting transient pain and that intra-articular anti-NGF given at injury, but not at later times, prevents development of long-lasting facet pain (Figure 5.5, 5.8, 5.9 & 5.10). Early anti-NGF treatment may prevent nociceptor priming by blocking the early intra-articular NGF after injury, a notion further supported by the finding that intra-articular anti-NGF given on day one when behavioral sensitivity is evident does not alleviate pain (Figure 5.10).

Indeed, intra-articular ketorolac, which disrupts synthesis of prostaglandins, has no effect on pain responses when given at the time of joint injury (Dong et al., 2013a), which is consistent with our finding that NGF is an early mediator of injury-induced joint pain. However, in contrast, intra-articular ketorolac *does* abolish facet pain when given later, after pain has developed (Dong et al., 2013a). The different effects of the anti-NGF and NSAID may be due to early NGF facilitating later $PGE_2$-mediated nociception; although NGF is sufficient to initiate pain, additional mediators may contribute to its maintenance.

Ablating joint afferents involved in peptidergic signaling prevents NGF-induced mechanical hypersensitivity, but eliminating non-peptidergic joint afferents has no effect (Figures 5.6 & 5.7). This is not surprising since the NGF receptor, trkA, is expressed mainly by peptidergic afferents (McMahon, 1996; Merighi et al., 2004), which comprise over 50% of the afferents innervating the rat's C6/C7 facet joint (Kras et al., 2013b). Increased peptidergic fiber density is reported in painful osteoarthritic joints (Saito et al., 2000), and peptidergic fibers sprout into the synovium in models of painful arthritis (Ghilardi et al., 2012; Longo et al., 2013). Neuropeptides are typically expressed by nociceptive C- and Aδ-fibers (Galeazza et al., 1995), so sprouting of peptidergic fibers in the facet may also induce joint pain. Our results demonstrate a role for peptidergic signaling among joint afferents in injury-induced pain since ablating them prior to injury prevents the development of behavioral sensitivity (Figure 5.4). Intra-articular NGF also increases thermal sensitivity, which is abolished when peptidergic signaling is disrupted prior to NGF injection (Figure 5.6). However, when non-peptidergic neurons are ablated, thermal sensitivity after NGF injection is not different from controls, confirming that non-peptidergic afferents also contribute to thermal pain (Figure 5.7). The transient

receptor potential vanilloid-1 responds to noxious thermal stimuli and is expressed on both peptidergic and non-peptidergic afferents in the rat (Okun et al., 2011; Yu et al., 2008), so both afferent populations may contribute to thermal sensitivity, which is also supported by our findings. Peptidergic signaling also contributes to mechanical sensitivity after NGF injection or after facet joint distraction; because non-peptidergic joint afferents do not contribute to NGF-induced mechanical sensitivity those afferents likely do not contribute to facet joint distraction-mediated mechanical sensitivity either. Together, these findings identify peptidergic signaling as having more influence than non-peptidergic signaling in both NGF- and injury-induced facet joint pain.

Intra-articular NGF also induces hyperexcitability in dorsal horn neurons, with equivalent noxious mechanical stimulation of the forepaw eliciting more spinal neuronal activity in the NGF-injected rats compared to control rats (Figure 5.5). This increased excitability is evident also when non-peptidergic joint afferents are eliminated before NGF injection (Figure 5.7). However, disruption of peptidergic signaling in the joint prevents NGF-induced hyperexcitability of spinal neurons (Figure 5.6). Many of the neurons in the deep dorsal horn are WDR neurons that respond to both non-noxious and noxious signals (Pezet et al., 1999; Seal et al., 2009). WDRs have an important role in central sensitization, the enhancement of the excitability or synaptic efficacy of neurons in the central nervous system, and contribute to many forms of persistent pain (Calvino et al., 1987; Latremoliere and Woolf, 2009; Martindale et al., 2007). With injection of intra-articular NGF, there is an increase in the number of neurons in the dorsal horn responding as WDRs to mechanical stimulation (Figure 5.5). The increases in spinal neuronal excitability and WDRs that are induced by NGF suggest that intra-articular NGF may

mediate the central modifications underlying joint pain. One common consequence of central sensitization is an expansion of the receptive fields of sensory neurons (Latremoliere and Woolf, 2009), which has been reported for monoarthritis in the rat knee with the neurons innervating the ipsilateral ankle becoming hyperexcitable (Martindale et al., 2007). Indeed, whiplash patients with neck pain experience hypersensitivity to mechanical stimuli in the neck, as well as in the shoulder, arm, and even the hand (Fernandez-Perez et al., 2012; Scott et al., 2005; Sterling et al., 2003). The finding that NGF injected in the facet joint induces behavioral hypersensitivity in the forepaw further supports central sensitization as an underlying mechanism in facet-mediated pain.

Painful facet joint distraction increases dorsal horn neuronal excitability and induces a shift from low threshold mechanosensitive neurons to WDRs (Crosby et al., 2013; Quinn et al., 2010). Together with our findings that NGF increases in the facet after its injury and is sufficient to induce pain and spinal neuronal hyperexcitability, early intra-articular NGF is strongly implicated as mediating injury-induced facet pain. Indeed, intra-articular application of an anti-NGF antibody prior to joint injury prevents the development of both behavioral hypersensitivity and spinal neuronal hyperexcitability (Figures 5.8 & 5.9). Although current systemic anti-NGF therapies show promise in alleviating joint pain from osteoarthritis and chronic low back pain, they are associated with adverse events, such as headache, hyperesthesia, paresthesia, and even joint degeneration (Brown et al., 2012; Katz et al., 2011; Lane et al., 2010). Our findings suggest *local* anti-NGF treatment to be effective at preventing the onset of joint pain. Of note, all rats receiving anti-NGF exhibited normal weight gain and grooming behavior

and were otherwise indistinguishable from control rats, with no obvious ill-effects associated with the local anti-NGF treatment.

In contrast to the findings that immediate intra-articular anti-NGF application prevents injury-induced pain and the spinal neuronal hyperexcitability associated with it (Figures 5.8 & 5.9), delayed application of intra-articular anti-NGF until one day after joint injury does not mitigate existing behavioral or spinal neuronal hypersensitivity (Figure 5.10). Only a single time point (day one) for post-injury anti-NGF treatment was assessed here, and there may be earlier post-injury time points at which intra-articular anti-NGF treatment is effective for preventing or alleviating pain. Indeed, blocking intra-articular sodium channel activation within four hours, but not later, after a known painful facet joint distraction prevents the development of both of these same behavioral and neuronal correlates (Crosby et al., 2014). As such, evaluation of additional time points for intra-articular delivery of anti-NGF after joint injury is necessary to determine if localized anti-NGF therapy is a feasible treatment for injury-induced joint pain. Moreover, only a single dose of the anti-NGF antibody was applied. Although the selected dose is effective when given immediately after injury, a higher dose may be required to alleviate existing pain. In fact, a dose-dependent alleviation of inflammatory and neuropathic pain is reported for systemic anti-NGF treatments in animal models of pain (Wild et al., 2007) as well as clinically for knee pain (Lane et al., 2010). Further, multiple injections of anti-NGF may be necessary to alleviate established facet joint-mediated pain. Although multiple anti-NGF injections have not been applied in pre-clinical models of joint pain, repeated anti-NGF treatment *does* alleviate sciatic nerve injury-induced pain in mice, while a single dose of anti-NGF only transiently relieves

pain (Wild et al., 2007). As such, additional work varying the dose and timing of anti-NGF treatment is needed to fully evaluate whether or not the more invasive, but more focused, local treatment is effective in alleviating facet joint pain and is associated with fewer adverse events than systemic anti-NGF treatment for joint pain. Nevertheless, the prevention of injury-induced pain and neuronal hyperexcitability achieved with intra-articular anti-NGF injection demonstrates that intra-articular NGF is necessary for the development of joint pain after facet injury.

Although further studies are necessary to determine if intra-articular anti-NGF is sufficient to alleviate established facet joint pain, additional pain mediators might also maintain facet pain. Substance P has an established role in a variety of pain modalities, including neuropathic and joint pain (Keeble and Brain, 2004; Nichols et al., 1999), promoting inflammation and potentiating glutamatergic neurotransmission (Keeble and Brain, 2004; Seybold, 2009; Sharif Naeini et al., 2005). Ablation of substance P sensitive spinal neurons prevents the development of pain following either nerve injury or an inflammatory stimulus in the rat (Nichols et al., 1999). In fact, ablation of spinal neurons expressing the NK1 receptor two weeks prior to a facet joint injury prevents the development of facet-mediated pain (Weisshaar and Winkelstein, 2014), suggesting the central release of substance P is required for pain maintenance after facet joint injury. Yet, the actions of substance P are not limited to the spinal cord; peripheral nerve terminals innervating targets such as joints also release substance P (Keeble and Brain, 2004). Similar to targeted elimination of NK1-bearing neurons in the spinal cord, ablation of substance P sensitive joint afferents prevents facet joint injury-induced pain (Figure 5.4). Further, both intra-articular and intrathecal antagonism of substance P signaling

separately alleviate established arthritis pain (Keeble and Brain, 2004; Uematsu et al., 2011), demonstrating that substance P in the periphery and in the spinal cord also maintains joint pain. Because expression and release of substance P from primary afferent neurons is regulated by NGF (Merighi et al., 2004), the increased intra-articular NGF that initiates pain following a facet joint injury likely stimulates substance P synthesis and release. In fact, substance P expression is increased in the DRG seven days after a painful facet joint injury (Lee and Winkelstein, 2009) in parallel with a similar increase in NGF expression (Figure 5.4). Moreover, ablation of joint afferents sensitive to substance P prevents both injury-induced and NGF-induced facet pain (Figures 5.4 & 5.6). Antagonism of the NK1 receptor in the spinal cord prevents the behavioral effects of NGF applied systemically (Thompson et al., 1995), demonstrating that substance P signaling is necessary for NGF-induced pain. That connection between NGF-induced behavioral hypersensitivity and substance P release suggests that treatments targeting substance P might be more effective in alleviating established facet pain than targeting intra-articular NGF. Although not included in this thesis, additional studies to assess whether or not blockade of substance P signaling, either alone or in combination with inhibition of intra-articular NGF, is sufficient to alleviate established pain after a facet joint injury would clarify the relationship, if any, between NGF, substance P, and facet pain maintenance.

## 5.6. Conclusions & Integration

In conclusion, these data demonstrate a role for intra-articular NGF and peptidergic joint afferents in the development of pain and spinal neuronal

hyperexcitability following injurious trauma to the cervical facet joint. Despite clinical reports of increased NGF in degenerative and arthritic joints (Barthel et al., 2009; Raychaudhuri et al., 2011) and in rat arthritis models (Aloe et al., 1992; Orita et al., 2011), this study is the first to establish that intra-articular NGF induces pain and central sensitization. Intra-articular anti-NGF given immediately after a joint injury prevents pain development; yet, when given one day after the injury, that same dose of intra-articular anti-NGF is ineffective in alleviating pain. Because only a single dose of anti-NGF was applied on day one after injury, further work applying a different anti-NGF treatment regimen, such as a higher dose and/or multiple injections, is needed to fully define whether or not intra-articular NGF contributes to the *maintenance* of joint pain. Additional pain mediators, such as prostaglandins and neuropeptides, are upregulated after joint injury (Kras et al., 2013c; Kras et al., 2014a; Lee and Winkelstein, 2009) and may contribute to pain maintenance. Regardless, this study provides the first evidence that intra-articular NGF is both necessary and sufficient for the development of facet joint-mediated pain.

Although findings in the current set of studies identify intra-articular NGF as an initiator of injury-induced facet pain and spinal neuronal hyperexcitability, the cellular responses initiated by NGF that lead to behavioral hypersensitivity and spinal sensitization after facet injury are not defined. Among the pain mediators regulated by NGF, brain-derived neurotrophic factor (BDNF) contributes to behavioral sensitivity resulting from tissue insults ranging from inflammation to nerve damage (Coull et al., 2005; Li et al., 2006; Mannion et al., 1999; Michael et al., 1997). BDNF is synthesized by peptidergic afferents in response to NGF signaling (Michael et al., 1997; Merighi et

al., 2008), so the finding that a majority of the afferents innervating the C6/C7 facet joint are peptidergic (Chapter 4) taken with the studies here demonstrating an injury-induced upregulation of NGF in the facet joint and DRG suggests that BDNF may be a downstream mediator of joint pain. In fact, BDNF produced in the primary afferents is transported to the spinal cord, where its release sensitizes spinal neurons via activation of trkB (Merighi et al., 2008; Pezet and McMahon, 2006; Zhou et al., 2008). Indeed, spinal BDNF contributes to pain and the central sensitization that maintains pain (Geng et al., 2010; Lu et al., 2009; Merighi et al., 2008; Zhou et al., 2008); moreover, inhibition of spinal BDNF signaling alleviates existing pain after nerve injury (Coull et al., 2005; Zhang et al., 2011). Because NGF has a prominent role in initiating facet-mediated pain and spinal neuronal hyperexcitability and BDNF is known to contribute to both pain and central sensitization, studies in Chapter 6 characterize the BDNF response in this model of painful facet joint loading, as well as identify whether or not BDNF maintains injury-induced joint pain.

# CHAPTER 6

# Facet Joint Injury and the Neurotrophin Response: A Role for Spinal BDNF in Persistent Pain

*Parts of this chapter are adapted from:*

Kras JV, Weisshaar CL, Quindlen J, Winkelstein BA (2013). Brain-Derived Neurotrophic Factor is Upregulated in the Cervical Dorsal Root Ganglia and Spinal Cord and Contributes to the Maintenance of Pain From Facet Joint Injury in the Rat. *Journal of Neuroscience Research*, 91(10): 1312-1321.

## 6.1. Overview

Although tensile loading of the cervical facet joint has been associated with inflammation and neuronal hyperexcitability (Crosby et al., 2013; Dong et al., 2013a; Quinn et al., 2010), the mechanisms of joint loading-induced pain remain unknown. Findings from the studies presented in Chapters 4 and 5 suggest a role for nerve growth factor (NGF) activation of the peptidergic joint afferents that innervate the C6/C7 facet joint in initiating the onset of sustained behavioral sensitivity and spinal neuronal hyperexcitability after mechanical joint injury (Kras et al., 2013b; Kras et al., 2014b). Further, expression of brain-derived neurotrophic factor (BDNF) is regulated by NGF and induces behavioral hypersensitivity and hyperexcitability of spinal neurons in models of both painful inflammation and nerve injury (Cho et al., 1997; Ha et al., 2001; Li et al., 2006; Lu et al., 2009; Mannion et al., 1999; Pezet and McMahon, 2006). BDNF is normally produced in peptidergic afferent neurons before undergoing anterograde

transport to the superficial dorsal horn of the spinal cord where its release is stimulus dependent (Hartmann et al., 2001; Merighi et al., 2008; Pezet and McMahon, 2006; Zhou et al., 1999). Upon release into the synaptic cleft, BDNF sensitizes neurons through both pre- and post-synaptic receptor activation, contributing to hypersensitivity in a wide range of tissue injuries and disease states (Geng et al., 2010; Matayoshi et al., 2005; Merighi et al., 2008; Pezet et al., 2002). In fact, BDNF is upregulated in primary afferents in the DRG in response to NGF signaling, as well as peripheral inflammation (Cho et al., 1997; Mannion et al., 1999; Michael et al., 1997). Pain models of inflamed tissues or arthritic joints demonstrate upregulation of BDNF (Mannion et al., 1999; Ohtori et al., 2002; Grimsholm et al., 2008). Despite increased BDNF expression being associated with inflammation (Mannion et al., 1999; Pezet and McMahon, 2006) and a reported contribution of inflammation to facet joint injury-induced pain (Dong et al., 2013a), no study has defined BDNF expression in the DRG and/or spinal cord following a painful mechanical joint injury. As such, characterization of the BDNF response in those tissues after facet joint injury can help identify whether or not BDNF contributes to the development and/or maintenance of injury-induced joint pain.

This chapter summarizes experiments under Aim 1b and Aim 3, which quantify the BDNF response to painful facet joint injury in the DRG (Aim 1b) and spinal cord (Aim 3). Intra-articular NGF is upregulated by mechanical facet joint injury and is necessary for the initiation of pain and neuronal hyperexcitability in the spinal cord after distraction of that joint (Chapter 5; Kras et al., 2014b). Because BDNF may be increased by NGF signaling and is associated with pain and neuronal hyperexcitability (Lu et al., 2009; Mannion et al., 1999; Merighi et al., 2004; Pezet and McMahon, 2006), studies in

this chapter test the hypothesis that BDNF increases in the DRG and spinal cord after a painful facet joint distraction and contributes to the maintenance of joint-mediated behavioral sensitivity. Accordingly, BDNF expression is quantified in the DRG (Aim 1b) and the spinal cord (Aims 3a & 3b) after a painful joint distraction at day one and day seven to evaluate if it is associated with behavioral hypersensitivity. Further, the functional role of BDNF in facet-mediated pain is evaluated using intrathecal sequestration of BDNF (Aim 3c) to directly assess the contribution of BDNF signaling to join injury-induced pain symptoms.

## 6.2. Relevant Background

Animal models of facet joint injury support the assertion that mechanical injury to the facet can cause pain and report altered inflammatory mediators in the joint and DRG, as well as neuronal hyperexcitability associated with behavioral sensitivity (Cavanaugh et al., 1996; Kras et al., 2013a; Lee et al., 2008; Lu et al., 2005; Quinn et al., 2010; Tachihara et al., 2007). The facet capsule is innervated by Aδ- and C-fibers that are activated by mechanical stimulation and inflammation (Cavanaugh et al., 1996; Ohtori et al., 2001; Lu et al., 2005; Cavanaugh et al., 2006). Both types of stimuli induce behavioral sensitivity (Dong et al., 2008; Dong et al., 2013a; Lee et al., 2008; Tachihara et al., 2007) and lead to upregulation of inflammatory cytokines in the DRG (Lee et al., 2008; Miyagi et al., 2006; Tachihara et al., 2007). The behavioral hypersensitivity induced by facet joint distraction is relieved by intra-articular application of the non-steroidal anti-inflammatory drug ketorolac (Dong et al., 2013a), implicating inflammation in painful mechanical joint injury. Moreover, because NGF is increased in inflamed

tissues (Merighi et al., 2004), the upregulation of NGF in the injured facet joint and its contribution to the initiation of facet-mediated pain that were identified in Chapter 5 (Kras et al., 2014b) further suggest that inflammation may be a key component of facet pain.

Peripheral inflammation and NGF increase the neurotrophin BDNF in the DRG (Cho et al., 1997; Mannion et al., 1999; Michael et al., 1997). The number of BDNF-expressing afferents innervating the facet joint has also been shown to increase seven days after inflammation induced by complete Freund's adjuvant (CFA) in that same facet joint compared to controls (Ohtori et al., 2002). Despite the association of inflammation with increases in BDNF (Cho et al., 1997; Mannion et al., 1999; Michael et al., 1997; Ohtori et al, 2002) and an established contribution of joint inflammation to facet loading-induced pain (Dong et al., 2013a), the relationships among facet joint injury, pain, and BDNF are unclear.

BDNF is involved in nociceptive signaling in many pain states (Cho et al., 1997; Li et al., 2006; Mannion et al., 1999; Michael et al., 1997; Zhou et al., 1999). BDNF released from primary afferents contributes to spinal hyperexcitability by activating its receptor, trkB (Lu et al., 2009; Merighi et al., 2008; Pezet and McMahon, 2006; Thompson et al., 1999), which in turn activates the MAP kinase, ERK, via phosphorylation (Ji et al., 2002; Pezet et al., 2002; Slack et al., 2004). Further, the amount of BDNF released in the spinal cord in response to neuronal stimulation is increased by exposure to NGF (Lever et al., 2001), suggesting that BDNF may be the central mediator of the NGF-dependent spinal hyperexcitability identified in Figure 5.8 (Kras et al., 2014b). Inhibition of spinal BDNF activity by the sequestering molecule,

trkB-Fc, which binds endogenously released BDNF and prevents it from activating functional membrane-bound trkB receptors, alleviates nerve injury-induced sensitivity (Coull et al., 2005; Zhang et al., 2011). That sequestering molecule also reduces the spinal ERK activation that is induced by chemical stimulation of peripheral nociceptors with capsaicin (Pezet et al., 2002). BDNF levels in the DRG and spinal cord both increase as soon as one day after a painful intraplantar injection of inflammatory CFA in the rat (Duric and McCarson, 2007; Mannion et al., 1999). Although animal models of joint inflammation and arthritis have demonstrated increased BDNF expression in the synovial tissue of the affected joints and their associated DRGs (Grimsholm et al., 2008; Ohtori et al., 2002), behavioral outcomes were not evaluated in those studies, so the functional role of BDNF in joint-mediated pain remains unclear.

Based on the role of BDNF in nociceptive signaling and its effects on spinal neuronal excitation, the objectives of this study are to evaluate whether or not BDNF increases following painful facet joint injury and to determine the functional role of BDNF in facet-mediated pain. Because BDNF is transcribed and synthesized in the DRG but is transported to, and released in, the spinal cord, BDNF mRNA and protein levels are quantified in the DRG and in the spinal cord using RT-PCR and immunolabeling techniques in separate animals at early (day one) and late (day seven) time points after the painful facet joint injury described in Chapter 3 and used in Chapters 4 and 5. Based on those characterization studies, additional studies administered trkB-Fc intrathecally to evaluate effects of sequestering spinal BDNF on hyperalgesia and spinal ERK activation.

## 6.3. Methods

### 6.3.1. Surgical Procedures & Behavioral Assessment

Male Holtzman rats (Harlan Sprague-Dawley, Indianapolis, IN) (402±24g) were housed under USDA- and AAALAC-compliant conditions with free access to food and water. All experimental procedures were approved by the University of Pennsylvania IACUC and carried out under the guidelines of the Committee for Research and Ethical Issues of the IASP (Zimmermann, 1983).

All surgical procedures were performed under inhalation isoflurane anesthesia (4% induction; 2.5% maintenance). The bilateral C6/C7 facet joints underwent a controlled distraction sufficient to induce sustained mechanical hypersensitivity using the same procedures described in Chapter 3 (Dong et al., 2008; Kras et al. 2013b). Briefly, the C6 and C7 laminae were exposed and attached to a loading device via microforceps to impose a distraction across the bilateral C6/C7 facet joints. Peak displacement of the C6 forceps during each distraction was recorded to quantify the severity of the applied injury. Separate groups of rats underwent joint distraction and were followed for one (n=13 rats) and seven days (n=12 rats), at which time both the C6 and C7 DRGs and C6-C7 spinal cord were harvested. Sham procedures that included device attachment with no joint distraction were performed in separate groups of rats (n=7 for day 1; n=10 for day 7). All wounds were closed using polyester suture and surgical staples, and rats were recovered in room air.

The response to mechanical stimulation was quantified in the forepaws of each rat to measure behavioral hypersensitivity after surgical procedures, using previously validated methods as described in Chapters 3, 4, and 5 (Dong et al., 2008; Hubbard and

Winkelstein, 2005; Lee and Winkelstein, 2009). Rats underwent behavioral testing on day one or days one, three, five, and seven, depending on the time of tissue harvest, as well as for three days prior to any surgical procedure in order to establish baseline responses. On each testing day, rats were acclimated to the testing environment for 15 minutes followed by three rounds of mechanical stimulation to each forepaw using a series of ascending von Frey filaments (Stoelting; Wood Dale, IL). Responses from the bilateral forepaws were averaged to obtain a single measure of mechanical sensitivity for each rat. Sensitivity after the surgical procedures was normalized to the baseline response for each rat and expressed as the fold-increase relative to baseline. A two-way ANOVA with Tukey's HSD test compared the normalized average mechanical sensitivity between distraction and sham groups with group and time point as factors, and significance at $p<0.05$.

### 6.3.2. DRG & Spinal Cord Processing & BDNF mRNA Quantification

In order to define the BDNF mRNA levels in the DRG and spinal cord, tissue was harvested at the C6 and C7 spinal levels from both of the sham and distraction groups at day one or day seven for RT-PCR analysis. After behavioral testing on day one (n=7 distraction; n=3 sham) or day seven (n=6 distraction; n=6 sham), rats were given an overdose of sodium pentobarbital (65mg/kg) and transcardially perfused with phosphate buffered saline (PBS). Because the injury is bilateral and behavioral responses are not different between the right and left sides, tissue responses to injury are also expected to not differ between right and left. As such, based on the symmetry assumption, only the left DRGs and spinal cord hemi-sections at the C6 and C7 levels were analyzed. Tissue

was harvested, immediately frozen on dry ice, and stored at -80ºC until further use. Tissue samples were homogenized in TRIzol® (Invitrogen; Carlsbad, CA). Total RNA was extracted and reverse-transcribed into single-stranded cDNA according to the manufacturer's instructions (Invitrogen). Taqman® real time RT-PCR reactions were carried out using an ABI-7300 system (Applied Biosystems; Foster City, CA) with primers specific to BDNF (Forward: 5'-GGA-CAT-ATC-CAT-GAC-CAG-AAA-GAA-A-3'; Reverse: 5'-GCA-ACA-AAC-CAC-AAC–ATT-ATC-GAG-3'; Probe: 5'-AGT-CAT-TTG-CGC-ACA-ACT-TTA-AAA-GTC-TGC-ATT-3') and the internal housekeeping gene 18S (Forward: 5'-CGG-CTA-CCA–CAT-CCA-AGG-AA-3'; Reverse: 5'-GCT-GGA–ATT-ACC-GCG-GCT-3'; Probe: 5'-CAC-CAG-ACT-TGC-CCT-C-3') (Gomez-Pinilla et al., 2002; Lossos et al., 2003). Cycle conditions were: 95°C for 10 minutes, 40 cycles at 95°C for 15 seconds and 60°C for 60 seconds. Samples were run in duplicate, and target gene expression was normalized to the internal housekeeping gene expression (18S) using the $2^{\Delta\Delta Ct}$ method (Kras et al., 2013c; Lee et al., 2008; Lee and Winkelstein, 2009; Livak and Schmittgen, 2001). The mRNA level for each tissue for the distraction group was calculated as the fold-change relative to the average levels for sham in that tissue. BDNF mRNA levels were separately compared between distraction and sham groups for each tissue (DRG; spinal cord) at each time point (day 1; day 7), using t-tests.

### 6.3.3. DRG & Spinal Cord Processing & BDNF Immunohistochemistry

BDNF is normally expressed in small and medium diameter neurons in the DRG, with less expression in the large diameter neurons (Zhou et al., 1999). Because injury or

inflammation shifts the neuronal phenotype that expresses BDNF towards larger diameter neurons (Ohtori et al., 2002; Zhou et al., 1999), painful facet joint injury is hypothesized to cause a similar phenotypic shift in BDNF expression. In order to identify any such phenotypic change, immunohistochemistry was used to evaluate BDNF protein in DRG neurons and in the superficial laminae of the spinal dorsal horn in additional separate groups of rats. After behavioral testing on day one (n=6 distraction; n=4 sham) or day seven (n=6 distraction; n=4 sham), rats were deeply anesthetized with an overdose of sodium pentobarbital (65mg/kg) and transcardially perfused with PBS followed by 4% paraformaldehyde in PBS.

Cervical spinal cords with bilateral DRGs were harvested en bloc from the C6 and C7 levels and were post-fixed overnight at 4°C. Tissue was transferred to 30% sucrose in PBS for at least 4 days at 4°C and embedded in Tissue-Tek® OCT Compound (Sakura Finetek; Torrance, CA). Serial DRG and spinal axial sections (14μm thick) were taken for immunofluorescent histochemistry and thaw-mounted onto slides, with 3-5 sections per slide. Tissue sections were washed and blocked with normal donkey serum (Chemicon; Temecula, CA) for 2 hours. DRG sections were incubated at 4°C overnight with a rabbit polyclonal antibody specific to BDNF (1:100; sc-20981; Santa Cruz Biotechnology; Santa Cruz, CA). The following day, slides were washed and incubated with a Cy3 donkey anti-rabbit secondary antibody (1:500; Jackson ImmunoResearch; West Grove, PA) for 2 hours at room temperature. After additional washes with PBS and $dH_2O$, slides were coverslipped with Fluoro-Gel anti-fade medium (Electron Microscopy Sciences; Hatfield, PA). Because there are multiple cellular sources for BDNF synthesis and release, including neurons, microglia, and astrocytes in the spinal cord and because

BDNF from *specific* cell types may underlie pain from different injuries (Coull et al., 2005; Merighi et al., 2008; Zhang et al., 2011; Zhou et al., 1999; Zhou et al., 2011), the cellular sources of spinal BDNF were identified in addition to quantifying overall BDNF expression in the spinal cord. Spinal cord sections were incubated at 4°C overnight with the rabbit antibody to BDNF and one of the following: mouse monoclonal antibody to glial fibrillary acidic protein (GFAP; as a marker of astrocytes) (1:500; Millipore; Billerica, MA), mouse polyclonal antibody to microtubule associated protein-2 (MAP2; as a marker of neurons) (1:200; SMI 52; Covance; Princeton, NJ), or mouse monoclonal antibody to OX-42 (CD11b; as a marker of microglia) (1:300; Serotec; Raleigh, NC). The following day, the slides were washed and incubated at room temperature for 2 hours with Cy3 donkey anti-rabbit (1:500; Jackson ImmunoResearch) and Alexa488 donkey anti-mouse (1:500; Invitrogen) secondary antibodies. Tissue sections that were not incubated with primary antibodies were included as negative controls for all assays.

Each DRG section was imaged using a fluorescent microscope equipped with a digital camera (Olympus; Center Valley, PA) with standardized exposure times for all studies. A blinded experimenter analyzed BDNF expression in at least three sections from each rat for a subset of distraction and sham rats at each time point (n=3 rats per group). For each section, at least 50 neurons were classified as being either positive or negative for BDNF immunoreactivity, and only those neurons with a visible nucleus were included in the count (Weisshaar et al., 2010). Mean signal intensity and cross-sectional area of the neurons were determined by manually outlining each neuron using ImageJ (NIH; Bethesda, MD). For each section, the BDNF intensity was normalized to the average background intensity calculated from the intensities of the BDNF-negative

neurons to determine the BDNF intensity ratio. BDNF-positive neurons were classified into seven neuronal sizes (from <200$\mu m^2$ to >700$\mu m^2$ in 100 $\mu m^2$ bins) based on their soma area (Zhou et al., 1999). The average BDNF intensity ratio was compared between distraction and sham groups using a two-way ANOVA, with group and neuronal size as the factors, at day one and day seven. Total and BDNF-positive neuron cell counts were also calculated for each section, and the percentage of neurons positive for BDNF was compared between distraction and sham groups using t-tests.

At least 6 images of the spinal dorsal horn were taken from each rat for analysis by immunolabeling, with all exposure times standardized. Automated densitometry was performed using Matlab code that quantifies the BDNF expression in a standardized pixel area (1360x510) corresponding to laminae I-IV in the dorsal horn (Weisshaar et al., 2010). Because BDNF expression data were positively skewed, the raw data were log-transformed to achieve an approximately normal distribution prior to statistical analysis. All statistical analyses were performed on the transformed data, but the means and 95% confidence intervals are presented. BDNF expression in the dorsal horn was compared between groups at each time point using a t-test.

### 6.3.4. BDNF Sequestration Study

To evaluate the role of spinal BDNF on behavioral sensitivity and phosphorylated ERK expression after pain has been established from facet joint injury, a separate study administered trkB-Fc intrathecally after injury in order to sequester spinal BDNF. Rats underwent a C6/C7 facet joint distraction as described in Chapter 3 (Dong et al., 2008; Kras et al., 2013b). Sensitivity to mechanical stimulation was quantified in the bilateral

forepaws as described in Chapter 3 before (day 0; baseline) and after joint distraction, on days one, three, five, six, and seven. Immediately after behavioral testing on day five, under inhalation isoflurane anesthesia, rats received a single injection of either the BDNF sequestering molecule trkB-Fc (trkB-Fc; n=6) or IgG-Fc as the matched vehicle control (vehicle; n=7) via lumbar puncture, which has previously been shown as capable of delivering agents to the cervical spinal cord in the rat (Rothman and Winkelstein, 2010). Both treatments (R&D Systems; Minneapolis, MN) were given at 5µg in 20µL of sterile PBS, a dose that was based on reports of its being an effective dose to prevent or alleviate behavioral sensitivity after nerve injury (Coull et al., 2005; Zhang et al., 2011). Mechanical response thresholds were compared to baseline responses using a repeated measures two-way ANOVA with Tukey's HSD and group and time as factors.

Cervical spinal cord hemi-sections were harvested from the left side from both treatment groups at day seven, as described above, to quantify ERK activation using Western blot. Tissue was homogenized in lysis buffer (150mM NaCl, 50mM tris Cl pH 8.0, 1mM EDTA, 1% Triton® X-100) in the presence of protease and phosphatase inhibitors and centrifuged at 12,000g for 15 minutes at 4˚C. Supernatants were collected and stored at -80˚C. Protein samples were combined with NuPAGE® LDS Sample Buffer, NuPAGE® Reducing Agent, and NuPAGE® Antioxidant (Invitrogen) and heated at 95˚C for 5 minutes before loading onto a NuPAGE® 4-12% Bis-Tris gel (Invitrogen). Proteins were separated and transferred to an Immobilon®-FL transfer membrane (Millipore) and blocked for 2 hours with 5% non-fat dry-milk in 0.1% Tween-20 Tris-buffered saline. Membranes were incubated overnight at 4˚C with rabbit anti-phospho-ERK1/2 (pERK) (4370; Cell Signaling Technology; Danvers, MA) and mouse anti-

ERK1/2 (ERK) (4696; Cell Signaling Technology) antibodies diluted at 1:500 and 1:2000, respectively. The following day, membranes were incubated at room temperature for 2 hours with goat anti-rabbit IRDye 800CW and goat anti-mouse IRDye 680 secondary antibodies (1:15,000; LI-COR; Lincoln, NE). Membranes were imaged using the Odyssey® Infrared Imaging System (LI-COR). Quantitative analysis of pERK and ERK fluorescent band intensity was performed using Odyssey Application Software v2.1. Expression of pERK1 and pERK2 was normalized to ERK1 and ERK2, respectively, as the loading control for each sample. pERK protein expression relative to ERK protein expression was compared between the trkB-Fc and vehicle groups using a two-way ANOVA with Tukey's HSD test, with group and molecular weight (44kDa pERK1/ERK1; 42kDa pERK2/ERK2) as factors.

## 6.4. Results

### 6.4.1. Behavioral Responses to Mechanical Stimuli Following Injury

All rats undergoing joint distraction received the same severity of mechanical injury. A summary of the individual injury mechanics data (C6 forceps displacement) defining the severity of the joint injury for each rat used in these studies can be found in Appendix B. The mean displacement of the C6 forceps for the day one distraction group is 2.32±0.17mm, which is not different from that displacement imposed for the day seven group (2.65±1.45mm). Similarly, the joint distractions applied in the trkB study are also not different from each other (2.53±0.01mm trkB-Fc; 2.49±0.03mm vehicle) or when compared to the injured rats used to define the BDNF responses.

For all studies, since the responses to mechanical stimulation are not different between the right and left forepaws, the responses are averaged between forepaws for each rat. Mechanical sensitivity after sham procedures is not changed from baseline at either time point (Figure 6.1). Yet, facet joint distraction induces an immediate increase in mechanical sensitivity compared to baseline on day one ($p<0.001$) that is also evident at day seven ($p<0.001$) (Figure 6.1). Forepaw mechanical sensitivity in the distraction group also is significantly greater than sham ($p<0.001$) at both time points, and not different between days one and seven ($p=0.183$). The individual normalized behavioral sensitivity responses for each rat are summarized in Appendix C.

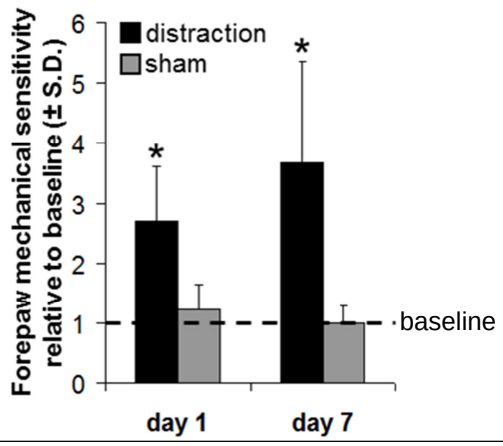


**Figure 6.1.** Mechanical sensitivity in the forepaw as measured by a fold-change from baseline sensitivity in response to von Frey filament stimulation. Sensitivity significantly increases (*$p<0.001$) after joint distraction compared to sham on the days when tissue was harvested.

### 6.4.2. BDNF mRNA Levels After Injury

Transcript levels of BDNF after a painful facet joint distraction differ from sham levels only in the spinal cord at day seven (Figure 6.2). BDNF mRNA is detected in the DRG and spinal cord in the distraction group, but is not different from sham in the DRG

at either day one or day seven (Figure 6.2A). After painful joint distraction, BDNF mRNA is significantly increased (p=0.031) over sham in the spinal cord at day seven (Figure 6.2B). Individual mRNA quantification data for each tissue response are provided for each rat in Appendix D.

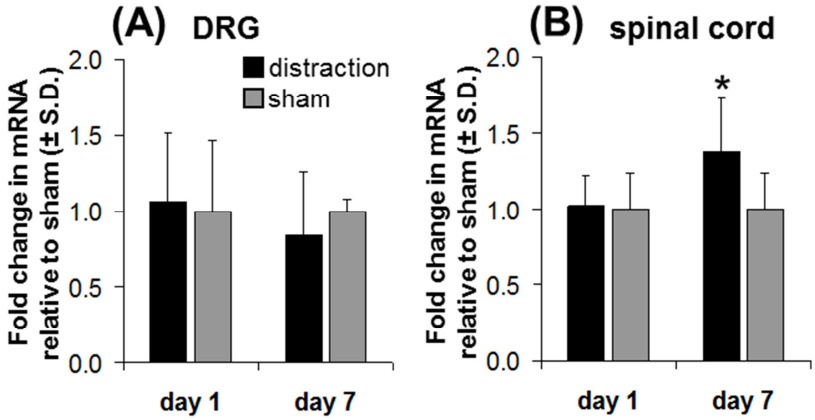


**Figure 6.2.** Quantification of BDNF mRNA in the DRG **(A)** and spinal cord **(B)** at days one and seven. **(A)** Painful joint distraction does not alter BDNF mRNA levels in the DRG. **(B)** Spinal BDNF mRNA increases (*p=0.031) at day seven after a painful joint distraction compared to sham.

### 6.4.3. BDNF Expression in the DRG Following Injury

Although neurons are identified in the DRG that express BDNF at both days one and seven for all rats, BDNF expression only increases in the DRG at day seven after painful distraction compared to sham (Figure 6.3). There is no change in the percentage of neurons expressing BDNF at either time point. The average BDNF-immunoreactive (BDNF-ir) intensity ratio across all neuron sizes is unchanged (p=0.078) after painful distraction compared to sham on day one (Figure 6.3A-6.3C). At day seven, the average BDNF-ir intensity ratio across all neuron sizes increases (p=0.016) after painful distraction compared to sham, but no change (p>0.338) in the response of neurons is

detected among the different sizes (p>0.338) (Figure 6.3D-6.3F). Individual neuronal size and BDNF labeling intensity data are detailed in Appendix E.

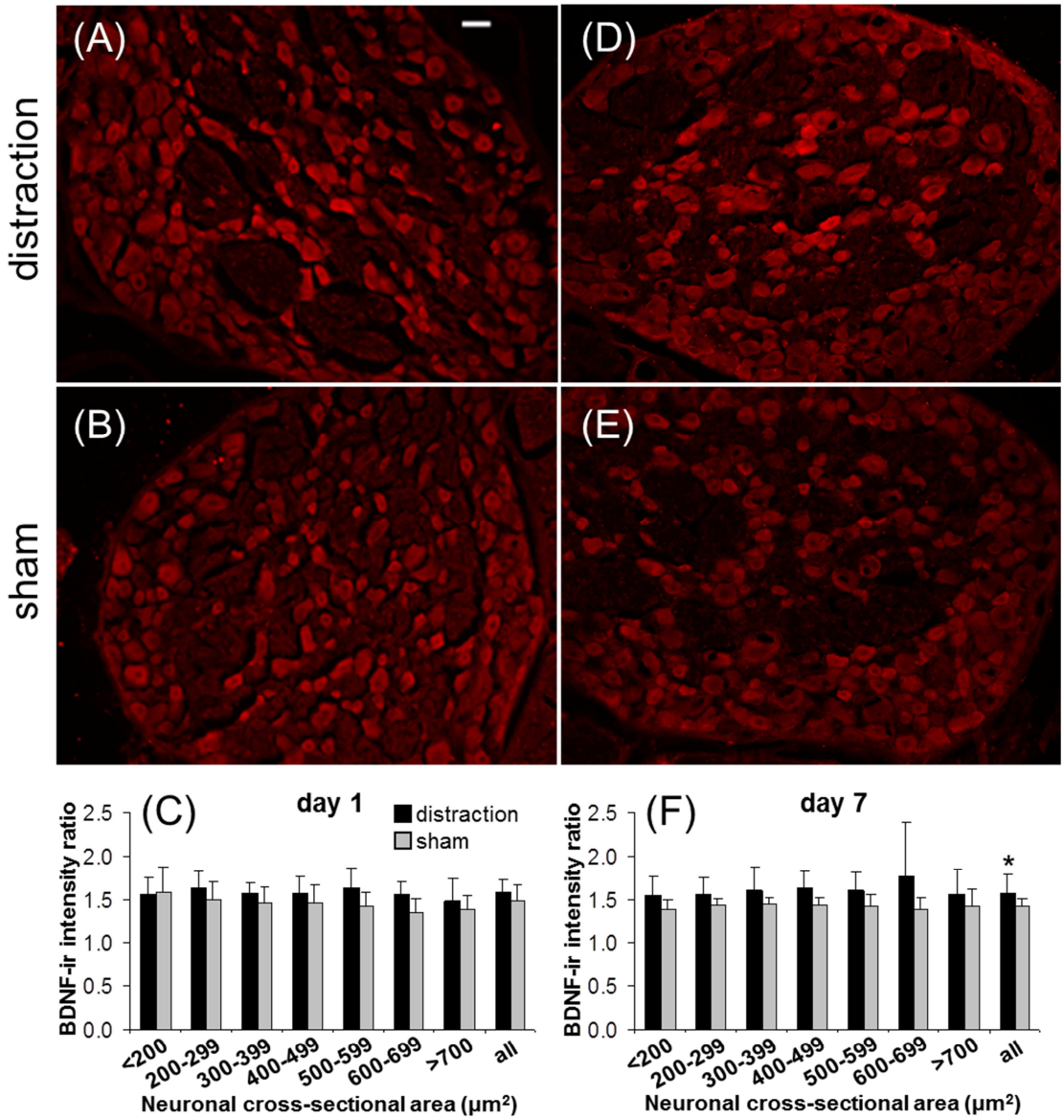


**Figure 6.3.** BDNF-ir intensity in neurons in the C6 DRG on day one **(A-C)** and seven **(D-F)**. Average BDNF-ir intensity is not different between distraction **(A)** and sham **(B)** groups at day one **(C)**. Average BDNF-ir intensity increases (*p=0.016) after distraction **(D)** relative to sham **(E)** on day seven **(F)**. Quantitative data for BDNF-ir intensity ratios **(C,F)** are average±standard deviation for three rats/group and at least three sections/rat; scale bar=50μm in **(A)** and applies to panels **(A,B,D,E)**.

### 6.4.4. BDNF Expression in the Spinal Dorsal Horn After Injury

BDNF protein also is detected in the spinal cords of all the rats receiving a joint distraction or sham procedure. Like the mRNA responses, there is no difference in BDNF in the superficial dorsal horn between distraction and sham at day one (p=0.252) (Figure 6.4). But, BDNF expression in the spinal cord at day seven after painful distraction is significantly increased (p=0.047) over expression in shams at that same time point (Figure 6.4). A summary of the quantitative densitometry for BDNF expression for individual rats is included in Appendix E.

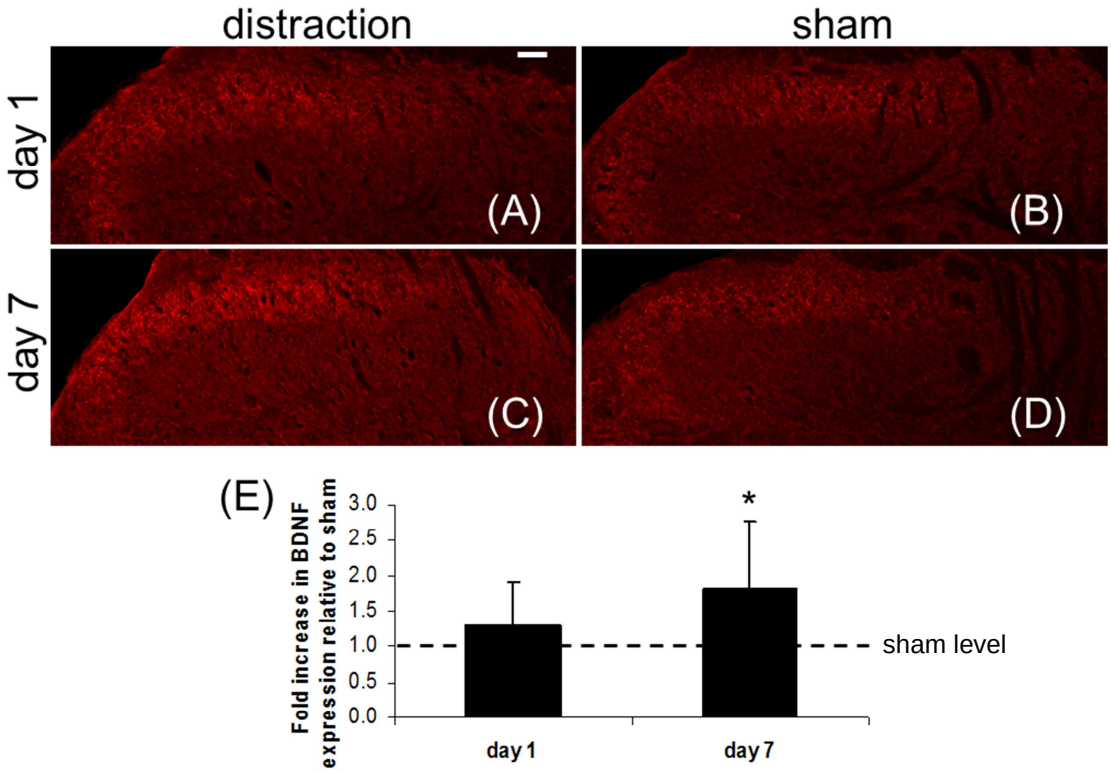


**Figure 6.4.** Representative images of BDNF in the spinal cord at day one **(A,B)** and day seven **(C,D)**, and its quantification **(E)**. **(A-B)** At day one, BDNF-ir intensity is not different between joint distraction and sham. **(C-D)** Joint distraction significantly (*p=0.047) increases BDNF-ir intensity over sham at day seven. Data in **(E)** are average±95% confidence limit. Scale bar=50μm in **(A)** and applies to panels **(A-D)**.

Double immunofluorescent labeling of spinal cord sections suggests that BDNF co-localizes with the neuronal marker MAP2 but not with the microglial marker OX-42 (CD11b) or the astrocytic marker GFAP at day seven (Figure 6.5). A limited amount of BDNF is also found to co-localize with neurons, but not microglia or astrocytes, in the spinal cord in the sham group at day seven (Figure 6.5). The same patterns are observed at day one for both groups (data not shown). All double-labeled spinal cord images for each rat on both days one and seven for the distraction and sham groups are also included in Appendix E.

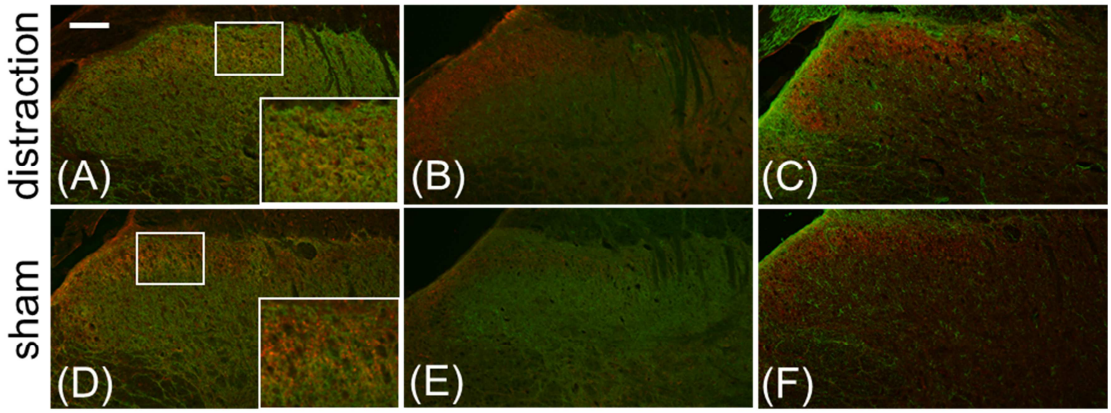


**Figure 6.5.** Representative co-labeling of BDNF with MAP2 **(A,D)**, OX-42 **(B,E)**, and GFAP **(C,F)**. **(A-C)** BDNF immunolabeling (red) co-localizes (yellow) with MAP2 **(A)** but not with OX-42 **(B)** or GFAP **(C)** on day seven after facet distraction. **(D-F)** Similarly, BDNF co-localizes with MAP2 **(D)** but not OX-42 **(E)** or GFAP **(F)** on day seven after sham. Scale bar=100μm in **(A)** and applies to panels **(A-F)**. MAP2, OX-42, GFAP label as green in **(A-F)**.

### 6.4.5. Behavioral Responses & ERK Activation After Spinal BDNF Sequestration

Before treatment, a joint distraction significantly reduces the withdrawal threshold compared to baseline responses in both the trkB-Fc ($p<0.017$) and vehicle ($p<0.005$) groups that is evident on all days up to and including day five (Figure 6.6A). The single

intrathecal injection of trkB-Fc increases the withdrawal threshold on both day six and day seven, returning it to baseline levels ($p>0.522$) for those rats (Figure 6.6A). However, the vehicle injection has no effect on the withdrawal threshold, which remains significantly decreased compared to baseline ($p<0.022$) at both days six and seven (Figure 6.6A).

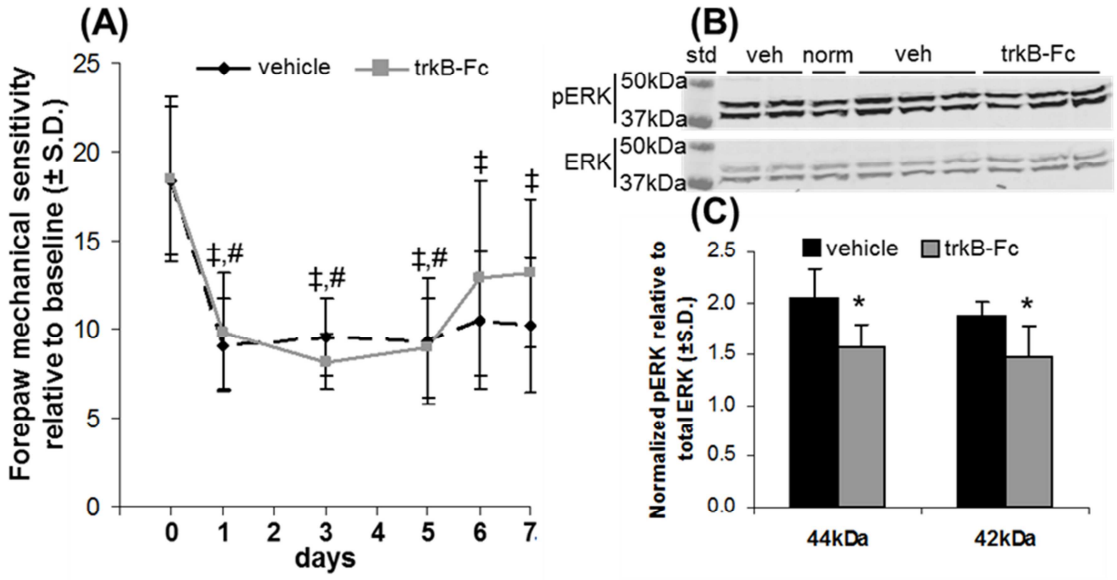


**Figure 6.6. (A)** The withdrawal threshold for von Frey filament stimulation is significantly reduced from baseline responses after joint distraction in both the trkB-Fc (#$p<0.017$; n=6) and vehicle (‡$p<0.005$; n=7) groups until treatment is given on day five. TrkB-Fc injection removes that decrease in the withdrawal threshold on days six and seven; vehicle injection has no effect on the withdrawal threshold, which remains significantly lower (‡$p<0.022$) than baseline on those days. **(B)** Representative immunoblots showing pERK1 (44kDa) & pERK2 (42kDa) and total ERK1 (44kDa) & total ERK2 (42kDa) in the spinal cord at day seven. **(C)** TrkB-Fc treatment significantly decreases both the ratio of pERK1/ERK1 (*$p=0.013$) and pERK2/ERK2 (*$p=0.047$). The pound symbol (#) indicates significant differences between trkB-Fc and the corresponding baseline response; the double-cross symbol (‡) indicates significant differences between vehicle and the corresponding baseline response; the asterisk (*) indicates significant differences between trkB-Fc and vehicle.

Both phosphorylated ERK1/2 and total ERK1/2 are detected at the expected molecular weights in the spinal cords of all rats receiving either intrathecal trkB-Fc or

vehicle (Figure 6.6B). Paralleling the behavioral outcomes, both spinal pERK1/ERK1 and pERK2/ERK2 are significantly decreased ($p<0.045$) at day seven after treatment with trkB-Fc. The individual behavioral data for each rat in this sequestration study are provided in Appendix C, and the quantification of ERK and pERK levels by Western blot is summarized in Appendix F.

## 6.5. Discussion

These findings demonstrate that BDNF is upregulated by day seven in both the DRG and spinal cord after a painful facet joint injury (Figures 6.2-6.4). Although increased BDNF is associated with a variety of painful conditions, ranging from plantar incision to spinal nerve transection (Cho et al., 1997; Li et al., 2006; Li et al., 2008; Mannion et al., 1999; Obata et al., 2006; Zhou et al., 1999), this is the first demonstration for *joint pain*. Synovial BDNF is elevated in arthritic joints, and inflammation of the lumbar facet joint can upregulate BDNF in afferents that innervate that joint (Grimsholm et al., 2008; Ohtori et al., 2001; Ohtori et al., 2002; Rihl et al., 2005). Yet, none of those studies define BDNF in the context of pain. Behavioral sensitivity increases nearly 3-fold immediately after a painful distraction and is sustained through day seven (Figure 6.1); however, increases in BDNF are not as robust and only evident at day seven (Figures 6.2-6.4). Sequestering spinal BDNF only partially attenuates the behavioral hypersensitivity after distraction (Figure 6.6). Spinal trkB-Fc significantly reduces spinal ERK activation, which is associated with pain and is known to be involved in BDNF-trkB signaling (Ji et al., 2002; Pezet et al., 2002; Slack et al., 2004). These findings indicate that a mechanical joint injury induces a functionally-relevant BDNF response but that it is not the sole

mediator of facet joint pain. Indeed, studies in Chapter 5 describe a contribution of NGF to the development of injury-induced joint pain (Kras et al., 2014b), and previous work with this injury model identified increased substance P levels in the DRG seven days after painful injury (Lee and Winkelstein, 2009). Expression of both BDNF and substance P are regulated by NGF signaling (Merighi et al., 2004; Pezet and McMahon, 2006), so it may be possible that NGF initiates joint pain but that substance P and BDNF are downstream messengers that contribute to its maintenance. Nevertheless, inflammatory and neuropeptide mechanisms in addition to spinal BDNF signaling are likely involved in the complex response to painful joint injury.

Although mRNA levels of BDNF are altered at day seven in the spinal cord, no changes are detected in the DRG at either day one or seven (Figure 6.2). BDNF mRNA has been reported to increase in the DRG as early as one day after a painful CFA-induced inflammatory stimulus not causing mechanical damage to afferents (Kobayashi et al., 2008; Mannion et al., 1999). A previous study using our same rat model found no change in substance P mRNA in the DRG after a *painful* joint injury but an increase over time after *non-painful* mechanical joint loading (Lee and Winkelstein, 2009). Because substance P and BDNF are produced in the same primary afferent neurons (Merighi et al., 2008; Michael et al., 1997; Pezet and McMahon, 2006) and substance P mRNA is not altered by a painful joint distraction (Lee and Winkelstein, 2009), the lack of change in BDNF mRNA levels observed here is not surprising. Further, because substance P mRNA only changes over time after a *non-painful*, but not a *painful*, joint distraction (Lee and Winkelstein, 2009), it is possible that *painful* mechanical facet injury may

disrupt mRNA transcription, possibly via damage to the afferents in the facet joint capsule.

The joint loading applied in our model produces mechanical strains in the capsule tissue that are similar to those (60-82%) that induce axonal damage in capsule afferents in a goat model of facet distraction (Kallakuri et al., 2008; Quinn et al., 2007). Further, axonal degeneration is not fully developed until day seven following axonal trauma (Hubbard and Winkelstein, 2008), suggesting that the absence of altered BDNF mRNA in the DRG that is observed here (Figure 6.2) may be due to the disruption of normal mRNA production via axonal damage from painful facet distraction. Although it has not been characterized in this model of facet joint injury in the rat, such loading-induced axonal damage to joint afferents may also contribute to elevated NGF in the DRG after facet injury (Figure 5.4). Neural tissue injuries, such as spinal nerve ligation or ventral root transection, increase expression of NGF in the DRG at the spinal level of the injured tissue (Lee et al., 1998; Obata et al., 2004). As such, characterization of the structural response of joint afferents to facet joint loading may provide further insight into the specific cellular mechanisms that are associated with facet pain from joint trauma. Alternatively, the lack of change in BDNF mRNA in the DRG after facet joint injury may be an artifact of the small number of joint afferents that are exposed to injurious loading relative to the total number of afferents with cell bodies in the DRG (Figure 4.2; Table 4.1; Kras et al., 2013b). Retrograde tracing studies in Chapter 4 identified only 208 facet joint afferents at the C7 level, the level with the highest number of joint afferents, from thirteen total rats included in that study (Table 4.1; Kras et al., 2013b). Yet, a single cervical DRG in the rat is estimated to contain on the order of ten thousand sensory

neurons (Bergman and Ulfhake, 1998). The quantification technique used in the current study analyzed mRNA from the entire DRG and may not be sensitive enough to detect changes in mRNA in the joint afferents. Additional studies combining retrograde neuronal tracing techniques with in situ hybridization that can detect mRNA in individual cells (Michael et al., 1999) would better identify whether or not BDNF mRNA levels are increased after facet joint injury.

BDNF mRNA increases in the spinal cord at day seven after painful distraction (Figure 6.2), which is consistent with observations of other acute and chronic pain models (Duric and McCarson, 2007; Li et al., 2006). Normally, BDNF mRNA is undetected in the dorsal horn, so *any* amount after injury is believed to be from novel expression (Li et al., 2006). Increased transcription of spinal BDNF after painful joint distraction supports the localized synthesis of BDNF in the spinal cord, though there are several possible cellular sources. Sensory and motor neurons, as well as activated microglia and astrocytes, can upregulate BDNF transcription after injury (Coull et al., 2005; Dougherty et al., 2000; Ikeda et al., 2001; Li et al., 2006; Merighi et al., 2008). Although a 1.3-fold increase in spinal BDNF mRNA is detected by RT-PCR (Figure 6.2), that measurement technique prevents the cellular and regional localization of mRNA. The increase may be due to a large increase in a small region of the spinal cord or from a generalized increase throughout, or may be in a specific cell type. Identification of the spatiotemporal cellular sources of spinal and DRG BDNF mRNA will further clarify the biochemical mechanisms mediating facet pain.

The same cells that upregulate transcription of BDNF at day seven may also increase BDNF protein after joint distraction. Spinal BDNF is nearly doubled after a joint

distraction (Figure 6.4). Yet, this increase corresponds to a less than 20% increase in BDNF in the afferents in the DRG (Figure 6.3). Because neurons in the DRG normally produce and transport BDNF to the spinal cord, the change in BDNF that is observed in those neurons after distraction suggests that increased transport from the DRG may contribute to the elevated spinal BDNF at day seven. A previous study has shown that the dorsal nerve roots must be intact for increased BDNF to be evident in *both* the DRG and spinal cord (Zhou et al., 1999), implying that anterograde transport of BDNF from the DRG is the source of spinal BDNF. Although BDNF is elevated in DRG neurons after joint distraction at day seven, the increase is only slight compared to the more robust spinal response (Figures 6.3 & 6.4). Together with the increase in BDNF mRNA in the spinal cord, it is likely that there are sources other than the primary afferents that contribute to the increased spinal BDNF at day seven. Spinal astrocytes, microglia, and oligodendrocytes also produce BDNF and show increases in their expression of BDNF after injury to the spinal cord (Dougherty et al., 2000). Although spinal BDNF does not co-localize with astrocytes or microglia after facet joint injury (Figure 6.5), oligodendrocytes were not labeled in this study. Further investigations of BDNF co-labeling in oligodendrocytes are needed to determine if these cells contribute to the injury-induced increase in spinal BDNF.

Although mRNA and protein were assayed using different groups of rats, all rats received the same magnitude joint distraction and exhibited the same behavioral outcomes; further, since tissue assays used the same spinal levels (C6/C7) for both techniques, they can be taken as the same. Nevertheless, it is possible that variability in the magnitude of the changes in BDNF mRNA and protein in the spinal cord may be due

to inter-animal variation; future work quantifying both mRNA and protein levels in the same animals will help clearly define the relationships of BDNF and other responses in painful joint injury. Further, the current study does not identify which DRG neurons specifically innervate the injured facet joint, but retrograde neuronal tracing in this same model has identified over 50% of the DRG neurons innervating the C6/C7 facet joint to be peptidergic (Chapter 4; Kras et al., 2013b). The high percentage of peptidergic joint afferents, which are known to express BDNF, supports an important role for BDNF and this class of neurons in joint pain. Also using tracing methods, Ohtori found that facet joint inflammation increases the number of joint afferents expressing BDNF (Ohtori et al., 2002), providing evidence that stimulation to the facet joint does induce changes in BDNF expression in its afferents. Although the afferents innervating the facet joint were not identified in the current study, such studies would help determine if the increased spinal BDNF at day seven is due to localized synthesis or increased transport from joint afferents. Exogenous NGF increases BDNF expression in the DRG as well as the spinal cord, and BDNF accumulates in the axons proximal to the DRG when the nerve root is ligated (Michael et al., 1997), suggesting that transport of BDNF from the DRG contributes to NGF-induced increases in spinal BDNF. Injury to the sciatic nerve similarly induces increased spinal BDNF that is blocked when the dorsal nerve root is ligated or transected (Zhou et al., 1996; Zhou et al., 1999), adding further support to the notion that transport of BDNF from the DRG is a major source of spinal BDNF. Taking these studies demonstrating anterograde transport of BDNF to the spinal cord after injury or NGF application together with loading-induced increases in NGF in the facet joint (Figure 5.3) suggests that increased transport of BDNF from the DRG likely contributes

to the increase in spinal BDNF that is seen after joint injury (Figure 6.4). Nevertheless, blocking BDNF transport from the DRG to the spinal cord is necessary to determine if facet injury-induced spinal BDNF increases are a result of retrograde transport from the DRG or localized synthesis in the spinal cord.

The increase in spinal BDNF protein (Figure 6.4) is consistent with other models of pain in the periphery (Cho et al., 1997; Mannion et al., 1999; Zhou et al., 2011). The increase in spinal BDNF at day 7 corresponds to a time point when spinal neurons are hyperexcitable and glutamate signaling is altered in this model (Chapter 5; Dong and Winkelstein, 2010; Kras et al., 2014b; Quinn et al., 2010). Elevated spinal BDNF has been associated with both neuronal and behavioral hyperexcitability through release from primary afferents and subsequent activation of glutamate receptors (Geng et al., 2010; Matayoshi et al., 2005; Slack et al., 2004). The co-localization of BDNF with the neuronal marker, MAP2, in the dorsal horn (Figure 6.5A) suggests that neurons may be responsible for the increase in spinal BDNF and supports a potential contribution of BDNF to the joint loading-induced neuronal hyperexcitability that is evident at day seven (Chapter 5; Kras et al., 2014b; Quinn et al., 2010). Yet, spinal hyperexcitability is also evident as early as one day after painful joint injury (Chapter 5; Crosby et al., 2013; Kras et al., 2014b), a time at which BDNF levels are no different from sham in either the DRG or spinal cord. Although BDNF may contribute to increased neuronal firing in the spinal cord, it is unlikely the sole mediator of facet injury-induced hyperexcitability. Indeed, $PGE_2$ contributes to the development, but not the maintenance, of joint inflammation-induced spinal neuronal hyperexcitability (Vasquez et al., 2001). In fact, since spinal $PGE_2$ is increased by day one after facet joint injury (Kras et al., 2014a), it likely

contributes to neuronal hyperexcitability at this early time point. Sequestering spinal BDNF partially alleviates injury-induced pain together with reducing spinal pERK (Figure 6.6), which supports BDNF's contribution to joint pain via an ERK-mediated pathway. In fact, the current data are in agreement with previous studies reporting reduced ERK activation due to BDNF sequestration (Pezet et al., 2002). ERK is activated when the BDNF receptor, trkB, is phosphorylated, as occurs during noxious mechanical stimulation of the paw (Pezet et al., 2002; Slack et al., 2004).

Since activation of ERK is associated with inflammatory pain and interference with its activation inhibits the development of mechanical hypersensitivity in the rat after inflammatory stimuli in the paws (Ji et al., 2002; Kawasaki et al. 2004), ERK activation is a key intracellular signaling mechanism leading to pain. The current findings that both ERK activation and behavioral sensitivity are reduced after BDNF sequestration in the spinal cord (Figure 6.6) are consistent with the notion of ERK as a key contributor to pain and support a role for BDNF-trkB signaling in joint pain. Since BDNF induces long-term potentiation in spinal neurons through an ERK-dependent mechanism (Zhou et al., 2008), elevated spinal BDNF may contribute to the neuronal hyperexcitability after painful joint distraction. Further, glutamate receptor activation contributes to BDNF-induced mechanical sensitivity (Geng et al., 2010), and ERK activation is associated with phosphorylation of glutamate receptors (Slack et al., 2004). Altered glutamate signaling, which also has been demonstrated to occur after a painful joint distraction (Dong and Winkelstein, 2010), may be a mechanism through which BDNF and ERK contribute to facet joint pain. Additional studies specifically determining the effects of BDNF on spinal neuronal excitability and glutamate signaling after painful and non-painful joint

injuries would further clarify the mechanism(s) through which spinal BDNF may contribute to facet joint-mediated pain.

## 6.6. Conclusions & Integration

Studies in this chapter support at least a partial role for spinal BDNF in the maintenance of pain from injurious facet joint loading. Yet, contributions from other neuropeptides and inflammatory mediators, such as prostaglandin $E_2$ and NGF, likely also contribute at both early and later time points (Kras et al., 2014a; Lee and Winkelstein, 2009). Indeed, intra-articular NGF has a critical role in the initiation of pain after facet joint injury (Chapter 5; Kras et al., 2014b), although the relationship between intra-articular NGF, neuronal BDNF, and chronic joint pain is not directly tested in this thesis. Yet, NGF is a regulator of BDNF expression that is capable of increasing BDNF levels in both the DRG and spinal cord (Apfel et al., 1996; Michael et al., 1997). This relationship between NGF and BDNF expression suggests that NGF signaling immediately following joint injury may induce upregulation of BDNF in the primary afferents and increase transport to the spinal cord at later time points, contributing to persistent pain. Although spinal BDNF sequestration attenuates pain after joint distraction, it does not fully abolish it (Figure 6.6). Further studies clarifying the mechanisms by which spinal BDNF and ERK activation contribute to pain after mechanical joint injury are needed to define the relationship between that neurotrophin and the complex mechanisms underlying facet-mediated pain. Nevertheless, an upregulation of BDNF and partial alleviation of hypersensitivity via BDNF sequestration provides the first evidence of a role for spinal BDNF in joint pain.

Although spinal neuronal hyperexcitability (Chapter 5) and upregulation of BDNF protein in the spinal cord (Chapter 6) are associated with joint pain, the spinal cord only represents the first relay of nociceptive signaling from the periphery to the central nervous system. Many higher order structures in the brain, such as the brainstem, periaqueductal gray matter, amygdala, thalamus and cortex, receive information related to nociception (Basbaum et al., 2009; Merighi et al., 2008; Steeds, 2009). Although there is no single region of the brain responsible for the perception of pain (Apkarian et al., 2005; Basbaum et al., 2009), the thalamus is a key structure in the processing of sensory information (Steeds, 2009), and the spinothalamic tract (STT) has traditionally been thought of as the main nociceptive pathway to the brain (Merighi et al., 2008). Models of painful arthritis report altered gene transcript levels and neuronal hyperexcitability in the thalamus in association with joint inflammation (Gautron and Guilbaud, 1982; Luo et al., 2014; Neto et al., 2008), supporting thalamic involvement in inflammatory joint pain. Further, the cellular responses to painful loading-induced facet joint injury, of which joint inflammation is a component, may also extend to the thalamus. In fact, neurons of the STT, which project from both the superficial (I-II) and deeper (IV-VI) laminae of the dorsal horn to the thalamus, express receptors for BDNF (Slack et al., 2005). Further, ERK is activated in STT neurons in response to BDNF release in the spinal cord (Slack et al., 2005). These anatomical observations suggest that facet joint injury-induced increases in spinal BDNF and ERK activation associated with neuronal hyperexcitability may also lead to increased activation of thalamic neurons. Although injury-induced spinal neuronal hyperexcitability (Chapter 5) and the role of spinal BDNF in the maintenance of joint pain (Chapter 6) support a central component for facet-mediated pain; studies in Chapter

7 further define the central modifications associated with persistent facet joint pain by assessing electrophysiological responses in the thalamus after injury at a time point when spinal BDNF expression is elevated.

# Chapter 7

# Thalamic Neuronal Hyperexcitability After Facet Joint Injury: Supraspinal Contributions to Facet-Mediated Pain

*Parts of this chapter are adapted from:*

Weisshaar CL, Kras JV, Pall PS, Kartha S, Winkelstein BA (2015). Non-peptidergic afferents in the facet joint mediate injury-induced pain and mediate thalamic hyperexcitability via supraspinal and spinal glutamate transporters. *Brain Research*, submitted.

## 7.1. Overview

Studies presented in Chapters 5 and 6 describe a joint injury-induced increase in spinal brain-derived neurotrophic factor (BDNF) (Chapter 6) at a time when spinal neurons are also hyperexcitable (Chapter 5) (Kras et al., 2013c; Kras et al., 2014b). Those findings support spinal neuronal hyperexcitability as contributing to facet-mediated pain. Hyperexcitability in neurons in the CNS can occur due to enhanced synaptic efficacy and membrane excitability, which are components of central sensitization (Latremoliere and Woolf, 2009). Such a sensitized state can result in normally innocuous stimuli being perceived as painful, even in the absence of any evidence of injury (Latremoliere and Woolf, 2009). However, the studies in Chapters 5 and 6 only evaluated joint injury-induced responses in the spinal cord. Yet, nociceptive information is transmitted from the spinal cord to many regions of the brain; among those brain regions, the thalamus has a

major role in relaying pain signals for sensation (Basbaum et al., 2009; Merighi et al., 2008; Steeds, 2009).

Neurons from laminae I and V in the spinal dorsal horn, which are regions that receive nociceptive sensory input from primary afferents, project to the thalamus via the lateral spinothalamic track (STT) and the anterior STT, respectively (Dostrovsky and Craig, 2013) (see Section 1.2.2). Thalamic neurons activated by mechanical joint stimulation become hyperexcitable in states of painful arthritis and joint inflammation (Gautron and Guilbaud, 1982; Luo et al., 2014). Further, the number of thalamocortical neurons that respond to graded stimulation as wide dynamic range (WDR) neurons increases in arthritis (Dostrovsky and Craig, 2013); when taken together with arthritis-induced thalamic neuronal hyperexcitability, supports enhanced thalamic neuronal activity in association with joint pain. Some thalamic neurons express the trkB receptor and are activated by spinal BDNF (Slack et al., 2005). Joint inflammation and elevated spinal levels of BDNF are associated with loading-induced facet pain (Dong et al., 2013a; Kras et al., 2013c). Despite documented activation and hyperexcitability of thalamic neurons in association with joint inflammation and spinal BDNF signaling (Gautron and Guilbaud, 1982; Slack et al., 2005), thalamic neuronal firing in facet joint injury-induced pain has not been evaluated.

Studies in this chapter characterize the evoked excitability of thalamic neurons after a painful facet joint distraction that is sufficient to induce sustained behavioral hypersensitivity and spinal neuronal hyperexcitability (Crosby et al., 2013; Dong et al., 2013a; Kras et al., 2013c; Quinn et al., 2010). This work specifically tests the hypothesis that painful mechanical injury of the cervical facet joint induces hyperexcitability in

neurons within the thalamus. As such, evoked thalamic neuronal excitability is quantified at day seven after a painful joint distraction using a stimulus train of both innocuous and noxious stimuli applied to the forepaw, where behavioral sensitivity is also measured. Based on those findings and to complement studies in Chapter 5 demonstrating that intact innervation of the facet joint is necessary for facet-mediated pain (Figure 5.4), a second study tests the hypothesis that non-peptidergic afferents in the facet joint contribute to the development and maintenance of joint injury-induced pain *and* thalamic neuronal hyperexcitability. Accordingly, non-peptidergic joint afferents were ablated prior to joint injury using the same methods of isolectin B4-conjugated saporin injection described in Chapter 5, followed by quantifying thalamic neuronal excitability at day seven after joint injury. Together, these studies aim to identify whether or not non-physiologic facet joint loading conditionally enhances activity in the thalamus when injury-induced behavioral hypersensitivity is evident.

## 7.2. Relevant Background

The facet joint is the most common source of neck pain (Bogduk, 2011; Lord et al., 1996), and biomechanical studies using cadavers as well as animal studies support non-physiologic loading of the facet joint capsular ligament as a potential initiator of pain (Barnsley et al., 1995; Bogduk and Aprill, 1993; Chen et al., 2006; Lu et al., 2005; Panjabi et al., 1998; Pearson et al., 2004; Sundararajan et al., 2004). Both Aδ- and C-fiber nociceptors innervate the cervical facet joint and are activated by tensile loading of that joint (Chen et al, 2006; Lu et al., 2005). Further, primary sensory neurons can be classified as peptidergic or non-peptidergic (see Section 1.2.2), and studies in Chapter 4

identified peptidergic afferents as representing greater than 50% of the neurons that innervate the C6/C7 facet joint in the rat (Chapter 4; Kras et al., 2013b; Merighi et al., 2008). Moreover, peptidergic signaling among joint afferents is necessary for the development of loading-induced facet joint pain (Figure 5.4) (Kras et al., 2014b). However, non-peptidergic afferents may also have a role in facet joint pain. Ishikawa reported that 11±2% of the neurons innervating lumbar facet joints bind isolectin B4 (IB4) and are non-peptidergic (Ishikawa et al., 2005). Up to one-third of nerve growth factor (NGF) sensitive neurons also bind IB4 (Joseph and Levine, 2010). Moreover, NGF facilitates inflammatory hyperalgesia by inducing a switch to a PKCε-dependent mechanism for $PGE_2$ signaling in IB4-positive neurons (Joseph and Levine, 2010; Parada et al., 2005). This contribution of non-peptidergic afferents to pain associated with NGF and $PGE_2$ signaling, taken in the context of facet joint loading-induced increases in NGF in the joint and $PGE_2$ in the spinal cord (Chapter 5; Kras et al., 2014a; Kras et al., 2014b), suggests that non-peptidergic afferents may regulate the expression of pain mediators following facet joint injury that contribute to behavioral hypersensitivity. Moreover, because each of NGF and $PGE_2$ are sufficient to induce hyperexcitability in the central nervous system in addition to behavioral hypersensitivity (Guilbaud et al., 1982; Hoheisel et al., 2007; Kras et al., 2014b; Vasquez et al., 2001), non-peptidergic afferents may have a role in the enhanced central neuronal excitability that maintains pain. Yet, no study has identified whether or not non-peptidergic joint afferents contribute to the neuronal hyperexcitability that is evident in the CNS after a painful facet joint injury.

Painful loading of the facet joint is associated with joint inflammation and spinal neuronal hyperexcitability and upregulates many pain mediators in the dorsal root

ganglion (DRG) and spinal cord, including $PGE_2$, NGF, and BDNF (Chapters 5 & 6; Crosby et al., 2013; Dong et al., 2008; Dong et al., 2013a; Kras et al., 2013c; Kras et al., 2014a; Kras et al., 2014b; Lee et al., 2008; Quinn et al., 2010). Spinal BDNF contributes to the maintenance of loading-induced facet pain and increases phosphorylation of the mitogen-activated protein kinase extracellular signal-regulated kinase (ERK) (Kras et al., 2013c), which has been implicated in inflammatory pain cascades (Ji et al., 2002; Kawasaki et al. 2004). Moreover, spinal BDNF signaling increases the excitability of neurons in the spinal cord after neural tissue injury (Geng et al., 2010; Lu et al., 2009). Yet, nociceptive sensory information in the spinal cord is relayed to the thalamus via the spinothalamic tract where it undergoes further processing before being relayed to the brain structures, such as the cortex, that are involved in the conscious perception of pain (Dostrovsky, 2000; Millan, 1999). Sensory neurons with cutaneous input, as well as neurons that innervate deep tissues like joints and viscera, converge in the thalamus (Millan, 1999). Indeed, this convergence of sensory information from multiple anatomical regions may serve as a potential mechanism for development of referred pain and suggests that alterations in thalamic neuronal excitability may mediate hypersensitivity measured in the forepaw after a facet joint injury (Dong et al., 2013a; Kras et al., 2013c; Kras et al., 2014b).

All nociceptive information that reaches the cortex is first received and processed by the thalamus (Dostrovsky, 2000; Merighi et al., 2008); the STT is the major ascending pathway for pain transmission (Purves et al., 2001). A majority of the STT neurons projecting from the superficial and deep laminae of the dorsal horn are sensitive to BDNF and exhibit increased activation of ERK in response to BDNF signaling (Slack et al.,

2005). Spinal BDNF is increased seven days after a painful facet joint injury (Figure 6.4), and sequestering spinal BDNF alleviates injury-induced pain and reduces spinal ERK activation (Figure 6.6) (Kras et al., 2013c), suggesting that increased spinal BDNF after joint injury may also activate thalamic neurons. In fact, alterations in thalamic neuronal firing patterns and evoked firing rates have been associated with inflammation- and neural tissue injury-induced pain (Huh et al., 2012; Iwata et al., 2011; Syré et al., 2014). Moreover, thalamic neurons receiving input from joints are hyperexcitable during arthritis and painful joint inflammation, such that normal joint movements or low threshold mechanical stimuli elicit neuronal firing in arthritic rats but not controls (Dostrovsky and Guilbaud, 1990; Gautron and Guilbaud, 1982; Luo et al., 2014). Since loading-induced facet joint pain is also associated with joint inflammation (Dong et al., 2013a), the excitability of thalamic neurons is hypothesized to increase after painful joint injury.

Considering that the thalamus is the major relay center for nociceptive information from the spinal cord to the rest of the brain, one objective of this work is to identify if facet joint injury induces hyperexcitability in thalamic neurons in association with pain. Of the thalamic nuclei that receive nociceptive input via the STT, neurons in the ventral posterolateral nucleus (VPL) encode the intensity and location of noxious stimuli, with receptive fields encompassing the forepaw (Francis et al., 2008; Millan, 1999). As such, excitability of thalamic neurons is quantified in the VPL in rats seven days after the painful facet joint injury that was described in detail in Chapter 3 and used for studies in Chapters 4-6. In addition, neurons were classified as either wide dynamic range (WDR), low threshold mechanoreceptive (LTM), or nociceptive specific (NS)

based on their responses to von Frey stimulation (Saito et al., 2008; Syré et al., 2014) since an increase in the number of neurons responding as WDR is believed to contribute to central sensitization (Coghill et al., 1993; Dostrovsky and Craig, 2013). Based on findings in that characterization study, a second study applied intra-articular IB4-saporin (as described in Chapter 5) two weeks prior to joint injury in order to ablate non-peptidergic joint afferents. The goal of those studies was to define if non-peptidergic joint afferents have a role in thalamic neuronal hyperexcitability following a facet joint distraction of identical magnitude to the one applied in the characterization study.

## 7.3. Methods

Male Holtzman rats (Harlan Sprague-Dawley, Indianapolis, IN) (405±25g) were housed under USDA- and AAALAC-compliant conditions with a 12-12 hour light-dark cycle and free access to food and water. Experimental procedures were approved by the IACUC and carried out under the guidelines of the Committee for Research and Ethical Issues of the International Association for the Study of Pain (Zimmermann, 1983).

### 7.3.1. Surgical Procedures for Characterization Study

All surgical procedures were performed under inhalation isoflurane anesthesia (4% induction, 2.5% maintenance). Rats included in the characterization study underwent either a painful cervical facet joint distraction injury (FJD n=4) or a sham procedure (sham n=3), as described in Section 3.3.1 and used in previously published studies (Dong et al., 2011; Kras et al., 2013a). Briefly, the C6 and C7 laminae were exposed and attached to a loading device via microforceps, and C6 was displaced rostrally while C7

was held in place. A camera mounted to a surgical dissecting scope tracked markers that were placed on the C6 and C7 laminae during the joint injury. Peak displacement of the C6 forceps and the corresponding peak capsular ligament distraction and maximum principal strain of the capsule during each distraction were quantified as measures of the severity of the applied injury. An additional group of rats underwent sham surgical procedures with device attachment but no applied joint distraction to serve as controls. Following surgery, the incision was closed and rats were recovered in room air.

### 7.3.2. Intra-Articular Saporin Injections & Facet Joint Distraction Procedures

Neurons that bind IB4 are typically non-peptidergic (Basbaum et al., 2009; Merighi et al., 2008) and are involved in pain from nerve injury and also separately from inflammation (Hucho et al., 2005; Parada et al., 2005; Tarpley et al., 2004). In order to identify the contribution, if any, of this population of sensory neurons in the joint to thalamic neuronal hyperexcitability in the case of facet pain, additional separate groups of rats received intra-articular injections of 5µg of saporin conjugated to isolectin B4 (IB4-Sap n=12) in 5µL of PBS to ablate the IB4-binding neurons (Chapter 5; Kras et al., 2014b). That dose of IB4-Sap was selected from a previously published report as sufficient to ablate non-peptidergic afferents (Tarpley et al., 2004) and is the same as the dose used in the earlier studies assessing intra-articular NGF-induced facet joint-mediated pain in Chapter 5. IB4-Sap was administered using established methods for intra-articular injection (Dong et al., 2013a; Kras et al., 2014b). Briefly, the bilateral C6/C7 facet joints were exposed as described above in Section 7.3.1. A 33-gauge beveled needle attached to a 10µL syringe (Hamilton Company; Reno, NV) was advanced manually into the facet

joint using a dorsal approach, and 5µg of IB4-Sap in 10µL of PBS was slowly injected into the bilateral facet joints. Following joint injections, wounds were closed with polyester suture and surgical staples, and the rats were recovered in room air.

Because saporin has been documented to induce cell death within fourteen days (Weisshaar et al., 2014; Wiley et al., 2007), that time period was waited prior to the rats undergoing either a facet joint distraction or sham procedure. Under inhalation isoflurane anesthesia, the surgical staples and suture were removed, and rats underwent either a facet joint distraction (IB4-Sap+FJD n=6) or sham (IB4-Sap+sham n=6) procedure as described in Section 7.3.1. For all rats in the IB4-Sap+FJD group, peak displacement of the C6 forceps and the corresponding peak capsular ligament distraction and maximum principal strain in the capsule during each distraction were quantified as measures of the injury severity to enable comparison to the rats in the characterization study. Wounds were closed again, and the rats were recovered in room air.

### 7.3.3. Behavioral Assessment of Mechanical Hyperalgesia

Bilateral forepaw mechanical hyperalgesia was evaluated in all rats using the methods described in Section 3.3.2 (Lee and Winkelstein, 2009; Quinn et al., 2010; Weisshaar et al., 2010). In the characterization study, baseline measurements were recorded for three days prior to any surgical procedure. Because the time course of behavioral hypersensitivity onset and maintenance following facet joint distraction has been well-documented in the rat (Chapters 3-6; Crosby et al., 2013; Dong et al., 2013a; Kras et al., 2013b; Lee and Winkelstein, 2009), in the current study, hyperalgesia was only measured on day seven after the injury or sham procedure in order to verify that

injury-induced behavioral hypersensitivity is evident on the day of electrophysiological assessment. For the saporin rats, forepaw mechanical withdrawal thresholds were measured for each rat at baseline (day 0) before surgery and on day seven following facet joint distraction or sham procedures. For assessing mechanical hyperalgesia, a given filament was recorded as the response threshold if the next higher filament also induced a positive response (Crosby et al., 2013; Lee and Winkelstein, 2009). Although the applied joint distraction induces a bilateral injury, response thresholds from only the right forepaw were considered for analysis in order to parallel the electrophysiological studies in the VPL that recorded only from those neurons with input from that forepaw. For the characterization study, response thresholds at day seven were compared between the distraction and sham groups and to each of their respective baseline values using a two-way repeated measures ANOVA with Tukey's HSD test, with time and group as the factors. Behavioral responses for the IB4-saporin study were similarly compared using a two-way repeated measures ANOVA with group (IB4-Sap+FJD, IB4-Sap+sham) and time (day 0, day 7) as factors with post hoc Tukey's HSD test.

### 7.3.4. Electrophysiological Recordings in the Thalamus

In order to quantify thalamic neuronal excitability after facet joint injury, all rats were prepared for electrophysiological recordings in the VPL after behavioral testing on day seven. All rats were anesthetized with sodium pentobarbital (45mg/kg, i.p.). A midline incision was made over the skull, and the soft tissue was removed to reveal the coronal, sagittal, and lambdoid cranial sutures (Figure 7.1A). In order to gain access to the VPL (Figure 7.1B), the cortex overlying the thalamus was exposed via an 8mm by

8mm craniotomy over the left hemisphere beginning at bregma and extending caudally and laterally (Syré et al., 2014). The mid-cervical trachea was exposed, cannulated, and ventilated (CWE Inc.; Ardmore, PA) with room air at approximately 40 breaths/minute, and the end tidal $CO_2$ concentration was monitored. The rat was mounted onto a stereotaxic frame with blunt ear bars (Figure 7.1C), and the head was adjusted so bregma and lambda were in the horizontal plane. The dura was removed, and the brain was bathed in 37°C mineral oil. The core temperature of the rat was maintained at 35-37°C using a feedback controlled heating plate with a rectal probe (Physitemp Instruments Inc.; Clifton, NJ). Anesthesia was maintained throughout all procedures with supplemental doses of sodium pentobarbital (5-10mg/kg, i.p.) as needed.

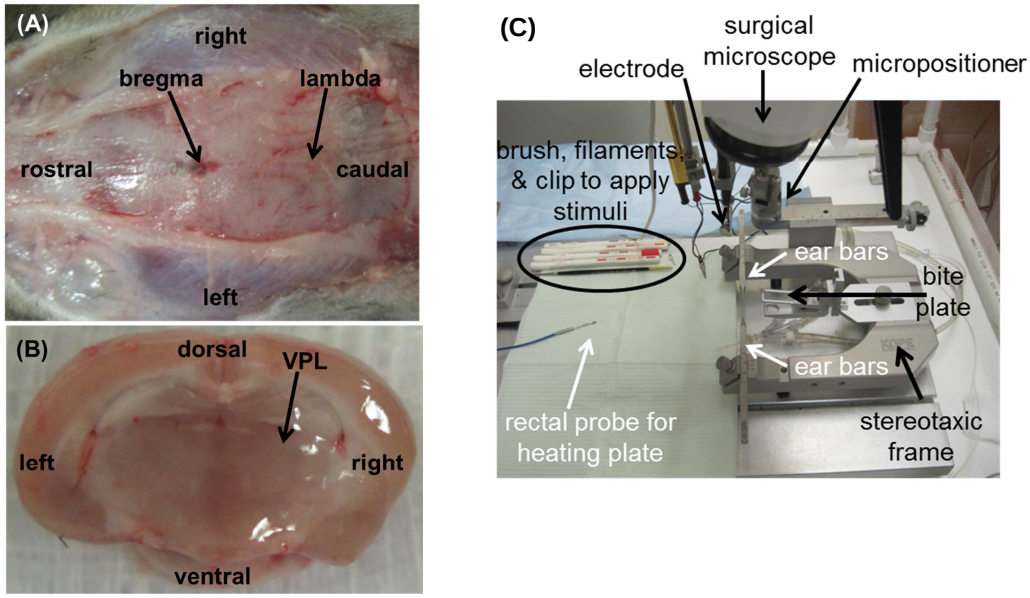


**Figure 7.1. (A)** Exposed rat skull illustrating bregma and lambda. **(B)** Cross-section of a rat brain illustrating the location of the VPL. **(C)** Instrumentation for extracellular recordings in the rat. A tungsten electrode measures extracellular signals in the VPL during stimulation of the forepaw with a series of mechanical stimuli, including four von Frey filaments, a non-noxious brush, and a noxious pinch by a microvascular clip. During each experiment, the temperature of the rat was monitored via the rectal probe attached to a feedback controlled heating plate.

Extracellular voltage potentials were recorded in the VPL using glass-insulated tungsten electrodes (FHC; Bowdoin, ME). The signal was amplified, processed, and digitally sampled and stored as described in Chapter 5 (Dong et al., 2013b; Syré et al., 2014). Beginning at -2.5mm from bregma and 2.2mm left lateral, the electrode was lowered 5-7mm below the pial surface (Figure 7.1). Subsequent locations were probed at 1mm intervals in the anterior-posterior and medial-lateral planes, based on known coordinates and somatatopy of the rat VPL (Francis et al., 2008; Paxinos and Watson, 2007). Neurons were identified by light brushing of the plantar surface of the right forepaw using a cotton swab. A stimulus train identical to that described in Chapter 5 was applied to the forepaw (Figure 7.2) (Crosby et al., 2013; Kras et al., 2014b; Syré et al., 2014). The stimulus train consists of a light brush (applied for 10 seconds), a series of non-noxious and noxious von Frey filaments (1.4g, 4g, 10g, 26g), and a noxious pinch (60g vascular clip (WPI; Sarasota, FL); applied for 10 seconds) (Figure 7.2).

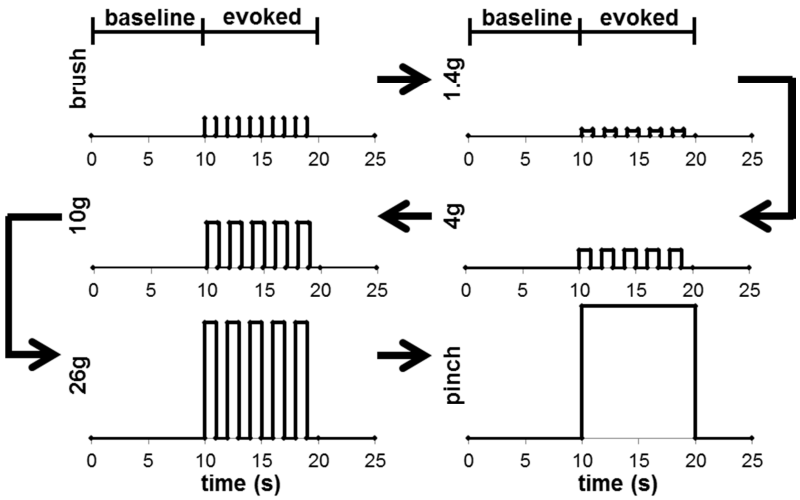


**Figure 7.2.** The stimulus train applied to the right forepaw consists of a light brush, von Frey filaments (1.4g, 4g, 10g, 26g), and a noxious pinch. Spikes are summed over the entire period of each stimulus application (evoked). Baseline spikes are summed over an equivalent time period (baseline) prior to the first application of each stimulus.

The strengths of the von Frey filaments used for the stimulus span the range used during mechanical withdrawal threshold testing for behavioral sensitivity. Each filament was applied for five stimulations of one second followed by one second of recovery. The different stimuli were applied at intervals of at least 60 seconds, and the evoked spikes were recorded.

To analyze individual neurons, recordings during the stimulus train were spike-sorted using Spike2 (CED; Cambridge, UK). Evoked spikes were summed over the continuous 10-second stimulus period for both the brush and pinch stimuli. The number of spikes evoked from the initial application of a von Frey filament until one second after the $5^{th}$ application of the filament were counted for each neuron (Figure 7.2). The duration of each stimulus was identified, and baseline firing was determined by counting the number of spikes over an equivalent time period (~10s) prior to initiation of the brush and pinch stimuli, as well as before the first application of each von Frey filament (Figure 7.2). Baseline spikes were subtracted from the total spike count for each stimulus in order to evaluate the evoked responses.

Neurons were classified based on their responses to von Frey stimulation (Saito et al., 2008; Syré et al., 2014). Wide dynamic range (WDR) neurons exhibited a graded response to increasing von Frey filament strength. Low threshold mechanoreceptors (LTM) responded to both non-noxious and noxious stimuli, and nociceptive specific (NS) neurons only responded to noxious von Frey filament stimulation. Because the distribution of spike totals for each stimulus exhibited a positive skew, spike counts were log-transformed to obtain a normal distribution for statistical analyses. Evoked firing for each stimulus was compared between groups using a two-way nested ANOVA, with

group and stimulus as factors, neurons nested within rats, and rats nested within group, with post hoc Tukey's HSD test. Within each study, evoked spike counts were compared between groups (FJD, sham; IB4-Sap+FJD, IB4-Sap+sham). Differences in the ratio of WDR neurons were also compared between groups in each study using Pearson's chi-square test.

## 7.4. Results

All rats undergoing joint distraction received the same severity of mechanical injury. The C6 forceps displacement, maximum capsular ligament distraction, and maximum principal strain across the ligament were compared between the IB4-Sap+FJD injury group and the FJD group using t-tests. The average displacement of the C6 forceps for the distraction group is 2.52±0.04mm, which is not different from the IB4-Sap+FJD group (2.51±0.03mm). Similarly, no differences are detected between injury groups for either the peak capsular ligament distraction (FJD 0.39±0.18mm; IB4-Sap+FJD 0.23±0.09mm) or the maximum principal strain in the ligament (FJD 40.31±9.48%; IB4-Sap+FJD 41.15±46.55%). These mechanical data demonstrate that the same magnitude of joint injury was applied to all groups undergoing an injury and that any differences in behavioral sensitivity or thalamic neuronal excitability are not due to differences in the injury itself. The maximum capsule distractions, as well as the associated maximum capsular ligament strains, for each rat included in this chapter are detailed in Appendix B.

The mechanical withdrawal threshold at day seven after sham procedures is not different from baseline (Figure 7.3). However, facet joint distraction induces hypersensitivity such that the withdrawal threshold is significantly reduced at day seven

compared to baseline ($p<0.036$) (Figure 7.3). Yet, despite a trend towards a reduced threshold ($p<0.631$) seven days after distraction compared to sham, statistical significance is not achieved between groups with these small group sizes (n=3-4 rats for each group). The individual mechanical withdrawal thresholds for each rat included in this study are summarized in Appendix C.

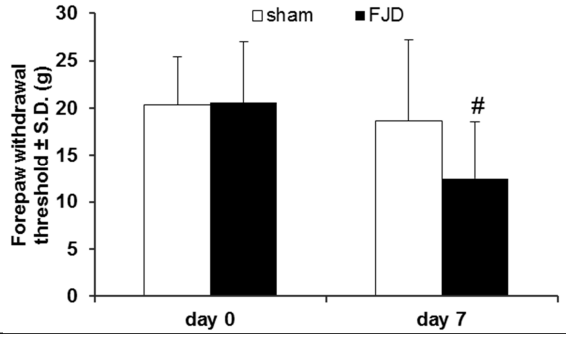


**Figure 7.3.** Mechanical sensitivity in the right forepaw as measured by the withdrawal threshold in response to von Frey filament stimulation. Withdrawal threshold decreases (#$p<0.034$) from baseline at day seven after facet joint distraction.

A total of 59 mechanosensitive neurons with input from the forepaw was recorded in the VPL at an average depth of 6.41±0.33mm below the pial surface in those rats that underwent distraction (24 neurons at 6.45±0.32mm depth) or sham (35 neurons at 6.38±0.33mm depth) procedures for the characterization study. Increased evoked firing is evident at day seven after injury, as observed in the representative traces during stimulation of the forepaw with the brush, von Frey, and pinch stimuli (Figure 7.4A). In fact, quantification of the neuronal firing in the left VPL demonstrates an increase in the number of spikes evoked by all of the von Frey filament strengths ($p<0.044$), except the non-noxious 1.4g filament after distraction (Figure 7.4B). Further, joint distraction induces an increase in the number of spikes evoked by both the brush ($p=0.003$) and the pinch ($p=0.001$) stimuli compared to the number evoked in sham animals (Figure 7.4C).

Despite an increase in neuronal excitability, there is no change in the proportion of neurons that respond to stimulation as WDR neurons. In the sham group, 63% of neurons were classified as WDR and 37% were LTM (Figure 7.4D); similarly, after distraction, 54% of neurons responded as WDR and 46% as LTM (Figure 7.4D). None of the recorded neurons were identified as nociceptive specific. The individual spinal neuronal firing data for each rat is summarized in Appendix G.

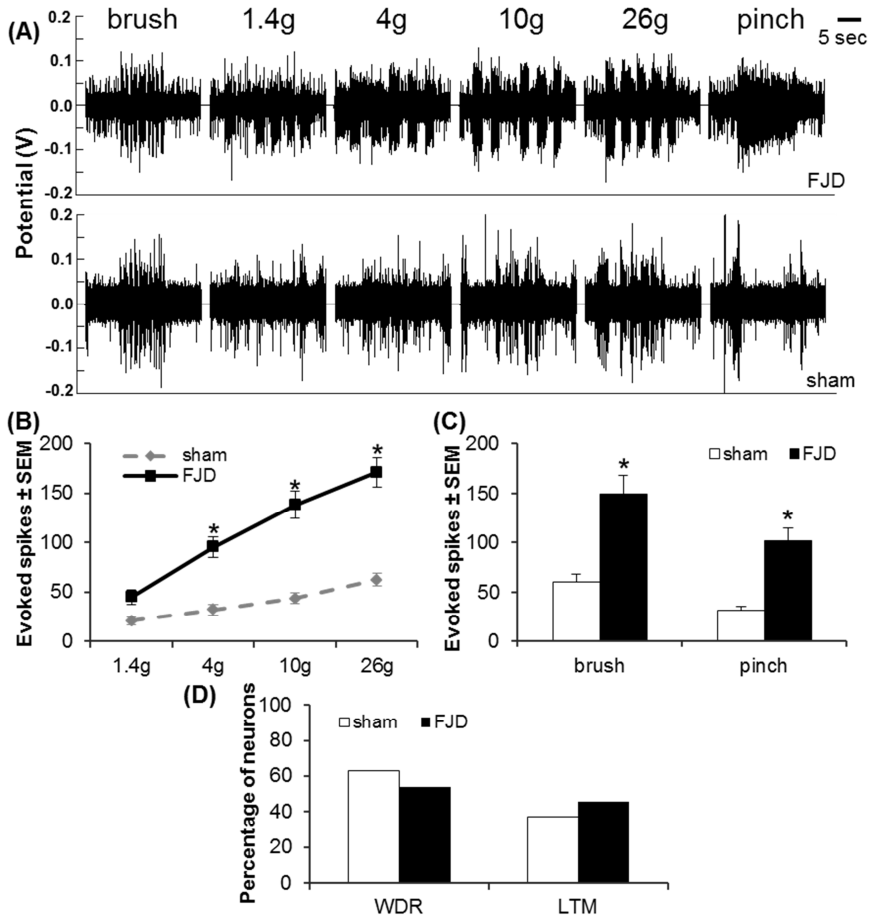


**Figure 7.4.** Hyperexcitability of thalamic neurons after distraction. **(A)** Representative traces illustrate increased evoked firing in the left VPL after distraction compared to sham. **(B & C)** Significantly more spikes are evoked by the 4g-26g von Frey filaments **(B)** and the brush and pinch **(C)** stimuli (*p<0.044) after FJD. **(D)** The percentage of neurons responding as WDR or LTM is unchanged between distraction and sham.

Ablating the IB4-positive joint afferents with saporin prior to a typically painful joint distraction prevents the development of mechanical hypersensitivity. On day seven, the withdrawal threshold to mechanical stimulation of the right forepaw is unchanged from baseline in both the IB4-Sap+FJD and the IB4-Sap+sham groups, and those two groups do not differ from each other (Figure 7.5A). Likewise, the excitability of VPL neurons also is not different between the IB4-Sap+FJD and the IB4-Sap+sham groups at day seven. In the VPL, 74 total neurons were recorded from both groups at an average depth of 6.27±0.42mm. The number of spikes evoked by each of the applied stimuli is not different between the IB4-Sap+FJD (33 neurons at 6.30±0.37mm depth) and the IB4-Sap+sham (41 neurons at 6.25±0.46mm depth) groups (Figure 7.5), and no differences are detected in the proportion of WDR neurons between groups (IB4-Sap+FJD 75.8%; IB4-Sap+sham 80.5%). Mechanical withdrawal thresholds for each rat are summarized in Appendix C; the individual spinal neuronal firing data for each rat is detailed in Appendix G.

## 7.5. Discussion

This study demonstrates that a painful facet joint injury induces hyperexcitability in the thalamus (Figures 7.3 & 7.4). Moreover, ablation of non-peptidergic joint afferents prevents the development of the behavioral hypersensitivity and thalamic neuronal hyperexcitability that are both evident seven days after a joint distraction (Figures 7.3-7.5). Hyperexcitability of thalamic neurons is associated with a variety of painful conditions, including injury to the peripheral nerve and nerve root (Syré et al., 2014; Zhao et al., 2006), but these data are the first evidence of increased thalamic activity in

*joint* pain from mechanical injury. Although increased evoked firing in the thalamus has been described for inflammatory arthritis (Gautron and Guilbaud, 1982), that study did not define neuronal excitability in the context of pain. Despite the association of thalamic neuronal hyperexcitability with joint pain, its functional role and the cellular mechanisms underlying the increased excitability are unknown.

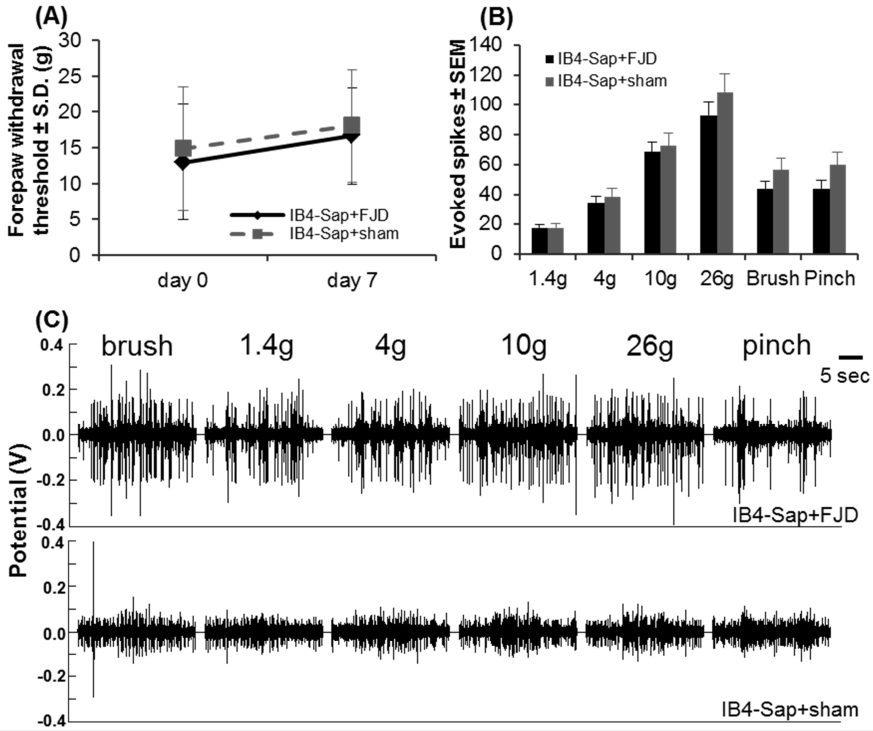


**Figure 7.5.** Ablation of non-peptidergic joint afferents prevents the development of injury-induced hypersensitivity and thalamic neuronal hyperexcitability. **(A)** Forepaw withdrawal threshold is unchanged after distraction (IB4-Sap+FJD) compared to baseline (day 0) or sham (IB4-Sap+sham) in rats given intra-articular IB4-Sap. **(B & C)** Excitability of neurons in the VPL is not different between IB4-Sap+FJD or IB4-Sap+sham rats for any of the applied stimuli.

Thalamic neuronal hyperexcitability at day seven after joint injury is evident for *both* noxious (10g, 26g, & pinch) and non-noxious (4g & brush) stimuli applied to the forepaw. Yet, evoked spikes induced by stimulation with the non-noxious 1.4g von Frey

filament are no different between the painful FJD and the non-painful sham groups. Of note, both the 1.4g and 4g von Frey filaments are considered non-noxious since they do not frequently evoke responses in normal rats (Dong et al., 2008; Dong and Winkelstein, 2010). The increased neuronal excitability that is observed in this study for mechanical forepaw stimuli greater than or equal to 4g is consistent with previous reports of facet joint injury-induced allodynia (Dong and Winkelstein, 2010; Dong et al., 2013a) in which significantly more forepaw withdrawals are evident for a 4g von Frey filament stimulus after a facet joint injury compared to sham controls. Since the average forepaw withdrawal threshold to mechanical stimulation has been reported to decrease to nearly 4g after painful facet joint distraction (Chapter 4; Crosby et al., 2014; Dong et al., 2011; Dong et al., 2013b), the neuronal hyperexcitability induced by stimulation with the 4g filament is not surprising. Yet, the withdrawal thresholds after injury do not approach 1.4g in those studies, so it is not surprising that the number of spikes evoked by the 1.4g filament is not elevated (Figure 7.4). Of note, in the current study, the withdrawal threshold for the forepaw is between 10g and 26g after joint injury (Figure 7.3). That withdrawal threshold suggests that thalamic neuronal hyperexcitability would not be evident for the 4g stimulus. However, only four rats were included in the injury group, and one of those rats (PSP11) exhibited an abnormally high withdrawal threshold (~20g; see Appendix C) after injury, shifting that group's average withdrawal threshold to over 10g. Including additional rats in the injury group would likely decrease the average withdrawal threshold, aligning it more with the electrophysiological findings in this study (Figures 7.3 & 7.4). A similar pattern of increased neuronal firing in response to both noxious (10g, 26g, & pinch) and normally non-noxious (4g & brush) stimuli is also

evident in the spinal cord at day seven in this model (Crosby et al., 2014; Quinn et al., 2010). Such similarities in neuronal responses between the two regions of the central nervous system may be a result of the neurons in the dorsal horn projecting to the thalamus. However, neuronal responses have not been quantified in both the thalamus and the spinal cord in the same animals. As such, it is not known if thalamic neuronal excitability is a direct result of spinal neuronal hyperexcitability. Because input from spinal neurons located in the deep laminae of the dorsal horn converges onto thalamic neurons, it is highly likely that hyperexcitability within spinal neurons drives the hyperexcitability of the thalamic neurons.

The apparent disconnect between evoked thalamic neuronal firing and the forepaw withdrawal threshold suggests that additional regions of the brain likely contribute to the overall response to forepaw stimulation. Indeed, the periaqueductal gray (PAG), the anterior cingulate cortex (ACC), and the primary somatosensory cortex (S1) are implicated in arthritis-mediated joint pain (Desantana et al., 2009; Guo et al., 2005; Lamour et al., 1983). The ACC has a role in the emotional aspect of pain sensation and contributes to the unpleasantness of pain (Guo et al., 2005); yet, activity in the ACC does not affect the threshold to withdrawal from a stimulus applied to the paw (Chen et al., 2012; LaGraize and Fuchs, 2007). Although hyperexcitability in the thalamus suggests the rats can detect the sensory aspect of the von Frey filament stimulation, the sensory information transmitted to the thalamus is further relayed to higher order regions involved in the sensory discriminative perception of pain, such as the primary somatosensory cortex. The excitability of neurons in S1 is increased during inflammation, and a lesion in this region alleviates inflammation-induced pain (Guilbaud

et al., 1993; Uhelski et al., 2012). Moreover, a unilateral noxious stimulus can activate neurons in S1 bilaterally, and this bilateral activity has been speculated to contribute to the motor responses to the stimulus (Wang et al., 2003). As such, the lack of a forepaw withdrawal in response to a stimulus that evoked thalamic neuronal hyperexcitability may be due to additional higher order processing of that sensory stimulus. Additional studies quantifying neuronal excitability in regions of the brain, such as the primary somatosensory cortex, are necessary to fully define the central responses to painful facet joint injury that mediate behavioral hypersensitivity and to contextualize the relationships between the threshold eliciting a forepaw withdrawal and that magnitude at which thalamic neuronal hyperexcitability is evident.

Thalamic neuronal hyperexcitability is not a central adaptation unique to painful facet joint injury. Rather, injury to additional soft tissues in the cervical spine like the cervical nerve roots also increases excitability of thalamic neurons. Neuronal firing in the VPL evoked by forepaw stimulation is increased in response to noxious stimuli (10g, 26g, & pinch) after a fifteen minute cervical nerve root compression in association with behavioral hypersensitivity (Syré et al., 2014), following the same pattern as in these studies (Figure 7.4). Yet, enhanced firing in the VPL is also evident for all non-noxious stimuli (1.4g, 4g, & brush) after the nerve root compression (Syré et al., 2014). However, enhanced firing is only evident for the 4g and brush stimuli following facet joint injury (Figure 7.4). The electrophysiological studies presented here were performed seven days after facet joint injury and those after nerve root injury were fourteen days after the initial injury (Syré et al., 2014). Any difference in the response to non-noxious stimuli between the two injuries may be due to differences in the injuries themselves or in the timing of

the measurements. Indeed, both painful nerve root compression and painful facet joint injury exhibit the same pattern of neuronal hyperexcitability in the spinal cord at day seven after injury, with all stimuli except the 1.4g von Frey filament evoking significantly more spikes after injury compared to controls (Nicholson et al., 2014; Quinn et al., 2010). Moreover, both spinal neurons and thalamic neurons exhibit the same pattern of hyperexcitability on day seven after facet joint injury (Figure 7.4; Quinn et al., 2010). As such, it may be that spinal and thalamic neurons also exhibit the same excitability pattern seven days after a nerve root injury. Alternatively, thalamic neuronal hyperexcitability may be evident across all stimuli (1.4g, 4g, 10g, 26g, brush, & pinch) on day seven after a nerve root compression.

The magnitude of behavioral hypersensitivity is the same at day seven and day fourteen after nerve root injury (Syré et al., 2014), so it follows that thalamic neuronal hyperexcitability may likewise be the same at those same time points after a nerve root injury. As such, painful facet joint and nerve root injuries would exhibit different patterns of thalamic neuronal hyperexcitability at day seven. Similarly, since facet joint injury induces behavioral hypersensitivity that is sustained at both days seven and fourteen to the same degree (Lee et al., 2004; Rothman et al., 2007), the pattern of thalamic neuronal hyperexcitability (4g, 10g, 26g, brush, & pinch) that is identified here at day seven might also be sustained at day fourteen and, thus, would be different from a nerve root injury at that same time (Syré et al., 2014). Further studies comparing these two painful cervical spine injuries at the same time points are needed to identify whether or not a common pattern of thalamic neuronal hyperexcitability exists across different pain etiologies and

origins. Such a common hyperexcitability pattern would support the potential for a single intervention at the thalamic level in alleviating pain from multiple types of injury.

The existence of hyperexcitability of neurons in the VPL supports central sensitization, which sustains ongoing pain and leads to referred pain, as a mediator of injury-induced facet pain. Yet, despite a trend towards a decrease in withdrawal threshold after joint distraction (Figure 7.3), this decrease did not reach significance when compared to sham. This lack of change in withdrawal threshold may be due to the small group sizes used in the characterization study because power analysis indicates that group sizes of at least six rats would be necessary to detect changes in behavioral responses between groups in this study. Regardless, the applied C6 forceps displacement (2.52±0.04mm) is similar to the C6 forceps displacements applied in Chapter 6 (2.65±1.45mm), and the capsule distraction (0.39±0.18mm) and maximum principal strains (40.31±9.48%) are consistent with those values of injury metrics (capsule distraction 0.23-0.34mm; maximum principal strain 21.5-31.2%) quantified in previously published reports of facet joint loading associated with behavioral hypersensitivity (Dong et al., 2008; Dong et al., 2011). It is, therefore, reasonable to assume that if the group sizes were expanded for the current study, such differences in behavioral responses between distraction and sham would be significant. As such, additional animals were not included in this study, but future studies identifying the specific cellular mechanisms responsible for thalamic neuronal hyperexcitability after joint injury should include larger group sizes.

Based on the findings in the characterization study, larger group sizes (n=6 for each group) were used in the IB4-saporin study to ensure sufficient power to detect any

potential differences in behavioral sensitivity between the IB4-Sap+FJD and IB4-Sap+sham groups. Such group sizes are sufficient to detect differences in behavioral sensitivity following painful facet joint loading (Chapters 4 & 6; Kras et al., 2013b; Kras et al., 2014a). Yet, no differences in withdrawal threshold are detected between the IB4-Sap+FJD and IB4-Sap+sham groups (Figure 7.5). The injury metrics quantified for the IB4-Sap+FJD rats (capsule distraction 0.23±0.09mm; maximum principal strain 41.1±46.5%; maximum rostrocaudal strain 22.4±18.2%) are not different from the respective distraction and strain values measured for either the SSP-Sap+FJD (0.23±0.07mm; 24.9±14.0%; 19.4±14.0%) or the Blank-Sap+FJD (0.22±0.06mm; 21.3±13.3%; 14.7±7.1%) groups that were used in Chapter 5 in which differences in behavioral sensitivity *were* detected. The lack of differences in the biomechanical metrics of applied injury severity across groups supports the injury applied to the IB4-Sap+FJD rats in this study to be sufficient to induce behavioral hypersensitivity. As such, the lack of difference in withdrawal threshold between the IB4-Sap+FJD and IB4-Sap+sham groups in the current study (Figure 7.5) can be taken as a result of the IB4-saporin treatment and not due to an insufficient injury. Further, running a power analysis on these groups indicates that group sizes in excess of 1,000 rats are required to detect differences in withdrawal threshold in the IB4-saporin treated groups. Such a large group size *far exceeds* the number of rats used to detect differences in behavioral sensitivity and confirms that the withdrawal thresholds between these groups are indeed the same, with the lack of difference not being an artifact of small group sizes.

In parallel with the withdrawal thresholds, the evoked spikes from thalamic neurons also are not different between the IB4-Sap+FJD and IB4-Sap+sham groups

(Figure 7.5). In a nerve root injury model, significant differences in thalamic neuronal excitability were detected between injury and control groups from 57 distinct neurons (Syré et al., 2014), suggesting the number of neurons recorded in the thalamus in the current study (74 neurons) would be sufficient to detect any differences between the IB4-Sap+FJD and IB4-Sap+sham groups. In fact, power analysis indicates that at least 900 neurons would be needed per group to detect differences in the number of spikes evoked by any of the brush, von Frey, and pinch stimuli. As such, the finding of no difference in thalamic neuronal excitability between the IB4-Sap+FJD and IB4-Sap+sham groups also is not likely a result of insufficient group sizes but rather reflects a true lack of difference between these groups. For comparisons of the ratio of WDR neurons between groups, Pearson's chi-square test requires a minimum of five observations for each group and classification. Since the number of neurons classified as WDR and LTM for the IB4-Sap+FJD and IB4-Sap+sham groups meet the required number of observations, the finding that the proportions of WDR neurons between the two injury groups are equivalent is not due to an insufficient number of neurons included in the test. Based on the sufficient power of these statistical tests, the ablation of the non-peptidergic joint afferents prior to injury can be taken as the underlying reason for the lack of difference in either the behavioral or the electrophysiological responses between the IB4-Sap+FJD and IB4-Sap+sham groups.

Despite sensitization of thalamic neurons in painful inflammatory conditions or following neural tissue injury (Huh et al., 2012; Syré et al., 2014; Zhao et al., 2006), the molecular responses underlying sensitization of neurons in the VPL are poorly defined. Because STT neurons express the trkB receptor for BDNF (Slack et al., 2005), spinal

BDNF may contribute to thalamic neuronal sensitization. Indeed, spinal BDNF induces long-term potentiation in spinal neurons via ERK mediated signaling (Zhou et al., 2008), and BDNF induces ERK activation in STT neurons (Slack et al., 2005). As such, the increased spinal BDNF observed at day seven after a painful facet joint distraction (Chapter 6) may also activate and sensitize STT neurons through a similar ERK-dependent mechanism. Moreover, NGF regulates BDNF expression (Merighi et al., 2004) and is increased in both the facet joint and the DRG after painful joint loading (Chapter 5). Accordingly, NGF may be a local initiator of joint pain and upregulation of neurotransmitters, such as BDNF expression, that can induce central sensitization. NGF mainly activates *peptidergic* afferents (McMahon, 1996; Merighi et al., 2004), but ablation of *non-peptidergic* joint afferents prevents the development of injury-induced behavioral sensitivity and thalamic hyperexcitability (Figure 7.5). Up to one-third of neurons that bind IB4 also express the NGF receptor trkA (Joseph and Levine, 2010), so it is possible that ablation of the IB4-expressing neurons may also disrupt NGF-mediated responses leading to joint pain after injury.

Additional mechanisms, such as those involving prostaglandin signaling, may also contribute to thalamic sensitization. Guilbaud identified disruption of prostaglandin synthesis as having a depressing effect on excitability of neurons in the thalamus of arthritic rats (Guilbaud et al., 1982). In fact, intra-articular ketorolac, a non-steroidal anti-inflammatory drug that disrupts prostaglandin synthesis, alleviates facet-mediated pain in this same injury model (Dong et al., 2013a). When taken together with the role for prostaglandins in thalamic sensitization (Guilbaud et al., 1982), the necessity of prostaglandins for the maintenance of facet-mediated pain suggests that prostaglandins

may also contribute to hyperexcitability in the VPL after painful facet joint injury. Non-peptidergic afferents have a role in potentiating behavioral responses to $PGE_2$ signaling (Joseph and Levine, 2010). In the context of the Joseph and Levine study, the current findings that ablating non-peptidergic joint afferents prevents the development of behavioral hypersensitivity and thalamic neuronal hyperexcitability after a facet joint injury (Figure 7.5) further supports $PGE_2$ as a mediator of thalamic excitability induced by facet injury. Although both BDNF and prostaglandins are potential mediators of thalamic sensitization, further studies specifically disrupting BDNF and prostaglandin signaling are necessary to define which cellular responses in the primary afferents and/or the spinal cord contribute to pain and central sensitization after facet joint injury.

Regardless of the cellular mechanisms involved, the finding of injury-induced hyperexcitability in the VPL demonstrates that facet joint injury elicits central modifications in the brain and suggests that interventions targeting the brain may have therapeutic potential for facet pain. Structural differences have been identified in the brains of pain patients with persistent low back pain or painful osteoarthritis (Gwilym et al., 2010; Saab, 2012; Seminowicz et al., 2011), and interventions like facet joint injections that alleviate pain also mitigate differences in brain structure between pain patients and control subjects (Seminowicz et al., 2011). As such, following painful facet joint injury, localized interventions in the facet joint that alleviate pain may also normalize brain modifications such as VPL hyperexcitability. Indeed, targeted ablation of non-peptidergic joint afferents prevents injury-induced thalamic hyperexcitability (Figure 7.5). Yet, it is unknown if VPL hyperexcitability is maintained by continuous input from the injured facet joint or if the initial injury is sufficient to sensitize thalamic neurons via

the joint afferents, spinal circuits, or gene expression changes within the thalamic neurons themselves. The effectiveness of radiofrequency neurotomy, which eliminates neurons innervating painful facet joints, in alleviating pain (Smith et al., 2014) supports a role for ongoing input from the joint afferents in the *maintenance* of facet pain.

In addition to neuronal ablation, deep brain stimulation (DBS) may provide an additional therapeutic option for alleviating facet pain. DBS in the thalamus has shown effectiveness in reducing pain and neuronal hyperexcitability in a rat neuropathic pain model (Iwata et al., 2011). Similarly, burst stimulation of the thalamus is effective in alleviating inflammatory pain associated with thalamic neuronal hyperexcitability in mice (Huh and Cho, 2013). Clinically, enhanced local field potentials are evident in the thalamus, periventricular gray (PVG), and periaqueductal gray (PAG) in patients experiencing pain (Llinás et al., 1999; Pereira et al., 2013). Stimulation of such brain regions as the VPL, PVG, and PAG reduces clinical pain in a variety of conditions, including low back pain, chronic regional pain syndrome, brachial plexus injury, and phantom limb pain (Pereira et al., 2013; Rasche et al., 2006). Further, stimulation of the anterior cingulate cortex to reduce the emotional impact of chronic pain has also been implemented in those patients for which thalamic or PVG/PAG DBS is ineffective (Pereira et al., 2013). DBS has not previously been applied to treat joint pain, either clinically or in pre-clinical studies. Because thalamic neurons are hyperexcitable in association with facet joint pain, further investigation of the relationship between thalamic neuronal activity and injury-induced pain is warranted. Implanting electrodes into the VPL to regulate thalamic neuronal firing would determine that relationship, as well as any therapeutic potential of DBS in alleviating established facet joint pain. Yet,

before such complicated studies are undertaken, additional studies are first needed to establish the time course of facet joint injury-induced thalamic neuronal hyperexcitability at times longer than seven days. If thalamic neuronal hyperexcitability is only transient, then an invasive treatment such as DBS would likely be inappropriate for alleviating facet-mediated hypersensitivity.

## 7.6. Conclusions & Integration

Studies in this chapter support modifications in the brain, specifically in the VPL, as likely contributing to facet joint injury-induced pain. Specifically, the prevention of both behavioral sensitivity and thalamic neuronal hyperexcitability that are normally evident after facet joint injury by ablating non-peptidergic joint afferents supports a contribution of VPL sensitization to facet-mediated pain. Moreover, the increase in thalamic excitability is evident at a time when spinal BDNF, which is capable of activating thalamic neurons, is also elevated (Chapter 6; Kras et al., 2013c). In fact, sequestration of spinal BDNF alleviates facet pain (Figure 6.6), but excitability of thalamic neurons was not assessed after BDNF sequestering. As such, it is not known if thalamic hyperexcitability after a painful facet joint injury is mediated by increased spinal BDNF signaling, nor is it known if the mechanism through which spinal BDNF contributes to behavioral hypersensitivity involves increased neuronal firing in the thalamus. Nevertheless, BDNF activates neurons projecting to the thalamus and is regulated by NGF (McMahon, 1996; Merighi et al., 2004; Slack et al., 2005). The increases in NGF in the joint and DRG (Figures 5.2 & 5.3) and increases in BDNF in the DRG and spinal cord (Figures 6.3 & 6.4) (Kras et al., 2013c; Kras et al., 2014b) that are

induced by facet injury imply that a neurotrophin-mediated mechanism is involved in both the initiation and maintenance of facet pain. Since disruption of intra-articular NGF signaling immediately after a facet joint injury prevents the development of spinal hyperexcitability at day seven (Chapter 5), it might also prevent the development of thalamic hyperexcitability at that same time. Yet, blocking intra-articular NGF signaling also prevents the development of spinal hyperexcitability at day one after injury. If neurotrophins drive hyperexcitability of neurons in the thalamus after facet joint injury, then it is likely that thalamic hyperexcitability would also be evident at earlier time points than day seven in parallel with the development of spinal neuronal hyperexcitability. Thalamic neuronal hyperexcitability was only assessed at day seven after joint injury, so it is not known if the excitability of thalamic neurons also increases at earlier time points when spinal neuronal hyperexcitability develops. Behavioral hypersensitivity and spinal neuronal hyperexcitability are evident as early as one day after a facet joint injury (Crosby et al., 2013; Kras et al., 2014b). $PGE_2$ is increased in the spinal cord at day one after facet joint injury (Kras et al., 2014a). Since $PGE_2$ is both sufficient to induce hyperexcitability in spinal neurons and contributes to joint inflammation-induced thalamic hyperexcitability (Guilbaud et al., 1982; Vasquez et al., 2001), $PGE_2$ probably contributes to facet injury-induced hyperexcitability in the thalamus at early time points, likely at day one.

Further, behavioral hypersensitivity is maintained as late as six weeks after the facet joint injury (Rothman et al., 2007). Although the maintenance of behavioral sensitivity implies that thalamic neuronal excitability might also be maintained at later time points beyond day seven, the cellular mechanisms that might sustain such prolonged

hyperexcitability have not been investigated. However, activation of astrocytes in the spinal cord is evident at both day seven and day fourteen after a painful facet joint injury (Dong et al., 2013b; Lee et al., 2004). Astrocytes contribute to pain through several mechanisms, including release of inflammatory cytokines and regulation of extracellular glutamate levels (Gao and Ji, 2010). Further, astrocytic activation in the thalamus has been associated with both inflammatory and post-stroke pain (Raghavendra et al., 2004; Wasserman and Koeberle, 2009). Inflammatory cascades have a role in facet-mediated pain (Dong et al., 2013a; Kras et al., 2014a), so astrocyte activation might also occur in the VPL after a painful facet joint injury and may also contribute to the associated thalamic neuronal hyperexcitability that is observed there. Since astrocytes are activated in the spinal cord as late as day fourteen following facet joint injury, a similar long-term activation of astrocytes may exist in the VPL and contribute to sustained behavioral hypersensitivity and thalamic neuronal hyperexcitability. Yet, studies are needed to identify whether or not astrocytes are activated in the thalamus following facet joint injury, as well as to investigate the time course of thalamic neuronal hyperexcitability in the context of facet-mediated pain, before such a mechanism can be considered. Other pain mediators may contribute to thalamic neuronal hyperexcitability in mechanical facet joint injury, such as altered expression of voltage-gated sodium channels, as has been documented for neural tissue injury (Zhao et al., 2006). Regardless, these data are the first identifying hyperexcitability in thalamic neurons in the context of pain following facet joint injury, and as a result, the brain represents a potential target for the development of therapeutics to treat persistent joint pain.

# Chapter 8

# Synthesis and Future Work

## 8.1. Introduction

Clinically, the cervical facet joint is the most common source of neck pain, and non-physiological stretching of the capsular ligament that encloses the facet joint space is a mechanism of neck pain that is supported by biomechanical studies (Barnsley et al., 1995; Lord et al., 1996; Manchikanti et al., 2002; Pearson et al., 2004; Siegmund et al., 2001; van Eerd et al., 2010; Yoganandan et al., 2002). Previous studies utilizing a rat model of painful mechanical facet joint injury demonstrate that facet joint distraction sufficient to induce behavioral hypersensitivity also induces joint inflammation within one day of injury, upregulates the expression of neuropeptides and inflammatory cytokines, and sensitizes spinal neurons (Crosby et al., 2013; Dong et al., 2013a; Dong et al., 2013b; Kras et al., 2014a; Lee and Winkelstein, 2009; Quinn et al., 2010). More recent work has identified afferent activity from the joint early after facet distraction as being required for the development of behavioral hypersensitivity and spinal neuronal hyperexcitability (Crosby et al., 2014). Collectively, these findings suggest that the inflammation and spinal neuronal dysfunction that maintain pain develop in response to local pain mediators and associated afferent activity within the injured facet joint that initiate pain immediately after injury. However, no specific cellular mechanism in the joint had been identified in studies as an initiating factor in facet injury-induced pain. In

addition, the relationship between such a local mechanism and the subsequent spinal modifications that maintain facet-mediated pain was not previously defined. Therefore, the goal of this thesis was to investigate one such potential cellular mechanism local to the facet joint by defining the roles of intra-articular nerve growth factor (NGF) in the initiation of facet pain and spinal neuronal dysfunction and spinal brain-derived neurotrophic factor (BDNF) in the maintenance of facet-mediated pain after a mechanical joint injury in the rat. Since contributions of NGF to inflammation- and arthritis-induced pain have been reported both clinically and experimentally (Amaya et al., 2004; Ghilardi et al., 2012; Lane et al., 2010; Rukwied et al., 2014; Woolf et al., 1994), intra-articular NGF was investigated as a promising candidate molecule likely involved in the induction and/or maintenance of facet joint pain after traumatic joint injury.

## 8.2. Summary & Synthesis of Major Findings

Tensile loading of the C6/C7 facet joint at magnitudes simulating the magnitude of capsular ligament stretch that occurs during neck trauma that is associated with motor vehicle collisions induces referred pain in the forepaw of the rat (Dong et al., 2011; Kras et al., 2013b; Lee and Winkelstein, 2009), which is consistent with the hypersensitivity that is observed clinically in neck pain patients (Fernandez-Perez et al., 2012; Herren-Gerber et al., 2004; Scott et al., 2005). Mechanical hyperalgesia develops within one day of a painful facet joint distraction (Chapters 3 & 4) and is maintained for at least six weeks (Rothman et al., 2007). Such a time course of immediate and sustained pain parallels the appearance of clinical pain symptoms that have been reported approximately 24 hours after a motor vehicle collision-induced neck trauma (Chien et al., 2010), with up

to 50% of patients with whiplash-associated pain still reporting symptoms at one year after injury (Carroll et al., 2009). Initiation of persistent pain within 24 hours of an injury suggests there may be a brief time period during which the initial cellular responses to injury could be manipulated in order to effectively treat injury-induced joint pain. Indeed, systemic infusion of the corticosteroid, methylprednisolone, within eight hours after a traumatic neck injury reduces long-term disability in neck pain patients (Pettersson et al., 1998), and an intra-articular injection of the sodium channel blocker, bupivacaine, within eight hours of a facet joint injury in the rat prevents the development of pain symptoms after injury (Crosby et al., 2014). Together, those clinical and basic science studies highlight the importance of the timing of potential interventions in the treatment of injury-induced neck pain and suggest that the early cellular responses to injury are likely a *key* determinant in the long-term pain outcomes following ligament injury.

Capsular ligament strains as low as 10%, induced by tensile loading of the cervical facet joint, activate the primary afferent fibers that innervate the joint (Chen et al., 2006; Lu et al., 2005). Injury-induced firing of primary afferents is one mechanism thought to initiate pain (Ji et al., 2003). Because the animal model of tensile capsular ligament stretch utilized for studies throughout this thesis induces maximum principal strains of 22.18±13.57% in the joint capsule (Chapter 3), activation of joint afferents by capsule stretch is a likely mechanism for initiating mechanical facet joint pain. Further, a majority of the neurons that innervate the cervical facet joint capsule are peptidergic (Chapter 4; Kras et al., 2013b). Peptidergic afferents are typically small diameter nociceptors, contain the neuropeptides substance P and/or calcitonin gene-related peptide (CGRP), and are sensitive to NGF (Merighi et al., 2008). Injury-induced activation of

peptidergic afferents not only leads to propagation of action potentials to the central nervous system, but activation of one branch of a peptidergic afferent propagates the signal into adjacent branches of that neuron, resulting in peripheral release of neuropeptides − this phenomenon is known as neurogenic inflammation (Birklein and Schmelz, 2008; Ringkamp et al., 2013). Peripherally-released substance P sensitizes articular afferents (Heppelmann and Pawlak, 1997), but it also induces the degranulation of mast cells (Birklein and Schmelz, 2008; Kumar and Mahal, 2012; Levine et al., 1984; Ringkamp et al., 2013). Mast cells are sources of NGF, and their degranulation releases NGF into the inflamed tissue (McMahon, 1996; Nicol and Vasko, 2007). Because NGF itself sensitizes primary afferents and regulates the expression and release of neuropeptides from those same neurons, injury-induced activation of facet joint afferents could initiate a positive feedback loop whereby substance P and NGF promote their own release within the injured joint, sensitizing joint afferents and ultimately inducing pain.

In addition to mechanical activation of joint afferents, inflammation has a well-established role in afferent sensitization and pain (Schaible et al., 2002; Woolf et al., 1997). As such, inflammation may also, in and of itself, promote injury-induced facet joint pain. Indeed, within 24 hours of a traumatic injury of the knee in humans, there is upregulation of the inflammatory cytokines interleukin-1 (IL-1) and tumor necrosis factor-α (TNF-α) in the intra-articular space (Furman et al., 2014). Mechanical facet joint injury upregulates prostaglandin $E_2$ and inflammatory cytokines (Kras et al., 2014a; Lee et al., 2008), and the increased intra-articular NGF evident one day after painful facet distraction is further evidence of injury-induced joint inflammation (Figure 8.1) (Chapter 5; Kras et al., 2014b). NGF itself has a particularly important role in the development of

pain since exogenous NGF applied either subcutaneously or intra-dermally is sufficient to induce pain in both human volunteers and in animal models (Dyck et al., 1997; Woolf et al., 1994). Indeed, exogenous intra-articular NGF induces pain within 24 hours of its application to the facet joint (Chapter 5; Kras et al., 2014b). Further, increased NGF in the joint after injury parallels the induction of behavioral sensitivity at day one (Chapter 5; Kras et al., 2014b). In conjunction with that finding, the notion that elevated levels of NGF in the facet joint after its injury initiate joint pain is supported by the fact that blocking NGF at the time of injury *prevents* the development of pain (Chapter 5; Kras et al., 2014b).

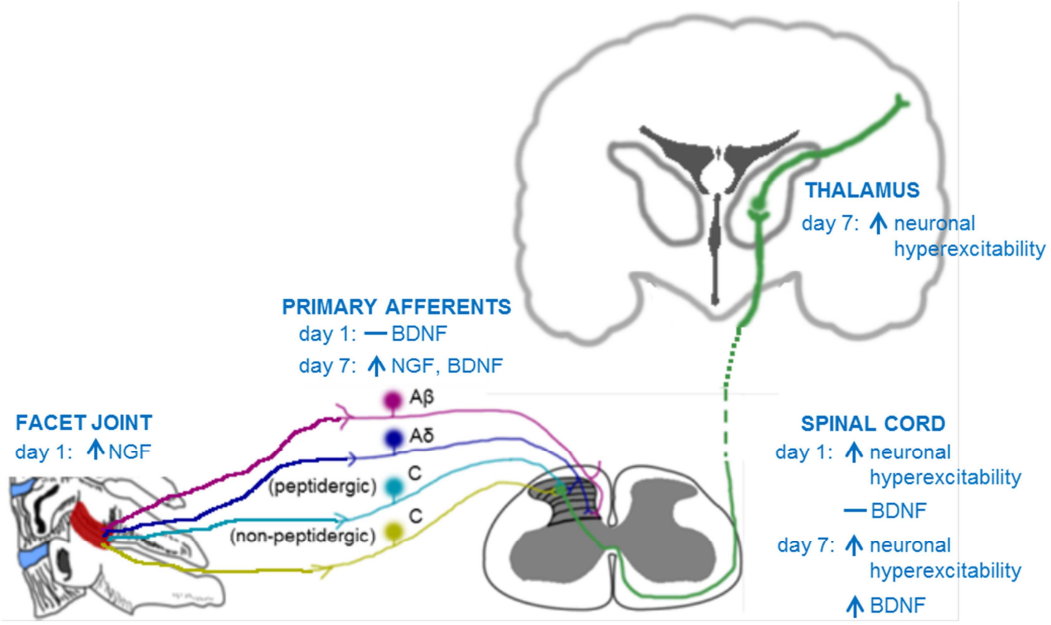


**Figure 8.1.** Painful facet joint distraction induces increased expression of neurotrophic factors in the facet joint, the primary afferents, and the spinal cord, as well as hyperexcitability in both spinal and thalamic neurons. NGF is elevated in the facet joint at day one after painful injury. Upregulation of NGF contributes to the spinal neuronal hyperexcitability also evident at day one. BDNF expression is unchanged in both the primary afferents and the spinal cord at one day after injury. At day seven, both NGF and BDNF are increased in the DRG, and spinal BDNF is also elevated after injury. Increases in spinal BDNF may be a central mediator of both spinal and thalamic neuronal hyperexcitability at day seven.

The elevated levels of intra-articular NGF identified clinically in inflamed and arthritic joints and the success of anti-NGF treatments in alleviating joint pain confirm that NGF signaling is a key mediator of arthritic joint pain (Barthel et al., 2009; Brown et al., 2012; Lane et al., 2010; Raychaudhuri et al., 2011; Schnitzer et al., 2014). Intra-articular NGF increases due to both arthritis and traumatic facet joint injury in the rat (Chapter 5; Kras et al., 2014b; McNamee et al., 2010; Orita et al., 2011). Further, NGF contributes to *pain* in both such joint conditions, as evidenced by the effectiveness of anti-NGF treatments applied either intra-articularly or systemically in preventing or alleviating pain (Chapter 5; Kras et al., 2014b; Lane et al., 2010; Schnitzer et al., 2014). In light of those parallels, NGF likely has a role in a broad range of painful joint conditions, possibly including other traumatic joint injuries or arthritis.

Despite the possibility that NGF may be a common factor in joint pain, the specific role of intra-articular NGF in persistent joint pain may vary across the different joint pain conditions. That notion is supported by the fact that intra-articular NGF seems to initiate, but not maintain, pain following facet joint injury since blocking it only prevents pain from developing after injury but does not alleviate facet pain that has already been established (Chapter 5; Kras et al., 2014b). In contrast, although chemically-induced joint osteoarthritis (OA) pain develops by day four after the initiating stimulus, NGF does not increase in the joint until day seven (Orita et al., 2011). However, that timing of increased NGF at day seven corresponds to when pain reaches its maximum in that OA model (Orita et al., 2011), suggesting that rather than initiating OA pain, intra-articular NGF may *exacerbate* existing pain. Indeed, intra-articular injection of NGF into osteoarthritic knees in the rat exacerbates existing OA pain (Ashraf et al., 2014).

Moreover, NGF as an amplifier of OA joint pain is consistent with clinical findings of relief, but not complete abolishment, of pain in patients (Brown et al., 2012; Lane et al., 2010; Schnitzer et al., 2014). Although growing evidence supports NGF as contributing to pain in multiple painful joint conditions, there may not be a single treatment paradigm (i.e. dose, timing, route of administration) for anti-NGF to effectively treat pain.

Although NGF levels increase in the facet joint one day after its painful injury, the source of NGF within the injured joint is still unknown. Immune cells, such as lymphocytes, macrophages, and mast cells, infiltrate inflamed joints in both animal models and patients with osteoarthritis and rheumatoid arthritis (Aloe et al., 1992; de Lange-Brokaar et al., 2012). Those immune cells are potential sources of NGF (McMahon, 1996). In addition to releasing NGF, macrophages and mast cells can also release inflammatory cytokines, such as IL-1β and TNF-α (de Lange-Brokaar et al., 2012), both of which are *themselves* mediators of behavioral hypersensitivity and potent inducers of NGF expression and release (Safieh-Garabedian et al., 1995; Woolf et al., 1997).

Interestingly, antagonism of either IL-1 or TNF-α via an intra-articular injection of a selective inhibitor for either cytokine at one day after a painful facet joint injury is ineffective in alleviating facet-mediated behavioral hypersensitivity (Dong, 2011). The ineffectiveness of cytokine antagonism suggests that neither of those pain mediators contributes to facet joint pain, although in that work, only a single dose of either antagonist was applied, leaving open the possibility that a higher dose or multiple doses might be effective in alleviating or attenuating pain. However, a study of IL-1β-induced knee pain also found that a single intra-articular injection of an IL-1 inhibitor failed to

alleviate pain despite the known overexpression of IL-1β within that joint (Allen et al., 2011). Moreover, the lack of pain relief following injection of the IL-1 inhibitor may be an artifact of the times selected for behavioral assessment. Safieh-Garabedian reported that injection of an IL-1 inhibitor reduced inflammatory pain 90 minutes after injection but that mechanical hyperalgesia returned within three hours of the initial injection (Safieh-Garabedian et al., 1995), which is well before behavioral responses were assessed following cytokine antagonism in the other studies (Allen et al., 2011; Dong, 2011). As such, it may be possible that intra-articular IL-1β contributes to facet-mediated pain and intra-articular NGF overexpression. Although, the cellular sources of increased NGF within the facet joint after its painful injury are still unknown, the documented role of inflammation in facet pain supports macrophages and mast cells as likely sources.

NGF induces sensitivity through post-translational modifications of ion channels as well as transcriptional regulation of neurotransmitters released at central and peripheral synapses (Mantyh et al., 2011). Within hours of exposure to NGF, modulation of ion channels such as voltage-gated sodium channels, potassium channels, and transient receptor potential vanilloid 1 (TRPV1) increases the excitability of primary afferent neurons that express the NGF receptor, trkA (Kerr et al., 2001; Mantyh et al., 2011; Zhang et al., 2002). Sensitization of the primary afferents innervating joints leads to a lower mechanical activation threshold for those neurons such that normally innocuous joint motions may activate nociceptors, and afferent activation releases more neurotransmitters into the spinal cord (Heppelmann and Pawlak, 1997; Schaible et al., 2002). Additionally, retrograde transport of the NGF-trkA receptor complex from the peripheral terminal to the cell body in the DRG increases synthesis of substance P,

CGRP, and BDNF, all of which are pro-algesic (Mantyh et al., 2011). Indeed, the increased NGF in the DRG seven days after painful facet joint injury (Chapter 5; Kras et al., 2014b) parallels the increased expression of both BDNF (Figure 8.1) (Chapter 6; Kras et al., 2013c) and substance P (Lee and Winkelstein, 2009) in the DRG at that same time.

Retrograde transport of NGF can take hours to days before alterations in protein synthesis are detected in the DRG (Mantyh et al., 2011), so the increased NGF in the facet joint that is evident on day one could be the source of the elevated NGF levels in the DRG at day seven. Yet, given the relatively close proximity of the cervical facet joint to the DRG and a reported rate of axonal NGF transport of approximately 3mm per hour in vitro (Delcroix et al., 2003), an effect of NGF on protein synthesis earlier than day seven is expected. Indeed, both BDNF and substance P expression exhibit trends towards elevation as early as day one after injury, although neither increase is significant (Kras et al., 2013c; Lee and Winkelstein, 2009). Such a trend suggests that NGF-induced synthesis of pain mediators in the primary afferents likely begins earlier than day seven, when injury-induced pain is already established. Nevertheless, the lack of changes in substance P and BDNF at day one does not preclude a contribution of those mediators to pain development at that time point since noxious stimulation of afferents induces the release of existing stores of substance P and BDNF from the central terminals of nociceptors (Lever et al., 2001; Pezet and McMahon, 2006).

Even though transcriptional regulation of BDNF and substance P by NGF at day one is too early to induce pain development, increased release of those pain mediators that is induced by NGF *can* initiate pain. Exposure to NGF increases evoked release of both BDNF and substance P in the spinal cord (Lever et al., 2001; Thompson et al.,

1995). Systemic NGF induces behavioral hypersensitivity and spinal neuronal sensitization within two hours after NGF exposure, and those effects are a result of an increased release of substance P into the dorsal horn (Thompson et al., 1995). Moreover, that NGF induced sensitivity is transient, lasting only 24 hours (Thompson et al., 1995). As such, substance P release likely has a role in the transient behavioral hypersensitivity and spinal neuronal hyperexcitability that are induced by exogenous intra-articular NGF application (Chapter 5; Kras et al., 2014b). Further, ablation of spinal cord neurons that express the NK1 receptor (NK1R) for substance P prevents the development of both pain and spinal hyperexcitability after a joint injury sufficient to elevate intra-articular NGF levels (Kras et al., 2014b; Weisshaar and Winkelstein, 2014). As described earlier, substance P release from primary afferents is not restricted to the spinal cord but is also evoked in the periphery when peptidergic afferents are activated (Birklein and Schmelz, 2008; Ringkamp et al., 2013). Substance P signaling has an established role in joint pain, with injection of substance P intra-articularly sensitizing joint afferents in otherwise normal rats (Heppelmann and Pawlak, 1997) and intra-articular inhibition of activation of NK1R alleviating established joint pain (Uematsu et al., 2011). Indeed, ablation of NK1 receptor-bearing joint afferents, but not non-peptidergic joint afferents, prevents both the behavioral hypersensitivity and the spinal neuronal hyperexcitability that are characteristic of intra-articular NGF application from developing (Figure 8.2) (Chapter 5). Similarly, ablation of those same joint afferents that express NK1R prior to facet joint injury prevents loading-induced pain from developing (Figure 8.2) (Chapter 5), in agreement with published reports that pre-emptive inhibition of NK1 receptor activation prevents inflammatory joint pain initiation (Keeble and Brain, 2004). Intra-articular NGF

may directly contribute to the onset of injury-induced facet pain by facilitating the release of substance P from primary afferents both peripherally within the joint and centrally within the spinal cord.

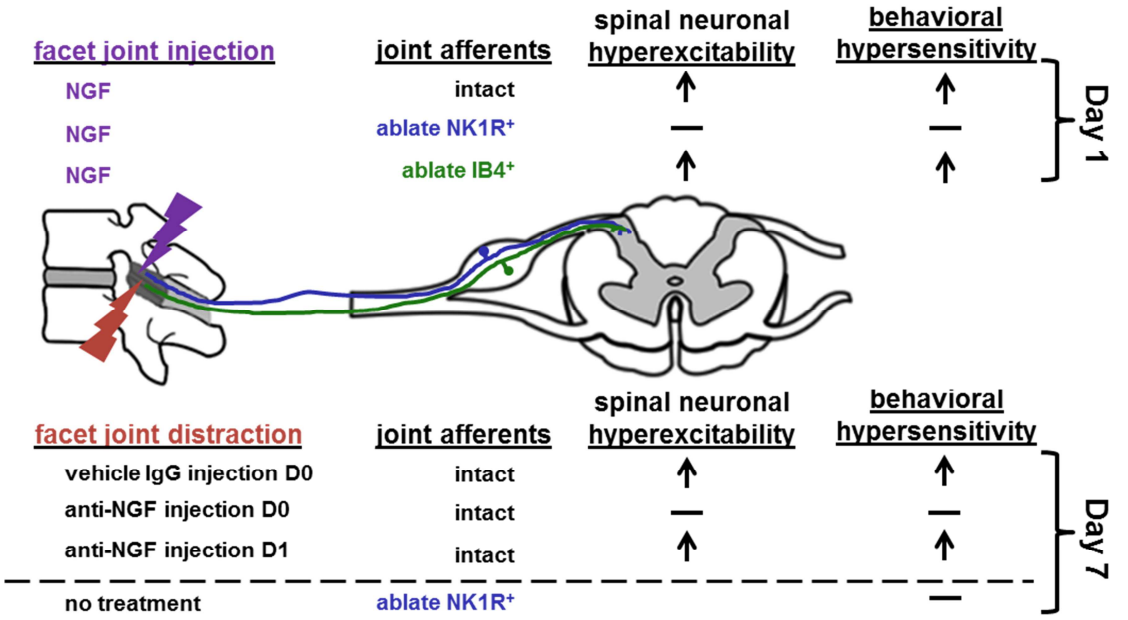


**Figure 8.2.** Intra-articular application of NGF is sufficient to induce both behavioral sensitivity and spinal neuronal hyperexcitability at day one after injection. Ablation of those neurons that express the NK1 receptor ($NK1R^+$) prior to NGF injection prevents the increases in behavioral sensitivity and excitability of spinal neurons; yet, ablating non-peptidergic afferents that bind IB4 ($IB4^+$) has no effect. Distraction of the facet joint increases behavioral sensitivity and induces spinal neuronal hyperexcitability at day seven. Selective inhibition of intra-articular NGF at the time of injury (D0), but not at a later time (D1), prevents the development of behavioral hypersensitivity and spinal neuronal hyperexcitability at day seven. Ablation of $NK1R^+$ joint afferents prior to a facet joint distraction with no other treatment prevents the initiation of behavioral hypersensitivity.

Regardless of the subpopulations of afferents that it activates, intra-articular NGF is necessary for facet joint injury-induced pain and the associated development of spinal neuronal hyperexcitability. Blocking NGF signaling with an anti-NGF antibody injected into the facet joint immediately after an otherwise painful injury prevents behavioral hypersensitivity and spinal hyperexcitability (Chapter 5; Kras et al., 2014b). Given that

pre-treatment with anti-NGF prior to a painful inflammatory stimulus prevents pain development (Safieh-Garabedian et al., 1995; Woolf et al., 1994) and that inflammation contributes to facet joint pain (Dong et al., 2013a; Kras et al., 2014a; Lee et al., 2008), it is not surprising that blocking NGF prevents injury-induced facet pain. Yet, the lack of effect when intra-articular NGF is blocked one day *after* injury, when pain and spinal hyperexcitability are already established, suggests that several mechanisms may induce persistent joint pain, with NGF as the initiator (Chapter 5; Kras et al., 2014b). $PGE_2$ is a known regulator of inflammation and pain and has a major role in joint pain (Lee et al., 2013; Lin et al., 2006). Intra-articular ketorolac, which disrupts synthesis of prostaglandins, reverses established facet joint pain, but only when given one day after injury when $PGE_2$ expression is elevated (Dong et al., 2013a; Kras et al., 2014a). In inflamed tissue, NGF promotes hyperalgesia by inducing a switch in $PGE_2$ signaling that increases the duration of $PGE_2$-mediated behavioral hypersensitivity (Joseph and Levine, 2010; Parada et al., 2005). Early anti-NGF treatment may prevent nociceptor priming by blocking intra-articular NGF after injury, a notion supported by the finding that intra-articular anti-NGF given one day after injury does not alleviate established pain (Chapter 5; Kras et al., 2014b). In fact, the different effects of anti-NGF and ketorolac may be due to early NGF facilitating later $PGE_2$-mediated nociception. As such, the timing of local joint interventions to correspond with the temporal contribution of their targeted mechanisms is crucial for effectively treating facet joint pain.

Within one day of facet joint injury, sensitization of spinal neurons is already evident (Chapter 5; Crosby et al., 2013; Kras et al., 2014b). Increased synaptic efficacy in the spinal cord is a hallmark of chronic pain that leads to reduced pain thresholds and

spreading of hypersensitivity to regions beyond the initial tissue injury (Ji et al., 2003; Latremoliere and Woolf, 2009). Facet joint injury in the rat induces hypersensitivity in anatomical regions that are remote from the neck, including the shoulder and forepaw (Chapter 3; Dong et al., 2013a; Lee and Winkelstein, 2009), similar to clinical neck trauma patients (Chien et al., 2009; Curatolo et al., 2001; Fernandez-Perez et al., 2012; Greening et al., 2005; Sterling and Kenardy, 2008; Sterling et al., 2002); that finding supports a spinal contribution to facet-mediated pain. Spinal maintenance of facet joint pain may explain why many current treatments for facet-mediated pain have proven to be effective only transiently (Barnsley, 2005; Manchikanti et al., 2008; van Eerd et al., 2014). They only treat the peripheral symptoms and do not alter the underlying spinal mechanisms that potentiate pain. Unlike the DRG and peripheral axons, the spinal cord is protected by the blood brain barrier (Sapunar et al., 2012), so treatments applied in the periphery are much less likely to penetrate into the spinal cord.

Since spinal neuronal hyperexcitability develops by day one after facet joint injury (Crosby et al., 2013; Kras et al., 2014b), peripheral treatment of facet pain is likely most effective prior to the onset of sensitization of spinal neurons. Indeed, anti-NGF treatment is only effective at the time of injury (Chapter 5; Kras et al., 2014b), and blocking activation of facet joint afferents via the sodium channel blocker bupivacaine is only effective when applied within eight hours of a joint injury (Crosby et al., 2014). However, the duration of the effects bupivacaine is only expected to be 8-12 hours when applied post-operatively (Skolnik and Gan, 2014). Because bupivacaine was applied intra-articularly at least 12 hours before behavioral sensitivity was measured in this model (Crosby et al., 2014), ongoing afferent input from the injured facet joint cannot be

ruled out as contributing to the maintenance of facet pain. Disruption of prostaglandin synthesis via intra-articular ketorolac alleviates facet pain when applied one day after injury (Dong et al., 2013a), suggesting that joint afferents *do* contribute to the maintenance of facet-mediated pain. Yet, unlike NGF, which is not transported to the spinal cord, prostaglandins are released in the spinal cord where they reduce transmission of inhibitory signals and increase release of neurotransmitters such as substance P from presynaptic primary afferents, both of which contribute to spinal neuronal excitability (Ji et al., 2003; Latremoliere and Woolf, 2009; Seybold, 2009; Vasquez et al., 2001). Spinal $PGE_2$ is increased at day one after painful facet joint injury (Kras et al., 2014a), supporting a spinal contribution for prostaglandins in facet pain. Intra-articular ketorolac could alleviate established facet pain by disrupting $PGE_2$ synthesis in primary afferents that would otherwise release it into the spinal cord. Antagonists of prostaglandin receptors have been developed (Jiang et al., 2013); using such antagonists to block spinal activation of $PGE_2$ receptors would clarify if spinal action of $PGE_2$ maintains facet-mediated pain. Regardless of whether or not $PGE_2$ contributes to pain via spinal signaling, the effectiveness of intra-articular ketorolac in alleviating facet pain at a time when anti-NGF treatment is *ineffective* supports different mechanisms being responsible for initiating and maintaining injury-induced facet pain.

Although intra-articular NGF *induces* the pain and spinal neuronal hyperexcitability that are associated with facet joint injury, multiple different mechanisms contribute to their *maintenance*. In the spinal cord, BDNF is generally localized to the superficial laminae (I-II) (Chapter 6), where nociceptors terminate. Its upregulation in that region of the spinal cord on day seven after painful injury implicates

BDNF as contributing to the spinal neuronal hyperexcitability that is evident at that time (Crosby et al., 2014; Kras et al., 2013c; Quinn et al., 2010). Spinal BDNF sensitizes neurons via activation of pre- and post-synaptic trkB receptors that leads to phosphorylation of glutamate receptors (Merighi et al., 2008; Slack et al., 2004) in an extracellular signal regulated kinase (ERK) dependent mechanism (Figure 8.3).

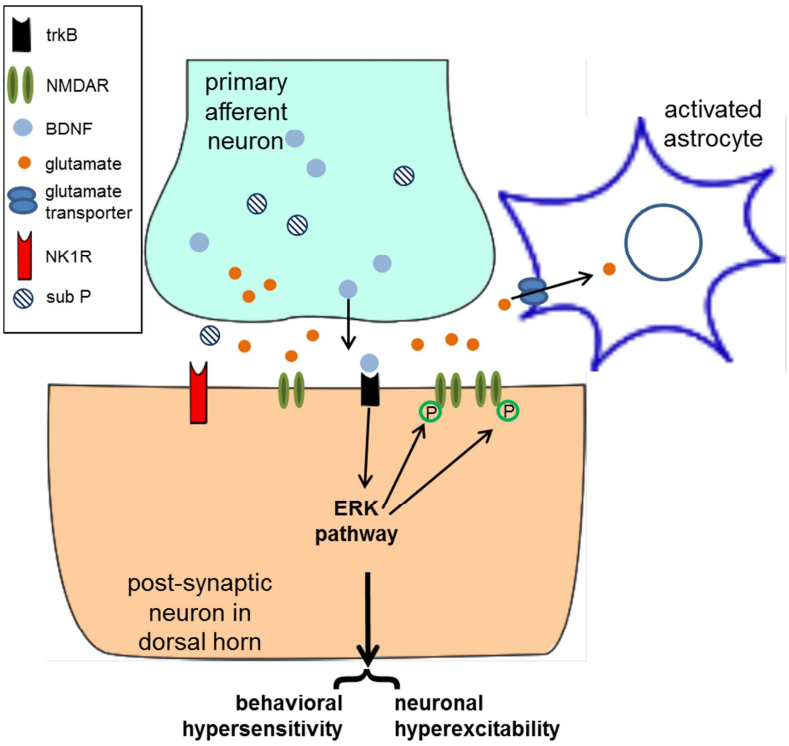


**Figure 8.3.** Schematic of BDNF release in the spinal cord at day seven. After a painful facet joint distraction, BDNF is upregulated in the superficial dorsal horn. BDNF released from primary afferent terminals activates post-synaptic trkB receptors, which leads to activation of ERK in second order sensory neurons in the dorsal horn and subsequent phosphorylation of NMDA receptors (NMDARs). Phosphorylation of the NMDARs leads to increased activation of the receptors and hyperexcitability of the spinal neuron. Downregulation of glutamate transporters on activated astrocytes prolongs the excitatory effects of glutamate binding the NMDARs. Because both BDNF and substance P (sub P) are released from the same pre-synaptic neurons, ablating spinal neurons expressing the substance P receptor NK1 (NK1R) will disrupt BDNF signaling mechanisms in the spinal cord as well.

Phosphorylation of the NR1 subunit of the NMDA glutamate receptor contributes to its activation and increases neuronal excitability. After facet joint injury, spinal BDNF is increased at the same time that both ERK and NR1 are phosphorylated in the spinal cord and spinal neurons are hyperexcitable (Crosby et al., 2014; Kras et al., 2013c), further supporting a contribution of spinal BDNF to neuronal hyperexcitability in the spinal cord. Moreover, selective inhibition of BDNF signaling in the spinal cord alleviates facet joint injury-induced behavioral hypersensitivity and reduces spinal ERK activation (Kras et al., 2013c), suggesting that increased spinal BDNF release will also underlie NR1 phosphorylation after injury.

Spinal BDNF is increased in the superficial dorsal horn where the number of excitatory synapses also increases after injury (Crosby et al., 2015; Kras et al., 2013c). Because BDNF released in synaptic clefts in the spinal cord is itself excitatory, the excitatory synapses in the superficial dorsal horn likely contain BDNF, and increases in the number of synapses may contribute to the overall increase in BDNF in that region. Spinal BDNF can contribute to sprouting of Aβ fibers, which normally transmit innocuous tactile information, from the deeper laminae into the superficial dorsal horn (Matayoshi et al., 2005). The sprouting Aβ fibers could form new synaptic connections with nociceptive circuits in the superficial dorsal horn and could, therefore, account for both the increase in excitatory synapses in that region and the increased excitability of spinal neurons. In either case, increased spinal BDNF contributes to facet joint injury-induced behavioral hypersensitivity (Chapter 6; Kras et al., 2013c) and likely contributes to spinal neuronal hyperexcitability either by directly sensitizing post-synaptic neurons or by inducing aberrant synaptic connections between Aβ fibers and nociceptive circuits in

the spinal cord. Since intrathecal inhibition of BDNF signaling after painful facet joint injury only partially alleviates behavioral hypersensitivity (Chapter 6; Kras et al., 2013c), BDNF may induce a combination of spinal neuronal sensitization and aberrant fiber sprouting. Disrupting BDNF signaling could block BDNF-mediated sensitization of spinal neurons at that time but would not disrupt existing aberrant synaptic connections. The continued activity of those aberrant synapses could be sufficient to maintain some pain. Interestingly, daily intrathecal injection of the BDNF inhibitor trkB-Fc started before a painful nerve injury does prevent the development of behavioral hypersensitivity and spinal neuronal hyperexcitability (Zhou et al., 2011). Continuous disruption of spinal BDNF signaling beginning early after facet injury when pain and spinal neuronal hyperexcitability are already established, but prior to any spinal synaptogenesis or increased BDNF (Crosby et al., 2015; Kras et al., 2013c; Kras et al., 2014b), would be needed to identify if spinal BDNF contributes to the neuronal hyperexcitability after a painful facet joint injury.

In the thalamus, neuronal hyperexcitability is also evident at day seven after a painful facet joint injury (Figure 8.1) (Chapter 7). Since the thalamus receives inputs from spinal neurons located in both the superficial (I-II) and deep (IV-VI) laminae of the dorsal horn, mechanisms mediating spinal neuronal hyperexcitability may also increase excitatory input to the thalamus. Indeed, inhibition of glutamate transporters increases the synaptic pool of glutamate and induces action potentials in neurons in the dorsal horn, including those that project to the thalamus (Nie et al., 2010). Further, many of the STT neurons are activated by BDNF (Slack et al., 2005) and substance P (Al-Khater et al., 2008), suggesting that those neurotransmitters may contribute to the thalamic neuronal

hyperexcitability that is observed in facet pain. Moreover, because STT neurons express NK1R, ablation of spinal neurons via SSP-saporin (SSP-Sap) may also ablate many STT neurons and modulate thalamic excitability in a similar manner to its effects on spinal neuronal hyperexcitability. Of note, ablation of non-peptidergic joint afferents via IB4-saporin (IB4-Sap) injection prior to facet joint injury prevented the development of thalamic neuronal hyperexcitability (Chapter 7), suggesting that peptidergic signaling that includes BDNF and substance P release is not the sole mediator of the excitability of thalamic neurons. However, up to a third of the neurons that bind IB4 can express the receptor for NGF and, so, may also express those neuropeptides that can sensitize STT neurons (Joseph and Levine, 2010). Despite these potential mediators of thalamic neuronal excitability, the specific mechanisms leading to thalamic neuronal hyperexcitability and its relationship to facet joint injury-induced pain remain uncertain at present.

## 8.3. Facet Joint Injury & Osteoarthritis

Osteoarthritis (OA) is a degenerative joint disease and is one of the most common forms of arthritis, affecting nearly 27 million Americans (Furman et al., 2014; Smelter and Hochberg, 2013). Although any joint can be affected by OA, the most frequent sites are load-bearing joints, such as those in the hand, knee, hip, and spine (Goldring and Goldring, 2007). Indeed, facet joint osteoarthritis is thought to be a common cause of back and neck pain (Gellhorn et al., 2013). OA is a leading source of physical disability in the United States and comes at a staggering economic cost, with healthcare costs alone of more than sixty billion dollars (Lee et al., 2013). Pain is the hallmark symptom of OA

and is a major contributor to the disability and healthcare costs associated with that disease (Neogi, 2013). Osteoarthritis does not resolve and typically progresses over the course of many years; in fact, age is one of the biggest risk factors for developing OA (Lee et al., 2013; Litwic et al., 2013). However, joint injury, including soft tissue injuries, also initiates degeneration within the joint (Dare and Rodeo, 2014; Furman et al., 2014). An estimated 12% of OA cases have a post-traumatic origin (Furman et al., 2014). Traumatic neck injuries induce chronic pain frequently originating from the facet joint (Barnsley et al., 1995; Carroll et al., 2009; Lord et al., 1996; Pedler et al., 2013); yet, the potential role of osteoarthritis in injury-induced facet pain has not been investigated.

In the normal joint, the extracellular matrix of articular cartilage perpetually undergoes a balance between anabolic and catabolic remodeling. During OA, the equilibrium is upset, so there is a progressive loss of joint cartilage (Goldring and Goldring, 2007; Lee et al., 2013). Chondrocytes proliferate in an attempt to repair the damage, but inflammatory cytokines and matrix-degrading enzymes cause further cartilage degradation (Buchanan and Kean, 2002; Goldring and Goldring, 2007). Eventual loss of cartilage exposes the subchondral bone, leading to alterations in bone density and the formation of new bone at the joint margins (osteophyte formation) (Buchanan and Kean, 2002; Lee et al., 2013). Progression of osteoarthritis can be confirmed radiographically, with joint space loss, osteophyte formation, and hardening of the subchondral bone visible (Swagerty et al., 2001).

Several mechanical factors contribute to the development of OA following an injury, including joint instability and/or malalignment, joint laxity, and altered load distribution (Dare and Rodeo, 2014; Goldring and Goldring, 2007; Litwic et al., 2013).

Biomechanical analysis of cervical facet joints identifies increased laxity after a traumatic neck injury (Ivancic et al., 2008), and increased capsular ligament laxity is thought to contribute clinically to chronic neck pain and instability (Ivancic et al., 2008; Panjabi et al., 1998; Steilen et al., 2014). Indeed, a similar increase in facet joint capsular ligament laxity is induced by painful facet joint injury in the rat (Quinn et al., 2007), and altered facet kinematics due to the increased laxity may contribute to the later development of joint degeneration. Yet, joint laxity is not the only risk factor for injury-induced OA associated with traumatic neck injury. Articular impact and/or fracture also lead to post-traumatic OA (Furman et al., 2014). Biomechanical simulations of traumatic neck injury using cadavers suggest that in addition to tensile stretch of the capsular ligament, facet joint compression occurs and can lead to articular impact (Pearson et al., 2004). Further, post-mortem analysis of cervical spines following fatal motor vehicle impacts reveals damage to articular cartilage and subchondral bone (Bogduk, 2011). Those findings further demonstrate additional risk factors for the development of OA during traumatic neck injuries that are not accounted for in the injury model utilized throughout this thesis. Nevertheless, the link between joint laxity and facet joint loading suggests that joint degeneration may be a long-term consequence of traumatic neck injury. Therefore, assessing whether or not degeneration develops after facet injury in association with joint laxity is needed since the long-term success of any treatments would depend not only on alleviating pain but also preventing further degeneration. Any laxity and subsequent altered distribution of stresses in the joint can lead to cartilage degradation (Lee et al., 2013; Lipowitz and Newton, 1985), which contributes to degeneration. In fact, increased joint laxity is reported in patients in the early stages of OA (Wada et al., 1996). Because

surgically-induced joint instability is sufficient to induce signs of joint degeneration within one week (Janusz et al., 2002) and pain is the hallmark symptom of OA (Neogi, 2013), evaluating joint degeneration after a mechanical facet joint injury like the one used in this thesis could determine if the pain after a facet joint and ligament injury can induce progressive joint degeneration.

Besides mechanical risk factors for developing OA, joint inflammation is a major contributor to joint degeneration and associated pain. Joint inflammation is evident in both post-traumatic and chemically-induced osteoarthritis (Bove et al., 2003; Furman et al., 2014; Gong et al., 2011; Huebner et al., 2014). Inflammatory cytokines are upregulated within the injured joint within 24 hours and not only sensitize joint afferents, but they also exacerbate catabolism within the joint (Dare and Rodeo, 2014; Furman et al., 2014; Lee et al., 2013). Interleukin-1 (IL-1) and tumor necrosis factor-α (TNF-α) are both potent promoters of cartilage breakdown and contribute to the pathophysiology of OA (Lee et al., 2013). For instance, IL-1 promotes expression of the collagen-degrading matrix metalloproteinases (MMPs) such as MMP-1, which degrades type II collagen, the predominant type of collagen in articular cartilage (Goldring and Goldring, 2007; Xu et al., 2013). In addition to promoting joint degeneration, both IL-1 and TNF-α are reported to induce behavioral sensitivity in the rat (Safieh-Garabedian et al., 1995; Woolf et al., 1997), suggesting that their expression in the joint after injury (Furman et al., 2014) also promotes joint pain. Although intra-articular inhibition of IL-1 or TNF-α failed to alleviate facet-mediated pain one day after injury (Section 8.2; Dong, 2011), inhibition of IL-1 impedes the progressive destruction of cartilage in experimental OA (Caron et al., 1996). Further evaluation of whether or not joint degeneration is a long-term

consequence of facet joint injury is necessary since joint inflammation contributes to OA as well as traumatic facet joint injury. If degeneration is evident, revisiting cytokine antagonism in facet pain could prove effective in minimizing progressive joint destruction.

In addition to promoting OA progression, both IL-1 and TNF-α increase the synthesis of $PGE_2$ and NGF within the osteoarthritic joint (Goldring and Goldring, 2007; Jacobs et al., 2011). Both $PGE_2$ and NGF are elevated within one day of a facet joint injury (Kras et al., 2014a; Kras et al., 2014b), and $PGE_2$ not only contributes to spinal neuronal sensitization and joint pain (Ji et al., 2003; Schaible et al., 2009), it also stimulates chondrocytes via the EP2 receptor and diminishes proteoglycan synthesis and type 2 collagen levels (Li et al., 2009). Following facet joint injury, intra-articular disruption of $PGE_2$ synthesis on day one after injury attenuates established pain (Dong et al., 2013a). Moreover, facet injury upregulates expression of the EP2 receptor at that same time (Kras et al., 2013a). Yet, that study quantified EP2 expression in the primary afferent neurons and so cannot necessarily be extended to altered receptor expression within the facet joint. Nevertheless, that finding, in combination with reports documenting upregulation of $PGE_2$ expression in the spinal cord and the role of $PGE_2$ in maintaining facet pain (Dong et al., 2013a; Kras et al., 2014a), clearly demonstrates that $PGE_2$ signaling is directly involved in the pathogenesis of injury-induced facet pain. In addition to maintaining facet pain, the catabolic properties of $PGE_2$ within joints could indicate that $PGE_2$ is also an initiator of post-traumatic facet joint degeneration. Although a contribution of NGF to OA progression is less clear, blocking NGF signaling in OA patients alleviates hip, knee, and low back pain (Katz et al., 2011; Lane et al., 2010;

Schnitzer et al., 2014). Indeed, increased levels of intra-articular NGF are a consequence of OA both clinically and in animal models (Lane et al., 2010; Surace et al., 2009; Orita et al., 2011). It is, therefore, possible that the upregulation of NGF within the injured facet joint, along with evidence of early inflammatory responses following facet injury (Dong et al., 2013a; Kras et al., 2014a), may reflect initial stages of a degenerative process.

Furthermore, the effectiveness of anti-NGF treatments in both OA and facet joint injury-induced pain suggest that facet joint distraction might also induce joint pathology that is similar to OA (Chapter 5; Kras et al., 2014b; Lane et al., 2010; Schnitzer et al., 2014); however, such a relationship is by no means certain. NGF contributes to multiple pain syndromes, such as neuropathic and inflammatory pain, including inflammatory joint pain (Ghilardi et al., 2012; Longo et al., 2013; Wild et al., 2007). Clinically, since NGF is detected in degenerative joints as well as in inflamed joints from rheumatoid arthritis patients (Barthel et al., 2009; Raychaudhuri et al., 2011; Surace et al., 2009), its potential for joint pain is not limited only to OA. Moreover, in clinical trials, the application of the same anti-NGF antibodies that are known to alleviate OA pain in patients experiencing lower back, neuropathic, and visceral pain has also shown positive outcomes for pain relief (Bramson et al., 2015; Evans et al., 2011; Katz et al., 2011). In light of the contribution of NGF to pain across a broad range of conditions both in animal models and clinically, its role in joint pain does not imply that joint degeneration is also involved. In fact, the mechanisms that lead to increasing NGF expression and pain may differ dramatically for OA and trauma-induced facet pain. Because facet joint injury induces joint inflammation within a day of ligament injury, it is hypothesized that

elevated intra-articular NGF is produced by, and released from, infiltrating immune cells in the joint (Aloe et al., 1992; de Lange-Brokaar et al., 2012; Dong et al., 2013a; McMahon, 1996). However, in vitro studies have identified chondrocytes subject to mechanical stress as sources of NGF (Pecchi et al., 2014). In fact, stress-induced production of NGF from chondrocytes could explain why NGF is not elevated one week after the induction of OA (Orita et al., 2011). Chondrocytes may not synthesize NGF until joint degeneration alters their local mechanical environment. In contrast, infiltrating immune cells can rapidly upregulate NGF within the inflamed facet joint after its injury, which could explain the increase in NGF that is evident at one day after injury (Chapter 5; Kras et al., 2014b). Yet, the cellular source of elevated intra-articular NGF is not known for either experimental OA or traumatic facet joint injury.

It is also unknown if intra-articular NGF expression is only transiently increased after a facet joint injury. NGF levels in the joint were only quantified at one time point after injury (Chapter 5; Kras et al., 2014b); yet, the increase in NGF expression that is evident in the DRG at day seven (Chapter 5) suggests that NGF may be transported to the DRG from the joint. Regardless, currently there is too little information available to establish temporal causative schema describing pain mechanisms for OA and facet joint trauma, despite a known contribution of NGF to pain in both joint conditions. Characterizing the spatiotemporal NGF expression in the facet joint and DRG, in parallel with joint degeneration, with long-term time points is needed to meaningfully understand NGF responses, joint degeneration, and pain in both OA and traumatic joint injuries.

Preventing onset of injury-induced facet joint pain by blocking intra-articular NGF supports anti-NGF as a potential treatment for trauma-induced neck pain (Chapter

5; Kras et al., 2014b). Yet, clinical trials administer the anti-NGF antibody systemically via intravenous injection and alleviate established pain (Brown et al., 2012; Katz et al., 2011; Lane et al., 2010; Schnitzer et al., 2014). In contrast, in our model of experimental facet joint injury-induced pain, NGF signaling was blocked locally within the facet joint; that local disruption of NGF signaling in the joint prevented pain onset after joint distraction when given at the time of injury but was ineffective when given even one day after the injury, when pain was already established (Chapter 5; Kras et al., 2014b). The lack of effect of anti-NGF treatment on established facet pain may be due to the dose being too small; 10µg of anti-NGF (~25µg/kg) was applied to each facet joint (Kras et al., 2014b); whereas anti-NGF applied to treat low back pain was given at a nearly ten-fold higher dose (200µg/kg) in humans (Katz et al., 2011). Yet, doses of anti-NGF as low as 10µg/kg are reported to effectively alleviate joint pain in OA in humans (Lane et al., 2010). As such, intra-articular anti-NGF not alleviating existing facet joint-mediated pain could be due to the fact that the site of action of NGF shifts from the joint immediately after its injury to the DRG once pain is established. Indeed, although NGF increases in the DRG by day seven after facet joint injury (Chapter 5; Kras et al., 2014b), it is not known if it is also elevated in the DRG at earlier time points. The serum half-life of IgG antibodies is reported to be nearly five days in the rat (Ishidate et al., 1990); but, it is unknown if intra-articularly injected antibodies are cleared from the joint quickly enough or if they reach the DRG. Intra-articular anti-NGF might not reach the DRG since even small molecular weight proteins (<50kDa) take hours to clear from the synovial fluid of joints (Allen et al., 2011), and IgG antibodies such as the one used in our studies are much larger (>150kDa). Since the DRG is not protected by the blood brain barrier

(Sapunar et al., 2012), systemic application of anti-NGF does reach it. As such, the systemic delivery of anti-NGF used clinically might be a more effective means of treating existing injury-induced facet pain.

Studies are ongoing to determine the optimal dose of anti-NGF to alleviate clinical OA pain while also minimizing the incidence of adverse events such as paresthesia, pain in the extremities, neuropathy, and even joint degeneration (Schnitzer et al., 2014; Schnitzer and Marks, 2015). In fact, in 2010, a hold was placed on the clinical studies utilizing anti-NGF treatments due to the risk of rapidly progressing joint degeneration; however, the hold was removed in 2012 following a thorough review of existing data (Schnitzer et al., 2014). The efficacy of anti-NGF treatments increases with increasing dose; however, the incidence of adverse events likewise increases (Schnitzer and Marks, 2015). Similarly, combination therapies including anti-NGF and oral NSAID treatment improve pain relief over either individual therapy, but they also incur a higher incidence of adverse events (Schnitzer et al., 2014). Experimentally, rats receiving intra-articular anti-NGF to prevent joint injury-induced pain exhibited normal weight gain and grooming behavior and were otherwise indistinguishable from control rats, with no obvious ill-effects associated with that local anti-NGF treatment (Chapter 5; Kras et al., 2014b). However, if systemic anti-NGF is administered in future studies with the goal of treating established pain after facet joint injury, close monitoring of animals for signs of adverse events similar to those identified during the treatment of clinical OA pain, such as pain and neuropathy in the extremities, will be necessary in order to identify an effective dose that also maximizes safety.

Administration of anti-NGF systemically, rather than intra-articularly, likely has greater potential for off-target effects as a result of its circulation throughout the entire body. In addition to blocking the effects of increased NGF in the painful joint, systemic anti-NGF also has the potential to disrupt normal NGF signaling in other tissues, such as the skin (McMahon, 1996). Indeed, loss of target-derived NGF available to sensory neurons and subsequent dysregulation of voltage-gated sodium channels is thought to contribute to pain after a nerve injury (Dib-Hajj and Waxman, 2010). A disruption of NGF signaling in peripheral tissues could underlie the reports of pain, paresthesia, and neuropathy in the extremities associated with anti-NGF treatment clinically (Brown et al., 2014; Schnitzer et al., 2014). Although paresthesia in the clinical trials was reported to be transient (Schnitzer et al., 2014) and would thus be difficult to quantify in the rat, pain in the extremities can be readily quantified using behavioral testing methods similar to those used throughout this thesis (Chapters 4, 5, & 6; Kras et al., 2013b; Kras et al., 2013c; Kras et al., 2014b). As such, in addition to monitoring weight gain and grooming behavior, rats receiving systemic anti-NGF should be evaluated behaviorally for signs of pain in the hindpaws since pain in the extremities is an adverse event associated with systemic anti-NGF clinically (Schnitzer et al., 2014).

In a rat model of facet joint osteoarthritis, injection of a chemical stimulus to induce OA is associated with inflammation and pain lasting only three days (Gong et al., 2011). However, three weeks after the initiating stimulus when joint degeneration is severe, pain returns and persists for at least an additional three weeks (Gong et al., 2011). Since the studies in this thesis were only through day seven, it is likely that joint degeneration itself may not contribute to the behavioral and electrophysiological

responses that are observed here. In experimental knee OA in the rat, surgical joint destabilization via transection of the meniscus induces joint degeneration by as early as one week (Janusz et al., 2002). Similarly, the first signs of joint degeneration following chemically-induced OA are visible within days of induction (Shuang et al., 2014). However, both surgically- and chemically-induced models of OA are designed to accelerate disease progression (Teeple et al., 2013), so joint degeneration following painful facet joint loading, in which no gross ligament damage is evident (Quinn et al., 2007), likely progresses more slowly, if at all. As such, a role for joint degeneration in the maintenance of injury-induced facet pain would likewise require more than a week to develop. Because behavioral hypersensitivity lasts for at least six weeks following facet joint distraction in this model (Rothman et al., 2007), additional studies extending on the order of weeks after injury are needed to define relationships between mechanical facet joint injury, joint degeneration, and persistent pain.

## 8.4. Limitations & Future Work

Collectively, the studies included in this thesis demonstrate contributions of NGF in the periphery, and BDNF in the central nervous system, to the development (NGF) and maintenance (BDNF) of facet-mediated pain and spinal neuronal hyperexcitability after a mechanical facet joint injury. Building upon previous studies utilizing this injury model that established inflammation and spinal neuronal hyperexcitability as contributing to facet pain (Crosby et al., 2013; Crosby et al., 2014; Dong et al., 2013a; Quinn et al., 2010), this work identifies NGF as one specific molecule in the joint that is an initiator of both persistent pain and spinal neuronal dysfunction associated with mechanical loading

of the facet joint. Yet, in this context, there are a number of limitations that warrant consideration. This section addresses several major limitations, including the use of purely tensile joint loading, evoked behavioral responses, and the lack of identifying a specific mechanism through which NGF induces behavioral hypersensitivity and spinal neuronal hyperexcitability. This section also suggests additional studies that would define the potential relationship between facet joint injury and OA and identify molecular pathways through which NGF contributes to persistent pain after injury.

The joint injury applied in this thesis imposes only tensile stretch of the facet joint capsular ligament. Although tensile stretch of the capsular ligament has been proposed as a mechanism underlying facet-mediated pain after a neck trauma (Panjabi et al., 1998; Pearson et al., 2004; Sundararajan et al., 2004), the facet joint also undergoes compression during a whiplash injury to the neck (Barnsley et al., 1994; Ono et al., 1997; Panjabi et al., 1998; Pearson et al., 2004). Simulations of whiplash-like neck trauma using cadaveric cervical spine specimens identify that the facet joint initially undergoes compression resulting from extension of the lower cervical spine (Pearson et al., 2004). Specifically, the inferior articular facet of the superior vertebra extends relative to the superior articular facet of the inferior vertebra, resulting in compression of the facet joint (Pearson et al., 2004). As discussed earlier (Section 8.3), compression of the facet joint can lead to articular impact and even fracture, damaging the joint cartilage and increasing the risk of OA development (Bogduk, 2011; Furman et al., 2014; Pearson et al., 2004). Biomechanical models of whiplash-like loading in the cervical spine identify the potential of articular impact during injury, but the magnitude of that compressive load has not been determined (Pearson et al., 2004). Because articular damage caused by impact is

a risk factor for OA (Furman et al., 2014), studying pain induced by isolated tensile loading of the facet joint neglects accounting for the possibility of cartilage damage that can lead to long-term degeneration of the joint.

Joint degeneration, including that of the facet joint, is a major source of pain clinically (Gellhorn et al., 2013; Lee et al., 2013). However, the contribution of degeneration of the joint to trauma-induced facet pain has not been investigated. Biomechanical simulations of traumatic neck injury using human spines demonstrates that maximum facet joint compression occurs nearly 40 milliseconds prior to the peak tensile strain in the capsular ligament (Pearson et al., 2004). If compressive loading to the facet joint were to be added to the injury model used in this thesis, in order to model neck trauma due to a motor vehicle collision, the compressive load would peak prior to distracting the facet joint. The magnitude of tensile loading applied to the rat throughout this thesis was scaled to be equivalent to distractions experienced by humans (Lee et al., 2004); as such, the magnitude of the *compressive* load experienced by humans during traumatic neck injury would also need to be appropriately scaled to the rat. Although that compressive load is unknown for humans, the peak magnitude of joint compression during neck trauma simulations in humans has been reported as 2.0±1.5mm for the C6/C7 facet joint (Pearson et al., 2004). That compression can be geometrically scaled between species by comparing the average facet joint space thickness in either species. In humans, the average thickness of the cervical facet space has been reported to be 1.9±0.5mm, computed using magnetic resonance imaging (Jaumard et al., 2014). Using a similar analysis, the corresponding joint space height in the rat could be used to develop a ratio of facet joint space thickness between the two species. That ratio could be used to

scale the magnitude of joint compression to be applied in the rat simulating the joint compression sustained during a motor vehicle collision-induced neck trauma. Inclusion of appropriately scaled compressive loading of the facet joint prior to tensile stretch of the capsular ligament in the rat will expand this model even more to be the first in vivo platform to study the contributions, if any, of facet joint articular impact to persistent pain and joint degeneration associated with traumatic neck injury.

Throughout this thesis, evoked measures of mechanical and thermal behavioral hypersensitivity are utilized as quantitative measures of pain, but spontaneous pain and activity-evoked pain are both major contributors to disability and a lower quality of life in chronic pain patients (Hagström et al., 1996; Mogil et al., 2010). Indeed, following neck trauma, spontaneous or ongoing pain is frequently reported (Hagström et al., 1996; Kosek and Januszewska, 2008; Mankovsky-Arnold et al., 2014). Further, in human volunteers, NGF sensitizes nociceptors and induces spontaneous pain (Rukwied et al., 2013). Because NGF is increased after a facet joint injury and is also necessary for the development of evoked behavioral hypersensitivity (Chapter 5; Kras et al., 2014b), spontaneous pain is also likely induced by the facet injury used in these studies. Yet, measures of spontaneous pain were not quantified. Metrics for quantifying spontaneous pain in animal models, such as food intake, grooming, and paw guarding, have proven unreliable in their specificity due to inherent susceptibility to confounding factors unrelated to pain (Mogil and Crager, 2004; Mogil et al., 2010). Due to the difficulty in quantifying spontaneous pain in experimental chronic pain models (Sotocinal et al., 2011), additional clinically-relevant measures of pain, such as activity-evoked pain, have been identified and implemented experimentally (Little and Zaki, 2012; Teeple et al.,

2013). Assessments of low back and osteoarthritis joint pain include, respectively, the Roland-Morris Disability Questionnaire (RMDQ) and the Western Ontario and McMaster Universities Osteoarthritis Index (WOMAC) questionnaires that assess the impact of pain on normal daily activities such as standing up, walking, and climbing stairs (Katz et al., 2011; Lane et al., 2010). Indeed, those questionnaires have been used to evaluate the effectiveness of anti-NGF therapies for low back and knee pain (Katz et al., 2011; Lane et al., 2010). Although measures of activity-evoked pain and functional deficits, including gait analysis, weight distribution, and locomotive activity (Larsen and Arnt, 1985; Matson et al., 2007; Teeple et al., 2013) have been quantified in animal models of OA, those measures are best suited to analysis of hindpaw function. Yet, neck trauma patients exhibit pain evoked by lifting objects with their arms (Mankovsky-Arnold et al., 2014), so assessment of activity-evoked pain in the upper limb is clinically relevant for facet pain.

Functionally, the grip strength of neck pain patients is diminished relative to healthy controls (Peolsson et al., 2014). A novel model of work-related repetitive use injury has been developed to study the effects of forelimb overuse on musculoskeletal and neural tissues (Barbe et al., 2013; Fisher et al., 2015). In that model, rats are trained to reach and pull a lever with their forelimbs in order to obtain a food pellet reward (Barbe et al., 2013). That protocol for that forelimb reaching task in the rat could be modified to assess voluntary use of and functional deficits in the forelimb after a painful facet joint injury in the rat. Since neck trauma patients exhibit diminished grip strength as well as pain evoked by lifting with their arms (Mankovsky-Arnold et al., 2014; Peolsson et al., 2014), a functional assay requiring *both* reaching and pulling in the rat is

translatable to the clinic. Implementation of that functional test in our facet joint injury model will not only increase its clinical relevance, but also enable assessment of whether or not interventions to treat pain also improve functional deficits.

Clinically, exposure to neck trauma initiates pain as early as 24 hours after the initial injury (Chien et al., 2010), and as many as 50% of those neck pain patients will report that their pain persists at one year after injury (Carroll et al., 2009). Yet, behavioral and cellular responses to facet joint injury in the rat were only investigated in this thesis as late as day seven post-injury, despite the fact that facet joint injury-induced pain is maintained as late as six weeks after the initiating injury (Rothman et al., 2007). Due to lifespan differences between the rat and the human, the persistence of pain for weeks in the rat approximates chronic pain in the human (Sengupta, 2013), with a single day in the life of a rat approximated as roughly equivalent to a month in the lifecycle of a human (Sengupta, 2013). Accordingly, pain maintained through seven days in the rat can be taken as persistent and is one of the primary reasons that rats were followed only through day seven after injury in this thesis. In addition, the abundance of data pertaining to the behavioral and molecular responses at that time after facet joint injury, including evidence for joint inflammation and the development and maintenance of spinal neuronal hyperexcitability (Crosby et al., 2013; Dong et al., 2013a; Quinn et al., 2010), enables comparison to previous work. However, by limiting studies to this time point, it is not possible to evaluate several potential long-term responses that have been uncovered in this work, such as joint degeneration that may develop over weeks in the rat. Indeed, facet joint injury induces mechanical laxity and inflammation ($PGE_2$, NGF upregulation) associated with joint degeneration and OA pain (Dare and Rodeo, 2014; Dong et al.,

2013a; Goldring and Goldring, 2007; Kras et al., 2014b; Lane et al., 2010; Orita et al., 2011; Quinn et al., 2007). However, the structural integrity of the joint was not investigated at any time point after injury in this thesis. Even if it was, day seven would likely be too early to detect signs of degeneration (Section 8.3). Nevertheless, the elevation of inflammatory mediators such as NGF and $PGE_2$ that are associated with OA suggests that degeneration may be initiated in the joint after injury. Because OA of the facet joints is a source of neck pain clinically (Gellhorn et al., 2013), joint degeneration should be evaluated following facet joint injury in the rat. Development of joint degeneration after a motor vehicle collision-induced neck trauma could explain why chronic facet-mediated pain is refractory to treatment; however, the relationship between loading-induced facet joint injury and degeneration is as yet undefined.

OA models of joint pain also demonstrate upregulation of inflammatory cytokines and NGF within the joint immediately following arthritis induction (Gong et al., 2011; McNamee et al., 2010; Orita et al., 2011), and blocking NGF prevents the initiation of pain (McNamee et al., 2010). Yet, NGF is also upregulated several weeks after induction of arthritis when degeneration is prominent, and blocking NGF also alleviates pain when OA is advanced (McNamee et al., 2010; Orita et al., 2011). Indeed, intra-articular levels of NGF are elevated in clinical OA patients, and disruption of NGF signaling via anti-NGF treatment alleviates clinical joint pain in patients with joint degeneration (Schnitzer et al., 2014). However, the temporal expression of intra-articular NGF is unknown after a facet joint injury. Chemical induction of OA in the knee increases intra-articular NGF by one week after the initiating stimulus and maintains that elevated level through at least four weeks (Orita et al., 2011). Similar chemical induction of OA in the facet joint

produces signs of degeneration, such as fissures in the cartilage and cartilage erosion, within one week and progressing to severe degeneration by four weeks (Gong et al., 2011). Chemically-induced OA may progress more rapidly than in models that surgically destabilize joints to induce OA, and differences in the time course of joint degeneration exist depending on the technique used to destabilize the joint (Teeple et al., 2013). Yet, even in surgically-induced OA in the knee, joint degeneration is evident by four weeks (Appleton et al., 2007). Because both chemically- and surgically-induced models of OA exhibit joint degeneration within four weeks but may show signs at one week (Appleton et al., 2007; Orita et al., 2011), preliminary investigations of joint degeneration and intra-articular NGF overexpression associated with facet joint loading should be investigated at both one week and four weeks after injury. Quantifying NGF expression in addition to joint degeneration should also identify additional time points at which disruption of NGF signaling might alleviate established facet pain.

In addition, the specific mechanism(s) through which NGF initiates facet joint injury-induced behavioral hypersensitivity and spinal neuronal hyperexcitability remain unknown. The upregulation of BDNF in the DRG and spinal cord at day seven in parallel with increased NGF in the DRG at that time after facet joint injury (Chapter 5; Kras et al., 2013c) demonstrates that transcriptional regulation of BDNF by NGF contributes to facet pain. Yet, gene regulation is only one mechanism through which NGF sensitizes neurons and induces pain. A major function of NGF is to promote axonal growth and survival of neurons; indeed, NGF knockout models are fatal perinatally (Chen et al., 2005). NGF applied to the spinal cord promotes sprouting of nociceptive afferents (Tang et al., 2004). Yet, the neurotrophic activity of elevated NGF expression in the facet joint

following its injury was not evaluated in this thesis. Rather, the relationship between intra-articular NGF and spinal neuronal hyperexcitability after a painful facet joint injury was the primary focus of the studies reported here. NGF expression was quantified within the joint capsule and synovium, and immunohistochemical labeling of the C6/C7 facet joint confirmed that expression of NGF in the soft tissues surrounding the joint is higher after injury than in sham control joints (Chapter 5; Kras et al., 2014b). Indeed, that overexpression of NGF suggests that afferent fiber sprouting might also occur after injury. Moreover, a majority of joint afferents are peptidergic and, thus, sensitive to NGF (Chapter 4; Kras et al., 2013b). Since targeted ablation of neurons involved in peptidergic signaling prevents both NGF- and injury-induced behavioral hypersensitivity and spinal neuronal hyperexcitability (Chapter 5), it is likely that any NGF-mediated fiber sprouting would also be specific to that subpopulation of afferents. Those findings demonstrate that intact innervation of the facet joint is necessary for NGF-induced pain and neuronal dysfunction in the spinal cord. Yet, those studies are unable to distinguish whether NGF mediates hyperexcitability of spinal neurons through increased transcription of pain mediators or if sprouting of joint afferents leads to joint hyperinnervation and thus increased sensitivity to motion of the joint.

Studies of arthritis pain report sprouting of peptidergic and sympathetic fibers within the joint that is blocked by anti-NGF treatment (Ghilardi et al., 2012; Longo et al., 2013). Moreover, blocking sympathetic fiber growth alleviates arthritis pain (Longo et al., 2013), demonstrating that hyperinnervation of the joint contributes to pain maintenance. Although those studies evaluated fiber growth four weeks after induction of arthritis, in vitro studies demonstrate that NGF promotes DRG neurite outgrowth within

days of exposure (Tang et al., 2013), so evidence of nerve growth such as increased expression of growth associated protein-43 (GAP-43) should be apparent by day seven after facet joint injury. Indeed, increased synaptogenesis in the spinal cord is evident at day seven after injury, with a trend toward significant increases as early as day one after injury (Crosby et al., 2015). It is likely that neuronal growth would also occur in the facet joint on a similar time frame. In light of the evidence for overexpression of NGF in the joint after injury and the abundance of NGF-responsive afferents innervating the joint, NGF-mediated fiber sprouting in the injured facet joint should be quantified in order to evaluate whether or not hyperinnervation of the joint contributes to long-term facet pain.

Interestingly, blocking intra-articular afferent activation with bupivacaine does not alleviate pain when it is done four days after the pain is initiated (Crosby et al., 2014); however, bupivacaine is only expected to alleviate clinical pain for 8-12 hours when applied post-operatively (Skolnik and Gan, 2014). As such, input from the facet joint might contribute to facet pain maintenance, as it does clinically (Barnsley, 2005; Manchikanti et al., 2008). It is possible that a block of the nerves lasting longer than 8-12 hours may be necessary to detect analgesic effects behaviorally in this rat model. Ablating joint afferents pharmacologically is one means of blocking joint afferent activity over an extended period of time. Ablation of NK1R-expressing joint afferents prior to injury via intra-articular application SSP-saporin prevents the development of pain after a subsequent facet joint injury (Figure 8.2). However, no study has identified whether or not ablation of joint afferents alleviates established pain after joint injury. Although saporin requires up to fourteen days to induce neuronal cell death (Weisshaar et al., 2014; Wiley et al., 2007), such a time course is not prohibitive to studying the potential

relationship between joint afferent signaling and the maintenance of facet pain since facet injury induces pain that lasts at least six weeks (Rothman et al., 2007). Indeed, ablation of the nerves innervating a painful facet joint alleviates facet pain in approximately 60% of patients, with pain relief lasting at least three months (Lord et al., 1996; Smith et al., 2014). Yet, clinical pain relief is not permanent after ablation of facet joint afferents. It may be that chronically elevated levels of NGF within the facet joint precipitate regrowth of afferent fibers back into the joint and, consequently, a return of the pain. As such, in addition to identifying whether or not intra-articular NGF induces fiber sprouting in the injured facet joint, studies assessing the role of joint afferents in the *maintenance* of facet pain should ablate joint afferents as well as inhibit NGF signaling to prevent any potential reinnervation of the joint. Those studies would further define the ongoing role of joint input to persistent pain, but they could also provide a means of prolonging the pain-alleviating effects of neuronal ablation currently used to treat clinical neck pain.

Recent reports promote the idea of nociceptive priming, referring to a transient insult causing a subsequent stimulus to elicit a prolonged pain state, as a potential mechanism underlying chronic pain. Several studies report that following exposure to stimuli such as carrageenan, TNF-α, or NGF that induce transient pain in the rat, $PGE_2$ injected into the paw can induce long-lasting pain (Joseph and Levine, 2010; Parada et al., 2003; Reichling and Levine, 2009). Indeed, following carrageenan-induced priming, administration of $PGE_2$ to the paw induces pain lasting several weeks, although in the unprimed state, $PGE_2$ induces only transient pain lasting on the order of hours (Aley et al., 2000; Reichling and Levine, 2009). Further, that purported primed state can last for weeks after the initial priming stimulus (Aley et al., 2000). Recent work in our rat model

demonstrates that priming in the spinal cord results in a facet joint distraction injury of a magnitude normally insufficient to induce pain to instead cause sustained behavioral hypersensitivity (Crosby et al., 2015). Moreover, preliminary work suggests that intra-articular NGF is sufficient to similarly prime the joint afferents in the rat (Figure 8.4). In pilot studies, NGF at a dose insufficient to induce pain (1µg in 5µL of sterile phosphate buffered saline) was injected into the bilateral C6/C7 facet joints (n=3 rats). On day two after the NGF injection, a normally non-painful facet joint distraction was applied (Crosby et al., 2015; Dong et al., 2012; Lee and Winkelstein, 2009); yet, the forepaw mechanical withdrawal threshold significantly decreased below baseline levels ($p<0.043$) and remained at the lower level through day seven (Figure 8.4).

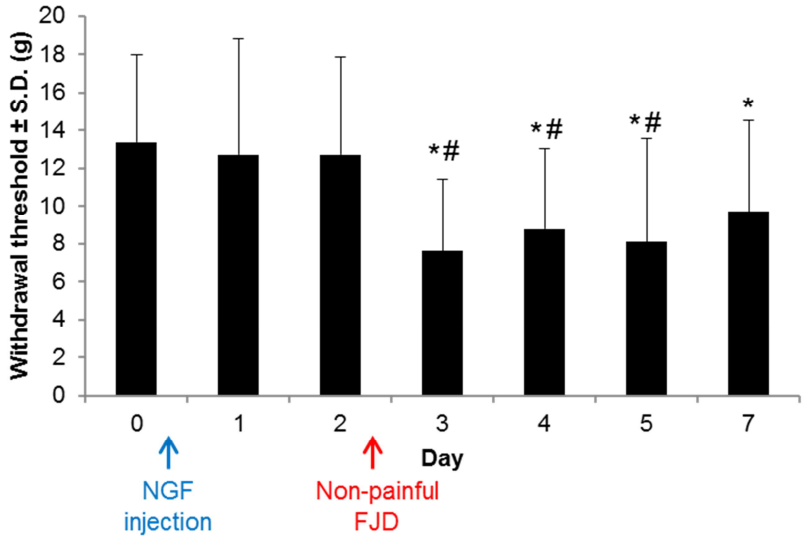


**Figure 8.4.** Mechanical sensitivity in the forepaw as measured by the withdrawal threshold in response to von Frey filament stimulation. Withdrawal threshold is unchanged from baseline on days one and two following intra-articular injections of 1µg NGF into the bilateral C6/C7 facet joints. Following a normally non-painful facet joint distraction (FJD) on day two, the withdrawal threshold significantly decreases from baseline at all subsequent time points (*$p<0.043$). On days three, four, and five, the withdrawal threshold also decreases relative the pre-distraction threshold on day two (#$p<0.028$).

Intra-articular NGF increases within the facet joint by day one after a painful facet joint injury (Chapter 5; Kras et al., 2014b); yet, it is unclear if a non-painful facet joint distraction is also sufficient to increase even slightly the intra-articular NGF levels. If so, a non-painful facet joint distraction could prime the sensory neurons such that a subsequent low-level joint distraction would induce a prolonged hypersensitivity. Indeed, mechanical or chemical priming is a potential and even likely mechanism through which an equivalent neck trauma in different patients induces transient pain in some but chronic pain in others (Jull et al., 2011; Sterling et al., 2003). It may be that a subset of those people undergoing a traumatic neck injury had previously sustained a minor neck trauma that primed them for experiencing a subsequent injury as painful. Although these findings are preliminary (Figure 8.4), the potential for intra-articular NGF to induce priming without inducing pain could profoundly shift the way neck trauma is treated. Rather than focusing only on the treatment of pain after an injury, interventions to disrupt neuronal priming would also then need to be developed so that even those trauma patients who do not experience pain after a neck trauma are not at greater risk of chronic pain in the event of a later trauma. Sustained activity of protein kinase C epsilon (PKCε) is reported as necessary for the maintenance of neuronal priming (Reichling and Levine, 2009). Antisense knockdown of PKCε expression eliminates priming and prevents its return even when PKCε levels return to normal (Reichling and Levine, 2009). Antagonists of PKCε have been developed (Inagaki et al., 2006). Further study is needed to determine if a non-painful facet joint injury upregulates intra-articular NGF and induces priming similar to that induced by a non-painful intra-articular injection of NGF. If priming is induced, PKCε antagonists could be evaluated for their potential to disrupt loading-

induced priming; such studies would be invaluable for developing therapies to prevent, rather than treat, trauma-induced chronic pain clinically.

## 8.5. Conclusions

In summary, studies presented in this thesis define contributions of the neurotrophins NGF and BDNF to mechanically-induced facet-mediated pain. Interestingly, a single molecule acting on a subpopulation of joint afferents is able to initiate facet pain. Intra-articular NGF is sufficient to induce both pain and spinal neuronal hyperexcitability, but only when those neurons involved in peptidergic signaling are intact. Painful facet joint injury upregulates NGF expression within the injured joint, which, in turn, can initiate both pain and spinal neuronal hyperexcitability at day one. Injury-induced elevation of NGF in the DRG by day seven stimulates overexpression of BDNF, which is released into the spinal cord where it maintains behavioral hypersensitivity and likely contributes to the long-term hyperexcitability of spinal neurons.

The work in this thesis is the first to identify a specific cellular mechanism within the joint that initiates pain and to define the relationship between that local mechanism and the spinal modifications that maintain facet-mediated pain. Since intra-articular NGF signaling is critical in increasing afferent excitability through translational and post-translation modifications and in stimulating neuronal growth (Longo et al., 2013; Nicol and Vasko, 2007), additional work characterizing the spontaneous component of facet-mediated pain as well as defining the contributions of neuronal priming and/or sprouting in the joint and spinal cord to the maintenance of pain is necessary. Moreover, NGF

signaling has a close relationship to joint pain from osteoarthritis; neck trauma that upregulates NGF also exhibits several risk factors for osteoarthritis. As such, identifying if there are potentially parallel mechanisms between osteoarthritis and facet joint trauma-induced pain involving NGF signaling would help determine if anti-NGF treatments that are being developed for OA may also be applicable to facet-mediated pain. However, joint laxity and inflammation, which are associated with facet joint loading sufficient to induce pain (Dong et al., 2013a; Quinn et al., 2007), also support joint degeneration as a factor that may contribute to long-term facet pain and disability. Yet, a role for degeneration in chronic facet pain has not been defined. The prevention of facet pain development and spinal neuronal hyperexcitability after injury with immediate anti-NGF treatment provides a foundation for future investigations into the specific molecular and structural mechanisms that promote neuronal hyperexcitability and persistent pain after facet joint injury. Although further studies are needed to identify the time course and optimal delivery method for effective anti-NGF treatment of facet pain, demonstrating that a single molecule in the facet joint is sufficient to initiate pain provides an important step toward developing targeted pharmacological therapies to effectively treat facet-mediated chronic pain.

# Appendix A

# Matlab Codes

This appendix contains the Matlab code that was used to generate the input file for LS-DYNA (LSTC; Livermore, CA) to calculate capsular ligament strains for all of the studies throughout this thesis. The Matlab code used to calculate the ratio of pixels positive for BDNF labeling relative to the total number of pixels in immunolabeled spinal cord sections for studies in Chapter 6 is also included. For the strain calculations, the Matlab code (Section A.1; Dyna_KatieFile.m) requires two input files containing: (1) the initial and final coordinates (i.e. $x_i$ $y_i$; $x_f$ $y_f$) for each capsule marker and (2) the start and stop times for the joint distraction. The user must separately input the number of rows and columns of markers that cover the joint capsule as a grid. The output file from the code is then input into LS-DYNA, which is used to generate a mesh of elements for the capsule and to calculate the strain in each element for the applied distraction.

The second Matlab code (Section A.2; densitometry_manual_threshold_fluor.m) included in this appendix was used for all densitometric quantifications of BDNF in the spinal cord (Chapter 6). This code requires that all of the images that are to be analyzed be located in the same file directory as the code file. In addition, this code requires the image files to be in the .tif format and must have 'BDNF' at the start of each file name. BDNF-labeled sections are imaged in the red channel; accordingly, this code only analyzes the red channel of images in the rgb format. A threshold for positive pixels (0-255) must be defined and manually applied to the pos_thresh variable in the code. In

order to define the positive pixel threshold for normal spinal BDNF expression, BDNF-labeled sections from a normal rat must be analyzed by running the script using a range of threshold values. The threshold that identifies positive pixels in the dorsal horn of the normal rat that most closely match the observed BDNF labeling in that region should be selected and then applied during analysis of all experimental groups. Although the positive pixel threshold must be defined separately for each immunolabeling study (day one, day seven) due to the inherent variability associated with immunohistochemical labeling, the positive pixel threshold applied for analysis of BDNF expression at day one and day seven in these studies (Chapter 6) is 95. An excel file that contains the ratio of positive pixels relative to all pixels for the red channel is generated for each image at the completion of the code.

**Section A.1. Dyna_KatieFile.m**

```
%MATLAB code to create a DYNA deck
%will allow for analysis of strain and generation of strain field data
%JUNE 2004: coded by Andrew Franklin (DYNA.m)
%JULY 2005: modified by Katie Lee (DYNA2.m) to allow for input of incremental data
%Modied by Ling Dong -
%% OBTAIN USER INPUT TO DEFINE VARIABLES

loadfile = input('Enter the name of the file containing incremental x & y coordinates
(with .txt extension): \n','s');
filename=loadfile;
timefile = input('Enter the name of the file containing a list of incremental times (in
seconds) (with .txt extension): \n','s');
rows = input('How many rows in the marker matrix? \n');
cols = input('How many cols in the marker matrix? \n');
timestep = input('Enter the analysis timestep.\nThe value must be greater than 0 and less
than 1.\nSuggest using a very small timestep for greater accuracy of results, i.e.
0.001.\n');
plotstep = input('Enter the timestep to be used for displaying results.\nIt should be at least
as big as the analysis timestep.\nSuggest using 0.1 to optimize plot display timing.\n');
% headerlines = input('How many lines of header or extraneous data are there?  \n ');

nodes = rows*cols;

%% IMPORT COORDINATE DATA
% initial x and y coordinates
loadfile=load(loadfile);
colxrow = size(loadfile);
numrows = colxrow(2);
numframes=numrows/2;
xini=loadfile(:,1);
yini=loadfile(:,2);

% generate x and y displacement matrices
xdisp=zeros(nodes,numframes);
ydisp=zeros(nodes,numframes);

for i=1:numframes
   for j=1:nodes
   xdisp(j,i)=loadfile(j,((2*i)-1))-xini(j);
   ydisp(j,i)=loadfile(j,(2*i))-yini(j);
   end
end

%% IMPORT TIMING DATA (TIME @ EACH LOADING STEP)
```

```
timefile=load(timefile);

%% *NODE
node_matrix = zeros(nodes,4);
for i = 1:nodes
   node_matrix(i,1) = i;
   node_matrix(i,2) = xini(i,1);
   node_matrix(i,3) = yini(i,1);
   node_matrix(i,4) = 0;
end

%% *ELEMENT_SHELL
elements = (rows - 1)*(cols - 1);
elem_matrix = zeros(elements,6);
pos = 1;
counter = 0;
for i = 1:rows - 1
  counter = counter + 1;
  for j = 1:cols - 1
   elem_matrix(pos,1) = pos;
   elem_matrix(pos,2) = 1;
   elem_matrix(pos,3) = counter;
   elem_matrix(pos,4) = counter+cols;
   elem_matrix(pos,5) = counter+cols+1;
   elem_matrix(pos,6) = counter+1;
   pos = pos + 1;
   counter = counter + 1;
  end
end

%% *BOUNDARY_PRESCRIBED_MOTION_NODE
motion_matrix = zeros((nodes*2),6);
% motion_matrix = zeros(nodes*3,6); %when the #of frames > nodes*2
counter = 1;
   for i = 1:nodes
%      for i = 1:(nodes+2);
      for j = 0:1
         motion_matrix((2*i)+j-1,1) = i;
         motion_matrix((2*i)+j-1,2) = j+1;
         motion_matrix((2*i)+j-1,3) = 2;
         motion_matrix((2*i)+j-1,4) = counter;
         motion_matrix((2*i)+j-1,5) = 1;
         motion_matrix((2*i)+j-1,6) = 0;
         counter = counter + 1;
      end
```

```
   end

%% CREATE LOADING CURVES
% generate first line of input (description of load curve)
load_matrix = zeros(nodes*2,7);
% load_matrix = zeros (nodes*3,7); %when the #of frames > nodes*2
counter = 1;
   for i = 1:(nodes*2)
%     for i = 1:nodes*3;       %when the #of frames > nodes*2
       load_matrix(i,1) = counter;
       load_matrix(i,2) = 0;
       load_matrix(i,3) = 1;
       load_matrix(i,4) = 1;
       load_matrix(i,5) = 0;
       load_matrix(i,6) = 0;
       load_matrix(i,7) = 0;
       counter = counter+1;
   end

load_matrix = load_matrix';

% generate remainder of loading curve input (incremental displacement)
step_matrix = zeros(numframes,(nodes*2));
% step_matrix = zeros(numframes,(nodes*3));
   for i = 1:nodes
     step_matrix(:,(i*2)-1) = xdisp(i,:);
     step_matrix(:,(i*2)) = ydisp(i,:);
   end

%% *CONTROL_TIMESTEP
control_timestep = [timestep,0.9,0,0,timestep,0,0,0];

%% *CONTROL_TERMINATION
control_termination = [timefile(length(timefile)),0,0,0,0];

%Printing the data to a dyna file
fileoutput = strrep(filename, 'txt', 'dyn');
fid = fopen(fileoutput, 'wt');
fprintf(fid,'*KEYWORD\n');
fprintf(fid,'*TITLE\n');
fprintf(fid,'FacetMarkers\n');
fprintf(fid,'*PART\n');
fprintf(fid,'PART PID = 1 NAME = FacetMarkers\n');
fprintf(fid,'1,1,1\n');
fprintf(fid,'*NODE\n');
```

```
fprintf(fid,'%5.0f,%5f,%5f,%5f\n',node_matrix');
fprintf(fid,'*SET_NODE_GENERAL\n');
fprintf(fid,'1,0,0,0,0\n');
fprintf(fid,'ALL\n');
fprintf(fid,'*ELEMENT_SHELL\n');
fprintf(fid,'%2.0f,%2.0f,%2.0f,%2.0f,%2.0f,%2.0f\n',elem_matrix');
fprintf(fid,'*MAT_ELASTIC\n');
fprintf(fid,'1,1,100000,0.2\n');
fprintf(fid,'*SECTION_SHELL\n');
fprintf(fid,'1,13,0.833\n');
fprintf(fid,'0,0,0,0\n');
fprintf(fid,'*CONTROL_SHELL\n');
fprintf(fid,'15,0,-1,0,13,2,1,0\n');
fprintf(fid,'*DATABASE_EXTENT_BINARY\n');
fprintf(fid,'0,0,3,1,1,1,2,1\n');
fprintf(fid,'0,0,0,0,0,3,1\n');
fprintf(fid,'*BOUNDARY_SPC_SET\n');
fprintf(fid,'1,0,0,0,1,1,1,1\n');
fprintf(fid,'*BOUNDARY_PRESCRIBED_MOTION_NODE\n');
fprintf(fid,'%2.0f,%2.0f,%2.0f,%2.0f,%2.0f,%2.0f\n',motion_matrix');
   for i = 1:length(step_matrix)
      fprintf(fid,'*DEFINE_CURVE\n');
      fprintf(fid,'%2.0f,%2.0f,%2.0f,%2.0f,%3f,%2.0f,%2.0f\n',load_matrix(:,i));
      for j=1:numframes
         fprintf(fid,'%5f,%6f\n',timefile(j),step_matrix(j,i));
      end
   end
fprintf(fid,'*DATABASE_NODOUT\n');
fprintf(fid,'%1.3f\n',plotstep);
fprintf(fid,'*DATABASE_BINARY_D3PLOT\n');
fprintf(fid,'%1.3f\n',plotstep);
fprintf(fid,'*CONTROL_TIMESTEP\n');
fprintf(fid,'%1.3f,%1.2f,%1.0f,%1.0f,%1.3f,%1.0f,%1.0f,%1.0f\n',control_timestep);
fprintf(fid,'*CONTROL_TERMINATION\n');
fprintf(fid,'%4f,%1.0f,%1.0f,%1.0f,%1.0f\n',control_termination);
fprintf(fid,'*END\n');
fclose(fid);

%end of program
```

**Section A.2. densitometry_manual_threshold_fluor.m**

```
%% This script was written to calculate and visualize percent positive
%% pixels per image. To run the file, u want to create an excel file that
%% has the detailed information abt the images to be analyzed, then number
%% those images with a common name that has an ordered numerical (1, 2...)
%% ending. NOTE: for the excel file, please have the following columns (in
%% order): rat #, tissue type, injury type, image no., threshold, raw
%% results, normalized results. Number normals last.

%% requires MATLAB 7.0 (or higher) and imaging toolbox.

%% Written by Ling Dong (modified from K. Quinn) on Feb 2, 2009.
%% Modified by Kristen Nicholson December 2009

clear all;
close all;

D = dir('BDNF*.tif');%specify which images to analyze (* = wildcard character)

for k=1:length(D);

   %reads file in
   file=D(k).name;

   % Load the image
   imag_orig = imread(file);
   % converts to grayscale
   imag_orig = imag_orig(:,:,1);%grab the red labeled image
   %imag_orig = imag_orig(:,:,2);%grab the green labeled image
   %imag_orig = rgb2gray(imag_orig);
   imag = imag_orig;
   invImag = (max(max(imag)) + min(min(imag))) - imag;
   imag = invImag;

   %calc number of pixels
   [a b]=size(imag);
   tsize=a*b;
   low=double(min(imag(:)));
   high=double(max(imag(:)));
   whiteSpace = 0.96*high;
   pos_thresh = 95; %input based on normal run, remember for DAB staining
   % higher value corresponds to a higher +ive threshold.

   backg=sum(sum(imag>whiteSpace));
   posp=sum(sum(imag<pos_thresh));
```

```
    %calc percent of positive pixels in tissue
    percpos(k)=  posp/(tsize-backg);

    %map out pos and neg pixels
    pmap=(imag<pos_thresh);
    nmap=(imag>whiteSpace);

    %   make figure for each image, if you are processing a bunch of images, you
    %   may want to comment this part out

    %make positive pixels more green, and background pixels less blue
    imag1(:,:,1)=double(imag)/255;
    imag1(:,:,2)=(1-pmap).*double(imag)/255+pmap;
    imag1(:,:,3)=double(imag)/255.*(1-nmap);


    h = figure;
    subplot(3,1,3);
    subimage(imag);
    axis image
    axis off
    subplot(3,1,2);
    subimage(imag1);
    axis image
    axis off
    colormap gray
    subplot(3,1,1);
    subimage(imag_orig);
    axis image;
    axis off;
    %drawnow;

    %save the gray-scale, inverted, and pos/neg images as a new figure
    saveas(h, ['densitometry-' D(k).name], 'jpg')

    clear imag imag1;
end
```

# Appendix B

# Facet Joint Distraction Mechanics

This appendix summarizes the loading parameters during facet joint injury, including the forces and displacements of the facet joint distraction device, the capsular ligament stretch, and the resultant strain fields across the capsule for all of the joint distractions for the rats used in this thesis. Table B.1.1 summarizes the C6 displacement and force responses across the C6/C7 facet joint during joint distraction measured for each rat in the studies in Chapter 3. The C6 displacement is measured by the linear variable differential transducer (LVDT) attached to the C6 forceps. A load cell attached to the C7 forceps captures the load imposed across the joint during distraction. The maximum principal strain fields were calculated at the peak joint distraction using LS-DYNA for each of the rats included in the studies in Chapter 3 and are presented in Table B.1.2. A Matlab program was used to generate the input files for calculating strain in LS-DYNA; that associated Matlab code is included separately in Appendix A. The strain values displayed with each strain field represent engineering strain, which is the default output for LS-DYNA. The maximum C6 displacements, the corresponding maximum vertebral and capsule distractions, and the maximum principal strain (MPS) and the maximum rostrocaudal strain for each rat presented in Chapter 3 are provided in Table B.1.3, in addition to Table 3.1. All of the strains presented have been converted to Lagrangian strain.

For all of the rats that underwent joint distraction in the studies presented in Chapters 4 and 5, only the C6 displacements, the vertebral and capsule distraction magnitudes, and the MPS and maximum rostrocaudal strain are summarized here. Table B.2 details the C6 displacements, vertebral and capsule distractions, and capsular ligament strains after facet joint injury for the rats used to characterize the innervation pattern of the C6/C7 facet joint (Chapter 4). Table B.3.1 provides the C6 displacements, vertebral and capsule distraction magnitudes, and capsule strains for the rats used to characterize nerve growth factor (NGF) expression in the facet joint and DRG after injury (Chapter 5). Specifically, the loading mechanics are summarized for the rats that underwent facet joint distraction (FJD), as well as for those that received intra-articular SSP-Sap (SSP-Sap+FJD) or Blank-Sap (Blank-Sap+FJD) prior to a joint distraction. Table B.3.2 summarizes the loading mechanics for all rats after FJD with immediate C6/C7 intra-articular anti-NGF (FJD+anti-NGF) or vehicle IgG (FJD+vehicle) injections as well as those rats receiving intra-articular anti-NGF one day after FJD (FJD+Anti-NGFD1) (Chapter 5).

For those rats that underwent joint distraction in the studies included in Chapter 6, technical difficulties prevented recording from several of the rats. As such, only the C6 displacements and vertebral distraction magnitudes are presented. Table B.4.1 summarizes the displacement and vertebral distraction values for the rats used to characterize BDNF expression in the spinal cord and dorsal root ganglion after FJD in Chapter 6. Table B.4.2 presents the displacements and vertebral distractions after painful joint loading with day 5 trkB-Fc (trkB-Fc) or vehicle IgG-Fc (vehicle) treatment in Chapter 6. Finally, the C6 displacements, vertebral and capsule distractions, and capsular

ligament strains after facet joint injury for rats used in Chapter 7, including those that underwent injury alone (FJD) and those that had intra-articular IB4-Saporin applied prior to injury (IB4-Sap+FJD), are summarized in Table B.5.

## Table B.1.1. Force-displacement plots for Chapter 3.

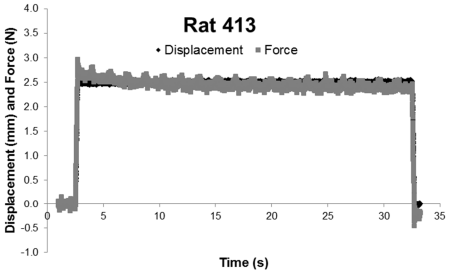


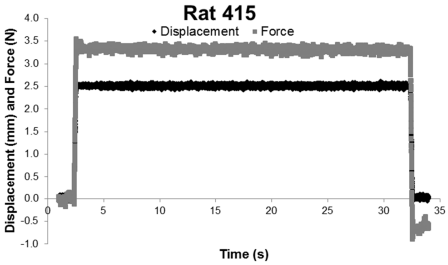


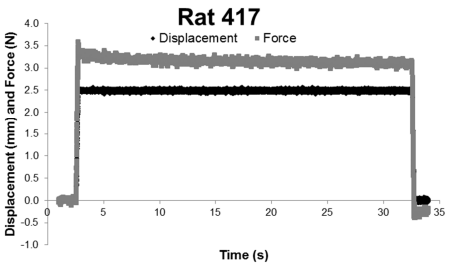


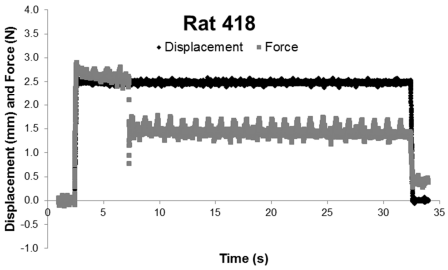


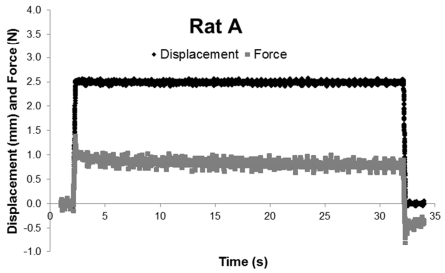


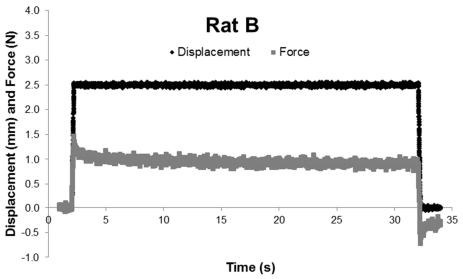


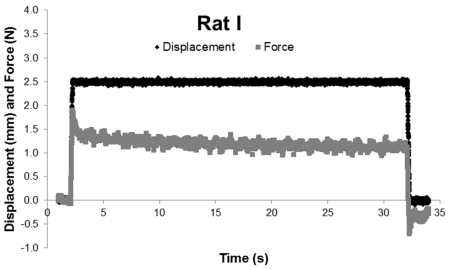


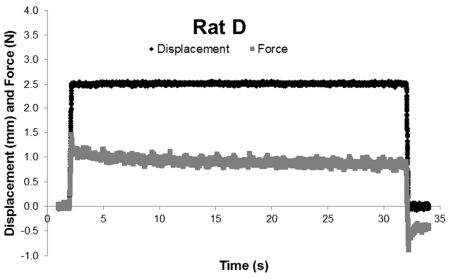


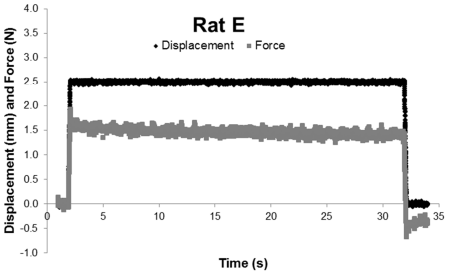


Note: For rats A-I, facet joint distraction procedures were performed by Ben A. Bulka, and the naming scheme reflects his records.

**Table B.1.2. Maximum principal strain fields for Chapter 3.**

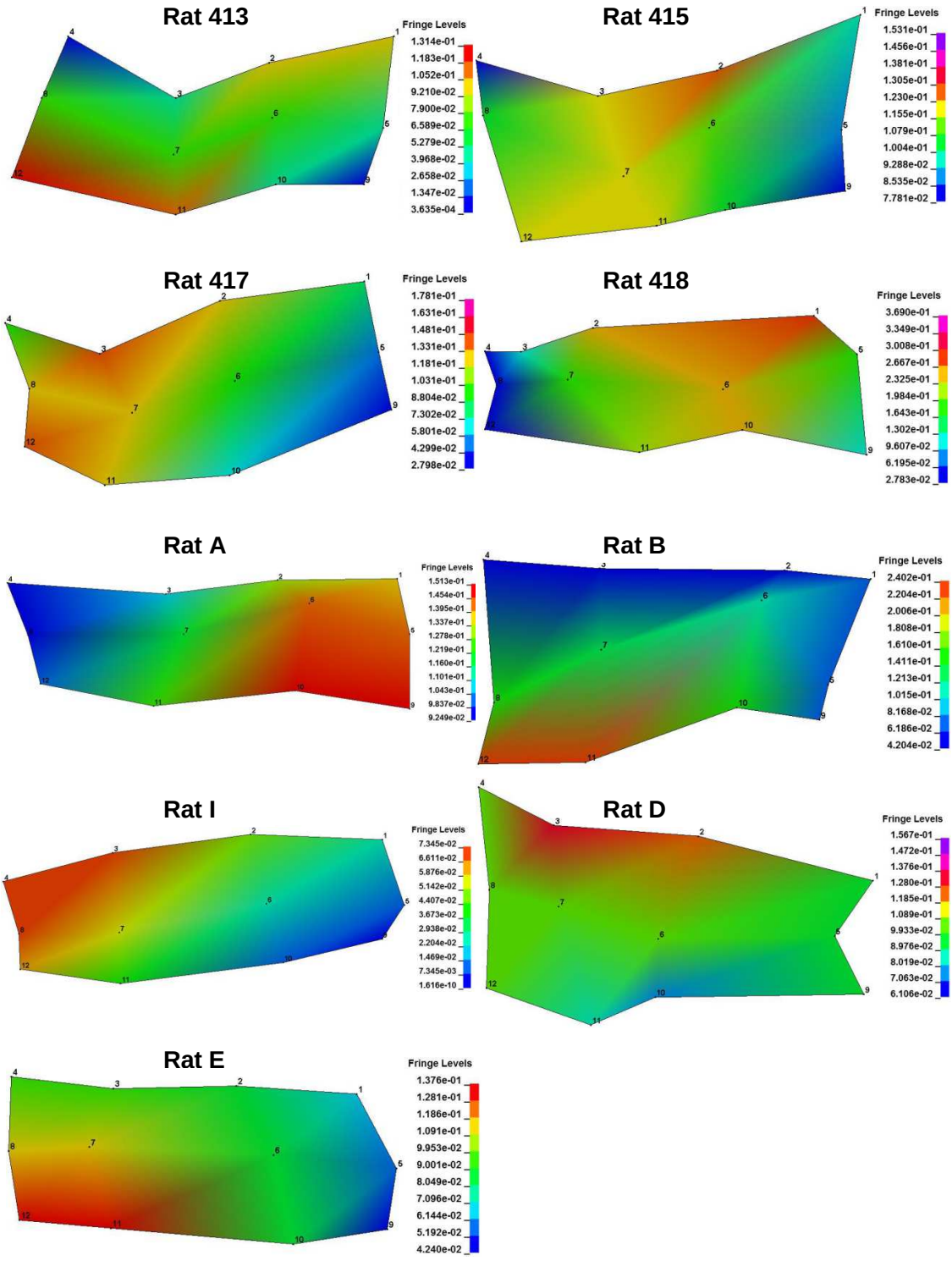

**Table B.1.3. C6 displacements, vertebral distractions, capsule distractions, and capsular ligament strains for Chapter 3.**

| Group | Rat | C6 displacement (mm) | Vertebral distraction (mm) | Capsule distraction (mm) | Maximum principal strain (%) | Maximum rostrocaudal strain (%) |
|---|---|---|---|---|---|---|
| FJD | 413 | 2.47 | 0.44 | 0.19 | 15.03 | 5.41 |
| | 415 | 2.50 | 0.36 | 0.25 | 17.92 | 17.81 |
| | 417 | 2.50 | 0.59 | 0.32 | 21.40 | 19.28 |
| | 418 | 2.50 | 0.96 | 0.59 | 54.59 | 40.97 |
| | A | 2.50 | 0.45 | 0.27 | 17.67 | 8.93 |
| | B | 2.53 | 0.45 | 0.17 | 30.84 | 8.68 |
| | I | 2.48 | 0.34 | 0.26 | 7.91 | 2.14 |
| | D | 2.51 | 0.55 | 0.25 | 18.41 | 18.00 |
| | E | 2.54 | 0.35 | 0.23 | 15.84 | 7.87 |

For rats A-I, facet joint distraction procedures were performed by Ben A. Bulka, and the naming scheme reflects his records.

**Table B.2. C6 displacements, vertebral distractions, capsule distractions, and capsular ligament strains for Chapter 4.**

| Group | Rat | C6 displacement (mm) | Vertebral distraction (mm) | Capsule distraction (mm) | Maximum principal strain (%) | Maximum rostrocaudal strain (%) |
|---|---|---|---|---|---|---|
| FJD | 134 | 2.51 | 0.48 | 0.22 | 17.84 | 17.70 |
| | 143 | 2.49 | 0.46 | 0.12 | 9.30 | 9.29 |
| | 152 | 2.52 | 0.40 | 0.15 | 11.17 | 10.88 |
| | 155 | 2.55 | 0.53 | 0.18 | 14.99 | 10.71 |

**Table B.3.1. C6 displacements, vertebral distractions, capsule distractions, and capsular ligament strains for rats used for NGF characterization (Chapter 5).**

| Group | Rat | C6 displacement (mm) | Vertebral distraction (mm) | Capsule distraction (mm) | Maximum principal strain (%) | Maximum rostrocaudal strain (%) |
|---|---|---|---|---|---|---|
| FJD | 381 | 2.50 | 0.34 | 0.19 | 13.81 | 3.00 |
| | 382 | 2.48 | 0.96 | 0.54 | 42.36 | 25.15 |
| | 386 | 2.50 | 0.89 | 0.44 | 35.39 | 26.13 |
| | 389 | 2.50 | 0.52 | 0.29 | 22.96 | 13.66 |
| | 390 | 2.50 | 0.64 | 0.30 | 25.48 | 25.48 |
| | 408 | 2.47 | 0.52 | 0.36 | 21.36 | 16.57 |
| | 409 | 2.51 | 0.84 | 0.53 | 24.74 | 22.98 |
| | 410 | 2.49 | 0.93 | 0.35 | 44.23 | 33.38 |
| SSP-Sap+ FJD | F136 | 2.49 | 0.44 | 0.18 | 20.61 | 9.69 |
| | F137 | 2.50 | 0.32 | 0.13 | 15.02 | 7.31 |
| | F138 | 2.50 | 0.86 | 0.31 | 30.32 | 29.12 |
| | F181 | 2.52 | 0.66 | 0.30 | 30.46 | 25.69 |
| | F185 | 2.55 | 0.25 | 0.25 | 51.77 | 44.38 |
| | F190 | 2.51 | 0.39 | 0.26 | 11.83 | 9.85 |
| | F199 | 2.51 | 0.39 | 0.20 | 14.54 | 9.98 |
| Blank-Sap+ FJD | F140 | 2.53 | 0.50 | 0.20 | 12.72 | 12.15 |
| | F141 | 2.51 | 0.31 | 0.17 | 19.89 | 5.00 |
| | F143 | 2.51 | 0.59 | 0.28 | 20.72 | 17.96 |
| | F179 | 2.51 | 0.29 | 0.19 | 14.36 | 13.32 |
| | F182 | 2.52 | 0.75 | 0.16 | 49.68 | 26.01 |
| | F196 | 2.56 | 0.93 | 0.20 | 10.03 | 8.72 |
| | F197 | 2.51 | 0.50 | 0.31 | 21.89 | 19.48 |

Note: Rats 385-390 were used to quantify NGF expression in the cervical facet joint using immunohistochemical labeling. Rats 381-382 and 408-410 were used to quantify NGF levels in the soft tissues of the cervical facet joint using Western blot. All rats in the SSP-Sap+FJD and Blank-Sap+FJD groups were generated by Christine L. Weisshaar, and the naming scheme reflects her records.

**Table B.3.2. C6 displacements, vertebral distractions, capsule distractions, and capsular ligament strains for rats used for anti-NGF injection studies (Chapter 5).**

| Group | Rat | C6 displacement (mm) | Vertebral distraction (mm) | Capsule distraction (mm) | Maximum principal strain (%) | Maximum rostrocaudal strain (%) |
|---|---|---|---|---|---|---|
| FJD+ anti-NGF | 250 | 2.54 | 0.55 | 0.32 | 59.06 | 41.89 |
| | 251 | 2.52 | 0.96 | 0.28 | 34.98 | 24.64 |
| | 254 | 2.53 | 0.73 | 0.35 | 44.25 | 23.18 |
| | 277 | 2.50 | 1.07 | 0.63 | 36.62 | 36.42 |
| | 279 | 2.50 | 0.55 | 0.28 | 28.19 | 26.45 |
| | 340 | 2.46 | 1.04 | 0.37 | 92.87 | 46.96 |
| | 306 | 2.48 | 0.85 | 0.42 | 44.58 | 43.08 |
| | 308 | 2.49 | 0.81 | 0.19 | 57.39 | 34.89 |
| | 353 | 2.50 | 0.83 | 0.34 | 50.98 | 50.91 |
| | 354 | 2.49 | 0.78 | 0.38 | 66.39 | 41.57 |
| | 355 | 2.48 | 0.54 | 0.30 | 47.58 | 31.17 |
| FJD+ vehicle | 272 | 2.47 | 0.38 | 0.26 | 19.01 | 15.59 |
| | 273 | 2.58 | 0.80 | 0.44 | 40.15 | 28.83 |
| | 274 | 2.53 | 0.92 | 0.36 | 46.10 | 35.19 |
| | 275 | 2.57 | 0.61 | 0.29 | 22.07 | 16.07 |
| | 276 | 2.53 | 0.63 | 0.26 | 19.43 | 18.30 |
| | 280 | 2.49 | 0.79 | 0.31 | 47.19 | 25.31 |
| | 305 | 2.49 | 0.58 | 0.18 | 16.97 | 15.80 |
| | 307 | 2.27 | 0.79 | 0.30 | 26.81 | 17.96 |
| | 309 | 2.52 | 0.82 | 0.30 | 35.16 | 27.89 |
| | 356 | 2.48 | 0.81 | 0.33 | 26.05 | 25.86 |
| | 357 | 2.46 | 0.69 | 0.31 | 21.89 | 17.45 |
| | 358 | 2.49 | 0.46 | 0.18 | 28.71 | 17.57 |
| FJD+ anti-NGFD1 | 345 | 2.47 | 1.18 | 0.45 | 41.16 | 41.16 |
| | 347 | 2.50 | 0.92 | 0.28 | 37.87 | 36.40 |
| | 359 | 2.46 | 1.03 | 0.57 | 30.06 | 29.24 |
| | 360 | 2.57 | 0.92 | 0.40 | 21.56 | 21.05 |
| | 361 | 2.56 | 0.66 | 0.35 | 38.65 | 27.78 |
| | 362 | 2.47 | 1.05 | 0.64 | 38.88 | 36.43 |
| | 363 | 2.48 | 0.93 | 0.46 | 58.41 | 58.25 |
| | 364 | 2.55 | 0.81 | 0.28 | 32.16 | 28.92 |

Note: For this study, rats highlighted in gray were used for electrophysiological recordings at day one. The remaining rats were used for electrophysiological recordings at day seven.

**Table B.4.1. C6 displacements and vertebral distractions for rats used for BDNF characterization studies (Chapter 6).**

| Group | Rat | C6 displacement (mm) | Vertebral distraction (mm) |
|---|---|---|---|
| FJD | 47 | 6.65 | 0.80 |
| | 48 | 1.43 | 0.58 |
| | 49 | 1.86 | 0.80 |
| | 52 | 1.29 | 0.68 |
| | 53 | 2.54 | 0.66 |
| | 54 | 1.44 | 0.72 |
| | KEL315 | 2.61 | 0.73 |
| | KEL316 | 3.00 | 0.72 |
| | KEL317 | 3.19 | 0.76 |
| | KEL318 | 1.65 | 0.73 |
| | KEL319 | 3.10 | 0.70 |
| | KEL320 | 3.06 | 0.70 |
| | F13 | 2.49 | 0.46 |
| | F14 | 2.46 | 0.57 |
| | F19 | 2.38 | 0.45 |
| | F20 | 2.49 | 0.55 |
| | F21 | 2.46 | 0.60 |
| | F24 | 2.44 | 0.54 |
| | F3 | 2.04 | - |
| | F4 | 2.05 | 0.47 |
| | F7 | 2.21 | 0.41 |
| | F8 | 2.28 | - |
| | F11 | 2.26 | - |

Note: For this study, tissue from rats highlighted in gray was harvested at day one. All rats that were harvested at day one were generated by Christine L. Weisshaar, and the naming scheme reflects her records. The remaining rats were harvested at day seven. For rats F3, F8, and F11, technical difficulties prevented video recording of the joint distraction, so vertebral distraction could not be calculated. Rats KEL315-KEL320 were generated by Kathryn E. Lee, and the numbering scheme reflects her records.

**Table B.4.2. C6 displacements and vertebral distractions for rats used for the spinal BDNF sequestration study (Chapter 6).**

| Group | Rat | C6 displacement (mm) | Vertebral distraction (mm) |
|---|---|---|---|
| trkB-Fc | **195** | 2.55 | 0.69 |
| | **196** | 2.59 | 0.59 |
| | **197** | 2.55 | 0.73 |
| | **202** | 2.51 | 0.56 |
| | **204** | 2.51 | 0.72 |
| | **206** | 2.52 | 0.69 |
| | **209** | 2.53 | 0.73 |
| vehicle | **203** | 2.52 | 0.87 |
| | **205** | 2.51 | 0.91 |
| | **207** | 2.53 | 0.64 |
| | **246** | 2.48 | 0.65 |
| | **247** | 2.49 | 1.01 |
| | **248** | 2.45 | 0.67 |
| | **249** | 2.48 | 0.73 |

**Table B.5. C6 displacements, vertebral distractions, capsule distractions, and capsular ligament strains for Chapter 7.**

| Group | Rat | C6 displacement (mm) | Vertebral distraction (mm) | Capsule distraction (mm) | Maximum principal strain (%) | Maximum rostrocaudal strain (%) |
|---|---|---|---|---|---|---|
| FJD | PSP1 | 2.55 | 0.66 | 0.24 | 38.09 | 27.39 |
| | PSP5 | 2.56 | 0.67 | 0.25 | 30.35 | 25.54 |
| | PSP7 | 2.49 | 0.99 | 0.50 | 39.66 | 39.65 |
| | PSP11 | 2.49 | 1.12 | 0.59 | 53.15 | 41.50 |
| IB4-Sap+ FJD | F240 | 2.50 | 0.34 | 0.26 | 15.31 | 13.33 |
| | F241 | 2.56 | 0.44 | 0.21 | 128.58 | 32.91 |
| | F242 | 2.54 | 0.27 | 0.18 | 9.97 | 9.94 |
| | F246 | 2.49 | 0.50 | 0.35 | 20.79 | 20.44 |
| | F249 | 2.50 | 0.54 | 0.10 | 12.84 | 4.18 |
| | F251 | 2.49 | 0.19 | 0.27 | 59.40 | 53.60 |

Note: For this study, electrophysiological recordings were performed by Parul S. Pall, which is reflected in the naming scheme of the rats included in the FJD group in accordance with my records. Surgical procedures for the IB4-Sap+FJD group were performed by Christine L. Weisshaar, and the naming scheme for those rats reflects her records.

# Appendix C

# Mechanical and Thermal Behavioral Sensitivity

This appendix details the individual responses for mechanical and thermal sensitivity for all of the rats included in the behavioral studies in Chapters 3-7. Mechanical hyperalgesia is reported as the response threshold (gram) averaged between the forepaws for each rat. The response threshold is determined by applying a series of von Frey filaments to each forepaw in an ascending series. The filament strength eliciting a response is recorded as the withdrawal threshold if the next consecutive filament also elicits a positive response (see Chapter 3 for further details). Thermal hyperalgesia is reported as the latency to forepaw withdrawal (seconds) from a radiant heat source averaged between forepaws for each rat. The heat source is applied separately to each forepaw, and a timer synchronized to the thermal stimulus measures the latency time between the initial application of the heat source and when the paw is withdrawn (i.e. the withdrawal latency) (see Chapter 3 for further details). The facet joint distraction (FJD) group refers to rats for which the C6 forceps was displaced by 2.5mm as recorded by the linear variable differential transducer (LVDT) (See Chapter 3 for details). The sham group underwent the same surgical procedure with no applied distraction.

Each table summarizes behavioral data for each group arranged by studies in the order they are presented in each chapter. Baseline responses (day 0) are included for all tables. Tables C.1.1 and C.1.2 itemize the individual responses to mechanical and thermal

stimulation, respectively, at all baseline and post-surgical time points for rats in the FJD and sham groups presented in Chapter 3. Table C.2 summarizes the mechanical withdrawal thresholds for the groups used to characterize the innervation pattern of the C6/C7 facet joint in the studies included in Chapter 4.

Tables C.3.1-C.3.9 report the behavioral response data for all of the rats included in the studies of intra-articular nerve growth factor (NGF)-mediated facet joint pain that are presented in Chapter 5. Table C.3.1 details the individual responses to mechanical stimulation of the forepaw following FJD or sham procedures for those rats used to identify and quantify NGF expression in the C6/C7 facet joint. Table C.3.2 contains the mechanical withdrawal thresholds for rats that received intra-articular [$Sar^{9}$,$Met(O_2)^{11}$]-substance P-saporin (SSP-Sap) or control saporin (Blank-Sap) prior to FJD or sham procedures. Table C.3.3 details the mechanical withdrawal thresholds following intra-articular injection of nerve growth factor (NGF) or phosphate buffered saline (vehicle). Tables C.3.4 and C.3.5 summarize the individual mechanical (Table C.3.4) and thermal (Table C.3.5) hyperalgesia responses for the rats that received intra-articular SSP-Sap or Blank-Sap prior to NGF (SSP-Sap+NGF, Blank-Sap+NGF) or vehicle (SSP-Sap+veh, Blank-Sap+veh) injection into the facet joint. Likewise, the next two tables report the mechanical (Table C.3.6) and thermal (Table C.3.7) responses for all rats that received intra-articular saporin conjugated to isolectin B4 (IB4-Sap) or unconjugated control saporin (Saporin) prior to application of intra-articular NGF (IB4-Sap+NGF, Saporin+NGF) or vehicle (IB4-Sap+NGF). Table C.3.8 details the forepaw withdrawal thresholds to mechanical stimulation for all rats that were given intra-articular anti-NGF or control immunoglobulin G immediately following FJD (FJD+anti-NGF, FJD+vehicle)

or sham (sham+anti-NGF, sham+vehicle) to identify if intra-articular NGF initiates facet joint loading-induced pain (see Chapter 5 for further details). Lastly, Table C.3.9 summarizes the mechanical hyperalgesia responses of those rats that underwent FJD followed by intra-articular anti-NGF on post-surgical day one.

Table C.4.1 details the mechanical sensitivity for each rat used to characterize BDNF responses at days one and seven following FJD or sham procedures (Chapter 6). Table C.4.2 contains the withdrawal thresholds for the rats that received intrathecal trkB-Fc (trkB-Fc) or control IgG-Fc (vehicle) on day five after distraction (Chapter 6). Table C.5 reports the individual mechanical hyperalgesia responses on all days tested for all of the rats used to quantify thalamic neuronal hyperexcitability in the studies presented in Chapter 7. Those rats underwent FJD or sham surgery. Additional rats received intra-articular IB4-Sap prior to distraction or sham surgery for those studies and are also detailed.

**Table C.1.1. Mechanical hyperalgesia thresholds (g) for one or seven days following facet joint distraction (FJD) (Chapter 3).**

| Group | Rat | day 0 | day 1 | day 3 | day 5 | day 7 |
|---|---|---|---|---|---|---|
| FJD | 413 | 24.17 | 13.33 | - | - | - |
| | 415 | 9.83 | 7.00 | - | - | - |
| | 417 | 14.17 | 8.83 | - | - | - |
| | 418 | 13.83 | 3.67 | - | - | - |
| | A | 15.17 | 10.17 | 7.67 | 7.67 | 6.67 |
| | B | 16.00 | 6.83 | 6.67 | 9.50 | 5.00 |
| | I | 13.00 | 7.33 | 7.00 | 8.83 | 7.33 |
| | D | 19.67 | 7.17 | 12.00 | 8.33 | 8.17 |
| | E | 16.00 | 8.33 | 8.50 | 8.83 | 8.50 |
| sham | 414 | 13.33 | 15.00 | - | - | - |
| | 416 | 14.00 | 14.83 | - | - | - |
| | G | 24.17 | 18.17 | 15.17 | 15.00 | 16.83 |
| | H | 17.83 | 14.00 | 11.83 | 12.17 | 15.17 |

Note: For this study, tissue from half of the rats was harvested at day one and at day seven for the other half of the rats. For rats A-I, facet joint distraction procedures were performed by Ben A. Bulka, and the naming scheme reflects his records.

**Table C.1.2. Thermal hyperalgesia latencies (sec) for one or seven days following facet joint distraction (Chapter 3).**

| Group | Rat | day 0 | day 1 | day 7 |
|---|---|---|---|---|
| FJD | 413 | 10.25 | 6.70 | - |
| | 415 | 9.45 | 9.46 | - |
| | 417 | 13.93 | 10.89 | - |
| | 418 | 13.84 | 11.59 | - |
| | A | 14.49 | 15.17 | 10.18 |
| | B | 8.61 | 8.97 | 7.97 |
| | I | 11.68 | 9.42 | 10.73 |
| | D | 10.02 | 10.96 | 9.75 |
| | E | 15.51 | 10.70 | 12.39 |
| sham | 414 | 10.85 | 11.29 | - |
| | 416 | 10.57 | 10.24 | - |
| | G | 12.26 | 6.86 | 7.81 |
| | H | 13.86 | 14.84 | 13.55 |

Note: Thermal behavioral testing was only performed at baseline, day one and day seven. As in Table C.1.1, only half of the rats were followed beyond day one. For rats A-I, facet joint distraction procedures were performed by Ben A. Bulka, and the naming scheme reflects his records.

**Table C.2. Mechanical hyperalgesia thresholds (g) following facet joint distraction (Chapter 4).**

| Group | Rat | day 0 | day 1 | day 3 | day 5 | day 7 |
|---|---|---|---|---|---|---|
| FJD | 134 | 8.67 | 3.67 | 5.00 | 3.67 | 3.67 |
| | 143 | 13.33 | 5.00 | 4.33 | 5.00 | 4.67 |
| | 152 | 20.50 | 3.23 | 5.67 | 6.67 | 6.33 |
| | 155 | 10.00 | 3.67 | 2.03 | 2.37 | 2.47 |
| sham | 132 | 18.67 | 11.50 | 20.50 | 19.67 | 22.33 |
| | 141 | 21.50 | 17.50 | 17.83 | 14.83 | 17.83 |
| | 142 | 17.00 | 18.67 | 19.67 | 16.83 | 16.83 |
| | 150 | 19.67 | 17.83 | 19.67 | 15.17 | 14.17 |
| | 154 | 14.00 | 12.17 | 11.33 | 15.67 | 13.67 |

**Table C.3.1. Mechanical hyperalgesia thresholds (g) following facet joint distraction (Chapter 5).**

| Group | Rat | day 0 | day 1 |
|---|---|---|---|
| FJD | 381 | 20.50 | 9.33 |
| | 382 | 19.67 | 9.17 |
| | 386 | 20.50 | 9.33 |
| | 389 | 16.00 | 10.83 |
| | 390 | 13.33 | 7.67 |
| | 408 | 22.33 | 8.67 |
| | 409 | 22.33 | 8.83 |
| | 410 | 18.67 | 8.17 |
| sham | 380 | 24.17 | 22.33 |
| | 383 | 22.33 | 21.50 |
| | 384 | 24.17 | 22.33 |
| | 385 | 19.67 | 22.33 |
| | 387 | 24.17 | 22.33 |
| | 388 | 21.50 | 17.50 |
| | 407 | 16.17 | 17.17 |
| | 411 | 20.50 | 16.83 |

Note: Rats 385-390 were used to identify NGF expression in the cervical facet joint using immunohistochemical labeling. All other rats were used to quantify NGF levels in the soft tissues of the cervical facet joint using Western blot.

**Table C.3.2. Mechanical hyperalgesia thresholds (g) after saporin treatment and following facet joint distraction (Chapter 5).**

| Group | Rat | day 0 | day 1 | day 3 | day 5 | day 7 |
|---|---|---|---|---|---|---|
| SSP-Sap+ FJD | F136 | 19.67 | 15.00 | 11.00 | 16.00 | 15.17 |
| | F137 | 14.33 | 11.00 | 12.17 | 15.67 | 12.17 |
| | F138 | 22.33 | 18.67 | 20.50 | 16.67 | 18.67 |
| | F181 | 18.67 | 18.50 | 20.50 | 17.00 | 21.50 |
| | F185 | 17.83 | 14.67 | 11.83 | 11.33 | 14.33 |
| | F190 | 22.33 | 24.17 | 13.00 | 18.83 | 22.33 |
| | F199 | 14.17 | 24.17 | 21.17 | 19.67 | 24.17 |
| Blank-Sap+ FJD | F140 | 10.00 | 4.67 | 2.80 | 3.13 | 4.67 |
| | F141 | 18.83 | 8.00 | 5.00 | 4.67 | 4.23 |
| | F143 | 20.50 | 6.00 | 6.33 | 6.33 | 4.67 |
| | F179 | 21.50 | 6.67 | 5.67 | 9.67 | 9.00 |
| | F182 | 17.00 | 5.67 | 5.67 | 3.67 | 5.00 |
| | F196 | 14.00 | 8.50 | 5.67 | 4.00 | 3.13 |
| | F197 | 16.33 | 4.57 | 5.00 | 5.67 | 5.33 |
| SSP-Sap+ sham | F188 | 24.17 | 26.00 | 18.83 | 22.33 | 17.00 |
| | F189 | 10.83 | 20.50 | 18.67 | 18.17 | 24.17 |
| | F198 | 16.00 | 21.50 | 22.33 | 18.67 | 20.50 |
| | F200 | 22.33 | 26.00 | 22.33 | 14.17 | 15.83 |

Note: All rats included in this study were generated by Christine L. Weisshaar, and the naming scheme reflects her records.

**Table C.3.3. Mechanical hyperalgesia thresholds (g) for one or seven days following NGF joint injection (Chapter 5).**

| Group | Rat | day 0 | day 1 | day 3 | day 5 | day 7 |
|---|---|---|---|---|---|---|
| NGF | **144** | 15.28 | 15.67 | 17.83 | 18.67 | 20.50 |
| | **145** | 20.44 | 10.83 | 22.33 | 20.50 | 17.83 |
| | **146** | 9.44 | 4.90 | 9.83 | 11.83 | 10.17 |
| | **147** | 20.89 | 14.50 | 23.00 | 18.67 | 21.50 |
| | **148** | 20.22 | 17.83 | 22.33 | 24.17 | 20.50 |
| | **149** | 16.78 | 12.33 | 16.67 | 19.67 | 18.83 |
| | **252** | 17.72 | 13.33 | - | - | - |
| | **253** | 22.06 | 7.17 | - | - | - |
| | **255** | 20.83 | 9.50 | - | - | - |
| | **256** | 13.94 | 8.00 | - | - | - |
| | **257** | 21.72 | 15.00 | - | - | - |
| | **278** | 16.08 | 9.67 | - | - | - |
| | **282** | 18.72 | 9.00 | - | - | - |
| vehicle | **341** | 21.50 | 21.50 | 24.17 | 16.00 | 22.33 |
| | **342** | 21.50 | 22.33 | 22.33 | 17.00 | 21.50 |
| | **344** | 18.17 | 15.83 | 17.00 | 18.17 | 21.17 |
| | **265** | 16.06 | 14.17 | - | - | - |
| | **266** | 25.08 | 22.33 | - | - | - |
| | **267** | 25.11 | 22.33 | - | - | - |
| | **268** | 16.00 | 16.83 | - | - | - |
| | **269** | 19.06 | 20.50 | - | - | - |
| | **281** | 17.33 | 18.67 | - | - | - |

Note: For this study, rats were followed for seven days after injection in order to characterize the time course of NGF-induced sensitivity. Additional NGF-injected rats were used for electrophysiological recordings at day one when sensitivity was evident.

**Table C.3.4. Mechanical hyperalgesia thresholds (g) at day one after SSP-saporin treatment followed by an NGF joint injection (Chapter 5).**

| Group | Rat | day 0 | day 1 | Group | Rat | day 0 | day 1 |
|---|---|---|---|---|---|---|---|
| Blank-Sap+ vehicle | **293** | 15.17 | 18.67 | Blank-Sap+ NGF | **212** | 13.00 | 7.00 |
| | **294** | 19.92 | 24.17 | | **213** | 22.33 | 12.50 |
| | **295** | 21.00 | 15.67 | | **216** | 19.67 | 14.00 |
| | **296** | 23.75 | 26.00 | | **217** | 24.17 | 18.83 |
| | **325** | 24.17 | 26.00 | | **299** | 6.33 | 4.33 |
| | **326** | 7.25 | 8.00 | | **300** | 10.33 | 4.67 |
| | **331** | 21.42 | 24.17 | | **303** | 13.42 | 6.33 |
| | **332** | 22.33 | 23.33 | | **304** | 10.92 | 4.33 |
| SSP-Sap+ NGF | **210** | 21.42 | 18.83 | | **321** | 13.17 | 7.00 |
| | **211** | 22.33 | 24.17 | | **322** | 19.67 | 12.17 |
| | **214** | 23.25 | 22.33 | | **329** | 21.00 | 8.83 |
| | **215** | 24.17 | 22.33 | | **330** | 16.83 | 5.00 |
| | **297** | 22.33 | 22.33 | SSP-Sap+ vehicle | **289** | 19.25 | 16.33 |
| | **298** | 17.50 | 20.50 | | **290** | 15.83 | 22.33 |
| | **301** | 21.50 | 22.33 | | **291** | 23.25 | 24.17 |
| | **302** | 7.67 | 8.33 | | **292** | 22.83 | 14.17 |
| | **319** | 6.17 | 7.33 | | **323** | 14.50 | 10.83 |
| | **320** | 20.08 | 20.50 | | **324** | 22.33 | 24.17 |
| | **327** | 24.17 | 20.50 | | **333** | 14.25 | 15.00 |
| | **328** | 12.00 | 8.67 | | **334** | 11.92 | 22.33 |
| | **391** | 20.50 | 14.83 | | **393** | 13.83 | 20.50 |
| | **392** | 16.83 | 20.50 | | **394** | 16.92 | 18.67 |
| | **395** | 26.00 | 24.17 | | **397** | 22.83 | 20.50 |
| | **396** | 18.42 | 18.50 | | **398** | 25.08 | 21.50 |

**Table C.3.5. Thermal hyperalgesia latencies (sec) at day one after SSP-saporin treatment followed by an NGF joint injection (Chapter 5).**

| Group | Rat | day 0 | day 1 |
|---|---|---|---|
| Blank-Sap+ NGF | 299 | 8.26 | 9.08 |
| | 300 | 10.28 | 8.17 |
| | 303 | 10.90 | 7.15 |
| | 304 | 12.26 | 5.54 |
| | 321 | 10.12 | 7.85 |
| | 322 | 10.54 | 9.19 |
| | 329 | 12.05 | 6.18 |
| | 330 | 9.44 | 7.49 |
| Blank-Sap+ vehicle | 325 | 11.56 | 8.82 |
| | 326 | 10.63 | 7.47 |
| | 333 | 10.18 | 12.52 |
| | 334 | 13.53 | 12.24 |
| SSP-Sap+ NGF | 297 | 9.83 | 11.05 |
| | 298 | 9.96 | 11.92 |
| | 301 | 13.00 | 9.59 |
| | 302 | 9.89 | 9.23 |
| | 319 | 9.85 | 10.13 |
| | 320 | 12.37 | 9.10 |
| | 327 | 10.92 | 12.25 |
| | 328 | 11.23 | 8.62 |
| SSP-Sap+ vehicle | 323 | 12.05 | 8.92 |
| | 324 | 10.72 | 11.45 |
| | 331 | 11.39 | 10.81 |
| | 332 | 14.73 | 13.01 |

**Table C.3.6. Mechanical hyperalgesia thresholds (g) at day one after IB4-saporin treatment followed by an NGF joint injection (Chapter 5).**

| Group | Rat | day 0 | day 1 |
|---|---|---|---|
| Saporin+ NGF | 311 | 23.25 | 11.83 |
| | 312 | 17.17 | 7.00 |
| | 313 | 11.42 | 7.67 |
| | 374 | 12.42 | 8.17 |
| | 375 | 22.33 | 10.67 |
| | 376 | 19.58 | 10.00 |
| | 377 | 20.50 | 10.67 |
| | 378 | 23.25 | 14.83 |
| IB4-Sap+ NGF | 315 | 12.50 | 9.67 |
| | 316 | 25.08 | 16.00 |
| | 317 | 13.92 | 7.33 |
| | 318 | 21.42 | 9.17 |
| | 346 | 20.08 | 5.33 |
| | 349 | 13.17 | 8.50 |
| | 350 | 17.33 | 7.33 |
| | 371 | 22.33 | 9.83 |
| | 372 | 13.17 | 4.33 |
| | 373 | 20.50 | 11.50 |
| | 399 | 13.61 | 8.83 |
| | 400 | 22.06 | 16.00 |
| IB4-Sap+ vehicle | 401 | 18.78 | 16.67 |
| | 402 | 20.56 | 20.50 |
| | 403 | 22.06 | 22.33 |
| | 404 | 10.33 | 13.67 |
| | 405 | 16.89 | 16.00 |
| | 406 | 20.72 | 19.67 |

**Table C.3.7. Thermal hyperalgesia latencies (sec) at day one after IB4-saporin treatment followed by an NGF joint injection (Chapter 5).**

| Group | Rat | day 0 | day 1 |
|---|---|---|---|
| Saporin+ NGF | 374 | 10.43 | 7.03 |
| | 375 | 13.17 | 6.35 |
| | 376 | 12.16 | 6.70 |
| | 377 | 12.82 | 7.96 |
| | 378 | 12.91 | 6.55 |
| IB4-Sap+ NGF | 346 | 9.80 | 10.29 |
| | 349 | 10.25 | 5.54 |
| | 350 | 14.99 | 9.00 |
| | 371 | 15.99 | 13.18 |
| | 372 | 10.15 | 7.74 |
| | 373 | 11.72 | 6.69 |
| | 399 | 13.24 | 6.17 |
| | 400 | 11.44 | 7.32 |
| IB4-Sap+ vehicle | 401 | 8.65 | 7.39 |
| | 402 | 8.79 | 6.53 |
| | 403 | 11.17 | 10.92 |
| | 404 | 14.93 | 13.57 |
| | 405 | 11.43 | 11.92 |
| | 406 | 10.08 | 10.26 |

**Table C.3.8. Mechanical hyperalgesia thresholds (g) for one or seven days following facet joint distraction and intra-articular treatments (Chapter 5).**

| Group | Rat | day 0 | day 1 | day 3 | day 5 | day 7 |
|---|---|---|---|---|---|---|
| FJD+ anti-NGF | 250 | 20.58 | 18.67 | 24.17 | 16.83 | 24.17 |
| | 251 | 23.56 | 20.50 | 22.33 | 24.17 | 24.17 |
| | 254 | 20.22 | 20.50 | 21.50 | 20.67 | 24.17 |
| | 277 | 13.33 | 17.83 | 15.17 | 18.67 | 18.67 |
| | 279 | 12.61 | 9.67 | 17.83 | 17.83 | 13.00 |
| | 340 | 22.06 | 24.17 | 22.33 | 26.00 | 22.33 |
| | 306 | 18.83 | 18.83 | - | - | - |
| | 308 | 21.72 | 17.00 | - | - | - |
| | 353 | 23.56 | 24.17 | - | - | - |
| | 354 | 19.17 | 19.33 | - | - | - |
| | 355 | 20.38 | 20.50 | - | - | - |
| FJD+ vehicle | 272 | 19.00 | 11.33 | 10.83 | 11.33 | 10.50 |
| | 273 | 15.33 | 8.33 | 8.50 | 8.50 | 9.67 |
| | 274 | 19.89 | 16.17 | 7.33 | 7.67 | 9.00 |
| | 275 | 13.06 | 8.17 | 4.00 | 5.33 | 7.00 |
| | 276 | 24.78 | 11.67 | 10.67 | 11.00 | 11.17 |
| | 280 | 19.61 | 9.17 | 9.50 | 9.83 | 9.83 |
| | 305 | 14.00 | 4.33 | - | - | - |
| | 307 | 16.00 | 8.50 | - | - | - |
| | 309 | 18.94 | 8.50 | - | - | - |
| | 356 | 13.72 | 8.50 | - | - | - |
| | 357 | 12.00 | 7.00 | - | - | - |
| | 358 | 15.78 | 10.17 | - | - | - |
| sham+ anti-NGF | 335 | 20.72 | 21.17 | 21.50 | 20.50 | 22.33 |
| | 336 | 22.33 | 22.33 | 18.67 | 17.83 | 22.33 |
| | 337 | 18.22 | 19.33 | 21.50 | 26.00 | 20.50 |
| | 338 | 16.44 | 20.50 | 20.50 | 17.83 | 17.00 |
| | 339 | 19.83 | 22.33 | 20.50 | 18.67 | 17.83 |
| sham+ vehicle | 283 | 20.17 | 21.50 | 22.33 | 20.50 | 19.67 |
| | 285 | 17.22 | 19.67 | 18.67 | 16.67 | 17.83 |
| | 286 | 21.78 | 24.17 | 26.00 | 24.17 | 24.17 |
| | 287 | 17.56 | 21.50 | 20.50 | 22.33 | 18.67 |
| | 288 | 19.33 | 22.33 | 24.17 | 24.17 | 24.17 |
| | 365 | 11.28 | 11.33 | - | - | - |
| | 366 | 26.00 | 24.17 | - | - | - |
| | 367 | 22.67 | 18.50 | - | - | - |
| | 368 | 17.50 | 19.33 | - | - | - |
| | 370 | 17.61 | 19.67 | - | - | - |

Note: For this study, some rats were used for electrophysiological recordings at day one, so withdrawal thresholds were only assessed at baseline and day one. The remaining rats were used for electrophysiological recordings at day seven.

**Table C.3.9. Mechanical hyperalgesia thresholds (g) following facet joint distraction and a delayed joint injection of anti-NGF at day one (Chapter 5).**

| Group | Rat | day 0 | day 1 | day 2 | day 3 | day 4 | day 5 | day 6 | day 7 |
|---|---|---|---|---|---|---|---|---|---|
| FJD+ anti-NGFD1 | **345** | 16.17 | 9.00 | 13.67 | 16.33 | 11.00 | 18.17 | 11.83 | 11.50 |
| | **347** | 14.00 | 5.33 | 11.50 | 20.50 | 10.00 | 8.33 | 11.33 | 8.67 |
| | **359** | 22.67 | 8.50 | 13.50 | 14.83 | 13.17 | 17.83 | 16.00 | 14.33 |
| | **360** | 19.44 | 14.00 | 11.67 | 10.00 | 10.83 | 16.00 | 13.00 | 11.50 |
| | **361** | 14.72 | 7.67 | 8.50 | 4.67 | 8.17 | 10.00 | 8.67 | 8.33 |
| | **362** | 19.83 | 9.67 | 7.83 | 4.67 | 6.17 | 6.83 | 9.00 | 7.83 |
| | **363** | 19.94 | 12.67 | 14.50 | 14.00 | 11.67 | 10.17 | 14.00 | 14.33 |
| | **364** | 19.44 | 13.00 | 13.00 | 18.67 | 20.50 | 12.83 | 8.00 | 9.83 |

Note: For this study, intra-articular anti-NGF was applied to the C6/C7 facet joints immediately following behavioral testing on day one.

**Table C.4.1. Mechanical sensitivity following facet joint distraction (Chapter 6).**

| Group | Rat | day 0 | day 1 | day 7 | Group | Rat | day 0 | day 1 | day 7 |
|---|---|---|---|---|---|---|---|---|---|
| FJD | 47 | 1.11 | 2.40 | 4.58 | sham | 50 | 0.83 | 0.88 | 0.91 |
| | 48 | 0.97 | 2.96 | 2.10 | | 55 | 1.23 | 1.12 | 1.40 |
| | 49 | 0.92 | 2.10 | 2.19 | | 56 | 0.84 | 0.81 | 0.81 |
| | 52 | 0.77 | 2.65 | 2.40 | | 60 | 1.25 | 1.13 | 1.13 |
| | 53 | 0.90 | 1.34 | 1.94 | | KEL307 | 1.04 | 0.64 | 1.25 |
| | 54 | 1.72 | 3.68 | 2.96 | | KEL308 | 1.04 | 1.43 | 1.37 |
| | KEL315 | 1.24 | 8.27 | 7.40 | | KEL309 | 1.81 | 2.02 | 1.49 |
| | KEL316 | 0.89 | 6.59 | 5.48 | | KEL310 | 0.67 | 1.23 | 0.61 |
| | KEL317 | 0.71 | 4.22 | 3.40 | | KEL321 | 0.69 | 1.14 | 0.77 |
| | KEL318 | 1.34 | 9.37 | 3.83 | | KEL322 | 1.72 | 1.72 | 1.43 |
| | KEL319 | 1.16 | 8.78 | 4.22 | | F15 | 0.88 | 0.76 | - |
| | KEL320 | 0.95 | 6.59 | 6.02 | | F17 | 0.88 | 1.03 | - |
| | F13 | 0.82 | 1.72 | - | | F22 | 1.47 | 1.04 | - |
| | F14 | 3.56 | 3.06 | - | | F23 | 0.97 | 1.16 | - |
| | F19 | 0.86 | 3.41 | - | | F9 | 1.20 | 1.80 | - |
| | F20 | 1.13 | 2.18 | - | | F10 | 0.60 | 1.20 | - |
| | F21 | 0.85 | 2.05 | - | | F12 | 1.20 | 1.80 | - |
| | F24 | 0.78 | 3.14 | - | | | | | |
| | CLW1 | 1.52 | 3.65 | - | | | | | |
| | F3 | 0.30 | 3.96 | - | | | | | |
| | F4 | 2.74 | 2.13 | - | | | | | |
| | CLW6 | 0.61 | 3.35 | - | | | | | |
| | F7 | 0.61 | 3.65 | - | | | | | |
| | F8 | 0.30 | 3.04 | - | | | | | |
| | F11 | 0.91 | 3.65 | - | | | | | |

Note: For this study, some rats were used to quantify BDNF expression in the spinal cord and dorsal root ganglion at day one, so sensitivity was only measured through day one. Rats 47-60 and F13-F24 were used to quantify BDNF expression using immunohistochemical labeling; all other rats were used to quantify BDNF mRNA using real time reverse-transcription polymerase chain reaction. All rats that were harvested at day one were generated by Christine L. Weisshaar, and the naming scheme reflects her records. Rats KEL307-KEL322 were generated by Kathryn E. Lee, and the numbering scheme reflects her records.

**Table C.4.2. Mechanical hyperalgesia thresholds (g) following facet joint distraction and intrathecal trkB-Fc injection at day five (Chapter 6).**

| Group | Rat | day 0 | day 1 | day 3 | day 5 | day 6 | day 7 |
|---|---|---|---|---|---|---|---|
| trkB-Fc | **195** | 22.06 | 8.00 | 6.67 | 7.00 | 5.00 | 10.00 |
| | **196** | 16.50 | 10.33 | 9.00 | 12.50 | 20.50 | 15.50 |
| | **197** | 21.11 | 15.83 | 10.67 | 11.83 | 12.33 | 20.50 |
| | **202** | 20.50 | 15.67 | 18.67 | 17.00 | 20.50 | 20.50 |
| | **204** | 14.83 | 7.50 | 6.67 | 6.33 | 10.00 | 11.83 |
| | **206** | 12.17 | 7.00 | 7.33 | 6.33 | 11.83 | 11.33 |
| | **209** | 24.17 | 10.67 | 8.67 | 9.83 | 17.50 | 9.83 |
| vehicle | **203** | 14.33 | 6.00 | 7.67 | 6.67 | 7.33 | 8.50 |
| | **205** | 12.50 | 8.00 | 8.17 | 7.33 | 9.83 | 11.00 |
| | **207** | 22.33 | 10.33 | 10.67 | 8.33 | 12.17 | 11.33 |
| | **246** | 18.67 | 8.50 | 9.00 | 7.33 | 7.00 | 6.33 |
| | **247** | 19.67 | 6.33 | 7.00 | 7.67 | 8.33 | 8.17 |
| | **248** | 16.83 | 12.50 | 12.67 | 16.67 | 18.17 | 17.83 |
| | **249** | 24.17 | 12.17 | 11.67 | 11.33 | 10.67 | 8.33 |

Note: For this study, rats received an intrathecal injection of trkB-Fc or vehicle immediately following behavioral testing on day five.

**Table C.5. Mechanical hyperalgesia thresholds (g) following facet joint distraction with or without prior intra-articular IB4-saporin treatment (Chapter 7).**

| Group | Rat | Day 0 | Day 1 | Day 3 | Day 5 | Day 7 |
|---|---|---|---|---|---|---|
| FJD | PSP1 | 13.33 | 16.33 | 18.67 | 8.67 | 7.33 |
| | PSP5 | 17.00 | 7.67 | 8.67 | 9.00 | 8.67 |
| | PSP7 | 26.00 | 10.00 | 8.67 | 13.33 | 13.33 |
| | PSP11 | 26.00 | 26.00 | 26.00 | 26.00 | 20.67 |
| sham | PSP4 | 16.33 | 9.33 | 9.33 | 6.67 | 9.33 |
| | PSP8 | 26.00 | 26.00 | 26.00 | 26.00 | 26.00 |
| | PSP12 | 18.67 | 15.30 | 10.33 | 13.33 | 20.67 |
| IB4-Sap+ FJD | F240 | 9.00 | 9.33 | - | - | 13.33 |
| | F241 | 9.50 | 8.00 | - | - | 9.33 |
| | F242 | 9.17 | 15.00 | - | - | 18.67 |
| | F246 | 22.33 | 22.33 | - | - | 26.00 |
| | F249 | 23.56 | 15.33 | - | - | 22.33 |
| | F251 | 4.00 | 11.00 | - | - | 10.33 |
| IB4-Sap+ sham | F244 | 4.67 | 11.00 | - | - | 7.33 |
| | F245 | 13.50 | 15.00 | - | - | 13.33 |
| | F247 | 11.67 | 22.33 | - | - | 22.33 |
| | F250 | 24.78 | 17.00 | - | - | 26.00 |
| | F252 | 26.00 | 26.00 | - | - | 26.00 |
| | F253 | 8.67 | 22.33 | - | - | 13.33 |

Note: For this study, withdrawal thresholds for rats that received IB4-saporin prior to facet joint distraction or sham procedures were quantified on day 1 to verify that behavioral sensitivity did not develop in either group and again on day 7 in order to confirm that behavioral sensitivity was not evident prior to electrophysiological assessment. Electrophysiological recordings were performed by Parul S. Pall, which is reflected in the naming scheme of the rats included in the FJD and sham groups in accordance with my records. Surgical procedures for the IB4-Sap+FJD and IB4-Sap+sham groups were performed by Christine L. Weisshaar, and the naming scheme for those rats reflects her records.

# Appendix D

# Quantification of Brain-Derived Neurotrophic Factor mRNA Using Real-Time RT-PCR

This appendix provides a summary of the brain-derived neurotrophic factor (BDNF) mRNA levels in the dorsal root ganglion (DRG) and spinal cord in the characterization study in Chapter 6. BDNF mRNA was quantified in both tissues at days one and seven after facet joint distraction or sham procedures using real-time reverse transcription polymerase chain reaction (RT-PCR). RT-PCR was carried out using primers specific to BDNF (Forward: 5'-GGA-CAT-ATC-CAT-GAC-CAG-AAA-GAA-A-3'; Reverse: 5'-GCA-ACA-AAC-CAC-AAC–ATT-ATC-GAG-3'; Probe: 5'-AGT-CAT-TTG-CGC-ACA-ACT-TTA-AAA-GTC-TGC-ATT-3') and the housekeeping gene 18S (Forward: 5'-CGG-CTA-CCA–CAT-CCA-AGG-AA-3'; Reverse: 5'-GCT-GGA–ATT-ACC-GCG-GCT-3'; Probe: 5'-CAC-CAG-ACT-TGC-CCT-C-3'). Separately for each tissue (DRG, spinal cord), BDNF mRNA levels for each rat at each time point were normalized to the housekeeping gene 18S and are reported as the fold-change relative to the average sham levels at that same time point. As such, the average of all of the samples in each sham group for each tissue and each time point that are presented in this appendix have an average BDNF mRNA value of 1. For rats in the facet joint distraction (FJD) group, the C6 forceps was displaced by 2.5mm as recorded by a linear variable differential transducer (LVDT) (See Chapter 3 for details). The sham group underwent the same surgical procedure with no applied distraction.

Table D.1 provides the quantification of BDNF mRNA levels in the C6 DRGs of separate groups of rats at days one and seven following facet joint distraction or sham procedures (Chapter 6). Table D.2 summarizes BDNF mRNA levels in the C6 spinal cord at both time points after distraction or sham procedures (Chapter 6).

**Table D.1. BDNF mRNA in the C6 DRG following painful facet joint distraction in separate groups of rats at day one and day seven (Chapter 6).**

| Group | Day | Rat | BDNF mRNA (fold-change relative to sham) |
|---|---|---|---|
| FJD | Day 1 | CLW1 | 0.70 |
| | | F3 | 1.96 |
| | | F4 | 0.62 |
| | | CLW6 | 0.94 |
| | | F7 | 1.34 |
| | | F8 | 0.84 |
| | | F11 | 0.97 |
| | Day 7 | 315 | 0.41 |
| | | 316 | 0.86 |
| | | 318 | 1.25 |
| sham | Day 1 | F9 | 1.52 |
| | | F10 | 0.62 |
| | | F12 | 0.86 |
| | Day 7 | 310 | 0.95 |
| | | 321 | 0.97 |
| | | 322 | 1.09 |

Note: All rats used in the day one study were generated by Christine L. Weisshaar, and the naming scheme reflects her records. All rats used in the day seven study were generated by Kathryn E. Lee, and the numbering scheme reflects her records.

**Table D.2. BDNF mRNA in the C6 spinal cord following painful facet joint distraction in separate groups of rats at day one and day seven (Chapter 6).**

| Group | | Rat | BDNF mRNA (fold-change relative to sham) |
|---|---|---|---|
| FJD | Day 1 | CLW1 | 1.32 |
| | | F3 | 0.87 |
| | | F4 | 0.74 |
| | | F7 | 1.09 |
| | | F8 | 1.12 |
| | | F11 | 0.95 |
| | Day 7 | 315 | 1.65 |
| | | 316 | 0.76 |
| | | 318 | 1.51 |
| | | 319 | 1.51 |
| | | 320 | 1.45 |
| sham | Day 1 | F9 | 0.92 |
| | | F10 | 1.26 |
| | | F12 | 0.82 |
| | Day 7 | 307 | 0.80 |
| | | 308 | 1.11 |
| | | 309 | 0.97 |
| | | 310 | 0.66 |
| | | 321 | 1.23 |
| | | 322 | 1.24 |

Note: All rats used in the day one study were generated by Christine L. Weisshaar, and the naming scheme reflects her records. All rats used in the day seven study were generated by Kathryn E. Lee, and the numbering scheme reflects her records.

# Appendix E

# Quantification of Nerve Growth Factor Protein in the DRG and Brain-Derived Neurotrophic Factor Protein in the DRG and Spinal Cord Using Immunohistochemistry

This appendix summarizes the quantification of immunolabeling of nerve growth factor (NGF) and brain-derived neurotrophic factor (BDNF) for the studies presented in Chapters 5 and 6. NGF expression was quantified in the C7 dorsal root ganglion (DRG) of rats that received intra-articular [$Sar^{9}$,$Met(O_2)^{11}$]-substance P-saporin (SSP-Sap) or control saporin (Blank-Sap) prior to facet joint distraction (FJD) or sham procedures (Chapter 5). At day seven after FJD or sham, four images of the C7 DRG were taken from each rat in the SSP-Sap+FJD, Blank-Sap+FJD, and SSP-Sap+sham groups for analysis by immunolabeling, with all exposure times standardized. Automated densitometry was performed using Matlab code (provided in Appendix A) that quantifies the NGF expression in the dorsal root ganglion (DRG) (Weisshaar et al., 2010). Each DRG image is digitally stored under the generalized file name Rat#_NGF_DRGside_20X_175ms_Section#.tif. The side distinction is either R (right) or L (left) for all sections. Because the injury is bilateral and behavioral responses are not different between the right and left sides, tissue responses to injury are also expected to not differ between right and left. As such, the distinction between right and left is only

made in this appendix for clarity in identifying the exact tissue location corresponding to each image.

In separate studies, BDNF expression was quantified in the DRG and spinal cord after FJD or sham procedures (Chapter 6). For analysis of the C6 dorsal root ganglion sections on either day one or day seven after facet joint distraction (FJD) or sham, the mean signal intensity and cross-sectional area of the neurons were determined by manually outlining each neuron using ImageJ (NIH; Bethesda, MD). For each tissue section, the BDNF intensity was normalized to the average background intensity, which was calculated from the intensities of the BDNF-negative neurons, in order to determine the BDNF intensity ratio. BDNF-positive neurons were classified into seven neuronal sizes (from $<200\mu m^2$ to $>700\mu m^2$ in 100 $\mu m^2$ bins) based on their soma area (Zhou et al., 1999), and the average BDNF intensity ratio is reported for each bin size, as well as the overall average for all neurons for each section (All). Each DRG image is digitally stored with a generalized file name of BDNF_Rat#_Section#_C6L DRG_20x.tif.

The C6 spinal cord was also assayed for BDNF expression on each of day one and day seven after FJD or sham. At least 6 images of the spinal dorsal horn were taken from each rat for analysis by immunolabeling, with all exposure times standardized. Automated densitometry was performed using Matlab code (provided in Appendix A) that quantifies the BDNF expression in a standardized pixel area (1360x510) corresponding to laminae I-IV in the dorsal horn (Weisshaar et al., 2010). Each spinal cord image is digitally stored under the generalized file name BDNF_Rat#_Section#_Side_20x_ExposureTime.tif. The side distinction is either RDH (right dorsal horn) or LDH (left dorsal horn) for all sections. As described above, the

distinction between right and left is only made for clarity in identifying the exact tissue location corresponding to each image because the injury is bilateral.

In order to identify the cellular sources of spinal BDNF on days one and seven after FJD or sham procedures, spinal cord sections were immunolabeled for BDNF and one of the following: glial fibrillary acidic protein (GFAP; as a marker of astrocytes), microtubule associated protein-2 (MAP2; as a marker of neurons), or OX-42 (CD11b; as a marker of microglia). Digital copies of spinal cord sections labeled for each cell type are also stored under the previously listed general file name Label_Rat#_Section#_Side_20x_ExposureTime.tif with the exception that 'Label' is replaced with either 'GFAP', 'MAP2', or 'OX42', accordingly. Throughout this appendix, the FJD group refers to rats for which the C6 forceps was displaced by 2.5mm as recorded by the linear variable differential transducer (LVDT); the sham group underwent the same surgical procedure with no applied distraction (Kras et al., 2013c).

The quantification of NGF expression in the C7 DRG seven days after FJD or sham with saporin treatment is reported in Table E.1. Figures E.1.A-E.1.C itemize each of the DRG sections in which NGF expression was quantified and reported in Table E.1. Tables E.2 and E.3 summarize the BDNF intensity ratio for the neuronal sizes described above in the C6 DRGs of both FJD and sham groups. Table E.2 details the intensity ratio on day one after surgical procedures, and Table E.3 reports the intensity ratio on day seven. Figures E.2 and E.3 present all of the DRG sections included in analyses for day one and day seven, respectively. Quantification of expression of BDNF in the C6 spinal cord one day after FJD or sham is provided in Table E.4.1. Because BDNF expression data were positively skewed, the raw data were log-transformed to achieve an

approximately normal distribution prior to statistical analysis, and the corresponding log-transformed data are presented in Table E.4.2. The log-transformation applied was: log(10,000*ratio of positive pixels). Figures E.4.A and E.4.B illustrate all of the spinal cord sections included in the analyses presented in Tables E.4.1 and E.4.2. Tables E.5.1 and E.5.2 summarize the raw BDNF expression and corresponding log-transformed data, respectively, at seven days following FJD or sham. The log-transformation applied was: log(100,000*ratio of positive pixels). Figures E.5.A and E.5.B present all of the spinal cord sections in which BDNF was quantified in Tables E.5.1 and E.5.2. Figure E.6 provides representative spinal cord images that are double-labeled for BDNF and each cell type for all of the rats included in the day one BDNF quantification study. Similarly, the corresponding representative double-labeled spinal cord images on day seven after FJD or sham are included in Figure E.7.

**Table E.1. Percentage of pixels positive for NGF in the C7 DRG seven days following FJD or sham with saporin treatment (Chapter 5).**

| Group | Rat | Section | Positive pixels (%) | Group | Rat | Section | Positive pixels (%) |
|---|---|---|---|---|---|---|---|
| SSP-Sap+ FJD | F136 | 2L | 2.30 | Blank-Sap+ FJD | F143 | 1L | 4.39 |
| | | 1R | 0.23 | | | 4L | 8.28 |
| | | 2R | 0.27 | | | 1R | 6.44 |
| | | 3R | 2.64 | | | 3R | 7.66 |
| | F137 | 1L | 0.93 | | F179 | 2L | 14.62 |
| | | 3L | 0.20 | | | 5L | 12.27 |
| | | 4L | 0.15 | | | 2R | 21.64 |
| | | 4R | 1.63 | | | 4R | 18.45 |
| | F138 | 1L | 0.00 | | F182 | 2L | 6.99 |
| | | 4L | 0.26 | | | 3L | 1.49 |
| | | 1R | 0.26 | | | 4R | 3.30 |
| | | 3R | 0.66 | | | 5R | 7.70 |
| | F181 | 3L | 0.44 | | F196 | 1L | 11.84 |
| | | 1R | 5.55 | | | 2L | 9.99 |
| | | 2R | 0.10 | | | 1R | 13.48 |
| | | 5R | 15.94 | | | 2R | 17.09 |
| | F185 | 3L | 1.94 | | F197 | 1L | 0.00 |
| | | 4L | 6.43 | | | 2L | 0.03 |
| | | 5L | 0.34 | | | 3L | 5.00 |
| | | 6L | 0.17 | | | 4L | 10.60 |
| | F190 | 5L | 1.50 | SSP-Sap+ sham | F188 | 1L | 1.26 |
| | | 6L | 3.02 | | | 4L | 2.81 |
| | | 3R | 1.44 | | | 6L | 0.14 |
| | | 4R | 3.61 | | | 3R | 4.44 |
| | F199 | 3L | 3.63 | | F189 | 5L | 1.33 |
| | | 2R | 3.67 | | | 1R | 0.24 |
| | | 3R | 0.00 | | | 3R | 1.33 |
| | | 4R | 0.00 | | | 6R | 2.23 |
| Blank-Sap+ FJD | F140 | 1L | 0.30 | | F198 | 4L | 0.00 |
| | | 4L | 1.54 | | | 5L | 0.00 |
| | | 1R | 11.33 | | F200 | 5L | 0.00 |
| | | 2R | 13.11 | | | 3R | 5.28 |
| | F141 | 3L | 3.24 | | | 5R | 0.00 |
| | | 5L | 6.12 | | | | |
| | | 4R | 6.95 | | | | |
| | | 6R | 4.87 | | | | |

Note: The section number refers to the position of the tissue section on each slide, beginning in the top left corner and proceeding in numerical order from top to bottom, then resuming at the top of the adjacent column to the right. The designators R and L indicate that the tissue section was from the right or left DRG, respectively. Tissue was generated by Christine L. Weisshaar, and the naming scheme for each rat reflects her records.

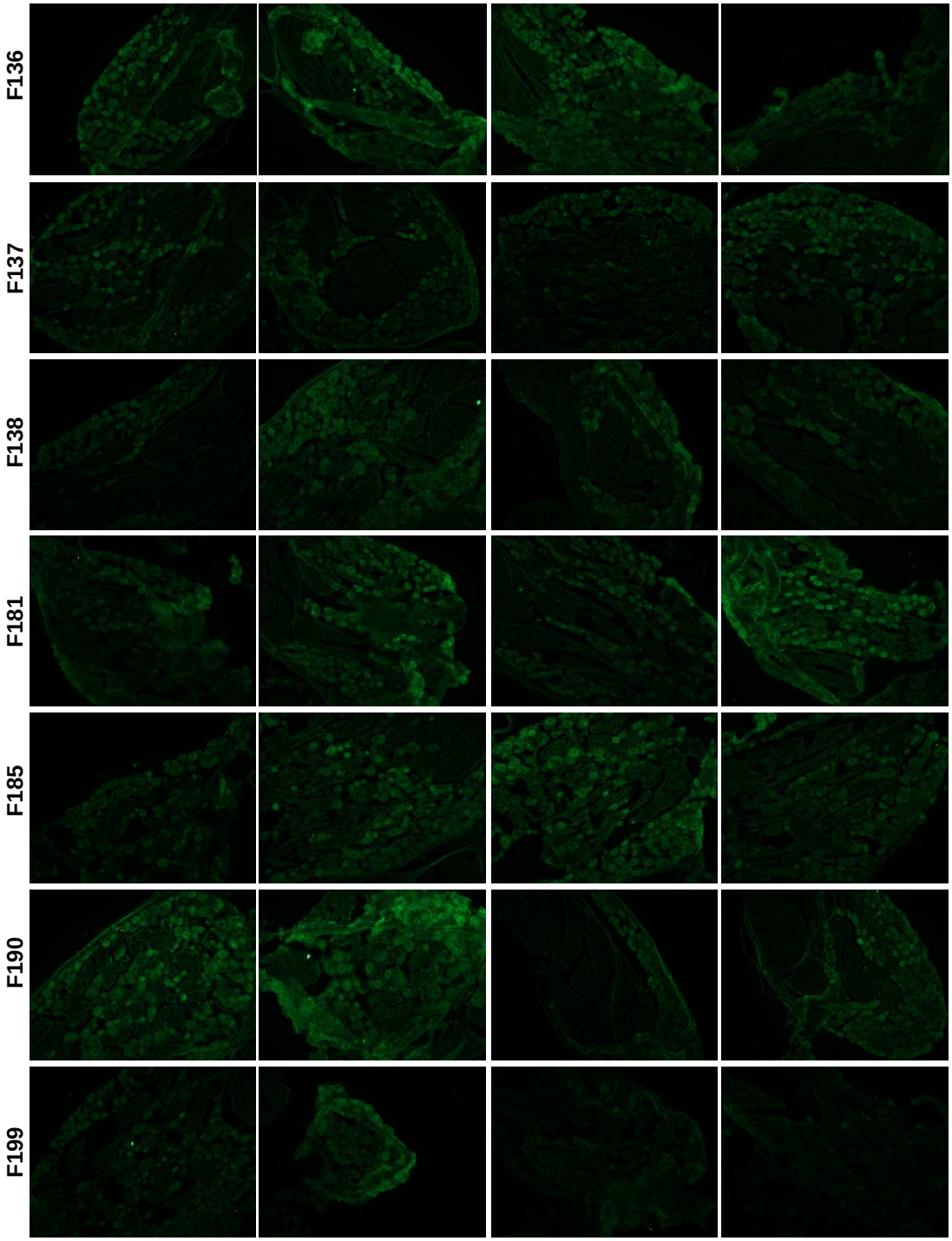


**Figure E.1.A.** NGF expression in the C7 DRG seven days after SSP-Sap+FJD (F136, F137, F138, F181, F185, 190, F199). For each rat, the sections presented correspond to those sections for which the percentage of NGF-positive pixels is summarized in Table E.1 with section number increasing from left to right.

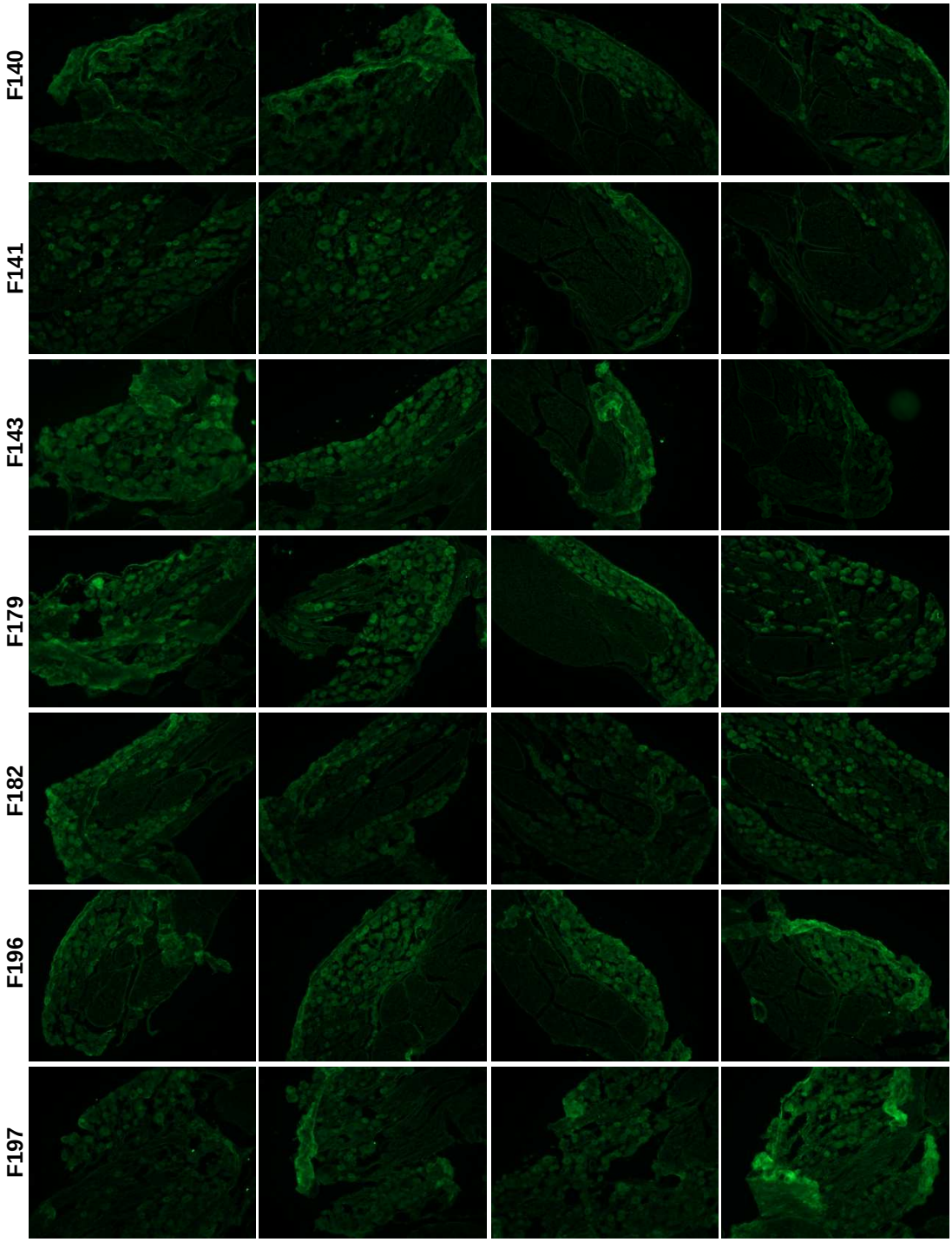


**Figure E.1.B.** NGF expression in the C7 DRG seven days after Blank-Sap+FJD (F140, F141, F143, F179, F182, F196, F197). For each rat, the sections presented correspond to those sections for which the percentage of NGF-positive pixels is summarized in Table E.1 with section number increasing from left to right.

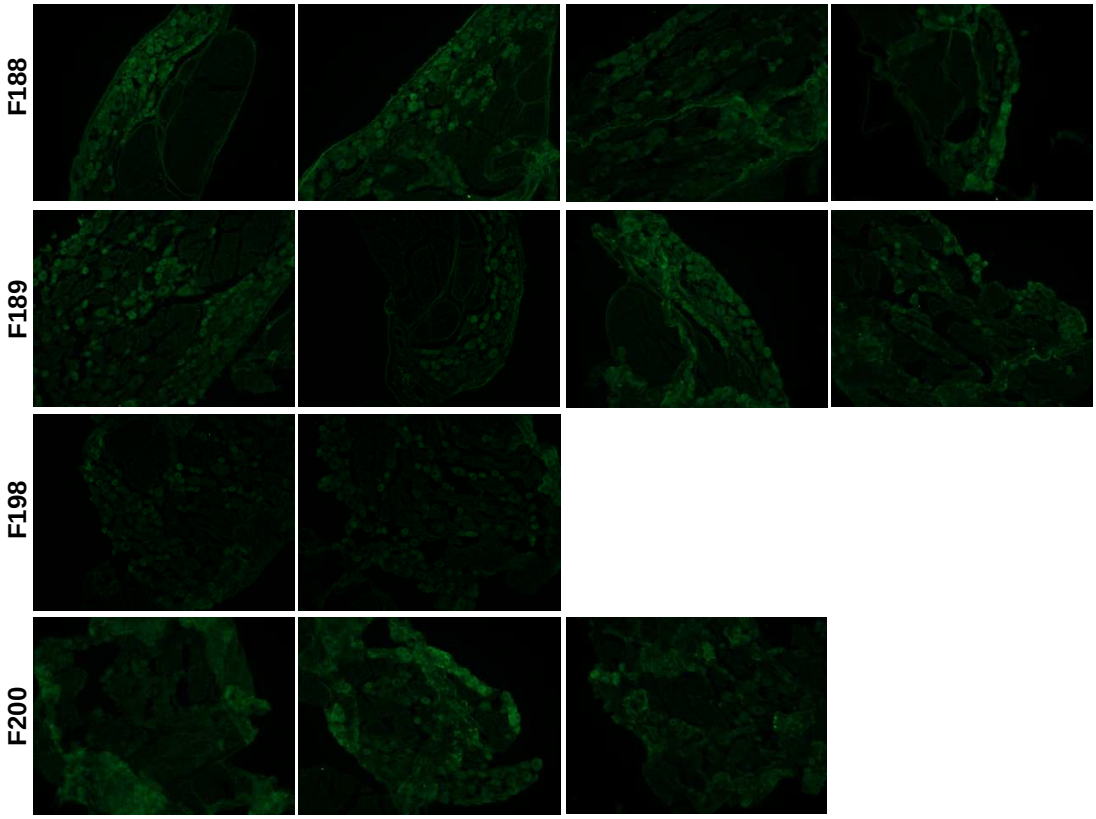


**Figure E.1.C.** NGF expression in the C7 DRG seven days after SSP-Sap+sham (F188, F189, F198, F200). For each rat, the sections presented correspond to those sections for which the percentage of NGF-positive pixels is summarized in Table E.1 with section number increasing from left to right.

**Table E.2. Average BDNF intensity ratio in neurons in the C6 DRG based on cell body area one day following painful FJD (Chapter 6).**

| | | | Neuronal cross-sectional area (μm$^2$) | | | | | | | |
|---|---|---|---|---|---|---|---|---|---|---|
| **Group** | **Rat** | **Section** | **<200** | **200-299** | **300-399** | **400-499** | **500-599** | **600-699** | **>700** | **All** |
| **FJD** | **F13** | 5 | 1.36 | 1.49 | 1.40 | 1.37 | 1.43 | 1.48 | 1.17 | 1.41 |
| | | 7 | 1.49 | 1.42 | 1.44 | 1.48 | 1.35 | 1.20 | 1.24 | 1.42 |
| | | 8 | 1.83 | 1.73 | 1.79 | 1.62 | 1.97 | | | 1.77 |
| | | 9 | 1.75 | 1.79 | 1.59 | 1.52 | | | | 1.68 |
| | **F20** | 7 | 1.77 | 2.07 | 1.53 | 1.98 | 1.84 | 1.68 | | 1.77 |
| | | 8 | 1.55 | 1.71 | 1.73 | 1.43 | 1.57 | 1.70 | 1.77 | 1.57 |
| | | 9 | 1.41 | 1.54 | 1.48 | 1.73 | 1.84 | 1.52 | | 1.58 |
| | | 10 | 1.39 | 1.57 | 1.53 | 1.51 | 1.81 | 1.50 | | 1.55 |
| | **F21** | 8 | 1.49 | 1.52 | 1.59 | 1.31 | 1.37 | 1.69 | 1.35 | 1.51 |
| | | 10 | 1.82 | 1.67 | 1.66 | 1.75 | 1.44 | 1.65 | 1.79 | 1.70 |
| | | 11 | 1.29 | 1.48 | 1.54 | 1.56 | 1.74 | 1.56 | 1.53 | 1.50 |
| **sham** | **F15** | 10 | 2.40 | 1.94 | 1.72 | 1.86 | 1.70 | | 1.39 | 1.90 |
| | | 11 | 1.40 | 1.25 | 1.32 | 1.25 | 1.20 | 1.27 | | 1.32 |
| | | 12 | 1.42 | 1.34 | 1.29 | 1.31 | 1.27 | 1.31 | | 1.33 |
| | | 15 | 1.66 | 1.65 | 1.52 | 1.52 | 1.47 | 1.44 | 1.38 | 1.56 |
| | **F22** | 5 | 1.48 | 1.43 | 1.42 | 1.40 | 1.36 | 1.13 | 1.58 | 1.41 |
| | | 6 | 1.54 | 1.37 | 1.28 | 1.47 | 1.29 | 1.30 | 1.33 | 1.41 |
| | | 9 | 1.59 | 1.55 | 1.67 | 1.29 | 1.36 | 1.33 | 1.53 | 1.47 |
| | | 10 | 1.49 | 1.48 | 1.34 | 1.45 | 1.53 | 1.45 | | 1.44 |
| | | 11 | 1.53 | 1.50 | 1.66 | 1.53 | 1.58 | 1.50 | 1.19 | 1.55 |
| | **F23** | 13 | 1.40 | 1.30 | 1.32 | 1.38 | 1.27 | 1.21 | 1.49 | 1.33 |
| | | 14 | 1.26 | 1.28 | 1.28 | 1.27 | 1.25 | 1.11 | 1.16 | 1.26 |
| | | 15 | 1.84 | 1.80 | 1.75 | 1.82 | 1.70 | 1.70 | 1.49 | 1.73 |

Note: The section number refers to the position of the tissue section on each slide, beginning in the top left corner and proceeding in numerical order from top to bottom, then resuming at the top of the adjacent column to the right. Gray boxes indicate that no neurons of the given size were analyzed in that section. The 'All' column provides the overall average BDNF intensity ratio for all neurons in the corresponding section, calculated by combining all neurons included in each of the seven bin sizes into a single group and taking the overall average. Tissue was generated by Christine L. Weisshaar, and the naming scheme for each rat reflects her records.

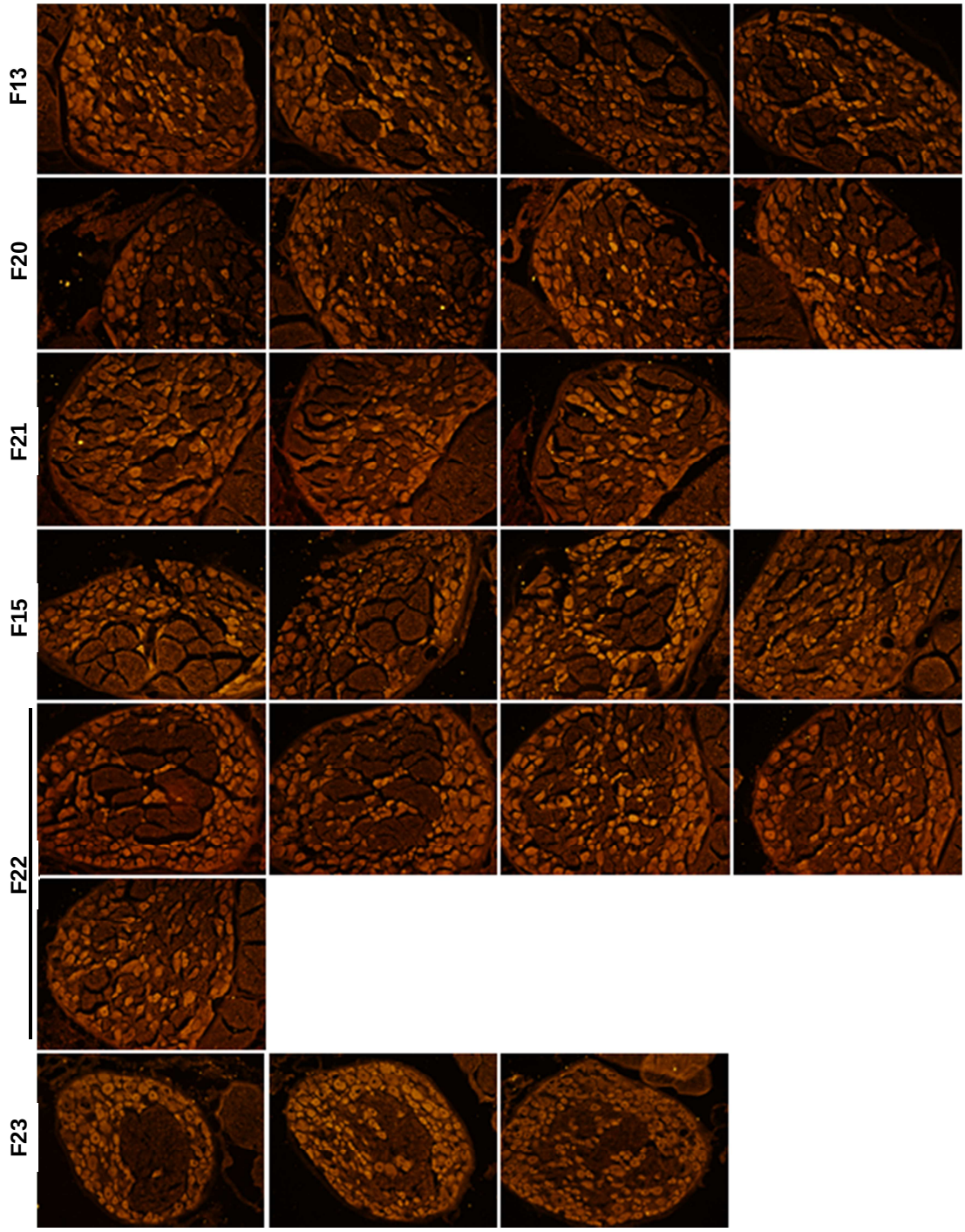


**Figure E.2.** BDNF expression in the C6 DRG one day after facet joint distraction (F13, F20, F21) or sham (F15, F22, F23). Tissue was generated by Christine L. Weisshaar, and the naming scheme for each rat reflects her records. For each rat, the sections presented correspond to those sections for which the BDNF-ir intensity ratio is summarized in Table E.2 with section number increasing from left to right.

**Table E.3. Average BDNF intensity ratio in neurons in the C6 DRG based on cell body area seven days following painful FJD (Chapter 6).**

| | | | Neuronal cross-sectional area (μm$^2$) | | | | | | | |
|---|---|---|---|---|---|---|---|---|---|---|
| **Group** | **Rat** | **Section** | **<200** | **200-299** | **300-399** | **400-499** | **500-599** | **600-699** | **>700** | **All** |
| **FJD** | **47** | 2 | 1.54 | 1.55 | 1.55 | 1.61 | 1.55 | | 1.31 | 1.53 |
| | | 3 | 1.56 | 1.40 | 1.55 | 1.63 | 1.76 | 1.59 | 1.26 | 1.52 |
| | | 4 | 1.90 | 1.88 | 2.19 | 1.96 | 1.95 | 3.43 | | 2.01 |
| | | 5 | 1.73 | 1.83 | 1.83 | 2.01 | 1.98 | 1.99 | 2.09 | 1.87 |
| | **48** | 1 | 1.68 | 1.73 | 1.68 | 1.53 | 1.65 | 1.93 | 1.86 | 1.71 |
| | | 2 | 1.45 | 1.52 | 1.34 | 1.65 | 1.58 | 1.48 | 1.75 | 1.51 |
| | | 4 | 1.38 | 1.42 | 1.42 | 1.52 | 1.47 | 1.52 | | 1.40 |
| | | 6 | 1.91 | 1.73 | 1.82 | 1.74 | 1.40 | 1.45 | 1.19 | 1.73 |
| | **49** | 3 | 1.42 | 1.44 | 1.45 | 1.47 | 1.47 | 1.46 | 1.58 | 1.45 |
| | | 4 | 1.39 | 1.52 | 1.70 | 1.70 | 1.53 | 1.29 | 1.62 | 1.51 |
| | | 5 | 1.26 | 1.41 | 1.54 | 1.45 | 1.58 | | 1.34 | 1.36 |
| | | 6 | 1.34 | 1.29 | 1.20 | 1.32 | 1.27 | 1.58 | 1.57 | 1.31 |
| **sham** | **55** | 4 | 1.36 | 1.37 | 1.37 | 1.37 | 1.38 | 1.30 | 1.16 | 1.36 |
| | | 6 | 1.24 | 1.34 | 1.34 | 1.27 | 1.15 | 1.27 | 1.40 | 1.27 |
| | | 7 | 1.64 | 1.56 | 1.42 | 1.46 | 1.66 | 1.36 | 1.66 | 1.56 |
| | | 8 | 1.39 | 1.48 | 1.44 | 1.47 | 1.35 | 1.39 | | 1.45 |
| | **56** | 8 | 1.35 | 1.39 | 1.35 | 1.37 | 1.26 | | 1.09 | 1.36 |
| | | 9 | 1.31 | 1.35 | 1.44 | 1.35 | 1.36 | 1.47 | 1.52 | 1.37 |
| | | 11 | 1.34 | 1.37 | 1.57 | 1.50 | 1.40 | 1.35 | 1.50 | 1.42 |
| | | 12 | 1.29 | 1.39 | 1.39 | 1.38 | | 1.40 | | 1.37 |
| | **60** | 5 | 1.43 | 1.46 | 1.43 | 1.54 | 1.59 | | | 1.50 |
| | | 6 | 1.47 | 1.52 | 1.56 | 1.48 | 1.49 | 1.67 | 1.44 | 1.52 |
| | | 7 | 1.41 | 1.52 | 1.52 | 1.46 | 1.52 | 1.49 | 1.56 | 1.49 |
| | | 8 | 1.41 | 1.36 | 1.54 | 1.55 | 1.40 | 1.24 | | 1.43 |

Note: As noted in Table E.2, the section number refers to the position of the tissue section on each slide, beginning in the top left corner and proceeding in numerical order from top to bottom, then resuming at the top of the adjacent column to the right. Gray boxes indicate that no neurons of the given size were analyzed in that section. The 'All' column provides the overall average BDNF intensity ratio for all neurons in the corresponding section, calculated by combining all neurons included in each of the seven bin sizes into a single group and taking the overall average.

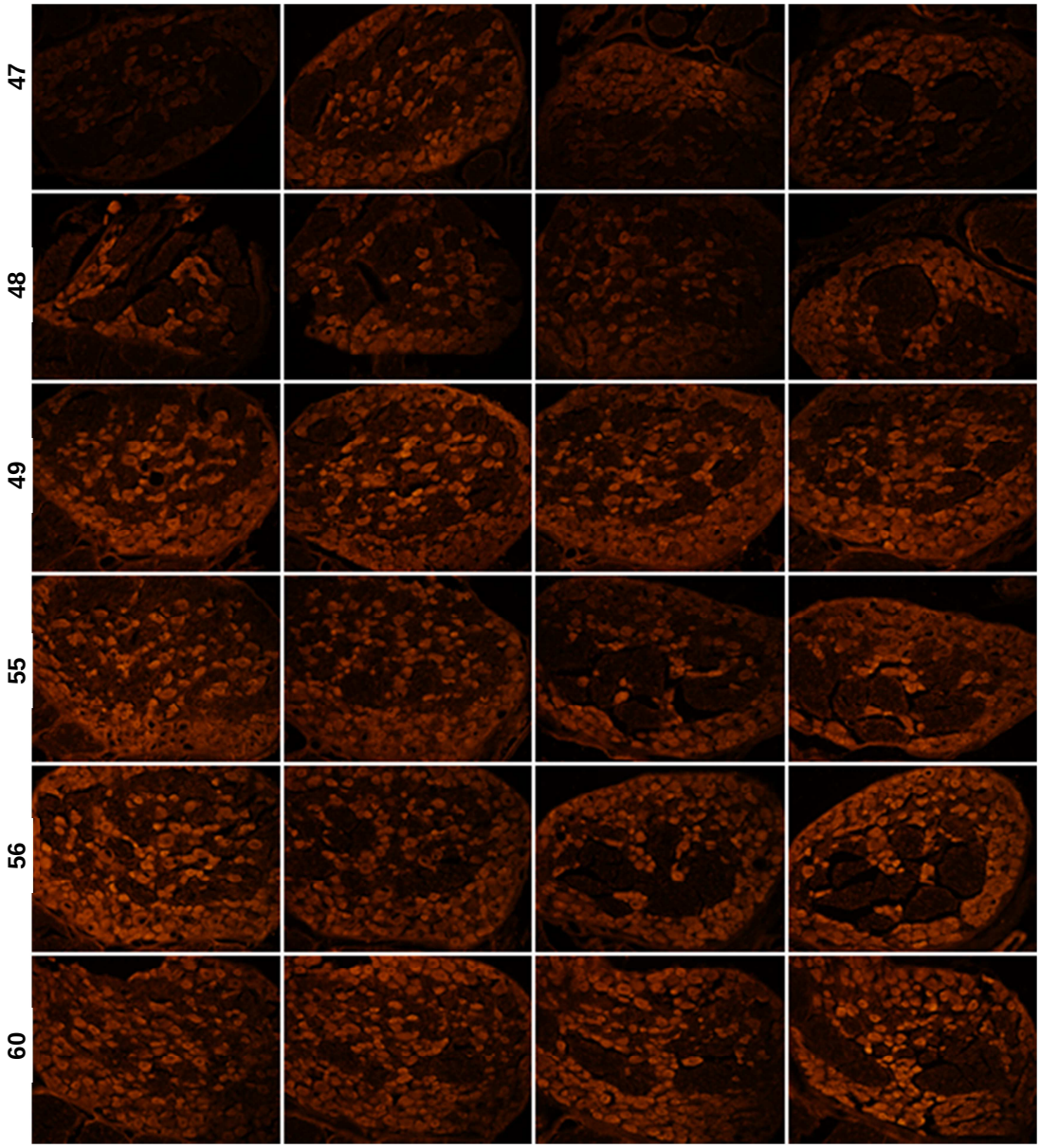


**Figure E.3.** BDNF expression in the C6 DRG seven days after facet joint distraction (47, 48, 49) or sham (55, 56, 60). For each rat, the sections presented correspond to those sections for which the BDNF-ir intensity ratio is summarized in Table E.3 with section number increasing from left to right.

**Table E.4.1. Ratio of pixels positive for BDNF in laminae I-IV in the dorsal horn one day following FJD or sham (Chapter 6).**

| | | Section | | | | | | | | | | | |
|---|---|---|---|---|---|---|---|---|---|---|---|---|---|
| **Group** | **Rat** | **1L** | **1R** | **2L** | **2R** | **3L** | **3R** | **4L** | **4R** | **5L** | **5R** | **6L** | **6R** |
| **FJD** | F13 | 0.005 | 0.000 | 0.009 | 0.006 | 0.003 | 0.003 | 0.010 | 0.006 | 0.015 | 0.079 | 0.005 | 0.007 |
| | F19 | 0.005 | 0.000 | 0.028 | 0.013 | 0.054 | 0.019 | 0.174 | 0.098 | 0.005 | 0.040 | 0.013 | 0.005 |
| | F20 | | 0.000 | | | 0.029 | | 0.103 | 0.001 | 0.008 | | 0.005 | |
| | F21 | 0.013 | | 0.033 | 0.038 | 0.147 | 0.049 | 0.001 | | 0.002 | 0.004 | 0.020 | 0.017 |
| | F24 | 0.001 | | 0.120 | 0.025 | 0.003 | 0.008 | 0.002 | 0.016 | 0.001 | 0.009 | 0.023 | |
| **sham** | F15 | | 0.134 | 0.119 | | 0.009 | 0.012 | 0.101 | 0.003 | 0.052 | 0.116 | | 0.002 |
| | F17 | 0.014 | 0.009 | 0.014 | 0.014 | 0.001 | 0.002 | 0.002 | 0.006 | 0.004 | 0.007 | 0.001 | 0.002 |
| | F22 | 0.002 | 0.000 | 0.001 | 0.008 | 0.027 | 0.009 | 0.001 | 0.000 | | 0.061 | | 0.018 |

Note: For each rat, six sections were analyzed, and both the right (R) and left (L) dorsal horns were included in analysis because of the assumption of a symmetric joint injury. Gray boxes indicate tissue sections that were excluded from analysis. All tissue was generated by Christine L. Weisshaar, and the naming scheme for each rat reflects her records.

**Table E.4.2. Log-transformation of the ratio of pixels positive for BDNF in laminae I-IV in the dorsal horn one day following FJD or sham (Chapter 6).**

| | | Section | | | | | | | | | | | |
|---|---|---|---|---|---|---|---|---|---|---|---|---|---|
| **Group** | **Rat** | **1L** | **1R** | **2L** | **2R** | **3L** | **3R** | **4L** | **4R** | **5L** | **5R** | **6L** | **6R** |
| **FJD** | F13 | 1.66 | 0.41 | 1.97 | 1.77 | 1.48 | 1.42 | 2.01 | 1.78 | 2.18 | 2.90 | 1.72 | 1.86 |
| | F19 | 1.70 | 0.58 | 2.45 | 2.12 | 2.73 | 2.28 | 3.24 | 2.99 | 1.70 | 2.61 | 2.11 | 1.73 |
| | F20 | | 0.07 | | | 2.47 | | 3.01 | 1.11 | 1.90 | | 1.72 | |
| | F21 | 2.10 | | 2.51 | 2.59 | 3.17 | 2.69 | 0.75 | | 1.33 | 1.59 | 2.30 | 2.23 |
| | F24 | 0.86 | | 3.08 | 2.39 | 1.48 | 1.88 | 1.22 | 2.20 | 1.03 | 1.97 | 2.36 | |
| **sham** | F15 | | 3.13 | 3.08 | | 1.95 | 2.10 | 3.00 | 1.45 | 2.72 | 3.06 | | 1.32 |
| | F17 | 2.14 | 1.96 | 2.16 | 2.13 | 1.05 | 1.39 | 1.29 | 1.80 | 1.61 | 1.84 | 1.13 | 1.22 |
| | F22 | 1.26 | 0.59 | 0.96 | 1.88 | 2.42 | 1.96 | 0.90 | 0.31 | | 2.78 | | 2.26 |

Note: Because BDNF expression data were positively skewed, the raw data were log-transformed to achieve an approximately normal distribution prior to statistical analysis. The log-transformation applied was: log(10,000*ratio of positive pixels). All tissue was generated by Christine L. Weisshaar, and the naming scheme for each rat reflects her records.

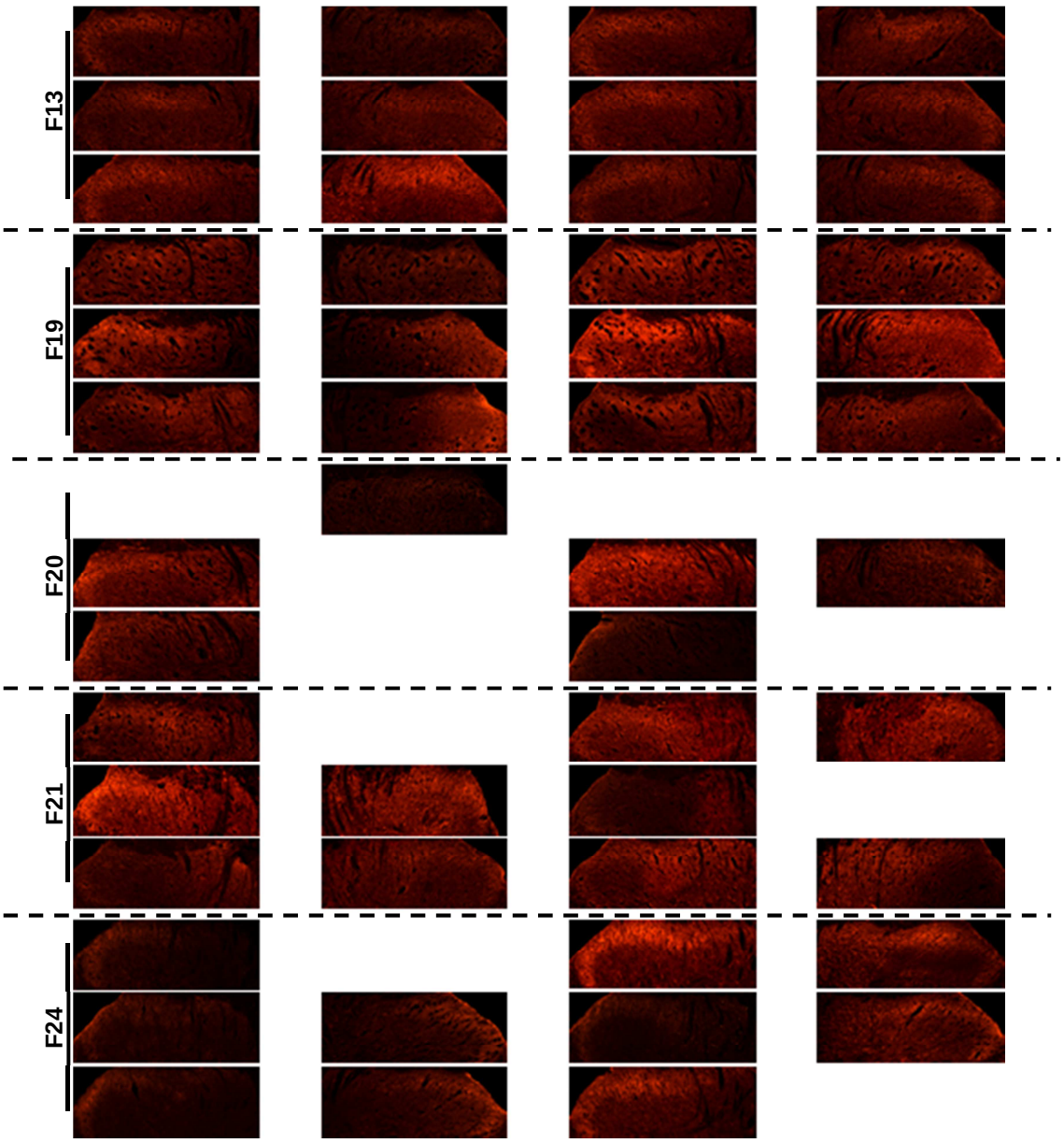


**Figure E.4.A.** BDNF expression in the C6 spinal cord one day after FJD (F13, F19, F20, F21, F24). Images are arranged in the order in which they appear in Table E.4.1. Six sections were analyzed per rat. For each rat, images from section 1 (left, right) and section 2 (left right) are presented in the first row. Sections 3 and 4 (second row) and 5 and 6 (third row) are also presented. Blank spaces represent tissue that was damaged and was not included in analyses. All tissue was generated by Christine L. Weisshaar, and the naming scheme for each rat reflects her records.

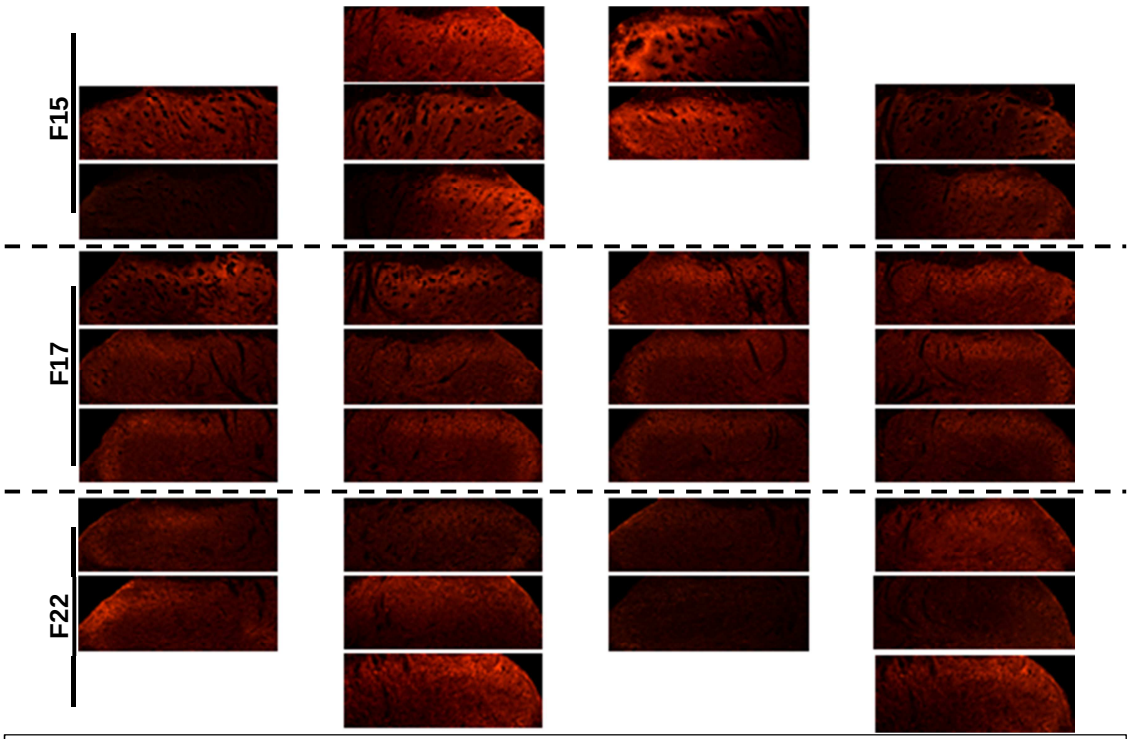


**Figure E.4.B.** BDNF expression in the C6 spinal cord one day after sham (F15, F17, F22). Images are arranged in the order in which they appear in Table E.4.1 as described in Figure E.4.A. All tissue was generated by Christine L. Weisshaar, and the naming scheme for each rat reflects her records.

**Table E.5.1. Ratio of pixels positive for BDNF in laminae I-IV in the dorsal horn seven days following FJD or sham (Chapter 6).**

| | | Section | | | | | | | | | | | |
|---|---|---|---|---|---|---|---|---|---|---|---|---|---|
| **Group** | **Rat** | **1L** | **1R** | **2L** | **2R** | **3L** | **3R** | **4L** | **4R** | **5L** | **5R** | **6L** | **6R** |
| **FJD** | 47 | 0.003 | 0.002 | 0.003 | 0.020 | 0.082 | | 0.015 | 0.071 | 0.006 | 0.162 | 0.029 | 0.030 |
| | 48 | | | 0.001 | 0.001 | 0.037 | 0.001 | | 0.002 | 0.006 | 0.013 | 0.033 | |
| | 49 | | | 0.002 | 0.001 | 0.001 | 0.002 | | | 0.001 | 0.011 | 0.001 | |
| | 52 | | 0.001 | 0.008 | 0.000 | 0.009 | | 0.003 | 0.022 | 0.007 | 0.068 | 0.002 | 0.003 |
| | 53 | | | | 0.001 | | | | 0.086 | 0.005 | 0.008 | 0.001 | 0.001 |
| | 54 | 0.020 | 0.046 | | | 0.064 | | | 0.145 | 0.073 | 0.096 | | 0.093 |
| **sham** | 50 | 0.005 | | 0.007 | 0.001 | 0.008 | 0.001 | 0.002 | 0.001 | 0.003 | 0.002 | | 0.001 |
| | 55 | 0.018 | 0.041 | 0.005 | 0.008 | 0.003 | 0.002 | 0.013 | | | 0.017 | 0.016 | 0.005 |
| | 56 | 0.015 | | 0.003 | 0.061 | 0.009 | | 0.009 | 0.004 | | 0.005 | 0.064 | 0.023 |
| | 60 | 0.008 | 0.074 | 0.000 | 0.005 | 0.010 | 0.000 | 0.000 | 0.001 | 0.004 | 0.002 | 0.000 | 0.000 |

Note: For each rat, six sections were analyzed, and both the right (R) and left (L) dorsal horns were included in analysis because of the assumption of a symmetric joint injury. Gray boxes indicate tissue sections that were excluded from analysis.

**Table E.5.2. Log-transformation of the ratio of pixels positive for BDNF in laminae I-IV in the dorsal horn seven days following FJD or sham (Chapter 6).**

| | | Section | | | | | | | | | | | |
|---|---|---|---|---|---|---|---|---|---|---|---|---|---|
| **Group** | **Rat** | **1L** | **1R** | **2L** | **2R** | **3L** | **3R** | **4L** | **4R** | **5L** | **5R** | **6L** | **6R** |
| **FJD** | 47 | 2.48 | 2.26 | 2.50 | 3.31 | 3.91 | | 3.16 | 3.85 | 2.79 | 4.21 | 3.46 | 3.47 |
| | 48 | | | 1.73 | 1.99 | 3.56 | 2.12 | | 2.39 | 2.79 | 3.12 | 3.52 | |
| | 49 | | | 2.39 | 2.03 | 2.05 | 2.29 | | | 1.90 | 3.04 | 1.79 | |
| | 52 | | 1.82 | 2.88 | 1.69 | 2.94 | | 2.45 | 3.35 | 2.83 | 3.83 | 2.28 | 2.43 |
| | 53 | | | | 2.02 | | | | 3.94 | 2.70 | 2.91 | 1.98 | 2.11 |
| | 54 | 3.30 | 3.66 | | | 3.81 | | | 4.16 | 3.86 | 3.98 | | 3.97 |
| **sham** | 50 | 2.71 | | 2.87 | 2.09 | 2.90 | 2.05 | 2.30 | 2.08 | 2.47 | 2.23 | | 1.79 |
| | 55 | 3.26 | 3.61 | 2.69 | 2.92 | 2.43 | 2.39 | 3.12 | | | 3.22 | 3.20 | 2.70 |
| | 56 | 3.16 | | 2.43 | 3.78 | 2.97 | | 2.93 | 2.57 | | 2.67 | 3.81 | 3.36 |
| | 60 | 2.92 | 3.87 | 1.66 | 2.74 | 3.00 | 1.51 | 1.64 | 2.01 | 2.60 | 2.28 | 1.47 | 0.95 |

Note: Because BDNF expression data were positively skewed, the raw data were log-transformed to achieve an approximately normal distribution prior to statistical analysis. The log-transformation applied was: log(100,000*ratio of positive pixels).

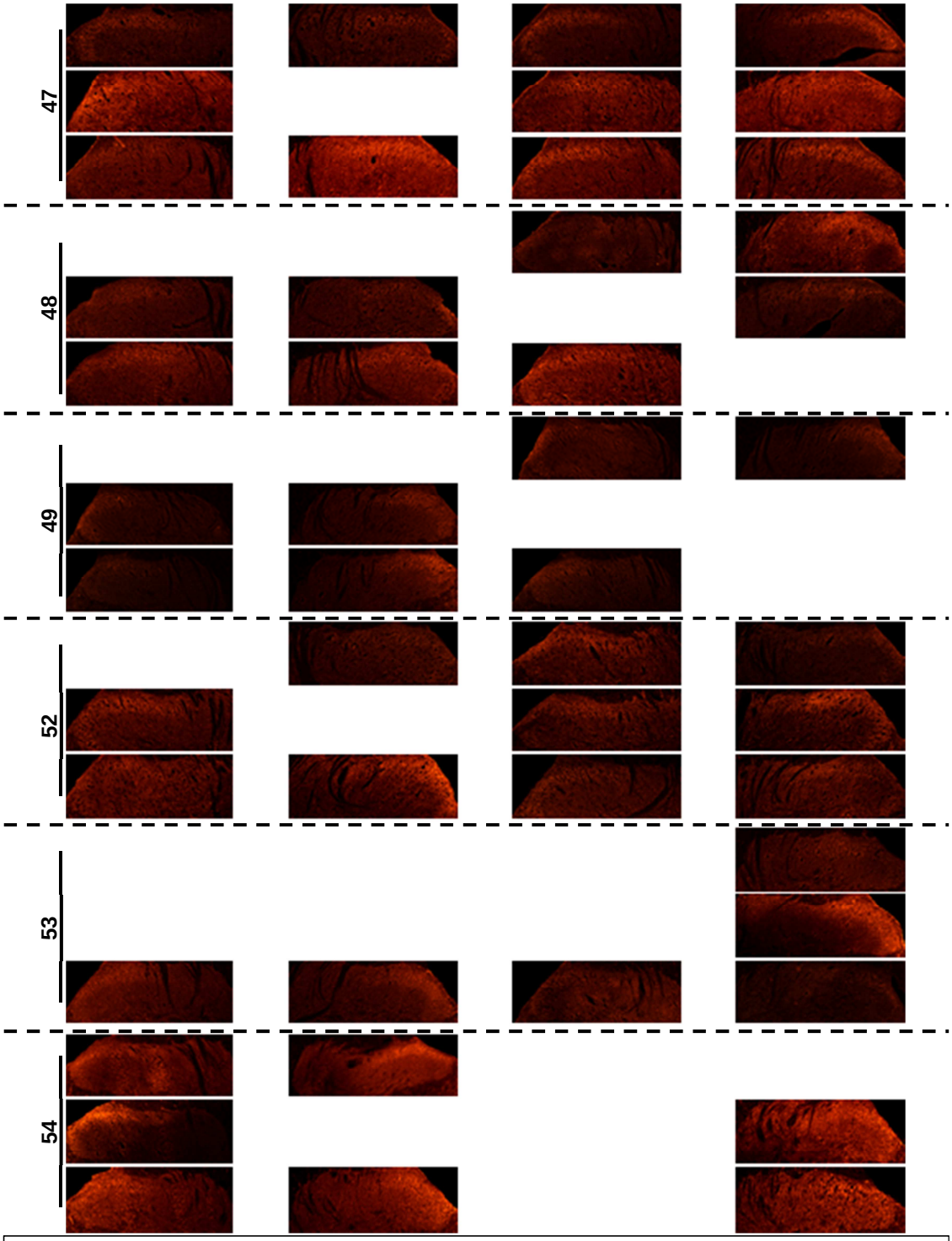


**Figure E.5.A.** BDNF expression in the C6 spinal cord seven days after FJD (47, 48, 49, 52, 53, 54). Images are arranged in the order in which they appear in Table E.5.1 and follow the pattern described in Figure E.4.

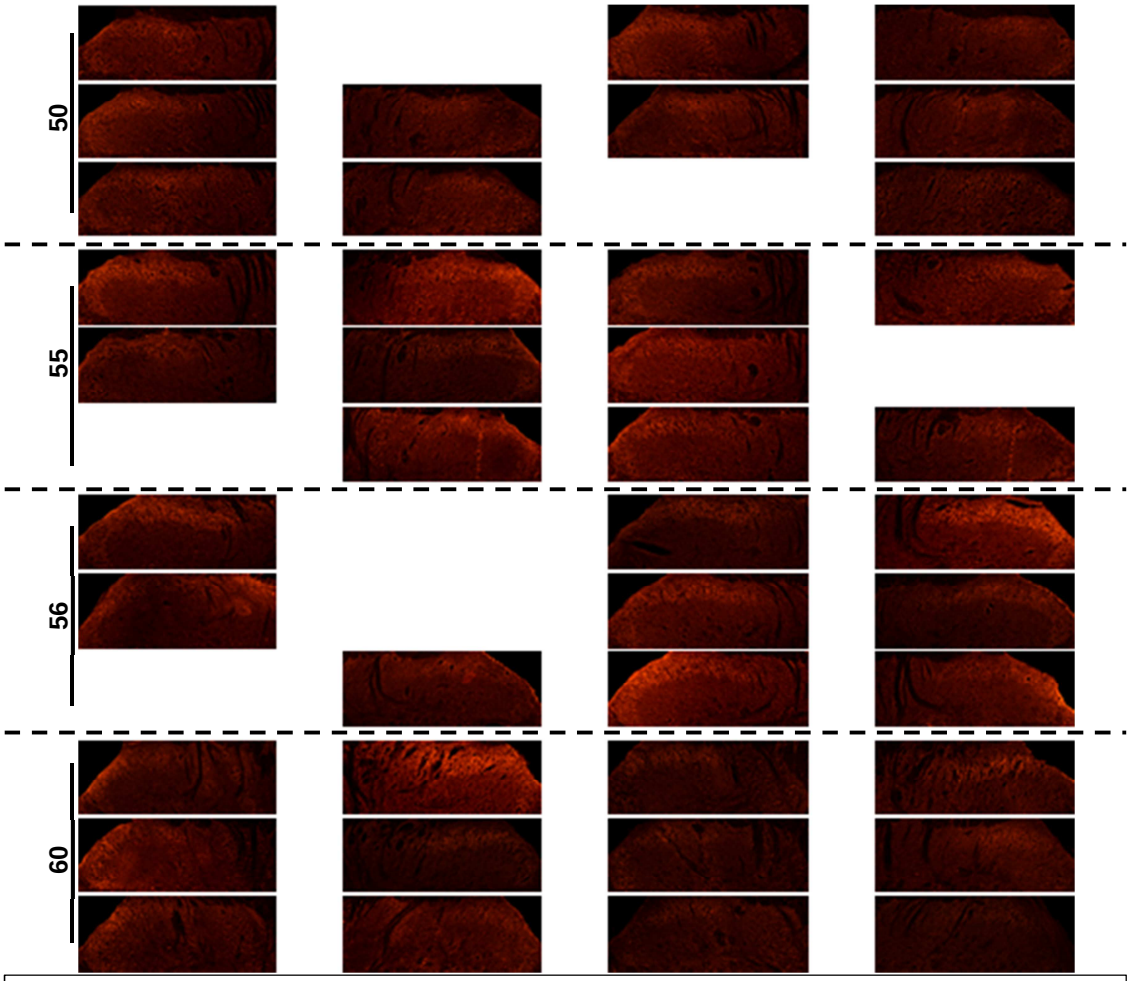


**Figure E.5.B.** BDNF expression in the C6 spinal cord seven days after sham (50, 55, 56, 60). Images are arranged in the order in which they appear in Table E.5.1 and follow the pattern described in Figure E.4.

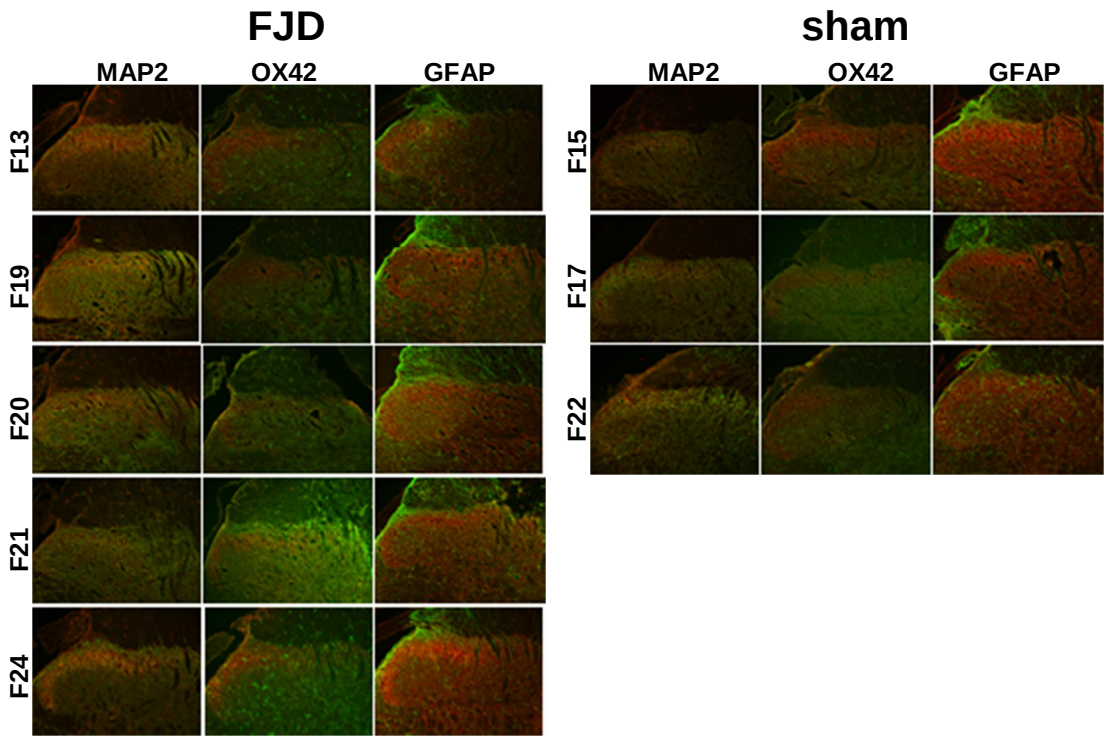


**Figure E.6.** Representative co-labeling of BDNF (red) with MAP2, OX-42, and GFAP (Green) one day after FJD or sham. All tissue was generated by Christine L. Weisshaar, and the naming scheme for each rat reflects her records.

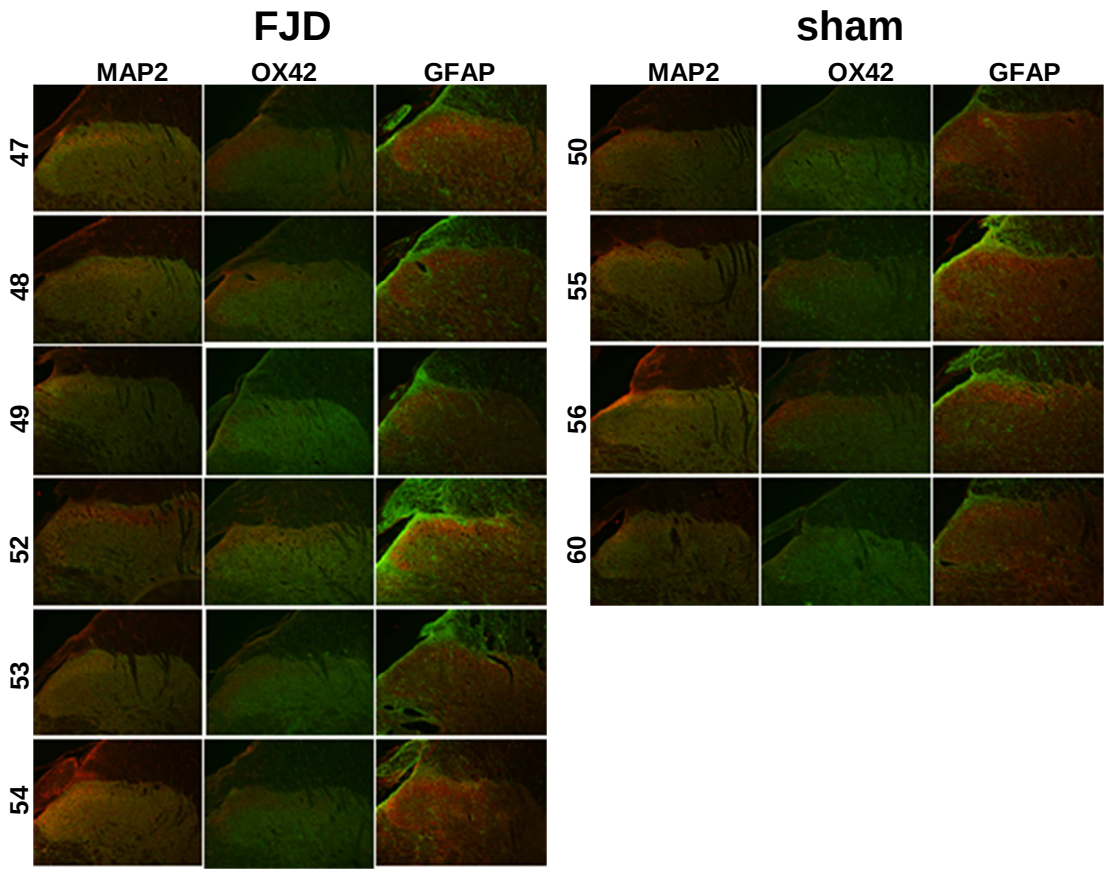


**Figure E.7.** Representative co-labeling of BDNF (red) with MAP2, OX-42, and GFAP (Green) seven days after FJD or sham.

# Appendix F

# Quantification of Proteins in the Facet Joint and Spinal Cord Using Western Blot

This appendix details the levels of protein expression determined using Western blot for individual rats included in the studies in Chapters 5 and 6. Specifically, levels of nerve growth factor (NGF) protein were quantified in the soft tissues of the C6/C7 facet joint at day one in the NGF characterization study in Chapter 5. In separate studies, spinal cord was assayed at day seven to assess activation of extracellular signal-regulated kinase (ERK) after facet joint distraction (FJD) with spinal sequestration of brain-derived neurotrophic factor (BDNF) in Chapter 6. For each blot, a loading control was included in addition to the experimental and study control groups. Levels of the target protein for each study are reported relative to expression of a housekeeping protein and are normalized to the loading control. The FJD group refers to rats for which the C6 forceps was displaced by 2.5mm as recorded by a linear variable differential transducer (LVDT). The sham group underwent the same surgical procedure with no applied distraction.

Table F.1 lists individual levels of NGF in the soft tissues of the C6/C7 facet joint, including the capsular ligament and synovial tissue, one day after FJD or sham procedures (Chapter 5). Table F.2 summarizes levels of phosphorylated ERK (pERK1/2) relative to total ERK in the spinal cord seven days after FJD with intrathecal trkB-Fc (trkB-Fc) or non-specific IgG-Fc (vehicle) injection that was given on day five (Chapter 6).

**Table F.1. NGF protein in the soft tissues of the C6/C7 facet joint one day after its painful distraction (Chapter 5).**

| Group | Rat | NGF (28kDa) relative to β-tubulin (normalized to loading control) |
|---|---|---|
| FJD | 381 | 2.98 |
| | 382 | 4.18 |
| | 408 | 4.39 |
| | 409 | 1.26 |
| | 410 | 5.71 |
| sham | 380 | 2.34 |
| | 383 | 2.81 |
| | 384 | 0.87 |
| | 407 | 2.12 |
| | 411 | 1.51 |

**Table F.2. Phosphorylated ERK (pERK) levels in the spinal cord after facet joint distraction and intrathecal trkB-Fc injection at day 5 (Chapter 6).**

| Group | Rat | pERK1 relative to total ERK1 (44kDa) (normalized to loading control) | pERK2 relative to total ERK2 (42kDa) (normalized to loading control) |
|---|---|---|---|
| trkB-Fc | 195 | 1.68 | 1.60 |
| | 196 | 1.86 | 1.76 |
| | 197 | 1.64 | 1.52 |
| | 204 | 1.42 | 1.58 |
| | 206 | 1.59 | 1.52 |
| | 209 | 1.19 | 0.88 |
| vehicle | 203 | 1.55 | 1.67 |
| | 205 | 2.00 | 1.85 |
| | 207 | 1.89 | 1.73 |
| | 246 | 2.18 | 2.07 |
| | 247 | 2.49 | 2.02 |
| | 248 | 2.18 | 1.89 |
| | 249 | 1.98 | 1.83 |

# Appendix G

# Quantification of Neuron Firing in the Dorsal Horn and Thalamus

This appendix summarizes the number of action potentials evoked during stimulation of the forepaw for individual spinal and thalamic neuronal recordings in the studies included in Chapters 5 and 7. All rats are separated into their respective experimental groups for the electrophysiology studies. For all tables, the neurons are numbered according to the rat from which they were recorded (Rat) and the order in which each neuron was identified within that rat's testing session (Neuron). Action potentials evoked by ten light brush strokes (Brush), five consecutive one second applications of each von Frey filament (vF), and a ten second pinch (Pinch) were counted; the total number of evoked action potentials for each stimulus is detailed in the tables.

All neurons were classified as wide dynamic range (WDR) or low threshold mechanoreceptive (LTM). For all neurons recorded in the spinal cord (Chapter 5), the electrode depth (μm) relative to the pial surface is also provided. The detailed protocol for electrophysiological recordings in the spinal cord is presented in Chapter 5. For all neurons recorded in the thalamus (Chapter 7), the electrode coordinates are provided for the left lateral distance from the midline (lateral, mm), the rostrocaudal distance from the intersection of the sagittal and coronal sutures (distance from Bregma, mm) with the

negative direction caudal to Bregma, and the depth relative to the pial surface (depth, µm), as presented previously (Syré et al., 2014). The protocol for electrophysiological recordings in the thalamus is detailed in Chapter 7. The facet joint distraction (FJD) group refers to rats for which the C6 forceps was displaced by 2.5mm as recorded by a linear variable differential transducer (LVDT) (See Chapter 3 for details). The sham group underwent the same surgical procedure with no applied distraction.

Table G.1 through Table G.6 detail the neuronal firing data for the studies included in Chapter 5. Table G.1 summarizes the evoked action potentials for rats that received intra-articular nerve growth factor (NGF) or sterile phosphate-buffered saline (vehicle) in the bilateral C6/C7 facet joints. For rats in which peptidergic signaling in joint afferents was disrupted prior to NGF (SSP-Sap+NGF) or vehicle (SSP-Sap+veh) facet joint injection, the evoked firing is detailed in Table G.2. Similarly, Table G.3 reports the evoked spikes for rats in which non-peptidergic joint afferents were ablated prior to NGF (IB4-Sap+NGF) or vehicle (IB4-Sap+veh) joint injections. Evoked firing quantified one day after facet joint distraction with an intra-articular anti-NGF antibody (FJD+anti-NGF) or a non-specific IgG (FJD+veh) facet joint injection are summarized in Table G.4. Rats that underwent sham procedures with the vehicle injection (sham+veh) are also included in Table G.4. Table G.5 details the action potentials evoked seven days after surgical procedures from additional rats in those same groups (FJD+anti-NGF, FJD+veh, sham+veh) as well as a sham group with an intra-articular anti-NGF injection (sham+anti-NGF). Additional rats underwent FJD and received intra-articular anti-NGF on day one after FJD (FJD+anti-NGFD1). For those rats, the spikes evoked seven days after the joint distraction are reported in Table G.6.

Table G.7 summarizes quantification of the evoked firing in thalamic neurons after FJD or sham procedures on day seven. Table G.8 details thalamic neuronal spikes on day seven in rats that were given intra-articular IB4-saporin to ablate non-peptidergic joint afferents prior to FJD (IB4-Sap+FJD) or sham (IB4-Sap+sham) procedures (see Chapter 7 for further details).

**Table G.1. Spinal neuronal firing counts at one day following intra-articular NGF application (Chapter 5).**

| Group | Rat | Neuron | Depth | Class | Pinch | Brush | 1.4g vF | 4g vF | 10g vF | 26g vF |
|---|---|---|---|---|---|---|---|---|---|---|
| NGF | 252 | 2 | 500 | LTM | 44 | 12 | 0 | 0 | 13 | 29 |
| | | 3 | 830 | WDR | 35 | 29 | 13 | 33 | 68 | 68 |
| | | 4 | 550 | WDR | 4 | 7 | 1 | 2 | 11 | 25 |
| | 253 | 2 | 610 | WDR | 69 | 24 | 6 | 21 | 67 | 47 |
| | | 3 | 150 | WDR | 17 | 12 | 10 | 11 | 36 | 39 |
| | | 4 | 500 | WDR | 139 | 73 | 54 | 97 | 195 | 238 |
| | | 5 | 510 | WDR | 59 | 3 | 2 | 5 | 56 | 84 |
| | | 7 | 1000 | WDR | 50 | 4 | 14 | 21 | 39 | 61 |
| | 255 | 1 | 150 | LTM | 44 | 34 | 28 | 56 | 87 | 73 |
| | | 3 | 950 | WDR | 67 | 20 | 49 | 89 | 79 | 122 |
| | | 4 | 830 | WDR | 31 | 26 | 79 | 75 | 76 | 97 |
| | | 6 | 820 | WDR | 74 | 10 | 18 | 22 | 30 | 62 |
| | | 7 | 800 | WDR | 109 | 85 | 15 | 14 | 44 | 72 |
| | | 8 | 780 | WDR | 69 | 24 | 57 | 19 | 32 | 87 |
| | 256 | 1 | 500 | WDR | 103 | 89 | 65 | 70 | 53 | 49 |
| | | 2 | 920 | WDR | 25 | 17 | 8 | 91 | 112 | 85 |
| | | 3 | 800 | WDR | 103 | 15 | 18 | 20 | 87 | 174 |
| | | 4 | 1000 | WDR | 99 | 13 | 7 | 7 | 30 | 121 |
| | | 5 | 840 | WDR | 279 | 29 | 6 | 13 | 45 | 90 |
| | | 6 | 740 | WDR | 91 | 71 | 41 | 55 | 104 | 95 |
| | | 8 | 800 | WDR | 151 | 38 | 18 | 65 | 80 | 148 |
| | 257 | 1 | 650 | WDR | 323 | 17 | 3 | 6 | 43 | 84 |
| | | 3 | 1010 | WDR | 83 | 32 | 11 | 7 | 15 | 62 |
| | | 4 | 700 | WDR | 155 | 4 | 46 | 75 | 68 | 82 |
| | | 5 | 870 | WDR | 278 | 44 | 16 | 30 | 88 | 273 |
| | | 6 | 1000 | WDR | 125 | 31 | 42 | 61 | 65 | 78 |
| | | 7 | 1090 | WDR | 145 | 41 | 10 | 38 | 69 | 95 |
| | 278 | 1 | 160 | LTM | 87 | 54 | 77 | 257 | 302 | 253 |
| | | 2 | 670 | WDR | 219 | 9 | 1 | 38 | 82 | 107 |
| | | 3 | 180 | WDR | 75 | 48 | 89 | 108 | 144 | 129 |
| | | 4 | 590 | WDR | 117 | 56 | 30 | 89 | 87 | 145 |
| | | 5 | 600 | WDR | 101 | 17 | 28 | 77 | 85 | 110 |
| | | 6 | 600 | WDR | 128 | 43 | 37 | 57 | 101 | 85 |
| | | 7 | 700 | WDR | 83 | 15 | 16 | 69 | 59 | 71 |
| | | 8 | 650 | WDR | 226 | 86 | 107 | 159 | 208 | 236 |
| | 282 | 3 | 300 | WDR | 34 | 42 | 83 | 96 | 83 | 91 |
| | | 4 | 650 | WDR | 132 | 86 | 49 | 142 | 157 | 217 |
| | | 5 | 580 | WDR | 169 | 47 | 39 | 102 | 69 | 81 |
| | | 6_1 | 860 | WDR | 372 | 0 | 1 | 2 | 17 | 190 |
| | | 6_2 | 860 | WDR | 206 | 3 | 2 | 5 | 205 | 226 |
| | | 7 | 630 | WDR | 387 | 32 | 14 | 9 | 35 | 133 |
| | | 8 | 740 | WDR | 127 | 49 | 23 | 43 | 88 | 138 |
| | | 9 | 770 | WDR | 72 | 8 | 20 | 46 | 88 | 98 |
| | | 10 | 500 | WDR | 43 | 40 | 35 | 99 | 192 | 196 |

Note: Table continued on next page.

| Group | Rat | Neuron | Depth | Class | Pinch | Brush | 1.4g vF | 4g vF | 10g vF | 26g vF |
|---|---|---|---|---|---|---|---|---|---|---|
| vehicle | 265 | 1 | 600 | WDR | 39 | 20 | 4 | 10 | 38 | 61 |
| | | 2 | 550 | WDR | 40 | 12 | 17 | 25 | 41 | 45 |
| | | 3 | 870 | WDR | 57 | 51 | 18 | 59 | 99 | 114 |
| | | 4 | 880 | WDR | 62 | 15 | 1 | 5 | 85 | 89 |
| | | 5 | 700 | WDR | 35 | 23 | 25 | 29 | 28 | 52 |
| | | 6 | 800 | LTM | 4 | 29 | 2 | 4 | 14 | 36 |
| | | 7 | 880 | LTM | 50 | 22 | 15 | 15 | 34 | 76 |
| | | 8 | 510 | WDR | 284 | 23 | 6 | 8 | 24 | 62 |
| | | 9 | 540 | WDR | 120 | 22 | 27 | 44 | 124 | 130 |
| | 266 | 1 | 800 | LTM | 38 | 45 | 8 | 14 | 25 | 54 |
| | | 2 | 660 | LTM | 21 | 17 | 4 | 96 | 30 | 21 |
| | | 3 | 500 | WDR | 18 | 22 | 15 | 7 | 52 | 45 |
| | | 4 | 480 | WDR | 33 | 7 | 3 | 48 | 85 | 71 |
| | | 5 | 720 | WDR | 42 | 22 | 16 | 40 | 73 | 109 |
| | | 7 | 580 | LTM | 10 | 13 | 3 | 0 | 12 | 30 |
| | | 8 | 530 | WDR | 60 | 9 | 6 | 5 | 40 | 69 |
| | 267 | 1 | 900 | LTM | 7 | 19 | 4 | 4 | 2 | 33 |
| | | 2 | 200 | LTM | 5 | 10 | 4 | 1 | 19 | 53 |
| | | 3 | 650 | WDR | 61 | 85 | 13 | 22 | 50 | 75 |
| | | 4 | 600 | WDR | 81 | 35 | 14 | 20 | 35 | 62 |
| | | 5 | 670 | WDR | 53 | 39 | 16 | 24 | 34 | 88 |
| | | 6 | 630 | WDR | 66 | 33 | 5 | 18 | 57 | 69 |
| | | 7 | 660 | WDR | 129 | 34 | 8 | 46 | 94 | 75 |
| | | 8 | 230 | LTM | 4 | 1 | 0 | 0 | 1 | 110 |
| | | 9 | 900 | WDR | 42 | 1 | 0 | 0 | 15 | 63 |
| | | 10 | 1010 | WDR | 37 | 28 | 11 | 11 | 43 | 51 |
| | 268 | 1 | 710 | WDR | 31 | 13 | 2 | 5 | 25 | 65 |
| | | 2 | 600 | WDR | 141 | 9 | 2 | 32 | 76 | 71 |
| | | 3 | 910 | WDR | 55 | 6 | 1 | 8 | 62 | 119 |
| | | 5 | 940 | LTM | 12 | 11 | 20 | 39 | 70 | 94 |
| | | 6 | 730 | WDR | 26 | 13 | 28 | 24 | 46 | 43 |
| | | 7 | 430 | WDR | 106 | 37 | 19 | 24 | 60 | 80 |
| | 269 | 1 | 570 | LTM | 24 | 21 | 14 | 26 | 29 | 38 |
| | | 2 | 840 | WDR | 35 | 0 | 0 | 3 | 43 | 75 |
| | | 3 | 740 | WDR | 30 | 24 | 93 | 64 | 71 | 75 |
| | | 4 | 680 | WDR | 160 | 24 | 15 | 31 | 62 | 92 |
| | | 5 | 1030 | WDR | 46 | 9 | 10 | 9 | 36 | 36 |
| | | 6 | 450 | WDR | 44 | 25 | 12 | 31 | 32 | 119 |
| | | 7 | 620 | WDR | 113 | 21 | 58 | 120 | 85 | 101 |
| | | 9 | 660 | WDR | 56 | 15 | 31 | 39 | 47 | 75 |
| | | 10 | 910 | LTM | 0 | 2 | 1 | 4 | 45 | 31 |
| | 281 | 1_1 | 550 | WDR | 304 | 45 | 0 | 12 | 55 | 150 |
| | | 1_2 | 550 | WDR | 77 | 25 | 6 | 15 | 66 | 158 |
| | | 2 | 660 | LTM | 29 | 10 | 82 | 88 | 193 | 204 |
| | | 3 | 650 | WDR | 58 | 10 | 6 | 131 | 168 | 106 |
| | | 4 | 760 | WDR | 186 | 10 | 9 | 33 | 117 | 130 |
| | | 5 | 470 | WDR | 56 | 21 | 3 | 64 | 168 | 157 |

**Table G.2. Spinal neuronal firing counts at one day following intra-articular NGF application in SSP-saporin treated rats (Chapter 5).**

| Group | Rat | Neuron | Depth | Class | Pinch | Brush | 1.4g vF | 4g vF | 10g vF | 26g vF |
|---|---|---|---|---|---|---|---|---|---|---|
| SSP-Sap+ NGF | 391 | 1 | 730 | WDR | 42 | 30 | 14 | 35 | 41 | 99 |
| | | 2 | 650 | WDR | 111 | 40 | 22 | 45 | 129 | 196 |
| | | 3 | 670 | WDR | 7 | 8 | 7 | 6 | 15 | 54 |
| | | 4 | 590 | WDR | 92 | 57 | 30 | 34 | 66 | 110 |
| | | 5_1 | 740 | WDR | 119 | 23 | 11 | 22 | 51 | 95 |
| | | 5_2 | 740 | LTM | 12 | 15 | 19 | 18 | 18 | 24 |
| | | 6 | 620 | WDR | 166 | 32 | 38 | 53 | 99 | 123 |
| | | 7 | 360 | WDR | 219 | 55 | 19 | 87 | 199 | 207 |
| | | 8_1 | 630 | WDR | 19 | 15 | 5 | 13 | 18 | 48 |
| | | 8_2 | 630 | WDR | 35 | 9 | 1 | 7 | 29 | 43 |
| | | 9 | 710 | WDR | 45 | 101 | 31 | 59 | 96 | 95 |
| | | 10_1 | 810 | WDR | 14 | 0 | 1 | 4 | 26 | 48 |
| | | 10_2 | 810 | WDR | 110 | 29 | 22 | 55 | 95 | 145 |
| | 392 | 1 | 540 | WDR | 91 | 8 | 24 | 44 | 91 | 96 |
| | | 2 | 890 | WDR | 26 | 42 | 23 | 36 | 50 | 79 |
| | | 3 | 630 | WDR | 165 | 37 | 12 | 14 | 22 | 48 |
| | | 4 | 500 | WDR | 161 | 38 | 34 | 44 | 70 | 92 |
| | | 5_1 | 700 | LTM | 98 | 2 | 5 | 13 | 6 | 9 |
| | | 5_2 | 700 | WDR | 17 | 50 | 29 | 40 | 58 | 64 |
| | | 6 | 840 | WDR | 128 | 0 | 0 | 1 | 38 | 262 |
| | 395 | 1 | 250 | WDR | 9 | 17 | 7 | 11 | 14 | 25 |
| | | 2 | 940 | WDR | 37 | 37 | 15 | 37 | 78 | 86 |
| | | 3 | 710 | WDR | 129 | 89 | 36 | 41 | 129 | 175 |
| | | 4 | 220 | WDR | 88 | 47 | 9 | 6 | 22 | 86 |
| | | 6_1 | 570 | WDR | 363 | 45 | 25 | 30 | 60 | 163 |
| | | 6_2 | 570 | WDR | 210 | 63 | 56 | 105 | 101 | 166 |
| | 396 | 1 | 590 | WDR | 25 | 12 | 20 | 32 | 57 | 58 |
| | | 3 | 870 | LTM | 5 | 40 | 29 | 41 | 24 | 15 |
| | | 4 | 550 | WDR | 122 | 20 | 11 | 12 | 19 | 61 |
| | | 5 | 770 | WDR | 135 | 39 | 10 | 73 | 122 | 130 |
| | | 6 | 800 | WDR | 56 | 9 | 0 | 44 | 94 | 120 |
| | | 7 | 720 | WDR | 55 | 55 | 15 | 24 | 39 | 101 |
| | | 8 | 450 | LTM | 139 | 146 | 73 | 55 | 83 | 97 |
| | | 10 | 800 | WDR | 4 | 52 | 19 | 1 | 12 | 66 |

Note: Table continued on next page.

| Group | Rat | Neuron | Depth | Class | Pinch | Brush | 1.4g vF | 4g vF | 10g vF | 26g vF |
|---|---|---|---|---|---|---|---|---|---|---|
| SSP-Sap+ veh | 393 | 1 | 430 | WDR | 19 | 27 | 6 | 17 | 33 | 60 |
| | | 2 | 670 | WDR | 24 | 19 | 7 | 8 | 50 | 72 |
| | | 3 | 710 | WDR | 282 | 92 | 119 | 189 | 238 | 297 |
| | | 7 | 470 | LTM | 284 | 48 | 53 | 83 | 106 | 80 |
| | | 8 | 700 | LTM | 36 | 13 | 14 | 40 | 33 | 32 |
| | | 9 | 430 | WDR | 53 | 44 | 25 | 27 | 59 | 61 |
| | | 10 | 800 | LTM | 348 | 13 | 73 | 45 | 56 | 102 |
| | 394 | 1 | 430 | LTM | 95 | 28 | 45 | 73 | 35 | 90 |
| | | 2 | 720 | WDR | 67 | 2 | 0 | 62 | 74 | 169 |
| | | 3 | 850 | WDR | 159 | 67 | 37 | 52 | 225 | 205 |
| | | 4 | 600 | WDR | 80 | 48 | 29 | 36 | 56 | 84 |
| | | 5 | 400 | WDR | 91 | 67 | 12 | 34 | 85 | 107 |
| | | 6 | 930 | WDR | 4 | 13 | 1 | 8 | 47 | 93 |
| | | 7 | 840 | WDR | 197 | 0 | 2 | 12 | 88 | 159 |
| | 397 | 1 | 750 | LTM | 248 | 89 | 96 | 133 | 170 | 153 |
| | | 2_1 | 620 | WDR | 41 | 8 | 1 | 4 | 8 | 34 |
| | | 2_2 | 620 | WDR | 32 | 11 | 1 | 6 | 25 | 58 |
| | | 3 | 620 | WDR | 87 | 37 | 10 | 15 | 37 | 63 |
| | | 4 | 700 | LTM | 112 | 130 | 85 | 96 | 63 | 161 |
| | | 5 | 940 | WDR | 27 | 11 | 3 | 27 | 126 | 230 |
| | | 6 | 1000 | WDR | 127 | 2 | 0 | 0 | 5 | 71 |
| | | 7 | 500 | WDR | 197 | 26 | 18 | 40 | 119 | 158 |
| | 398 | 1 | 910 | WDR | 89 | 7 | 3 | 5 | 17 | 63 |
| | | 2 | 880 | LTM | 12 | 25 | 18 | 18 | 36 | 35 |
| | | 3 | 900 | WDR | 103 | 27 | 18 | 49 | 71 | 100 |
| | | 4 | 650 | WDR | 136 | 21 | 24 | 79 | 140 | 134 |
| | | 5 | 750 | WDR | 105 | 16 | 15 | 19 | 21 | 60 |
| | | 6 | 800 | WDR | 58 | 42 | 1 | 5 | 18 | 34 |
| | | 7 | 750 | WDR | 133 | 6 | 0 | 5 | 38 | 196 |

**Table G.3. Spinal neuronal firing counts at one day following intra-articular NGF application in IB4-saporin treated rats (Chapter 5).**

| Group | Rat | Neuron | Depth | Class | Pinch | Brush | 1.4g vF | 4g vF | 10g vF | 26g vF |
|---|---|---|---|---|---|---|---|---|---|---|
| IB4-Sap+ NGF | 371 | 1 | 940 | WDR | 19 | 21 | 21 | 26 | 37 | 81 |
| | | 2 | 900 | LTM | 146 | 199 | 167 | 211 | 259 | 278 |
| | | 3 | 800 | WDR | 44 | 56 | 10 | 26 | 83 | 214 |
| | | 4 | 880 | WDR | 14 | 19 | 10 | 13 | 94 | 166 |
| | | 5 | 560 | WDR | 211 | 29 | 43 | 81 | 125 | 119 |
| | | 6 | 850 | WDR | 179 | 64 | 44 | 61 | 79 | 142 |
| | | 7 | 780 | WDR | 67 | 7 | 15 | 43 | 258 | 251 |
| | | 8 | 1100 | WDR | 7 | 29 | 6 | 10 | 32 | 168 |
| | | 9 | 820 | WDR | 30 | 9 | 70 | 55 | 122 | 186 |
| | 372 | 2 | 760 | WDR | 124 | 6 | 10 | 25 | 286 | 322 |
| | | 3 | 770 | WDR | 49 | 0 | 0 | 2 | 74 | 184 |
| | | 4 | 1000 | WDR | 21 | 9 | 10 | 20 | 65 | 164 |
| | | 5 | 830 | WDR | 313 | 36 | 19 | 74 | 187 | 323 |
| | | 6 | 860 | WDR | 92 | 12 | 20 | 39 | 75 | 189 |
| | | 7 | 940 | WDR | 6 | 13 | 6 | 4 | 22 | 60 |
| | | 8 | 900 | WDR | 20 | 36 | 17 | 30 | 56 | 81 |
| | 373 | 1_1 | 730 | WDR | 260 | 31 | 26 | 83 | 162 | 218 |
| | | 1_2 | 730 | WDR | 65 | 22 | 3 | 10 | 51 | 114 |
| | | 3 | 230 | WDR | 15 | 16 | 6 | 161 | 226 | 277 |
| | | 4 | 690 | WDR | 39 | 42 | 9 | 7 | 30 | 61 |
| | | 5 | 860 | WDR | 91 | 50 | 10 | 31 | 49 | 139 |
| | | 6 | 170 | LTM | 36 | 30 | 6 | 51 | 87 | 51 |
| | | 7 | 760 | LTM | 62 | 73 | 99 | 93 | 87 | 125 |
| | | 8 | 880 | WDR | 23 | 1 | 0 | 5 | 46 | 81 |
| | | 9 | 740 | WDR | 113 | 0 | 3 | 18 | 41 | 144 |
| | | 10 | 800 | WDR | 15 | 15 | 19 | 57 | 201 | 219 |
| | | 11 | 900 | WDR | 260 | 31 | 17 | 32 | 206 | 266 |
| | | 12 | 880 | WDR | 82 | 34 | 3 | 6 | 24 | 128 |
| | 399 | 1 | 710 | LTM | 468 | 65 | 75 | 190 | 196 | 180 |
| | | 2 | 680 | LTM | 203 | 170 | 200 | 169 | 178 | 222 |
| | | 3 | 610 | WDR | 93 | 20 | 39 | 45 | 129 | 108 |
| | | 4 | 830 | WDR | 100 | 7 | 0 | 7 | 57 | 98 |
| | | 5 | 890 | WDR | 63 | 5 | 5 | 47 | 80 | 108 |
| | | 6 | 690 | LTM | 89 | 35 | 117 | 147 | 133 | 144 |
| | | 7 | 670 | LTM | 56 | 15 | 23 | 113 | 141 | 150 |
| | | 9 | 870 | WDR | 391 | 30 | 1 | 18 | 71 | 308 |
| | 400 | 1 | 600 | LTM | 252 | 32 | 112 | 134 | 178 | 138 |
| | | 2 | 700 | LTM | 6 | 28 | 29 | 32 | 59 | 48 |
| | | 3 | 750 | WDR | 221 | 15 | 13 | 28 | 139 | 224 |
| | | 4 | 740 | WDR | 320 | 24 | 23 | 121 | 179 | 282 |
| | | 5 | 530 | LTM | 82 | 13 | 42 | 95 | 94 | 141 |
| | | 6 | 770 | WDR | 213 | 51 | 36 | 114 | 271 | 320 |

Note: Table continued on next page.

| Group | Rat | Neuron | Depth | Class | Pinch | Brush | 1.4g vF | 4g vF | 10g vF | 26g vF |
|---|---|---|---|---|---|---|---|---|---|---|
| IB4-Sap+ veh | 402 | 1 | 650 | LTM | 52 | 29 | 30 | 70 | 66 | 78 |
| | | 2 | 430 | LTM | 120 | 33 | 107 | 96 | 74 | 97 |
| | | 3_1 | 810 | WDR | 24 | 15 | 1 | 6 | 11 | 32 |
| | | 3_2 | 810 | WDR | 120 | 45 | 33 | 74 | 157 | 164 |
| | | 4 | 500 | WDR | 4 | 24 | 7 | 16 | 25 | 24 |
| | | 5 | 700 | WDR | 62 | 38 | 58 | 171 | 230 | 285 |
| | | 6 | 910 | LTM | 10 | 52 | 51 | 34 | 32 | 56 |
| | | 7 | 950 | WDR | 168 | 16 | 7 | 15 | 76 | 132 |
| | | 9 | 760 | LTM | 206 | 43 | 120 | 196 | 247 | 181 |
| | | 10 | 900 | WDR | 11 | 29 | 5 | 19 | 44 | 41 |
| | 403 | 1 | 760 | LTM | 6 | 16 | 12 | 13 | 25 | 12 |
| | | 2 | 710 | LTM | 85 | 35 | 98 | 117 | 76 | 102 |
| | | 3 | 720 | LTM | 30 | 51 | 33 | 67 | 53 | 59 |
| | | 4 | 500 | WDR | 93 | 63 | 22 | 51 | 132 | 171 |
| | | 5 | 430 | WDR | 45 | 46 | 22 | 28 | 51 | 50 |
| | | 6_1 | 700 | WDR | 135 | 0 | 3 | 4 | 2 | 25 |
| | | 6_2 | 700 | WDR | 169 | 8 | 3 | 9 | 22 | 74 |
| | | 6_3 | 700 | WDR | 115 | 11 | 5 | 39 | 66 | 74 |
| | | 7 | 740 | LTM | 46 | 36 | 40 | 17 | 48 | 65 |
| | | 8 | 810 | WDR | 61 | 3 | 7 | 33 | 49 | 57 |
| | | 10 | 890 | LTM | 54 | 35 | 16 | 38 | 42 | 47 |
| | | 11 | 490 | LTM | 16 | 35 | 14 | 18 | 26 | 27 |
| | 404 | 1_1 | 510 | WDR | 66 | 67 | 30 | 28 | 65 | 75 |
| | | 1_2 | 510 | LTM | 28 | 67 | 26 | 75 | 50 | 31 |
| | | 2 | 780 | WDR | 27 | 15 | 17 | 31 | 52 | 48 |
| | | 3 | 420 | LTM | 28 | 51 | 50 | 76 | 80 | 46 |
| | | 4 | 820 | LTM | 5 | 34 | 9 | 26 | 38 | 30 |
| | | 5 | 850 | WDR | 245 | 15 | 36 | 122 | 245 | 237 |
| | | 7 | 290 | WDR | 220 | 57 | 125 | 167 | 287 | 267 |
| | 405 | 1 | 620 | WDR | 53 | 32 | 4 | 47 | 114 | 131 |
| | | 2 | 700 | WDR | 35 | 14 | 8 | 16 | 28 | 35 |
| | | 3 | 550 | LTM | 292 | 17 | 104 | 203 | 172 | 163 |
| | | 4 | 690 | WDR | 57 | 51 | 6 | 24 | 47 | 66 |
| | | 5 | 770 | LTM | 63 | 21 | 35 | 148 | 146 | 155 |
| | | 6 | 950 | WDR | 564 | 51 | 31 | 137 | 201 | 232 |
| | | 7 | 890 | WDR | 284 | 23 | 20 | 22 | 39 | 106 |

**Table G.4. Spinal neuronal firing counts in rats at one day following facet joint distraction and immediate intra-articular anti-NGF application (Chapter 5).**

| Group | Rat | Neuron | Depth | Class | Pinch | Brush | 1.4g vF | 4g vF | 10g vF | 26g vF |
|---|---|---|---|---|---|---|---|---|---|---|
| FJD+veh | 305 | 1 | 410 | LTM | 4 | 2 | 14 | 79 | 73 | 231 |
| | | 2 | 840 | WDR | 13 | 1 | 1 | 34 | 42 | 49 |
| | | 3 | 630 | WDR | 54 | 5 | 39 | 227 | 288 | 228 |
| | | 4 | 880 | WDR | 55 | 48 | 9 | 6 | 24 | 108 |
| | 309 | 1 | 910 | WDR | 42 | 13 | 6 | 20 | 84 | 91 |
| | | 2_1 | 780 | WDR | 65 | 10 | 3 | 4 | 63 | 90 |
| | | 2_2 | 780 | WDR | 249 | 97 | 82 | 156 | 261 | 355 |
| | | 3 | 1000 | WDR | 111 | 22 | 16 | 23 | 47 | 211 |
| | | 4 | 330 | WDR | 55 | 50 | 8 | 30 | 50 | 104 |
| | | 5_1 | 260 | WDR | 68 | 6 | 72 | 69 | 80 | 77 |
| | | 5_2 | 260 | WDR | 46 | 17 | 60 | 70 | 66 | 63 |
| | | 6 | 700 | WDR | 239 | 11 | 66 | 169 | 221 | 248 |
| | | 7 | 850 | WDR | 16 | 1 | 0 | 2 | 59 | 55 |
| | | 8 | 640 | WDR | 87 | 50 | 18 | 58 | 105 | 133 |
| | | 9 | 850 | WDR | 45 | 38 | 31 | 78 | 80 | 89 |
| | | 10 | 760 | WDR | 186 | 17 | 15 | 12 | 54 | 198 |
| | 356 | 1 | 640 | WDR | 361 | 58 | 25 | 100 | 256 | 297 |
| | | 2 | 810 | WDR | 166 | 50 | 32 | 33 | 94 | 131 |
| | | 3 | 690 | LTM | 18 | 50 | 23 | 56 | 49 | 52 |
| | | 4 | 890 | WDR | 169 | 31 | 40 | 61 | 140 | 101 |
| | | 5 | 450 | WDR | 35 | 67 | 103 | 20 | 24 | 18 |
| | | 6 | 870 | WDR | 89 | 0 | 3 | 14 | 215 | 567 |
| | | 7 | 450 | LTM | 10 | 7 | 3 | 5 | 32 | 95 |
| | | 8 | 800 | WDR | 98 | 16 | 15 | 16 | 121 | 169 |
| | | 9 | 950 | WDR | 264 | 21 | 7 | 18 | 185 | 267 |
| | | 10_1 | 800 | LTM | 15 | 75 | 61 | 190 | 170 | 182 |
| | | 10_2 | 800 | WDR | 100 | 25 | 36 | 42 | 99 | 114 |
| | 357 | 1 | 910 | WDR | 12 | 3 | 0 | 3 | 4 | 69 |
| | | 2 | 690 | WDR | 119 | 42 | 41 | 98 | 108 | 169 |
| | | 3 | 660 | WDR | 253 | 96 | 78 | 228 | 346 | 393 |
| | | 4 | 150 | LTM | 13 | 12 | 1 | 25 | 141 | 123 |
| | | 5 | 750 | WDR | 44 | 18 | 10 | 13 | 112 | 175 |
| | | 6 | 690 | WDR | 37 | 51 | 48 | 44 | 67 | 87 |
| | | 7 | 940 | LTM | 49 | 24 | 24 | 43 | 94 | 210 |
| | | 8 | 820 | WDR | 61 | 19 | 12 | 33 | 69 | 316 |
| | | 9_1 | 700 | WDR | 40 | 17 | 8 | 12 | 34 | 136 |
| | | 9_2 | 700 | WDR | 66 | 32 | 68 | 85 | 101 | 59 |

Note: Table continued on next page.

| Group | Rat | Neuron | Depth | Class | Pinch | Brush | 1.4g vF | 4g vF | 10g vF | 26g vF |
|---|---|---|---|---|---|---|---|---|---|---|
| FJD+ anti-NGF | 306 | 1 | 740 | WDR | 28 | 14 | 3 | 3 | 7 | 123 |
| | | 2 | 820 | WDR | 241 | 24 | 43 | 83 | 119 | 157 |
| | | 3 | 790 | WDR | 133 | 29 | 35 | 145 | 124 | 102 |
| | | 4 | 700 | WDR | 62 | 80 | 25 | 50 | 61 | 97 |
| | | 5 | 410 | WDR | 26 | 17 | 13 | 16 | 26 | 41 |
| | | 6_1 | 590 | WDR | 26 | 24 | 14 | 22 | 42 | 44 |
| | | 6_2 | 530 | WDR | 49 | 23 | 19 | 24 | 41 | 68 |
| | 308 | 1 | 620 | WDR | 86 | 35 | 27 | 38 | 101 | 176 |
| | | 2 | 640 | WDR | 132 | 36 | 6 | 17 | 72 | 148 |
| | | 3 | 650 | LTM | 0 | 20 | 0 | 0 | 1 | 54 |
| | 353 | 1 | 860 | LTM | 22 | 8 | 6 | 20 | 55 | 97 |
| | | 2 | 880 | LTM | 5 | 0 | 0 | 0 | 3 | 6 |
| | | 3 | 920 | LTM | 5 | 9 | 5 | 3 | 19 | 39 |
| | | 4 | 140 | LTM | 16 | 1 | 0 | 30 | 114 | 129 |
| | | 5 | 500 | WDR | 32 | 31 | 59 | 136 | 84 | 69 |
| | | 6 | 910 | WDR | 12 | 42 | 24 | 7 | 29 | 80 |
| | | 7 | 670 | WDR | 32 | 57 | 56 | 49 | 119 | 84 |
| | | 8 | 600 | LTM | 20 | 40 | 33 | 58 | 176 | 204 |
| | 354 | 1 | 590 | LTM | 46 | 47 | 20 | 41 | 69 | 191 |
| | | 2 | 750 | WDR | 70 | 28 | 15 | 11 | 95 | 66 |
| | | 3 | 620 | LTM | 20 | 16 | 20 | 62 | 171 | 136 |
| | | 5 | 850 | LTM | 31 | 10 | 10 | 18 | 21 | 42 |
| | | 6 | 970 | LTM | 48 | 20 | 16 | 22 | 44 | 111 |
| | 355 | 1 | 80 | LTM | 2 | 16 | 3 | 1 | 27 | 117 |
| | | 2 | 770 | WDR | 50 | 15 | 9 | 18 | 53 | 136 |
| | | 4_1 | 730 | LTM | 33 | 11 | 7 | 26 | 94 | 119 |
| | | 4_2 | 730 | WDR | 59 | 0 | 10 | 27 | 144 | 169 |
| | | 5 | 700 | WDR | 230 | 17 | 18 | 48 | 117 | 438 |
| | | 6 | 800 | WDR | 33 | 19 | 19 | 22 | 30 | 39 |

Note: Table continued on next page.

| Group | Rat | Neuron | Depth | Class | Pinch | Brush | 1.4g vF | 4g vF | 10g vF | 26g vF |
|---|---|---|---|---|---|---|---|---|---|---|
| sham+ veh | 365 | 1 | 870 | LTM | 14 | 38 | 11 | 15 | 38 | 123 |
| | | 2_1 | 880 | WDR | 20 | 21 | 9 | 24 | 32 | 50 |
| | | 2_2 | 880 | WDR | 326 | 14 | 10 | 21 | 98 | 83 |
| | | 4 | 1050 | LTM | 20 | 36 | 20 | 26 | 38 | 112 |
| | | 5 | 950 | WDR | 9 | 28 | 26 | 26 | 31 | 21 |
| | | 6 | 950 | LTM | 15 | 25 | 10 | 13 | 14 | 78 |
| | | 7 | 790 | WDR | 37 | 25 | 20 | 21 | 30 | 89 |
| | | 8 | 630 | LTM | 21 | 26 | 16 | 13 | 23 | 63 |
| | | 9 | 650 | WDR | 36 | 13 | 27 | 97 | 130 | 124 |
| | 366 | 1 | 820 | WDR | 24 | 15 | 16 | 38 | 50 | 51 |
| | | 2 | 500 | WDR | 0 | 10 | 14 | 37 | 27 | 70 |
| | | 3 | 900 | WDR | 46 | 3 | 10 | 12 | 99 | 71 |
| | | 4 | 980 | WDR | 30 | 16 | 24 | 88 | 228 | 141 |
| | | 5 | 950 | LTM | 10 | 11 | 4 | 6 | 13 | 21 |
| | | 6 | 900 | LTM | 9 | 1 | 0 | 2 | 31 | 164 |
| | | 7 | 930 | WDR | 15 | 24 | 14 | 31 | 48 | 47 |
| | | 8 | 910 | LTM | 9 | 17 | 1 | 4 | 19 | 24 |
| | 367 | 1 | 840 | WDR | 252 | 34 | 18 | 93 | 168 | 211 |
| | | 3 | 300 | WDR | 10 | 18 | 9 | 10 | 28 | 81 |
| | | 5 | 830 | LTM | 33 | 22 | 1 | 2 | 6 | 38 |
| | | 6 | 860 | LTM | 16 | 10 | 5 | 7 | 65 | 75 |
| | | 7 | 900 | WDR | 119 | 0 | 0 | 35 | 180 | 221 |
| | | 8 | 700 | WDR | 10 | 26 | 27 | 61 | 40 | 41 |
| | 368 | 1 | 860 | WDR | 32 | 52 | 29 | 48 | 40 | 62 |
| | | 2 | 670 | WDR | 27 | 26 | 14 | 45 | 42 | 48 |
| | | 3 | 800 | WDR | 117 | 31 | 68 | 74 | 82 | 114 |
| | | 4 | 450 | LTM | 7 | 4 | 3 | 10 | 56 | 85 |
| | | 5 | 590 | WDR | 82 | 44 | 81 | 89 | 151 | 214 |
| | | 6 | 850 | LTM | 0 | 36 | 9 | 27 | 58 | 81 |
| | | 8 | 500 | WDR | 16 | 36 | 9 | 17 | 24 | 38 |
| | | 9 | 900 | WDR | 73 | 13 | 11 | 17 | 32 | 81 |
| | | 10 | 950 | WDR | 62 | 20 | 11 | 8 | 39 | 148 |
| | 370 | 1 | 560 | WDR | 126 | 29 | 118 | 237 | 256 | 230 |
| | | 2 | 700 | WDR | 49 | 19 | 29 | 86 | 61 | 63 |
| | | 3_1 | 900 | LTM | 3 | 10 | 4 | 9 | 34 | 70 |
| | | 3_2 | 900 | WDR | 61 | 25 | 17 | 40 | 54 | 88 |
| | | 4 | 980 | LTM | 24 | 31 | 23 | 27 | 70 | 107 |
| | | 5 | 780 | LTM | 31 | 26 | 7 | 6 | 36 | 77 |
| | | 6 | 750 | LTM | 23 | 9 | 0 | 6 | 9 | 22 |
| | | 8 | 760 | LTM | 6 | 10 | 8 | 13 | 15 | 18 |
| | | 9 | 700 | WDR | 15 | 4 | 8 | 31 | 138 | 178 |

**Table G.5. Spinal neuronal firing counts in rats at seven days following facet joint distraction and immediate intra-articular anti-NGF application (Chapter 5).**

| Group | Rat | Neuron | Depth | Class | Pinch | Brush | 1.4g vF | 4g vF | 10g vF | 26g vF |
|---|---|---|---|---|---|---|---|---|---|---|
| FJD+veh | 272 | 1 | 440 | WDR | 105 | 54 | 13 | 70 | 145 | 146 |
| | | 3 | 650 | WDR | 325 | 5 | 13 | 39 | 259 | 244 |
| | | 4 | 790 | WDR | 33 | 31 | 11 | 7 | 68 | 120 |
| | | 5 | 570 | WDR | 57 | 64 | 76 | 74 | 86 | 98 |
| | 274 | 1 | 500 | WDR | 251 | 89 | 39 | 104 | 192 | 159 |
| | | 2 | 620 | WDR | 61 | 35 | 8 | 12 | 49 | 111 |
| | | 3 | 560 | WDR | 135 | 129 | 98 | 180 | 237 | 169 |
| | | 4 | 360 | WDR | 350 | 44 | 39 | 156 | 139 | 145 |
| | | 5 | 440 | WDR | 64 | 41 | 55 | 61 | 92 | 160 |
| | | 6 | 530 | WDR | 72 | 81 | 14 | 23 | 78 | 155 |
| | | 7 | 310 | WDR | 195 | 34 | 72 | 322 | 419 | 381 |
| | | 8 | 70 | WDR | 35 | 3 | 12 | 57 | 94 | 68 |
| | 275 | 1_1 | 450 | WDR | 182 | 6 | 4 | 8 | 177 | 219 |
| | | 1_2 | 450 | WDR | 224 | 64 | 51 | 109 | 112 | 181 |
| | | 3 | 530 | WDR | 135 | 36 | 9 | 67 | 116 | 166 |
| | | 4 | 680 | WDR | 247 | 25 | 15 | 64 | 63 | 150 |
| | | 5 | 570 | WDR | 305 | 180 | 60 | 116 | 246 | 186 |
| | | 6 | 780 | WDR | 150 | 2 | 11 | 22 | 115 | 243 |
| | | 7_1 | 530 | WDR | 272 | 34 | 7 | 36 | 84 | 132 |
| | | 7_2 | 530 | WDR | 120 | 64 | 3 | 65 | 137 | 132 |
| | | 8 | 580 | WDR | 123 | 93 | 48 | 200 | 217 | 199 |
| | | 9 | 600 | WDR | 215 | 47 | 33 | 141 | 144 | 203 |
| | | 10 | 670 | WDR | 111 | 48 | 32 | 55 | 69 | 81 |
| | 276 | 1 | 480 | WDR | 193 | 28 | 42 | 119 | 153 | 156 |
| | | 2 | 590 | WDR | 119 | 75 | 9 | 26 | 70 | 175 |
| | | 3 | 530 | WDR | 127 | 14 | 21 | 102 | 111 | 87 |
| | | 4 | 680 | WDR | 55 | 89 | 20 | 40 | 69 | 95 |
| | | 5 | 450 | WDR | 128 | 108 | 20 | 42 | 182 | 210 |
| | | 7 | 580 | WDR | 80 | 37 | 21 | 37 | 90 | 77 |
| | | 8_1 | 490 | WDR | 151 | 42 | 19 | 34 | 71 | 116 |
| | | 8_2 | 490 | WDR | 63 | 10 | 12 | 39 | 64 | 52 |
| | | 9 | 640 | WDR | 69 | 33 | 10 | 67 | 85 | 85 |
| | 280 | 1 | 560 | WDR | 242 | 58 | 32 | 43 | 98 | 250 |
| | | 2_1 | 550 | WDR | 159 | 39 | 45 | 47 | 115 | 231 |
| | | 2_2 | 550 | WDR | 1 | 52 | 31 | 46 | 49 | 51 |
| | | 3 | 510 | WDR | 647 | 1 | 0 | 1 | 134 | 374 |
| | | 4 | 610 | WDR | 55 | 25 | 68 | 55 | 99 | 171 |
| | | 5 | 470 | WDR | 72 | 24 | 12 | 28 | 96 | 70 |
| | | 6_1 | 650 | WDR | 435 | 90 | 29 | 14 | 141 | 202 |
| | | 6_2 | 650 | WDR | 27 | 19 | 5 | 7 | 51 | 139 |
| | | 7 | 780 | WDR | 145 | 7 | 13 | 24 | 101 | 146 |
| | | 8 | 820 | WDR | 79 | 33 | 96 | 76 | 147 | 155 |

Note: Table continued on next page.

| Group | Rat | Neuron | Depth | Class | Pinch | Brush | 1.4g vF | 4g vF | 10g vF | 26g vF |
|---|---|---|---|---|---|---|---|---|---|---|
| FJD+ anti-NGF | 250 | 1 | 210 | LTM | 0 | 35 | 20 | 63 | 54 | 58 |
| | | 2 | 750 | WDR | 97 | 5 | 2 | 3 | 7 | 14 |
| | | 3 | 580 | WDR | 89 | 163 | 34 | 54 | 64 | 86 |
| | | 4 | 760 | WDR | 34 | 47 | 7 | 3 | 32 | 36 |
| | | 5 | 140 | LTM | 20 | 14 | 0 | 7 | 25 | 57 |
| | | 6 | 600 | WDR | 45 | 51 | 19 | 32 | 50 | 42 |
| | | 7 | 600 | WDR | 5 | 26 | 11 | 10 | 11 | 36 |
| | | 8 | 580 | WDR | 8 | 28 | 10 | 39 | 19 | 44 |
| | | 9 | 690 | WDR | 104 | 21 | 8 | 20 | 10 | 68 |
| | | 10 | 750 | WDR | 166 | 44 | 21 | 31 | 51 | 104 |
| | | 11 | 70 | WDR | 73 | 3 | 0 | 14 | 21 | 80 |
| | | 12 | 470 | WDR | 26 | 106 | 13 | 24 | 48 | 36 |
| | | 13 | 280 | WDR | 93 | 6 | 20 | 44 | 81 | 107 |
| | | 14 | 590 | LTM | 12 | 25 | 8 | 16 | 26 | 21 |
| | | 15 | 830 | WDR | 85 | 25 | 23 | 44 | 91 | 56 |
| | 251 | 1 | 640 | WDR | 90 | 41 | 8 | 7 | 11 | 27 |
| | | 2 | 710 | WDR | 51 | 38 | 20 | 35 | 65 | 53 |
| | | 3 | 850 | LTM | 21 | 19 | 5 | 10 | 20 | 36 |
| | | 4 | 550 | WDR | 69 | 18 | 14 | 20 | 27 | 36 |
| | | 5 | 820 | WDR | 24 | 19 | 9 | 16 | 15 | 49 |
| | 254 | 1 | 530 | WDR | 30 | 68 | 28 | 66 | 87 | 35 |
| | | 2 | 730 | WDR | 165 | 79 | 13 | 36 | 76 | 152 |
| | | 3 | 620 | WDR | 65 | 43 | 26 | 37 | 50 | 63 |
| | | 4 | 860 | WDR | 61 | 56 | 10 | 10 | 29 | 63 |
| | | 5 | 450 | WDR | 131 | 46 | 7 | 30 | 48 | 91 |
| | | 6 | 690 | WDR | 121 | 7 | 9 | 38 | 94 | 82 |
| | | 7 | 650 | WDR | 60 | 11 | 17 | 32 | 65 | 115 |
| | | 8 | 490 | WDR | 134 | 7 | 3 | 12 | 37 | 106 |
| | | 9 | 760 | WDR | 251 | 19 | 12 | 33 | 119 | 142 |
| | | 10 | 620 | WDR | 98 | 41 | 25 | 16 | 44 | 59 |
| | 277 | 1 | 670 | WDR | 38 | 12 | 3 | 12 | 12 | 62 |
| | | 2 | 560 | WDR | 186 | 73 | 31 | 129 | 100 | 97 |
| | | 3 | 610 | WDR | 14 | 15 | 11 | 1 | 39 | 55 |
| | | 4 | 480 | WDR | 425 | 43 | 37 | 177 | 123 | 246 |
| | | 5 | 300 | WDR | 97 | 14 | 16 | 79 | 88 | 113 |
| | | 6 | 60 | LTM | 11 | 9 | 0 | 36 | 156 | 255 |
| | | 7 | 710 | LTM | 0 | 30 | 125 | 170 | 142 | 154 |
| | | 8_1 | 530 | WDR | 342 | 52 | 56 | 78 | 142 | 272 |
| | | 8_2 | 530 | WDR | 6 | 14 | 15 | 29 | 18 | 31 |
| | | 9 | 590 | WDR | 76 | 16 | 8 | 29 | 91 | 118 |
| | | 10 | 450 | WDR | 44 | 23 | 2 | 18 | 44 | 50 |
| | | 11 | 400 | WDR | 58 | 14 | 54 | 47 | 50 | 52 |
| | 279 | 1_1 | 590 | WDR | 44 | 40 | 4 | 30 | 68 | 69 |
| | | 1_2 | 590 | WDR | 24 | 43 | 13 | 18 | 51 | 49 |
| | | 2_1 | 930 | WDR | 91 | 4 | 1 | 1 | 10 | 109 |
| | | 2_2 | 930 | WDR | 90 | 64 | 32 | 17 | 54 | 73 |
| | | 3 | 500 | WDR | 292 | 18 | 23 | 40 | 89 | 117 |
| | | 4 | 770 | WDR | 34 | 1 | 45 | 81 | 113 | 68 |
| | | 5 | 720 | WDR | 36 | 23 | 7 | 15 | 42 | 58 |
| | | 6 | 580 | WDR | 58 | 37 | 109 | 116 | 113 | 166 |
| | | 7 | 620 | WDR | 144 | 28 | 15 | 21 | 50 | 158 |
| | | 8 | 700 | WDR | 65 | 70 | 68 | 73 | 131 | 210 |
| | 340 | 1 | 630 | WDR | 103 | 89 | 6 | 11 | 18 | 54 |
| | | 2 | 530 | LTM | 10 | 91 | 11 | 13 | 25 | 23 |
| | | 3 | 660 | LTM | 19 | 11 | 5 | 6 | 20 | 122 |
| | | 4 | 640 | WDR | 94 | 46 | 9 | 11 | 80 | 101 |
| | | 5 | 500 | WDR | 16 | 34 | 4 | 16 | 67 | 97 |
| | | 6 | 660 | LTM | 30 | 25 | 14 | 50 | 69 | 48 |
| | | 7 | 570 | WDR | 146 | 69 | 29 | 52 | 131 | 109 |
| | | 8 | 660 | LTM | 49 | 51 | 9 | 8 | 116 | 166 |
| | | 9 | 610 | LTM | 8 | 15 | 11 | 9 | 71 | 71 |
| | | 10 | 700 | WDR | 94 | 57 | 32 | 26 | 79 | 135 |
| | | 11_1 | 250 | WDR | 18 | 4 | 7 | 45 | 93 | 174 |
| | | 11_2 | 250 | WDR | 0 | 29 | 0 | 27 | 19 | 21 |
| | | 12 | 700 | WDR | 183 | 27 | 16 | 30 | 58 | 86 |

Note: Table continued on next page.

| Group | Rat | Neuron | Depth | Class | Pinch | Brush | 1.4g vF | 4g vF | 10g vF | 26g vF |
|---|---|---|---|---|---|---|---|---|---|---|
| sham+ veh | 283 | 1 | 500 | WDR | 124 | 29 | 7 | 22 | 74 | 98 |
| | | 2 | 610 | WDR | 125 | 15 | 1 | 3 | 32 | 118 |
| | | 3 | 800 | WDR | 86 | 26 | 39 | 75 | 102 | 85 |
| | | 4 | 520 | WDR | 78 | 2 | 51 | 49 | 60 | 59 |
| | | 5 | 450 | WDR | 231 | 34 | 72 | 118 | 173 | 198 |
| | | 6 | 310 | LTM | 21 | 0 | 5 | 21 | 83 | 119 |
| | | 7 | 480 | WDR | 33 | 16 | 1 | 42 | 34 | 41 |
| | 284 | 1 | 620 | WDR | 32 | 38 | 51 | 97 | 83 | 98 |
| | | 2 | 620 | WDR | 118 | 32 | 24 | 59 | 88 | 101 |
| | | 3 | 910 | WDR | 74 | 18 | 3 | 10 | 32 | 61 |
| | | 4 | 780 | WDR | 18 | 10 | 11 | 19 | 56 | 78 |
| | | 5 | 760 | LTM | 64 | 5 | 2 | 2 | 19 | 69 |
| | | 6 | 240 | LTM | 34 | 2 | 1 | 41 | 78 | 73 |
| | | 7 | 750 | WDR | 146 | 86 | 20 | 54 | 215 | 227 |
| | | 8 | 770 | WDR | 84 | 37 | 20 | 35 | 83 | 116 |
| | 285 | 1 | 670 | WDR | 26 | 21 | 12 | 10 | 62 | 102 |
| | | 2 | 630 | WDR | 50 | 24 | 9 | 19 | 40 | 100 |
| | | 3 | 750 | WDR | 27 | 42 | 1 | 6 | 24 | 57 |
| | | 4 | 640 | WDR | 56 | 24 | 21 | 43 | 66 | 73 |
| | | 5 | 700 | WDR | 149 | 20 | 13 | 23 | 49 | 70 |
| | 286 | 1 | 720 | WDR | 103 | 15 | 63 | 131 | 149 | 178 |
| | | 2 | 700 | WDR | 104 | 19 | 23 | 28 | 137 | 162 |
| | | 3 | 820 | WDR | 116 | 58 | 61 | 183 | 123 | 224 |
| | | 4 | 880 | WDR | 41 | 71 | 29 | 48 | 51 | 57 |
| | | 5 | 790 | WDR | 195 | 49 | 43 | 61 | 141 | 238 |
| | | 7 | 610 | WDR | 62 | 9 | 6 | 8 | 18 | 57 |
| | | 8 | 600 | WDR | 62 | 20 | 11 | 17 | 27 | 100 |
| | 287 | 1 | 730 | WDR | 38 | 18 | 10 | 20 | 40 | 55 |
| | | 2 | 230 | LTM | 40 | 0 | 0 | 0 | 134 | 163 |
| | | 3 | 910 | LTM | 39 | 38 | 2 | 11 | 72 | 123 |
| | | 4 | 590 | WDR | 24 | 49 | 15 | 19 | 43 | 62 |
| | | 5 | 580 | WDR | 12 | 26 | 7 | 14 | 50 | 99 |
| | | 6 | 840 | LTM | 16 | 25 | 20 | 33 | 52 | 74 |
| | | 7 | 550 | WDR | 133 | 40 | 25 | 45 | 108 | 167 |
| | | 8 | 870 | WDR | 45 | 8 | 4 | 8 | 31 | 137 |
| | | 9 | 820 | LTM | 21 | 25 | 19 | 59 | 42 | 36 |
| | | 10 | 950 | WDR | 91 | 6 | 4 | 26 | 165 | 70 |

Note: Table continued on next page.

| Group | Rat | Neuron | Depth | Class | Pinch | Brush | 1.4g vF | 4g vF | 10g vF | 26g vF |
|---|---|---|---|---|---|---|---|---|---|---|
| sham+ anti-NGF | 335 | 1 | 850 | WDR | 14 | 41 | 20 | 34 | 32 | 37 |
| | | 2 | 690 | WDR | 23 | 2 | 3 | 3 | 9 | 61 |
| | | 3 | 900 | WDR | 40 | 22 | 27 | 27 | 110 | 166 |
| | | 4 | 750 | WDR | 55 | 177 | 8 | 37 | 116 | 293 |
| | | 5 | 680 | LTM | 26 | 42 | 21 | 73 | 149 | 155 |
| | | 6 | 330 | LTM | 10 | 6 | 3 | 128 | 105 | 104 |
| | | 7 | 880 | WDR | 48 | 108 | 5 | 51 | 84 | 169 |
| | | 8 | 830 | WDR | 26 | 5 | 30 | 69 | 82 | 66 |
| | | 9 | 960 | LTM | 49 | 40 | 10 | 15 | 46 | 97 |
| | 336 | 1 | 630 | WDR | 103 | 4 | 17 | 105 | 177 | 195 |
| | | 2_1 | 900 | WDR | 20 | 7 | 29 | 73 | 88 | 57 |
| | | 2_2 | 900 | WDR | 6 | 55 | 18 | 31 | 22 | 23 |
| | | 3 | 740 | WDR | 62 | 34 | 38 | 87 | 109 | 128 |
| | | 4 | 830 | LTM | 4 | 6 | 31 | 111 | 87 | 47 |
| | | 5 | 640 | WDR | 31 | 20 | 23 | 110 | 141 | 207 |
| | | 6 | 920 | WDR | 81 | 37 | 3 | 26 | 156 | 161 |
| | | 7 | 720 | WDR | 17 | 18 | 45 | 25 | 20 | 19 |
| | | 8 | 960 | LTM | 4 | 70 | 34 | 21 | 33 | 22 |
| | | 9 | 590 | WDR | 97 | 1 | 3 | 12 | 174 | 203 |
| | 337 | 1 | 630 | WDR | 44 | 25 | 52 | 29 | 73 | 91 |
| | | 2 | 750 | WDR | 115 | 10 | 15 | 25 | 86 | 126 |
| | | 4 | 740 | WDR | 27 | 22 | 0 | 3 | 24 | 59 |
| | | 5_1 | 870 | LTM | 6 | 24 | 10 | 11 | 16 | 44 |
| | | 5_2 | 870 | WDR | 27 | 16 | 20 | 15 | 10 | 65 |
| | | 6 | 600 | WDR | 99 | 8 | 2 | 13 | 29 | 75 |
| | 338 | 1 | 240 | WDR | 1 | 6 | 8 | 6 | 13 | 38 |
| | | 2 | 820 | LTM | 34 | 25 | 18 | 20 | 33 | 55 |
| | | 3 | 460 | LTM | 37 | 28 | 27 | 44 | 78 | 115 |
| | | 4_1 | 700 | WDR | 31 | 0 | 0 | 1 | 12 | 9 |
| | | 5_2 | 700 | WDR | 98 | 56 | 39 | 97 | 81 | 99 |
| | | 6_1 | 570 | WDR | 92 | 4 | 19 | 29 | 69 | 119 |
| | | 6_2 | 570 | WDR | 65 | 31 | 63 | 60 | 71 | 68 |
| | 339 | 2 | 360 | LTM | 13 | 52 | 25 | 18 | 74 | 137 |
| | | 3_1 | 750 | LTM | 20 | 37 | 21 | 22 | 36 | 49 |
| | | 3_2 | 750 | WDR | 5 | 4 | 10 | 7 | 19 | 7 |
| | | 4 | 490 | WDR | 52 | 20 | 40 | 79 | 79 | 75 |
| | | 5 | 550 | WDR | 69 | 28 | 33 | 41 | 56 | 45 |
| | | 6 | 780 | LTM | 45 | 87 | 21 | 36 | 65 | 119 |
| | | 7 | 470 | WDR | 25 | 14 | 16 | 16 | 33 | 38 |
| | | 8_1 | 310 | WDR | 18 | 1 | 7 | 9 | 10 | 48 |
| | | 8_2 | 310 | WDR | 80 | 46 | 24 | 16 | 41 | 25 |
| | | 9 | 600 | WDR | 84 | 38 | 3 | 9 | 30 | 92 |

**Table G.6. Spinal neuronal firing counts in rats at seven days following facet joint distraction with intra-articular anti-NGF application on day one (Chapter 5).**

| Group | Rat | Neuron | Depth | Class | Pinch | Brush | 1.4g vF | 4g vF | 10g vF | 26g vF |
|---|---|---|---|---|---|---|---|---|---|---|
| FJD+ anti-NGFD1 | 345 | 1 | 780 | LTM | 44 | 45 | 10 | 34 | 93 | 111 |
| | | 2 | 760 | WDR | 35 | 110 | 36 | 75 | 280 | 192 |
| | | 3 | 720 | WDR | 17 | 73 | 28 | 51 | 78 | 74 |
| | | 4 | 930 | LTM | 76 | 5 | 1 | 1 | 0 | 232 |
| | 347 | 1 | 680 | LTM | 14 | 1 | 1 | 45 | 70 | 84 |
| | | 2 | 550 | WDR | 98 | 55 | 37 | 116 | 145 | 241 |
| | | 3_1 | 720 | WDR | 10 | 0 | 0 | 1 | 11 | 45 |
| | | 3_2 | 720 | WDR | 42 | 18 | 14 | 13 | 152 | 281 |
| | | 4 | 850 | WDR | 162 | 61 | 49 | 47 | 203 | 193 |
| | | 5 | 570 | WDR | 225 | 17 | 20 | 51 | 142 | 174 |
| | | 6 | 290 | LTM | 9 | 0 | 1 | 18 | 131 | 172 |
| | | 7 | 610 | WDR | 32 | 31 | 11 | 10 | 45 | 47 |
| | | 8 | 690 | LTM | 47 | 1 | 2 | 3 | 11 | 90 |
| | 359 | 2 | 840 | WDR | 8 | 24 | 42 | 70 | 64 | 89 |
| | | 3 | 610 | LTM | 17 | 15 | 4 | 21 | 23 | 32 |
| | | 4 | 700 | WDR | 37 | 49 | 16 | 120 | 213 | 178 |
| | | 5 | 550 | WDR | 142 | 75 | 120 | 189 | 240 | 178 |
| | | 6 | 810 | WDR | 138 | 74 | 96 | 174 | 352 | 450 |
| | | 7 | 750 | WDR | 59 | 87 | 29 | 28 | 106 | 242 |
| | | 8 | 930 | WDR | 195 | 45 | 37 | 52 | 85 | 244 |
| | 360 | 1 | 420 | WDR | 23 | 42 | 0 | 1 | 28 | 34 |
| | | 2 | 900 | LTM | 9 | 1 | 0 | 1 | 5 | 58 |
| | | 3 | 300 | WDR | 35 | 58 | 18 | 32 | 32 | 102 |
| | | 4 | 970 | WDR | 10 | 33 | 37 | 26 | 60 | 52 |
| | | 5 | 650 | LTM | 31 | 55 | 1 | 15 | 51 | 80 |
| | 361 | 1 | 280 | WDR | 33 | 8 | 52 | 100 | 75 | 120 |
| | | 2 | 600 | WDR | 79 | 74 | 29 | 86 | 125 | 130 |
| | | 3 | 810 | WDR | 43 | 23 | 24 | 26 | 136 | 190 |
| | | 4 | 820 | WDR | 58 | 31 | 145 | 193 | 240 | 275 |
| | | 5 | 570 | WDR | 185 | 4 | 1 | 12 | 293 | 325 |
| | | 6 | 950 | WDR | 79 | 37 | 47 | 103 | 86 | 144 |
| | | 7 | 820 | WDR | 48 | 70 | 35 | 133 | 143 | 278 |
| | | 8 | 720 | WDR | 13 | 32 | 9 | 10 | 75 | 107 |
| | | 9 | 620 | LTM | 18 | 15 | 2 | 14 | 71 | 136 |
| | | 10 | 800 | WDR | 37 | 54 | 24 | 46 | 60 | 129 |
| | 362 | 1 | 710 | WDR | 19 | 22 | 52 | 58 | 73 | 114 |
| | | 2 | 880 | LTM | 57 | 8 | 23 | 25 | 40 | 82 |
| | | 3 | 740 | WDR | 0 | 52 | 61 | 120 | 176 | 120 |
| | | 4 | 740 | WDR | 39 | 60 | 51 | 79 | 107 | 107 |
| | | 5 | 800 | WDR | 28 | 4 | 16 | 36 | 67 | 40 |
| | | 6 | 250 | LTM | 12 | 15 | 11 | 28 | 60 | 58 |
| | | 7 | 770 | WDR | 89 | 28 | 154 | 173 | 110 | 100 |
| | | 8 | 770 | WDR | 109 | 37 | 8 | 26 | 103 | 81 |
| | | 9 | 1000 | WDR | 93 | 45 | 41 | 67 | 170 | 178 |
| | | 10 | 930 | WDR | 54 | 27 | 13 | 36 | 85 | 151 |
| | | 11 | 950 | LTM | 10 | 3 | 26 | 93 | 105 | 124 |
| | 363 | 1 | 870 | WDR | 111 | 57 | 107 | 153 | 169 | 171 |
| | | 2 | 610 | WDR | 51 | 32 | 49 | 74 | 118 | 101 |
| | | 3 | 830 | WDR | 109 | 20 | 16 | 74 | 103 | 203 |
| | | 4 | 760 | WDR | 16 | 11 | 21 | 49 | 57 | 36 |
| | | 5 | 500 | LTM | 15 | 36 | 33 | 75 | 106 | 115 |
| | | 6 | 690 | LTM | 14 | 13 | 5 | 9 | 51 | 80 |
| | | 7 | 960 | WDR | 26 | 4 | 15 | 32 | 153 | 153 |
| | | 8 | 890 | WDR | 168 | 16 | 21 | 59 | 96 | 180 |
| | | 9 | 860 | WDR | 14 | 116 | 35 | 58 | 67 | 69 |
| | | 10 | 940 | LTM | 29 | 83 | 41 | 69 | 139 | 215 |
| | 364 | 1 | 980 | WDR | 57 | 34 | 22 | 52 | 136 | 159 |
| | | 2 | 680 | WDR | 97 | 47 | 66 | 72 | 137 | 112 |
| | | 3 | 60 | LTM | 14 | 116 | 27 | 51 | 73 | 83 |
| | | 4 | 850 | WDR | 66 | 59 | 13 | 47 | 83 | 100 |
| | | 5 | 870 | WDR | 38 | 22 | 23 | 58 | 79 | 105 |

**Table G.7. Thalamic neuronal firing counts in rats at seven days following facet joint distraction (Chapter 7).**

| Group | Rat | Neuron | Lateral (mm) | Distance from Bregma (mm) | Depth (µm) | Class | Pinch | Brush | 1.4g vF | 4g vF | 10g vF | 26g vF |
|---|---|---|---|---|---|---|---|---|---|---|---|---|
| FJD | PSP1 | 1 | 3.4 | -2.5 | 6780 | LTM | 269 | 386 | 133 | 217 | 186 | 209 |
| | | 2 | 3.6 | -2.5 | 6100 | LTM | 76 | 99 | 21 | 77 | 78 | 95 |
| | | 3 | 2.4 | -3.1 | 7000 | LTM | 66 | 161 | 78 | 75 | 90 | 117 |
| | PSP5 | 1 | 2.0 | -2.5 | 6000 | WDR | 76 | 102 | 44 | 73 | 130 | 175 |
| | | 3 | 2.2 | -3.1 | 6650 | LTM | 24 | 74 | 45 | 93 | 95 | 129 |
| | | 4 | 2.4 | -3.1 | 6900 | LTM | 54 | 163 | 61 | 92 | 97 | 111 |
| | | 5 | 2.6 | -3.1 | 6400 | WDR | 109 | 218 | 23 | 70 | 190 | 162 |
| | PSP7 | 1 | 3.6 | -3.3 | 6550 | LTM | 94 | 137 | 22 | 93 | 111 | 144 |
| | | 10_1 | 2.4 | -3.5 | 6750 | WDR | 113 | 97 | 15 | 48 | 83 | 168 |
| | | 11 | 2.6 | -3.5 | 5950 | LTM | 125 | 68 | 96 | 49 | 82 | 174 |
| | | 12 | 2.6 | -3.5 | 6400 | WDR | 26 | 91 | 1 | 82 | 121 | 163 |
| | | 14 | 2.8 | -3.5 | 6550 | LTM | 61 | 86 | 3 | 147 | 128 | 126 |
| | | 16 | 2.8 | -3.7 | 6275 | LTM | 31 | 126 | 0 | 100 | 115 | 118 |
| | | 17 | 2.8 | -3.7 | 6275 | WDR | 110 | 159 | 108 | 157 | 224 | 264 |
| | | 18 | 2.6 | -3.7 | 6200 | WDR | 66 | 161 | 14 | 36 | 90 | 117 |
| | | 19 | 2.6 | -3.7 | 6650 | WDR | 44 | 52 | 30 | 45 | 70 | 113 |
| | PSP11 | 1 | 2.0 | -3.1 | 6450 | LTM | 189 | 391 | 68 | 222 | 179 | 316 |
| | | 9 | 2.4 | -3.4 | 6550 | WDR | 136 | 275 | 45 | 95 | 212 | 241 |
| | | 11 | 2.6 | -3.5 | 5850 | WDR | 96 | 173 | 68 | 78 | 128 | 203 |
| | | 12 | 2.6 | -3.5 | 6700 | WDR | 209 | 101 | 71 | 158 | 391 | 392 |
| | | 13 | 2.4 | -3.5 | 5900 | WDR | 63 | 108 | 47 | 56 | 151 | 143 |
| | | 14 | 2.2 | -3.5 | 6400 | LTM | 86 | 187 | 13 | 98 | 109 | 144 |
| | | 15 | 2.2 | -3.5 | 6950 | WDR | 75 | 69 | 43 | 62 | 125 | 107 |
| | | 17 | 2.0 | -3.5 | 6400 | WDR | 234 | 97 | 32 | 72 | 129 | 173 |

Note: Table continued on next page. The naming scheme for these rats refers to the fact that they were generated for electrophysiological recordings that were performed by Parul S. Pall.

| Group | Rat | Neuron | Lateral (mm) | Distance from Bregma (mm) | Depth (µm) | Class | Pinch | Brush | 1.4g vF | 4g vF | 10g vF | 26g vF |
|---|---|---|---|---|---|---|---|---|---|---|---|---|
| sham | PSP4 | 3 | 3.8 | -3.1 | 5725 | LTM | 61 | 43 | 0 | 48 | 41 | 71 |
| | | 4 | 3.8 | -3.1 | 6350 | WDR | 33 | 2 | 12 | 0 | 5 | 28 |
| | | 6 | 3.4 | -3.1 | 7100 | LTM | 41 | 15 | 37 | 0 | 0 | 25 |
| | | 7 | 3.2 | -3.1 | 6340 | WDR | 22 | 30 | 0 | 9 | 18 | 59 |
| | | 8 | 3.2 | -3.1 | 6150 | WDR | 16 | 2 | 5 | 1 | 17 | 35 |
| | | 10 | 3.0 | -3.1 | 5750 | WDR | 65 | 30 | 0 | 10 | 39 | 100 |
| | | 11 | 3.0 | -3.1 | 6350 | LTM | 34 | 43 | 24 | 32 | 46 | 24 |
| | | 12 | 3.0 | -3.1 | 6800 | LTM | 11 | 31 | 24 | 25 | 28 | 27 |
| | | 13 | 2.8 | -3.1 | 6100 | LTM | 35 | 53 | 20 | 39 | 1 | 1 |
| | | 14 | 3.6 | -3.3 | 6200 | LTM | 32 | 184 | 70 | 95 | 80 | 89 |
| | | 15 | 3.2 | -3.3 | 7050 | WDR | 12 | 106 | 9 | 60 | 68 | 131 |
| | | 16 | 3.0 | -3.3 | 6800 | WDR | 17 | 36 | 6 | 11 | 13 | 17 |
| | PSP8 | 1 | 3.2 | -3.1 | 6050 | WDR | 63 | 133 | 3 | 24 | 61 | 100 |
| | | 2 | 3.2 | -3.1 | 6100 | WDR | 26 | 75 | 25 | 27 | 29 | 56 |
| | | 3 | 3.2 | -3.1 | 6250 | LTM | 14 | 45 | 32 | 31 | 39 | 41 |
| | | 4 | 3.2 | -3.1 | 6300 | WDR | 26 | 58 | 9 | 23 | 49 | 52 |
| | | 5 | 3.4 | -3.1 | 5800 | WDR | 27 | 32 | 10 | 13 | 37 | 36 |
| | | 8 | 3.4 | -3.3 | 6200 | WDR | 15 | 74 | 9 | 3 | 25 | 53 |
| | | 11_1 | 3.2 | -3.3 | 6100 | WDR | 14 | 7 | 34 | 43 | 70 | 84 |
| | | 12 | 3.2 | -3.3 | 6250 | LTM | 103 | 46 | 65 | 128 | 107 | 150 |
| | | 14 | 3.0 | -3.3 | 6350 | LTM | 16 | 37 | 31 | 34 | 38 | 59 |
| | | 15 | 3.0 | -3.3 | 6600 | WDR | 67 | 87 | 70 | 111 | 166 | 187 |
| | | 16 | 3.0 | -3.5 | 6500 | WDR | 14 | 51 | 5 | 24 | 46 | 68 |
| | | 17 | 3.0 | -3.5 | 6400 | WDR | 31 | 179 | 30 | 41 | 49 | 76 |
| | | 19 | 3.2 | -3.5 | 6350 | WDR | 9 | 45 | 8 | 13 | 18 | 30 |
| | | 20 | 3.2 | -3.5 | 6500 | LTM | 3 | 27 | 15 | 10 | 15 | 11 |
| | PSP12 | 1_1 | 2.2 | -3.5 | 6000 | WDR | 12 | 29 | 1 | 3 | 15 | 47 |
| | | 2 | 2.2 | -3.5 | 6500 | WDR | 78 | 22 | 7 | 4 | 57 | 135 |
| | | 3 | 2.4 | -3.5 | 6450 | WDR | 17 | 55 | 0 | 10 | 27 | 33 |
| | | 4 | 2.4 | -3.5 | 6625 | LTM | 49 | 123 | 105 | 107 | 57 | 84 |
| | | 5 | 2.4 | -3.3 | 6675 | LTM | 23 | 162 | 29 | 57 | 69 | 52 |
| | | 7 | 2.5 | -3.5 | 6750 | WDR | 47 | 35 | 1 | 15 | 49 | 71 |
| | | 8 | 2.6 | -3.5 | 6550 | WDR | 21 | 37 | 10 | 21 | 67 | 64 |
| | | 9 | 2.7 | -3.5 | 6350 | WDR | 10 | 89 | 11 | 21 | 37 | 54 |
| | | 14 | 2.5 | -3.6 | 6800 | LTM | 25 | 65 | 14 | 37 | 41 | 44 |

**Table G.8. Thalamic neuronal firing counts in rats following facet joint distraction for seven days with IB4-saporin pretreatment (Chapter 7).**

| Group | Rat | Neuron | Lateral (mm) | Distance from Bregma (mm) | Depth (µm) | Class | Pinch | Brush | 1.4g vF | 4g vF | 10g vF | 26g vF |
|---|---|---|---|---|---|---|---|---|---|---|---|---|
| IB4-Sap+ FJD | F240 | 1_1 | 2.2 | -3.5 | 6100 | WDR | 9 | 21 | 6 | 9 | 19 | 37 |
| | | 2 | 2.0 | -3.5 | 6375 | WDR | 117 | 35 | 0 | 7 | 146 | 180 |
| | | 3 | 2.4 | -3.5 | 6350 | LTM | 33 | 142 | 40 | 50 | 60 | 34 |
| | | 4 | 2.3 | -3.5 | 6325 | WDR | 141 | 21 | 19 | 62 | 109 | 130 |
| | | 5 | 2.0 | -3.6 | 6475 | WDR | 100 | 54 | 9 | 52 | 70 | 93 |
| | | 6 | 2.2 | -3.6 | 6540 | WDR | 39 | 52 | 23 | 40 | 44 | 86 |
| | | 7 | 2.2 | -3.6 | 6675 | LTM | 58 | 80 | 48 | 35 | 68 | 81 |
| | F241 | 1 | 2.0 | -3.5 | 6325 | WDR | 41 | 45 | 10 | 32 | 69 | 98 |
| | F242 | 1_1 | 2.0 | -3.1 | 5900 | LTM | 0 | 15 | 0 | 8 | 3 | 3 |
| | | 2 | 2.0 | -3.3 | 6250 | LTM | 4 | 11 | 8 | 38 | 58 | 43 |
| | | 3 | 2.2 | -3.3 | 5500 | WDR | 58 | 6 | 1 | 8 | 13 | 43 |
| | | 5 | 2.4 | -3.3 | 5400 | LTM | 46 | 43 | 42 | 23 | 33 | 49 |
| | | 6 | 2.6 | -3.3 | 6200 | WDR | 46 | 17 | 20 | 45 | 59 | 106 |
| | | 7 | 2.8 | -3.3 | 5350 | WDR | 19 | 14 | 10 | 37 | 70 | 32 |
| | | 8 | 2.0 | -3.0 | 6150 | LTM | 46 | 48 | 25 | 122 | 134 | 179 |
| | F246 | 1 | 3.4 | -3.5 | 6000 | WDR | 38 | 53 | 4 | 7 | 56 | 98 |
| | | 3 | 3.4 | -3.7 | 6650 | WDR | 81 | 33 | 1 | 33 | 64 | 122 |
| | | 4 | 3.3 | -3.7 | 6450 | WDR | 37 | 25 | 11 | 34 | 43 | 69 |
| | | 5 | 3.1 | -3.7 | 6050 | WDR | 43 | 79 | 26 | 38 | 97 | 138 |
| | | 6 | 2.9 | -3.7 | 6450 | WDR | 8 | 20 | 0 | 1 | 59 | 67 |
| | | 7 | 2.7 | -3.7 | 7000 | WDR | 27 | 28 | 22 | 28 | 71 | 195 |
| | | 8 | 2.5 | -3.7 | 6820 | WDR | 23 | 25 | 12 | 23 | 23 | 35 |
| | F249 | 2 | 3.2 | -3.5 | 6630 | WDR | 33 | 69 | 16 | 15 | 56 | 114 |
| | | 3 | 3.4 | -3.5 | 6500 | WDR | 21 | 55 | 26 | 45 | 104 | 103 |
| | | 4 | 3.4 | -3.5 | 6650 | WDR | 57 | 100 | 31 | 48 | 82 | 97 |
| | | 5 | 3.4 | -3.7 | 6250 | LTM | 26 | 34 | 29 | 37 | 32 | 54 |
| | | 6 | 3.4 | -3.7 | 6150 | WDR | 42 | 55 | 17 | 28 | 57 | 75 |
| | | 7_1 | 3.2 | -3.7 | 6500 | WDR | 75 | 99 | 19 | 71 | 105 | 171 |
| | | 8 | 3.2 | -3.7 | 6650 | WDR | 60 | 50 | 22 | 64 | 88 | 135 |
| | | 9 | 3.0 | -3.7 | 6250 | WDR | 30 | 7 | 1 | 5 | 57 | 114 |
| | | 10 | 3.2 | -3.8 | 6450 | LTM | 71 | 52 | 53 | 61 | 119 | 102 |
| | F251 | 1 | 2.2 | -3.3 | 6200 | WDR | 20 | 24 | 1 | 15 | 140 | 129 |
| | | 2 | 2.4 | -3.3 | 6250 | WDR | 4 | 27 | 14 | 24 | 44 | 50 |

Note: Table continued on next page. All surgical procedures for these rats were performed by Christine L. Weisshaar, and the naming scheme reflects her records.

| Group | Rat | Neuron | Lateral (mm) | Distance from Bregma (mm) | Depth (µm) | Class | Pinch | Brush | 1.4g vF | 4g vF | 10g vF | 26g vF |
|---|---|---|---|---|---|---|---|---|---|---|---|---|
| IB4-Sap+ sham | F244 | 2 | 2.0 | -3.1 | 6650 | WDR | 61 | 81 | 21 | 83 | 171 | 230 |
| | | 3 | 2.2 | -3.1 | 5500 | LTM | 4 | 8 | 4 | 0 | 3 | 8 |
| | | 4 | 2.2 | -3.1 | 5600 | WDR | 10 | 53 | 13 | 60 | 124 | 160 |
| | | 5 | 2.4 | -3.1 | 5550 | WDR | 0 | 27 | 3 | 33 | 65 | 90 |
| | | 6 | 2.6 | -3.1 | 5425 | WDR | 28 | 32 | 8 | 0 | 26 | 24 |
| | | 8 | 2.4 | -3.0 | 5150 | WDR | 133 | 57 | 41 | 58 | 127 | 159 |
| | | 9 | 2.2 | -3.0 | 5200 | WDR | 33 | 24 | 10 | 28 | 48 | 61 |
| | | 10 | 2.0 | -3.0 | 5950 | WDR | 29 | 1 | 0 | 16 | 24 | 41 |
| | F247 | 1 | 2.0 | -3.1 | 6200 | LTM | 29 | 18 | 21 | 22 | 30 | 31 |
| | | 2 | 2.2 | -3.1 | 6000 | WDR | 235 | 184 | 27 | 95 | 129 | 215 |
| | | 3 | 2.4 | -3.1 | 6300 | WDR | 32 | 25 | 2 | 4 | 41 | 86 |
| | | 6 | 2.3 | -3.3 | 6235 | WDR | 5 | 13 | 8 | 21 | 59 | 133 |
| | | 7 | 2.3 | -3.4 | 6300 | WDR | 45 | 20 | 9 | 21 | 46 | 54 |
| | | 8 | 2.3 | -3.4 | 6500 | WDR | 16 | 50 | 52 | 129 | 168 | 182 |
| | | 10 | 2.1 | -3.4 | 6250 | WDR | 150 | 54 | 9 | 28 | 102 | 166 |
| | | 11 | 2.1 | -3.4 | 6350 | WDR | 87 | 124 | 0 | 4 | 132 | 135 |
| | | 12 | 2.0 | -3.5 | 6650 | LTM | 24 | 61 | 13 | 55 | 69 | 75 |
| | F250 | 1 | 2.4 | -3.0 | 6200 | WDR | 118 | 36 | 5 | 12 | 38 | 144 |
| | | 2 | 2.6 | -3.0 | 6650 | WDR | 27 | 21 | 0 | 0 | 16 | 85 |
| | | 3 | 2.8 | -3.0 | 5650 | WDR | 45 | 73 | 32 | 42 | 53 | 119 |
| | | 4 | 2.8 | -3.0 | 6250 | WDR | 32 | 169 | 5 | 19 | 41 | 34 |
| | F252 | 1 | 3.0 | -3.0 | 6700 | LTM | 26 | 54 | 20 | 15 | 22 | 36 |
| | | 2 | 3.2 | -3.0 | 6300 | WDR | 20 | 64 | 20 | 24 | 33 | 50 |
| | | 3 | 3.4 | -3.0 | 6550 | WDR | 86 | 132 | 41 | 60 | 94 | 134 |
| | | 4 | 3.6 | -3.0 | 6850 | WDR | 49 | 74 | 34 | 52 | 68 | 80 |
| | | 5 | 3.0 | -2.8 | 6350 | WDR | 103 | 60 | 11 | 51 | 87 | 113 |
| | | 6 | 2.8 | -2.8 | 6200 | LTM | 47 | 52 | 2 | 20 | 17 | 40 |
| | | 7 | 2.8 | -2.8 | 6850 | WDR | 51 | 33 | 74 | 140 | 190 | 252 |
| | | 8 | 3.2 | -2.8 | 6400 | WDR | 19 | 5 | 0 | 4 | 11 | 43 |
| | | 9 | 2.6 | -2.8 | 6200 | WDR | 107 | 105 | 21 | 77 | 114 | 186 |
| | F253 | 1 | 2.6 | -3.0 | 6200 | LTM | 58 | 74 | 56 | 76 | 117 | 102 |
| | | 3 | 2.8 | -3.1 | 6750 | WDR | 25 | 22 | 0 | 22 | 22 | 48 |
| | | 4 | 2.6 | -3.1 | 6800 | WDR | 88 | 185 | 51 | 115 | 167 | 172 |
| | | 6 | 2.3 | -3.1 | 6450 | WDR | 95 | 76 | 15 | 39 | 82 | 147 |
| | | 7 | 2.3 | -3.3 | 7200 | LTM | 32 | 46 | 2 | 45 | 58 | 40 |
| | | 9 | 2.8 | -3.3 | 6400 | WDR | 15 | 11 | 6 | 10 | 17 | 25 |
| | | 10 | 2.8 | -2.9 | 6200 | WDR | 172 | 1 | 2 | 3 | 155 | 368 |
| | | 11 | 2.6 | -2.9 | 6000 | WDR | 67 | 20 | 4 | 12 | 32 | 83 |
| | | 12_1 | 2.4 | -2.9 | 6300 | WDR | 28 | 31 | 7 | 14 | 40 | 67 |
| | | 13 | 2.2 | -2.9 | 6050 | WDR | 210 | 119 | 46 | 46 | 112 | 218 |
| | | 14 | 2.2 | -2.9 | 6750 | LTM | 6 | 15 | 8 | 26 | 16 | 22 |

# Appendix H

# Identification of C6/C7 Facet Joint Afferents and Calcitonin Gene-Related Peptide Expression in the DRG Using Immunohistochemistry

This appendix summarizes the characterization of afferents that innervate the right C6/C7 facet joint for the studies presented in Chapter 4. Each tissue section throughout the entire dorsal root ganglion (DRG) for each spinal level from C5 to C8 was analyzed visually to identify afferents labeled positively for cholera toxin subunit b (CTb) at day seven after facet joint distraction (FJD) or sham procedures; normal tissues were also included. CTb was injected into the joint three days prior to FJD or sham procedures, so tissues harvested at day seven post-injury correspond to day ten after the CTb injection. For further details on the labeling technique, see Section 4.3.1 in Chapter 4. The total number of CTb-positive neurons was summed for each rat at each DRG level. Each DRG image was digitally stored with a generalized file name of CTb_Rat#_SpinalLevel_ Slide#_Section#_ExposureTime_20x.tif. For all sections from a given spinal level in each individual rat, the exposure time was standardized. However, due to the large number of sections that were labeled and analyzed, immunolabeling experiments were separately undertaken for each spinal level of each individual rat. As such, the exposure times vary between rats and spinal levels. On each slide, sections were numbered beginning in the top left corner and proceeding in numerical order from top to bottom, then resuming at

the top of the adjacent column to the right. Throughout this appendix, the FJD group refers to rats for which the C6 forceps was displaced by 2.5mm as recorded by the linear variable differential transducer (LVDT); the sham group underwent the same surgical procedure with no applied distraction (Kras et al., 2013c).

In order to identify the joint afferents as peptidergic, all tissue sections also were immunolabeled for the neuropeptide calcitonin gene-related peptide (CGRP) in addition to the fluorescent CTb label. For all CTb-positive neurons, the mean CGRP signal intensity and cross-sectional area ($\mu m^2$) of the neurons were determined by manually outlining each neuron using ImageJ (NIH; Bethesda, MD). Each neuron was identified as being either CGRP-positive or CGRP-negative based on its intensity of CGRP labeling. Further details about these analysis methods can be found in Section 4.3.2 of Chapter 4 (Kras et al., 2013b). The number of CTb-positive neurons also positively labeled for CGRP was counted at each level for each rat. Each CGRP-labeled image corresponding to an image containing a CTb-positive neuron was digitally stored with a generalized file name of CGRP_Rat#_SpinalLevel_Slide#_Section#_ExposureTime_20x. For all sections from individual rats at each spinal level, the exposure times were standardized as described above.

Table H.1 summarizes the total number of CTb-positive neurons for each rat at each spinal level. Table H.2 reports the total number of those CTb-positive neurons that are also positively labeled for CGRP for each rat and spinal level. Exposure times for all CTb and CGRP labeled images for each rat and each spinal level are tabulated in Table H.3. The size ($\mu m^2$) and the CGRP classification (+/-) for each CTb-positive neuron for all rats in the FJD group are detailed in Table H.4. Figures H.1.A-H.1.D itemize each of

the DRG tissue sections at each spinal level containing at least one CTb-positive neuron as well as the CGRP-labeled image corresponding to each CTb-labeled section for all four of the rats in the FJD group. Table H.5 provides the size and CGRP classification for the CTb-positive neurons of rats in the sham group. All of the DRG sections containing CTb-positive neurons and the corresponding CGRP-labeled images for each section for the five rats in the sham group are presented in Figures H.2.A-H.2.D. For the normal group, the neuronal size and CGRP classification of CTb-positive joint afferents are provided in Table H.6; Figures H.3.A-H.3.D illustrate all CTb-positive neurons in DRG sections that were also immunolabeled for CGRP for all rats in the normal group. In all figures, the DRG images are presented such that the CGRP-labeled image of each section containing a CTb-positive neuron is provided immediately below the corresponding CTb-labeled image.

**Table H.1. Summary of the number of CTb-labeled joint afferents for each rat at each cervical level at seven days after FJD (Chapter 4).**

| Group | Rat | C5 | C6 | C7 | C8 | Total |
|---|---|---|---|---|---|---|
| FJD | 134 | 1 | 2 | 17 | 4 | 24 |
| | 143 | 1 | 2 | 15 | 10 | 28 |
| | 152 | 0 | 2 | 9 | 4 | 15 |
| | 155 | 1 | 5 | 23 | 13 | 42 |
| sham | 132 | 0 | 2 | 8 | 13 | 23 |
| | 141 | 0 | 0 | 4 | 3 | 7 |
| | 142 | 2 | 11 | 15 | 4 | 32 |
| | 150 | 0 | 3 | 14 | 6 | 23 |
| | 154 | 2 | 5 | 20 | 15 | 42 |
| normal | 135 | 0 | 3 | 29 | 13 | 45 |
| | 136 | 1 | 3 | 15 | 6 | 25 |
| | 138 | 4 | 11 | 22 | 11 | 48 |
| | 140 | 1 | 10 | 17 | 15 | 43 |

**Table H.2. Summary of the number of CGRP-positive CTb-labeled joint afferents for each rat at each cervical level at seven days after FJD (Chapter 4).**

| Group | Rat | C5 | C6 | C7 | C8 | Total |
|---|---|---|---|---|---|---|
| FJD | 134 | 1 | 1 | 9 | 3 | 14 |
| | 143 | 1 | 1 | 5 | 5 | 12 |
| | 152 | 0 | 0 | 7 | 2 | 9 |
| | 155 | 0 | 4 | 14 | 9 | 27 |
| sham | 132 | 0 | 1 | 5 | 7 | 13 |
| | 141 | 0 | 0 | 2 | 3 | 5 |
| | 142 | 0 | 7 | 6 | 0 | 13 |
| | 150 | 0 | 3 | 10 | 6 | 19 |
| | 154 | 1 | 5 | 15 | 14 | 35 |
| normal | 135 | 0 | 2 | 11 | 6 | 19 |
| | 136 | 0 | 0 | 6 | 5 | 11 |
| | 138 | 1 | 6 | 9 | 10 | 26 |
| | 140 | 1 | 7 | 11 | 12 | 31 |

**Table H.3. Summary of the exposure times for all CTb and CGRP images from all sections from each rat at each spinal level (Chapter 4).**

| Group | Rat | Spinal level | CTb (ms) | CGRP (ms) | Group | Rat | Spinal level | CTb (ms) | CGRP (ms) |
|---|---|---|---|---|---|---|---|---|---|
| FJD | 134 | C5 | 100 | 200 | normal | 135 | C5 | N/A | N/A |
| | | C6 | 120 | 60 | | | C6 | 100 | 65 |
| | | C7 | 200 | 80 | | | C7 | 150 | 60 |
| | | C8 | 200 | 100 | | | C8 | 200 | 150 |
| | 143 | C5 | 150 | 70 | | 136 | C5 | 200 | 200 |
| | | C6 | 150 | 100 | | | C6 | 100 | 65 |
| | | C7 | 150 | 100 | | | C7 | 150 | 60 |
| | | C8 | 150 | 150 | | | C8 | 200 | 150 |
| | 152 | C5 | N/A | N/A | | 138 | C5 | 200 | 150 |
| | | C6 | 150 | 70 | | | C6 | 200 | 100 |
| | | C7 | 150 | 80 | | | C7 | 200 | 100 |
| | | C8 | 150 | 70 | | | C8 | 200 | 150 |
| | 155 | C5 | 100 | 30 | | 140 | C5 | 200 | 150 |
| | | C6 | 100 | 60 | | | C6 | 200 | 100 |
| | | C7 | 180 | 80 | | | C7 | 200 | 100 |
| | | C8 | 200 | 80 | | | C8 | 200 | 150 |
| sham | 132 | C5 | N/A | N/A | | | | | |
| | | C6 | 120 | 60 | | | | | |
| | | C7 | 200 | 80 | | | | | |
| | | C8 | 200 | 100 | | | | | |
| | 141 | C5 | N/A | N/A | | | | | |
| | | C6 | N/A | N/A | | | | | |
| | | C7 | 150 | 100 | | | | | |
| | | C8 | 150 | 150 | | | | | |
| | 142 | C5 | 150 | 70 | | | | | |
| | | C6 | 150 | 100 | | | | | |
| | | C7 | 150 | 100 | | | | | |
| | | C8 | 150 | 150 | | | | | |
| | 150 | C5 | N/A | N/A | | | | | |
| | | C6 | 150 | 70 | | | | | |
| | | C7 | 150 | 80 | | | | | |
| | | C8 | 150 | 70 | | | | | |
| | 154 | C5 | 100 | 30 | | | | | |
| | | C6 | 100 | 60 | | | | | |
| | | C7 | 180 | 80 | | | | | |
| | | C8 | 200 | 80 | | | | | |

Note: For exposure times labeled N/A, no CTb-positive neurons were detected for that rat at that spinal level.

**Table H.4. Neuronal size and CGRP classification for each CTb-positive neuron for each rat at day seven after FJD (Chapter 4).**

| Level | Rat | Slide | Section | Area ($\mu m^2$) | CGRP expression |
|---|---|---|---|---|---|
| C5 | 134 | 8 | 9 | 410.6 | + |
| | 143 | 2 | 6 | 909.4 | + |
| | 152 | N/A | N/A | N/A | N/A |
| | 155 | 2 | 6 | 1019.7 | - |
| C6 | 134 | 1 | 6 | 524.2 | - |
| | | 2 | 1 | 1139.1 | + |
| | 143 | 2 | 5 | 777.1 | - |
| | | 3 | 9 | 636.9 | + |
| | 152 | 5 | 3_top left | 621.1 | - |
| | | | 3_bottom | 1389.5 | - |
| | 155 | 6 | 9 | 906.1 | + |
| | | 8 | 1 | 408.1 | - |
| | | | 4 | 613.2 | + |
| | | | 7 | 914.4 | + |
| | | 9 | 7 | 545.8 | + |
| C7 | 134 | 4 | 5 | 625.7 | - |
| | | 5 | 4 | 582.4 | + |
| | | 6 | 5 | 602.8 | - |
| | | | 6 | 717.2 | - |
| | | | 9 | 587.8 | - |
| | | 7 | 2 | 1098.3 | + |
| | | | 4_left | 572.9 | + |
| | | | 5_middle | 789.6 | + |
| | | | 6_left | 791.3 | + |
| | | | 10 | 804.2 | - |
| | | 8 | 4 | 738.4 | - |
| | | | 8_right | 895.3 | - |
| | | | 8_left | 918.6 | - |
| | | | 10 | 922.7 | + |
| | | 9 | 8 | 991.0 | + |
| | | | 27 | 460.1 | + |
| | | | 33 | 663.6 | + |
| | 143 | 1 | 5 | 648.6 | - |
| | | | 6 | 470.9 | + |
| | | 2 | 6 | 309.9 | - |
| | | 3 | 1 | 349.9 | - |
| | | | 4 | 332.4 | - |
| | | | 10 | 461.4 | + |
| | | 4 | 4 | 690.2 | - |
| | | 5 | 1 | 329.1 | - |
| | | | 8 | 679.8 | - |
| | | | 9 left | 754.3 | + |
| | | | 9 right | 809.2 | - |
| | | 6 | 4 | 592.0 | - |
| | | | 9 left | 639.4 | + |
| | | | 9 right | 809.2 | - |
| | | | 10 | 1005.5 | + |

Note: Table continued on next page. In the Section column, designators such as left, right, top, & bottom are used to specify a single neuron when multiple CTb-positive neurons are evident in that section. For cells labeled N/A, no CTb-positive neurons were detected for that rat at that spinal level.

| Level | Rat | Slide | Section | Area ($\mu m^2$) | CGRP expression |
|---|---|---|---|---|---|
| C7 | 152 | 5 | 2 | 765.5 | + |
| | | 7 | 6 | 861.6 | + |
| | | | 8 | 1111.6 | + |
| | | 8 | 2 | 725.1 | - |
| | | | 4 | 896.1 | + |
| | | 9 | 4 | 1157.8 | + |
| | | | 6 | 832.1 | - |
| | | | 7_top | 1023.0 | + |
| | | 10 | 9 | 869.5 | + |
| | 155 | 2 | 8 | 521.7 | + |
| | | | 9 | 932.7 | - |
| | | 3 | 4_top | 535.0 | + |
| | | | 4_low right | 707.7 | - |
| | | | 5_left | 482.2 | - |
| | | | 5_right | 676.5 | + |
| | | | 6_low left | 923.6 | - |
| | | | 9 | 589.5 | - |
| | | 4 | 4 | 701.0 | + |
| | | | 7 | 973.1 | + |
| | | | 10 | 796.7 | - |
| | | 5 | 2 | 626.5 | + |
| | | | 6 | 657.7 | - |
| | | | 8_top right | 580.8 | + |
| | | | 9_bottom | 628.6 | + |
| | | 6 | 5_left | 867.4 | - |
| | | | 5_right | 549.2 | + |
| | | 7 | 2 | 816.2 | + |
| | | 8 | 1 | 523.8 | + |
| | | | 4 | 512.1 | + |
| | | | 10 | 753.4 | + |
| | | 9 | 2 | 598.7 | + |
| | | | 4 | 483.0 | - |
| C8 | 134 | 5 | 1 | 686.4 | - |
| | | 6 | 6 | 715.6 | + |
| | | 8 | 5 | 1118.7 | + |
| | | 9 | 6 | 876.6 | + |
| | 143 | 3 | 10_1 | 580.4 | - |
| | | | 10_2 | 598.7 | - |
| | | | 12 | 494.2 | - |
| | | 4 | 1 | 383.2 | + |
| | | | 3 | 756.7 | + |
| | | | 6 | 1008.9 | + |
| | | | 14 | 823.3 | + |
| | | 5 | 10 | 713.1 | + |
| | | | 12 | 1213.5 | - |
| | | 7 | 13 | 1158.2 | - |

Note: Table continued on next page. In the Section column, designators such as left, right, top, & bottom are used to specify a single neuron when multiple CTb-positive neurons are evident in that section. A Section number followed by a numerical designator (i.e. 10_1 & 10_2) indicates a section that contains multiple neurons that could not be captured in one image frame. As such, two separate images had to be taken for that section.

| Level | Rat | Slide | Section | Area ($\mu m^2$) | CGRP expression |
|---|---|---|---|---|---|
| C8 | 152 | 4 | 1 | 833.3 | - |
| | | 8 | 3 | 1032.6 | + |
| | | | 9 | 675.2 | + |
| | | 9 | 10 | 813.3 | - |
| | 155 | 3 | 2_left | 781.7 | + |
| | | | 2_right | 1031.7 | + |
| | | | 8 | 392.7 | - |
| | | 4 | 3 | 691.8 | - |
| | | | 10 | 591.6 | + |
| | | 7 | 7 | 865.3 | - |
| | | | 9 | 781.7 | + |
| | | 8 | 4 | 1221.9 | + |
| | | | 6 | 870.3 | + |
| | | | 9 | 639.4 | + |
| | | 9 | 1 | 617.4 | + |
| | | | 5 | 702.3 | + |
| | | | 6 | 1218.1 | - |

Note: In the Section column, designators such as left, right, top, & bottom are used to specify a single neuron when multiple CTb-positive neurons are evident in that section.

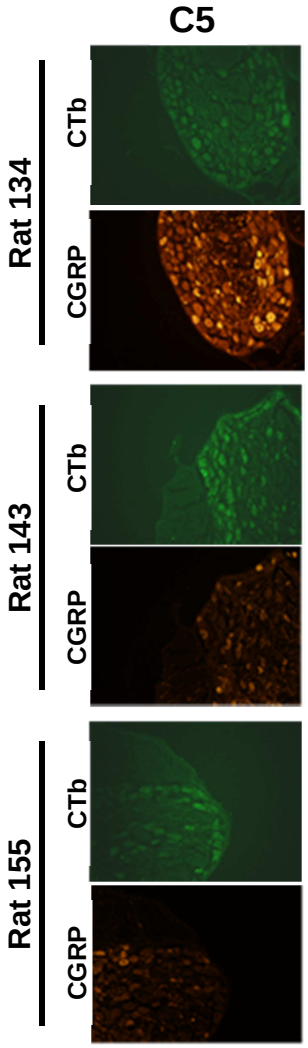


**Figure H.1.A.** CTb and CGRP-labeled sections of the C5 DRG from Rats 134, 143, and 155 in the FJD group. For each rat, the images presented correspond to those sections for which CTb-labeled neurons were identified as summarized in Table H.4. For each CTb-labeled image, the corresponding CGRP-labeled image is presented immediately below it.

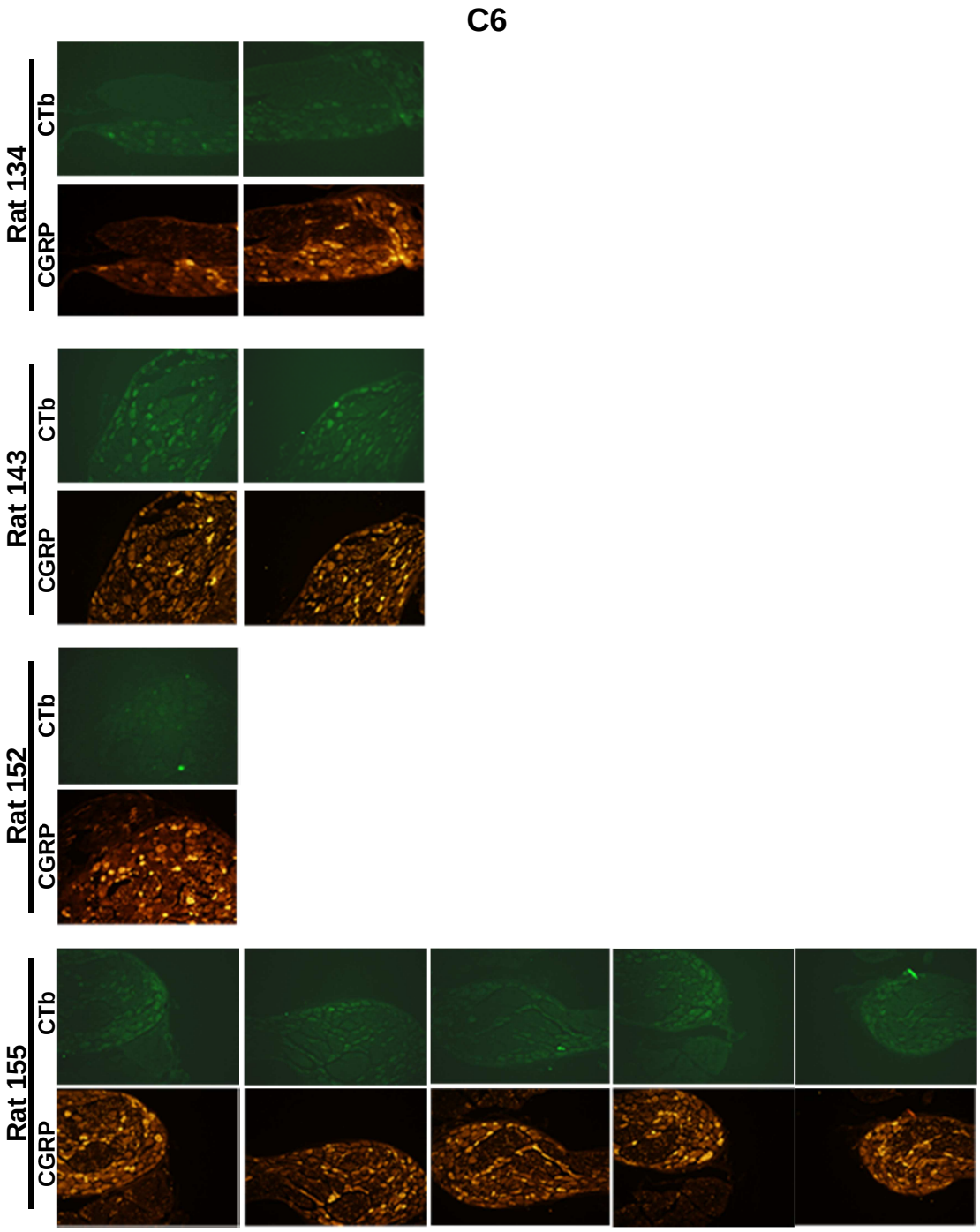


**Figure H.1.B.** CTb and CGRP-labeled sections of the C6 DRG from rats in the FJD group. For each rat, the images presented correspond to those sections for which CTb-labeled neurons were identified as summarized in Table H.4. For each rat, slide number and section number increase from left to right. For each CTb-labeled image, the corresponding CGRP-labeled image is presented immediately below it.

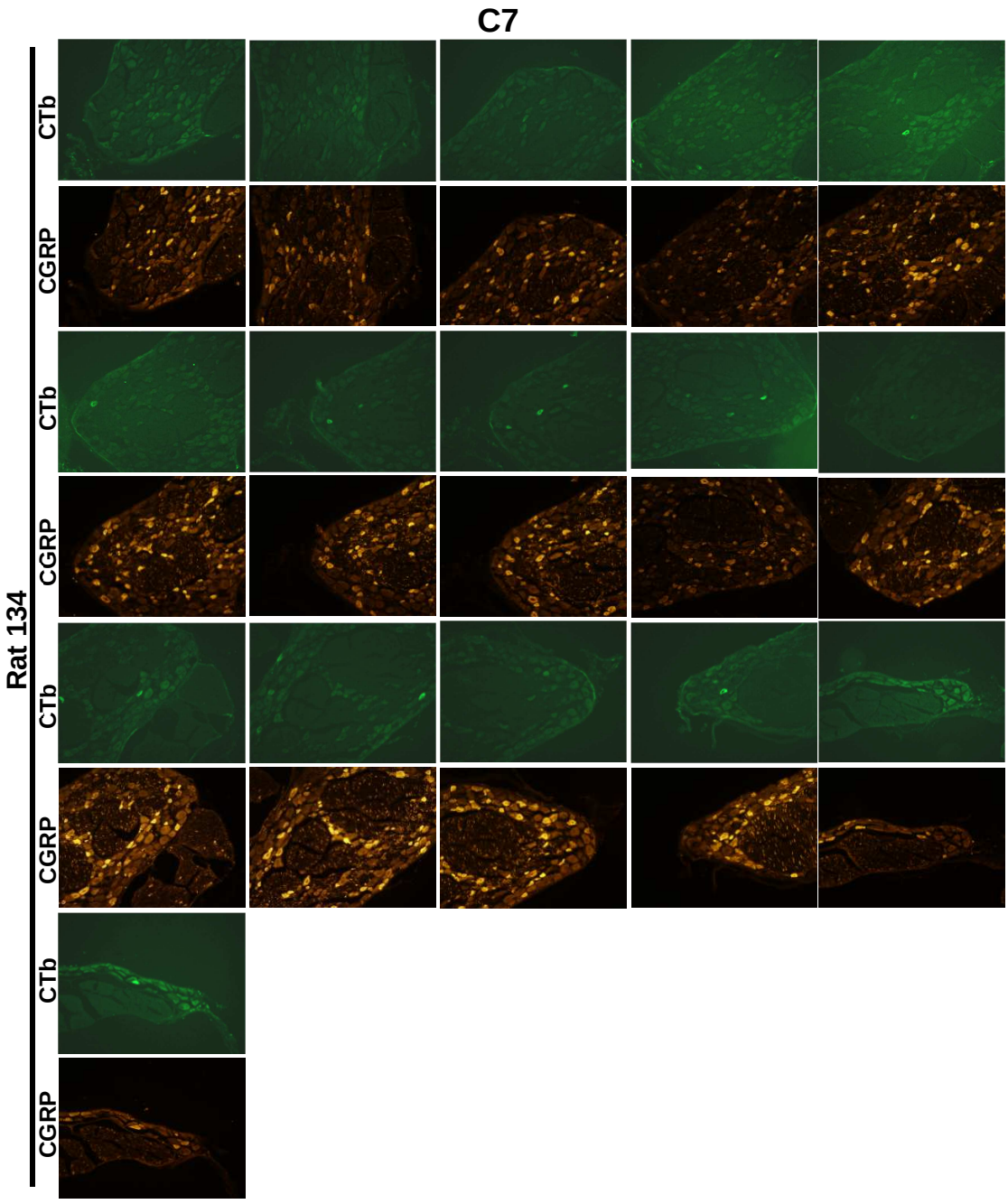


**Figure H.1.C.** CTb and CGRP-labeled sections of the C7 DRG from Rat 134 in the FJD group. For each rat, the images presented correspond to those sections for which CTb-labeled neurons were identified as summarized in Table H.4. For each rat, slide number and section number increase from left to right. For each CTb-labeled image, the corresponding CGRP-labeled image is presented immediately below it. Figure is continued on the next page.

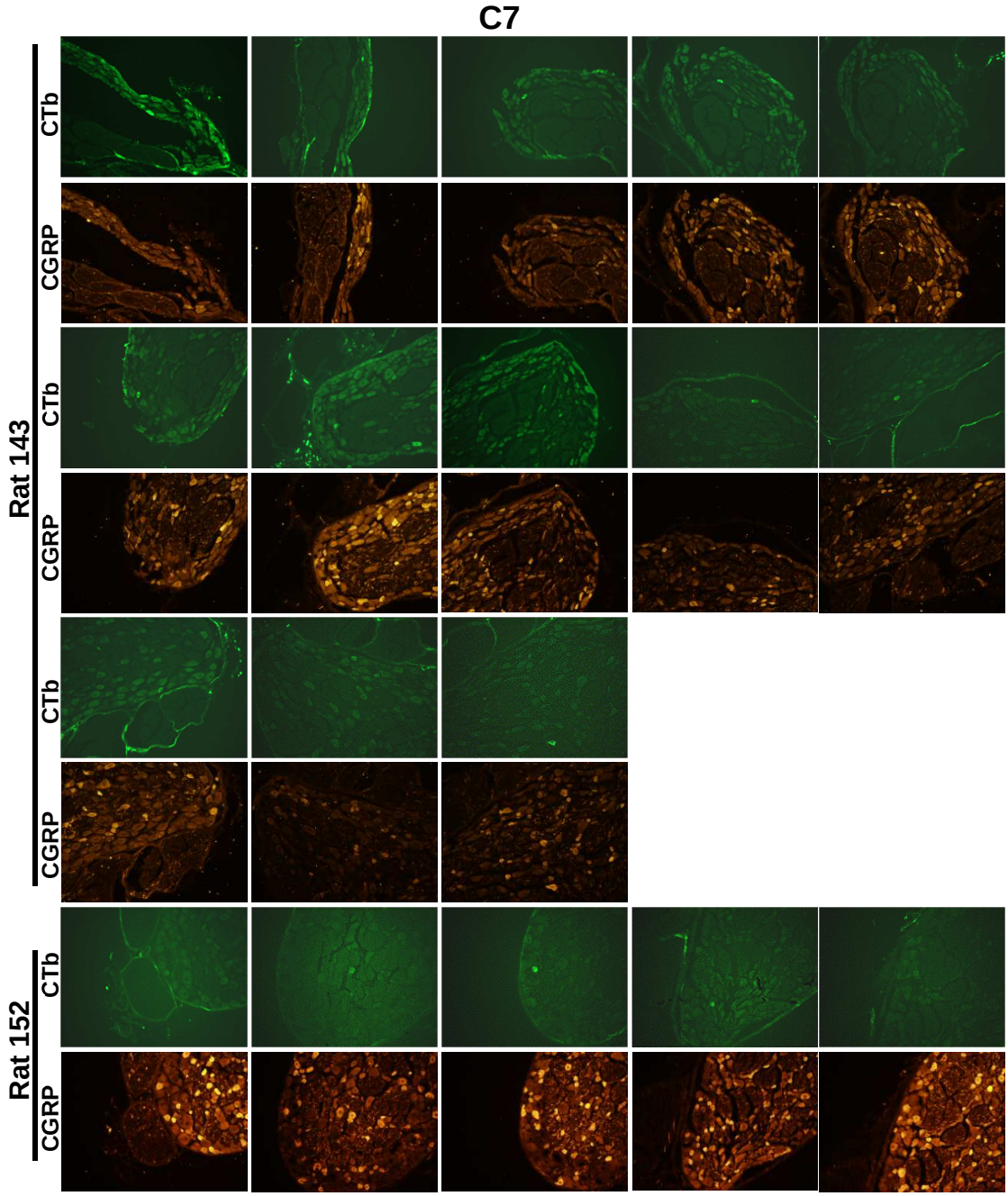


**Figure H.1.C.** CTb and CGRP-labeled sections of the C7 DRG from Rats 143 and 152 in the FJD group. For each rat, the images presented correspond to those sections for which CTb-labeled neurons were identified as summarized in Table H.4. For each rat, slide number and section number increase from left to right. For each CTb-labeled image, the corresponding CGRP-labeled image is presented immediately below it. Figure is continued on the next page.

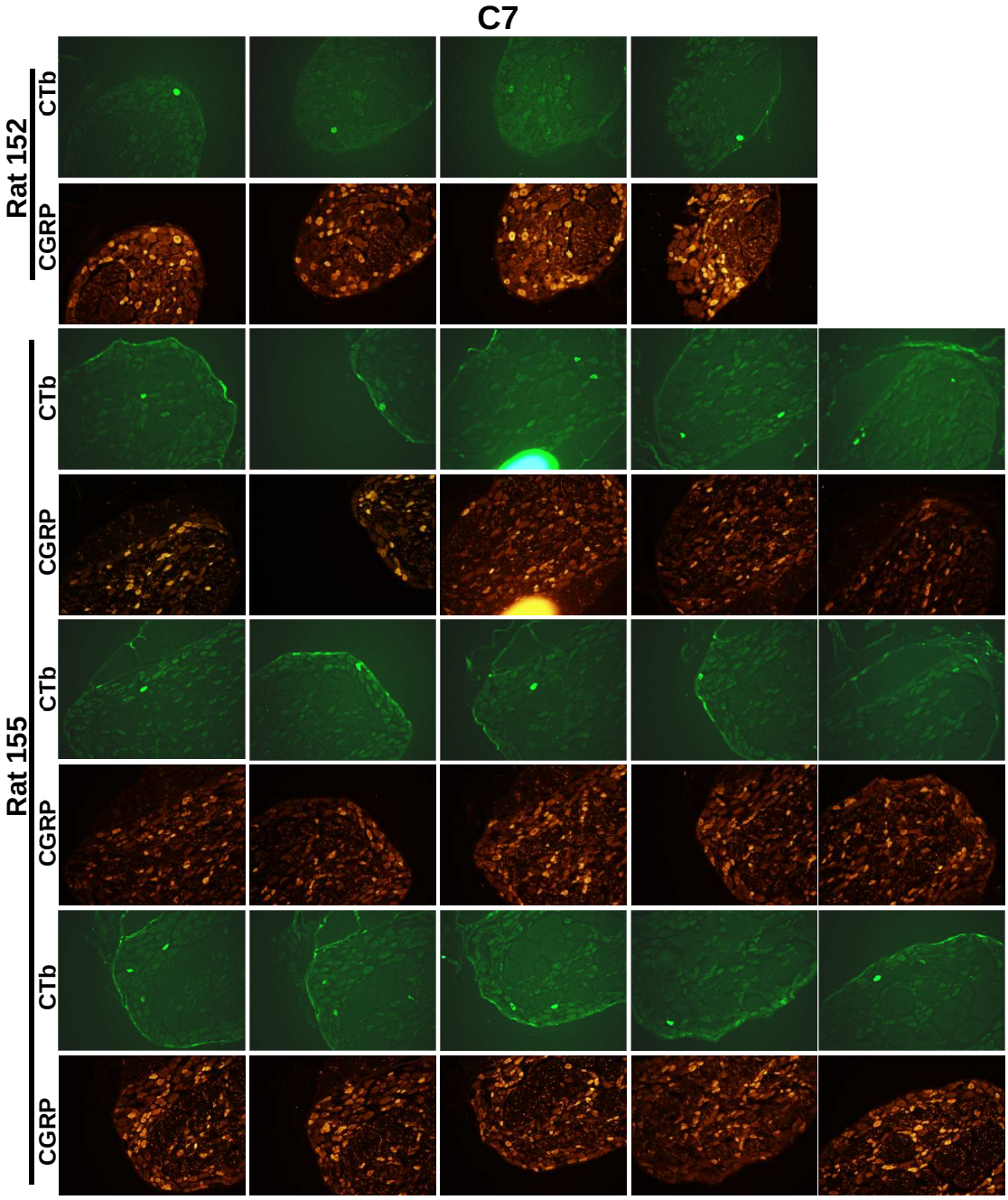


**Figure H.1.C.** CTb and CGRP-labeled sections of the C7 DRG from Rats 152 and 155 in the FJD group. For each rat, the images presented correspond to those sections for which CTb-labeled neurons were identified as summarized in Table H.4. For each rat, slide number and section number increase from left to right. For each CTb-labeled image, the corresponding CGRP-labeled image is presented immediately below it. Figure is continued on the next page.

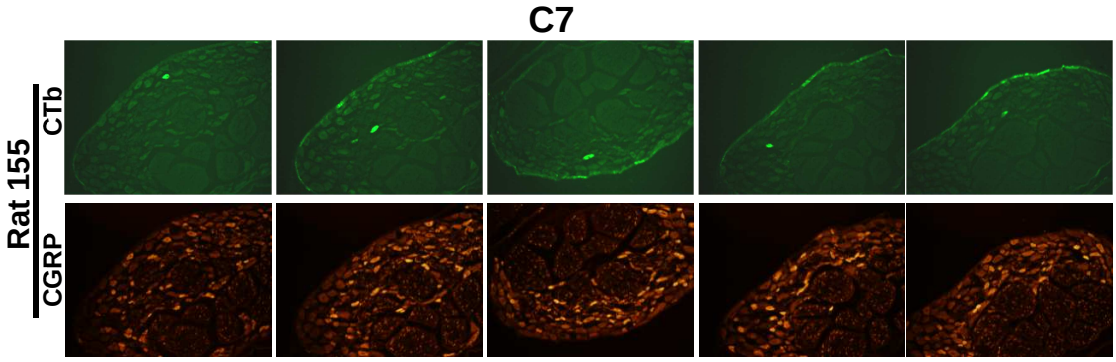


**Figure H.1.C.** CTb and CGRP-labeled sections of the C7 DRG from Rat 155 in the FJD group. For each rat, the images presented correspond to those sections for which CTb-labeled neurons were identified as summarized in Table H.4. For each rat, slide number and section number increase from left to right. For each CTb-labeled image, the corresponding CGRP-labeled image is presented immediately below it.

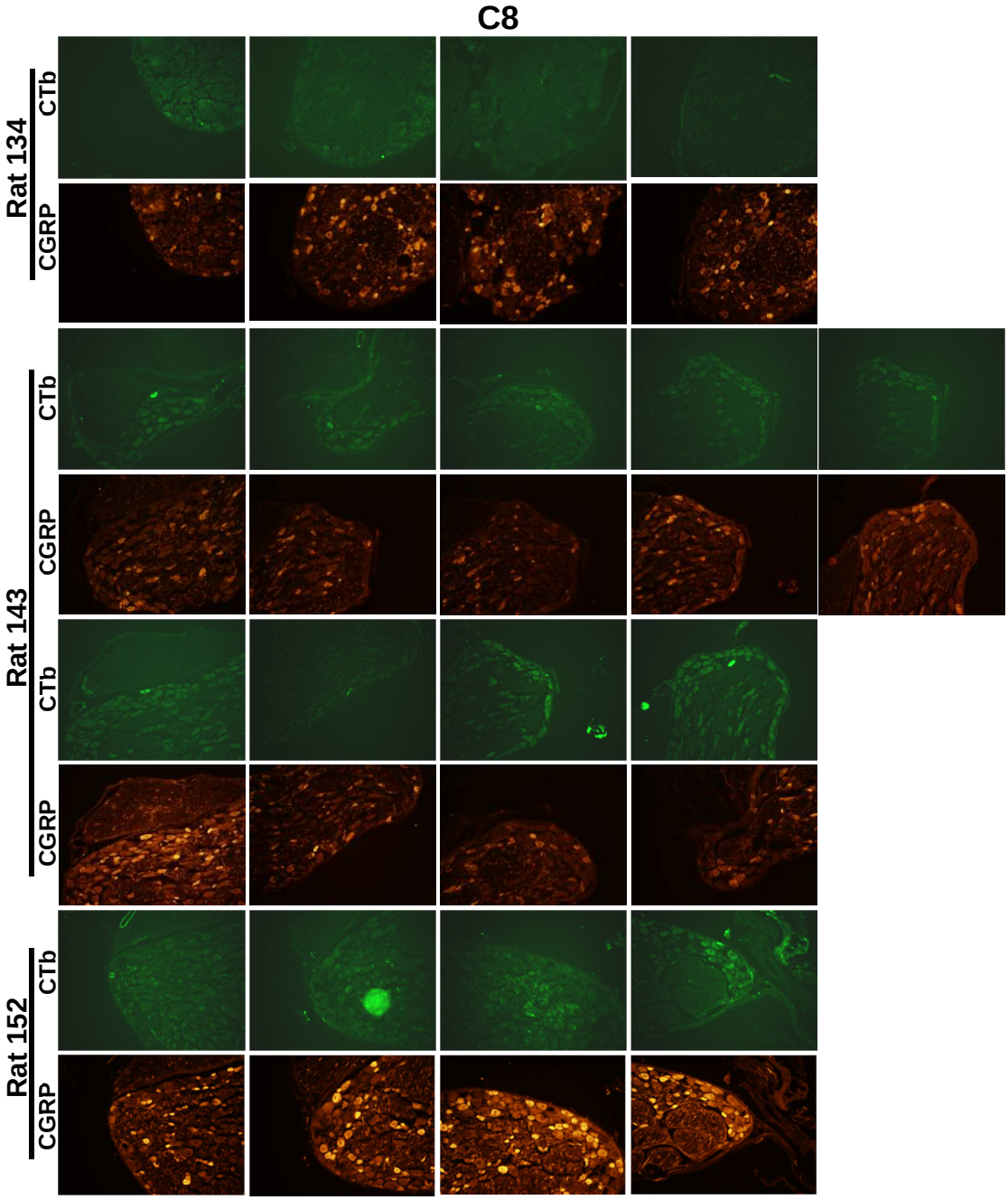


**Figure H.1.D.** CTb and CGRP-labeled sections of the C8 DRG from Rats 134, 143, and 152 in the FJD group. For each rat, the images presented correspond to those sections for which CTb-labeled neurons were identified as summarized in Table H.4. For each rat, slide number and section number increase from left to right. For each CTb-labeled image, the corresponding CGRP-labeled image is presented immediately below it. Figure is continued on the next page.

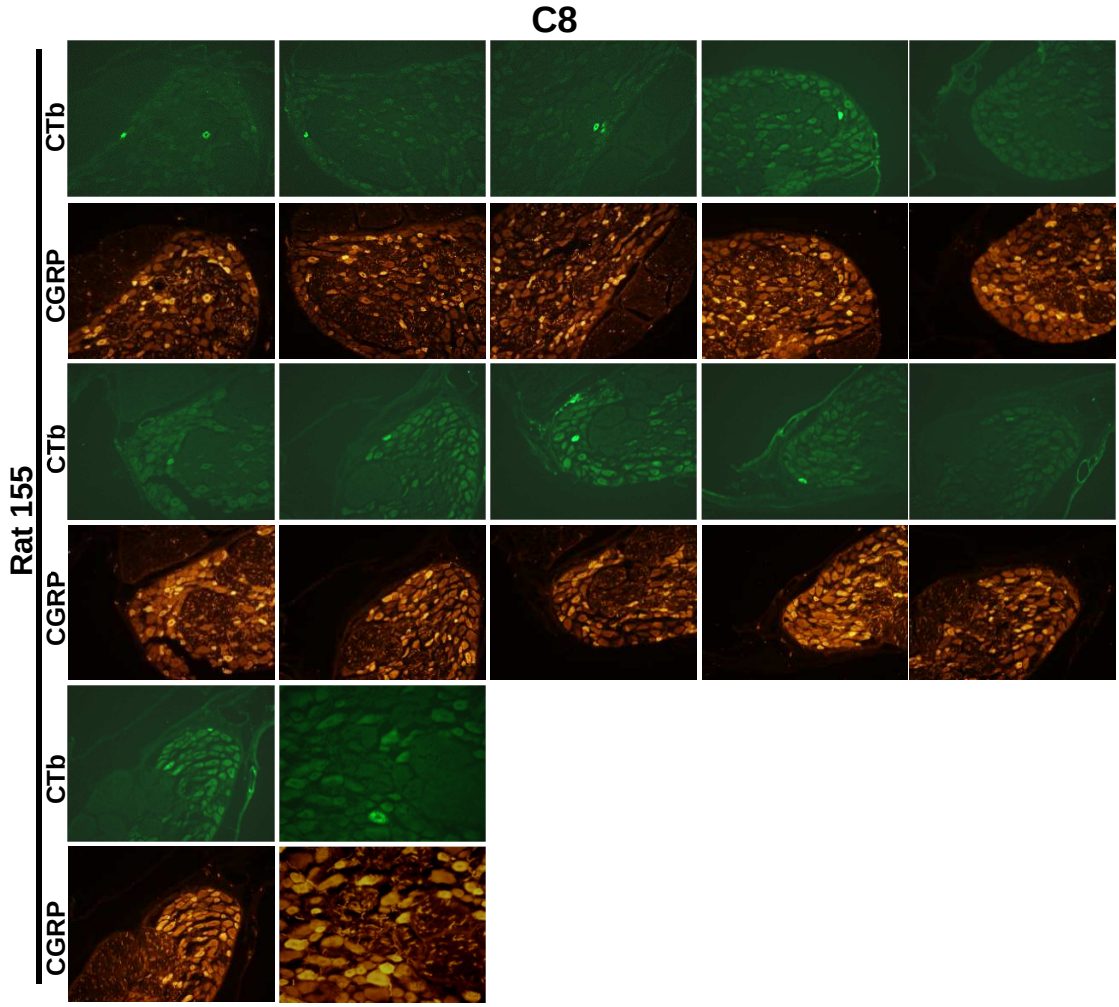


**Figure H.1.D.** CTb and CGRP-labeled sections of the C8 DRG from Rat 155 in the FJD group. For each rat, the images presented correspond to those sections for which CTb-labeled neurons were identified as summarized in Table H.4. For each rat, slide number and section number increase from left to right. For each CTb-labeled image, the corresponding CGRP-labeled image is presented immediately below it.

**Table H.5. Neuronal size and CGRP classification for each CTb-positive neuron for each rat at day seven after sham (Chapter 4).**

| Level | Rat | Slide | Section | Area ($\mu m^2$) | CGRP expression |
|---|---|---|---|---|---|
| C5 | 132 | N/A | N/A | N/A | N/A |
| | 141 | N/A | N/A | N/A | N/A |
| | 142 | 1 | 1 | 604.9 | - |
| | | 3 | 1 | 503.4 | - |
| | 150 | N/A | N/A | N/A | N/A |
| | 154 | 5 | 2 | 863.7 | - |
| | | 6 | 7 | 740.5 | + |
| C6 | 132 | 4 | 4 | 727.6 | - |
| | | 7 | 2 | 697.7 | + |
| | 141 | N/A | N/A | N/A | N/A |
| | 142 | 4 | 9 | 412.7 | + |
| | | | 11 | 551.6 | + |
| | | | 12 | 332.0 | + |
| | | 5 | 1 | 463.0 | + |
| | | | 3 | 585.8 | - |
| | | | 6 | 455.5 | + |
| | | | 7 | 457.6 | + |
| | | | 12 | 596.2 | + |
| | | 7 | 2 | 399.4 | - |
| | | | 8 | 378.6 | - |
| | | 8 | 4 | 632.8 | - |
| | 150 | 1 | 2 | 1419.9 | + |
| | | 5 | 2 | 747.2 | + |
| | | 9 | 3 | 842.5 | + |
| | 154 | 4 | 7 | 532.5 | + |
| | | 7 | 9 | 1115.4 | + |
| | | | 10 | 978.5 | + |
| | | 8 | 3 | 703.1 | + |
| | | | 10 | 463.0 | + |
| C7 | 132 | 2 | 7 | 426.0 | + |
| | | | 9 | 458.5 | - |
| | | 4 | 4 | 560.4 | + |
| | | 5 | 12 | 557.9 | - |
| | | 6 | 3 | 394.4 | - |
| | | | 6 | 672.7 | + |
| | | | 7 | 648.2 | + |
| | | 7 | 11 | 554.6 | + |
| | 141 | 2 | 7 | 641.5 | - |
| | | | 9 | 461.8 | - |
| | | 3 | 7 | 515.9 | + |
| | | 4 | 10 | 542.1 | + |

Note: Table continued on next page. For cells labeled N/A, no CTb-positive neurons were detected for that rat at that spinal level.

| Level | Rat | Slide | Section | Area ($\mu m^2$) | CGRP expression |
|---|---|---|---|---|---|
| C7 | 142 | 1 | 12 | 672.3 | + |
| | | 3 | 3 | 988.5 | + |
| | | 3 | 7_1 | 405.2 | - |
| | | | 7_2 | 398.6 | - |
| | | 4 | 5 | 748.4 | - |
| | | | 8 | 647.3 | - |
| | | | 10_1 right | 478.0 | + |
| | | | 10_2 middle | 432.7 | - |
| | | | 11 left | 428.5 | - |
| | | | 11 right | 671.9 | + |
| | | | 12 | 717.6 | + |
| | | 5 | 12 | 521.7 | - |
| | | 6 | 6 | 558.7 | - |
| | | 8 | 2 | 808.8 | + |
| | | | 8 | 358.6 | - |
| | 150 | 1 | 2 | 902.8 | + |
| | | 3 | 2 | 708.9 | + |
| | | | 8 | 1124.9 | + |
| | | 5 | 3 | 782.1 | + |
| | | | 5_1 | 714.7 | - |
| | | | 6 | 1205.6 | + |
| | | | 9 | 913.2 | + |
| | | 6 | 1 | 1266.8 | + |
| | | | 9 | 1193.6 | - |
| | | 7 | 1 | 1105.8 | - |
| | | 9 | 1 | 778.8 | + |
| | | | 3 | 1120.8 | + |
| | | | 6 | 1039.6 | - |
| | | | 10 | 872.4 | + |
| | 154 | 2 | 2 | 459.3 | - |
| | | | 6 | 602.0 | - |
| | | 3 | 10 | 553.3 | + |
| | | 4 | 8 | 410.6 | + |
| | | 5 | 3 | 341.1 | + |
| | | | 8 | 602.8 | + |
| | | 6 | 4 | 595.3 | + |
| | | 7 | 1 | 522.9 | + |
| | | | 4 | 1058.0 | + |
| | | | 9 | 409.4 | + |
| | | | 10 | 446.0 | + |
| | | 8 | 1 | 583.7 | + |
| | | | 6 | 859.5 | + |
| | | | 8_2 | 658.6 | - |
| | | | 9 | 1013.0 | + |
| | | 9 | 4 right | 843.3 | + |
| | | | 5 left | 713.1 | - |
| | | 10 | 1 | 807.5 | + |
| | | | 3 | 767.6 | - |
| | | | 6 | 645.7 | + |

Note: Table continued on next page. In the Section column, designators such as left, right, top, & bottom are used to specify a single neuron when multiple CTb-positive neurons are evident in that section. A Section number followed by a numerical designator (i.e. 7_1 & 7_2) indicates a section that contains multiple neurons that could not be captured in one image frame. As such, two separate images had to be taken for that section.

| Level | Rat | Slide | Section | Area ($\mu m^2$) | CGRP expression |
|---|---|---|---|---|---|
| C8 | 132 | 5 | 1 | 825.8 | - |
| | | | 2 | 1097.1 | - |
| | | | 9 | 788.0 | - |
| | | 6 | 6 | 852.4 | + |
| | | 7 | 6 | 966.4 | - |
| | | 8 | 8 | 927.3 | + |
| | | | 10 | 805.8 | + |
| | | 9 | 4 | 754.3 | + |
| | | | 5 | 693.9 | - |
| | | 10 | 4_top | 839.1 | + |
| | | | 4_bottom | 899.0 | - |
| | | | 7 | 642.8 | + |
| | | | 10 | 369.8 | + |
| | 141 | 5 | 6 | 610.3 | + |
| | | | 8 | 662.3 | + |
| | | 6 | 5 | 632.4 | + |
| | 142 | 3 | 11 | 643.6 | - |
| | | 4 | 7 | 790.4 | - |
| | | 5 | 3 | 373.2 | - |
| | | 7 | 9 | 1200.6 | - |
| | 150 | 5 | 7 | 1213.1 | + |
| | | | 10 | 827.1 | + |
| | | 6 | 7 | 1296.7 | + |
| | | 9 | 7 | 1180.3 | + |
| | | | 9 | 800.4 | + |
| | | 10 | 7 | 1122.0 | + |
| | 154 | 3 | 8 | 1083.7 | + |
| | | 5 | 4_1 low left | 411.4 | + |
| | | | 4_2 top right | 816.7 | + |
| | | 6 | 5 | 716.0 | + |
| | | | 7 | 836.2 | + |
| | | 7 | 5 | 815.8 | + |
| | | 8 | 1 | 490.1 | + |
| | | 9 | 3_1 | 645.7 | - |
| | | | 3_2 left | 738.9 | + |
| | | | 10 | 689.4 | + |
| | | 10 | 3 | 955.6 | + |
| | | | 6 | 808.8 | + |
| | | | 8 | 654.4 | + |
| | | | 14 top right | 569.5 | + |
| | | | 14 bottom left | 1029.7 | + |

Note: In the Section column, designators such as left, right, top, & bottom are used to specify a single neuron when multiple CTb-positive neurons are evident in that section.

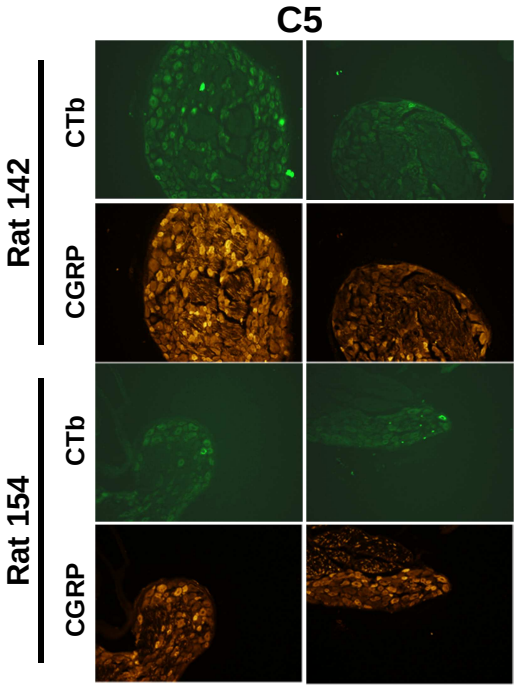


**Figure H.2.A.** CTb and CGRP-labeled sections of the C5 DRG from Rats 142 and 154 in the sham group. For each rat, the images presented correspond to those sections for which CTb-labeled neurons were identified as summarized in Table H.5. For each rat, slide number and section number increase from left to right. For each CTb-labeled image, the corresponding CGRP-labeled image is presented immediately below it.

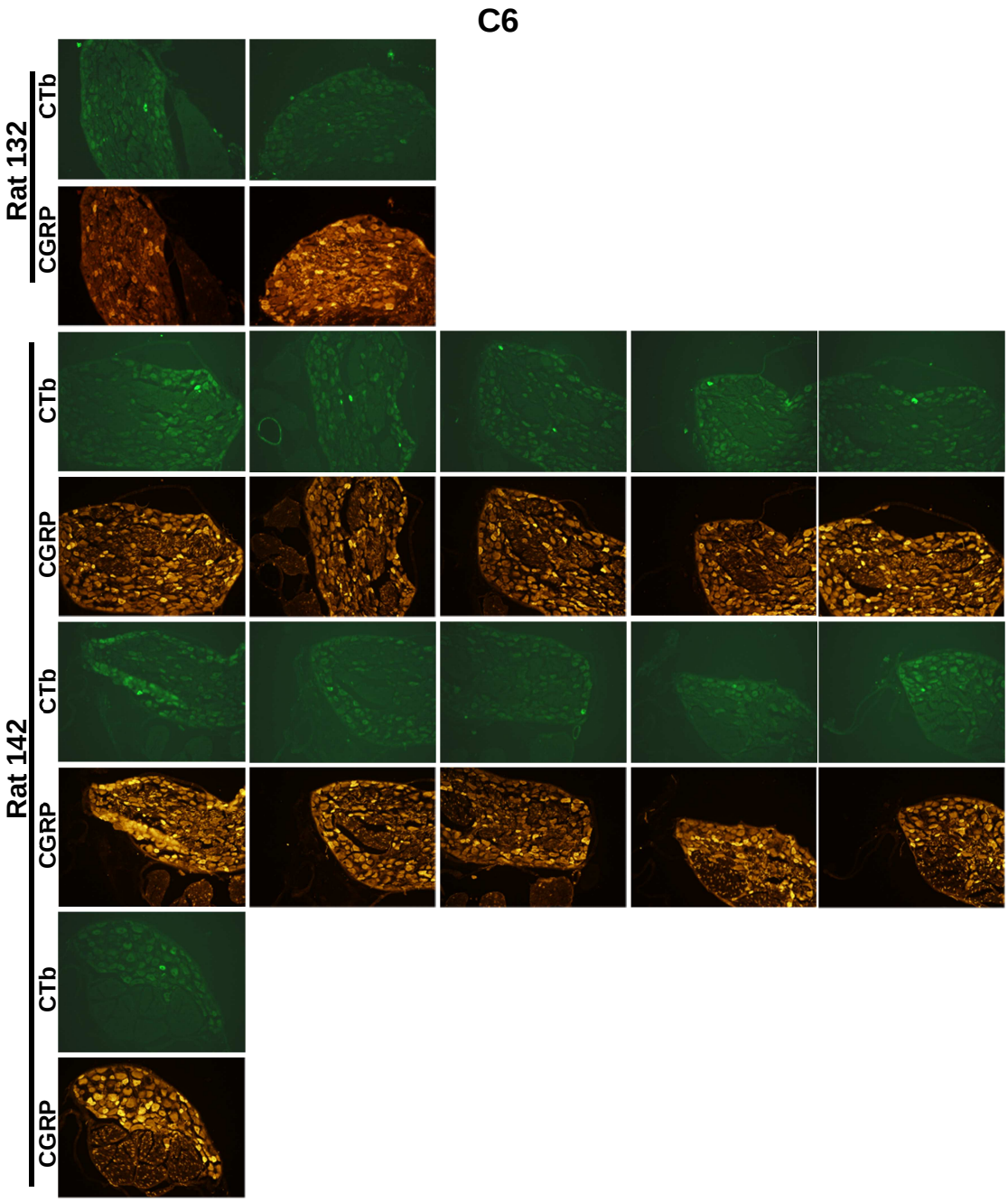


**Figure H.2.B.** CTb and CGRP-labeled sections of the C6 DRG from Rats 132 and 142 in the sham group. For each rat, the images presented correspond to those sections for which CTb-labeled neurons were identified as summarized in Table H.5. For each rat, slide number and section number increase from left to right. For each CTb-labeled image, the corresponding CGRP-labeled image is presented immediately below it. Figure is continued on the next page.

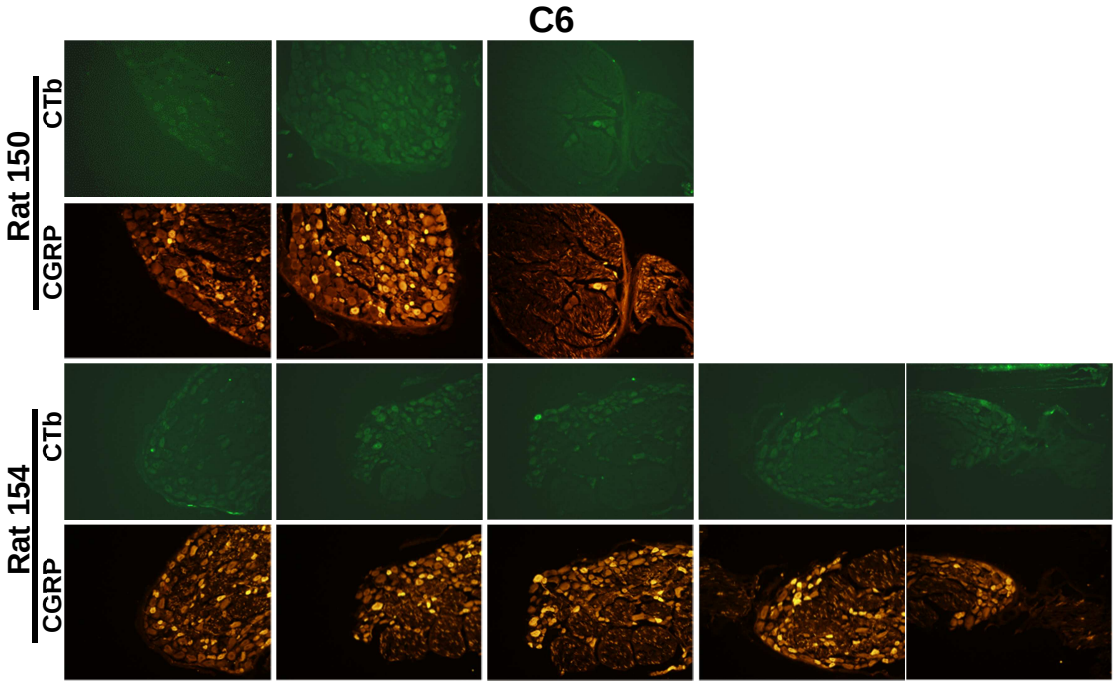


**Figure H.2.B.** CTb and CGRP-labeled sections of the C6 DRG from Rats 150 and 154 in the sham group. For each rat, the images presented correspond to those sections for which CTb-labeled neurons were identified as summarized in Table H.5. For each rat, slide number and section number increase from left to right. For each CTb-labeled image, the corresponding CGRP-labeled image is presented immediately below it.

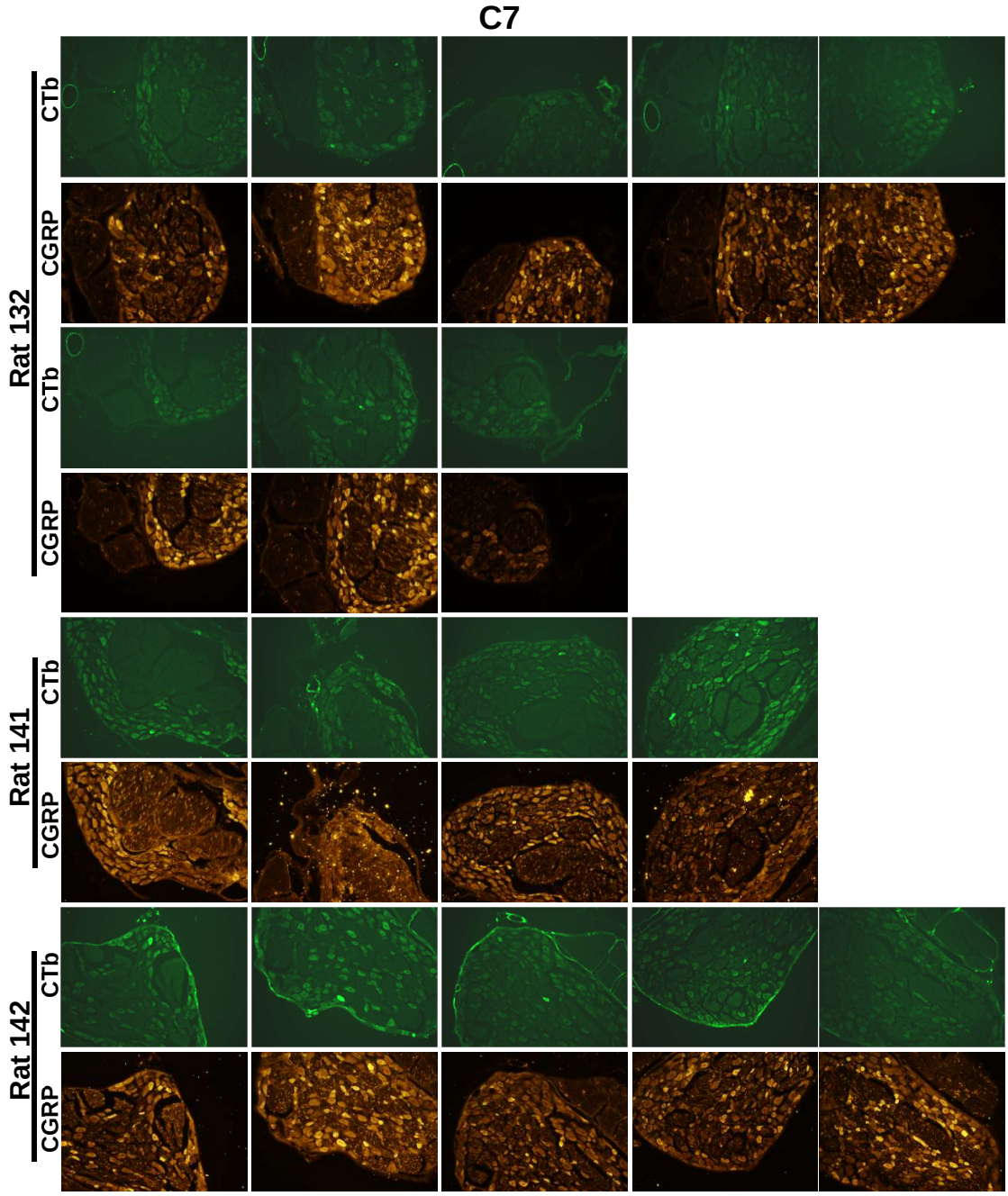


**Figure H.2.C.** CTb and CGRP-labeled sections of the C7 DRG from Rats 132, 141, and 142 in the sham group. For each rat, the images presented correspond to those sections for which CTb-labeled neurons were identified as summarized in Table H.5. For each rat, slide number and section number increase from left to right. For each CTb-labeled image, the corresponding CGRP-labeled image is presented immediately below it. Figure is continued on the next page.

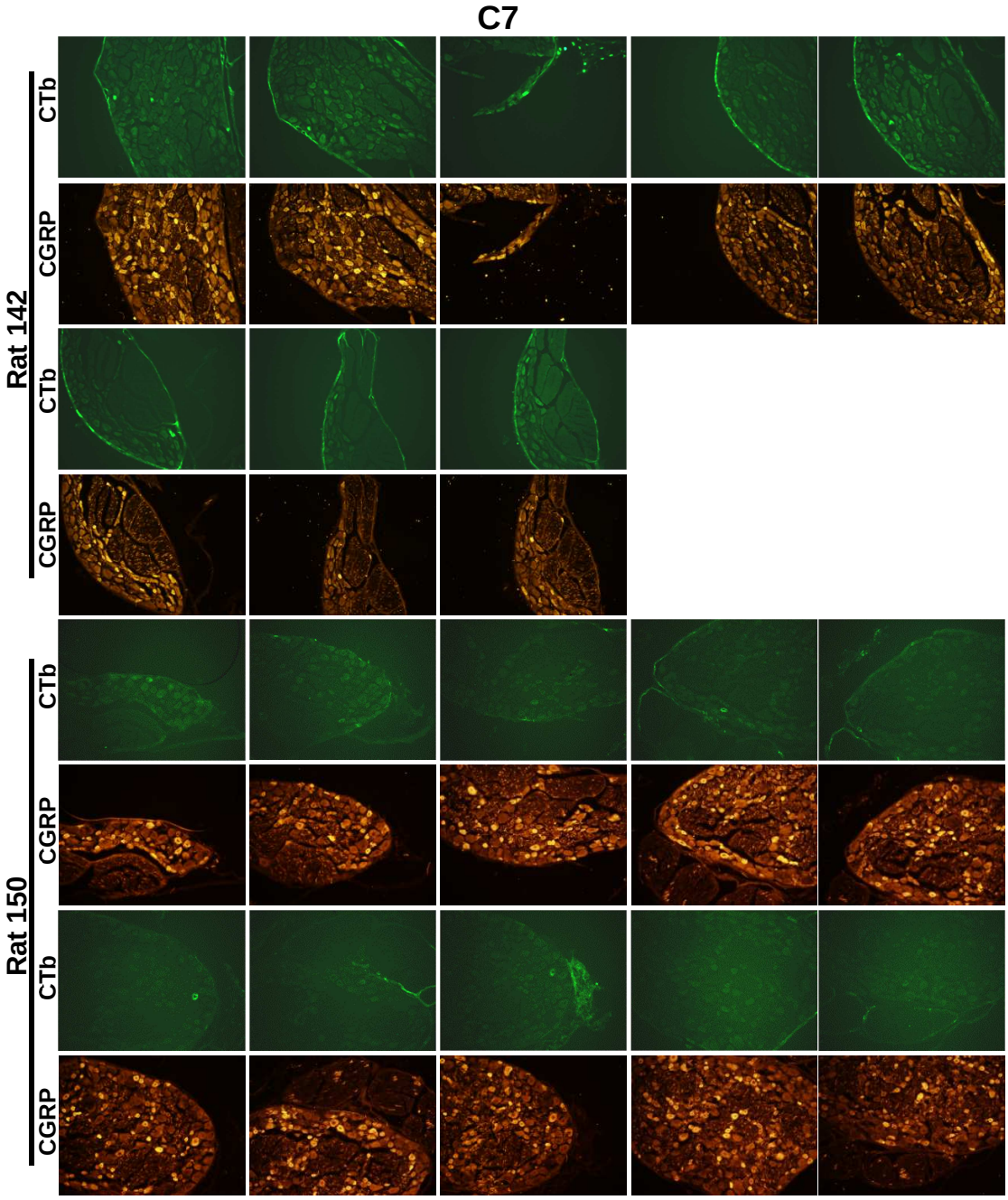


**Figure H.2.C.** CTb and CGRP-labeled sections of the C7 DRG from Rats 142 and 150 in the sham group. For each rat, the images presented correspond to those sections for which CTb-labeled neurons were identified as summarized in Table H.5. For each rat, slide number and section number increase from left to right. For each CTb-labeled image, the corresponding CGRP-labeled image is presented immediately below it. Figure is continued on the next page.

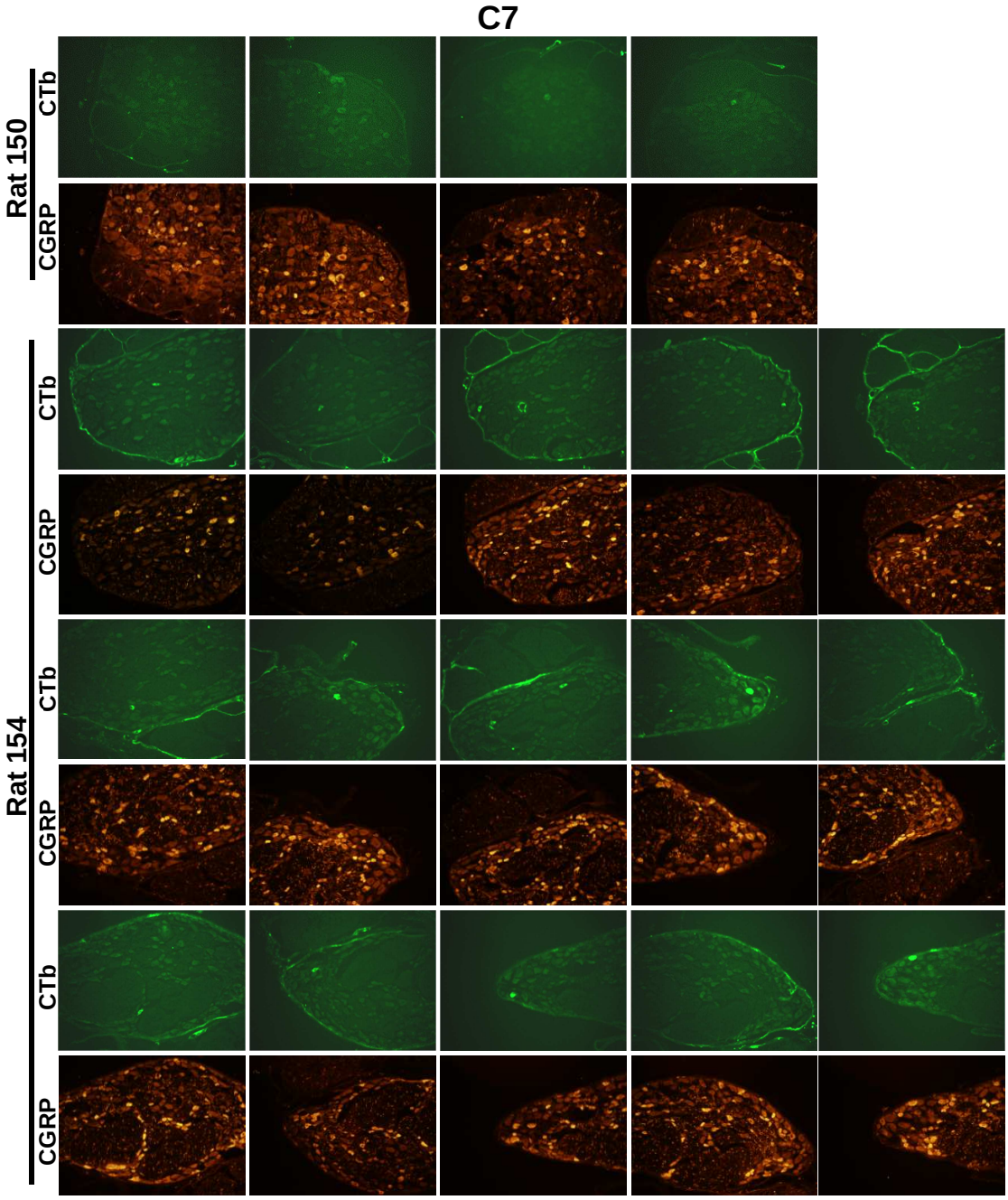


**Figure H.2.C.** CTb and CGRP-labeled sections of the C7 DRG from Rats 150 and 154 in the sham group. For each rat, the images presented correspond to those sections for which CTb-labeled neurons were identified as summarized in Table H.5. For each rat, slide number and section number increase from left to right. For each CTb-labeled image, the corresponding CGRP-labeled image is presented immediately below it. Figure is continued on the next page.

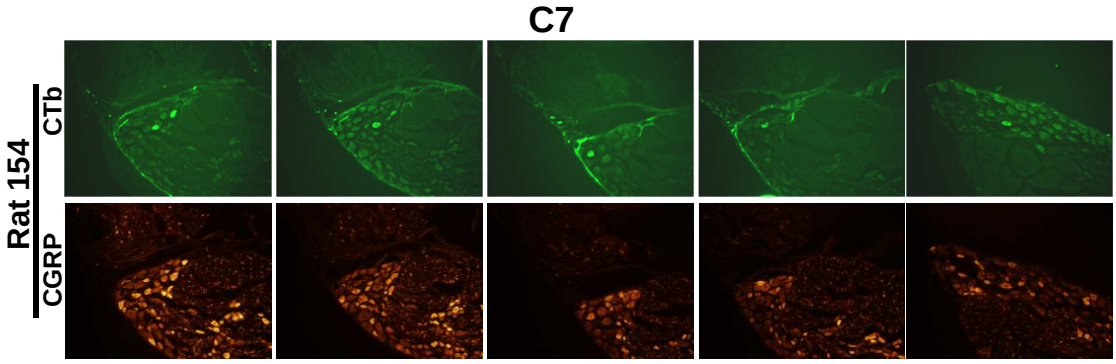


**Figure H.2.C.** CTb and CGRP-labeled sections of the C7 DRG from Rat 154 in the sham group. For each rat, the images presented correspond to those sections for which CTb-labeled neurons were identified as summarized in Table H.5. For each rat, slide number and section number increase from left to right. For each CTb-labeled image, the corresponding CGRP-labeled image is presented immediately below it.

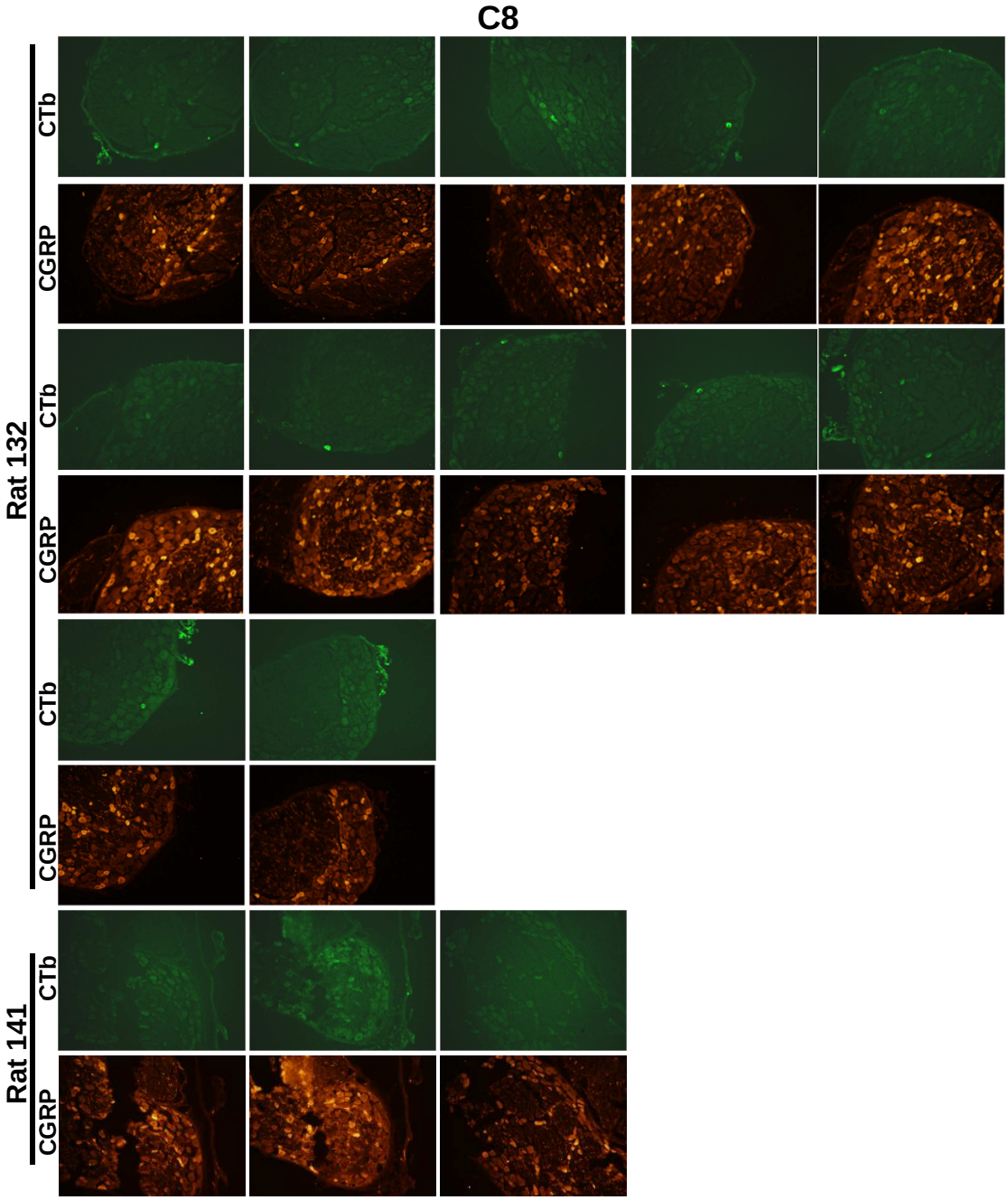


**Figure H.2.D.** CTb and CGRP-labeled sections of the C8 DRG from Rats 132 and 141 in the sham group. For each rat, the images presented correspond to those sections for which CTb-labeled neurons were identified as summarized in Table H.5. For each rat, slide number and section number increase from left to right. For each CTb-labeled image, the corresponding CGRP-labeled image is presented immediately below it. Figure is continued on the next page.

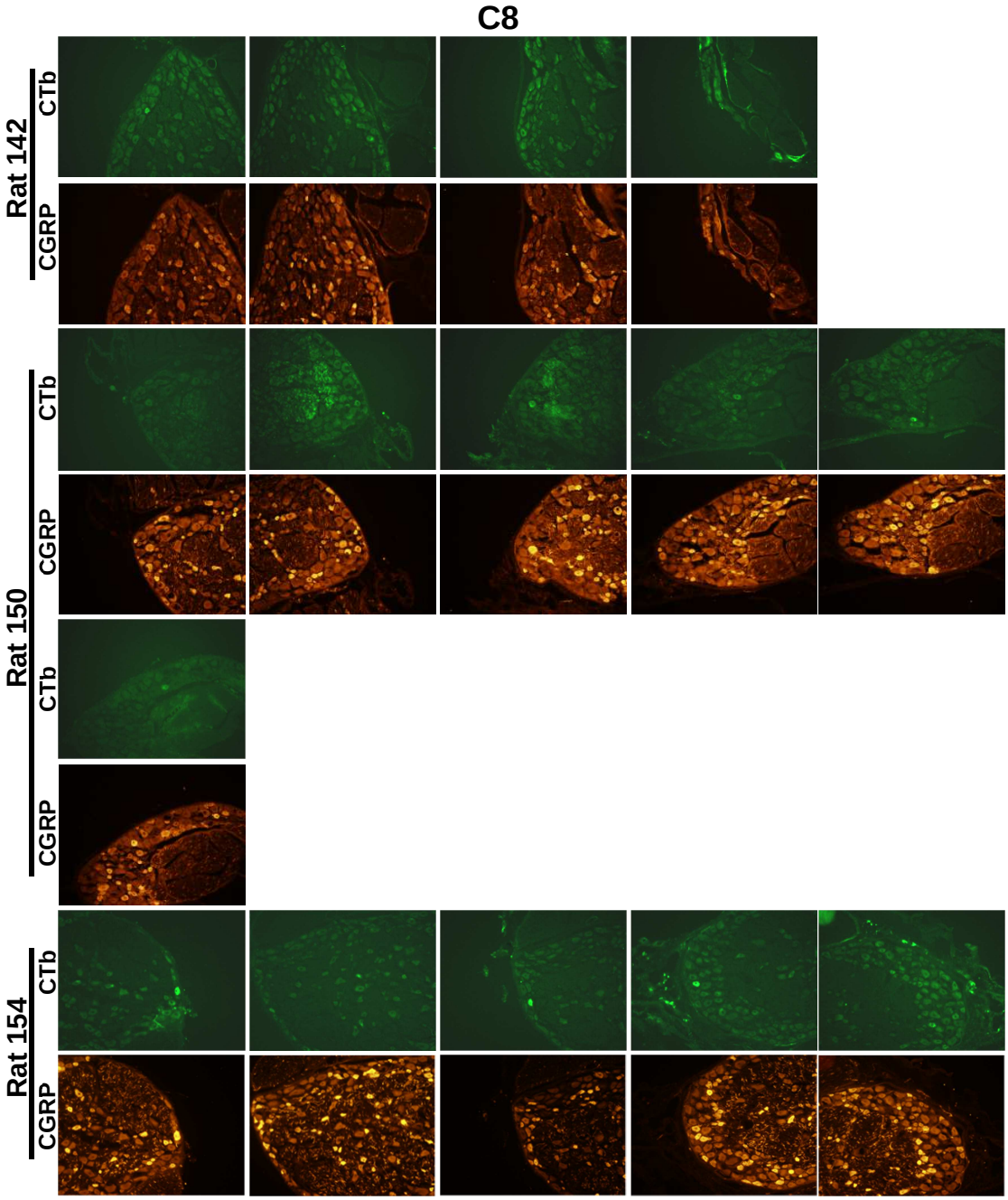


**Figure H.2.D.** CTb and CGRP-labeled sections of the C8 DRG from Rats 142, 150, and 154 in the sham group. For each rat, the images presented correspond to those sections for which CTb-labeled neurons were identified as summarized in Table H.5. For each rat, slide number and section number increase from left to right. For each CTb-labeled image, the corresponding CGRP-labeled image is presented immediately below it. Figure is continued on the next page.

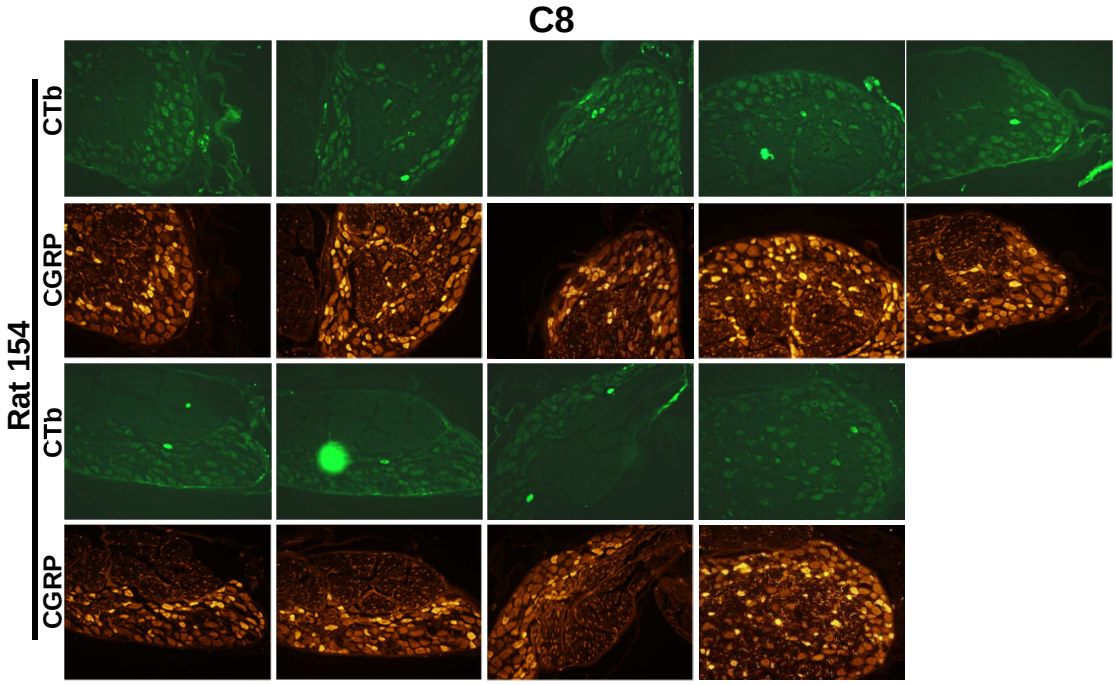


**Figure H.2.D.** CTb and CGRP-labeled sections of the C8 DRG from Rat 154 in the sham group. For each rat, the images presented correspond to those sections for which CTb-labeled neurons were identified as summarized in Table H.5. For each rat, slide number and section number increase from left to right. For each CTb-labeled image, the corresponding CGRP-labeled image is presented immediately below it.

**Table H.6. Neuronal size and CGRP classification for each CTb-positive neuron for each rat in the normal group (Chapter 4).**

| Level | Rat | Slide | Section | Area ($\mu m^2$) | CGRP expression |
|---|---|---|---|---|---|
| C5 | 135 | N/A | N/A | N/A | N/A |
| | 136 | 5 | 3 | 664.0 | - |
| | 138 | 1 | 13_top right | 744.3 | + |
| | | | 13_bottom left | 1109.5 | - |
| | | 2 | 6 | 950.2 | - |
| | | | 9 | 760.9 | - |
| | 140 | 4 | 4 | 453.1 | + |
| C6 | 135 | 1 | 5 | 451.4 | - |
| | | 6 | 4 | 683.1 | + |
| | | 8 | 7 | 814.6 | + |
| | 136 | 2 | 8 | 1216.5 | - |
| | | 3 | 8 | 1626.2 | - |
| | | 5 | 1 | 833.3 | - |
| | 138 | 1 | 8_bottom | 483.0 | - |
| | | | 8_top | 974.7 | - |
| | | | 10 | 664.0 | + |
| | | 2 | 3 | 877.4 | + |
| | | | 6 | 1142.0 | - |
| | | | 8 | 561.6 | + |
| | | | 10 | 869.9 | - |
| | | | 14 | 1125.8 | - |
| | | 3 | 1 | 835.4 | + |
| | | | 4 | 1137.4 | + |
| | | 4 | 5 | 869.9 | + |
| | 140 | 1 | 9 | 1266.4 | - |
| | | 2 | 10 | 1061.3 | - |
| | | | 14 | 309.5 | - |
| | | 3 | 2 | 1214.0 | + |
| | | | 11_top right | 656.5 | + |
| | | | 11_bottom left | 713.5 | + |
| | | 4 | 2 | 466.4 | + |
| | | | 4 | 1474.4 | + |
| | | 5 | 15 | 1147.8 | + |
| | | | 16 | 1456.1 | + |

Note: Table continued on next page. In the Section column, designators such as left, right, top, & bottom are used to specify a single neuron when multiple CTb-positive neurons are evident in that section. For cells labeled N/A, no CTb-positive neurons were detected for that rat at that spinal level.

| Level | Rat | Slide | Section | Area ($\mu m^2$) | CGRP expression |
|---|---|---|---|---|---|
| C7 | 135 | 1 | 2 | 926.1 | + |
| | | | 5 | 723.5 | - |
| | | | 9 | 847.4 | - |
| | | | 10 | 485.9 | + |
| | | 2 | 3 | 882.8 | - |
| | | | 5 | 611.6 | + |
| | | | 8 | 810.8 | - |
| | | | 9 | 852.0 | - |
| | | 3 | 1 | 681.0 | - |
| | | | 2 | 570.4 | - |
| | | | 5 | 702.3 | + |
| | | | 6 | 1520.6 | + |
| | | 4 | 2 | 580.4 | - |
| | | | 5 | 590.8 | - |
| | | 5 | 2 | 586.2 | - |
| | | | 8 | 727.6 | - |
| | | | 9 | 708.1 | - |
| | | 6 | 2 | 459.7 | - |
| | | | 7 | 709.3 | - |
| | | | 8_top | 746.3 | + |
| | | | 8_bottom left | 946.9 | + |
| | | | 8_bottom right | 587.4 | + |
| | | 7 | 2_top left | 525.0 | - |
| | | | 2_bottom right | 864.1 | + |
| | | | 10 | 432.7 | - |
| | | 8 | 2 | 591.2 | - |
| | | | 4 | 676.0 | + |
| | | | 6_top | 628.2 | + |
| | | | 6_bottom | 582.0 | - |
| | 136 | 2 | 10 | 953.1 | + |
| | | 3 | 5 | 1426.5 | - |
| | | 4 | 5 | 421.4 | + |
| | | | 9 | 663.1 | - |
| | | 5 | 9 | 1016.8 | - |
| | | 6 | 6_top | 892.4 | - |
| | | | 6_bottom | 587.0 | - |
| | | | 8 | 694.3 | - |
| | | 7 | 5 | 597.4 | + |
| | | | 6 | 998.9 | - |
| | | 8 | 1 | 796.7 | - |
| | | | 6 | 764.7 | - |
| | | | 7 | 903.2 | + |
| | | 9 | 2_top left | 669.8 | + |
| | | | 2_bottom right | 842.0 | + |

Note: Table continued on next page. In the Section column, designators such as left, right, top, & bottom are used to specify a single neuron when multiple CTb-positive neurons are evident in that section.

| Level | Rat | Slide | Section | Area ($\mu m^2$) | CGRP expression |
|---|---|---|---|---|---|
| C7 | 138 | 3 | 12 | 765.9 | + |
| | | | 13 | 934.8 | + |
| | | | 15 | 719.3 | - |
| | | 4 | 1 | 822.9 | - |
| | | | 5 | 685.6 | + |
| | | | 8 | 949.4 | - |
| | | | 10 | 932.3 | + |
| | | | 13_left | 633.2 | - |
| | | | 13_right | 1014.7 | + |
| | | | 15 | 627.8 | + |
| | | 5 | 1_top | 590.8 | - |
| | | | 2 | 840.4 | - |
| | | | 6 | 815.0 | - |
| | | | 14_middle | 660.6 | - |
| | | | 14_top left | 1356.2 | - |
| | | 6 | 1 | 696.8 | - |
| | | | 3 | 745.1 | - |
| | | | 10 | 361.9 | - |
| | | | 13 | 842.9 | + |
| | | 7 | 7 | 881.1 | + |
| | | 8 | 2_top | 527.5 | + |
| | | | 2_bottom | 815.8 | - |
| | 140 | 1 | 9 | 651.5 | + |
| | | 2 | 10 | 428.1 | + |
| | | 3 | 5 | 425.2 | + |
| | | 4 | 4_right | 1015.9 | + |
| | | | 4_left | 615.3 | + |
| | | | 5_top left | 689.4 | - |
| | | | 5_bottom right | 669.8 | + |
| | | | 6 | 632.8 | - |
| | | | 8_right | 518.8 | - |
| | | | 8_left | 615.3 | + |
| | | | 11 | 773.4 | + |
| | | | 13 | 527.9 | - |
| | | 5 | 1 | 368.6 | - |
| | | | 2_right | 473.0 | + |
| | | | 2_left | 712.2 | - |
| | | | 3 | 808.8 | + |
| | | | 11 | 449.3 | + |
| C8 | 135 | 2 | 6 | 384.0 | + |
| | | 3 | 6 | 628.2 | - |
| | | 4 | 4 | 347.0 | - |
| | | | 5 | 712.7 | - |
| | | | 7 | 470.9 | + |
| | | 5 | 2_left | 709.3 | - |
| | | | 3 | 510.0 | + |
| | | 6 | 5 | 596.6 | + |
| | | 7 | 8 | 773.4 | + |
| | | 8 | 1 | 644.4 | + |
| | | | 2 | 800.8 | - |
| | | | 8 | 800.4 | - |
| | | | 11 | 629.9 | - |

Note: Table continued on next page. In the Section column, designators such as left, right, top, & bottom are used to specify a single neuron when multiple CTb-positive neurons are evident in that section.

| Level | Rat | Slide | Section | Area ($\mu m^2$) | CGRP expression |
|---|---|---|---|---|---|
| C8 | 136 | 2 | 6 | 902.4 | + |
| | | 6 | 9 | 738.4 | + |
| | | 7 | 1 | 674.4 | + |
| | | | 7 | 795.4 | - |
| | | 9 | 4 | 945.2 | + |
| | | | 6 | 546.7 | + |
| | 138 | 2 | 6 | 852.4 | - |
| | | | 7_bottom | 909.8 | + |
| | | | 10 | 627.4 | + |
| | | 3 | 12 | 981.8 | + |
| | | | 13_top | 1056.7 | + |
| | | 4 | 8 | 964.3 | + |
| | | | 13 | 1037.6 | + |
| | | 5 | 5 | 492.2 | + |
| | | | 10 | 593.7 | + |
| | | | 11 | 674.0 | + |
| | | | 14 | 1039.2 | + |
| | 140 | 2 | 9 | 784.2 | + |
| | | 3 | 8 | 842.0 | + |
| | | | 9 | 677.3 | + |
| | | | 11 | 635.7 | - |
| | | | 12_top right | 732.2 | + |
| | | | 12_bottom left | 677.3 | - |
| | | | 14_top | 993.5 | + |
| | | | 14_bottom | 745.9 | + |
| | | 4 | 3 | 991.4 | + |
| | | | 4 | 487.6 | - |
| | | | 13 | 800.0 | + |
| | | | 14 | 734.3 | + |
| | | 5 | 7 | 808.3 | + |
| | | | 8 | 1430.7 | + |
| | | | 10 | 716.8 | + |

Note: In the Section column, designators such as left, right, top, & bottom are used to specify a single neuron when multiple CTb-positive neurons are evident in that section.

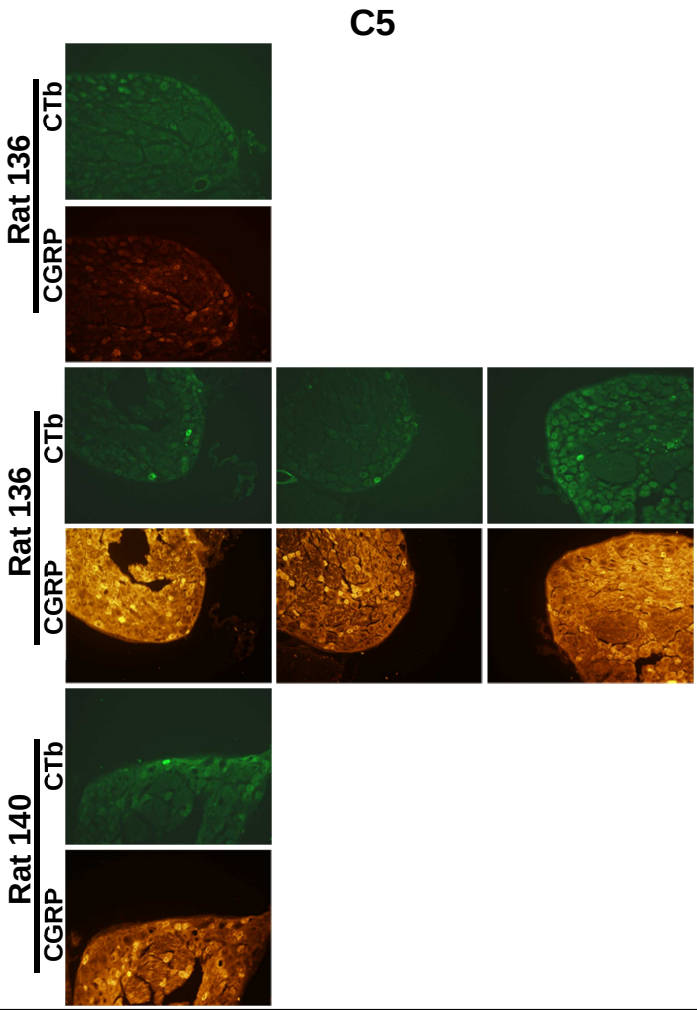


**Figure H.3.A.** CTb and CGRP-labeled sections of the C5 DRG from Rats 136 and 140 in the normal group. For each rat, the images presented correspond to those sections for which CTb-labeled neurons were identified as summarized in Table H.6. For each rat, slide number and section number increase from left to right. For each CTb-labeled image, the corresponding CGRP-labeled image is presented immediately below it.

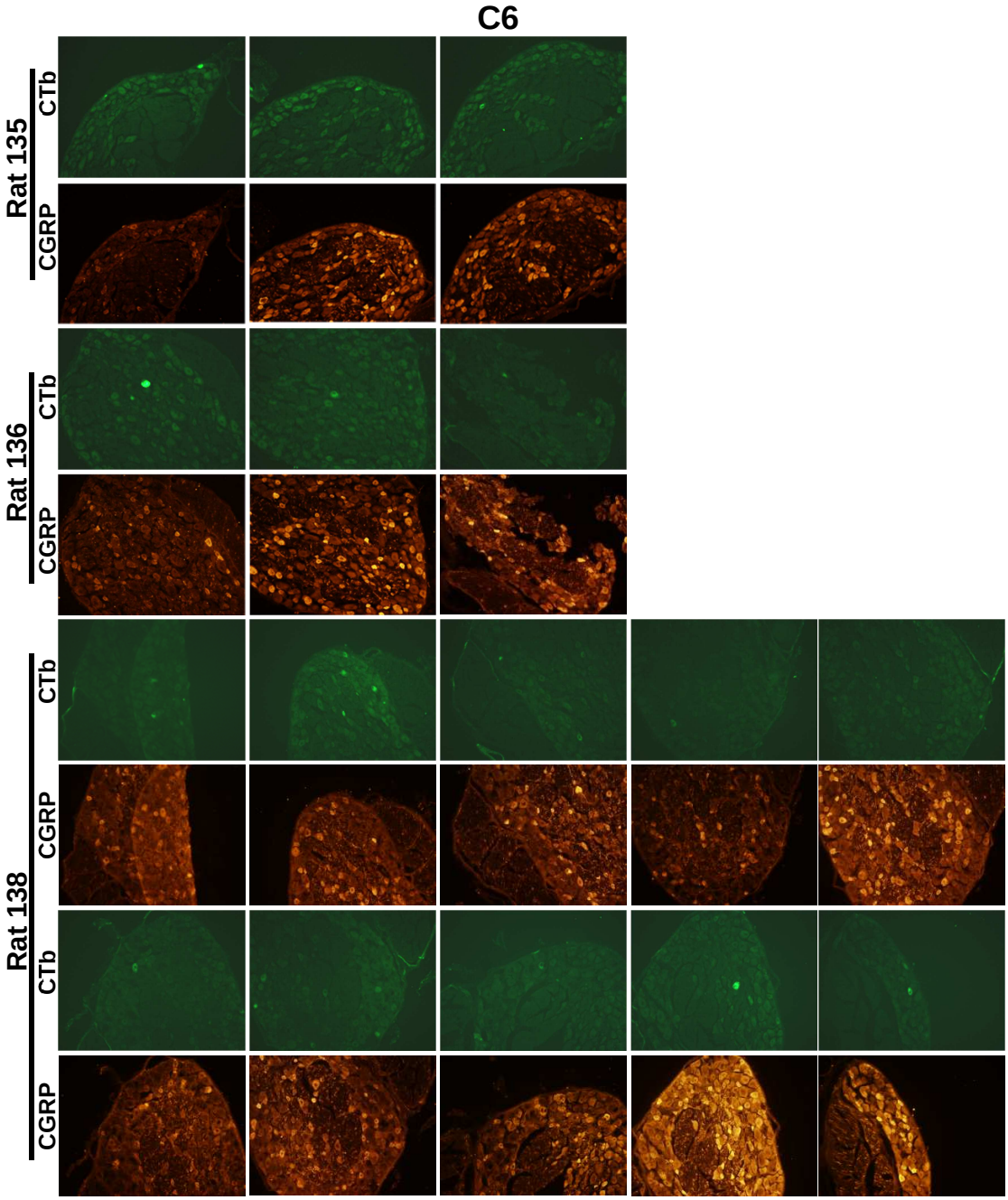


**Figure H.3.B.** CTb and CGRP-labeled sections of the C6 DRG from Rats 135, 136, and 138 in the normal group. For each rat, the images presented correspond to those sections for which CTb-labeled neurons were identified as summarized in Table H.6. For each rat, slide number and section number increase from left to right. For each CTb-labeled image, the corresponding CGRP-labeled image is presented immediately below it. Figure is continued on the next page.

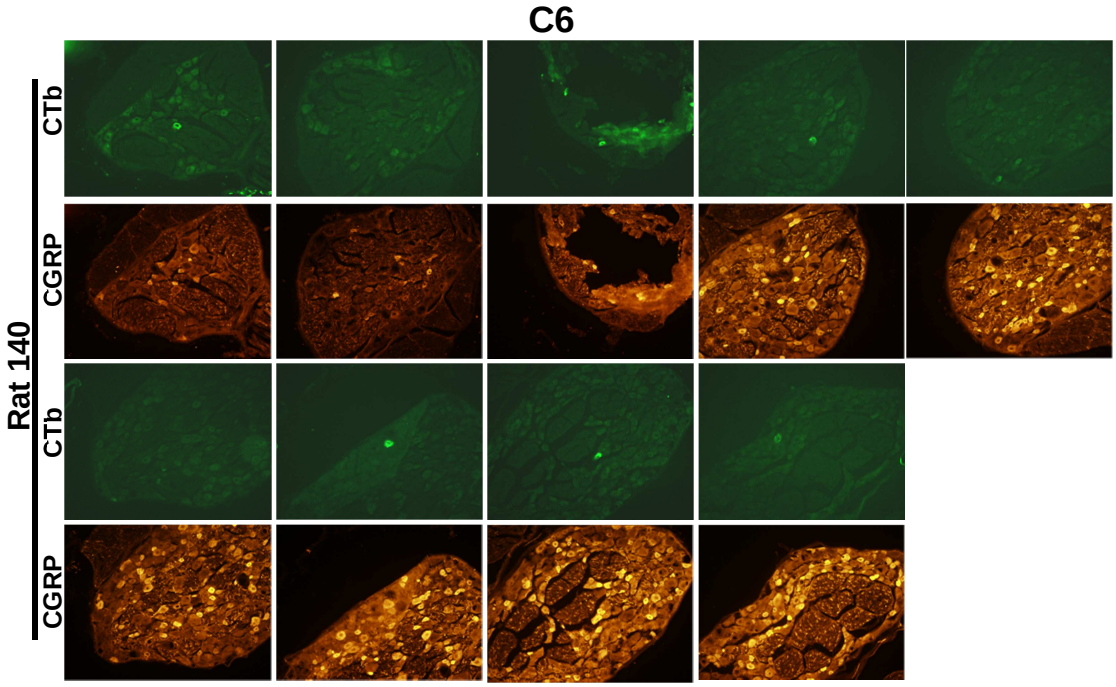


**Figure H.3.B.** CTb and CGRP-labeled sections of the C6 DRG from Rat 140 in the normal group. For each rat, the images presented correspond to those sections for which CTb-labeled neurons were identified as summarized in Table H.6. For each rat, slide number and section number increase from left to right. For each CTb-labeled image, the corresponding CGRP-labeled image is presented immediately below it.

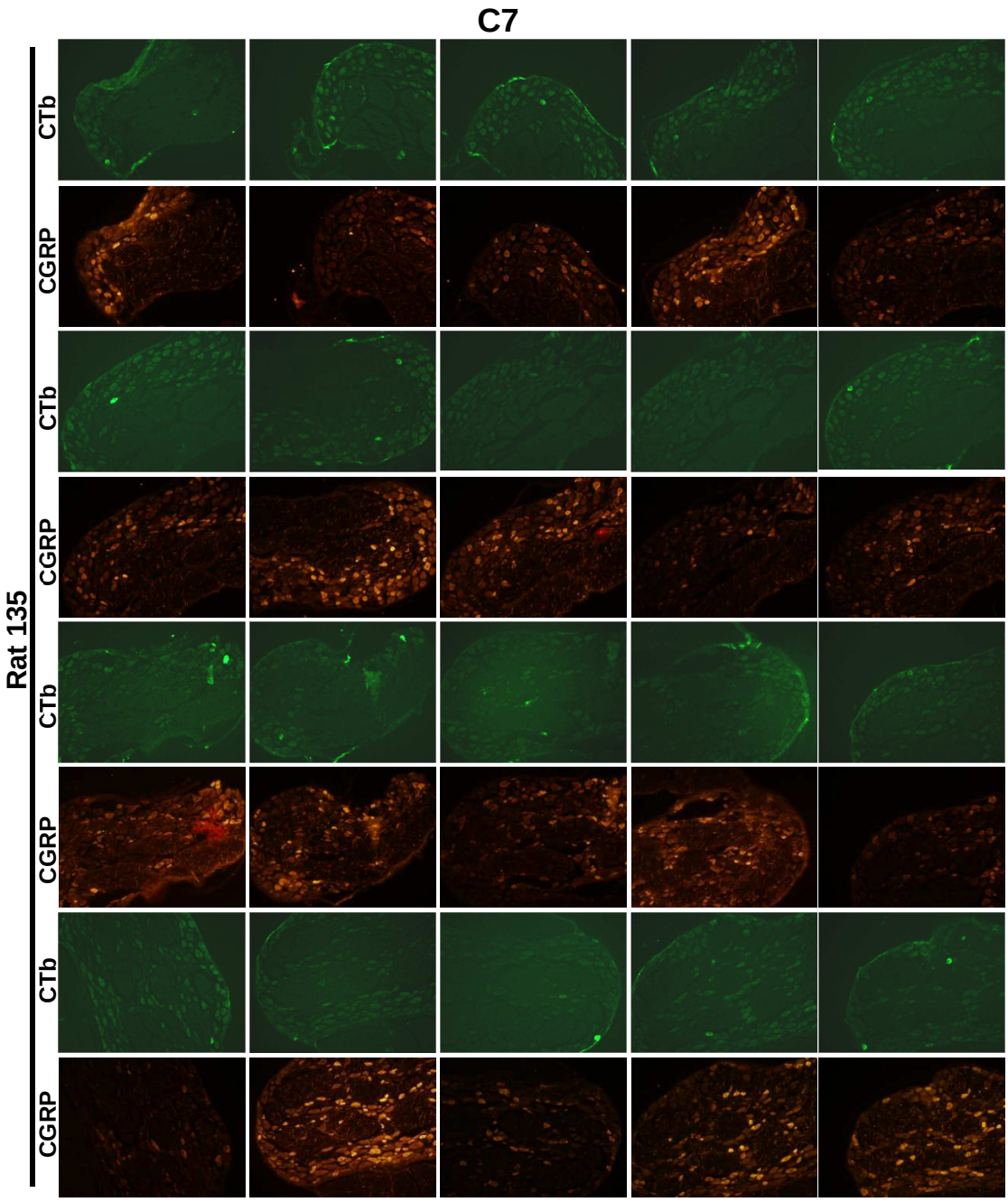


**Figure H.3.C.** CTb and CGRP-labeled sections of the C7 DRG from Rat 135 in the normal group. For each rat, the images presented correspond to those sections for which CTb-labeled neurons were identified as summarized in Table H.6. For each rat, slide number and section number increase from left to right. For each CTb-labeled image, the corresponding CGRP-labeled image is presented immediately below it. Figure is continued on the next page.

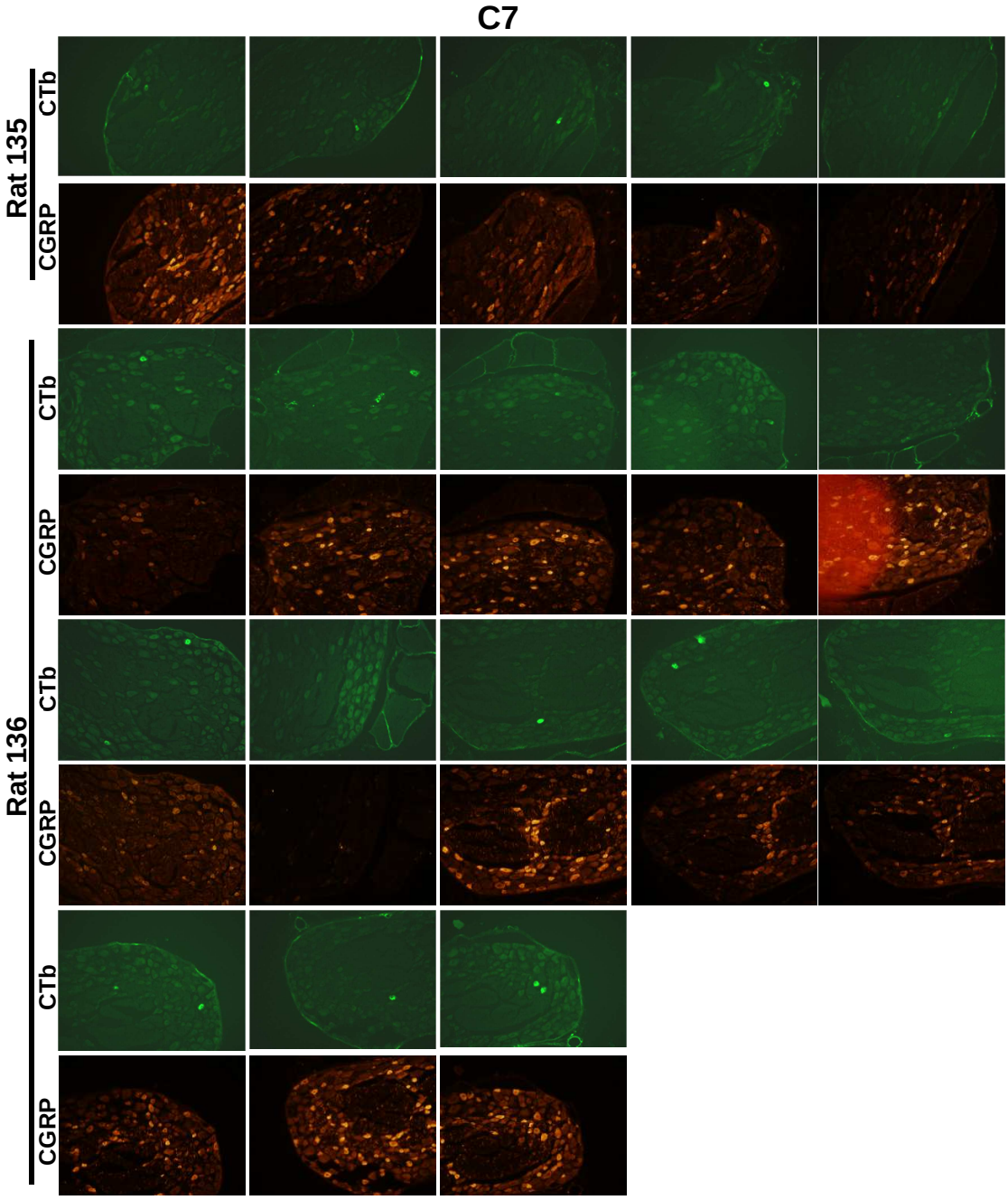


**Figure H.3.C.** CTb and CGRP-labeled sections of the C7 DRG from Rats 135 and 136 in the normal group. For each rat, the images presented correspond to those sections for which CTb-labeled neurons were identified as summarized in Table H.6. For each rat, slide number and section number increase from left to right. For each CTb-labeled image, the corresponding CGRP-labeled image is presented immediately below it. Figure is continued on the next page.

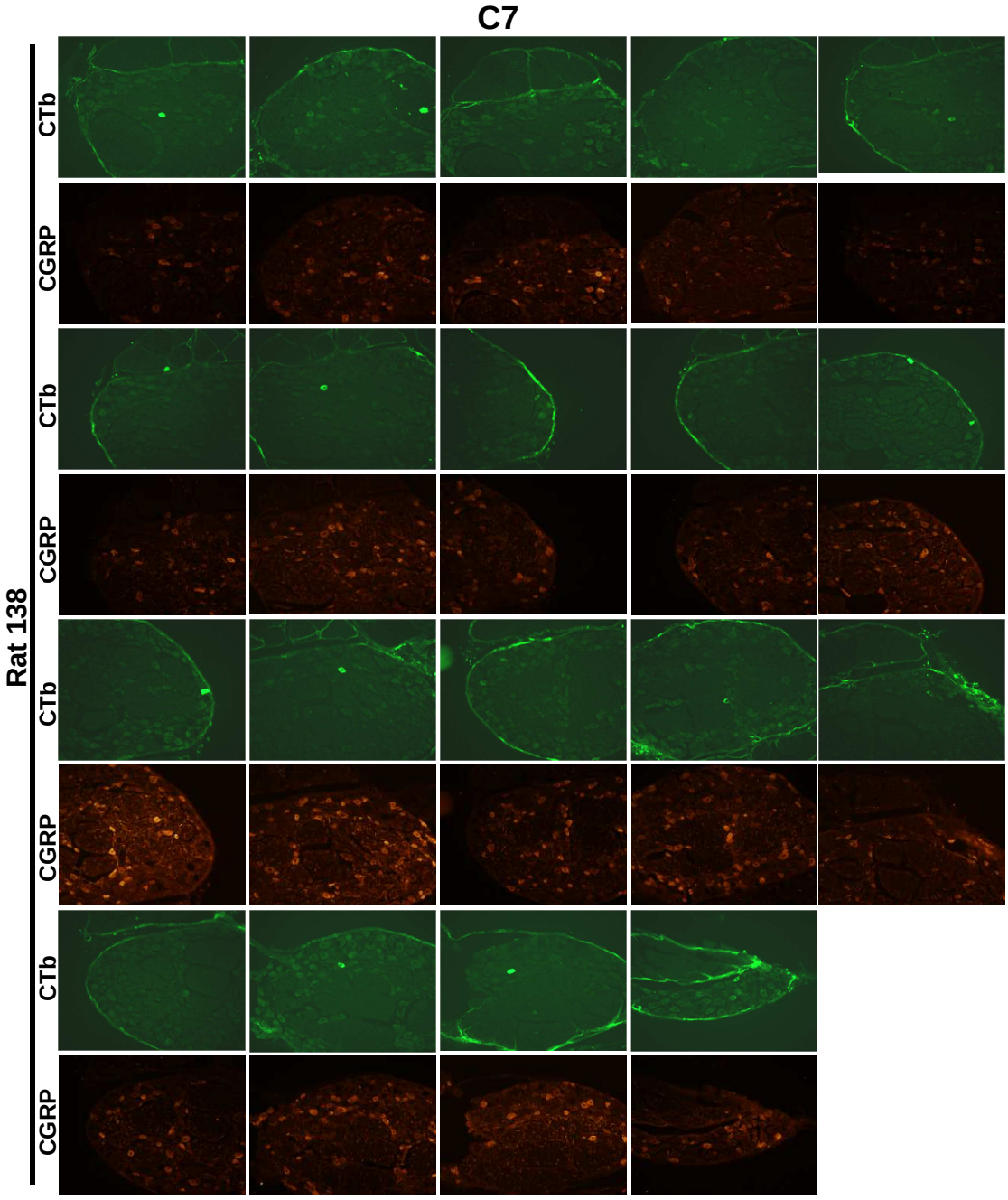


**Figure H.3.C.** CTb and CGRP-labeled sections of the C7 DRG from Rat 138 in the normal group. For each rat, the images presented correspond to those sections for which CTb-labeled neurons were identified as summarized in Table H.6. For each rat, slide number and section number increase from left to right. For each CTb-labeled image, the corresponding CGRP-labeled image is presented immediately below it. Figure is continued on the next page.

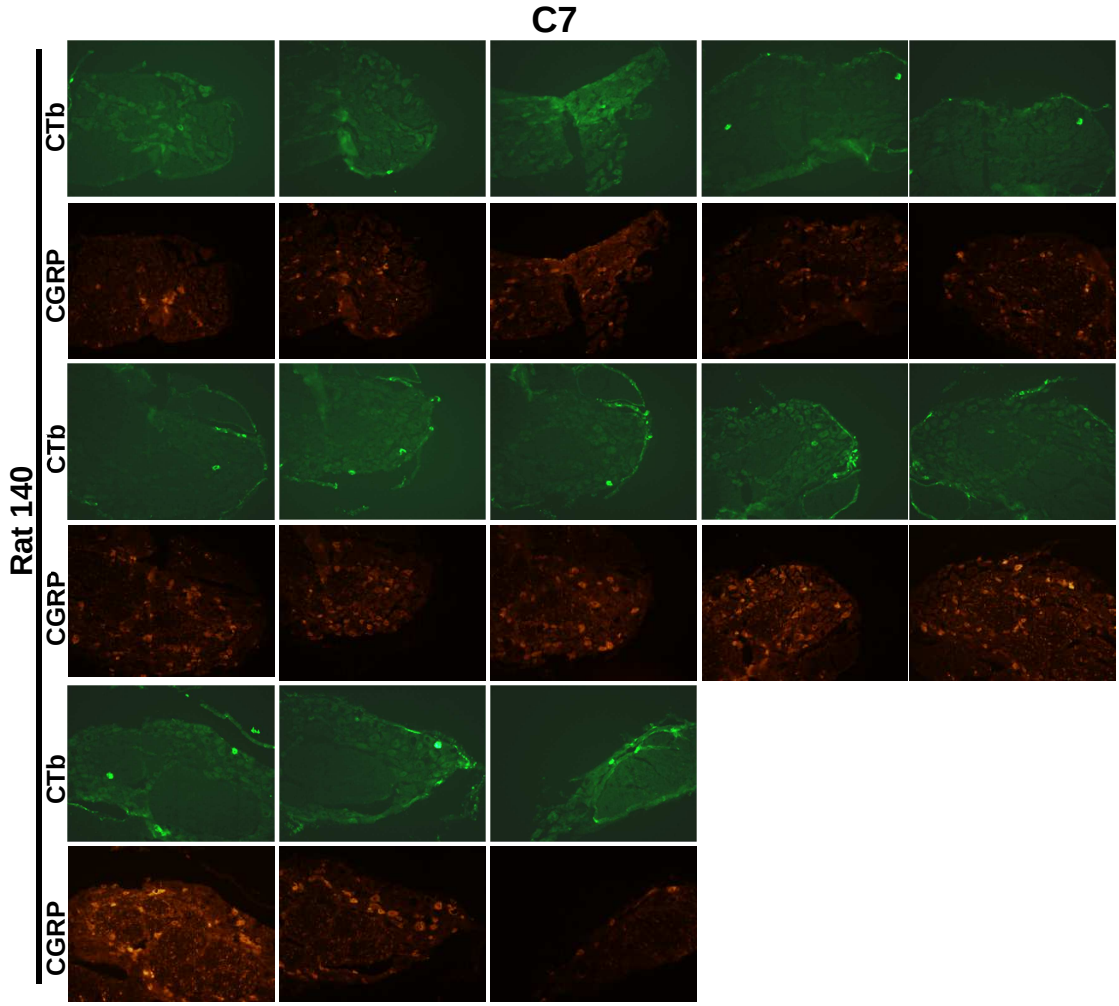


**Figure H.3.C.** CTb and CGRP-labeled sections of the C7 DRG from Rat 140 in the normal group. For each rat, the images presented correspond to those sections for which CTb-labeled neurons were identified as summarized in Table H.6. For each rat, slide number and section number increase from left to right. For each CTb-labeled image, the corresponding CGRP-labeled image is presented immediately below it.

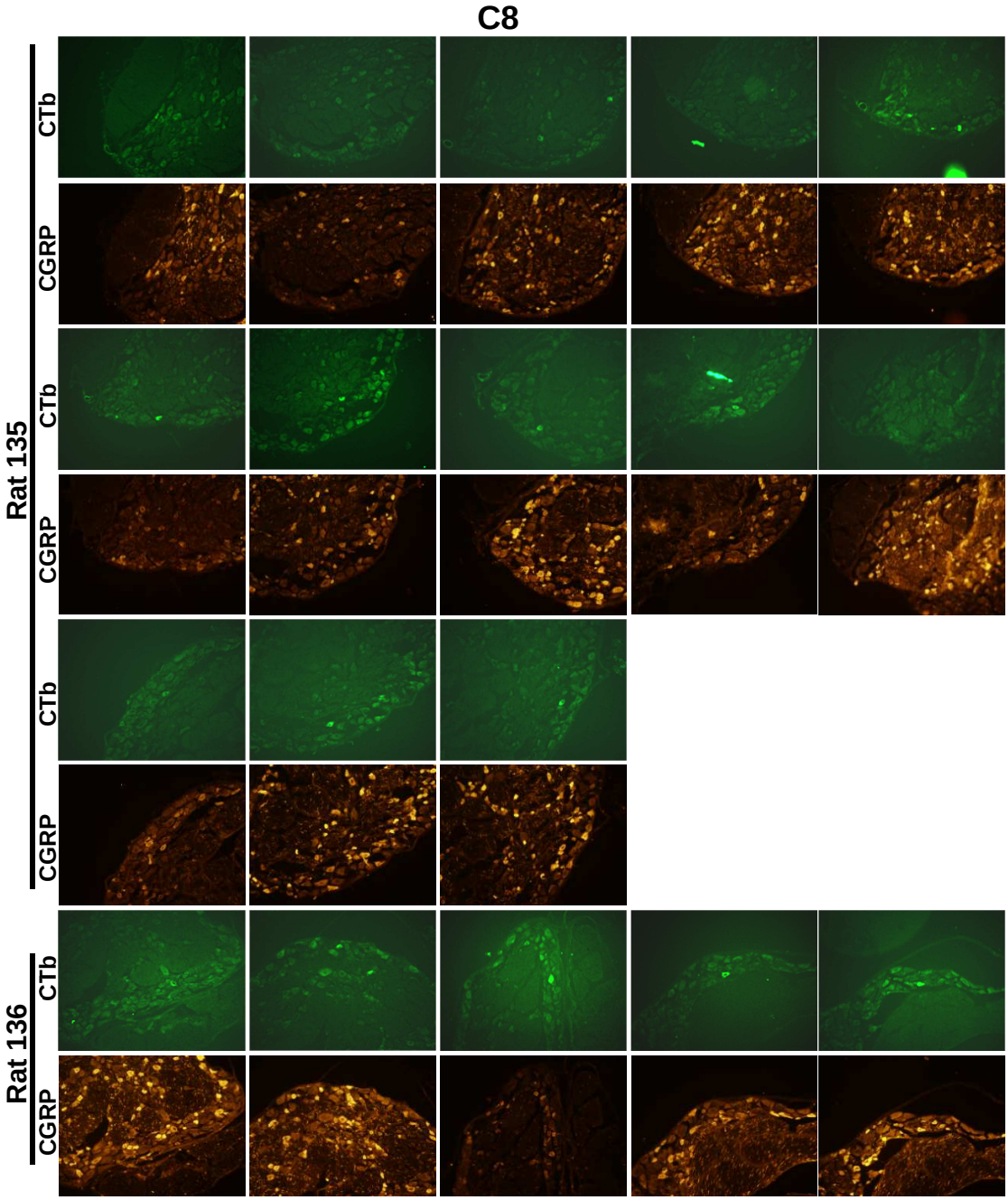


**Figure H.3.D.** CTb and CGRP-labeled sections of the C8 DRG from Rats 135 and 136 in the normal group. For each rat, the images presented correspond to those sections for which CTb-labeled neurons were identified as summarized in Table H.6. For each rat, slide number and section number increase from left to right. For each CTb-labeled image, the corresponding CGRP-labeled image is presented immediately below it. Figure is continued on the next page.

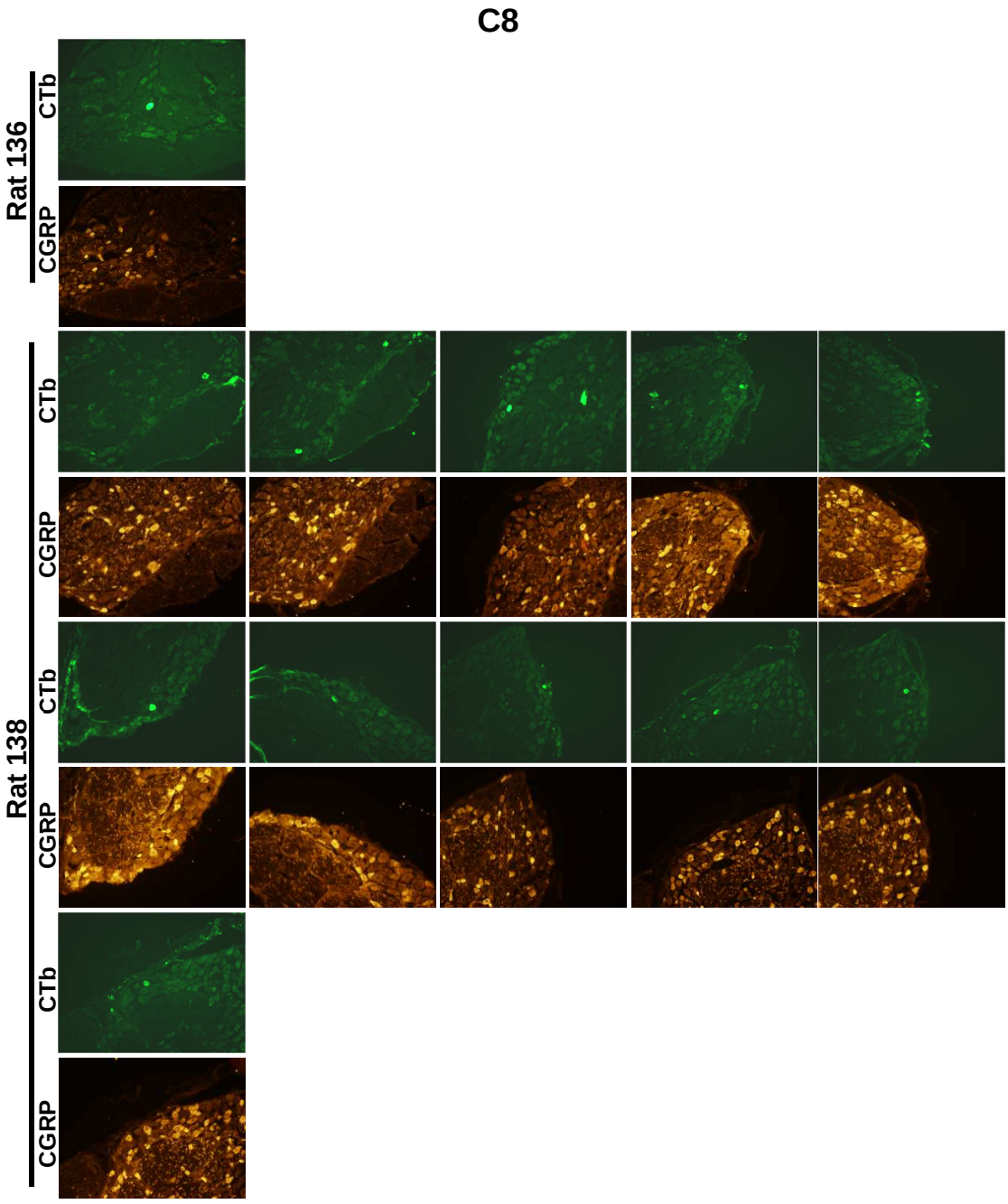


**Figure H.3.D.** CTb and CGRP-labeled sections of the C8 DRG from Rats 136 and 138 in the normal group. For each rat, the images presented correspond to those sections for which CTb-labeled neurons were identified as summarized in Table H.6. For each rat, slide number and section number increase from left to right. For each CTb-labeled image, the corresponding CGRP-labeled image is presented immediately below it. Figure is continued on the next page.

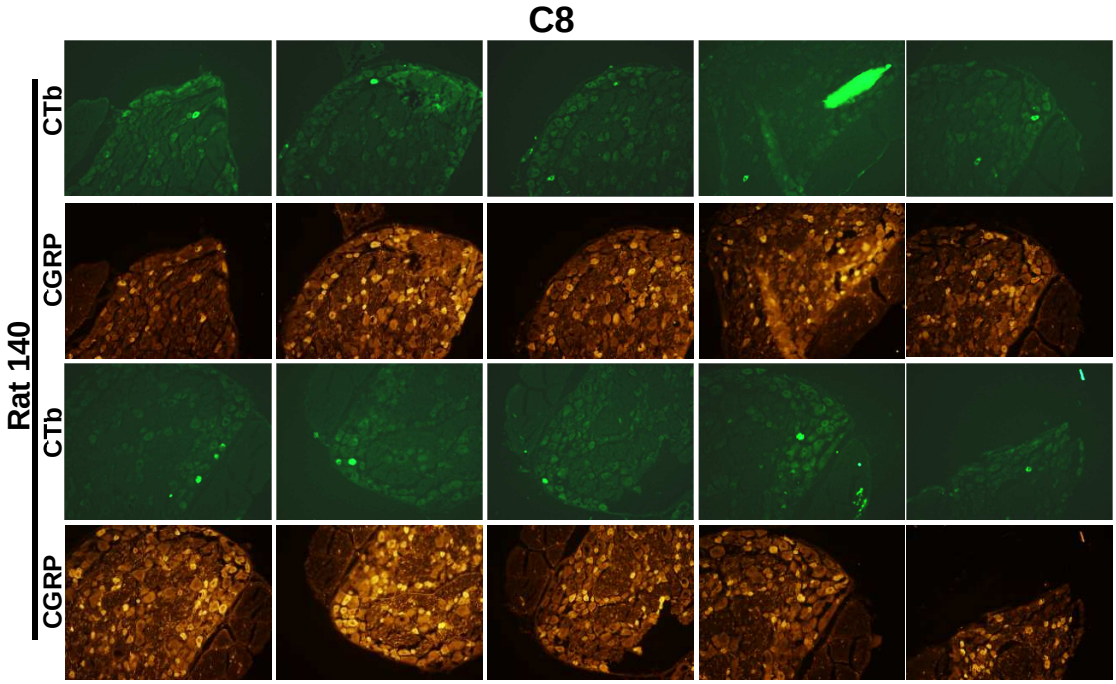


**Figure H.3.D.** CTb and CGRP-labeled sections of the C8 DRG from Rat 140 in the normal group. For each rat, the images presented correspond to those sections for which CTb-labeled neurons were identified as summarized in Table H.6. For each rat, slide number and section number increase from left to right. For each CTb-labeled image, the corresponding CGRP-labeled image is presented immediately below it.

# REFERENCES

Aley KO, Messing RO, Mochly-rosen D, Levine JD. Chronic hypersensitivity for inflammatory nociceptor sensitization mediated by the epsilon isozyme of protein kinase C. *J Neurosci* 2000; 20: 4680-4685.

Al-Khater KM, Kerr R, Todd AJ. A quantitative study of spinothalamic neurons in laminae I, III, and IV in lumbar and cervical segments of the rat spinal cord. *J Comp Neurol* 2008; 511: 1-18.

Allen KD, Adams SB Jr, Mata BA, Shamji MF, Gouze E, Jing L, Nettles DL, Latt LD, Setton LA. Gait and behavior in an IL1β-mediated model of rat knee arthritis and effects of an IL1 antagonist. *J Orthop Res* 2011; 29: 694-703.

Aloe L, Tuveri MA, Levi-Montalcini R. Studies on carrageenan-induced arthritis in adult rats: presence of nerve growth factor and role of sympathetic innervation. *Rheumatol Int* 1992; 12: 213-216.

Amann R, Schuligoi R, Herzeg G, Donnerer J. Intraplantar injection of nerve growth factor into the rat hind paw: local edema and effects on thermal nociceptive threshold. *Pain* 1996; 64: 323-329.

Amaya F, Shimosato G, Nagano M, Ueda M, Hashimoto S, Tanaka Y, Suzuki H, Tanaka M. NGF and GDNF differentially regulate TRPV1 expression that contributes to development of inflammatory thermal hyperalgesia. *Eur J Neurosci* 2004; 20: 2303-2310.

Apfel SC, Wright DE, Wiideman AM, Dormia C, Snider WD, Kessler JA. Nerve growth factor regulates the expression of brain-derived neurotrophic factor mRNA in the peripheral nervous system. *Mol Cell Neurosci* 1996; 7: 134-142.

Apkarian AV, Bushnell MC, Treede RD, Zubieta JK. Human brain mechanisms of pain perception and regulation in health and disease. *Eur J Pain* 2005; 9: 463-484.

Appleton CT, McErlain DD, Henry JL, Holdsworth DW, Beier F. Molecular and histological analysis of a new rat model of experimental knee osteoarthritis. *Ann N Y Acad Sci* 2007; 1117: 165-174.

Ashraf S, Mapp PI, Burston J, Bennett AJ, Chapman V, Walsh DA. Augmented pain behavioural responses to intra-articular injection of nerve growth factor in two animal models of osteoarthritis. *Ann Rheum Dis* 2014; 73: 1710-1718.

Barbe MF, Gallagher S, Massicotte VS, Tytell M, Popoff SN, Barr-Gillespie AE. The interaction of force and repetition on musculoskeletal and neural tissue responses and sensorimotor behavior in a rat model of work-related musculoskeletal disorders. *BMC Musculoskelet Disord* 2013; 14: 303.

Barnsley L, Bogduk N. Medial branch blocks are specific for the diagnosis of cervical zygapophyseal joint pain. *Reg Anesth* 1993; 18: 343-350.

Barnsley L, Lord S, Bogduk N. Comparative local anaesthetic blocks in the diagnosis of cervical zygapophysial joint pain. *Pain* 1993; 55: 99-106.

Barnsley L, Lord SM, Wallis BJ, Bogduk N. Lack of effect of intraarticular corticosteroids for chronic pain in the cervical zygapophyseal joints. *N Engl J Med* 1994; 330: 1047-1050.

Barnsley L, Lord SM, Wallis BJ, Bogduk N. The prevalence of chronic cervical zygapophyseal joint pain after whiplash. *Spine* 1995; 20: 20-26.

Barnsley L. Percutaneous radiofrequency neurotomy for chronic neck pain: outcomes in a series of consecutive patients. *Pain Med* 2005; 6: 282-286.

Barthel C, Yeremenko N, Jacobs R, Schmidt RE, Bernateck M, Zeidler H, Tak PP, Baeten D, Rihl M. Nerve growth factor and receptor expression in rheumatoid arthritis and spondyloarthritis. *Arthritis Res Ther* 2009; 11: R82.

Basbaum AI, Bautista DM, Scherrer G, Julius D. Cellular and molecular mechanisms of pain. *Cell* 2009; 139: 267-284.

Berge O. Animal models of pain. In: Textbook of Pain, McMahon SB, Koltzenburg M, Tracey I, Turk DC, Eds., *Philadelphia: Saunders*, 2013; 170-181.

Berglund A, Alfredsson L, Cassidy JD, Jensen I, Nygren A. The association between exposure to a rear-end collision and future neck or shoulder pain: a cohort study. *J Clin Epidemiol* 2000; 53: 1089-1094.

Bergman E, Ulfhake B. Loss of primary sensory neurons in the very old rat: neuron number estimates using the dissector method and confocal optical sectioning. *J Comp Neurol* 1998; 396: 211-222.

Bird GC, Han JS, Fu Y, Adwanikar H, Willis WD, Neugebauer V. Pain-related synaptic plasticity in spinal dorsal horn neurons: role of CGRP. *Mol Pain* 2006; 2: 31.

Birklein F, Schmelz M. Neuropeptides, neurogenic inflammation and complex regional pain syndrome (CRPS). *Neurosci Lett* 2008; 437: 199-202.

Boettger MK, Hensellek S, Richter F, Gajda M, Stöckigt R, von Ganchet GS, Bräuer R, Schaible HG. Antinociceptive effects of tumor necrosis factor alpha neutralization in a rat model of antigen-induced arthritis: evidence of a neuronal target. *Arthritis Rheum* 2008; 58: 2368-2378.

Bogduk N, Aprill C. On the nature of neck pain, discography and cervical zygapophysial joint blocks. *Pain* 1993; 54: 213-7.

Bogduk N, Yoganandan N. Biomechanicsl of the cervical spine Part 3: minor injuries. *Clin Biomech* 2001; 16: 267-275.

Bogduk N. On cervical zygapophysial joint pain after whiplash. *Spine* 2011; 36: S194-S199.

Boivie J. Central pain and the role of quantitative sensory testing (QST) in research and diagnosis. *Eur J Pain* 2003; 7: 339-343.

Borchgrevink GE, Kaasa A, McDonagh D, Stiles TC, Haraldseth O, lereim I. Acute treatment of whiplash neck sprain injuries. A randomized trial of treatment during the first 14 days after a car accident. *Spine* 1998; 23: 25-31.

Bove SE, Calcaterra SL, Brooker RM, Huber CM, Guzman RE, Juneau PL, Schrier DJ, Kilgore KS. Weight bearing as a measure of disease progression and efficacy of anti-inflammatory compounds in a model of monosodium iodoacetate-induced osteoarthritis. *Osteoarthritis Cartilage* 2003; 11: 821-830.

Bramson C, Herrmann DN, Carey W, Keller D, Brown MT, West CR, Verburg KM, Dyck PJ. Exploring the role of tanezumab as a novel treatment for the relief of neuropathic pain. *Pain Med* 2015; Epub ahead of print.

Bradesi S. Role of spinal cord glia in the central processing of peripheral pain perception. *Neurogastroenterol Motil* 2010; 22: 499-511.

Brown MT, Herrmann DN, Goldstein M, Burr AM, Smith MD, West CR, Verburg KM, Dyck PJ. Nerve safety of tanezumab, a nerve growth factor inhibitor for pain treatment. *J Neurol Sci* 2014; 345: 139-147.

Brown MT, Murphy FT, Radin DM, Davignon I, Smith MD, West CR. Tanezumab reduces osteoarthritic knee pain: results of a randomized, double-blind, placebo-controlled phase III trial. *J Pain* 2012; 13: 790-798.

Buchanan WW, Kean WF. Osteoarthritis II: pathology and pathogenesis. *Inflammopharmacology* 2002; 10: 23-52.

Calvino B, Villanueva L, Le Bars D. dorsal horn (convergent) neurons in the intact anaesthetized arthritic rat. I. Segmental excitatory influences. *Pain* 1987; 28: 81-98.

Caron JP, Fernandes JC, Martel-Pelletier J, Tardif G, Mineau F, Geng C, Pelletier JP. Chondroprotective effect of intraarticular injections of interleukin-1 receptor antagonist in experimental osteoarthritis. Suppression of collagenase-1 expression. *Arthritis Rheum* 1996; 39: 1535-1544.

Carr FB, Geranton SM, Hunt SP. Descending controls modulate inflammatory joint pain and regulate CXC chemokine and iNOS expression in the dorsal horn. *Mol Pain* 2014; 10: 39.

Carroll LJ, Holm LW, Hogg-Johnson S, Cote P, Cassidy JD, Haldeman S, Nordin M, Hurwitz EL, Carragee EJ, van der Velde G, Peloso PM, Guzman J. Course and prognostic factors for neck pain in whiplash-associated disorders (WAD): results of the Bone and Joint Decade 2000-2010 Task Force on Neck Pain and Its Associated Disorders. *J Manipulative Physiol Ther* 2009; 32: S97-S107.

Cavanaugh JM, el-Bohy A, Hardy WN, Getchell TV, Getchell ML, King AI. Sensory innervation of soft tissues of the lumbar spine in the rat. *J Orthop Res* 1989; 7: 378-388.

Cavanaugh JM, Lu Y, Chen C, Kallakuri S. Pain generation in lumbar and cervical facet joints. *J Bone Joint Surg Am* 2006; 88: 63-67.

Cavanaugh JM, Ozaktay AC, Yamashita HT, King AI. Lumbar facet pain: biomechanics, neuroanatomy and neurophysiology. *J Biomech* 1996; 29: 1117-1129.

Cavanaugh JM, Ozaktay AC, Yamashita T, Avramov A, Getchell TV, King AI. Mechanisms of low back pain: a neurophysiologic and neuroanatomic study. *Clin Orthop Relat Res* 1997; 335: 166-180.

Chaplan SR, Bach FW, Pogrel JW, Chung JM, Yaksh TL. Quantitative assessment of tactile allodynia in the rat paw. *J Neurosci Methods* 1994; 53: 55-63.

Chen C, Lu Y, Kallakuri S, Patwardhan A, Cavanaugh JM. Distribution of A-delta and C-fiber receptors in the cervical facet joint capsule and their response to stretch. *J Bone Joint Surg Am* 2006; 88: 1807-1816.

Chen FL, Dong YL, Zhang ZJ, Cao DL, Xu J, Hui J, Zhu L, Gao YJ. Activation of astrocytes in the anterior cingulate cortex contributes to the affective component of pain in an inflammatory pain model. *Brain Res Bull* 2012; 87: 60-66.

Chien A, Eliav E, Sterling M. Hypoaesthesia occurs with sensory hypersensitivity in chronic whiplash--further evidence of a neuropathic condition. *Man Ther* 2009; 14: 138-146.

Chien A, Eliav E, Sterling M. Whiplash (grade II) and cervical radiculopathy share a similar sensory presentation: an investigation using quantitative sensory testing. *Clin J Pain* 2008; 24: 595-603.

Cho HJ, Kim JK, Zhou XF, Rush RA. Increased brain-derived neurotrophic factor immunoreactivity in rat dorsal root ganglia and spinal cord following peripheral inflammation. *Brain Res* 1997; 764: 269-272.

Coghill RC, Mayer DJ, Price DD. Wide dynamic range but not nociceptive-specific neurons encode multidimensional features of prolonged repetitive heat pain. *J Neurophysiol* 1993; 69: 703-716.

Coull JA, Beggs S, Boudreau D, Boivin D, Tsuda M, Inoue K, Gravel C, Salter MW, De Koninck Y. BDNF from microglia causes the shift in neuronal anion gradient underlying neuropathic pain. *Nature* 2005; 538: 1017-1021.

Crosby ND, Gilliland TM, Winkelstein BA. Early afferent activity from the facet joint after painful trauma to its capsule potentiates neuronal excitability and glutamate signaling in the spinal cord. *Pain* 2014; 155: 1878-1887.

Crosby ND, Weisshaar CL, Winkelstein BA. Spinal neuronal plasticity is evident within 1 day after a painful cervical facet joint injury. *Neurosci Lett* 2013; 542: 102-106.

Crosby ND, Zaucke F, Kras JV, Dong L, Luo ZD, Winkelstein BA. Thrombospondin-4 and excitatory synaptogenesis promote spinal sensitization after painful mechanical joint injury. *Exp Neurol* 2015; 264: 111-120.

Curatolo M, Petersen-Felix S, Arendt-Nielsen L, Giani C, Zbinden AM, Radanov BP. Central hypersensitivity in chronic pain after whiplash injury. *Clin J Pain* 2001; 17: 306-315.

Dare D, Rodeo S. Mechanisms of post-traumatic osteoarthritis after ACL injury. *Curr Rheumatol Rep* 2014; 16: 448.

Dawes JM, Andersson DA, Bennett DLH, Bevan S, McMahon SB. Inflammatory mediators and modulators of pain. In: Textbook of Pain, McMahon SB, Koltzenburg M, Tracey I, Turk DC, Eds., *Philadelphia: Saunders*, 2013; 48-67.

de Lange-Brokaar BJ, Ioan-Facsinay A, van Osch GJ, Zuurmond AM, Schoones J, Toes RE, Huizinga TW, Kloppenburg M. Synovial inflammation, immune cells and their cytokines in osteoarthritis: a review. *Osteoarthritis Cartilage* 2012; 20: 1484-1499.

Decosterd I, Woolf CJ. Spared nerve injury: an animal model of persistent peripheral neuropathic pain. *Pain* 2000; 87: 149-158.

Delcroix JD, Valletta JS, Wu C, Hunt SJ, Kowal AS, Mobley WC. NGF signaling in sensory neurons: evidence that early endosomes carry NGF retrograde signals. *Neuron* 2003; 39: 69-84.

DeSantana JM, Da Silva LF, De Resende MA, Sluka KA. Transcutaneous electrical nerve stimulation at both high and low frequencies activates ventrolateral periaqueductal grey to decrease mechanical hyperalgesia in arthritic rats. *Neuroscience* 2009; 163: 1233-1241.

Dib-Hajj SD, Cummins TR, Black JA, Waxman SG. Sodium channels in normal and pathological pain. *Annu Rev Neurosci* 2010; 33: 325-347.

Dina OA, Chen X, Reichling D, Levine JD. Role of protein kinase Cepsilon and protein kinase A in a model of paclitaxel-induced painful peripheral neuropathy in the rat. *Neuroscience* 2001; 108: 507-515.

Dirig DM, Salami A, Rathbun ML, Ozaki GT, Yaksh TL. Characterization of variables defining hindpaw withdrawal latency evoked by radiant thermal stimuli. *J Neurosci Meth* 1997; 76: 183-191.

Dong L, Crosby ND, Winkelstein BA. Gabapentin alleviates facet-mediated pain in the rat through reduced neuronal hyperexcitability and astrocytic activation in the spinal cord. *J Pain* 2013b; 14: 1564-1572.

Dong L, Guarino BB, Jordan-Sciutto KL, Winkelstein BA. Activating transcription factor 4, a mediator of the integrated stress response, is increased in the dorsal root ganglia following painful facet joint distraction. *Neuroscience* 2011; 193: 377-386.

Dong L, Odeleye AO, Jordan-Sciutto KL, Winkelstein BA. Painful facet joint injury induces neuronal stress activation in the DRG: implications for cellular mechanisms of pain. *Neurosci Lett* 2008; 443: 90-94.

Dong L, Quindlen JC, Lipschutz DE, Winkelstein BA. Whiplash-like facet joint loading initiates glutamatergic responses in the DRG and spinal cord associated with behavioral hypersensitivity. *Brain Res* 2012; 1461: 51-63.

Dong L, Smith JR, Winkelstein BA. Ketorolac reduces spinal astrocytic activation and PAR1 expression associated with attenuation of pain after facet joint injury. *J Neurotrauma* 2013a; 30: 818-825.

Dong L, Winkelstein BA. Simulated whiplash modulates expression of the glutamatergic system in the spinal cord suggesting spinal plasticity is associated with painful dynamic cervical facet loading. *J Neurotrauma* 2010; 27: 163-174.

Dong L. Inflammatory and neuronal mechanisms of facet-mediated pain in the context of neck injury (Doctoral Dissertation). 2011. *Dissertations available from ProQuest*. Paper AAI3497973.

Dostrovsky JO, Craig AD. Ascending projection systems. In: Textbook of Pain, McMahon SB, Koltzenburg M, Tracey I, Turk DC, Eds., *Philadelphia: Saunders*, 2013; 182-198.

Dostrovsky JO, Guilbaud G. Nociceptive responses in medial thalamus of the normal and arthritic rat. *Pain* 1990; 40: 93-104.

Dostrovsky JO. Role of thalamus in pain. *Prog Brain Res* 2000; 129: 245-257.

Dougherty KD, Dreyfus CF, Black IB. Brain-derived neurotrophic factor in astrocytes, oligodendrocytes, and microglia/macrophages after spinal cord injury. *Neurobiol Dis* 2000; 7: 574-585.

Dunk NM, Nicholson KJ, Winkelstein BA. Impaired performance on the angle board test is induced in a model of painful whiplash injury but is only transien in a model of cervical radiculopathy. *J Orthop Res* 2011; 29: 562-566.

Duric V, McCarson KE, Neurokinin-1 (NK-1) receptor and brain-derived neurotrophic factor (BDNF) gene expression is differentially modulated in the rat spinal dorsal horn and hippocampus during inflammatory pain. *Mol Pain* 2007; 3: 32.

Dyck PJ, Peroutka S, Rask C, Burton E, Baker MK, Lehman KA, Gillen DA, Hokanson JL, O'Brien PC. Intradermal recombinant human nerve growth factor induces pressure allodynia and lowered heat-pain threshold in humans. *Neurology* 1997; 48: 501-505.

Eck JC, Hodges SD, Humphreys SC. Whiplash: a review of a commonly misunderstood injury. *Am J Med* 2001; 110: 651-656.

Elliott JM, Noteboom JT, Flynn TW, Sterling M. Characterization of acute and chronic whiplash-associated disorders. *J Orthop Sports Phys Ther* 2009; 39: 312-323.

Evans RJ, Moldwin RM, Cossons N, Darekar A, Mills IW, Scholfield D. Proof of concept trial of tanezumab for the treatment of symptoms associated with interstitial cystitis. *J Urol* 2011; 185: 1716-1721.

Fang X, Djouhri L, McMullan S, Berry C, Waxman SG, Okuse K, Lawson SN. Intense isolectin-B4 binding in rat dorsal root ganglion neurons distinguishes C-fiber nociceptors with borad action potential and high Nav1.9 expression. *J Neurosci* 2006; 26: 7281-7292.

Fernandez-Perez AM, Villaverde-Gutierrez C, Mora-Sanchez A, Alonso-Blanco C, Sterling M, Fernandez-de-Las-Penas C. Muscle trigger points, pressure pain threshold, and cervical range of motion in patients with high level of disability related to acute whiplash injury. *J Orthop Sports Phys Ther* 2012; 42: 634-641.

Ferrari LF, Bogen O, Levine JD. Nociceptor subpopulations involved in hyperalgesic priming. *Neuroscience* 2010; 165: 896-901.

Ferrari R, Russell AS, Carroll LJ, Cassidy JD. A re-examination of the whiplash associated disorders (WAD) as a systemic illness. *Ann Rheum Dis* 2005; 64: 1337-1342.

Fischer MJ, Btesh J, McNaughton PA. Disrupting sensitization of transient receptor potential vanilloid subtype 1 inhibits inflammatory hyperalgesia. *J Neurosci* 2013; 33: 7407-7414.

Fisher PW, Zhao Y, Rico MC, Massicotte VS, Wade CK, Litvin J, Bove GM, Popoff SN, Barbe MF. Increased CCN2, substance P and tissue fibrosis are associated with sensorimotor declines in a rat model of repetitive overuse injury. *J Cell Commun Signal* 2015; Epub ahead of print.

Francis JT, Xu S, Chapin JK. Proprioceptive and cutaneous representations in the rat ventral posterolateral thalamus. *J Neurophysiol* 2008; 99: 2291-2304.

Freeman MD, Croft AC, Rossignol AM, Weaver DS, Reiser M. A review of methodologic critique of the literature refuting whiplash syndrome. *Spine* 1999; 24: 86-96.

Furman BD, Mangiapani DS, Zeitler E, Bailey KN, Horne PH, Huebner JL, Kraus VB, Guilak F, Olson SA. Targeting pro-inflammatory cytokines following joint injury: acute intra-articular inhibition of interleukin-1 following knee injury prevents post-traumatic arthritis. *Arthritis Res Ther* 2014; 16: R134.

Galeazza MT, Garry MG, Yost HJ, Strait KA, Hargreaves KM, Seybold VS. Plasticity in the synthesis and storage of substance P and calcitonin gene-related peptide in primary afferent neurons during peripheral inflammation. *Neuroscience* 1995; 66: 443-458.

Gao YJ, Ji RR. Targeting astrocyte signaling for chronic pain. *Neurotherapeutics* 2010; 7: 482-493.

Gautron M, Guilbaud G. Somatic responses of ventrobasal thalamic neurons in polyarthritic rats. *Brain Res* 1982; 237: 459-471.

Gellhorn AC, Katz JN, Suri P. Osteoarthritis of the spine: the facet joints. *Nat Rev Rheumatol* 2013; 9: 216-224.

Geng SJ, Liao FF, Dang WH, Ding X, Liu XD, Cai J, Han JS, Wan Y, Xing GG. Contribution of the spinal cord BDNF to the development of neuropathic pain by activation of the NR2B-containing NMDA receptors in rats with spinal nerve ligation. *Exp Neurol* 2010; 222: 256-266.

Gerber RK, Nie H, Arendt-Nielsen L, Curatolo M, Graven-Nielsen T. Local pain and spreading hyperalgesia induced by intramuscular injection of nerve growth factor are not reduced by local anesthesia of the muscle. *Clin J Pain* 2011; 27: 240-247.

Ghilardi JR, Freeman KT, Jimenez-Andrade JM, Coughlin KA, Kaczmarska MJ, Castaneda-Corral G, Bloom AP, Kuskowski MA, Mantyh PW. Neuroplasticity of sensory and sympathetic nerve fibers in a mouse model of a painful joint. *Arthritis Rheum* 2012; 64: 2223-2232.

Goldring MB, Goldring SR. Osteoarthritis. *J Cell Physiol* 2007; 213: 626-634.

Gomez-Pinilla F, Ying Z, Roy RR, Molteni R, Edgerton VR. Voluntary exercise induces a BDNF-mediated mechanism that promotes neuroplasticity. *J Neurophysiol* 2002; 88: 2187-2195.

Gong K, Shao W, Chen H, Wang Z, Luo ZJ. Rat model of lumbar facet joint osteoarthritis associated with facet-mediated mechanical hyperalgesia induced by intra-articular injection of monosodium iodoacetate. *J Formos Med Assoc* 2011; 110: 145-152.

Gong Y, Tagawa Y, Lunn MP, Laroy W, Heffer-Lauc M, Li CY, Griffin JW, Schnaar RL, Sheikh KA. Localization of major gangliosides in the PNS: implications for immune neuropathies. *Brain* 2002; 125: 2491-2506.

Greening J, Dilley A, Lynn B. In vivo study of nerve movement and mechanosensitivity of the median nerve in whiplash and non-specific arm pain patients. *Pain* 2005; 115: 248-253.

Gregory NS, Harris AL, Robinson CR, Dougherty PM, Fuchs PN, Sluka KA. An overview of animal models of pain: disease models and outcome measures. *J Pain* 2013; 14: 1255-1269.

Grimsholm O, Guo Y, Ny T, Forsgren S. Expression patterns of neurotrophins and neurotrophin receptors in articular chondrocytes and inflammatory infiltrates in knee joint arthritis. *Cells Tissues Organs* 2008; 188: 299-309.

Guilbaud G, Benoist JM, Condes-Lara M, Gautron M. Further evidence for the involvement of SmI cortical neurons in nociception: their responsiveness at 24 hr after arrrageenin-induced hyperalgesic inflammation in the rat. *Somatosens Mot Res* 1993; 10: 229-244.

Guilbaud G, Benoist JM, Gautron M, Kayser V. Aspirin clearly depresses responses of ventrobasal thalamus neurons to joint stimuli in arthritic rats. *Pain* 1982; 13: 153-163.

Guilbaud G, Iggo A, Tegnér R. Sensory receptors in ankle joint capsules of normal and arthritic rats. *Exp Brain Res* 1985; 58: 29-40.

Guo JD, Wang H, Zhang YQ, Zhao ZQ. Alterations of membrane properties and effects of D-serine on NMDA-induced current in rat anterior cingulate cortex neurons after monoarthritis. *Neurosci Lett* 2005; 384: 245-249.

Gwilym SE, Filippini N, Douaud G, Carr AJ, Tracey I. Thalamic atrophy associated with painful osteoarthritis of the hip is reversible after arthroplasty: a longitudinal voxel-based morphometric study. *Arthrits Rheum* 2010; 62: 2930-2940.

Ha SO, Kim JK, Hong HS, Kim DS, Cho HJ. Expression of brain-derived neurotrophic factor in rat dorsal root ganglia, spinal cord and gracile nuclei in experimental models of neuropathic pain. *Neuroscience* 2001; 107: 301-309.

Hagström Y, Carlsson J. Prolonged functional impairments after whiplash injury. *Scand J Rehabil Med* 1996; 28: 139-146.

Hargreaves K, Dubner R, Brown F, flores C, Joris J. A new and sensitive method for measuring thermal nociception in cutaneous hyperalgesia. *Pain* 1988; 32: 77-88.

Hartmann M, Heumann R, Lessmann V. Synaptic secretion of BDNF after high-frequency stimulation of glutamatergic synapses. *EMBO J* 2001; 20: 5887-5897.

Hauser RA, Phillips HJ. Treatment of joint hypermobility syndrome, including Ehlers-Danlos syndrome, with Hackett-Hemwall prolotherapy. *Journal of Prolotherapy* 2011; 3: 612-629.

Heppelmann B, Pawlak M. Sensitisation of articular afferents in normal and inflamed knee joints by substance P in the rat. *Neurosci Lett* 1997; 223: 97-100.

Herren-Gerber R, Weiss S, Arendt-Nielsen L, Petersen-Felix S, Di Stefano G, Radanov BP, Curatolo M. Modulation of central hypersensitivity by nociceptive input in chronic pain after whiplash injury. *Pain Med* 2004; 5: 366-376.

Hincapié CA, Cassidy JD, Côté P, Carroll LJ, Guzmán J. Whiplash injury is more than neck pain: a population-based study of pain localization after traffic injury. *J Occup Environ Med* 2010; 52: 434-440.

Hogg-Johnson S, van der Velde G, Carroll LJ, Holm LW, Cassidy JD, Guzman J, Côté P, Haldeman S, Ammendolia C, Carragee E, Hurwitz E, Nordin M, Peloso P. The burden and determinants of neck pain in the general population: results of the Bone and Joint Decade 2000-2010 Task Force on Neck Pain and Its Associated Disorders. *Spine* 2008; 33: S39-S51.

Hoheisel U, Unger T, Mense S. Sensitization of rat dorsal horn neurons by NGF-induced subthreshold potentials and low-frequency activation. A study employing intracellular recordings in vivo. *Brain Res* 2007; 1169: 34-43.

Hubbard RD, Winkelstein BA. Dorsal root compression produces myelinated axonal degeneration near the biomechanical thresholds for mechanical behavioral hypersensitivity. *Exp Neurol* 2008; 212: 482-489.

Hubbard RD, Winkelstein BA. Transient cervical nerve root compression in the rat induces bilateral forepaw allodynia and spinal glial activation: Mechanical factors in painful neck injuries. *Spine* 2005; 301: 1924-1932.

Hucho TB, Dina OA, Levine JD. Epac mediates a cAMP-to-PKC signaling in inflammatory pain: an isolectin B4(+) neuron-specific mechanism. *J Neurosci* 2005; 25: 6119-6126.

Huebner KD, Shrive NG, Frank CB. Dexamethasone inhibits inflammation and cartilage damage in a new model of post-traumatic osteoarthritis. *J Orthop Res* 2014; 32: 566-572.

Huh Y, Bhatt R, Jung D, Shin HS, Cho J. Interactive responses of a thalamic neuron to formalin induced lasting pain in behaving mice. *PLoS One* 2012; 7: e30699.

Huh Y, Cho J. Discrete pattern of burst stimulation in the ventrobasal thalamus for anti-nociception. *PLoS One* 2013; 8: e67655.

Ikeda O, Murakami M, Ino H, Yamazaki M, Nemoto T, Koda M, Nakayama C, Moriya H. Acute up-regulation of brain-derived neurotrophic factor expression resulting from experimentally induced injury in the rat spinal cord. *Acta Neuropathol* 2001; 102: 239-245.

Inagaki K, Churchill E, Mochly-Rosen D. Epsilon protein kinase C as a potential therapeutic target for the ischemic heart. *Cardiovasc Res* 2006; 70: 222-230.

Ishidate T, Ward HJ, Hoyer JR. Quantitative studies of tubular immune complex formation and clearance in rats. *Kidney Int* 1990; 38: 1075-1084.

Ishikawa T, Miyagi M, Ohtori S, Aoki Y, Ozawa T, Doya H, Saito T, Moriya H, Takahashi K. Characteristics of sensory DRG neurons innervating the lumbar facet joints in rats. *Eur Spine J* 2005; 14: 559-564.

Ivancic PC, Ito S, Tominaga Y, Rubin W, Coe MP, Ndu AB, Carlson EJ, Panjabi MM. Whiplash causes increased laxity of cervical capsular ligament. *Clin Biomech (Bristol, Avon)* 2008; 23: 159-165.

Ivanusic JJ, Beaini D, Hatch RJ, Staikopoulos V, Sessle BJ, Jennings EA. Peripheral N-methyl-d-aspartate receptors contribute to mechanical hypersensitivity in a rat model of inflammatory temporomandibular joint pain. *Eur J Pain* 2011; 15: 179-185.

Iwakura N, Ohtori S, Orita S, Yamashita M, Takahashi K, Kuniyoshi K. Role of low-affinity nerve growth factor receptor inhibitory antibody in reducing pain behavior and calcitonin gene-related peptide expression in a rat model of wrist joint inflammatory pain. *J Hand Surg Am* 2010; 35: 267-73.

Iwata M, LeBlanc BW, Kadasi LM, Zerah ML, Cosgrove RG, Saab CY. High-frequency stimulation in the ventral posterolateral thalamus reverses electrophysiologic changes and hyperalgesia in a rat model of peripheral neuropathic pain. *Pain* 2011; 152: 2505-2513.

Jacobs LJ, Vo N, Kang JD. Identifying inflammatory targets for biologic therapies for spine pain. *PM R* 2011; 3: S12-S17.

Jansen GB, Edlund C, Grane P, Hildingsson C, Karlberg M, Link H, Måwe U, Portala K, Rydevik B, Sterner Y. Whiplash injuries: diagnosis and early management. The Swedish Society of Medicine and the Whiplash Medical Task Force. *Eur Spine J* 2008; Suppl 3: S355-S417.

Janusz MJ, Bendele AM, Brown KK, Taiwo YO, Hsieh L, Heitmeyer SA. Induction of osteoarthritis in the rat by surgical tear of the meniscus: inhibition of joint damage by a matrix metalloproteinase inhibitor. *Osteoarthritis Cartilage* 2002; 10: 785-791.

Jaumard NV, Udupa JK, Welch WC, Winkelstein BA. Kinematic magnetic resonance imaging to define the cervical facet joint space for the spine in neutral and torsion. *Spine* 2014; 39: 664-672.

Ji RR, Befort K, Brenner GJ, Woolf CJ. ERK MAP kinase activation in superficial spinal cord neurons induces prodynorphin and NK-1 upregulation and contributes to persistent inflammatory pain hypersensitivity. *J Neurosci* 2002; 22: 478-485.

Ji RR, Kohno T, Moore KA, Woolf CJ. Central Sensitization and LTP: do pain and memory share similar mechanisms? *Trends Neurosci* 2003; 26: 696-705.

Jiang J, Quan Y, Ganesh T, Pouliot WA, Dudek FE, Dingledine R. Inhibition of the prostaglandin receptor EP2 following status epilepticus reduces delayed mortality and brain inflammation. *Proc Natl Acad Sci U S A* 2013; 110: 3591-3596.

Johannes CB, Le TK, Zhou X, Johnston JA, Dworkin RH. The prevalence of chronic pain in United States adults: results of an internet-based survey. *J Pain* 2010; 11: 1230-1239.

Joseph EK, Levine JD. Hyperalgesic priming is restricted to isolectin B4-positive nociceptors. *Neuroscience* 2010; 169: 431-435.

Jull GA, Söderlund A, Stemper BD, Kenardy J, Gross AR, Côté P, Treleaven J, Bogduk N, Sterling M, Curatolo M. Toward optimal early management after whiplash injury to lessen the rate of transition to chronicity: discussion paper 5. *Spine* 2011; 36: S335-S342.

Kallakuri S, Li Y, chen C, Cavanaugh JM. Innervation of cervical ventral facet joint capsule: Histological evidence. *World J Orthop* 2012; 3: 10-14.

Kallakuri S, Singh A, Chen C, Cavanaugh JM. Demonstration of substance P, calcitonin gene-related peptide, and protein gene product 9.5 containing nerve fibers in human cervical facet joint capsules. *Spine* 2004; 29: 1182-1186.

Kallakuri S, Singh A, Lu Y, Chen C, Patwardhan A, Cavanaugh JM. Tensile stretching of cervical facet joint capsule and related axonal changes. *Eur Spine J* 2008; 17: 556-563.

Kartha S, Zeeman ME, Baig HA, Guarino BB, Winkelstein BA. Upregulation of BDNF & NGF in cervical intervertebral discs exposed to painful whole body vibration. *Spine* 2014; 39: 1542-1548.

Katz N, Borenstein DG, Birbara C, Bramson C, Nemeth MA, Smith MD, Brown MT. Efficacy and safety of tanezumab in the treatment of chronic low back pain. *Pain* 2011; 152: 2248-2258.

Kawasaki Y, Kohno T, Zhuang Zy, Brenner GJ, Wang H, Van Der Meer C, Befort K, Woolf CJ, Ji RR. Ionotropic and metabotropic receptors, protein kinase A, protein kinase C, and Src contribute to C-fiber-induced ERK activation and cAMP Response element-binding protein phosphorylation in dorsal horn neurons, leading to central sensitization. *J Neurosci* 2004; 24: 8310-8321.

Keeble JE, Brain SD. A role for substance P in arthritis? *Neurosci Lett* 2004; 361: 176-179.

Kerr BJ, Bradbury EJ, Bennett DLH, Trivedi PM, Dassan P, French J, Shelton DB, McMahon SB, Thompson SWN. Brain-derived neurotrophic factor modulates nociceptive sensory inputs and NMDA-evoked responses in the rat spinal cord. *J Neurosci* 1999; 19: 5138-5148.

Kerr BJ, Souslova V, McMahon SB, Wood JN. A role for the TTX-resistant sodium channel Nav 1.8 in NGF-induced hyperalgesia, but not neuropathic pain. *Neuroreport* 2001; 12: 3077-3080.

Khasar SG, Lin YH, Martin A, Dadgar J, McMahon T, Wang D, Hundle B, Aley KO, Isenberg W, McCarter G, Green PG, Hodge CW, Levine JD, Messing RO. A novel nociceptor signaling pathway revealed in protein kinase C epsilon mutant mice. *Neuron* 1999; 24: 253-260.

Kidd BL, Morris VH, Urban L. Pathophysiology of joint pain. *Ann Rheum Dis* 1996; 55: 276-283.

Kirpalani D, Mitra R. Cervical facet joint dysfunction: a review. *Arch Phys Med Rehabil* 2008; 89: 770-774.

Kobayashi H, Yokoyama M, Matsuoka Y, Omori M, Itano Y, Kaku R, Morita K, Ichikawa H. Expression changes of multiple brain-derived neurotrophic factor transcripts in selective spinal nerve ligation model and complete Freund's adjuvant model. *Brain Res* 2008; 1206: 13-19.

Kosek E, Januszewska A. Mechanisms of pain referral in patients with whiplash-associated disorder. *Eur J Pain* 2008; 12: 650-660.

Kras JV, Dong L, Winkelstein BA. Increased interleukin-1α and prostaglandin E2 expression in the spinal cord at 1 day after painful facet joint injury: evidence of early spinal inflammation. *Spine* 2014a; 39: 207:212.

Kras JV, Dong L, Winkelstein BA. The prostaglandin E2 receptor, EP2, is upregulated in the dorsal root ganglion after painful cervical facet joint injury in the rat. *Spine* 2013a; 38: 217-222.

Kras JV, Tanaka K, Gilliland TM, Winkelstein BA. An anatomical and immunohistochemical characterization of afferents innervating the C6-C7 facet joint after painful joint loading in the rat. *Spine* 2013b; 38: E325-E331.

Kras JV, Weisshaar CL, Quindlen J, Winkelstein BA. Brain-derived neurotrophic factor is upregulated in the cervical dorsal root ganglia and spinal cord and contributes to the maintenance of pain from facet joint injury in the rat. *J Neurosci Res* 2013c; 91: 1312-1321.

Kras JV, Kartha S, Winkelstein BA. Intra-Articular Nerve Growth Factor Regulates Development, But Not Maintenance, of Injury-Induced Facet Joint Pain & Spinal Neuronal Hypersensitivity. *Osteoarthritis Cartilage* 2014b, submitted.

Kumar V, Mahal BA. NGF – the TrkA to successful pain treatment. *J Pain Res* 2012; 5: 279-287.

LaBuda CJ, Fuchs PN. A behavioral test paradigm to measure the aversive quality of inflammatory and neuropathic pain in rats. *Exp Neurol* 2000; 163: 490-494.

LaGraize SC, Fuchs PN. GABAA but not GABAB receptors in the rostral anterior cingulate cortex selectively modulate pain-induced escape/avoidance behavior. *Exp Neurol* 2007; 204: 182-194.

Lamour Y, Guilbaud G, Willer JC. Altered properties and laminar distribution of neuronal responses to peripheral stimulation in the SmI cortex of the arthritic rat. *Brain Res* 1983; 273: 183-187.

Lane NE, Schnitzer TJ, Birbara CA, Mokhtarani M, Shelton DL, Smith MD, Brown MT. Tanezumab for the treatment of pain from osteoarthritis of the knee. *N Engl J Med* 2010; 363: 1521-1531.

Langford DJ, Bailey AL, Chanda ML, Clarke SE, Drummond TE, Echols S, Glick S, Ingrao J, Klassen-Ross T, Lacroix-Fralish ML, Matsumiya L, Sorge RE, Sotocinal SG, Tabaka JM, Wong D, van den Maagdenberg AM, Ferrari MD, Craig KD, Mogil JS. Coding of facial expressions of pain in the laboratory mouse. *Nat Methods* 2010; 7: 447-449.

Larsen JJ, Arnt J. Reduction in locomotor activity of arthritic rats as parameter for chronic pain: effect of morphine, acetylsalicylic acid and citalopram. *Acta Pharmacol Toxicol (Copenh)* 1985; 57: 345-351.

Latremoliere A, Woolf CJ. Central sensitization: a generator of pain hypersensitivity by central neural plasticity. *J Pain* 2009; 10: 895-926.

Le Bars D, Gozariu M, Cadden SW. Animal models of nociception. *Pharmacol Rev* 2001; 53: 597-652.

LeBlanc BW, Zerah ML, Kadasi LM, Chai N, Saab CY. Minocycline injection in the ventral posterolateral thalamus reverses microglial reactivity and thermal hyperalgesia secondary to sciatic neuropathy. *Neurosci Lett* 2011; 498: 138-142.

Lee AS, Ellman MB, Yan D, Kroin JS, Cole BJ, van Wijnen AJ, Im HJ. A current review of molecular mechanisms regarding osteoarthritis and pain. *Gene* 2013; 527: 440-447.

Lee KE, Davis MB, Mejilla RM, Winkelstein BA. In vivo cervical facet capsule distraction: mechanical implications for whiplash and neck pain. *Stapp Car Crash J* 2004; 48: 373-396.

Lee KE, Davis MB, Winkelstein BA. Capsular ligament involvement in the development of mechanical hyperalgesia after facet joint loading: behavioral and inflammatory outcomes in a rodent model of pain. *J Neurotrauma* 2008; 25: 1383-1393.

Lee KE, Winkelstein BA. Joint distraction magnitude is associated with different behavioral outcomes and substance P levels for cervical facet joint loading in the rat. *J Pain* 2009; 10: 436-445.

Lee MW, McPhee RW, Stringer MD. An evidence-based approach to human dermatomes. *Clin Anat* 2008; 21: 363-373.

Lee SE, Shen H, Taglialatela G, Chung JM, Chung K. Expression of nerve growth factor in the dorsal root ganglion after peripheral nerve injury. *Brain Res* 1998; 796: 99-106.

Lee Y, Takami K, Kawai Y, Girgis S, Hillyard CJ, MacIntyre I, emson PC, Tohyama M. Distribution of calcitonin gene-related peptide in the rat peripheral nervous system with reference to its coexistence with substance P. *Neuroscience* 1985; 15: 1227-1237.

Lever IJ, Bradbury EJ, Cunningham JR, Adelson DW, Jones MG, McMahon SB, Marvizon JC, Malcangio M. Brain-derived neurotrophic factor is released in the dorsal horn by distinctive patterns of afferent fiber stimulation. *J Neurosci* 2001; 21: 4469-4477.

Levine JD, Clark R, Devor M, Helms C, Moskowitz MA, Basbaum AI. Intraneuronal substance P contributes to the severity of experimental arthritis. *Science* 1984; 226: 547-549.

Lewin GR, Rueff A, Mendell LM. Peripheral and central mechanisms of NGF-induced hyperalgesia. *Eur J Neurosci* 1994; 6: 1903-1912.

Li CQ, Xu JM, Liu D, Zhang JY, Dai RP. Brain derived neurotrophic factor (BDNF) contributes to the pain hypersensitivity following surgical incision in the rats. *Mol Pain* 2008; 4: 27.

Li J, Muehleman C, Abe Y, Masuda K. Prevalence of facet joint degeneration in association with intervertebral joint degeneration in a sample of organ donors. *J Orthop Res* 2011; 29: 1267-1274.

Li L, Xian CJ, Zhong JH, Zhou XF. Upregulation of brain-derived neurotrophic factor in sensory pathway by selective motor nerve injury in adult rats. *Neurotox Res* 2006; 9: 269-283.

Li X, Ellman M, Muddasani P, Wang JH, Cs-Szabo G, van Wijnen AJ, Im HJ. Prostaglandin E2 and its cognate EP receptors control human adult articular cartilage homeostasis and are linked to the pathophysiology of osteoarthritis. *Arthritis Rheum* 2009; 60: 513-523.

Lin CR, Amaya F, Barrett L, Wang H, Takada J, Samad TA, Woolf CJ. Prostaglandin E2 receptor EP4 contributes to inflammatory pain hypersensitivity. *J Pharmacol Exp Ther* 2006; 319: 1096-1103.

Lipowitz AJ, Newton CD. Degenerative joint disease and traumatic arthritis. In: Textbook of Small Animal Orthopedics, Newton CD, Nunamaker DM, Eds., *Philadelphia: Lippincott Williams & Wilkins*, 1985.

Litwic A, Edwards MH, Dennison EM, Cooper C. Epidemiology and burden of osteoarthritis. *Br Med Bull* 2013; 105: 185-199.

Little CB, Zaki S. What constitutes an “animal model of osteoarthritis” -- the need for consensus? *Osteoarthritis Cartilage* 2012; 20: 261-267.

Livak KJ, Schmittgen TD. Analysis of relative gene expression data using real-time quantitative PCR and the 2(-Delta Delta C(T)) method. *Methods* 2001; 25: 402-408.

Llinás RR, ribary U, Jeanmonod D, Kronberg E, Mitra PP. Thalamocoritcal dysrhythmia: A neurological and neuropsychiatric syndrome characterized by magnetoencephalography. *Proc Natl Acad Sci USA* 1999; 96: 15222-15227.

Loeser JD, Treede RD. The Kyoto protocol of IASP basic pain terminology. *Pain* 2008; 137: 473-477.

Longo G, Osikowicz M, Ribeiro-da-Silva A. Sympathetic fiber sprouting in inflamed joints and adjacent skin contributes to pain-related behavior in arthritis. *J Neurosci* 2013; 33: 10066-10074.

Lord SM, Barnsley L, Wallis BJ, McDonald GJ, Bogduk N. Percutaneous radio-frequency neurotomy for chronic cervical zygapophyseal-joint pain. *N Engl J Med* 1996; 335: 1721-1726.

Lossos IS, Czerwinski DK, Wechser MA, Levy R. Optimization of quantitative real-time RT-PCR parameters for the study of lymphoid malignancies. *Leukemia* 2003; 17: 789-795.

Lu VB, Biggs JE, Stebbing MJ, Balasubramanyan S, Todd KG, Lai AY, Colmers WF, Dawbarn D, Ballanyi K, Smith PA. Brain-derived neurotrophic factor drives the changes in excitatory synaptic transmission in the rat superficial dorsal horn that follow sciatic nerve injury. *J Physiol* 2009; 587(Pt 5): 1013-1032.

Lu Y, Chen C, Kallakuri S, Patwardhan A, Cavanaugh JM. Neurophysiological and biomechanical characterization of goat cervical facet joint capsules. *J Orthop Res* 2005; 23: 779-787.

Luo JG, Zhao XL, Xu WC, Zhao XJ, Wang JN, Lin XW, Sun T, Fu ZJ. Activation of spinal NF-κB/p65 contributes to peripheral inflammation and hyperalgesia in rat adjuvant-induced arthritis. *Arthritis Rheumatol* 2014; 66: 896-906.

Ma QP, Woolf CJ. The progressive tactile hyperalgesia induced by peripheral inflammation is nerve growth factor dependent. *Neuroreport* 1997; 8: 807-810.

Malik-Hall M, Dina OA, Levine JD. Primary afferent nociceptor mechanisms mediating NGF-induced mechanical hyperalgesia. *Eur J Neurosci* 2005; 21: 3387-3394.

Manchikanti L, Pampati V, Fellows B, Bakhit CE. Prevalence of lumbar facet joint pain in chronic low back pain. *Pain Physician* 1999; 2: 59-64.

Manchikanti L, Pampati V, singh V, Falco FJ. Assessment of the escalating growth of facet joint interventions in the medicare population in the United States from 2000 to 2011. *Pain Physician* 2013; 6: E365-378.

Manchikanti L, Singh V, Falco FJ, Cash KM, Fellows B. Cervical medial branch blocks for chronic cervical facet joint pain: a randomized, double-blind, controlled trial with one-year follow-up. *Spine* 2008; 33: 1813-1820.

Manchikanti L, Singh V, Rivera J, Pampati V. Prevalence of cervical facet joint pain in chronic neck pain. *Pain Physician* 2002; 5: 243-249.

Mankovsky-Arnold T, Wideman TH, Lariviere C, Sullivan MJL. Measures of spontaneous and movement-evoked pain are associated with disability in patients with whiplash injuries. *J Pain* 2014; 15: 967-975.

Mannion RJ, Costigan M, Decosterd I, Amaya F, Ma QP, Holstege JC, Ji RR, Acheson A, Lindsay RM, Wilkinson GA, Woolf CJ. Neurotrophins: peripherally and centrally acting modulators of tactile stimulus-induced inflammatory pain hypersensitivity. *Proc Natl Acad Sci USA* 1999; 96: 9385-9390.

Mantyh PW, Koltzenburg M, Mendell LM, Tive L, Shelton DL. Antagonism of nerve growth factor-TrkA signaling and the relief of pain. *Anesthesiology* 2011; 115: 189-204.

Martindale JC, Wilson AW, Reeve AJ, Chessell IP, Headley PM. Chronic secondary hypersensitivity of dorsal horn neurons following inflammation of the knee joint. *Pain* 2007; 133: 79-86.

Matayoshi S, Jiang N, Katafuchi T, Koga K, Furue H, Yasaka T, Nakatsuka T, Zhou XF, Kawasaki Y, Tanaka N, Yoshimura M. Actions of brain-derived neurotrophic factor on spinal nociceptive transmission during inflammation in the rat. *J Physiol* 2005; 569(Pt2): 685-695.

Matson DJ, Broom DC, Carson SR, Baldassari J, Kehne J, Cortright DN. Inflammation-induced reduction of spontaneous activity by adjuvant: A novel model to study the effect of analgesics in rats. *J Pharmacol Exp Ther* 2007; 320: 194-201.

McMahon SB. NGF as a mediator of inflammatory pain. *Philos Trans R Soc Lond B Biol Sci* 1996; 351: 431-440.

McNamee KE, Burleigh A, Gompels LL, Feldmann M, Allen SJ, Williams RO, Dawbarn D, Vincent TL, Inglis JJ. Treatment of murine osteoarthritis with TrkAd5 reveals a pivotal role for nerve growth factor in non-inflammatory joint pain. *Pain* 2010; 149: 386-392.

Merighi A, Carmignoto G, Gobbo S, Lossi L, Salio C, Vergnano AM, Zonta M. Neurotrophins in spinal cord nociceptive pathways. *Prog Brain Res* 2004; 146: 291-321.

Merighi A, Salio C, Ghirri A, Lossi L, Ferrini F, Betelli C, Bardoni R. BDNF as a pain modulator. *Prog Neurobiol* 2008; 85: 297-317.

Michael GJ, Averill S, Nitkunan A, Rattray M, Bennett DL, Yan Q, Priestley JV. Nerve growth factor treatment increases brain-derived neurotrophic factor selectively in TrkA-expressing dorsal root ganglion cells and in their central terminations within the spinal cord. *J Neurosci* 1997; 17: 8476-8490.

Michael GJ, Averill S, Shorland PJ, Yan Q, Priestley JV. Axotomy results in major changes in BDNF expression by dorsal root ganglion cells: BDNF expression in large trkB and trkC cells, in pericellular baskets, and in projections to deep dorsal horn and dorsal column nuclei. *Eur J Neurosci* 1999; 11: 3539-3551.

Millan MJ. Descending control of pain. *Prog Neurobiol* 2002; 66: 355-474.

Millan MJ. The induction of pain: an integrative review. *Prog Neurobiol* 1999; 57: 1-164.

Miyagi M, Ohtori S, Ishikawa T, Aoki Y, Ozawa T, Doya H, Saito T, Moriya H, Takahashi K. Up-regulation of TNFalpha in DRG satellite cells following lumbar facet joint injury in rats. *Eur Spine J* 2006; 15: 953-958.

Mogil JS, Crager SE. What should we be measuring in behavioral studies of chronic pain in animals? *Pain* 2004; 112: 12-15.

Mogil JS, Davis KD, Derbyshire SW. The necessity of animal models in pain research. *Pain* 2010; 151: 12-17.

Moog M, Quintner J, Hall T, Zusman M. The late whiplash syndrome: a psychophysical study. *Eur J Pain* 2002; 6: 283-294.

Neogi T. The epidemiology and impact of pain in osteoarthritis. *Osteoarthritis Cartilage* 2013; 21: 1145-1153.

Neto FL, Carvalhosa AR, Ferreira-Gomes J, Reguenga C, Castro-Lopes JM. Delta opioid receptor mRNA expression is changed in the thalamus and brainstem of monoarthritic rats. *J Chem Neuroanat* 2008; 36: 122-127.

Nichols ML, Allen BJ, Rogers SD, Ghilardi JR, Honore P, Luger NM, Finke MP, Li J, Lappi DA, Simone DA, Mantyh PW. Transmission of chronic nociception by spinal neurons expressing the substance P receptor. *Science* 1999; 286: 1558-1561.

Nicholson KJ, Zhang S, Gilliland TM, Winkelstein BA. Riluzole effects on behavioral sensitivity and the development of axonal damage and spinal modifications that occur after painful nerve root compression. *J Neurosurg Spine* 2014; 20: 751-762.

Nicol GD, Vasko MR. Unraveling the story of NGF-mediated sensitization of nociceptive sensory neurons: ON or OFF the Trks? *Mol Interv* 2007; 7: 26-41.

Nie H, Zhang H, Weng HR. Bidirectional neuron-glia interactions triggered by deficiency of glutamate uptake at spinal sensory synapses. *J Neurophysiol* 2010; 104: 713-725.

Nuki G. Osteoarthritis: a problem of joint failure. *Z Rheumatol* 1999; 58: 142-147.

Obata K, Yamanaka H, dai Y, Mizushima T, Fukuoka T, Tokunaga A, Noguchi K. Activation of extracellular signal-regulated protein kinase in the dorsal root ganglion following inflammation near the nerve cell body. *Neuroscience* 2004; 126: 1011-1021.

Obata K, Yamanaka H, Dai Y, Mizushima T, Fukuoka T, Tokunaga A, Yoshikawa H, Noguchi K. Contribution of degeneration of motor and sensory fibers to pain behavior and the changes in neurotrophic factors in rat dorsal root ganglion. *Exp Neurol* 2004; 188: 149-160.

Obata K, Yamanaka H, Dai Y, Tachibana T, Fukuoka T, Tokunaga A, Yoshikawa H, Noguchi K. Differential activation of extracellular signal-regulated protein kinase in primary afferent neurons regulates brain-derived neurotrophic factor expression after peripheral inflammation and nerve injury. *J Neurosci* 2003; 23: 4117-4126.

Obata K, Yamanaka H, Kobayashi K, Dai Y, Mizushima T, Katsura H, Fukuoka T, Tokunaga A, Noguchi K. The effect of site and type of nerve injury on the expression of brain-derived neurotrophic factor in the dorsal root ganglion and on neuropathic pain behavior. *Neuroscience* 2006; 137: 961-970.

Ohtori S, Moriya H, Takahashi K. Calcitonin gene-related peptide immunoreactive sensory DRG neurons innervating the cervical facet joints in rats. *J Orthop Sci* 2002; 7: 258-261.

Ohtori S, Takahashi K, Chiba T, Yamagata M, Sameda H, Moriya H. Sensory innervation of the cervical facet joints in rats. *Spine* 2001; 26: 147-50.

Ohtori S, Takahashi K, Moriya H. Calcitonin gene-related peptide immunoreactive DRG neurons innervating the cervical facet joints show phenotypic switch in cervical facet injury rats. *Eur Spine J* 2003; 12: 211-215.

Ohtori S, Takahashi K, Moriya H. Inflammatory pain mediated by a phenotypic switch in brain-derived neurotrophic factor-immunoreactive dorsal root ganglion neurons innervating the lumbar facet joints in rats. *Neurosci Lett* 2002; 323: 129-132.

Okun A, DeFelice M, Eyde N, Ren J, Mercado R, King T, Porreca F. Transient inflammation-induced ongoing pain is driven by TRPV1 sensitive afferents. *Mol Pain* 2011; 7: 4.

Ono K, Kaneoka K, Wittek A, Kajzer J. Cervical injury mechanism based on the analysis of human cervical vertebral motion and head-neck-torso kinematics during low speed rear impacts. *Stapp Car Crash J* 1997; 41: 339-356.

Orita S, Ishikawa T, Miyagi M, Ochiai N, Inoue G, Eguchi Y, Kamoda H, Arai G, Toyone T, Aoki Y, Kubo T, Takahashi K, Ohtori S. Pain-related sensory innervation in monoiodoacetate-induced osteoarthritis in rat knees that gradually develops neuronal injury in addition to inflammatory pain. *BMC Musculoskelet Disord* 2011; 12: 134.

Panjabi MM, Cholewicki J, Nibu K, Grauer J, Vahldiek M. Capsular ligament stretches during in vitro whiplash simulations. *J Spinal Disord* 1998; 11: 227-232.

Panjabi MM, Cholewicki J, Nibu K, Grauer JN, Babat LB, Dvorak J. Mechanism of whiplash injury. *Clin Biomech (Bristol, Avon)* 1998; 13: 239-249.

Panjabi MM, Nibu K, Cholewicki J. Whiplash injuries and the potential for mechanical instability. *Eur Spine J* 1998c; 7: 484-492.

Parada CA, Yeh JJ, Joseph EK, Levine JD. Tumor necrosis factor receptor type-1 in sensory neurons contributes to induction of chronic enhancement of inflammatory hyperalgesia in rat. *Eur J Neurosci* 2003; 17: 1847-1852.

Parada CA, Rechling DB, Levine JD. Chronic hyperalgesic priming in the rat involves a novel interaction between cAMP and PKCepsilon second messenger pathways. *Pain* 2005; 113: 185-190.

Paxinos G, Watson C. The Rat Brain in Stereotaxic Coordinates. 6th edition. San Diego (CA): Academic Press; 2007.

Pearson AM, Ivancic PC, Ito S, Panjabi MM. Facet joint kinematics and injury mechanisms during simulated whiplash. *Spine* 2004; 29: 390-397.

Pecchi E, Priam S, Gosset M, Pigenet A, Sudre L, Laiguillon MC, Berenbaum F, Houard X. Induction of nerve growth factor expression and release by mechanical and inflammatory stimuli in chondrocytes: possible involvement in osteoarthritis pain. *Arthritis Res Ther* 2014; 16: R16.

Pedler A, Sterling M. Patients with chronic whiplash can be subgrouped on the basis of symptoms of sensory hypersensitivity and posttraumatic stress. *Pain* 2013; 154: 1640-1648.

Peolsson A, Ludvigsson ML, Wibault J, Dedering Å, Peterson G. Function in patients with cervical radiculopathy or chronic whiplash-associated disorders compared with healthy volunteers. *J Manipulative Physiol Ther* 2014; 37: 211-218.

Pereira EA, Green AL, Aziz TZ. Deep brain stimulation for pain. *Handb Clin Neurol* 2013; 116: 277-294.

Pettersson K, Toolanen G. High-dose methylprednisolone prevents extensive sick leave after whiplash injury. A prospective, randomized, double-blind study. *Spine* 1998; 23: 984-989.

Pezet S, Malcangio M, Lever IJ, Perkinton MS, Thompson SWN, Williams RJ, McMahon SB. Noxious stimulation induces trk receptor and downstream ERK phosphorylation in spinal dorsal horn. *Mol Cell Neurosci* 2002; 21: 684-695.

Pezet S, Malcangio M, McMahon SB. BDNF: a neuromodulator in nociceptive pathways? *Brain Res Brain Res Rev* 2002; 40: 240-249.

Pezet S, McMahon SB. Neurotrophins: mediators and modulators of pain. *Annu rev Neurosci* 2006; 29: 507-538.

Pezet S, Onteniente B, Grannec G, Calvino B. Chronic pain is associated with increased TrkA immunoreactivity in spinoreticular neurons. *J Neurosci* 1999; 19: 5482-5492.

Pizzo PA, Clark NM, Carter-Pokras O, Christopher M, Farrar JT, Follett KA, Heitkemper MM, Inturrisi C, Keefe F, Kerns RD, Lee JS, Loder E, Mackey S, Marinelli R, Payne R, Thernstrom M, Turk DC, Wesselmann U, Zeltzer L. Relieving pain in america: a blueprint for transforming prevention, care, education, and research. 2011; Washington, DC: National Academies Press (US).

Purves D, Augustine GJ, Fitzpatrick D, et al., editors. Neuroscience. 2nd edition. Sunderland (MA): Sinauer Associateds; 2001. Central Pain Pathwasy: The Spinothalamic Tract.

Quinlan KP, Annest JL, Myers B, Ryan G, Hill H. Neck strains and sprains among motor vehicle occupants-United States 2000. *Accid Anal Prev* 2004; 36: 21-27.

Quinn KP, Dong L, Golder FJ, Winkelstein BA. Neuronal hyperexcitability in the dorsal horn after painful facet joint injury. *Pain* 2010; 151: 414-421.

Quinn KP, Lee KE, Ahaghotu CC, Winkelstein BA. Structural changes in the cervical facet capsular ligament: potential contributions to pain following subfailure loading. *Stapp Car Crash J* 2007; 51: 169-187.

Raghavendra V, Tanga FY, DeLeo JA. Complete Freunds adjuvant-induced peripheral inflammation evokes glial activation and proinflammatory cytokine expression in the CNS. *Eur J Neurosci* 2004; 20: 467-473.

Rambaransingh B, Stanford G, Burnham R. The effect of repeated zygapophysial joint radiofrequency neurotomy on pain, disability, and improvement duration. *Pain Med* 2010; 11: 1343-7.

Rasche D, rinaldi PC, Young RF, Tronnier VM. Deep brain stimulation for the treatment of various chronic pain syndromes. *Neurosurg Focus* 2006; 21: E8.

Raychaudhuri SP, Raychaudhuri SK, Atkuri KR, Herzenberg LA, Herzenberg LA. Nerve growth factor: a key local regulator in the pathogenesis of inflammatory arthritis. *Arthritis Rheum* 2011; 63: 3243-3252.

Reichling DB, Levine JD. Critical role of nociceptor plasticity in chronic pain. *Trends Neurosci* 2009; 32: 611-618.

Rihl M, Kruithof E, Barthel C, De Keyser F, Veys EM, Zeidler H, Yu DT, Kuipers JG, Baeten D. Involvement of neurotrophins and their receptors in spondyloarthritis synovitis: relation to inflammation and response to treatment. *Ann Rheum Dis* 2005; 64: 1542-1549.

Ringkamp M, Raja SN, Campbell JN, Meyer RA. Peripheral mechanisms of cutaneous nociception. In: Textbook of Pain, McMahon SB, Koltzenburg M, Tracey I, Turk DC, Eds., *Philadelphia: Saunders*, 2013; 1-30.

Rothman SM, Hubbard RD, Lee KE, Winkelstein BA. Detection, transmission, and perception of pain. In: Interventional Spine: An Algorithmic Approach. Slipman C, Simeone F, Derby R, Eds., Philadelphia: Elsevier, 2007; 29-37.

Rothman SM, Winkelstein BA. Cytokine antagonism reduces pain and modulates spinal astrocytic reactivity after cervical nerve root compression. *Ann Biomed Eng* 2010; 38: 2563-2576.

Rothstein JD, Dykes-Hoberg M, Pardo CA, Bristol LA, Jin L, Kunci RW, Kanai Y, Hediger MA, Wang Y, Schielke JP, Welty DF. Knockout of glutamate transporters reveals a major role for astroglial transport in excitotoxicity and clearance of glutamate. *Neuron* 1996; 16: 675-686.

Rukwied R, Mayer A, Kluschina O, Obreja O, Schley M, Schmelz M. NGF induces non-inflammatory localized and lasting mechanical and thermal hypersensitivity in human skin. *Pain* 2010; 148: 407-413.

Rukwied R, Weinkauf B, Main M, Obreja O, Schmelz M. Inflammation meets sensitization -- an explanation for spontaneous nociceptor activity? *Pain* 2013; 154: 2707-2714.

Rukwied R, Weinkauf B, Main M, Obreja O, Schmelz M. Axonal hyperexcitability after combined NGF sensitization and UV-B inflammation in humans. *Eur J Pain* 2014; 18: 785-793.

Saab CY. Pain-related changes in the brain: diagnostic and therapeutic potentials. *Trends Neurosci* 2012; 35: 629-637.

Safieh-Garabedian B, Poole S, Allchorne A, Winter J, Woolf CJ. Contribution of interleukin-1 beta to the inflammation-induced increase in nerve growth factor levels and inflammatory hyperalgesia. *Br J Pharmacol* 1995; 115: 1265-1275.

Sah DW, Ossipo MH, Porreca F. Neurotrophic factors as novel therapeutics for neuropathic pain. *Nat Rev Drug Discov* 2003; 2: 460-472.

Saito K, Hitomi S, Suzuki I, Masuda Y, Kitagawa J, Tsuboi Y, Kondo M, Sessle BJ, Iwata K. Modulation of trigeminal spinal subnucleus caudalis neuronal activity following regeneration of transected inferior alveolar nerve in rats. *J Neurophysiol* 2008; 99: 2251-2263.

Saito T, Koshino T. Distribution of neuropeptides in synovium of the knee with osteoarthritis. *Clin Orthop Relat Res* 2000; 376: 172-182.

Sakuma Y, Ohtori S, Miyagi M, Ishikawa T, Inoue G, Doya H, Koshi T, Ito T, Yamashita M, Yamauchi K, Suzuki M, Moriya H, Takahashi K. Up-regulation of p55 TNF alpha-receptor in dorsal root ganglia neurons following lumbar facet joint injury in rats. *Eur Spine J* 2007; 16: 1273-1278.

Sameda H, Takahashi Y, Takahashi K, et al. Primary sensory neurons with dichotomizing axons projecting to the facet joint and the sciatic nerve in rats. *Spine* 2001; 26: 1105-9.

Sapunar D, Kostic S, Banozic A, Puljak L. Dorsal root ganglion – a potential new therapeutic target for neuropathic pain. *J Pain Res* 2012; 5: 31-38.

Schaible HG, Grubb BD. Afferent and spinal mechanisms of joint pain. *Pain* 1993; 55: 5-54.

Schaible HG, Richter F, Ebersberger A, Boettger MK, Vanegas H, Natura G, Vazquez E, von Banchet GS. Joint pain. *Exp Brain Res* 2009; 196: 153-162.

Schnitzer TJ, ekman EF, Spierings EL, Greenberg HS, Smith MD, Brown MT, West CR, Verburg KM. Efficacy and safety of tanezumab monotherapy or combined with non-steroidal anti-inflammatory drugs in the treatment of knee or hip osteoarthritis pain. *Ann Rheum Dis* 2014; Epub ahead of print.

Schnitzer TJ, Marks JA. A systematic review of the efficacy and general safety of antibodies to NGF in the treatment of OA of the hip or knee. *Osteoarthritis Cartilage* 2015; 23: S8-S17.

Scott D, Jull G, Sterling M. Widespread sensory hypersensitivity is a feature of chronic whiplash-associated disorder but not chronic idiopathic neck pain. *Clin J Pain* 2005; 21: 175-181.

Seal RP, Wang X, Guan Y, Raja SN, Woodbury CJ, Basbaum AI, Edwards RH. Injury-induced mechanical hypersensitivity requires C-low threshold mechanoreceptors. *Nature* 2009; 462: 651-655.

Seminowicz DA, Wideman TH, Naso L, Hatami-Khoroushahi Z, Fallatah S, Ware MA, Jarzem P, Bushnell MC, Shir Y, Ouellet JA, Stone LS. Effective treatment of chronic low back pain in humans reverses abnormal brain anatomy and function. *J Neurosci* 2011; 31: 7540-7550.

Sengupta P. The laboratory rat: relating its age with human's. *Int J Prev Med* 2013; 4: 624-630.

Seybold VS. The role of peptides in central sensitization. *Handb Exp Pharmacol* 2009; 194: 451-491.

Sharif Naeini R, Cahill CM, Ribeiro-da-Silva A, Ménard HA, Henry JL. Remodelling of spinal nociceptive mechanisms in an animal model of monoarthritis. *Eur J Neurosci* 2005; 22: 2005-2015.

Shuang F, Zhu J, Song K, Hou S, Liu Y, Zhang C, Tang J. Establishment of a rat model of adjuvant-induced osteoarthritis of the lumbar facet joint. *Cell Biochem Biophys* 2014; 70: 1545-1551.

Siegmund GP, Myers BS, Davis MB, Bohnet HF, Winkelstein BA. Mechanical evidence of cervical facet capsule injury during whiplash: a cadaveric study using combined shear, compression, and extension loading. *Spine* 2001; 26: 2095-2101.

Skolnik A, Gan TJ. New formulations of bupivacaine for the treatment of postoperative pain: liposomal bupivacaine and SABER-Bupivacaine. *Expert Opin Pharmacother* 2014; 15: 1535-1542.

Slack SE, Grist J, Mac Q, McMahon SB, Pezet S. TrkB expression and phosphor-ERK activation by brain-derived neurotrophic factor in rat spinothalamic tract neurons. *J Comp Neurol* 2005; 489: 59-68.

Slack SE, Pezet S, McMahon SB, Thompson SW, Malcangio M. Brain-derived neurotrophic factor induces NMDA receptor subunit one phosphorylation via ERK and PKC in the rat spinal cord. *Eur J Neurosci* 2004; 20: 1769-1778.

Smelter E, Hochberg MC. New treatments for osteoarthritis. *Curr Opin Rheumatol* 2013; 25: 310-316.

Smith AD, Jull G, Schneider G, Frizzell B, Hooper RA, Sterling M. Cervical radiofrequency neurotomy reduces central hyperexcitability and improves neck movement in individuals with chronic whiplash. *Pain Med* 2014; 15: 128-141.

Sotocinal SG, Sorge RE, Zaloum A, Tuttle AH, Martin LJ, Wieskopf JS, Mapplebeck JC, Wei P, Zhan S, Zhang S, McDougall JJ, King OD, Mogil JS. The Rat Grimace Scale: a partially automated method for quantifying pain in the laboratory rat via facial expressions. *Mol Pain* 2011; 7: 55.

Staton PC, Wilson AW, Bountra C, Chessell IP, Day NC. Changes in dorsal root ganglion CGRP expression in a chronic inflammatory model of the rat knee joint: differential modulation by rofecoxib and paracetamol. *Eur J Pain* 2007; 11: 283-289.

Steeds CE. The anatomy and physiology of pain. *Surgery – Oxford International Edition* 2009; 27: 507-511.

Steilen D, Hauser R, Woldin B, Sawyer S. Chronic neck pain: making the connection between capsular ligament laxity and cervical instability. *Open Orthop J* 2014; 8: 326-345.

Sterling M, Jull G, Vicenzino B, Kenardy J. Sensory hypersensitivity occurs soon after whiplash injury and is associated with poor recovery. *Pain* 2003; 104: 509-517.

Sterling M, Kenardy J. Physical and psychological aspects of whiplash: Important considerations for primary care assessment. *Man Ther* 2008; 13: 93-102.

Sterling M, Treleaven J, Edwards S, Jull G. Pressure pain thresholds in chronic whiplash associated disorder: Further evidence of altered central pain processing. *J Musculoskelet Pain* 2002; 10: 69-81.

Strine TW, Hootman JM. US national prevalence and correlates of low back and neck pain among adults. *Arthritis Rheum* 2007; 57: 656-65.

Stucky CL, Lewin GR. Isolectin B(4)-positive and –negative nociceptors are functionally distinct. *J Neurosci* 1999; 19: 6497-6505.

Summer GJ, Puntillo KA, Miaskowski C, Dina OA, Green PG, Levine JD. TrkA and PKC-epsilon in thermal burn-induced mechanical hyperalgesia in the rat. *J Pain* 2006; 7: 884-891.

Sun RQ, Tu YJ, Lawand NB, Yan JY, Lin Q, Willis WD. Calcitonin gene-related peptide receptor activation produces PKA- and PKC-dependent mechanical hyperalgesia and central sensitization. *J Neurophysiol* 2004; 92: 2859-2866.

Sundararajan S, Prasad P, Demetropoulos CK, Tashman S, Begeman PC, Yang KH, King AI. Effect of head-neck position on cervical facet stretch of post mortem human subjects during low speed rear end impacts. *Stapp Car Crash J* 2004; 48: 331-372.

Surace MF, Prestamburgo D, Campagnolo M, Fagetti A, Murena L. Presence of NGF and its receptor TrkA in degenerative lumbar facet joint specimens. *Eur Spine J* 2009; 18 Suppl 1: 122-125.

Svensson P, Cairns BE, Wang K, Arendt-Nielsen L. Injection of nerve growth factor into human masseter muscle evokes long-lasting mechanical allodynia and hyperalgesia. *Pain* 2003; 104: 241-247.

Swagerty DL Jr, Hellinger D. Radiographic assessment of osteoarthritis. *Am Fam Physician* 2001; 64: 279-286.

Syré PP, Weisshaar CL, Winkelstein BA. Sustained neuronal hyperexcitability is evident in the thalamus after a transient cervical radicular injury. *Spine* 2014; 39: E870-E877.

Tachihara H, Kikuchi S, Konno S, Sekiguchi M. Does facet joint inflammation induce radiculopathy?: an investigation using a rat model of lumbar facet joint inflammation. *Spine* 2007; 32: 406-412.

Takahashi Y, Nakajima Y. Dermatomes in the rat limbs as determined by antidromic stimulation of sensory C-fibers in spinal nerves. *Pain* 1996; 67: 197-202.

Tang S, Zhu J, Xu Y, Xiang AP, Jiang MH, Quan D. The effects of gradients of nerve growth factor immobilized PCLA scaffolds on neurite outgrowth in vitro and peripheral nerve regeneration in rats. *Biomaterials* 2013; 34: 7086-7096.

Tang XQ, Tanelian DL, Smith GM. Semaphorin3A inhibits nerve growth factor-induced sprouting of nociceptive afferents in adult rat spinal cord. *J Neurosci* 2004; 24: 819-827.

Tarpley JW, Kohler MG, Martin WJ. The behavioral and neuroanatomical effects of IB4-saporin treatment in rat models of nociceptive and neuropathic pain. *Brain Res* 2004; 1029: 65-76.

Teeple E, Jay GD, Elsaid KA, Gleming BC. Animal models of osteoarthritis: challenges of model selection and analysis. *AAPS J* 2013; 15: 438-446.

Thompson SW, Dray A, McCarson KE, Krause JE, Urban L. Nerve growth factor induces mechanical allodynia associated with novel A fibre-evoked spinal reflex activity and enhanced neurokinin-1 receptor activation in the rat. *Pain* 1995; 62: 219-231.

Thompson SW, Bennett DL, Kerr BJ, Bradbury EJ, McMahon SB. Brain-derived neurotrophic factor is an endogenous modulator of nociceptive responses in the spinal cord. *Proc Natl Acad Sci USA* 1999; 96: 7714-7718.

Uematsu T, Sakai A, Ito H, Suzuki H. Intra-articular administration of tachykinin $NK_1$ receptor antagonists reduces hyperalgesia and cartilage destruction in the inflammatory joint in rats with adjuvant-induced arthritis. *Eur J Pharmacol* 2011; 668: 163-168.

Uhelski ML, Davis MA, Fuchs PN. Pain affect in the absence of pain sensation: evidence of asomaesthesia after somatosensory cortex lesions in the rat. *Pain* 2012; 153: 885-892.

Umimura T, Miyagi M, Ishikawa T, Kamoda H, Wakai K, Sakuma T, sakai R, Kuniyoshi K, Ochiai N, Kishida S, Nakamura J, Eguchi Y, Iwakura N, Kenmoku T, Arai G, Orita S, Suzuki M, Sakuma Y, Kubota G, Oikawa Y, Inoue G, Aoki Y, Toyone T, Takahashi K, Ohtori S. Investigation of dichotomizing sensory nerve fibers projecting to the lumbar multifidus muscles and intervertebral disc or facet joint or sacroiliac joint in rats. *Spine* 2012; 37: 557-562.

van Eerd M, Patijn J, Lataster A, Rosenquist RW, van Kleef M, Mekhail N, Van Zundert J. Cervical facet pain. *Pain Pract* 2010; 10: 113-123.

van Eerd M, de Meij N, Dortangs E, Kessels A, van Zunderty J, Lataster A, Patijn J, van Kleef M. Long-term follow-up of cervical facet medial branch radiofrequency treatment with the single posterior-lateral approach: an exploratory study. *Pain Pract* 2014; 14: 8-15.

Vasquez E, Bär KJ, Ebersberger A, Klein B, Vanegas H, Schaible HG. Spinal prostaglandins are involved in the development but not the maintenance of inflammation-induced spinal hyperexcitability. *J Neurosci* 2001; 21: 9001-9008.

von Banchet GS, Schaible HG. Localization of the neurokinin 1 receptor on a subset of substance P-positive and isolectin B4-negative dorsal root ganglion neurons of the rat. *Neurosci Lett* 1999; 274: 175-178.

Wada M, Imura S, Baba H, Shimada S. Knee laxity in patients with osteoarthritis and rheumatoid arthritis. *Br J Rheumatol* 1996; 35: 560-563.

Wang JY, Luo F, Chang JY, Woodward DJ, Han JS. Parallel pain processing in freely moving rats revealed by distributed neuron recording. *Brain Res* 2003; 992: 263-271.

Wasserman JK, Koeberle PD. Development and characterization of a hemorrhagic rat model of central post-stroke pain. *Neuroscience* 2009; 161: 173-183.

Watkins LR, Maier SF, Goehler LE. Immune activation: the role of pro-inflammatory cytokines in inflammation, illness responses and pathological pain states. *Pain* 1995; 63: 289-302.

Weisshaar CL, Dong L, Bowman AS, Perez FM, Guarino BB, Sweitzer SM, Winkelstein BA. Metabotropic glutamate receptor-5 and protein kinase C-epsilon increase in dorsal

root ganglion neurons and spinal glial activation in an adolescent rat model of painful neck injury. *J Neurotrauma* 2010; 27: 2261-2271.

Weisshaar CL, Winkelstein BA. Ablating spinal NK1-bearing neurons eliminates the development of pain and reduces spinal neuronal hyperexcitability and inflammation from mechanical joint injury in the rat. *J Pain* 2014; 15: 378-386.

Weissner W, Winterson BJ, Stuart-Tilley A, Devor M, Bove GM. Time course of substance P expression in dorsal root ganglia following complete spinal nerve transection. *J Comp Neurol* 2006; 497: 78-87.

Wild KD, Bian D, Zhu D, Davis J, Bannon AW, Zhang TJ, Louis JC. Antibodies to nerve growth factor reverse established tactile allodynia in rodent models of neuropathic pain without tolerance. *J Pharmacol Exp Ther* 2007; 322: 282-287.

Wiley RG, Kline RH 4$^{th}$, Vierck CJ Jr. Anti-nociceptive effects of selectively destroying substance P receptor-expressing dorsal horn neurons using [Sar9,Met(O2)11]-substance P-saporin: behavioral and anatomical analyses. *Neuroscience* 2007; 146: 1333-1345.

Winkelstein BA, Nightingale RW, Richardson WJ, Myers BS. The cervical facet capsule and its role in whiplash injury: a biomechanical investigation. *Spine* 2000; 25: 1238-1246.

Winkelstein BA, Santos DG. An intact facet capsular ligament modulates behavioral sensitivity and spinal glial activation produced by cervical facet joint tension. *Spine* 2008; 33: 856-862.

Woolf CJ, Allchorne A, Safieh-Garabedian B, Poole S. Cytokines, nerve growth factor and inflammatory hyperalgesia: the contribution of tumour necrosis factor alpha. *Br J Pharmacol* 1997; 121: 417-424.

Woolf CJ, Safieh-Garabedian B, Ma QP, Crilly P, Winter J. Nerve growth factor contributes to the generation of inflammatory sensory hypersensitivity. *Neuroscience* 1994; 62: 327-331.

Woolf CJ, Wall PD. Relative effectiveness of C primary afferent fibers of different origins in evoking a prolonged facilitation of the flexor reflex in the rat. *J Neurosci* 1986; 6: 1433-1442.

Woolf CJ. Phenotypic modification of primary sensory neurons: the role of nerve growth factor in the production of persistent pain. *Philos Trans R Soc Lond B Biol Sci* 1996; 351: 441-448.

Xu D, Sun Y, Bao G, Liu W, Zhu X, Cui S, Fan J, Cui Z. MMP-1 overexpression induced by IL-1β: possible mechanism for inflammation in degenerative lumbar facet joint. *J Orthop Sci* 2013; 18: 1012-1019.

Yeomans DC, Pirec V, Proudfit HK. Nociceptive responses to high and low rates of noxious cutaneous heating are mediated by different nociceptors in the rat: behavioral evidence. *Pain* 1996; 68: 133-140.

Yoganandan N, Pintar FA, Cusick JF. Biomechanical analyses of whiplash injuries using an experimental model. *Accid Anal Prev* 2002; 34: 663-671.

Yu L, Yang F, Luo H, Liu FY, Han JS, Xing GG, Wan Y. The role of TRPV1 in different subtypes of dorsal root ganglion neurons in rat chronic inflammatory nociception induced by complete Freund's adjuvant. *Mol Pain* 2008; 4: 61.

Zhang X, Wang J, Zhou Q, Xu Y, Pu S, Wu J, Xue Y, tian Y, Lu J, Jiang W, Du D. Brain-derived neurotrophic factor-activated astrocytes produce mechanical allodynia in neuropathic pain. *Neuroscience* 2011; 199: 452-460.

Zhang YH, Vasko MR, Nicol GD. Ceramide, a putative second messenger for nerve growth factor, modulates the TTX-resistant Na(+) current and delayed rectifier K(+) current in rat sensory neurons. *J Physiol* 2002; 544(Pt2): 385-402.

Zhao P, Waxman SG, Hains BC. Sodium channel expression in the ventral posterolateral nucleus of the thalamus after peripheral nerve injury. *Mol Pain* 2006; 2: 27.

Zhou LJ, Yang T, Wei X, Liu Y, Xin WJ, Chen Y, Pang RP, Zang Y, Li YY, Liu XG. Brain-derived neurotrophic factor contributes to spinal long-term potentiation and mechanical hypersensitivity by activation of spinal microglia in rat. *Brain Behav Immun* 2011; 25: 322-334.

Zhou LJ, Zhong Y, Ren WJ, Li YY, Zhang T, Liu XG. BDNF induces late-phase LTP of C-fiber evoked field potentials in rat spinal dorsal horn. *Exp Neurol* 2008; 212: 507-514.

Zhou XF, Chie ET, Deng YS, Zhong JH, Zue Q, rush RA, Xian CJ. Injured primary sensory neurons switch phenotype for brain-derived neurotphic factor in the rat. *Neuroscience* 1999; 92: 841-853.

Zhou XF, Rush RA. Endogenous brain-derived neurotrophic factor is anterogradely transported in primary sensory neurons. *Neuroscience* 1996; 74: 945-953.

Ziegler EA, Magerl W, Meyer RA, Treede RD. Secondary hyperalgesia to punctuate mechanical stimuli. Central sensitization to A-fibre nociceptor input. *Brain* 1999; 122: 2245-2257.

Zimmermann M. Ethical guidelines for investigations of experimental pain in conscious animals. *Pain* 1983; 16: 109-110.

Zuby DS, Lund AK. Preventing minor neck injuries in rear crashes – forty years of progress. *J Occup Environ Med* 2010; 52: 428-433.